Quantitative proteomic analysis of the effect of 24(S),25-epoxycholesterol on SN4741 neuron cells.

Gilmore, Ian Richard

Quantitative Proteomic Analysis of the Effect of 24(*S*),25-Epoxycholesterol on SN4741 Neuron Cells.

IAN RICHARD GILMORE

SUBMITTED TO SWANSEA UNIVERSITY IN FULFILMENT OF THE REQUIREMENTS FOR THE DEGREE PROGRAMME OF DOCTOR OF PHILOSOPHY

SWANSEA UNIVERSITY

2013

ProQuest LLC.
789 East Eisenhower Parkway
P.O. Box 1346
Ann Arbor, MI 48106 – 1346

SUMMARY

Oxysterols are oxygenated derivatives of cholesterol or its precursors. One oxysterol, 24(*S*),25-epoxycholesterol (24(*S*),25-EC), which results from a shunt in the cholesterol synthesis pathway has been found at higher than expected levels in embryonic murine brain. Interestingly, the receptor that 24(*S*),25-EC is a ligand for, Liver X Receptor (LXR), has been implicated in neurogenesis in the ventral mid brain region of embryonic brain; an area with a high density of dopaminergic neurons. The mechanism by which LXR induces this effect is unclear. Therefore, proteomic and phosphoproteomic studies were performed using a stable isotope labelled in amino acid in cell culture (SILAC) approach in order to quantify changes in the proteome between different treatment groups in a mouse substantia nigra dopaminergic cell line (SN4741)

SN4741 cells were cultured in SILAC media containing differentially isotope labelled arginine and lysine. For protein expression studies SN4741 cells were treated in serum free media with vehicle, 10μM 24(*S*),25-EC, or 1μM GW3965, a synthetic ligand of LXR, for 24 hours. For analysis of changes in the phosphoproteome SN4741 cells were treated in serum free media with vehicle, 10μM 24(*S*),25-EC, or 30μM 25-hydroxycholesterol for 6 hours. Cells were lysed and protein combined in a 1:1 ratio before trypsin digestion and peptide separation via strong cation exchange chromatography. Phosphopeptides were enriched using immobilised metal affinity chromatography (IMAC). Resulting fractions were analysed, using a data dependent LC-MS/MS method. Data was quantified using MaxQuant software in conjunction with Mascot using an IPI mouse database.

In protein expression analysis known oxysterol regulated genes, via SREBP or LXR, were differentially expressed. Oxysterol treatment induced global changes in proteins involved in lipid (cholesterol, fatty acid, phospholipid, triglyceride) synthesis. LXRβ protein expression increased after GW3965 and 24(*S*),25-EC treatment, though no change was seen on LXRβ mRNA, implying that ligand binding protects LXRβ from degradation. 24(*S*),25-EC induced changes in expression and localisation of the membrane protein caveolin-1. Also, phosphoethanolamine cytidylyltransferase and collagen type IV alpha-3-binding protein, 2 proteins involved in phospholipid synthesis, had an altered expression after 24(*S*),25-EC treatment suggesting a role for oxysterols in membrane homeostasis. A cytokine, macrophage colony stimulating factor, which is required for normal neuronal development and macrophage differentiation had an LXR independent increased expression after 24(*S*),25-EC treatment. Quantitative RT-PCR data demonstrated that proteomic changes were due to both transcriptional and post-transcriptional effects of oxysterol. In addition, studies examining changes in the mouse phosphoproteome identified a number of novel phosphorylation sites.

DECLARATION AND STATEMENTS

DECLARATION

This work has not previously been accepted in substance for any degree and is not being concurrently submitted in candidature for any degree.

Signed .... (candidate)

Date ..... 23/12/13 .....

STATEMENT 1

This thesis is the result of my own investigations, except where otherwise stated. Where correction services have been used, the extent and nature of the correction is clearly marked in a footnote(s).

Other sources are acknowledged by footnotes giving explicit references. A bibliography is appended.

Signed ... . (candidate)

Date ..... 23/12/13 .....

STATEMENT 2

I hereby give consent for my thesis, if accepted, to be available for photocopying and for inter-library loan, and for the title and summary to be made available to outside organisations.

Signed .... (candidate)

Date ..... 23/12/13 .....

CONTENTS

	Page
CHAPTER 1: INTRODUCTION	1
1.1 Oxysterols	1
1.1.1 Cholesterol	1
1.1.2 Oxysterols	5
1.1.3 Synthesis of Oxysterols	8
1.1.3.1. Auto-oxidation and photo-oxidation of cholesterol	8
1.1.3.2. Enzymatic Formation of Oxysterols	9
1.1.3.3. 24(*S*),25-epoxycholesterol Synthesis	10
1.1.4. Differential distribution of oxysterols	10
1.1.5. Biological Functions of Oxysterols	12
1.1.5.1. Regulation of SREBP	12
1.1.5.2. Activation of Liver X Receptor	14
1.1.5.3. Regulation of Protein Degradation	15
1.1.5.4. Cell signalling	16
1.1.6. Role of Oxysterols in Disease	17
1.1.6.1. Role of Oxysterols in Cardiovascular Disease	17
1.1.6.2. Role of Oxysterols in Eye Disease	18
1.1.6.3. Role of Oxysterols in Neurodegenerative Diseases	19
1.1.7. Role of Oxysterols in Immunity	22
1.1.8. Role in development	26
1.2. Proteomics	29
1.2.1. Phosphoproteomics	30
1.2.2. Mass Spectrometry	31
1.2.2.1. Electrospray Ionization	31
1.2.2.2. Mass Analyzer	33
1.2.2.3. Precursor Ion	33
1.2.2.4. Tandem Mass Spectrometry (MS/MS)	34
1.2.2.5. Multistage activation	35

1.2.3. Quantitative Proteomics 35
1.2.3.1. Stable Isotope Labelling with Amino Acids in Cell Culture (SILAC) 36
1.2.3.2. Isobaric Tagging 37
1.2.3.3. Label Free Quantification 38
1.2.4. Peptide Mixture Complexity Reduction 38
1.2.4.1. Reverse Phase High Performance Liquid Chromatography 39
1.2.4.2. Strong Cation Exchange 39
1.2.4.3. Phosphoenrichment 40
1.2.5. Proteomic Bioinformatics 40
1.2.6. Experimental Considerations of Proteomic Studies 43
1.2.6.1 SN4741 Cell Line. 43
1.2.6.2. Proteomic Profiling Validation of Existing Knowledge 43
1.2.6.3. Identification of Novel 24(*S*),25-epoxycholesterol Regulated Genes 43
1.2.6.4. Identification of Novel 24(*S*),25-epoxycholesterol Regulated Protein Phosphorylation 44
1.3. Aims and Objectives 45

CHAPTER 2: MATERIALS AND METHODS 46
2.1. Cell Culture 46
2.1.1. SN4741 Cell Culture 46
2.1.2 Hela Cell Culture 47
2.1.3. THP1 Cell Culture 47
2.1.4. Freezing Cells 48
2.1.5. SILAC Cell Culture 49
2.2. Cell Culture Treatments. 50
2.2.1. Oxysterol Treatment 50
2.2.1.1. Adherent cells - SN4741 50
2.2.1.2. Suspension cells - THP1 50
2.2.2. GW3965 Treatment 51

2.2.2.1. Adherent cells - SN4741 51
2.2.2.2. Suspension cells - THP1 51
2.3. SN4741 viability assays 51
2.3.1. Cell Viability Assay: XTT 52
2.3.2. Cell Viability Assay: CellTiter Blue 52
2.4. Cell Lysis – Protein Extraction 52
2.5. Protein Estimation 53
2.6. Stable Isotope Labelling in Cell Culture (SILAC) 54
2.6.1. SILAC Treatment(s) - SN4741 54
2.6.2. SILAC Sample Reduction and Methylation 54
2.6.3. Strong Cation Exchange (SCX) Chromatography 54
2.6.4. Desalting 55
2.6.5. LTQ-Orbitrap Calibration Electrospray Positive Ion Mode 55
2.6.6. LTQ-Orbitrap Nanospray 56
2.6.7. Liquid Chromatography 56
2.6.8. Liquid Chromatography Validation - Bovine Serum Albumin 56
2.6.9. LTQ-Orbitrap LC-MS/MS 57
2.6.10. Orbitrap Velos LC-MS/MS 57
2.6.11. Analysis of SILAC LC-MS/MS data 58
2.7. PhosphoSILAC 59
2.7.1. PhosphoSILAC Treatments - SN4741 59
2.7.2. phosphoSILAC Sample Reduction and Methylation 59
2.7.3. Strong Cation Exchange Chromatography 59
2.7.4. Desalting 59
2.7.5. Peptide Methylation 60
2.7.6. Immobilised Metal Affinity Chromatography (IMAC) Phosphoenrichment 60
2.7.7. LTQ-Orbitrap Calibration Electrospray Positive Ion Mode 61
2.7.8. LTQ-Orbitrap Nanospray 61
2.7.9. Liquid Chromatography 61

2.7.10. Liquid Chromatography Validation - Bovine Serum Albumin 61
2.7.11. LTQ-Orbitrap LC-MS/MS 61
2.7.12. Analysis of phosphoSILAC LC-MS/MS data 62
2.8. Western Blotting 63
2.8.1. Polyacrylamide Gel Casting 63
2.8.2. Polyacrylamide Gel Electrophoresis Sample Loading 64
2.8.3. Protein Transfer to Nitrocellulose Membrane 65
2.8.4. Blocking Non-Specific Binding 65
2.8.5. Primary Antibody Incubation 66
2.8.6. Secondary Antibody Incubation 66
2.8.7. Detection 66
2.9. Fixed Cell Confocal Microscopy 67
2.10. Real Time Reverse Transcription PCR 69
2.10.1. RNA Extraction – Adherent cells 69
2.10.2. RNA Extraction – Suspension Cells 69
2.10.3. RNA Concentration Estimation 70
2.10.4. Reverse transcription 70
2.10.5. Primers 71
2.10.6. Real Time Polymerase Chain Reaction 73
2.10.7. Data Analysis 75
2.11. Mouse MCSF Enzyme Linked Immunosorbant Assay 77
2.12. Human MCSF Enzyme Linked Immunosorbant Assay 78
2.13 Statistical Analysis 79

CHAPTER 3: PROTEOMIC ANALYSIS OF 24*S*,25-EPOXYCHOLESTEROL TREATMENT IN SN4741 NEURONS 80
3.1. Introduction 80
3.2. Results 82
3.2.1. Analysis of 24(*S*),25-epoxycholesterol Treatment on SN4741 Growth 82
3.2.2. Analysis of 24(*S*),25-epoxycholesterol Treatment on SN4741 Viability 83

3.2.3. LXR Expression in SN4741 cells.
3.2.4. Strong Cation Exchange Fractionation of SILAC peptides 85
3.2.5. C18 Reverse Phase LC-MS/MS of SILAC peptides 87
3.2.6. Peptide and Protein Identifications 91
3.2.7. Expression of Neurotrophins and Neuronal Markers in SN4741 Cells 94
3.2.8. Analysis of proteomic data 98
100

CHAPTER 4: FURTHER ANALYSIS OF 24(*S*),25-EPOXYCHOLESTEROL INDUCED PROTEIN EXPRESSION CHANGES IN SN4741 NEURONS 136

4.1. Introduction 136
4.2. Results 138
4.2.1. Validation of Known Oxysterol Regulated Genes Identified by SILAC 138
4.2.2. Ligand Binding Induces Up-Regulation of Liver X Receptor β (LXRβ) 140
4.2.3. Fatty Acid Synthesis 141
4.2.4. Phospholipid Synthesis 142
4.2.5. Decreased expression of Ethanolamine-phosphate cytidylyltransferase 143
4.2.6. Increased expression of Collagen type IV alpha-3-binding protein 145
4.2.7. 24(*S*),25-epoxycholesterol Effects Caveolin-1 Expression and Localisation 146
4.2.8. Changes in miscellaneous proteins 151
4.2.8.1 Golgi sialoglycoprotein MG-160 151
4.2.8.2. Increased Expression of Macrophage Colony Stimulating Factor 152
4.2.9. Increased MCSF mRNA expression in THP1 human monocytes. 156

4.3. Discussion 160

CHAPTER 5: PHOSPHOPROTEOMIC ANALYSIS OF 24*S*,25-EPOXYCHOLESTEROL AND 25-HYDROXYCHOLESTEROL TREATMENT IN SN4741 CELLS 165

5.1. Introduction.. 165

5.2. Results 170

5.2.1. Effect of 25-hydroxycholesterol on ERK Phosphorylation 170

5.2.2. Strong Cation Exchange and IMAC 171

5.2.3. C18 Reverse Phase LC-MS/MS of SILAC phosphopeptides 176

5.2.4. Phosphopeptide Identifications 184

5.2.5. Analysis of Phosphopeptides For Novel Phosphorylation Sites 185

5.2.6. Analysis of Phosphopeptide Motifs 191

5.2.7. Quantitative Analysis of Changes in Phosphorylation 193

5.2.8. Peptide Methylation 208

5.3. Discussion 210

CHAPTER 5: GENERAL DISCUSSION 214

REFERENCES 220

APPENDIX 1: ALL PROTEINS IDENTIFIED AS DOWN-REGULATED IN ≥1 BIOLOGICAL REPLICATE 240

APPENDIX 2: ALL PROTEINS IDENTIFIED AS UP-REGULATED IN ≥1 BIOLOGICAL REPLICATE 258

APPENDIX 3. ALL PHOSPHOPEPTIDES IDENTIFIED AS DOWN-REGULATED AFTER TREATMENT WITH 24(*S*),25-EPOXYCHOLESTEROL 280

APPENDIX 4. ALL PHOSPHOPEPTIDES IDENTIFIED AS UP-REGULATED AFTER TREATMENT WITH 24(*S*),25-EPOXYCHOLESTEROL (24(*S*),25-EC) IN ≥ 1 BIOLOGICAL REPLICATE. 282

APPENDIX 5. ALL PHOSPHOPEPTIDES IDENTIFIED AS DOWN-REGULATED AFTER TREATMENT WITH 25-HYDROXYCHOLESTEROL (25-OHCHOL) IN ≥1 BIOLOGICAL REPLICATE. 284

APPENDIX 6. ALL PHOSPHOPEPTIDES IDENTIFIED AS UP-REGULATED AFTER TREATMENT WITH 25-HYDROXYCHOLESTEROL (25-OHCHOL) IN ≥1 BIOLOGICAL REPLICATE. 286

ACKNOWLEDGEMENTS

With love to my parents for their unflinching support and Louise for putting things in perspective.

List of Figures and Tables

Page

Figures

Chapter 1: Introduction

Figure 1.1. Structure of cholesterol and bioactive molecules for which cholesterol is the starting material. 2
Figure 1.2. The cholesterol synthesis pathway. 4
Figure 1.3. Chemical structure of oxysterols. 6
Figure 1.4. Simplified overview of bile acid synthesis. 7
Figure 1.5. Peptide fragmentation notation. 34
Figure 1.6. Schematic of SILAC experimental design. 37

Chapter 2: Materials and Methods

Figure 2.1. Typical plate set up for real time RT-PCR. 74

Chapter 3: Proteomic analysis of 24*S*,25-epoxycholesterol treatment in SN4741 Neurons

Figure 3.1. Effect of 24(*S*),25-epoxycholesterol on the rate of growth of SN4741 cells. 83
Figure 3.2. 24(*S*),25-epoxycholesterol is not toxic in SN4741 cells as measured by XTT assay. 84
Figure 3.3. 24(*S*),25-epoxycholesterol is not toxic in SN4741 cells as measured by Cell Titer Blue assay. 85
Figure 3.4. The protein level of ABCA1 is increased after 24 hours treatment with either 10μM 24(*S*),25-epoxycholesterol or 1μM GW3965 indicating that SN4741 cells express LXRα/β. 86
Figure 3.5. Strong Cation Exchange chromatography validation. 88
Figure 3.6. Strong Cation Exchange chromatography trace of SILAC peptides. 90
Figure 3.7. Reverse Phase LC-MS/MS validation. 91
Figure 3.8. Reverse Phase LC-MS/MS SILAC peptide separation. 92
Figure 3.9. Example SILAC spectra for lysine and arginine containing peptides. 93

Figure 3.10. There was a large overlap between runs of the same biological replicate on different instruments (A,B,C); 90% (A), 91% (B) and 86% (C) of leading proteins identified on the LCQ-Orbitrap with ≥2 peptides were also identified on the Orbitrap Velos with ≥2 peptides 97

Figure 3.11. Overlap of leading proteins identified and quantified with ≥2 peptides using MaxQuant. 130

Figure 3.12. Flowchart of data analysis showing the process by which protein expression data was rejected in order to identify reproducible changes in the proteome.

CHAPTER 4: FURTHER ANALYSIS OF 24(*S*),25-EPOXYCHOLESTEROL INDUCED PROTEIN EXPRESSION CHANGES IN SN4741 NEURONS

Figure 4.1. SN4741 reverse transcription qPCR. 139

Figure 4.2. IDOL is expressed in SN4741 cells. 140

Figure 4.3. Synthesis of the monounsaturated fatty acid oleic acid. 142

Figure 4.4. Simplified schematic of phospholipid synthesis. 143

Figure 4.5. Western blotting confirmed the observed down-regulation of phosphoethanolamine cytidylyltransferase (PCyt2) in SN4741 cells. 144

Figure 4.6. Western blotting confirmed the observed down-regulation of caveolin-1 in SN4741 cells. 147

Figure 4.7. Confocal microscopy performed on paraformaldehyde fixed SN4741 cells. 149

Figure 4.8. Confocal microscopy performed on paraformaldehyde fixed SN4741 cells. 150

Figure 4.9. Western blotting of SN4741 lysates probing for MCSF. 153

Figure 4.10. qPCR showing mean fold change in MCSF expression in SN4741 cells. 154

Figure 4.11. ELISA assay of secreted MCSF concentration in SN4741 cell supernatant. 155

Figure 4.12. qPCR showing mean fold change in MCSF expression in THP1 monocytes. 157

Figure 4.13. Western blot showing no change in MCSF protein expression in THP1 monocytes. 158

Figure 4.14. ELISA assay of secreted MCSF concentration in THP1 cell supernatant. 159

CHAPTER 5: PHOSPHOPROTEOMIC ANALYSIS OF 24*S*,25-EPOXYCHOLESTEROL AND 25-HYDROXYCHOLESTEROL TREATMENT IN SN4741 CELLS

Figure 5.1 25-hydroxycholesterol treatment increases ERK1/2 phosphorylation in Hela cells. 170

Figure 5.2. Strong Cation Exchange chromatography trace of SILAC peptides and phosphopeptides from the first biological replicate. 173

Figure 5.3. Strong Cation Exchange chromatography trace of SILAC peptides and phosphopeptides from the second biological replicate. 175

Figure 5.4. Reverse Phase LC-MS/MS SILAC phosphopeptide separation. 177

Figure 5.5. Phosphopeptide SILAC MS scan and multistage activation. 179

Figure 5.6. Phosphopeptide SILAC multistage activation MS/MS spectra. 181

Figure 5.7. Phosphopeptide SILAC multistage activation scans for the phosphopeptide AS(ph)EDESDLEDEEEKSQEDTEQK. 183

Figure 5.8. Venn diagram of phosphopeptides identified with unique sequence and site of modification. 185

Figure 5.9. Distribution of phosphopeptide 'best motif' with SILAC ratio. 193

Figure 5.10. Poor correlation in peptide ratio between biological replicates. 206

CHAPTER 6: GENERAL DISCUSSION

Figure 6.1. The effect of 24(*S*),25-epoxycholesterol on SN4741 neuronal cells. 217

TABLES Page

CHAPTER 1: INTRODUCTION

Table 1.1. Summary of important oxysterols and disease states in which they have been implicated. 22

CHAPTER 2: MATERIALS AND METHODS

Table 2.1. SN4741 full media. 46
Table 2.2. Hela full media. 47
Table 2.3. THP1 full media. 48
Table 2.4. SN4741 SILAC media. 49
Table 2.5. Dilutions of BSA for Bradford Assay standard curve 53
Table 2.6. Reagents used in preparation of resolving gel. 63
Table 2.7. Reagents used in preparation of the stacking gel. 64
Table 2.8.Primers used for reverse transcription qPCR. 71
Table 2.9. Conditions for real time PCR 75
Table 2.10. Summary of RT-PCR primer efficiencies. Efficiency shown as mean with standard deviation. 76

CHAPTER 3: PROTEOMIC ANALYSIS OF 24*S*,25-EPOXYCHOLESTEROL TREATMENT IN SN4741 NEURONS

Table 3.1. Threshold cycle for LXRα and LXRβ after RT-qPCR. 86
Table 3.2. Comparison of proteins identified between LTQ-Orbitrap and Orbitrap Velos instruments. 94
Table 3.3. Neurotrophins and neuronal markers expressed in SN4741 cells identified in SILAC experiments. 99
Table 3.4. Number of proteins identified as 'no change', 'up-regulated or 'down regulated' from each biological replicate on LTQ-Orbitrap or Orbitrap Velos instruments after treatment with 24(*S*),25-epoxycholesterol. 100
Table 3.5. Proteins identified as down-regulated. 102
Table 3.6. Proteins identified as up-regulated 115
Table 3.7. Gene Ontology terms identified as enriched after DAVID bio-informatic analysis. 126

Table 3.8. KEGG Pathways identified as enriched by DAVID bio-informatic analysis of down regulated proteins. 128

Table 3.9. Kegg Pathways identified as enriched by DAVID bio-informatic analysis of up-regulated proteins. 129

Table 3.10. Summary of reproducible changes in protein expression. 132

CHAPTER 5: PHOSPHOPROTEOMIC ANALYSIS OF 24*S*,25-EPOXYCHOLESTEROL AND 25-HYDROXYCHOLESTEROL TREATMENT IN SN4741 CELLS

Table 5.1. Summary of studies analysing effects of oxysterol treatment or cyclodextrin cholesterol depletion on ERK phosphorylation 167

Table 5.2. Summary of Western blot experiments analysing effect of 25-hydroxycholsterol on SN4741 cell phospho-ERK levels. 171

Table 5.3. The number of peptides identified in 2 biological replicates. 184

Table 5.4. Phosphopeptides identified in both replicates that are currently listed, on Uniprot.org (accessed 02/04/12), as not having experimental evidence to demonstrate post-translational modification at these phosphorylation sites. 187

Table 5.5. Probabilities of phosphopeptides identified in both replicates that are not currently listed, on Uniprot.org (accessed 02/04/12), as not phosphorylated at these sites. 189

Table 5.6. Frequency of phosphopeptide 'best motif' in each biological replicate. 192

Table 5.7. Median SILAC un-normalised ratios for the 2 phosphoproteomic data sets. 195

Table 5.8. Phosphopeptides identified as down-regulated after treatment with 24(*S*),25-epoxycholesterol (24(*S*),25-EC). 196

Table 5.9. Phosphopeptides identified as up-regulated after treatment with 24(*S*),25-epoxycholesterol (24(*S*),25-EC). 198

Table 5.10. Phosphopeptides identified as down-regulated after treatment with 25-hydroxycholesterol (25-OHChol). 200

Table 5.11. Phosphopeptides identified as up-regulated after treatment with 25-hydroxycholesterol (25-OHChol). 202

Table 5.12. Phosphopeptides identified as having change in expression after treatment with 25-hydroxycholesterol (25-OHChol) or 24(*S*),25-epoxycholesterol (24(*S*),25-EC). 204

Table 5.13. Incomplete methylation increases complexity of the peptide mixture. 209

Table 5.14. Phosphopeptides with a novel site of phosphorylation identified in 3 independent experiments. 209

ABBREVIATIONS

19-OHChol	19-hydroxycholesterol
22-OHChol	22-hydroxycholesterol
22(R)-OHChol	22(R)-hydroxycholesterol
24(*S*),25-EC	24(*S*),25-epoxycholesterol
24(*S*)-OHChol	24(*S*)-hydroxycholesterol
25-OHChol	25-hydroxycholesterol
27-OHChol	25-hydroxycholesterol
7α-OHChol	7α-hydroxycholesterol
7β-OHChol	7β-hydroxycholesterol
Aβ	Amyloid β peptide
ABCA1	ATP binding cassette A1
ABCG1	ATP binding cassette G1
ANOVA	analysis of variance
ApoE	apolipoprotein E
APS	ammonium persulphate
ATP	adenosine-5'- triphosphate
BSA	bovine serum albumin
Cav-1	caveolin-1
CH25H	cholesterol 25-hydroxylase
CHO	Chinese hamster ovary
CID	collision induced dissociation
CoA	coenzyme A
Col4a3bp	collagen type IV alpha-3-binding protein
Ct	cycle threshold
CTX	cerebrotendinous xanthamatosis
CYP11A1	cholesterol side-chain cleavage enzyme
CYP27A1	sterol 27-hydroxylase
CYP46A1	cholesterol 24-hydroxylase
CYP7A	cholesterol 7-alpha-hydroxylase
CYP7B1	25-hydroxycholesterol 7-alpha-hydroxylase
DMEM	Dulbecco's modified Eagle medium

DMSO	dimethyl sulfoxide
DTT	dithiothreitol
EBI2	Epstein-Barr virus-induced gene 2
EC50	half maximal effective concentration
EDTA	ethylenediaminetetraacetic acid
EGF	epidermal growth factor
ELISA	enzyme-linked immunosorbent assay
ERK	extracellular signal regulated kinase
ESI	electrospray ionisation
FBS	foetal bovine serum
FDR	false discovery rate
FT	Fourier transform
FTICR	Fourier transform ion cyclotron resonance
FXR	farnesoid X receptor
HβCD	2-hydroxypropyl-β-cyclodextrin
HMG-CoA	3-hydroxy-3-methylglutaryl-CoA
HPLC	high performance liquid chromatography
HRP	horseradish peroxidase
IFN	interferon
IgA	immunoglobulin A
IgG	immunoglobulin G
IMAC	immobilised metal affinity chromatography
Insig	Insulin-induced gene
IPI	International protein index
Ki	binding affinity
LC	liquid chromatography
LDLR	low density lipoprotein receptor
LPS	lipopolysaccharide
LTQ	linear trap quadrupole
LXR	liver X receptor
MALDI	matrix assisted laser desorption ionisation
MAPK	mitogen activated protein kinase
MβCD	methyl-β-cyclodextrin

MCSF	macrophage colony stimulating factor
MOAC	metal oxide affinity chromatography
MS	mass spectrometry
NF-κB	nuclear factor kappa-light-chain-enhancer of activated B cells
OSBP	oxysterol binding protein
PBS	phosphate buffered saline
PCyt2	phosphoethanolamine cytidylyltransferase
Poly I:C	polyinosinic:polycytidylic acid
PPAR	peroxisome proliferator-activated receptor
PTM	post-translational modification
qPCR	quantitative polymerase chain reaction
Q-TOF	quadrupole – time of flight
RF	radio frequency
RT	reverse transcription
RXR	retinoid X receptor
SCAP	SREBP cleavage activating protein
SCX	strong cation exchange
SILAC	stable isotope labelling with amino acids in cell culture
SREBP	sterol response element binding protein
StarD4	StAR-related lipid transfer protein 4
TEMED	N,N,N',N' – tetramethylethylenediamine
TH	tyrosine hydroxylase
TLR	Toll-like receptor
TOF	time of flight
TRIF	TR-domain-containing adapter-inducing interferon-β
UniprotKB	Uniprot knowledgebase
UV	ultraviolet
XTT	2,3-bis-(2-methoxy-4-nitro-5-sulfophenyl)-2H-tetrazolium-5-carboxanilide
w/o	without

CHAPTER 1: INTRODUCTION

1.1 Oxysterols

1.1.1 Cholesterol

Cholesterol is a molecule that is an essential component of the eukaryotic cell membrane, where it plays a key role in the maintenance of permeability and fluidity.. Cholesterol orientates itself inside the membrane between phospholipids so that the hydroxyl group at position 3 of the ring structure is adjacent to the polar head group of phospholipids with the hydrophobic part of the molecule in the hydrophobic core of the membrane. The steroid ring structure interacts with the aliphatic chains of the phospholipid reducing the mobility of the membrane and its permeability to water soluble small molecules. Cholesterol reduces the fluidity of the membrane but this also prevents possible phase transitions. Phase transitions occur when lipid components of the liquid membrane crystallise at reduced temperatures. Thus, cholesterol plays a role in the membrane that allows the bilayer to control entry of water soluble small molecules and to maintain the membrane in a liquid, albeit less fluid, state (Olsen *et al.* 2012).

In addition, cholesterol is an important precursor for a number of other active bio-molecules. Cholesterol is the starting material for androgens (e.g. testosterone), progestogens (e.g. progesterone), oestrogens (e.g. oestradiol) glucocorticosteroids (e.g. hydrocortisone), mineralocorticoids (e.g. aldosterone) and bile acids (e.g. cholic acid) (fig. 1.1.). Cholesterol and its derivatives are therefore important molecules that play a multifunctional role in cellular function. However, increased levels of cholesterol are also associated with artherosclerosis and an increased risk of cardiovascular disease. For healthy adults a blood cholesterol level of <5mmol/l is considered normal and concentrations above this considered high (http://www.nhs.uk/Conditions/Cholesterol/Pages/Diagnosis.aspx accessed 10-4-2013). Therefore, homeostasis is necessary to maintain a balance between cholesterol uptake and excretion.

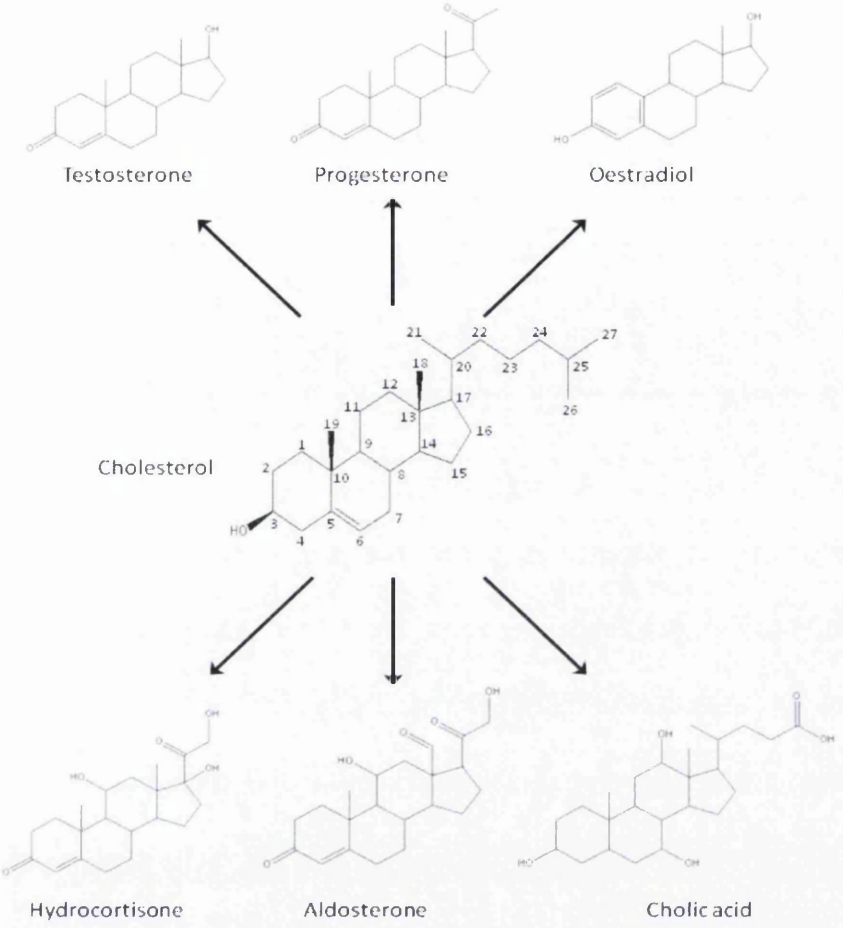

Figure 1.1. Structure of cholesterol and bioactive molecules for which cholesterol is the starting material. Cholesterol contains 27 carbon atoms and is numbered as shown in the figure. Cholesterol is transformed via multistep biochemical reactions to form androgens (e.g. testosterone), progestogens (e.g. progesterone), oestrogens (e.g. oestradiol), glucocorticosteroids (e.g. hydrocortisone), mineral corticosteroids (e.g. aldosterone) and bile acids (e.g. cholic acid). It is apparent that the 4 ring structure of cholesterol is the basis of these molecules; changes in the ring structure, side chain or oxygenation can lead to profound differences in biological activity.

Cholesterol is obtained from two principal sources – diet and from *de novo* synthesis. The majority of the daily requirement of cholesterol is achieved from the activity of a number of enzymes involved in a multistep synthesis occurring at the endoplasmic reticulum (fig. 1.2.). The starting material for cholesterol synthesis is acetyl CoA that is linked to another acetyl CoA to form acetoacetyl CoA. It is converted early in the pathway to 3-hydroxy-3-methylglutaryl-CoA (HMG-CoA). HMG-CoA is then reduced to yield mevalonate by the action of HMG-CoA reductase; this is the rate

limiting step in cholesterol synthesis and is inhibited by statins, an extensively used family of drugs for reducing cholesterol level.

Therefore, the homeostasis of cholesterol is crucial to balance the essential functions of the molecule with the negative consequences that high levels induce. Cholesterol itself has a role to play by end product negative feedback but, importantly, cholesterol can be metabolised to form oxysterols which regulate intercellular cholesterol levels.

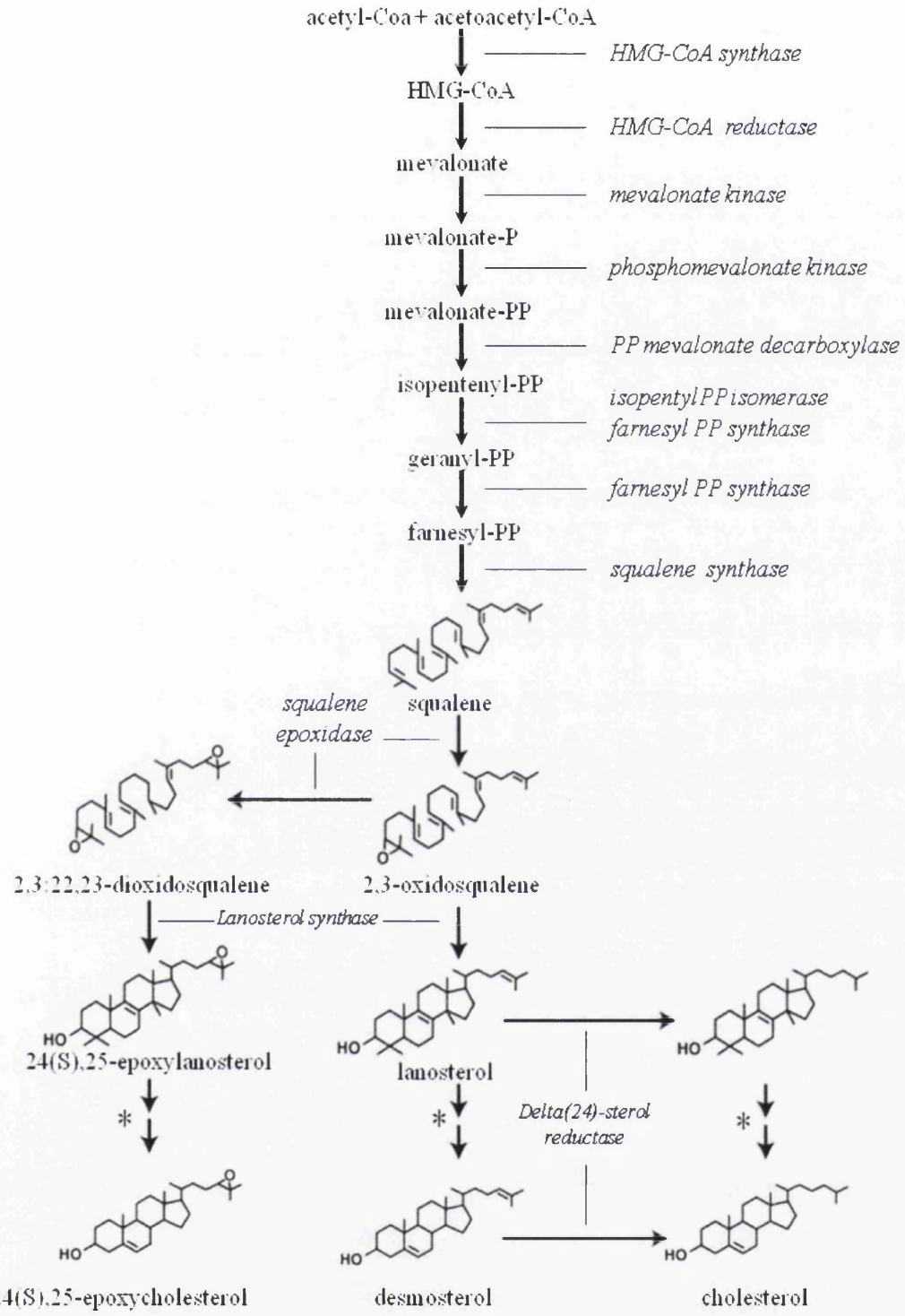

Figure 1.2. The cholesterol synthesis pathway. A shunt in the pathway results in the formation of 24(*S*),25-epoxycholesterol (* = multiple steps). Enzymes responsible for the reactions are shown in italics.

1.1.2 Oxysterols

Oxysterols are biologically active oxidized derivatives of cholesterol. The oxysterols are diverse as they can be oxidised in different positions on the molecule either by auto-oxidation or by enzymatic means. The oxygen can be introduced onto the sidechain (*e.g.* 22(*R*)-hydroxycholesterol, 24(*S*)-hydroxycholesterol, 25-hydroxycholesterol, 24(*S*),25-epoxycholesterol) or onto the cholesterol ring structure (*e.g.* 7α-hydroxycholesterol, 7-ketocholesterol) (fig 1.3). *In vivo* oxysterols are produced via auto-oxidation, enzymatically via various cytochrome P450 and cholesterol hydroxylase enzymes (section 1.1.3.) or by a shunt in the cholesterol synthesis pathway that leads to the formation of 24*S*,25-epoxycholesterol (fig 1.2.). The formation of oxysterols is the first step in the synthesis of bile acids from cholesterol (fig. 1.4.)

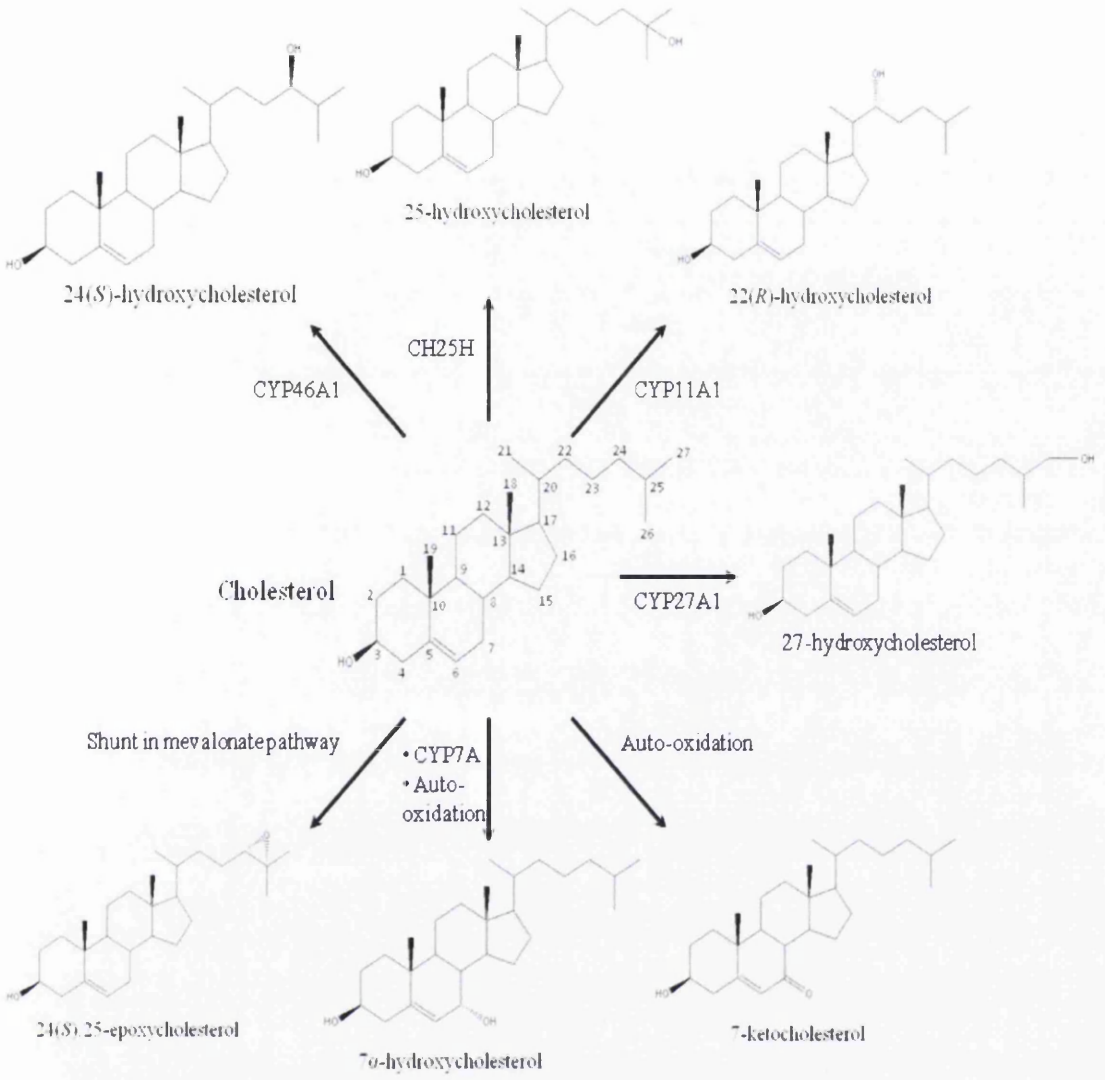

Figure 1.3. Chemical structure of oxysterols. Oxygen is introduced to the molecule to the sidechain or ring structure by auto-oxidation or enzymatic activity. The enzymes responsible for the generation of different oxysterols are shown. Biological activity of the oxysterols is dependent on the location of the oxygenation with profound differences in efficacy as ligands.

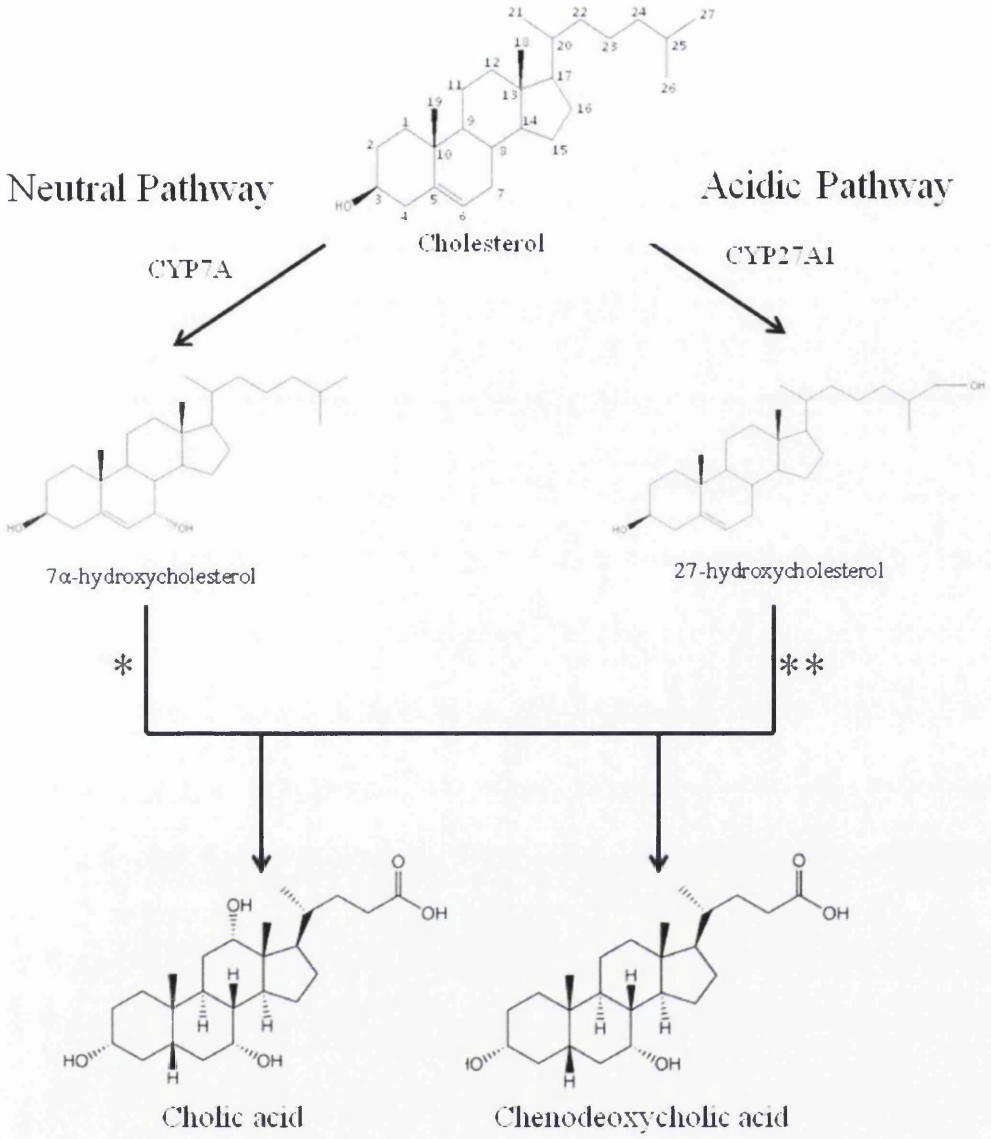

Figure 1.4. Simplified overview of bile acid synthesis. The initial step in the formation of bile acids of both the neutral and acidic pathways is the synthesis of oxysterols. In the neutral pathway cholesterol is metabolised by CYP7A to form 7α-hydroxycholesterol before multiple steps (indicated by *) to form bile acids (cholic and chenodeoxycholic acid). In the acidic pathway the initial oxysterol formed is 27-hydroxycholesterol by the action of CYP27A1. Multiple steps (indicated by **) convert 27-hydroxychoelsterol to bile acids.

The location of the modification is important as although the oxysterols share characteristics, such as a reduced hydrophobicity compared with the cholesterol parent, the location, and stereochemistry play a role in the biological function of the molecules. There are differences between them in terms of activity due to differences in protein binding. The activation of Liver X receptor (LXR), for which oxysterols are the natural ligand, varies considerably depending on where cholesterol is oxidised with EC_{50} values ranging from 4 or 3μM for LXRα/β respectively for 24(*S*)-hydroxycholesterol but below the detection limit for 7-ketocholesterol (Janowski *et al.* 1999). The biological roles of oxysterols will be discussed further in section 1.1.5 but they have been shown to be important in cholesterol homeostasis and in disease. Oxysterols have been associated with artherosclerotic cardiovascular disease (section 1.1.6.1) and, in addition, they have also been implicated in neurodegenerative conditions such as Alzheimer's disease (see section 1.1.6.3; Olkkonen & Lehto 2004, Vaya *et al.* 2007).

1.1.3 Synthesis of Oxysterols

Oxysterols are synthesised from cholesterol by a number of mechanisms. These include auto-oxidation, photo-oxidation and enzymatic formation.

1.1.3.1. Auto-oxidation and photo-oxidation of cholesterol

When exposed to the atmosphere cholesterol can be auto-oxidised to form oxysterols (Weiner *et al.* 1972). The most commonly encountered oxysterols generated in this manner are the 7-position modified oxysterols that includes 7α-hydroxycholesterol, 7β-hydroxycholesterol and 7-ketocholesterol. In addition, 5,6α- or 5,6β-epoxycholesterol can be produced which is converted to 5α,6β-dihydroxycholesterol. All these oxysterols are modified on the ring structure of cholesterol and have poor activity with regard to liver X receptor (LXR), the nuclear receptor for which oxysterols are the natural ligand (Janowski *et al.* 1999). With the exception of 7α-hydroxycholesterol (section 1.1.3.2) they are not produced enzymatically. In addition cholesterol is also oxidised by photo-oxidation. This process predominantly yields 5α-hydroperoxycholesterol which can be transformed to 7-position oxygenated oxysterols. Thus, the major products of both forms of non-enzymatic production of oxysterols are the same.

It has been shown that some auto-oxidation products are toxic (7β-hydroxycholesterol, 7-ketocholesterol) and therefore their presence may lead to harmful biological effects (Hughes *et al.* 1994). In a laboratory context it is important to recognise the importance of auto-oxidation with regard to artefacts generated by processing of cholesterol in the course of experimental methodology as they could potentially lead to false positive conclusions.

1.1.3.2. Enzymatic Formation of Oxysterols

Cholesterol is metabolised to oxysterols enzymatically via a number of different enzymes. 24(*S*)-hydroxycholesterol, the predominant oxysterol found in the brain, is generated by the action of the cytochrome P450 CYP46A1 (Lund *et al.* 1999). Unsurprisingly, in both mice and humans it is predominantly expressed in the brain with very low expression in other tissues. Human brain was analysed in more depth and expression was found across a number of subsections of the brain. Expression was stronger however in grey matter compared with white matter. In mouse brain *cyp46a1* immunohistochemical staining showed localisation to neurons. The expression of CYP46A1 varies with aging. Initially the protein level in the brain, measured by Western blotting, of both mouse and human is low in the early stages of postpartum development and increases over time until reaching a steady state.

The activity of the cytochrome P450 enzyme cholesterol 7α-hydroxylase (CYP7A) results in the formation of 7α-hydroxycholesterol. This oxysterol, which is also a product of auto-oxidation, is a precursor in the formation of bile acids. It is predominantly expressed in the liver (Jelinek *et al.* 1990) and is the predominant location of its activity (Chiang *et al.* 1990).

The enzymatic formation of 25-hydroxycholesterol is due to the activity of cholesterol 25-hydroxylase (Lund *et al.* 1998). This polytopic membrane protein, unlike CYP7A and CYP46A1 which are responsible for the formation of 7α-hydroxycholesterol and 24(*S*)-hydroxycholesterol respectively, is not a cytochrome P450. Instead, it belongs to a family of enzymes that require di-iron co-factors as a catalyst. Murine cholesterol 25-hydroxylase was found in lung, heart and kidney. In comparison, human cholesterol 25-hydroxylase was found at very low levels in all tissues tested. Recently however, it has been reported that the expression of cholesterol 25-hydroxylase

increases dramatically in response to certain stimuli (see section 1.1.7 for a full discussion of this effect).

1.1.3.3. 24(*S*),25-epoxycholesterol Synthesis

24(*S*),25-epoxycholesterol is an unique oxysterol as it not a metabolite of cholesterol but instead is a final product made by a shunt in the cholesterol synthesis mevalonate pathway (fig 1.2.; Nelson *et al.* 1981). However, the measured level of 24(*S*),25-epoxycholesterol is much lower than that of cholesterol with levels between 0.1% and 1% total cholesterol reported (Spencer *et al.* 1985; Wong *et al.* 2004; Wong *et al.* 2007). In the synthesis of cholesterol squalene epoxidase (AKA squalene monooxygenase) introduces an epoxide moiety to squalene to produce 2,3*(S)*-monooxidosqualene. This molecule is then cyclised by 2,3-oxidosqualene cyclase to form lanosterol and then processed, via a number of steps, to cholesterol. However, it is possible for the 2,3*(S)*-monooxidosqualene to be oxygenated further by squalene epoxidase to form 2,3*(S)*;22(*S*),23-dioxidosqualene. This molecule can then be cyclised to oxidolanosterol by 2,3-oxidosqualene cyclase before being processed using the same enzymes as those used in the synthesis of cholesterol to form 24(*S*),25-epoxycholesterol as an end product. This implies that any cell that synthesises cholesterol has the potential to synthesise 24(*S*),25-epoxycholesterol. Indeed, in a variety of cell types such as macrophages, fibroblasts and astrocytes this has been shown to be the case (Wong *et al.* 2004; Spencer *et al.* 1985; Wong *et al.* 2007).

1.1.4. Differential distribution of oxysterols

Just as the expression of oxysterol generating enzymes vary across different tissues (section 1.1.3.2) the abundance of the different oxysterols vary depending on the tissue or biological fluid examined. A number of studies have been conducted to investigate the plasma levels of different oxysterols in humans (summarised in Schroepfer 2000). Although the values identified by different research groups had variation between them clear trends were also present. The predominant oxysterols identified in plasma were 27-hydroxycholesterol (a naturally occurring oxysterol derived from the activity of a mitochondrial cytochrome P450 sterol 27-hydroxylase (CYP27A1, Andersson *et al.* 1989)), 24(*S*)-hydroxycholesterol and 7α-

hydroxycholesterol. In addition, other oxysterols, such as 25-hydroxycholesterol, were identified at lower concentrations.

In the central nervous system the predominant oxysterol is 24(*S*)-hydroxycholesterol due to the high expression of CYP46A1 (see section 1.1.3.2; (Lund *et al.* 1999)). 24(*S*)-hydroxycholesterol has been identified as a component of cerebrospinal fluid (Lütjohann *et al.* 1996). The level of 24(*S*)-hydroxycholesterol in cerebrospinal fluid was ~10% that in plasma. The ratio of 24(*S*)-hydroxycholesterol to cholesterol was measured at 1690±600 ng/mg in children but lower in adults with a ratio of 390±50 ng/mg. The ratios were 10-fold higher than the ratio of 24(*S*)-hydroxycholesterol to cholesterol in plasma but 50% lower than the ratio found in brain. No other sidechain modified oxysterols were reported by the authors. In contradiction a recent paper showed that the oxysterol profile of cerebrospinal fluid was a lot more complex with numerous oxysterols identified by charge tagging mass spectrometry (Ogundare *et al.* 2010). Oxysterols identified included 24(*S*)-hydroxycholesterol, 25-hydroxycholesterol, 27-hydroxycholesterol and bile acids. In this study 24(*S*)-hydroxycholesterol was not the highest concentration oxysterol identified.

24(*S*)-hydroxycholesterol has been identified in the brain of a number of different species including rat, cow, horse and human. 24(*S*)-hydroxycholesterol was measured in various tissues but was at a highest concentration in the cerebrum and cerebellum. In human adult brain the level analysed post mortem the level of 24(*S*)-hydroxycholesterol (Lütjohann *et al.* 1996) was measured at 0.27-0.58 ng/μg cholesterol in cerebrum and 0.68 - 2.19 ng/μg cholesterol in cerebellum. In addition, it was reported (thought the data was not presented) that 27-hydroxycholesterol and 25-hydroxycholesterol were also found in brain though at lower levels - 5 to 30% and <3% respectively.

It is unclear at present whether the distribution of oxysterols to specific tissues, such as 24(*S*)-hydroxycholesterol to the central nervous system, leads to distinct, specific effects dependent on the isomer present. However, there has been a large amount of work conducted on the biological importance of oxysterols.

1.1.5. Biological Functions of Oxysterols

The major, well studied, biological functions of oxysterols are as important regulatory molecules. Due to the presence of oxysterols cholesterol synthesis is inhibited via negative feedback by down-regulation of the synthesis of enzymes in the synthetic pathway (Gill *et al.* 2008). In addition, they can affect the homeostasis of cholesterol by increasing the expression levels of cholesterol exporters (*e.g.* ATP binding cassette A1 (ABCA1)) and reducing the low density lipoprotein receptor mediated uptake of cholesterol in the form of low density lipoprotein. Oxysterols, generally, exert their effects through three methods; regulation of protein transcription through inhibition of SREBP (Sterol Response Element Binding Protein) processing, acting as a ligand for the nuclear receptor Liver X Receptor (LXR), and by altering the rate of protein degradation.

However, the functions of oxysterols are not limited to their classical roles as it has recently been shown that oxysterols can affect other diverse processes. Oxysterols can alter intracellular cell signalling by altering post-translational protein phosphorylation. In addition, it appears that oxysterols are important in the innate immune response, embryonic development, and disease progression.

1.1.5.1. Regulation of SREBP

The SREBP family are transcription factors that contain a basic helix loop helix leucine zipper motif ((bHLH-Zip). The family of proteins consists of 3 subtypes SREBP1a, 1c and 2 (Brown and Goldstein 1997). Each subtype consists of a pair of membrane spanning domains that allow the N and C terminus domains to project into the cytoplasm. However, SREBP1 and 2 differ in their function. SREBP1 is predominantly expressed in the liver and adrenal gland and is involved in the regulation of fatty acid and triglyceride metabolism and *de novo* lipogenesis whereas SREBP2 is ubiquitously expressed and regulates the transcription of the enzymes involved in the cholesterol synthesis pathway (Brown and Goldstein 1997). Despite the divergence in their role the SREBPs are processed to their active form by a common transport and proteolytic mechanism.

SREBP1/2 in the presence of sterols is retained in the endoplasmic reticulum (Yang *et al.* 2002). As the intracellular cholesterol levels falls SREBP1/2 is transported, via the Golgi apparatus where it is made active due to proteolysis, to the nucleus. Two proteolytic cleavages are required to convert SREBP1/2 to its mature form. The first S1P (site-1 protease) splits SREBP1/2 in two but is unable to release the active bHLH-Zip domain (Espenshade *et al.* 1999). A second protease, S2P (site-2 protease), then converts SREBP1/2 into a transcription factor (Zelenski *et al.* 1999). Active SREBP1/2 is transferred to the nucleus where it can exert its effect and promote the expression of responsive genes.

SREBP1/2 itself does not contain a sterol binding domain and therefore its regulation is reliant on two other proteins – SCAP (SREBP cleavage activating protein) and Insig (Insulin induced gene) (Radhakrishnan *et al.* 2007). In cholesterol depleted cells SCAP transports SREBP1/2 from the ER to the Golgi apparatus where it is processed to its active from as described above. However, SCAP contains a sterol binding domain that allows it to bind cholesterol (Radhakrishnan *et al.* 2004). The presence of cholesterol alters SCAPs conformation and results in effects on SREBP1/2 processing. SREBP1/2 is bound to SCAP by an interaction between the c-terminus of both proteins that, in the presence of cholesterol, ensures that SREBP1/2 is tethered to the endoplasmic reticulum membrane. Thus, the interaction of cholesterol and SCAP results in a down regulation in expression of SREBP1/2 regulated genes. SCAP is only affected by cholesterol; 25-hydroxycholesterol had no effect on its conformation. However, a second protein Insig exerts a similar effect mediated by oxysterols. Insig, of which there are two closely related proteins Insig-1 and Insig-2, binds oxysterols but does not bind cholesterol (Radhakrishnan *et al.* 2007). In the presence of oxysterols Insig binds to SCAP and prevents the SCAP/SREBP1/2 complex from being transported to the Golgi for processing. Thus, the action of SREBP1/2 can be modified by cholesterol and oxysterols.

In addition, as another layer of regulation SREBP stimulates the production of Insig1 mRNA. Therefore, SREBP promotes the expression of an inhibitor of its processing to maturation. Stimulation of Insig expression promotes inhibition of SREBP regulated gene transcription (Horton *et al.* 2003).

1.1.5.2. Activation of Liver X Receptor

The liver X receptor (LXR) is a transcription factor and a nuclear receptor with strong similarity to other nuclear receptors such as PPAR, FXR and RXR. LXR was classified, initially, as an orphan receptor as its natural ligand was unknown (Apfel *et al.* 1994, Song *et al.* 1994). LXR exists as two isoforms α and β which have a large (77%) homology between the two. There are, however, differences in expression with LXRα being the predominant isoform in the liver whilst LXRβ is ubiquitously expressed. Oxysterols have been shown to be the endogenous ligand for both LXRα and LXRβ (Janowski *et al.* 1998). The potency of different oxysterols vary depending on where on the ring or side chain of cholesterol the oxygen is added and the stereochemistry of the modification. Structure activity relationships have shown that the most potent ligands for LXR are oxysterols with modified side chain (Janowski *et al.* 1998). Indeed, the most potent naturally occurring oxysterol ligands for LXR, 24(*S*),25-epoxycholesterol and 24(*S*)-hydroxycholesterol, had an EC50 of <5μM for both LXRα and β. In comparison, 7α-hydroxycholesterol, a naturally occurring oxysterol, had an efficacy of ≤10% at 40μM. In addition to the position the number and stereochemistry of the modifications are also important as cholesterol hydroxylated twice were substantially less potent (e.g. K_i 24(*S*),25-dihydroxycholesterol for LXRα = 1200nM) as were enantiomers of active oxysterols (e.g. K_i 24(R),25-epoxycholesterol for LXRα = 1200nM). This can be explained by the structure of the oxysterol binding pocket of LXR (Svensson *et al.* 2003). The crystal structure of LXR shows the orientation of the hydrophobic ring structure into a hydrophobic cavity. Hydrogen bonding between the hydroxyl at position 3 and arginine-305 holds the ring in the correct position. A second hydrogen bond between active sidechain oxygenated oxysterols, (e.g. 22(*R*)-hydroxycholesterol, 24(*S*)-hydroxycholesterol, 24(*S*),25-epoxycholesterol) and either histidine-421 or tryptophan-443 residues in the binding pocket results in stronger binding of these ligands. Inactive oxysterols such as 22(*S*)-hydroxycholesterol and 24(*R*)-hydroxycholesterol are prevented from binding efficiently in the pocket due to steric effects preventing hydrogen bonding to either the histidine-421 or tryptophan-443.

Retinoid x receptor (RXR) is a nuclear receptor that is activated in the presence of 9-cis retinoic acid. It can heterodimerise with a number of other nuclear receptors

depending on which activating ligands are present. In the presence of oxysterols activated LXR forms heterodimers with RXR. This heterodimer can then activate transcription of genes containing a LXR response element in their promoter region. The LXR response element is a nucleotide sequence that has the idealised nucleotide sequence 5'-AGGTCANXXXXAGGTCA-3' in the promoter region of LXR activated genes. Genes that are regulated by LXR include a number of genes that are associated with cholesterol and lipid homeostasis. Examples of genes regulated by LXR include ATP binding cassette A1 (ABCA1) which is a cholesterol efflux protein, ApoE a transporter of cholesterol and other hydrophobic compounds, and SREBP1c which controls the synthesis of fatty acid synthesising enzymes (e.g. fatty acid synthase).

1.1.5.3. Regulation of Protein Degradation

In addition to their roles in altering the transcription of genes, either by LXR or SREBP, oxysterols can alter the rate of protein degradation. HMG-CoA reductase, a membrane bound enzyme and a rate limiting step in the synthesis of cholesterol, is transcriptionally regulated by SREBP2. However, it has also been shown that oxysterols lead to a increased rate of HMG-CoA degradation (Chin *et al.* 1985; Gil *et al.* 1985; Nakanishi *et al.* 1988). This effect is mediated by Insig, the oxysterol sensing protein that causes SREBP retention in the endoplasmic reticulum (Sever *et al.* 2003a; Sever *et al.* 2003b). In the presence of sterols HMG-CoA reductase is ubiquitinated which is reliant on Insig; RNAi knockout of Insig 1 and 2 mitigated this effect (Sever *et al.* 2003a; Sever *et al.* 2003b). Therefore, these synergistic effects increase the rapidity of response to changes in cholesterol levels; the rate of synthesis of new protein is reduced and the removal of previously synthesised HMG-CoA reductase is accelerated.

Another protein that is targeted for degradation by the presence of oxysterols is low density lipoprotein receptor (LDLR). Regulation of LDLR expression is by modification of SREBP; the LDLR mRNA level is rapidly reduced in the presence of oxysterols (Metherall *et al.* 1989). Similarly to HMG-CoA reductase the protein, due to oxysterols, is ubiquitinated and then degraded. However, the mechanism of action by which oxysterols achieve this effect differs between the 2 proteins. In the case of LDLR stimulation of LXR induces Idol which ubiquitinates LDLR. LDLR is then

degraded (Zelcer *et al.* 2009). Thus like HMG-CoA reductase these effects, at the protein and mRNA level, are additive.

In the presence of oxysterols the rate of degradation of LXRα and LXRβ is slowed. Overexpressed FLAG-tagged LXRα/β in the presence of oxysterols (i.e. in the presence of ligand) degraded at a lower rate after protein synthesis was inhibited with cycloheximide (Kim *et al.* 2009). It has not been shown whether this effect leads to a change in the level of endogenous LXR levels after treatment with oxysterols. Again this effect, in the case of LXRα, is potentially additive as the LXRα mRNA expression has been shown to be auto regulated in some, but not all, cell types.

Thus, it is potentially possible to affect protein expression levels by treatment with oxysterols without altering the level of mRNA expression. Either by inducing ubiquitination, as in the examples of HMG-CoA reductase and LDLR, or by preventing ubiquitination, in the case of LXR, it is clear that the role of oxysterols in protein regulation goes beyond that of transcriptional inhibition/activation via SREBP and LXR respectively. Indeed, it has recently been shown that the oxysterols play a role in the regulation of post transcriptional cell signalling.

1.1.5.4. Cell signalling

In addition to their regulatory role oxysterols can affect protein phosphorylation in particular the phosphorylation of extracellular signal regulated kinase (ERK1/2) (Yoon *et al.* 2004, Lemaire-Ewing *et al.* 2009). Cholesterol stabilises a phosphatase complex containing oxysterol binding protein (OSBP) as a scaffold, the serine/threonine phosphatase PP2A and the tyrosine phosphatase HePTP that decreases the phosphorylation of ERK 1/2 (Wang *et al.* 2003, Wang *et al.* 2005). By competing with cholesterol oxysterols cause the disassembling of the phosphatase complex and, therefore, the presence of oxysterol up-regulates ERK 1/2 phosphorylation at the thr202/tyr204 amino acid residues. ERK 1/2 is an important signalling molecule and a known oncogene. It has roles in a number of different biological functions including cell growth, differentiation and apoptosis (Avruch 2007). The up-regulation of ERK1/2 phosphorylation by disassembly of this phosphatase has been shown in a number of different cell lines either by depletion of cholesterol with cyclodextrin or with treatment with oxysterols (Furuchi & Anderson

1998, Yoon *et al.* 2004, Agassandian *et al.* 2005, Calleros *et al.* 2006, Kim *et al.* 2007, Jin *et al.* 2008, Lemaire-Ewing *et al.* 2009). This effect seems to be a feature of oxysterols generally as a number of different, dissimilar oxysterols have been shown to initiate this effect including 7β-hydroxycholesterol, 22-hydroxycholesterol (not specified *R/S*), and 25-hydroxycholesterol.

It is unclear whether treatment with oxysterols only affects ERK1/2 of the mitogen activated protein kinase (MAPK) family as there has been contradictory evidence regarding other MAPKs (e.g. JNK) (Ares *et al.* 2000, Yoon *et al.* 2004). In addition, it is unclear as to what pathways downstream of ERK1/2 are up/down-regulated due to the activation of ERK1/2.

1.1.6. Role of Oxysterols in Disease

Oxysterols have been hypothesised to play a role in a number of disease states. These include cardiovascular disease, eye disease and neurodegenerative diseases.

1.1.6.1. Role of Oxysterols in Cardiovascular Disease

Artherosclerosis is a condition characterised by the hardening and thickening of the arterial wall caused by the accumulation of cholesterol, and other substances, in the wall of the artery leading to the formation of areas of hardening called plaques. Oxysterols have been shown to be cytotoxic to endothelial and arterial smooth muscle cells *in vitro* and have therefore been hypothesised to be artherogenic (Ares *et al.* 2000). However, *in vivo* the situation appears to be equivocal as treatment of animals with dietary oxysterols resulted in variable responses. Some articles detailed increased levels of artherosclerosis, some reported no change whilst others observed reduced levels of disease progression. However, as oxidized low density lipoprotein has high levels of non-enzymatically formed oxysterols it is a possibility that these molecules have a role to play in the pathology of the disease. Indeed the most cytotoxic oxysterol in oxidized low density lipoprotein is 7-hydroperoxycholesterol (Chisholm *et al.* 1994). This oxysterol is rapidly decomposed to other 7-modified oxysterols and therefore true concentration of 7-hydroperoxycholesterol is probably under estimated but 7-modified oxysterols are found in high concentration in foam cells and artheromas. The pathogenic importance may be due to uptake oxidized low density

lipoprotein and accumulation of toxic molecules. However, the dominant oxysterol in artheroma is a enzymatically produced one - 27-hydroxycholesterol. It has been hypothesised that 27-hydroxycholesterol might act as a defence to large concentrations of cholesterol (Bjorkhem *et al.* 1994; Babiker *et al.* 1997). Evidence supporting this is found in analysis of the disease cerebrotendinous xanthamatosis (CTX). In this disease, which is a genetic autosomal recessive disease that results in the absence of cholesterol 27-hydroxylase (the enzyme responsible for the synthesis of 27-hydroxycholesterol), there is an early onset of artherosclerosis despite most CTX patients having normal cholesterol plasma levels (Fujiyama *et al.* 1991). The majority of oxysterols in artherosclerotic plaques are comprised of 4 oxysterols. Together, these four oxysterols, 27-hydroxycholesterol, 7-ketocholesterol, 7β-hydroxycholesterol and 7α-hydroxycholesterol, account for ~80% of the total amount of oxysterol in artherosclerotic plaques (Bjorkhem *et al.* 1994; Crisby *et al.* 1997). At present there is no direct evidence of the involvement of oxysterols in the disease. However, they are cytotoxic and oxysterols have been demonstrated to be pro-apotopic. Therefore, it appears that oxysterols have a role to play in the progression of this condition.

1.1.6.2. Role of Oxysterols in Eye Disease

Oxysterols have been associated with disease of the eye with implied roles in age related macular degeneration and glaucoma. Age-related macular degeneration is a disease that, as its name suggests, involves the degradation of the macula, a specialised structure of the retina with a high concentration of cone photoreceptors and ganglion cells, and can lead to blindness. The disease is classified as two forms wet (or exudative) and dry (or atrophic). The wet form of the disease is due to increased choroidal vascularisation. The dry form of the disease is the more common, but generally less severe, form of the disease. It is characterised by the formation of drusen, extracellular deposits between the retinal pigment epithelium and Bruch's membrane. These deposits can induce retinal pigment epithelial atrophy in the central part of the eye. Currently there are no treatments for this form of age-related macular dystrophy. It is this form that has been associated with oxysterols as it has recently been hypothesised that 7-ketocholesterol is a key player in the development of the disease (Rodriguez *et al.* 2004).

In cultured retinal pigment epithelium cells treatment with low density lipoprotein caused toxicity after 72 hours. In order to determine if this effect was mediated by oxysterols the cells were treated with 50μM oxysterol and cell viability measured after 72 hours (Rodriguez *et al.* 2004) Of the oxysterols tested (25-hydroxycholesterol, 20-hydroxychoelsterol, 7-ketocholesterol, 7α-hydroxycholesterol, 7β-hydroxycholesterol) the most cytotoxic were 20-hydroxycholesterol and 7-ketocholesterol. In addition, 7-ketocholesterol has been identified in monkey retina (Moreira *et al.* 2009) and in retina of albino rat (Rodriguez and Fliesler 2009) at a level of 0.5-1.5 pmol per nmol cholesterol and 1-4 pmol per nmol cholesterol respectively. As other sidechain hydroxylated oxysterols were below the detection limit (100fmol/nmol cholesterol) it is unclear whether these concentrations are in the correct range or whether auto-oxidation artefacts have artificially elevated them. However, despite no definitive evidence for a role for oxysterols in the disease oxysterol binding protein 2 (OSBP2) has been implicated (Torrini *et al.* 2007).

Another eye disease with which oxysterols have been associated is glaucoma. Glaucoma is a chronic disease that can lead to permanent loss of sight due to optic nerve damage and often presents as an increased pressure of the aqueous humour inside the eye. A mutation in CYP46A1 was associated with incidence of primary open angle glaucoma (Fourgeaux *et al.* 2009). Though there was a genetic link between the polymorphism and the disease this was not identified by changes in the plasma level of 24(*S*)-hydroxycholesterol and therefore cannot be used as a biomarker for primary open angle glaucoma.

1.1.6.3. Role of Oxysterols in Neurodegenerative Diseases

Alzheimer's disease is characterised by neuronal loss and the accumulation of amyloid beta (Aβ) peptide deposits resulting in plaque formation. Aβ peptide is formed from cleavage of amyloid precursor protein by α-secretase, β-secretase or γ-secretase. α-secretase results in the formation of Aβ40 a soluble form that does not result in amyloid plaques. In comparison, β-secretase or γ-secretase activity synthesises Aβ42 which then forms insoluble aggregates. Oxysterols have been

implicated in Alzheimer's disease as a biomarker of the disease and as neuroprotective agents.

In cerebrospinal fluid the level of 24(*S*)-hydroxycholesterol was increased in 14 newly diagnosed Alzheimer's patients compared with 10 healthy controls. In Alzheimer's a level of 2.6±1.1ng/ml was recorded in cerebrospinal fluid compared with 1.6±0.6ng/ml in healthy controls (Schönknecht *et al.* 2002). This difference was considered statistically significant ($p<0.05$). However, no difference was observed in the plasma level of 24(*S*)-hydroxycholesterol with levels of 60.5±19.3ng/ml and 53.6±14.3ng/ml measured in Alzheimer's disease and healthy controls respectively. This change in cerebrospinal fluid level of 24(*S*)-hydroxycholesterol appeared independent of plasma cholesterol as both Alzheimer's disease and control subjects had normal plasma cholesterol levels (150-230mg/dl) (Schönknecht *et al.* 2002). In another study analysing the plasma level of 24(*S*)-hydroxycholesterol in a greater number of newly diagnosed Alzheimer's patients (n=30) showed an increase in plasma 24(*S*)-hydroxycholesterol levels as compared to control (Lütjohann *et al.* 2000). In Alzheimer's patients the concentration measured was 75±18ng/ml (range 42-116) compared with 60±21ng/ml (range 24-105) of healthy control ($p<0.001$, ANCOVA). In this study however there was no statistical difference between Alzheimer's and vascular dementia. Vascular dementia patients had a 24(*S*)-hydroxycholesterol plasma level of 78±20 (range 43-114) (Lütjohann *et al.* 2000). In a separate study using a larger number of patients (n=40) it was shown that there was a significant decrease in the plasma level of 24(*S*)-hydroxycholesterol in Alzheimer's disease patients who had been diagnosed for at least 4 years (Bretillon *et al.* 2000). This decrease was modest (~18%) but statistically significant ($p<0.01$). Thus, from these studies it appears that the level of plasma 24(*S*)-hydroxycholesterol is an indication of disease progression with newly diagnosed patients having increased levels of plasma 24(*S*)-hydroxycholesterol but with a decrease over time.

Analysis of the expression of two oxysterol generating enzymes, cholesterol 24-hydroxylase (CYP46A1) and cholesterol 27-hydroxylase (CYP27A1), showed differences between Alzheimer's disease patients' brain (n=7) and control subjects (n=7) (Brown 3rd *et al.* 2004). Both enzymes, in control brain, are expressed in neurons and some astrocytes. Cholesterol 27-hydroxylase is also found in

oligodendrocytes. However, in Alzheimer's disease this pattern of distribution changes with expression of cholesterol 24-hydroxylase predominantly in astrocytes and around the amyloid plaques. Cholesterol 27-hydroxylase expression decreases in neurons but increases in oligodendrocytes. Analysis of the effect of 24(*S*)-hydroxycholesterol and 27-hydroxycholesterol showed that both oxysterols reduced the rate of production of Aβ peptide in rat primary cortical neurons transfected with adenovirus expressed amyloid precursor protein. 24(*S*)-hydroxycholesterol was the more potent of the two oxysterols. After 24 hours treatment with 10μM 24(*S*)-hydroxycholesterol there was a reduction in Aβ(40/42) peptide of ~70% whereas 15μM 27-hydroxycholesterol reduced the Aβ(40/42) secretion by ~40%.

Interestingly, 24(*S*)-hydroxycholesterol and 27-hydroxycholesterol have been shown to modulate the production of Aβ in human neuroblastoma SH-SY5Y cells (Prasanthi *et al.* 2009). 24(*S*)-hydroxycholesterol did not affect the generation of Aβ42 while treatment with 5μM 27-hydroxycholesterol increased the level of this peptide ~2 fold. This increase in Aβ42 level due to 27-hydroxycholesterol treatment was associated with increases in both amyloid precursor protein, the source of Aβ peptide, and beta-secretase the enzyme that generates Aβ42. In comparison, 24(*S*)-hydroxycholesterol treatment promoted the alpha secretase pathway that generates non-amyloidogenic soluble APP and therefore it appears that 24(*S*)-hydroxycholesterol plays a neuroprotective role to prevent the formation of amyloid plaques. Conversely, it appears that 27-hydroxycholesterol promotes the formation of insoluble Aβ42.

Questions remain regarding the role of oxysterols in Alzheimer's disease as it is still unclear the biological role that oxysterols play in the disease state. It appears that oxysterols, such as 24(*S*)-hydroxycholesterol, can have a neuroprotective role due to changes in Aβ processing (Prasanthi *et al.* 2009, Brown 3rd *et al.* 2004). However, it has yet to be determined if changes in oxysterol concentration measured in cerebrospinal fluid and plasma of Alzheimer's patients is a reflection of the cause of neuronal loss or merely a by-product of the disease state as a neuroprotective homeostatic mechanism.

Table 1.1. Summary of important oxysterols and disease states in which they have been implicated.

Oxysterol	Formed	Enzyme	Implicated in disease state
7-ketocholesterol	Auto-oxidation	n/a	Cardiovascular disease. Glaucoma. Age related macular degeneration
7α-hydroxycholesterol	Enzymatically. Auto-oxidation.	CYP7A	Cardiovascular disease.
7β-hydroxycholesterol	Auto-oxidation	n/a	Cardiovascular disease.
22R-hydroxycholesterol	Enzymatically	CYP11A1	n/a
24S-hydroxycholesterol	Enzymatically	CYP46A1	Alzheimer's disease.
25-hydroxycholesterol	Enzymatically	CH25H	n/a
27-hydroxycholesterol	Enzymatically	CYP27A1	Cardiovascular disease (proposed protective role). Alzheimer's disease.
24(*S*),25-epoxycholesterol	Enzymatically	Shunt in mevalonate pathway	n/a

1.1.7. Role of Oxysterols in Immunity

It has recently emerged that oxysterols have a role to play in the innate immune response. In has been shown it that the mRNA encoding cholesterol 25-hydroxylase is up-regulated significantly (35x) in mouse macrophages after a short (2 hour) incubation with 10ng/ml lipopolysaccharide (LPS; Diczfalusy *et al.* 2009). Lipopolysaccharide is an important component of Gram-negative bacteria and a potent activator of the mammalian immune response. In contrast, lipopolysaccharide had no effect on the mRNA level of 2 other oxysterol generating enzymes (CYP27A1 and CYP7B1). This increase in cholesterol 25-hydroxylase mRNA corresponded with a ~6fold increase in intracellular 25-hydroxycholesterol. In addition, the intravenous

injection of lipopolysaccharide into healthy human volunteers resulted in an increased level of 25-hydroxycholesterol in the plasma.

Another study, conducted independently (Bauman *et al.* 2009), showed a similar increase in cholesterol 25-hydroxylase (CH25H) and 25-hydroxycholesterol after treatment with Kdo2-Lipid A, a selective toll-like receptor 4 (TLR4) agonist, in peritoneal and bone marrow derived murine macrophages. This effect appeared to be a general response to toll-like receptor activation as lipopolysaccharide, peptidoglycan (a selective agonist for TLR2), polyinosinic:polycytidylic acid (poly I:C, a selective agonist for TLR3) and lipoteichoic acid (an agonist for TLR2/6) also induced the expression of cholesterol 25-hydroxylase and 25-hydroxycholesterol. The Kdo2-Lipid A induced changes were inhibited by co-incubation with either MAPK inhibitors or NF-κB inhibitors.

This effect of Kdo2-Lipid A was also observed *in vivo* in wild-type mice after interperitoneal injection. Induction of CH25H mRNA was observed in all tissues tested with a maximum response (~250fold) in the liver. Protein levels of CH25H were also elevated in liver and lung after Kdo2-Lipid A treatment coupled with an increase in concentration of 25-hydroxycholesterol in lungs and serum. In CH25H-/- knockout mice the level of IgA heavy chain mRNA was increased compared to wild-type mice. This was corroborated as the IgA level was increased in serum, lungs and intestinal mucosa in CH25H-/- knockout mice. These changes were shown to not be due to a increase in the total number of leukocytes in the CH25H-/- knockout mice compared with wild type mice. Conversely knockout mice lacking oxysterol 7α-hydroxylase (CYP7B1-/-), which in normal circumstances rapidly metabolises 25-hydroxycholesterol, showed significant reductions in the IgA level in the lung, serum and mucosa. This effect of 25-hydroxycholesterol suppressing IgA release was also shown *in vitro* in splenic B220+ cells with an IC50 of ~50nM. This effect appears to be independent of LXR and cellular cholesterol levels as 22(*R*)-hydroxycholesterol and 24(*R/S*)-hydroxycholesterol were inactive and co-incubation of cholesterol with 25-hydroxycholesterol did not reverse the effect.

The toll-like receptor 3 (TLR3) ligand poly I:C and the toll-like receptor 4 (TLR4) ligand LPS increase the mRNA expression of cholesterol 25-hydroxylase (CH25H) in

dendritic cells and macrophages derived from mouse bone marrow (Park and Scott 2010). It appears that this is primarily a TRIF (TR-domain-containing adapter-inducing interferon-β), a TLR3/4 adapter molecule, dependent mechanism as in TRIF-/- mice the up-regulation of CH25H after treatment with polyI:C or LPS was abolished. In addition, TRIF signaling results in increases in interferon-β (IFNβ) expression; both polyI:C and LPS increased expression of IFNβ in bone marrow derived dendritic cells and macrophages. Similarly to the effect on CH25H expression this effect is abolished in dendritic cells from TRIF-/- mice. In addition, the increase in CH25H expression can be induced by direct stimulation with interferons α, β or γ. Further investigation of the pathway showed that increased expression of CH25H in macrophage and dendritic cells is reliant on JAK signalling as JAK inhibitors prevented the effects of polyI:C, LPS and interferon-β. In addition, JAK inhibition reduces TLR3/4 ligand and interferon-β induced STAT1 phosphorylation. The absence of STAT1 in knockout models abolishes the increase in CH25H expression by polyI:C, LPS and interferons α, β, and γ in dendritic cells and macrophages.

Recently two groups have reported independently and concurrently the role of 7α,25-hydroxycholesterol in inducing the migration of immune cells via Epstein-Barr virus-induced gene 2 (EBI2) a G-protein coupled receptor (Hannedouche *et al.* 2011,Liu *et al.* 2011). EBI2, whose natural ligand was previously unknown, is a key regulator of the migration of B-cells in lymphoid organs.

7α,25-hydroxycholesterol was identified as the naturally occurring receptor ligand of EBI2 (Hannedouche *et al.* 2011). Modification of cholesterol by hydroxylation at both positions increased the potency of the oxysterol greatly (~1000-fold) compared with the mono-hydroxylated 7α-hydroxycholesterol or 25-hydroxycholesterol. In addition, 7α,25-hydroxycholesterol is a potent chemoattractant of immune cells expressing EBI2 including B cells and dendritic cells. Blocking $G\alpha_i$-coupled receptors with pertussis toxin blocked the chemoattraction of B-cells induced by 7α,25-hydroxycholesterol. The synthesis of 7α,25-hydroxycholesterol requires the activity of both cholesterol 25-hydroxylase (CH25H) and 25-hydroxycholesterol 7-alpha-hydroxylase (CYP7B1); two enzymes shown to be present at high levels in both spleen and lymph nodes. Therefore, to further investigate the biological relevance and

function of 7α,25-hydroxycholesterol CH25H-/- knockout mice were used. The concentration of 7α,25-hydroxycholesterol was increased in the spleen of lipopolysaccharide treated wild type mice but not in CH25H-/- mice. In addition, CH25H-/- mice had attenuated *in vivo* migration of B-cells in the spleen. The absence of CH25H also decreased the level of IgG1 response to the presence of antigen by ~3 fold.

A second, independent, paper (Liu *et al.* 2011) also identified 7α,25-hydroxycholesterol as the natural ligand of EBI2 with a EC50 value of 140pM measured by 35S-GTP-γS incorporation. 7α,25-hydroxycholesterol was the most potent of the oxysterols tested (EC50; 7α,25-hydroxycholesterol = 0.14±0.03nM; 7α,27-hydroxycholesterol = 1.3±0.28nM; 7β,25-hydroxycholesterol = 2.1±0.51nM; 7β,27-hydroxycholesterol = 51±1.78nM; 7α-hydroxycholesterol = 82±13.3; 7β-hydroxycholesterol = 1763±262; 25-hydroxycholesterol = 127±26.6; 27-hydroxycholesterol = 3029±571). 7α,25-hydroxycholesterol treatment of CHO cells transfected with V5 tagged human EBI2 induced receptor internalisation indicating that 7α,25-hydroxycholesterol is the natural ligand of the receptor. The biological relevance was demonstrated *in vitro* as B-cell and CD4+ T-cell migration in response to 7α,25-hydroxycholesterol was observed. This response was also observed *in vivo* in LPS activated B-cells, CD4+ T-cells, CD8+ T-cells and dendritic cells. All of these cells were characterised as expressing EBI2. However, this effect appears cell type specific as there was no response *in vitro* to natural killer cells, neutrophils and macrophages despite all three cell types of the immune system being EBI2 positive. 7α,25-hydroxycholesterol desensitises EBI2 receptor. The observed effects in cell migration in wild-type mice were absent in EBI2-/- mice with no migratory response to 7α,25-hydroxycholesterol. Heterozygous EBI2+/- mice had a reduced response (~50%) to 7α,25-hydroxycholesterol compared with wild type mice.

It is clear therefore that an emerging, important role for oxysterols in the innate immune response is slowly being elucidated. However, it appears that oxysterols, in particular those hydroxylated at the 25- position, are key players in this mechanism.

1.1.8. Role in development

A large number of oxysterols are found in the central nervous system (Wang *et al.* 2009), but the predominant oxysterol produced in adult brain is 24*S*-hydroxycholesterol (C^5-3β,24*S*-diol), a CYP46A1 oxidised metabolite of cholesterol that is exclusively synthesised in the brain (Lund *et al.* 1999). It has recently been shown that in murine embryonic brain 24(*S*),25-epoxycholesterol (C^5-3β-ol-24*S*,25-epoxide) is present at relatively high levels compared to other oxysterols (Wang *et al.* 2009). As previously described (section 1.1.3.3), unlike other oxysterols 24(*S*),25-epoxycholesterol is not a metabolite of cholesterol but a final product in a shunt of the mevalonate pathway of cholesterol synthesis.

24(*S*),25-epoxycholesterol has a potential role in the development of the embryonic brain as it has been shown that the level of 24(*S*),25-epoxycholesterol is present at relatively high levels in comparison to other oxysterols in the cortex and spinal cord of embryonic mice (Wang *et al.* 2009). The predominant oxysterol in adult mouse brain is 24(S)-hydroxycholesterol with level of 2.53±0.05ng/μg 24(*S*)-hydroxycholesterol to cholesterol (Lütjohann *et al.* 2002). In the embryonic murine brain this level is greatly reduced; at embryonic day 11 there was an observed level of 0.026μg/g (wet weight) in the cerebral cortex and 0.013μg/g (wet weight) in the spinal cord. In comparison, the concentration of 24(*S*),25-epoxycholesterol was 0.165μg/g (wet weight) in the cerebral cortex and 0.091μg/g (wet weight) in the spinal cord. In comparison in human primary neurons, derived from 14-18 week old foetuses, 24(*S*),25-epoxycholesterol synthesis has been detected (Wong *et al.* 2007). The overall level of 24(*S*),25-epoxycholesterol was not measured though the rate of synthesis of the oxysterol was 0.001-0.05% of the rate of synthesis of cholesterol (Wong *et al.* 2007). It is unclear the role this increased concentration plays in murine embryonic neural development. However, LXRα/β is present in embryonic brain (Sacchetti *et al.* 2009) and as 24(*S*),25-epoxycholesterol is a potent ligand for this nuclear receptor (Janowski *et al.* 1999) it might play a role in neural development. Indeed, there is evidence to suggest that the presence of LXR is essential to dopaminergic neurogenesis in the ventral midbrain (Sacchetti *et al.* 2009).

LXR is expressed in embryonic mice (Annicotte *et al.* 2004). LXRα was observed to be abundant in the liver, intestines and adipose tissue whereas LXRβ was more ubiquitously expressed with strong expression in neuronal and endocrine tissue. LXR is expressed in ventral midbrain progenitor cells (Sacchetti *et al.* 2009). In addition to this these cells also express oxysterol generating enzymes (e.g. CYP46A1, oxidosqualene lanosterol cyclase) and ABCA1, whose expression is reliant on LXR activation. LXRα/β knockout mice showed down regulation of two genes that control dopaminergic neuron development Lmx1b and Wnt1. These reduced expressions, consequently, caused the down-regulation of Pitx3 a gene regulated by Lmx1b and Wnt1. The effect of LXRα/β knockout cased a reduced number of cells in the marginal zone where dopaminergic neurons are present. These effects result in impaired dopaminergic neuron development in LXRα/β knockout mice.

The reduction in dopaminergic neurogenesis was reliant on LXRα/β as there was no increase in apoptosis and oxysterols did not have a direct effect on neurogenesis in LXRα/β knockout mice. However, at embryonic day 11.5 dopaminergic neurogenesis was impaired in the floor plate midbrain, the area of the brain where dopaminergic neurons are derived. In LXRα/β knockout mice there were less tyrosine hydroxylase positive (TH^+) neurons. Tyrosine hydroxylase is the rate-limiting enzyme for dopamine synthesis. In ventral midbrain primary cultures 22(*R*)-hydroxycholesterol and GW3965, a synthetic LXR ligand, increased the number of TH^+ cells in wild type but not in LXRα/β knockout cells.

In addition, the efficiency of the differentiation of mouse embryonic stem cells to dopaminergic neurons treated with 22(*R*)-hydroxycholesterol was increased. Overexpressing LXRβ had a similar effect and interestingly the combination of 22(*R*)-hydroxycholesterol treatment and LXRβ was additive. The balance between, and organisation of, different cell types was disrupted by LXRα/β knockout as the number $RC2^+$ glia increased whilst there was disorganisation of $GFAP^+$ astrocytes. However the primary defect caused by LXRα/β knockout is on ventral midbrain dopaminergic neurogenesis.

LXRα/β knockout also disrupted the cell cycle (Sacchetti *et al.* 2009) as there was an increase in cells entering the active stages of mitosis, measured by Ki67+ staining, but

no subsequent increase in Brdu incorporation and cell cycle exit was decreased. In LXRα/β knockout cells were held at G2/M with an increased percentage of progenitor cells and reduced neurogenesis.

In human embryonic stem cells LXRα/β are expressed and increases during differentiation. The number of Tuj1+ neurons was increased by 70% and TH+ neurons increased by 300% after treatment with 22(*R*)-hydroxycholesterol during differentiation (Sacchetti *et al.* 2009). The number of Tuj1+ that also stained positive for TH cells was also increased. This effect was at its maximum at a concentration of 0.1-0.5μM 22(R)-hydroxycholesterol. There were no signs of toxicity at these concentrations and TH+ oxysterol treated cells expressed midbrain dopaminergic markers (LMX1a, ENGRAILED1, NURR1, PITX3, GIRK2, DAT). In contrast, very few GABA+, serotonin+, and dopamine beta-hydroxylase (DBH)+ neurons were detected indicating that treatment with 22(*R*)-hydroxycholesterol gave a specific enhancement of dopaminergic neuron development. In addition there was reduced progenitor proliferation and in the number of astrocytes whilst increasing the generation of midbrain dopaminergic neurons.

More recently it has been shown that 24(*S*),25-epoxycholesterol is a potent ligand of LXR during ventral midbrain neurogenesis and specifically promotes dopaminergic neurogenesis (Theofilopoulos *et al.* 2013). In embryonic mouse midbrain neurons organotypic cultures treatment with 24(*S*),25-epoxycholesterol increased the number of tyrosine hydroxylase positive neurons by 88% *c.f.* vehicle. Similarly 24(*S*),25-epoxycholesterol treatment increased the number of tyrosine hydroxylase positive neurons in mouse primary progenitor cultures. In addition, 24(*S*),25-epoxycholesterol promoted the differentiation of mouse embryonic stem cells into dopaminergic neurons. Thus, it appears that 24(*S*),25-epoxycholesterol is a critical ligand for normal dopaminergic neurogenesis.

However, the mechanism(s) by which 24(*S*),25-epoxycholesterol/LXR acts to result in this effect on neuron proliferation is unclear. Increased concentrations of 24(*S*),25-epoxycholesterol could alter protein expression directly through transcriptional modification of known or unknown LXR. In addition, 24(*S*),25-epoxycholesterol could have indirect effects by inhibiting SREBP2 and decreasing biosynthesis of

cholesterol and other members of the mevalonate pathway or inducing downstream effects of differentially expressed proteins.

In addition, oxysterols have been shown to affect Hedgehog signalling, a pathway that is involved in embryonic development. Cholesterol and oxysterols have been shown to increase proliferation of medulloblastoma cells through Hedgehog signalling with 20(*S*)-hydroxycholesterol and 22(*S*)-hydroxycholesterol having the greatest effect (Corcoran and Scott 2006). It has also been demonstrated independently that 20(*S*)-hydroxycholesterol and 22(*S*)-hydroxycholesterol activate the Hedgehog pathway and induce an osteoinductive effect (Dwyer *et al.* 2007). In addition, it has been demonstrated that 20(*S*)-hydroxycholesterol inhibits the differentiation of bone marrow stromal cells into adipocytes through a Hedgehog dependent mechanism and that 20(*S*)-hydroxycholesterol can induce expression of Notch target genes (Kim *et al.* 2007; Kim *et al.* 2010). The mechanism by which 20(*S*)-hydroxycholesterol effects Hedgehog signalling is by activating the protein Smoothened; Smoothened mediates the signal induced by Hedgehog ligands (Nachtergaele *et al.* 2012). Thus, there is evidence for a role for oxysterols in the regulation of embryonic development.

1.2. Proteomics

Proteomics is the study of global protein expression (Wilkins *et al.* 1996). As proteins are the macromolecules that implement cellular biological processes the analysis of changes in their expression can identify gross changes in cell function. The proteins expressed, including any post-translational modifications, at any given point is called the cell's proteome. The proteome is more complex than the genome. The genome can be considered as a stable constant whereas the proteome is highly variable. The proteome varies with cell type, with time and as a response to stresses or stimuli (Dix *et al.* 2008). In addition, mRNA splice variants of genes add further complexity as do post-translational modifications of proteins such as phosphorylation (Uhlen & Ponten 2005). Indeed, some proteins are able to have multiple different post-translational modifications illustrating the complexity of a proteomic sample at any given point.

The analysis of the proteome can be analysed as whole proteins or more commonly as peptides. It is common to digest protein enzymatically by using, for example, the enzyme trypsin. Trypsin hydrolyses the peptide bond on the carboxylic side of the

amino acids lysine and arginine. Thus, peptides are fragments of the protein backbone that have been generated from intact proteins. Peptides are analysed by mass spectrometry and their sequence identified using bioinformatic software. From this information the proteins present can be deduced.

A strength of proteomics is the direct analysis of protein expression rather than extrapolating from mRNA data *e.g.* microarray; it has been shown that changes in mRNA expression need not correlate with a change in protein expression (Rogers *et al.* 2008). It has the advantage over immunoblotting (Western blotting) as the expression of a large number of proteins can be analysed in one run. In addition, post-translational modifications of the proteome can be analysed giving information regarding signalling pathways or the response to a given stimulus (Olsen *et al.* 2006). Proteins can be modified after translation to alter their function, localization or interactions with other proteins. These alterations are termed post-translational modifications. Post-translational modifications significantly increase the diversity of the proteome as they can be initiated in response to a given stimulus to regulate cellular processes. A large number of diverse modifications have been identified including phosphorylation, glycosylation and ubiquitination. Proteomics allows the analysis of changes in post-translation modifications that would not be possible using immunoblotting due to no commercially available specific antibody (Jensen 2004).

1.2.1. Phosphoproteomics

Phosphoproteomics is a specialized branch of proteomics examining phosphorylated proteins. In the case of phosphorylation, an extensively studied post-translational modification, it has been demonstrated to be involved in the regulation of diverse cellular processes (*e.g.* apoptosis, cell cycle).

Phosphorylation, is a reversible post translational modification and plays a role in a variety of cellular processes and it is a common mechanism for cell signalling and protein regulation. In eukaryotic cells phosphorylation of protein occurs on the side chains of serine, threonine and tyrosine residues. These amino acids have in common a nucleophilic hydroxyl group that reacts with adenosine triphosphate (ATP) resulting in the covalent attachment of a phosphate to the amino acid side chain. Phosphorylation is often associated with protein activity as the addition of the

phosphate can result in conformational changes in the newly phosphorylated protein and can regulate the activation or inactivation of an enzyme. In addition, phosphorylation can induce proteins to associate and is important in signal transduction as it can allow an enzyme to bind its substrate. The phosphorylation and dephosphorylation of protein(s) is regulated by kinases and phosphatases respectively. The balance between the activities of these two enzyme families influences the dynamic phosphorylation state of a cell. At any given point the phosphorylation state of a cell's proteins is called its phosphoproteome.

Phosphoproteomics is the analysis of the phosphorylation state of the entire proteome. This can be done in order to identify novel post-translational modification sites or to identify activation or deactivation of signalling pathways (Olsen *et al.* 2006). The technical challenge of phosphoproteomics is high. Phosphopeptides are present in low abundance compared to their non-phosphorylated counterparts. In addition they are poorly ionized. These two factors mean that phosphoenrichment is required in order to examine these molecules.

1.2.2. Mass Spectrometry

Mass spectrometry measures an ion's mass to charge ratio (*m/z*). Mass spectrometers generally consist of an ionisation source (*e.g.* electrospray), a mass analyzer and an ion detector. In combination these components allow the detection ions of different mass to charge ratios.

1.2.2.1. Electrospray Ionization

The ability to investigate global protein expression has blossomed since the invention of 2 soft ionising techniques – matrix assisted laser desorption ionisation (MALDI; Tanaka *et al.* 1989) and electrospray ionisation (ESI). These techniques have the advantage of ionizing macromolecules without inducing fragmentation. Therefore, these techniques have become essential for proteomic analysis as they allow the ionization of amino acid chains without disrupting the peptide bonds and thus conserving sequence information.

Electrospray ionization was developed to ionise macromolecules without inducing fragmentation (Fenn *et al.* 1989). The analyte, *e.g.* a peptide mixture, dissolved in a

solvent is subjected to an electrical voltage that induces generation of a Taylor cone and the formation of a fine aerosol spray. Volatile organic solvents such as acetonitile or methanol are commonly used as they evaporate easily facilitating ion formation of the analyte. In addition, the ionisation of large flow electrospray can be improved by using an inert gas in order to help remove solvent. However, electrospray ionisation is more efficient at low flow rates due to the lower size of initial droplets. A flow rate of 300-800nl/min resulted in an increased performance of HPLC-MS analyses (Emmett and Caprioli 1994). The flow rate can even be reduced even further to a nanoflow of ~25nl/min and still generate efficient electrospray (Wilm and Mann 1996).

Mass spectrometer design also promotes ionisation *e.g.* a heated capillary that ions follow into the mass spectrometer helps evaporation. Evaporation continues until the droplet becomes unstable upon reaching its Rayleigh limit and emits charged jets in Coulomb fission. Two theories have been proposed to explain the production of gas phase ions. The first, the ion evaporation model theorises that that as the radius of the droplet decreases the surface of the droplet increases to assist in the field desorption of solvated ions. The second model is the charge residue model suggests that electrospray droplets as the solvent evaporates and splits until the droplets contain one analyte ion. The solvent evaporates leaving the analyte carrying the charge. Whichever theory is correct the end result of this ionisation technique is the formation of gas phase ions.

The ions produced by electrospray ionization can either be due to the addition of a proton [M+H] or the removal of a proton [M-H]. These modes are termed positive and negative modes respectively. In order to promote protonation or deprotonation, in positive and negative modes respectively, an acid (*e.g.* formic acid) or base (*e.g.* ammonia solution) can be added to the solvent. Positive mode is generally used for the analysis of proteins and peptides in proteomic experiments. In the case of peptides multiply charged ions are commonly seen. This is because both the N-terminus and arginine and lysine residue sidechains can act as proton acceptors thus creating ions carrying a +2 charge.

1.2.2.2. Mass Analyzer

A large number of different mass analyzer technologies exist including quadrupole, time of flight (TOF), Fourier transform ion cyclotron resonance (FTICR) and Orbitrap instruments. Hybrid instruments also exist that consist of a number of analyzers combined e.g. triple quadrupole, Q-TOF. These mass analyzers vary in how they measure ion *m/z* and technical specifications. In addition, the choice of mass analyzer is often determined by the application.

In proteomic studies high resolution LTQ-Orbitrap instruments are commonly used. The Orbitrap consists of 2 electrodes - a central electrode kept at a high voltage when ions are being trapped and a second electrode surrounding the first at ground potential (Hu *et al.* 2005, Scigelova *et al.* 2011). The frequencies of the oscillating ions can be detected and following a Fourier transform can be displayed as a mass spectrum. An Orbitrap instrument has a high resolution (>100,000) and a high mass accuracy (<5ppm) making it suitable for proteomic studies. The use of an Orbitrap mass analyzer for high mass accuracy MS spectra is in commercial instruments coupled with a linear ion trap (Hu *et al.* 2005). The ion trap acts as an accumulation device that stores ions before introduction to the Orbitrap and therefore allows the use of continuous electrospray ionisation. In addition, the ion trap allows MS^n that fragments the precursor ion and therefore allows elucidation of structural information.

1.2.2.3. Precursor Ion

The initial mass spectrometry scan identifies all ionisable components of a sample. These ions identified in the MS scan give an indication of the molecular weight of analyte. Importantly, a precursor ion can be selected for fragmentation by selecting an ion at a given *m/z*. Fragmentation of an ion yields structural information about it. Peptides have a distinctive isotope envelope due to the fact that peptides can accept multiple protons inducing charge states of +2, +3 or more. Thus, in the example of a doubly charged peptide each isotopic peak that is 1Da apart will be 0.5*m/z* apart. Therefore an analyte can be deduced to be a peptide by examining its precursor ion. However, an MS/MS scan is required for sequence information.

1.2.2.4. Tandem Mass Spectrometry (MS/MS)

Tandem mass spectrometry allows further analysis of an ion identified in the initial MS spectra. A precursor ion of interest is selected, based on its *m/z* and is fragmented e.g. collision induced dissociation (CID) yield structural information about the analyte. In the case of peptides by colliding the precursor ion with an inert gas, *e.g.* nitrogen, the peptide bonds break leading to information regarding the amino acid sequence (Mann & Wilm 1994). Thus, the fragmentation pattern of a peptide's amino acid backbone allows database searching (e.g. Mascot) to identify the peptide sequence and the protein from which it was derived by comparing it to predicted peptide sequence. Depending on the distribution of charge post-fragmentation (*i.e.* to the N- or C-terminus) b- and y- ions are predominantly generated (though a, c, x and z ions can also be formed; fig. 1.5; Roepstorff & Fohlman 1984) that allow identification of the sequence due to specific *m/z* changes that correspond to each amino acid. A subscript number indicates which peptide bond is broken. Thus, the mass differences between the b and y fragmentation ions (e.g. b_1 and b_2 fig 1.5) generated indicate which amino acid residue is lost. From the generated y- and b- ions a peptide's sequence from a given MS^2 can be deduced.

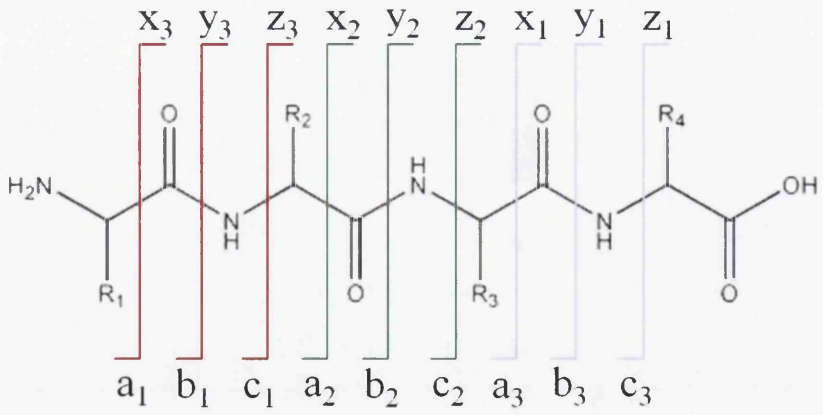

Fig 1.5. Peptide fragmentation notation. The dominant ions in MS/MS spectra are b and y ions.

1.2.2.5. Multistage activation

The analysis of phosphopeptides is dependent on detecting the phosphorylation modification of the peptide and fragmentation of the amino acid backbone of the peptide to deduce its sequence. The phosphate group of a phosphopeptide is relatively weak and they are liable to break instead of peptide bonds. Thus, phosphopeptides in a CID MS/MS spectrum are likely to exhibit a large neutral loss peak 98Da (H_3PO_4) or 80Da (HPO_3) less than the precursor peak. This leads to inability to deduce sequence information from the MS/MS spectra. Therefore a second step of activation is required in order to obtain this information required for identification. This can be achieved by using MS^3 when a dominant neutral loss peak is identified in the MS/MS spectra and is subsequently selected for fragmentation yielding a spectra displaying sequence information.

A second method that can be used to identify and sequence phosphopeptides is multistage activation and has the advantage of having a shorter time for analysis than MS^3. In this method a pseudo-MS^3 spectrum is generated. A precursor ion is selected for fragmentation at both its observed *m/z* and, critically, at the *m/z* where the neutral loss ion is theoretically present. This yields a spectrum with no neutral loss ion peak. The spectrum contains b and y ions allowing identification of the peptide sequence. In addition b-98 and y-98 ions are present derived from fragmentation of the neutral loss peak. Therefore, multistage activation generates a hybrid pseudo-MS^3 spectrum showing both MS^2 and MS^3 fragmentation on the same spectrum that can be analysed for both peptide sequence and phosphorylation.

1.2.3. Quantitative Proteomics

After protein identification the next step is quantification to give an indication for the level of protein expression and how it differs in cells with different treatments. To this end a number of different approaches have been developed including isotope labelled and label free methodologies. In label free methods each sample is run individually and then subsequently compared. However, in the case of isotope labelling each group is labelled with a different isotope marker and thus they are distinguishable by mass spectrometry. Due to this ability to distinguish different groups it is possible to combine samples and compare them in a single mass spectrometry analysis.

1.2.3.1. Stable Isotope Labelling with Amino Acids in Cell Culture (SILAC)

SILAC is a quantitative proteomic technique that allows the identification of relative changes in protein expression using non-radioactive isotope labelling (Ong & Mann 2006). SILAC can be used in many applications and can be used in order to monitor changes in gene expression, post-translational modification and protein-protein interactions. In this technique cells are grown in cell culture and are split into 2 or 3 populations (fig. 1.6.). The first population is cultured in growth media that contains normal, non-isotope labelled amino acids. However, the second population is grown in the presence of amino acids, commonly arginine and lysine, labelled with stable, non-radioactive isotopes. Commonly used are $^{13}C_6$ and $^{13}C_6$ $^{15}N_4$ arginine (R_6/R_{10}) together with D_4 and $^{13}C_6$ $^{15}N_2$ lysine (K_4/K_8). These are termed light (unlabelled R and K), medium (K_4/R_6) and heavy (K_8/R_{10}). Due to the mechanism of action of trypsin that cleaves peptide bonds to the C-terminus side of arginine and lysine. Thus, each peptide generated, except the C-terminus, theoretically results in only having a single label.

As the cell population increases, and is passaged, the heavier amino acids are incorporated into the proteome. Eventually all proteins contain the isotope labelled amino acids and are heavier than their normal counterparts. Thus, they are distinguishable by mass spectrometry but otherwise chemically and biologically identical. It is therefore possible to combine the protein derived from different SILAC states and analyse it simultaneously as pairs or triplets of peptides that co-elute from HPLC columns. Therefore this methodology allows 3 treatment groups to be simultaneously analysed. The ratio of the peak intensities of the peptides can then be analysed and their relative abundance determined. Peptide ratios can then be extrapolated to protein expression ratios.

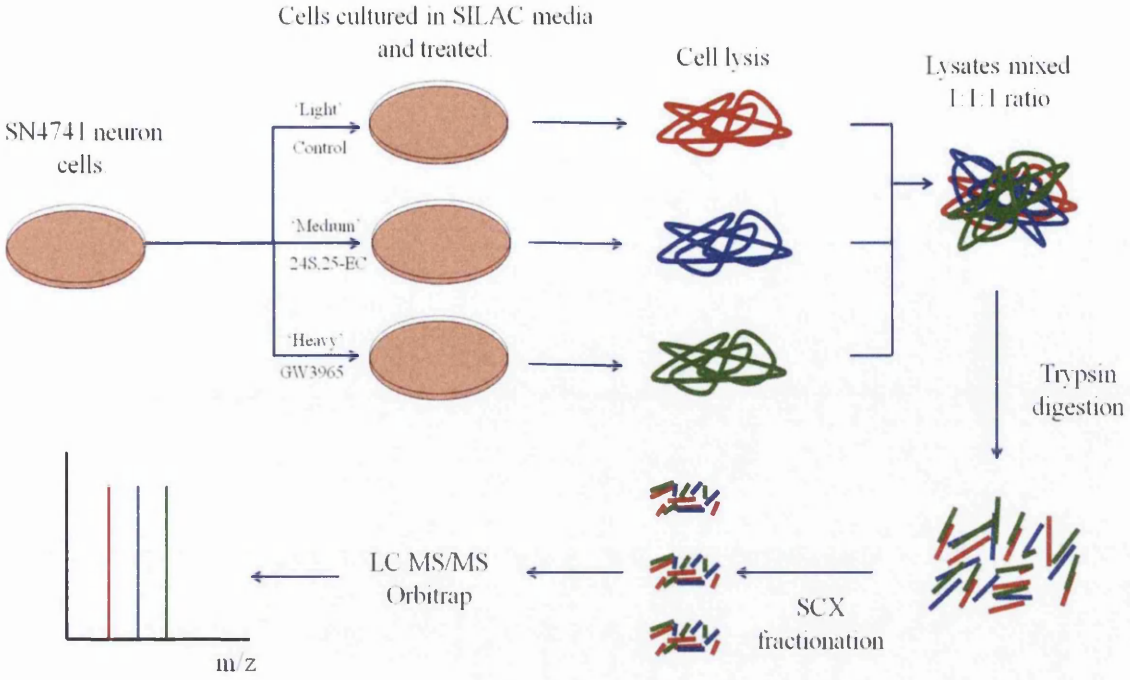

Figure 1.6. Schematic of SILAC experimental design. In this study SN4741 cells were cultured in isotope labelled amino acid containing media. This approach can be extended to any cells grown in culture. Cells are then treated, in this case with vehicle (control), 24(*S*),25-epoxycholesterol (24(*S*),25-EC) and GW3965, before cells are lysed and protein harvested. The protein lysates are then mixed on a 1:1 ratio before trypsin digestion and strong cation exchange (SCX) fractionation. Fractions are then analysed using LC-MS/MS. Due to the isotope labelling it is possible to distinguish between the 'light', 'medium' and 'heavy' peptides. Mass spectra of SILAC peptides result in a characteristic triplet envelope and the intensity of the signal from each SILAC state can be used for relative quantification.

1.2.3.2. Isobaric Tagging

Isobaric tagging (e.g. iTraq) is a relative quantitative proteomic technique that allows identification of chemically tagged peptides from different treatment groups (Ross *et al.* 2004). In iTraq a N-succinimide ester group on the tag that reacts with primary amines. The workflow of the experimental approach means that the labelling occurs after trypsin digestion but before mixing and assumes that the labelling between different treatment groups is equal. The total molecular weight of tag remains constant but is split into a reporter moiety and a balance moiety. Thus, tagged

peptides have the same molecular weight and all identical sequence peptides co-elute during liquid chromatography. In addition, the precursor ion is the same molecular weight in all groups. Upon fragmentation low molecular weight reporter ions distinguish between the different groups and allow relative quantification. An advantage of iTraq over SILAC is that more treatment groups, up to 8, can be analysed at the same time.

1.2.3.3. Label Free Quantification

Label-free quantification of proteins does not rely on an isotope label. These approaches are suitable for identifying large changes (>2 orders of magnitude) but less reliable for identifying smaller, subtle changes. Due to the lack of an isotope label samples can't be run simultaneously and require the detection of the corresponding peptide across different LC-MS or LC-MS/MS runs for quantification. Thus, care is required to account for experimental variation. Two methods used for label free quantification are ion peak intensity and spectral counting (Bantscheff *et al.* 2007).

Ion peak intensity relies on precursor signal intensity in order to quantify peptides and therefore relies on LC-MS only. Thus, high mass precision spectrometers are required for this approach as high resolution power is required for identifying peptide signals at the MS level. Peptides are differentiated from noise due to their isotopic pattern. The peptide precursor ion is tracked over time gives a chromatographic profile of the monoisotopic peak which is integrated to estimate original peptide concentration. No MS/MS spectra are generated and thus peptides with a similar *m/z* and coincidentally eluting at the same point or overlapping may be confused. The second method, spectral counting, compares the total number of MS/MS spectra for a given peptide between samples. The number of spectra is correlated with the abundance of the protein. Both techniques require significant normalization.

1.2.4. Peptide Mixture Complexity Reduction

Peptide mixtures generated from the protein digestion are complex and techniques to simplify these mixtures are commonly used. In the case of both proteomics and phosphoproteomics the peptide mixtures derived from proteome digestion are inherently complex. In order to reduce this complexity prior to mass spectrometric

analysis a number of techniques can be used. These include polyacrylamide gel electrophoresis, 2D-gel electrophoresis, affinity chromatography, ion exchange chromatography and reverse phase liquid chromatography. These steps help to maximize the number of peptides observed by mass spectrometry and thus increase the number of proteins identified. Low abundance peptides (and therefore low abundance proteins) are more likely to be identified in less complex mixtures. The techniques utilized in this work (strong cation exchange chromatography, reverse phase high performance liquid chromatography, phosphoenrichment) are discussed in more detail below.

1.2.4.1. Reverse Phase High Performance Liquid Chromatography

High performance liquid chromatography (HPLC) is a chromatography technique to separate analytes in complex mixtures. HPLC utilizes a stationary phase in column and a mobile phase that is pumped through the column carrying analytes. The retention time of an analyte is dependent on its interaction with the stationary phase and the mobile phase. Commonly $C_{18}H_{37}$ modified stationary phases are used and the technique is known, for historical reasons, as reverse phase HPLC. In reverse phase chromatography the retention of hydrophobic compounds is increased. Conversely, more polar analytes are eluted quicker. The retention of a given analyte can be adjusted by adding increased levels of organic solvent, such as acetonitrile or methanol, and is commonly manipulated using a solvent gradient on a HPLC instrument. Importantly, liquid chromatography can be coupled to a mass spectrometer so that analytes eluting from the column and transferred directly to the spectrometer for ionization and subsequent analysis.

1.2.4.2. Strong Cation Exchange

Strong cation exchange chromatography is a form of ion exchange chromatography. This form of chromatography separates of molecules on the basis of their charge. The stationary phase of the column has anionic functional groups (e.g. polysulphoethyl aspartamide (PolyLC Inc.)) that interact with cationic analytes. A chromatography gradient increases the salt concentration (e.g. NH_4Cl) in the solvent and results in the cationic molecules in the solvent competing for the anionic sites on the strong cation exchange column. Thus, cationic molecules are displaced and elute from the column.

Therefore, during strong cation exchange chromatography anionic analytes are eluted first off the column whereas strongly cationic analytes take longer. Strong cation exchange can be used for sample fractionation to reduce complexity prior to further analysis.

1.2.4.3. Phosphoenrichment

Phosphorylated peptides require enrichment prior to mass spectrometry analysis due to their low abundance and poor ionization (Zhou *et al.* 2000). Strategies to extract phosphorylated peptides from a peptide mixture include immobilised metal ion affinity chromatography (IMAC) and metal oxide affinity chromatography (MOAC). Both techniques use metal ligands to interact with phosphate groups in order to retain phosphopeptides whilst allowing non-phosphorylated peptides to elute.

Immobilised metal ion affinity chromatography (IMAC) relies on the phosphate group's oxygen interacting with an immobilized metal ion. A high affinity for phosphate groups has been shown with chelated iron(III) and gallium(III) ions (Zhou *et al.* 2000). During chromatography this results in the retention of the phosphopeptides on the column and washing of the non-phosphorylated peptide mixture through. The phosphopeptides can then be washed off the column by changing the pH of the mobile phase or adding a competitor. Thus, IMAC increases the concentration of phosphopeptides.

Titanium dioxide is used for metal oxide affinity chromatography (MOAC) phosphoenrichment (Larsen *et al.* 2005). Similarly to IMAC titanium dioxide chelated resins are used to form complexes with phosphate groups. MOAC can be combined with IMAC in order to increase the number of phosphopeptides in the sample. In addition both IMAC and MOAC can be used after fractionation (e.g. strong cation exchange) to improve the phosphoenrichment by reducing sample complexity.

1.2.5. Proteomic Bioinformatics

The identification of peptides and therefore proteins by using the mass spectrometric data is reliant on bio-informatic software. It is possible to analyse spectra manually although this is prohibitively time consuming when considering the many thousands of spectra typically generated in one experiment. Therefore, database searching has

become an integral part of proteomics experiments. This search is conducted using software such as Mascot that identifies peptides from the raw mass spectrometry data. The data is analysed bio-informatically to identify peptides by comparing sequence information derived from MS/MS spectra to a sequence database containing all theoretical peptide sequences. The peptidase, such as trypsin, can be defined before searching so that the generated experimental peptides match the theoretical. The database search can be constructed so that any modifications, such as phosphorylation and SILAC, are taken into account. Peptides are identified and can be assigned a score that indicates the probability of a correct identification.

The database used for the Mascot search is not limited to one and a number of databases are available for various species from different sources. International protein index (IPI) is a database from the European Bioinformatics Institute founded to catalogue the disparate databases and act as a link between them. Since its inception a concerted effort has led to a significant synchronization of data. In light of this, the IPI database has recently been retired and IPI numbers are currently being superseded by Uniprot numbers. Uniprot is comprehensive database managed by a consortium of the European Bioinformatics Institute, the Swiss Institute of Bioinformatics and the Protein Information Resource (Uniprot Consortium 2011). These consortium members each individually maintained a database but joined forces to produce a curated protein database Uniprot knowledgebase (UniprotKB). UniProtKB comprises 2 sections Uniport/Swissprot that is reviewed and manually annotated and Uniprot/Trembl that is unreviewed and annotated automatically. UniprotKB/Swissprot gives indication of a large range of factors and has the ultimate aim of providing all known, relevant information in a single place. Therefore, Uniprot is currently the canonical reference set of proteins for a number of organisms.

In our study the quantification of peptides was performed using MaxQuant software. MaxQuant is specialised software designed for the analysis of SILAC MS spectra (Cox *et al.* 2009). MaxQuant identifies the characteristic doublet/triplet isotope envelopes of SILAC labelled peptides. The software tracks these precursor ions over time that allows the merger of the separate signal intensity peaks into a 3D representation. The volumes of the 3D peaks are then compared allowing the generation of ratios between the different SILAC states (e.g. medium:light,

heavy:light). To identify peptides MS/MS data is analysed. The data is then combined to give an identified and quantified peptide. In the case of phosphopeptides this means that they can be identified and when coupled with SILAC labelling can give an indication of the relative levels of phosphorylation at a specific site between control and treatment groups. In addition to quantifying each individual peptide the quantified peptide is combined with others derived from the same protein and extrapolated in order to generate the ratio between the SILAC states of the protein. Thus, the relative quantification of proteins between different SILAC states is identified and further analysed to identify changes in protein expression.

1.2.6. Experimental Considerations of Proteomic Studies

1.2.6.1 SN4741 Cell Line.

Due to the limited amount of primary dopaminergic neurons from mouse embryonic brain available for large-scale proteome wide screening in the experimental work presented here the differentiated neuronal cell line SN4741 was used. SN4741 cells are dopaminergic neurons derived form the substantia nigra of embryonic mice (Son *et al* 1999). It has previously been shown that SN4741 cells are tyrosine hydroxylase positive and express other neuronal markers (Son *et al* 1999). Dopaminergic neuronal markers, such as tyrosine hydroxylase, can be searched for in the proteomic data set to validate the model.

In order to achieve large-scale accurate protein quantification stable isotope labelling approaches such as SILAC or iTraq are the preferred choices. The use of a SILAC approach allows the harvesting of a large amount of protein (mg scale) for use in the proteomic experiments easily. Thus, by having a large amount of starting material the probability of identifying low abundance proteins is improved and therefore SILAC is the most appropriate choice.

1.2.6.2. Proteomic Profiling Validation of Existing Knowledge

One of the strengths of proteomic studies is the ability to analyse the proteome as a whole. This provides the opportunity for the experimental data to validate previously identified changes in protein expression as a response to a given treatment. Oxysterols have known regulatory roles for SREBP2 and LXR controlled genes. However, no previous work has been conducted analysing the effect of oxysterols in SN4741 cells. Indeed, it can be anticipated that 24(*S*),25-epoxycholesterol will induce changes in the cholesterol synthesis pathway in SN4741 cells through inhibition of SREBP2 and induction of LXR regulated genes such as ABCA1.

1.2.6.3. Identification of Novel 24(*S*),25-epoxycholesterol Regulated Genes

It is difficult, if not impossible, to predict novel 24(*S*),25-epoxycholesterol regulated genes in the context of proteomic studies. The basic hypothesis of the experiments is broad; 24(*S*),25-epoxycholesterol induces protein expression changes in SN4741 cells via SREBP, LXR or other unknown oxysterol receptors. Early studies suggest that oxysterols promote dopaminergic neurogenesis through LXR (Sacchetti *et al.* 2009;

Theofilopoulos *et al.* 2013). However, which LXR regulated proteins induce this effect is not clear. The aim of the work is to pinpoint the protein pathways which are affected by 24(*S*),25-epoxycholesterol by employing a quantitative proteomics approach. This is essential to fully understand the mechanism(s) of 24(*S*),25-epoxycholesterol in promoting dopaminergic neurogenesis. The data generated from the proteomic studies will also be analysed for the presence of neurotrophins, proteins that have an important regulatory role in neuron development, survival and function (Hempstead 2006), and any changes in their expression. In addition, neuronal markers from different stages of neuronal development will be analysed to determine if 24(*S*),25-epoxycholesterol has an effect on the maturation of neurons.

1.2.6.4. Identification of Novel 24(*S*),25-epoxycholesterol Regulated Protein Phosphorylation

Oxysterols have been shown to induce changes in ERK phosphorylation (section 1.1.5.4) a pathway associated with dopaminergic neurogenesis (Kim *et al.* 2006; Kim *et al.* 2008; Yoon *et al.* 2011; Jaeger *et al.* 2011). We speculate that 24(*S*),25-epoxycholesterol could promote dopaminergic neurogenesis at multiple levels *i.e.* via activation of LXR and also, possibly, by activation of the ERK signalling pathway Thus, a phosphoproteomic approach will be used to identify novel 24(*S*),25-epoxycholesterol regulated protein phosphorylation either downstream of ERK or any other kinase pathways. These data will provide further insight into the mechanism of oxysterol activity in addition to the quantitative proteomics study. Again, the basic hypothesis of the experiments is broad; 24(*S*),25-epoxycholesterol induces protein phosphorylation changes in SN4741 cells. Therefore, the data generated from the phosphoproteomic studies will be analysed to identify changes, if any, in cell signalling pathways.

1.3. Aims and Objectives

The work presented here is founded on the previously reported requirement of LXR in normal neuronal development (Sacchetti *et al.* 2009) and the above expected level of 24(*S*),25-epoxycholesterol in embryonic mouse brain (Wang *et al.* 2009b). Therefore, three main hypotheses form the basis of this work:

- 24(*S*),25-epoxycholesterol is an important molecule in normal murine neuronal development.
- 24(*S*),25-epoxycholesterol exerts an influence on neuronal development by inducing LXR dependent and independent changes in protein expression.
- 24(*S*),25-epoxycholesterol induces changes in the phosphoproteome and exerts an influence on neuronal development by affecting cell signalling.

In order to examine these hypotheses a SILAC experimental model was followed in order to examine the proteome and phosphoproteome as a whole. A differentiated dopaminergic neuronal cell line was chosen, SN4741, for *in vitro* experiments due to the fact they are derived from the ventral midbrain region of embryonic mice (Son *et al.* 1999) – the same area of the brain where LXR was observed to be important in normal development (Sacchetti *et al.* 2009),

CHAPTER 2: MATERIALS AND METHODS

2.1. Cell Culture

Mammalian cell culture was performed aseptically in a cell culture flow hood. All single use cell culture apparatus used were sterile (Greinier BioOne). Items transferred into the cell culture hood were sprayed with 70% ethanol.

2.1.1. SN4741 Cell Culture

SN4741 murine dopaminergic neuronal cells were cultured on 90mm tissue culture dishes (Greinier) in full media (see table 2.1) with incubation at 5% CO_2/ 37°C. For routine SN4741 cell culture media was removed before the cells were washed once with pre-warmed phosphate buffered saline (37°C, PBS, Lonza). Trypsin/EDTA (approx. 2.5ml, Invitrogen) was incubated with the cells for 30s at room temperature before removal of the majority of the trypsin/EDTA and a further incubation of the cells for 4 min at 37°C/5% CO_2. Detachment of the cells was observed using an inverted light microscope. Detached cells were re-suspended in 10ml of pre-warmed (37°C) full media and mixed thoroughly to ensure a homogenous cell suspension. Cells were then counted using a Neubauer haemocytometer (Fisher) with 10µl of cell suspension in each chamber. Cells were seeded to new 90mm tissue culture plates containing 15ml of full media. Plates were incubated at 37°C/5% CO_2 until ready.

Table 2.1. SN4741 full media. Dulbecco's modified Eagle medium (DMEM) with L-glutamine and glucose, and without sodium pyruvate was modified by adding the reagents shown below. Serum free media is as below with the exception that foetal bovine serum is omitted.

Component	Manufacturer	Volume
DMEM + glucose, L-glutamine w/o sodium pyruvate	Invitrogen	500ml
Foetal bovine serum	Invitrogen	50ml
Penicillin/streptomycin/L-glutamine	Sigma	5ml
20% glucose solution	Sigma	15ml

2.1.2 Hela Cell Culture

Hela human cervical cancer cells were cultured on 90mm tissue culture dishes (Greinier) in full media (see table 2.2) with incubation at 5% CO_2/ 37°C. For routine Hela cell culture media was removed before the cells were washed once with pre-warmed phosphate buffered saline (37°C, PBS, Lonza). Trypsin/EDTA (approx. 2.5ml, Invitrogen) was incubated with the cells for 30s at room temperature before removal of the majority of the trypsin/EDTA and a further incubation of the cells for 4 min at 37°C/5% CO_2. Detachment of the cells was observed using an inverted light microscope (Zeiss). Detached cells were resuspended in 10ml of pre-warmed (37°C) full media and mixed thoroughly to ensure a homogenous cell suspension. Cells were then counted using a haemocytometer with 10µl of cell suspension in each chamber. Cells were then seeded to new 90mm tissue culture plates containing 15ml of full media. Plates were incubated at 37°C/5% CO_2 until ready for use or further culture.

Table 2.2. Hela full media. Dulbecco's modified Eagle medium (DMEM) with L-glutamine and glucose, and without sodium pyruvate was modified by adding the reagents shown below. Serum free media is as below with the exception that foetal bovine serum is omitted.

Component	Manufacturer	Volume
DMEM	Invitrogen	500ml
Foetal bovine serum	Invitrogen	50ml
Penicillin/streptomycin/L-glutamine	Sigma	5ml

2.1.3. THP1 Cell Culture

THP1 human monocytes were cultured in 25cm^2 tissue culture flasks (Corning) in full media (see table 2.3) with incubation at 5% CO_2/ 37°C. THP1 cells grow in suspension. For routine culture, the cell suspension was transferred to a 15ml centrifuge tube and centrifuged at 700g for 5min. The media was discarded without

disruption of the cell pellet before resuspension in 10ml of full media. A 0.5ml aliquot of the cell suspension was taken and diluted 20x with full media. This diluted cell suspension was then counted using a Scepter automated hand held cell counter (Millipore) using 60μm sensor tips. Cells were then transferred to a new $25cm^2$ or $75cm^2$ tissue culture flask for a final concentration of 200,000 cells/ml and a final volume of 10ml or 25ml respectively. Cells were incubated at 37°C/5% CO_2 until ready for use or further culture.

Table 2.3. THP1 full media. RPMI-1640 media w/o L-Glutamine was modified by adding the reagents shown below. Serum free media is as below with the exception that no foetal bovine serum is added.

Component	Manufacturer	Volume
RPMI-1640 W/O L-Glutamine	Invitrogen	500ml
Foetal bovine serum	Invitrogen	50ml
Penicillin/streptomycin/L-glutamine	Sigma	5ml
50mM 2-mercaptoethanol in PBS	Sigma	500μl

2.1.4. Freezing Cells

For long term storage cells were stored in liquid nitrogen. To freeze cells the protocol for culturing was followed with the following exceptions. The cells were resuspended after treatment with trypsin (after centrifugation in the case of THP1 cells) in 1ml of freezing media (10% dimethyl sulfoxide (DMSO; Sigma) in foetal bovine serum) per 90mm tissue culture plate ($25cm^2$ flask for THP1 cells). The cell suspension was transferred to a freezing vial and stored at -80°C overnight in a bicell biofreezing vessel (Nihon) before transfer to liquid nitrogen.

2.1.5. SILAC Cell Culture

SN4741 murine dopaminergic neuronal cells grown for stable isotope labelling in cell culture (SILAC) experiments were cultured as previously described for 5 passages in SILAC DMEM (Pierce) supplemented with dialysed foetal bovine serum (Invitrogen), Penicillin/Streptomycin/L-glutamine (Sigma), and glucose (Sigma, table 4). SILAC DMEM was also supplemented with isotopically labelled arginine and lysine to a concentration of 0.398mM and 0.44mM respectively ('light', $^{12}C_6$ K_0,$^{12}C_6$ R_0 (Sigma); 'medium', $^{2}H_4$ K_4,$^{13}C_6$ K_6 (Cambridge Isotope Laboratories Inc.); 'heavy', $^{13}C_6$ R_6, $^{13}C_6$ $^{15}N_2$ K_8, $^{13}C_6$ $^{15}N_4$ R_{10} (Cambridge Isotope Laboratories Inc.)). Amino acid solutions were made to a 1000X stock solution of 0.398M and 0.44M for arginine and lysine respectively in PBS.

Table 2.4. SN4741 SILAC media. SILAC Dulbecco's modified Eagle medium (DMEM) was modified by adding the reagents shown below. Serum free media is as below with the exception that no dialyzed foetal bovine serum is added.

Component	Manufacturer	Volume
SILAC DMEM	Invitrogen	45ml
Dialyzed foetal bovine serum (dFBS),	Invitrogen	4.5ml
Penicillin/streptomycin/L-glutamine (PSG)	Sigma	0.45ml
20% glucose solution	Sigma	1.35ml
L-arginine (0.398M) in PBS	Sigma/Cambridge Isotope Laboratories Inc.	45µl
L-lysine (0.44M) in PBS	Sigma/Cambridge Isotope Laboratories Inc.	45µl

2.2. Cell Culture Treatments.

In all cases appropriate volumes of vehicle (EtOH, 45% hydroxypropyl-β-cyclodextrin in 0.9% NaCl or both) were also added to media to act as controls between treatments.

2.2.1. Oxysterol Treatment

2.2.1.1. Adherent cells - SN4741

Oxysterols (24(*S*),25-epoxycholesterol (Enzo Life Sciences), 7α-hydroxycholesterol (Steraloids), 7β-hydroxycholesterol (Sigma), 19-hydroxycholesterol (Steraloids), 24*S*-hydroxycholesterol (Avanti Polar Lipids), 25-hydroxycholesterol (Sigma), 27-hydroxycholesterol (Avanti Polar Lipids)) were prepared at a 10mM concentration in 45% hydroxypropyl-β-cyclodextrin/0.9% saline (both Sigma) before dilution to 10μM in serum free media. Solutions were vortexed to ensure thorough mixing before sterile filtration.

SN4741 cells were washed twice with PBS before addition of 10ml of treatment per 90mm tissue culture plate and incubated for 24 hours at 37°C/5% CO_2.

2.2.1.2. Suspension cells - THP1

Oxysterols (24(*S*),25-epoxycholesterol, 7α-hydroxycholesterol, 7β-hydroxycholesterol, 24*S*-hydroxycholesterol, 25-hydroxycholesterol) was prepared at a 10mM concentration in 45% hydroxypropyl-β-cyclodextrin/0.9% saline (both Sigma) before dilution of 11.1μl in 10ml serum free media. These solutions were vortexed to ensure thorough mixing before sterile filtration. 9ml of sterile treatment was added per $25cm^2$ flask as appropriate.

THP1 cells were transferred to a centrifuge tube before being spun at 700g for 5min. The media supernatant was discarded and cells resuspended in 10ml PBS. Cells were then spun at 700g for 5min. The PBS was discarded and the wash step repeated. The cells were then resuspended in 10ml serum free media. An aliquot of the cell suspension was diluted 1:40 with serum free media and then counted using a Scepter automated hand held cell counter (Millipore) using 60μm sensor tips. Cells were then diluted to $6x10^6$ with serum free media before addition of 1ml per flask as appropriate

for a final concentration of $6x10^5$ cells/ml and incubated for 24 hours at 37°C/5% CO_2.

2.2.2. GW3965 Treatment

2.2.2.1. Adherent cells - SN4741

GW3965 (Sigma) prepared as a 10mM solution in ethanol before dilution to 1_M with serum free media. This 1μM solution was vortexed to ensure thorough mixing before sterile filtration. SN4741 cells were then washed twice with PBS before addition of 10ml of appropriate treatment was added per 90mm plate and incubated for 24 hours at 37°C/5% CO_2.

2.2.2.2. Suspension cells - THP1

GW3965 (Sigma) prepared as a 10mM solution in ethanol before dilution of 1.1μl in 10ml serum free media. This solution was vortexed to ensure thorough mixing before sterile filtration. 9ml of sterile treatment was added per $25cm^2$ flask as appropriate.

THP1 cells were transferred to a centrifuge tube before being spun at 700g for 5min. The media supernatant was discarded and cells resuspended in 10ml PBS. Cells were then spun at 700g for 5min. The PBS was discarded and the wash step repeated. The cells were then resuspended in 10ml serum free media. An aliquot of the cell suspension was diluted 1:40 with serum free media and then counted using a Scepter automated hand held cell counter (Millipore) using 60μm sensor tips. Cells were then diluted to $6x10^6$ with serum free media before addition of 1ml per flask as appropriate for a final concentration of $6x10^5$ cells/ml and incubated for 24 hours at 37°C/5% CO_2.

2.3. SN4741 viability assays

SN4741 cells were seeded at 200μl/well, 50,000 cells/ml in 96 well plates and incubated for 24 hours at 37°C/5% CO_2. After incubation the cells were washed twice with PBS before addition of 100μl of treatment (vehicle, 1μM GW3965, 10μM 24(*S*),25-epoxycholesterol or 10μM 24*S*-hydroxycholesterol) in charcoal stripped serum containing media and incubated at 37°C for the desired time.

2.3.1. Cell Viability Assay: XTT

Cell viability was measured using XTT Cell proliferation Assay Kit (ATCC) following the manufacturer's instructions. XTT, in the presence of viable cells, is reduced to an orange colour formazan derivative that can be read by absorbance on a plate reader. Briefly, to 5ml of XTT solution 100µl of activating solution was added and mixed. To 100µl media (per well on a 96 well plate) 50µl of activated XTT reagent was added and incubated for 2-4 hours at 37°C. The plate was then read at 475nm (test) and 660nm (control) using a POLARstar Omega plate reader (BMG Labtech). Wells containing media only (i.e. no cells) served as a blank control and the average from these wells were deducted from test wells. The reading measured at 660nm was then deducted from the 475nm reading.

2.3.2. Cell Viability Assay: CellTiter Blue

Cell viability was then measured using CellTiter Blue assay (Promega) following the manufacturer's instructions. CellTiter blue is a resazurin based assay; in the presence of viable cells resazurin can be reduced to resorufin, a fluorescent compound. Briefly, to 100µl media (per well on a 96 well plate) 20µl of CellTiter Blue reagent was added and incubated for 2-4 hours at 37°C. If the treatment was in a larger volume then the volume of CellTiter Blue reagent was scaled up accordingly. Fluorescence was then measured using a POLARstar Omega plate reader (excitation 544nm; emission 590nm). Wells containing media only (i.e. no cells) served as a blank control and the average from these wells were deducted from test wells.

2.4. Cell Lysis – Protein Extraction

Cells were washed twice with ice cold PBS before lysis was performed with 200µl ice cold lysis buffer (200mM ammonium bicarbonate, 0.1% sodium dodecyl sulphate (SDS, Invitrogen), 1% phosphatase inhibitor cocktail 1 (Sigma), 1% phosphatase inhibitor cocktail 2 (Sigma)) per plate. A cell scraper (Greinier) was used in order to ensure thorough lysis before transfer to a 1.5ml microcentrifuge tube. The lysate was then centrifuged at 4°C, 14000 rpm for 30min. The supernatant was transferred to a new microcentrifuge tube for further analysis/storage and the cell pellet was discarded. Samples intended for Western blotting were supplemented with Complete

protease EDTA-free inhibitors (Roche) at a 1:25 dilution from a stock 25x solution. Lysates were stored at –20°C for short term or –80°C for longterm.

2.5. Protein Estimation

Protein lysate concentration was estimated using Bradford assay. A bovine serum albumin (BSA) linear standard curve of known concentrations (table 2.5) is measured in order to allow regression of the absorbance of the unknown samples. To achieve this 60µl of 2mg/ml BSA (Bio-Rad) is mixed with 60µl of water in a 1.5ml microcentrifuge tube. This 1µg/µl solution is then used to create the standards to test. The standards were prepared in duplicate.

Table 2.5. Dilutions of BSA for Bradford Assay standard curve

BSA concentration (µg/µl)	Volume 1µg/µl BSA (µl)	Volume H_2O (µl)
1	20	0
0.75	15	5
0.5	10	10
0.25	5	15
0.125	2.5	17.5
0	0	20

The lysate sample of unknown concentration were vortexed and centrifuged briefly before 2µl was taken and diluted 1:10 with water. These dilutions were prepared in duplicate for each sample. The Bradford dye reagent (Bio-Rad) was then diluted from a 5x stock to a 1x working solution with distilled water. 1ml of 1x Bradford reagent was then added to each standard and sample, vortexed, and are left to incubate for 5min. Once the incubation is complete 250µl of each standard or sample were transferred in duplicate to a 96-well flat-bottomed tissue culture plate (Greinier) and the absorbance measured at 595nm on an iMark plate reader (Bio-Rad). A linear standard curve was generated and the concentration of the 1:10 diluted sample

solutions were calculated from their observed absorbance. These concentrations are then multiplied by 10 to take into account the dilution of the sample and the volume required for a given weight of protein (e.g. 20μg) can be calculated.

2.6. Stable Isotope Labelling in Cell Culture (SILAC)

Changes in protein expression were examined using SILAC. SN4741 cells were cultured for SILAC as described earlier (section 2.1.5.).

2.6.1. SILAC Treatment(s) - SN4741

Treatments (24(*S*),25-epoxycholesterol 10μM, GW3965 1μM) intended for SILAC cells were prepared as described previously (sections 2.2.1, 2.2.2) in the appropriate serum free SILAC media ('light', 'medium', 'heavy'). To ensure that the isotope labelling itself led to no change in protein expression the treatments assigned to each SILAC state were rotated with each biological replicate (*i.e.* if 24(*S*),25-epoxycholesterol used to treat 'light' SILAC cells in first experiment then for next experiment 24(*S*),25-epoxycholesterol used to treat 'medium' SILAC cells.

2.6.2. SILAC Sample Reduction and Methylation

Protein from the different SILAC states were mixed at a 1:1:1 ratio for 2mg total protein before incubation for 1hour at 60°C with an appropriate volume of 50mM tris(2-carboxyethyl)phosphine hydrochloride (TCEP, Sigma) in HPLC grade H_2O to give a final concentration of 5mM. To block the thio groups of cysteine amino acid residue the sample was then incubated for 15min at room temp with an appropriate volume of 200mM *S*-Methyl methanethiosulfonate (MMTS, Sigma) in HPLC grade isopropanol to give a final concentration of 10mM. Protein was digested using 200μg sequencing grade trypsin (Promega) with incubation overnight at 37°C.

2.6.3. Strong Cation Exchange (SCX) Chromatography

Strong cation exchange chromatography was performed on a Dionex Ultimate 3000 HPLC system using a Polysulfoethyl A column (200mmx4.6mm, 5μm, 200Å, Poly LC Inc; solvent A = 2% HPLC grade acetonitrile (Fisher), 0.1% formic acid; solvent B = 0.6M NH_4Cl, 2% HPLC grade acetonitrile, 0.2% formic acid). 50μg of trypsin

digested BSA was used to validate SCX performance before sample was loaded onto the column. Samples were diluted 10x using solvent A and then, if required, adjusted to pH 2.5-3 with formic acid prior to loading. Loading of the sample was performed by injecting 2ml sample at 5 min intervals with a flow rate of 800µl/min of solvent B. Once the sample was fully loaded LC gradient was run over 70 min (0-10min 2% B, 10-15min 2-15% B, 15-45min 15-30% B, 45-55min 30-50% B, 55-60min, 50-100% B, 60-65min 100% B, 65-66min 100-2% B, 66-70min 2% B) at a flow rate of 800µl/min with fraction collection performed from 15 to 70min. Fraction collection was more frequent (90s per fraction) at the beginning of the run (see fig. 3.6). A UV trace was recorded in order to visualise the fractionation of the loaded peptide mixture.

2.6.4. Desalting

Sep-Pak Vac 3cc C18 cartridges (Waters) were activated with 1ml 80% acetonitrile/0.1% formic acid before equilibration with 4ml H_2O/0.1% formic acid. SCX fractions were diluted 1:1 with H_2O/0.1% formic acid before loading onto the Sep-Pak C18 cartridge and washed with 4ml H_2O/0.1% formic acid. Peptides were eluted from C18 with 1ml 80% acetonitrile/0.1% formic acid before drying overnight under vacuum. Dry samples were resuspended in 45µl H_2O/0.1% formic acid.

2.6.5. LTQ-Orbitrap Calibration Electrospray Positive Ion Mode

The LTQ-Orbitrap (Thermo) instrument was calibrated prior to use by using the electrospray source in positive ion mode. Calmix (Caffeine, MRFA, Ultramark) was injected to the source at 3µl/min and the instrument was tuned on the 524.3m/z peak. The tune file was then saved. The ion trap settings calibrated initially were multipole RF frequency, main RF frequency, electron multiplier gain. After successful calibration of these parameters the following were calibrated:- mass calibration-normal scan rate types; mass calibration – enhanced scan rate types; Mass and resolution calibration- normal scan rate type; Isolation wave form; Activation wave form. Following successful calibration the following Fourier transform (FT, i.e. Orbitrap) parameters were checked only:- transfer multipole RF frequency; storage multipole RF frequency; positive ion mode- storage transmission; positive ion mode – FT transmission. The only FT parameter calibrated was Positive ion mode – mass

calibration. The calibration was then backed up. The ion trap was calibrated as least once a month and the Orbitrap calibrated at least twice a week. After calibration spectra were recorded of the calmix in the FT and ion trap modes to allow an audit trail of performance.

2.6.6. LTQ-Orbitrap Nanospray

After calibration the electrospray source was removed and replaced with the nanospray source. A solution of [Glu^1]-fibrinopeptide B human (Glufib, Sigma) 100fmole/µl was required for tuning and was prepared by diluting 10µl of a 1pmole/µl stock with 90µl 40% acetonitrile/0.1% formic acid. The glufib was injected at a rate of 0.3µl/min. The ion trap was then tuned on 785.8m/z. Spectra were then acquired in the FT and ion trap (MS and MS^2) modes to allow an audit trail of performance.

2.6.7. Liquid Chromatography

Liquid chromatography was performed in nanoflow mode on a Dionex Ultimate 3000 HPLC system using as solvent A1 2% acetonitrile/0.1% formic acid and as solvent B1 90%acetonitrile/0.1% formic acid. For loading H_2O/0.1% formic acid was used as the solvent. Lines were purged prior to LC flow commencing for 300 seconds at a flow rate of 2000µl/min. The LC system was attached to the mass spectrometer and the flow started; 4%B 0.3µl/min for micropump 1 and 15µl/min for micropump 2

2.6.8. Liquid Chromatography Validation - Bovine Serum Albumin

To evaluate liquid chromatography (LC) performance 5µl of 20fmol/µl trypsin digested BSA was injected to test the instrument. The method for the LTQ-Orbitrap was an n^{th} order double play method analysing the top 6 peaks. The method consisted of 2 scan events. Scan event 1 was a MS scan in the FT mode with the following settings – acquire time = 35min, lock mass = 445.1200, scan range =400-2000m/z, data format = profile, resolution = 60,000. Scan event 2 was a MS^2 scan performed in the ion trap with the following settings – centroid; activation - type = CID, default charge state = 2, isolation width m/z = 3, normalised collision energy = 35, activation Q = 0.25, activation time = 30, minimum signal required = 500, top n peaks = 6;

enable charge state screening, enable monoisotopic precursor selection, reject charge state = 1; enable dynamic exclusion, repeat = 1, repeat duration = 30s, exclusion list size = 500, exclusion duration = 30s, exclusion mass width = ±7ppm, early expiration enabled. Contact closure was used to synchronise the LC to the mass spectrometer.

2.6.9. LTQ-Orbitrap LC-MS/MS

10µl of each fraction was analysed by LC-MS/MS over a 120min gradient (0-3min 4% B, 3-99min 4-50% B, 99-100min 50-90% B, 100-105min 90% B, 105min 90-4% B, 105-120min 4% B). For the first 3min of the gradient samples were loaded at 15µl/min onto a Symmetry300 C18 trap column (Waters) before separation on a RSLCnano column C18 column (75µm i.d. x 15cm, Dionex) at a ~250nl/min flow rate. Separated peptides were analysed on a LTQ-Orbitrap over 4 mass ranges (400-610 m/z, 590-800 m/z, 780-1010 m/z and 990-2000 m/z) using an Orbitrap resolution of 60,000 and an n^{th} order double play 'top 6' method to select ions for CID MS/MS (singly charged precursors ions or those with signal <500 not selected).

The method consisted of 2 scan events. Scan event 1 was a MS scan in the FT mode with the following settings – acquire time = 118 min, lock mass = 445.12, scan range = 4 mass ranges (400-610 m/z, 590-800 m/z, 780-1010 m/z and 990-2000 m/z), data format = profile, resolution = 60,000. Scan event 2 was a MS^2 scan performed in the ion trap with the following settings – data format = centroid; activation - type = CID, default charge state = 2, isolation width m/z = 3, normalised collision energy = 35, activation Q = 0.25, activation time = 30, minimum signal required = 500, top n peaks = 6; enable charge state screening, enable monoisotopic precursor selection, reject charge state = 1; enable dynamic exclusion, repeat = 1, repeat duration = 20, exclusion list size = 500, exclusion duration = 90s, exclusion mass width = ±5ppm, early expiration enabled. Contact closure was used to synchronise the LC to the mass spectrometer.

2.6.10. Orbitrap Velos LC-MS/MS

Dry samples were resuspended in 100µl H_2O/0.1% formic acid. 10µl of each fraction was analysed by LC-MS/MS over a 120min gradient (solvent A H_2O/0.1% formic acid, solvent B acetonitrile/0.1% formic acid; 0-5min 2% B, 5-85min 2-40% B, 85-

100min 40-80% B, 100-104min 80% B, 104-105min 80-2% B, 105-120min 2% B). For the first 5min of the gradient samples were loaded at 10µl/min onto a trap column (CapTrap, Michrom Bioresources) before separation on a Reprosil C18 column (100µm i.d. x 15cm, Nikkyo Technos Co. Ltd) at a ~200nl/min flow rate. Separated peptides analysed on a LTQ-Orbitrap Velos over a mass range of 400-2000 m/z using an Orbitrap resolution of 60,000 and a data dependent (singly charged precursors ions or those with signal <500 not selected) 'top 20' method to select ions for CID MS/MS.

2.6.11. Analysis of SILAC LC-MS/MS data

SILAC data was analysed using MaxQuant software (v.1.0.13.8 downloaded from www.maxquant.org). Thermo-Finnigan RAW files transformed to msm files using MaxQuant Quantify (v.1.0.13.8) software using appropriate triplet SILAC states. Parameters used were Orbitrap; Triplet (Arg6, Lys4, Arg10, Lys 8); maximum of 3 labelled amino acids; variable modifications = oxidation (M), acetyl (protein n-term), methylthio (C); trypsin/P; MS/MS tolerance = 0.5Da; maximum msm file size = 350Mb; maximum missed cleavages = 2; top ms/ms peaks per 100Da = 6.

Database used was IPI mouse v3.52 modified using Maxquant SequenceReverser (v.1.0.13.8). Database searching was performed using Mascot (Matrix Science v.2.2.2) using parameters generated by MaxQuant. MaxQuant Identify (v.1.0.13.8) was used to generate data tables for further analysis. Parameters used were peptide false discovery rate (FDR) = 0.01; site FDR = 0.01; protein FDR = 0.01; apply site FDR separately; maximum peptide PEP = 1; minimum peptides = 1; minimum unique peptides = 1; minimum peptide length = 6; reverse string =REV_; contaminant string = CON_; use only unmodified peptides and oxidation (M), acetyl (protein N-term), methylthio (C); use razor and unique peptides; discard unmodified counterpart peptides; minimum ratio count =1; use least modified peptides; number of threads = 1; re-quantify; filter labelled amino acids; low scoring version of identified peptides not kept.

MaxQuant generated protein ratios were analysed by following the method reported by Graumann *et al.*. Low and high z-values of ≥2 (the equivalent of 2 standard

deviations away from the median) were treated as up- or down-regulated. Three biological replicates were performed.

2.7. PhosphoSILAC

Changes in protein phosphorylation after treatment with oxysterols were examined using a quantitative proteomic approach (SILAC). The following experimental protocols were used to examine changes in the phosphoproteome. SN4741 cells were cultured for SILAC as described earlier (section 2.1.5.).

2.7.1. PhosphoSILAC Treatments - SN4741

Treatments (24(*S*),25-epoxycholesterol 10μM, 25-hydroxycholesterol 30μM) intended for phosphoSILAC studies were prepared as described previously (sections 2.2.1, 2.2.2) in the appropriate serum free SILAC media ('light', 'medium', 'heavy') with the following exceptions - oxysterols were dissolved in ethanol; 25-hydroxycholesterol was used at a higher concentration and therefore prepared as a 30mM stock solution before dilution to 30μM; cells incubated with treatment for 6 hours. To ensure that the isotope labelling itself led to no change in protein expression the treatments assigned to each SILAC state were rotated with each biological replicate.

2.7.2. phosphoSILAC Sample Reduction and Methylation

As section 2.6.1.

2.7.3. Strong Cation Exchange Chromatography

As section 2.6.2. With the exception that fraction collection was more frequent (1minute per fraction) at the beginning of the run (see figures. 4.2 and 4.3)

2.7.4. Desalting

As section 2.6.3.

2.7.5. Peptide Methylation

In one phosphoSILAC experiment methanolic HCl (hydrochloric acid in methanol; Sigma) was used to methylate acidic moieties. 3N methanolic HCl was diluted to 2N with HPLC grade methanol. 900µl 2N methanolic acid was added to each desalted dried fraction and incubated for 2 hours at room temperature with sonication every 15 minutes before being dried under vacuum.

2.7.6. Immobilised Metal Affinity Chromatography (IMAC) Phosphoenrichment

IMAC was performed using Phos-Select Iron Affinity gel (Sigma). 150µl of gel slurry (≈75µl gel; suitable for ~150µg phosphopeptide) was added to a Mobicol spin column (Mobitec) with a 10µm pore filter inserted (Mobitec).To the slurry 500µl 30% acetonitrile, 250mM acetic acid was added, vortexed and centrifuged at 8200g for 1 minute. The flow through was discarded and this step repeated twice. Dry phosphoSILAC samples were resuspended in 500µl 30% acetonitrile, 250mM acetic acid, and vortexed. The resuspended samples were added to the spin columns and then shaken with end over end rotation (30rpm) for 2 hours at room temperature. The columns were then centrifuged at 8200g for 1 minute. The gel was then washed by adding 500µl 30% acetonitrile, 250mM acetic acid, vortexing and then centrifuging at 8200g for 1 minute. A second wash was the performed by adding 500µl HPLC grade H_2O, vortexing and then centrifuging at 8200g for 1 minute. For elution 500µl 400mM ammonium hydroxide (pH = 11) was added to the gel, vortexed and shaken with end over end rotation (30rpm) for 5 minutes at room temperature. This was then eluted by centrifuging at 8200g for 1 minute to a 2ml microcentrifuge tube. A second elution was performed by adding 200µl 400mM ammonium hydroxide (pH = 11) to the gel, vortexed and shaken with end over end rotation (30rpm) for 5 minutes at room temperature. This was then eluted by centrifuging at 8200g for 1 minute to a 1.5ml Protein Lo-Bind microcentrifuge tube (Eppendorf). The two sequential elutions were combined in a 1.5ml Protein Lo-Bind microcentrifuge tube and 5µl of formic acid was added to neutralise the ammonium hydroxide. The samples were then dried overnight under vacuum. Samples were re-suspended in 60µl H_2O/0.1% formic acid.

2.7.7. LTQ-Orbitrap Calibration Electrospray Positive Ion Mode

As section 2.6.4.

2.7.8. LTQ-Orbitrap Nanospray

As section 2.6.5.

2.7.9. Liquid Chromatography

As section 2.6.6.

2.7.10. Liquid Chromatography Validation - Bovine Serum Albumin

As section 2.6.7.

2.7.11. LTQ-Orbitrap LC-MS/MS

20µl of each fraction was analysed by LC-MS/MS over a 120min gradient (0-3min 4% B, 3-99min 4-50% B, 99-100min 50-90% B, 100-105min 90% B, 105min 90-4% B, 105-120min 4% B). For the first 3min of the gradient samples were loaded at 15µl/min onto a Symmetry300 C18 trap column (Waters) before separation on a RSLCnano column C18 column (75µm i.d. x 15cm, Dionex) at a ~250nl/min flow rate. Each phosphopeptide fraction was analysed twice (i.e. two 20µl injections) on a LTQ-Orbitrap over 2 mass ranges (400-760 m/z, 740-2000 m/z) using an Orbitrap resolution of 60,000 and a data dependent 'top 6' MS/MS method to select ions for CID MS/MS(singly charged precursors ions or those with signal <500 not selected). Multistage activation was used for fragmentation (neutral loss within top 10 of 32.70 m/z, 49.00 m/z, 65.30 m/z, 98.00 m/z).

The method consisted of 7 scan events. Scan event 1 was a MS scan in the FT mode with the following settings – acquire time = 118 min, lock mass = 445.12, scan range = 2 mass ranges (400-760 m/z, 740-2000 m/z), data format = profile, resolution = 60,000. Scan event 2 was a MS^2 scan performed in the ion trap with the following settings – data format = centroid; activation - type = CID, default charge state = 2, isolation width m/z = 3, normalised collision energy = 35, activation Q = 0.25, activation time = 30, current scan event = 500, n^{th} most intense ion = 1; enable

multistage activation; product mass range = 400; neutral loss within top 10 of 32.70 m/z, 49.00 m/z, 65.30 m/z, 98.00 m/z; enable charge state screening, enable monoisotopic precursor selection, reject charge state = 1; enable dynamic exclusion, repeat = 1, repeat duration = 30, exclusion list size = 500, exclusion duration = 45s, exclusion mass width = ±5ppm; early expiration enabled. Subsequent scans (3-7) repeated scan 2 with the next 5 most intense ions (i.e. in scan 3 n^{th} most intense ion = 2, scan 4 n^{th} most intense ion = 3 etc.). Contact closure was used to synchronise the LC to the mass spectrometer.

2.7.12. Analysis of phosphoSILAC LC-MS/MS data

SILAC data was analysed using MaxQuant software (v.1.0.13.8 downloaded from www.maxquant.org). Thermo-Finnigan RAW files transformed to msm files using Maxquant Quantify (v.1.0.13.8) software using appropriate triplet SILAC states. Settings used were Orbitrap; Triplet (Arg6, Lys4, Arg10, Lys 8); maximum of 3 labelled amino acids; variable modifications = oxidation (M), acetyl (protein n-term), methylthio (C), phosphorylation (ST), phosphorylation (Y); trypsin/P; MS/MS tolerance = 0.5Da; maximum msm file size = 350Mb; maximum missed cleavages = 2; top ms/ms peaks per 100Da = 6.

Database used was IPI mouse v3.52 modified using Maxquant SequenceReverser (v.1.0.13.8). Database searching was performed using Mascot (Matrix Science v.2.2.2) using parameters generated by MaxQuant. MaxQuant Identify (v.1.0.13.8) was used to generate data tables for further analysis. Parameters used were peptide FDR = 0.01; site FDR = 0.01; protein FDR = 0.01; apply site FDR separately; maximum peptide PEP = 1; minimum peptides = 1; minimum unique peptides = 1; minimum peptide length = 6; reverse string =REV_; contaminant string = CON_; use only unmodified peptides and oxidation (M), acetyl (protein N-term), methylthio (C), Phospho (ST), Phospho (Y); use razor and unique peptides; discard unmodified counterpart peptides; minimum ratio count =1; use least modified peptides; number of threads = 1; re-quantify; filter labelled amino acids; low scoring version of identified peptides not kept.

2.8. Western Blotting

2.8.1. Polyacrylamide Gel Casting

The electrophoresis apparatus was assembled and the resolving gel prepared (see table 2.6 for the required reagents for one $10cm^2$ plate, 1mm spacers, and a final concentration of 10% acrylamide). The 10% acrylamide solution was then transferred to the glass plates avoiding the generation of air bubbles and 1ml of water-saturated n-butanol was gently added to the top of the gel. The resolving gel was then left to polymerise.

Table 2.6. Reagents used in preparation of resolving gel. Volumes are for one $10cm^2$ glass plate, 1mm spacers, and a final concentration of 10% acrylamide. 4X Resolving Gel Tris consists of 1.5M Tris HCl pH 8.8, 0.4% SDS adjusted to pH 8.8 with 1M HCl. TEMED = N,N,N',N'–tetramethylethylenediamine (Sigma).

Reagent	**Volume**
Distilled water	3.15ml
Acrylamide 30% solution (Sigma)	2.5ml
4x Resolving Tris solution	1.875ml
10% w/v ammonium persulphate (APS; for electrophoresis ≥98%; Sigma)	75µl
TEMED (for electrophoresis approx. 99%) (Sigma)	7.5µl

Once the resolving gel had polymerised the water saturated n-butanol was removed and the gel washed using distilled water. The stacking gel was then prepared (see table 2.7 for the required reagents for one $10cm^2$ plate, 1mm spacers, and a final concentration of 3% acrylamide). The solution was then transferred to the glass plates avoiding the generation of air bubbles. The comb was added and the stacking gel was then left to polymerise.

Table 2.7. Reagents used in preparation of the stacking gel. Volumes are for one $10cm^2$ glass plate, 1mm spacers, and a final concentration of 3% acrylamide. 4X Stacking Gel Tris solution consists of 0.5M Tris HCl pH 6.8, 0.4% SDS adjusted to pH 6.8 with 1M HCl. TEMED = N,N,N',N' – tetramethylethylenediamine.

Reagent	**Volume**
MilliQ distilled water	2.1ml
Acrylamide 30% solution (Sigma)	0.325ml
4x Stacking gel Tris solution	0.8ml
10% w/v ammonium persulphate (APS; for electrophoresis ≥98%; Sigma)	34µl
TEMED (for electrophoresis approx. 99%) (Sigma)	3.4µl

2.8.2. Polyacrylamide Gel Electrophoresis Sample Loading

From the concentration given by the protein estimation the volume required for 20µg of protein was calculated. The sample was combined with 4x sample buffer (Invitrogen), 100mM dithiothreitol (DTT, Sigma), and distilled H_2O in a microcentrifuge tube. For a 20µl reaction - x µl sample, 5µl 4x sample buffer, 2µl 100mM DTT, H_2O to 20µl are combined, vortexed to ensure thorough mixing and then spun briefly in a microcentrifuge. The samples were then heated to 70°C for 5 min, vortexed and then spun briefly in a microcentrifuge to collect the sample at the bottom of the tube prior to loading.

The wells were washed before loading by gently pipetting 1ml of running buffer (1X Tris-glycine tank buffer – SDS = 200ml 4x tris-glycine tank buffer-SDS (36g Tris base, 172.8g glycine, distilled H_2O to 3l), 8ml 10% SDS, distilled H_2O to 800ml) into the wells removing any loose polyacrylamide. The inner chamber was then filled with running buffer and 20µl sample added to the appropriate lanes using gel-loading tips.

7µl of Novex sharp stain molecular weight ladder (Invitrogen) was added to one lane. Any surplus lanes were loaded with 10µl of 4x sample buffer (Invitrogen). Once loading is complete the outer tank is filled with running buffer and electrophoresis is performed at 125V for 130min at room temperature noting the current initially and on completion.

2.8.3. Protein Transfer to Nitrocellulose Membrane

Protein transfer was performed using XCell II™ Blot Module (Invitrogen) Western blotting apparatus using XCell SureLock Mini-Cell (Invitrogen). Fibre blotting pads and the nitrocellulose membrane were soaked in transfer buffer (1.456g Tris base, 7.2g glycine, 200ml methanol, distilled water to 1000ml) prior to use. Filter paper was soaked briefly in transfer buffer prior to placing in the cassette. Care was taken throughout to ensure that there are no air bubbles between the components that could affect protein transfer. Working from the cathode core of the blotting module the transfer cassette was assembled by placing two fibre blotting pads, filter paper and the gel were assembled in order. A small amount of transfer buffer was then used to wet the gel before addition of the nitrocellulose membrane. A second piece of filter paper was then added on top of the nitrocellulose and finally, two fibre blotting pads were added. The anode core is then placed onto the assembly ensuring that the components are held firmly and with a complete connection. The whole assembly is then slid into the transfer tank and braced into position. Transfer buffer is added to the transfer chamber until the gel/membrane assembly is covered. The outer chamber is filled with H_2O. Electrophoresis is then performed at 16V overnight at room temperature noting the current (in mA) initially and on completion.

2.8.4. Blocking Non-Specific Binding

After protein transfer the nitrocellulose membrane is removed from the transfer cassette and washed with H_2O to remove any polyacrylamide residue. The membrane is stained with 1x Ponceau S solution (1% Ponceau S (Sigma) in 5% acetic acid) to ensure successful transfer has occurred. The membrane was washed with PBS-Tween and then blocked to prevent non-specific binding by using 2% blocking reagent (Amersham) in PBS-Tween. at room temperature for 1hr with gentle shaking.

2.8.5. Primary Antibody Incubation

Primary antibodies were incubated with the membrane overnight at 4°C or at room temperature for 3 hours with gentle shaking (Caveolin-1, 1:5000, Cell Signalling Technologies; ATP binding cassette A1 (ABCA1), 1:500, Novus; Actin, 1:200, Sigma; phosphoethanolamine cytidylyltransferase (PCyt2), 0.5μg/ml, Abcam; Macrophage colony stimulating factor, 0.2μg/ml, Abcam; p44/p42 MAP kinase, 1:1000, Cell Signalling Technologies; phospho-p44/p42 MAP kinase (Thr202/Tyr204), 1:1000, Cell Signalling Technologies). Sodium azide was added to the primary antibody solution to give a final w/v concentration of 0.05% to prevent bacterial growth and allow the reuse of the antibody solution after storage at 4°C.

2.8.6. Secondary Antibody Incubation

After primary antibody incubation the membrane was then washed three times for 10 minutes each with 2% Amersham blocking reagent in PBS-Tween before incubation with appropriate horseradish peroxidase (HRP)-linked secondary antibody (donkey anti-rabbit HRP-linked (Amersham) unless otherwise noted); Caveolin-1, 1:5000; ABCA1, 1:10,000; Actin, 1:50,000; phosphoethanolamine cytidylyltransferase (PCyt2), 1:20,000; Macrophage colony stimulating factor, 1:2000 donkey anti-goat HRP-linked (Santa Cruz) p44/p42 MAP kinase 1:2000; phospho-p44/p42 MAP kinase (Thr202/Tyr204) 1:1000) for 1 hour at room temperature. The nitrocellulose was then washed three times for 15min with PBS Tween at room temperature with gentle shaking. Before detection the nitrocellulose membrane was then washed with 20ml PBS for at least 5min.

2.8.7. Detection

Enhanced chemiluminescence (ECL) is used for detection using ECL Advance kit (GE Amersham). An equal volume of reagent 1 and 2 are mixed (typically 1000μl of each for 1 blot) and are then added to the nitrocellulose. The detection reagent is incubated with the nitrocellulose for 5min at room temp before visualisation using a Biorad ChemiDoc XRS and Quantity One software (Bio-Rad). Tracker tape (Amersham) is used to visualise the position of the Novex sharp stain molecular weight ladder on the Chemidoc system.

2.9. Fixed Cell Confocal Microscopy

Glass cover slips (Fisher) were placed in each well of a 24 well tissue culture plate (Greinier) before incubation for 10 min with 250µl poly-L-lysine (0.01% BioReagent, mol wt 150,000 – 300,000 sterile filtered suitable for cell culture; Sigma). The poly-L-lysine was then removed and the cover slips left to dry for 20min at room temperature. SN4741 cells were trypsinised and counted, as previously described, before being seeded at a density of 50,000 cells per well in 1ml full media and incubated for 24 hours prior to treatment.

Oxysterols (24(*S*),25-epoxycholesterol (Enzo Life Sciences), 7α-hydroxycholesterol (Steraloids), 19-hydroxycholesterol (Steraloids), 24(*S*)-hydroxycholesterol (Avanti Polar Lipids), 25-hydroxycholesterol (Sigma), 27-hydroxycholesterol (Avanti Polar Lipids)) were prepared at a 10mM concentration in 45% hydroxypropyl-_-cyclodextrin/0.9% saline (both Sigma) before dilution to 10µM in serum free media. GW3965 (Sigma) prepared as a 10mM solution in ethanol before dilution to 1µM with serum free media. These solutions were vortexed to ensure thorough mixing before sterile filtration.

SN47471 cells were then treated with vehicle, 0.5ml GW3965 1µM (Sigma), or 0.5ml 10µM oxysterol (24(*S*),25-epoxycholesterol, 7α-hydroxycholesterol, 19-hydroxycholesterol, 24(*S*)-hydroxycholesterol, 25-hydroxycholesterol or 27-hydroxycholesterol) in the presence or absence of 250µM cholesterol (Sigma) for 24 hours at 37°C/5% CO2. After incubation cells were washed twice with 1ml PBS prior to fixing by incubating with 250µl 4% paraformaldehyde (Sigma) in PBS for 15 minutes.

Fixed cells were washed three times with 1ml of Hank's Balanced Salt Solution (HBSS; Invitrogen) and then stained with 250µl of 1µg/ml Alexa-555 labelled wheat germ agglutinin (Invitrogen) per well for 5min at room temperature. After incubation the cells were washed twice for 5minutes with 1ml HBSS then permeabilised by incubating with 250µl PBS Triton-X100 0.2% (Sigma) in for 10min at room temperature. Non-specific binding was blocked with incubation for 30min with 250µl blocking buffer (0.5% essentially fat free BSA (Sigma) in PBS Triton-X100 0.1%)

per well before treatment with anti-caveolin-1 antibody (1:200 in blocking buffer, Cell Signalling Technologies) for 1hour at room temperature. The primary antibody was removed and the cells washed three times with 1ml PBS Triton-X100 0.1% for 5min. Alexa 488 linked anti-Rabbit secondary antibody (1:2000 in blocking buffer; Invitrogen) was incubated with the cells for 1 hour at room temperature before washing three times with 1ml PBS Triton-X100 0.1%. The cover slips were then mounted onto glass slides (Fisher) using Mowiol 4-88 mounting medium and left to dry overnight. Slides were imaged on a Zeiss LSM 510 Meta microscope.

2.10. Real Time Reverse Transcription PCR

2.10.1. RNA Extraction – Adherent cells

RNA extraction was performed using RNeasy Mini Kit (Qiagen) following the manufacturer's instructions. Treatments were removed from cells and stored for future ELISA assays. Cells (on 90mm tissues culture dishes (Greinier)) were washed twice with ~10ml ice cold PBS (Lonza) before addition of 600µl RLT lysis buffer (Qiagen). Cells were scraped using a cell scraper (Greinier) before transfer of the lysate to a certified RNase/DNase free 2ml microcentrifuge tube (Eppendorf). The lysate was then homogenised using a 1ml syringe with a BD Microfine 23G, 1_" needle by drawing the lysate up then expelling 10 times.

After homogenisation 600µl of 70% ethanol was added to the lysate and mixed by pipetting (no centrifugation). The lysate was then loaded to a RNeasy spin column (Qiagen) placed in a 2ml collection tube. 600µl of sample was loaded and then spun in a microcentrifuge for 15s at 13,000 rpm. The flow through was discarded and the loading was repeated until all lysate was transferred to column. 700µl of RW1 buffer was added to the column and spun for 15s at 13,000 rpm to wash the sample and the flow through was discarded. A second wash was performed; 500µl of RPE buffer was added to the column, spun for 15s at 13,000 rpm and the flow through was discarded. For the final wash 500µl of RPE buffer was added to the column, spun for 2min at 13,000 rpm and the flow through was discarded. The column was transferred to a clean 2ml collection tube and then spun again for 1min at 13,000 rpm to ensure removal of all wash buffers.

RNA was eluted from the column with 40µl RNase free water to a clean 1.5ml centrifuge tube. The water was added directly to the membrane of the column and then spun for 1min at 13,000 rpm. To ensure a good yield of RNA the flow through was reloaded onto the column and then spun again for 1min at 13,000 rpm. RNA was stored at -80°C.

2.10.2. RNA Extraction – Suspension Cells

RNA extraction was performed using RNeasy Mini Kit (Qiagen) following the manufacturer's instructions. The cell suspension was transferred from the tissue

culture flask to 15ml centrifuge tube and then centrifuged at 700g for 5min. The supernatant, i.e. the treatment media, was stored for future ELISA assays at -80°C. The cell pellet was washed by resuspending cells in 10ml ice cold PBS (Lonza) before centrifugation for 5min at 700g. This was repeated once before addition of 600µl RLT lysis buffer (Qiagen). The lysate was then transferred to a certified RNase/DNase free 2ml microcentrifuge tube (Eppendorf) and homogenised using a 1ml syringe (BD) with a BD Microfine 23G, 1_" needle (BD) by drawing the lysate up then expelling 10 times.

The remainder of the extraction follows same method as adherent cells (2.9.1).

2.10.3. RNA Concentration Estimation

RNA concentration was estimated using a Nanodrop ND-1000 spectrophotometer (Labtech). The capillary was cleaned before use using water. The option to measure nucleic acid was chosen and 1µl of water was loaded and used to initialise the instrument. The setting was switched to 'RNA' and 1µl of water was loaded and measured as a blank. 1µl of sample(s) were then loaded sequentially and measured. The RNA concentration was recorded (ng/µl) and the 260nm/280nm and 260/230 ratios that indicates the quality of the RNA.

2.10.4. Reverse transcription

Reverse transcription was performed using a Quantitect Reverse Transcription kit (Qiagen) following the manufacturer's instructions. All components were kept on ice until used. Before the reverse transcription a step to remove genomic DNA was undertaken; for each sample 900ng of RNA was taken and diluted to 12µl with RNase free water and 2µl of genomic DNA wipeout buffer added (Qiagen) for a total volume of 14µl. This mixture was mixed and centrifuged briefly before incubation at 42°C for 2min (iCycler, Bio-Rad). A master mix for the reverse transcription reaction was then prepared consisting of 4µl 5x Quantiscript RT buffer, 1µl Quantiscript reverse transcriptase and 1µl of primers (all Qiagen) per sample. After incubation the sample was centrifuged briefly 6µl of reverse transcription master mix was added per sample to give a final volume of 20µl. The samples were mixed, centrifuged briefly and then incubated at 42°C for 15min followed by 95°C for 3min (iCycler, Bio-Rad) to

generate cDNA. No reverse transcriptase control reactions were performed as above but with the Quantitect reverse transcriptase enzyme in the reaction mixture replaced with water.

2.10.5. Primers

Each primer set (table 2.8., Sigma (unless otherwise noted)) was evaluated to ensure that they amplified the target while avoiding the generation of primer dimers and that a linear standard curve was generated across a broad range by dilution with water (cDNA neat, 1:10 , 1:100, 1:1000). Primers were reconstituted from lyophilised powder to a 100μM concentration with H_2O.

Table 2.8.Primers used for reverse transcription qPCR. The primers for LXRα and LXRβ were obtained from the Nuclear Receptor Signalling Atlas website (www.nursa.org/10.1621/datasets.02001 - accessed 13-12-2010). Primers for StarD4 self designed using NCBI Primer-Blast primer designing tool (http://www.ncbi.nlm.nih.gov/tools/primer-blast). The primers for FADS2 were taken from the RTprimerDB website (http://medgen.ugent.be/rtprimerdb/assay_report.php?assay_id=8122 – accessed 17-1-2011). Primers for CERT were obtained from Qiagen. No sequence information was provided. * Mismatch in primer sequence in referenced manuscript. Possible typographical error therefore primer sequence used 100% complementary.

Primer Name	Species	Sequence (5'-3')	Reference
LXRα forward	Mouse	AGG AGT GTC GAC TTC GCA AA	See table legend
LXRα reverse	Mouse	CTC TTC TTG CCG TTC AGT TT	See table legend
LXRβ forward	Mouse	AAG CAG GTG CCA GGG TTC T	See table legend
LXRβ reverse	Mouse	TGC ATT CTG TCT CGT GGT TGT	See table legend
SREBP1c forward	Mouse	ATC GGC GCG GAA GCT GTC GGG GTA GCG TC	Shimomura *et al.* 1997

SREBP1c reverse	Mouse	ACT GTC TTG GTT GTT GAT GAG CTG GAG CAT	Shimomura *et al.* 1997
Cav-1 forward	Mouse	AAC GAC GAC GTG GTC AAG A	Bailey & Liu 2008
Cav-1 reverse	Mouse	CAC AGT GAA GGT GGT GAA GC	Bailey & Liu 2008
LDLR forward	Mouse	CAT GCA GCA GGA ACG AGT TC*	Masson *et al.* 2004
LDLR reverse	Mouse	GGA GTC AGG AAT GCA TCG GC	Masson *et al.* 2004
StarD4 forward	Mouse	ATG CGT TAC ACC ACT GCT GGG C	See table legend
StarD4 reverse	Mouse	TCT GGT CTC GTC TCA CTC CAC TCA	See table legend
MCSF forward	Mouse	GAA CAC TGT AGC CAC ATG ATT GG	Wang *et al.* 2009
MCSF reverse	Mouse	TGG CAT GAA GTC TCC ATT TGA C	Wang *et al.* 2009
Col4a3bp forward	Mouse	Unknown	See table legend
Col4a3bp reverse	Mouse	Unknown	See table legend
β-actin forward	Mouse	GGT CGT ACC ACA GGC ATT GTG ATG	Shimomura *et al.* 1997
β-actin reverse	Mouse	GGA GAG CAT AGC CCT CGT AGA TGG	Shimomura *et al.* 1997
IDOL forward	Mouse	AGG AGA TCA ACT CCA CCT TCT G	Zelcer *et al.* 2009
IDOL reverse	Mouse	ATC TGC AGA CCG GAC AGG	Zelcer *et al.* 2009
MCSF forward	Human	TGC AGC GGC TGA TTG ACA	Razzaque *et al.* 2002
MCSF reverse	Human	TTC AAC TGT TCC TGG TCT ACA AAC TC	Razzaque *et al.* 2002
β-actin forward	Human	GAT GGC CAC GGC TGC TTC	Cronin *et al.* 2011
β-actin reverse	Human	TGC CTC AGG GCA GCG GAA	Cronin *et al.* 2011

2.10.6. Real Time Polymerase Chain Reaction

Primers (table 2.8) were diluted from a 100μM stock solution to 10μM with water, vortexed and centrifuged. A master mix was then prepared for each gene. For each well 12.5μl of QuantiFast SYBR green PCR master mix 2x (Qiagen), 2.5μl forward primer (i.e. 1μM final concentration), 2.5μl reverse primer (i.e. 1μM final concentration), 5.5μl RNase free water was required and therefore these values were multiplied by the number of wells to be used (plus an overage). The master mix was then mixed and centrifuged briefly.

cDNA was taken from each sample and pooled in order to be used to generate a standard curve. The pooled cDNA used for the standard curve was diluted 1:10, 1:100 and 1:1000 using serial dilutions. Samples to be analysed for gene expression (and noRT controls) were diluted 1:4 with water so that they fell within the limits of the standard curve. At each stage the cDNA was mixed and centrifuged to give a homogenous mixture. Each sample was analysed in triplicate. The master mix was then transferred into the PCR plate with 23μl per well as appropriate. 2μl of cDNA (or water for no template controls (NTC)) was added to each well as appropriate (see figure 2.1 for example of plate set up).

	1	2	3	4	5	6	7	8	9	10	11	12
A	1:1000, Pooled, Target			1:4, sample A, Target			1:4, sample E, Target			1:4, sample D, Target noRT		
B	1:100, Pooled, Target			1:4, sample A, β-actin			1:4, sample E, β-actin			1:4, sample D, β-actin noRT		
C	1:10, Pooled, Target			1:4, sample B, Target			1:4, sample A, Target noRT			1:4, sample E, Target, noRT		
D	Undiluted, Pooled, Target			1:4, sample B, β-actin			1:4, sample A, β-actin noRt			1:4, sample E, β-actin, noRT		
E	1:1000, Pooled, β-actin			1:4, sample C, Target			1:4, sample B, Target noRt					
F	1:100, Pooled, β-actin			1:4, sample C, β-actin			1:4, sample B, β-actin noRT					
G	1:10, Pooled, β-actin			1:4, sample D, Target			1:4, sample C, Target noRT			NTC target		
H	Undiluted, Pooled, β-actin			1:4, sample D, β-actin			1:4, sample C, β-actin noRT			NTC β-actin		

Figure 2.1. Typical plate set up for real time RT-PCR. All samples were run in triplicate. A standard curve derived form pooled cDNA from the samples was generated using 4 serial dilutions. Samples for analysis of expression were diluted 1:4 with DNase/RNase free water. NoRt = No reverse transcriptase added to sample in the RT step. NTC = No template control

The plate was then centrifuged briefly to ensure that samples were collected at the bottom of the well and then checked to ensure that no air bubbles were present. The plate was then transferred to an iQ5 real time PCR detection system (Bio-Rad) to be analysed using the conditions shown in table 2.9.

Table 2.9. Conditions for real time PCR

Cycle	Cycle Repeated	Temperature (°C)	Dwell Time (s)	Additional information
1	1x	95°C	300	
2.1	45x	95°C	10	
2.2		60°C	30	Real time analysis
3	1x	95°C	60	
4	1x	55°C	60	
5	81x	Start at 55°C with a 0.5°C increase per cycle	10	Melt curve analysis

2.10.7. Data Analysis

The standard curve derived from the pooled cDNA was used to monitor primer efficiency. Primer efficiency expressed as a percentage was generated using the Bio-Rad iQ5 software. Primer efficiencies summarised in table 2.10.

Table 2.10. Summary of RT-PCR primer efficiencies. Efficiency shown as mean with standard deviation.

Gene	Species	Primer efficiency
LXRα	Mouse	93.5±5.2
LXRβ	Mouse	109.7±6.8
SREBP1c	Mouse	93.1±4.0
Cav-1	Mouse	88.2±0.64
LDLR	Mouse	100.8±8.2
StarD4	Mouse	100.0±2.3
MCSF	Mouse	98.4±7.6
Col4a3bp	Mouse	102.9±2.0
IDOL	Mouse	94.1±1.3
β-actin	Mouse	97.4±6.7
MCSF	Human	102.8±4.3
β-actin	Human	102.0±1.3

Analysis of the data was performed using ΔΔCt method. The cycle threshold value (Ct) of the gene of the interest was subtracted from the Ct value of the reference gene (β-actin) from the same sample giving the ΔCt value.

$$\Delta Ct = Ct_{(sample)} - Ct_{(reference)}$$

This was repeated for each experimental condition. The ΔCt values for the treatment were then subtracted from the control value giving a ΔΔCt value.

$$\Delta\Delta Ct = \Delta Ct_{(treatment)} - \Delta Ct_{(control)}$$

The ΔΔCt value was then converted into fold induction; as the amount of product amplified theoretically doubles with each PCR cycle this can be written as:-

$$\text{Fold induction c.f. control} = 2^{-\Delta\Delta Ct}$$

2.11. Mouse MCSF Enzyme Linked Immunosorbant Assay

A mouse MCSF Quantikine kit assay (R&D Systems) was performed following the manufacturer's instructions. Briefly, a mouse MCSF standard was reconstituted with 2ml of calibrator diluent RD5-16 (R&D Systems) giving a stock solution of 2000pg/ml. This solution was incubated at room temperature for 5min with gentle shaking before being used to create samples for a standard curve by using serial dilution. Calibrator diluent RD5-16 was used as a diluent. The concentrations for the standard curve were 2000pg/ml (stock solution), 1000pg/ml, 500pg/ml, 250pg/ml, 125pg/ml, 62.5pg/ml, 31.25pg/ml, 0pg/ml (Calibrator diluent RD5-16). The kit's supplied mouse MCSF internal control was reconstituted in 1ml ddH_2O. This internal control should yield a reading of 175-291pg/ml. For unknown concentration samples, 0.5ml of cell culture supernatant was vortexed then centrifuged at 14,000 rpm for 2min at 4°C.

50µl of assay diluent RD1N (R&D systems) was added to each well of the MCSF antibody pre-coated microplate supplied with the kit. 50µl of standard, control or sample was then added to each well as appropriate. To ensure thorough mixing the plate was tapped gently for one minute. The plate was then covered with an adhesive strip and incubated for 2 hours at room temperature. After incubation each well was aspirated and washed (~400µl) with 1x wash buffer (supplied as a 25x concentrated solution, R&D Systems). This wash step was repeated four times (i.e. 5 washes in total). The plate was then gently blotted against a clean paper towel to ensure removal of remaining wash buffer. 100µl of mouse MCSF conjugate (R&D Systems) was then added to each well and the plate covered with a new adhesive strip. The plate was then incubated at room temperature for 2 hours. After incubation the wells were washed as described previously.

Substrate solution was prepared by mixing equal volumes of colour reagent A and B (both R&D systems). 100µl of substrate solution was then added to each well and incubated for 30 min at room temperature protecting the plate from light. 100µl of stop solution was added to each well. The plate was gently tapped in order to ensure thorough mixing and the development of a uniform colour. The optical density of each well was then read on an iMark microplate reader (Bio-Rad) set at a wavelength

of 450nm. The plate was then read at 595nm to correct for optical imperfections of the plate.

2.12. Human MCSF Enzyme Linked Immunosorbant Assay

A human MCSF Quantikine kit assay (R&D Systems) was performed following the manufacturer's instructions. Precautionary measures were taken to prevent contamination from MCSF found in human saliva – a facemask and gloves were worn. Briefly, a human MCSF standard was reconstituted with 1ml of calibrator diluent RD5-18 (R&D Systems) giving a stock solution of 50,000pg/ml. This solution was incubated at room temperature for 15min with gentle shaking before being used to create samples for a standard curve by using serial dilution. Calibrator diluent RD5-18 was used as a diluent. The concentrations for the standard curve were 5000pg/ml (stock solution), 2500pg/ml, 1250pg/ml, 625pg/ml, 312.5pg/ml, 156.25pg/ml, 78.125pg/ml, 0pg/ml (Calibrator diluent RD5-18). For unknown concentration samples, 0.5ml of cell culture supernatant was vortexed then centrifuged at 14,000 rpm for 2min at 4°C.

100µl of assay diluent RD1-56 (R&D systems) was added to each well of the MCSF antibody pre-coated microplate supplied with the kit. 100µl of standard or sample was then added to each well as appropriate. To ensure thorough mixing the plate was tapped gently for one minute. The plate was then covered with an adhesive strip and incubated for 2 hours at room temperature. After incubation each well was aspirated and washed (~400µl) with 1x wash buffer (supplied as a 25x concentrated solution, R&D Systems). This wash step was repeated three times (i.e. 4 washes in total). The plate was then gently blotted against a clean paper towel to ensure removal of remaining wash buffer. 200µl of human MCSF conjugate (R&D Systems) was then added to each well and the plate covered with a new adhesive strip. The plate was then incubated at room temperature for 2 hours. After incubation the wells were washed as described previously.

Substrate solution was prepared by mixing equal volumes of colour reagent A and B (both R&D systems). 200µl of substrate solution was then added to each well and incubated for 30 min at room temperature protecting the plate from light. 50µl of stop solution was added to each well. The plate was gently tapped in order to ensure

thorough mixing and the development of a uniform colour. The optical density of each well was then read on an iMark microplate reader (Bio-Rad) set at a wavelength of 450nm. The plate was then read at 595nm to correct for optical imperfections of the plate.

2.13 Statistical Analysis

Statistical analysis was performed on the data using Microsoft Excel 2007 software using Student's two-tailed t-test. p values below 0.05 were considered a significant change.

CHAPTER 3: PROTEOMIC ANALYSIS OF 24(*S*),25-EPOXYCHOLESTEROL TREATMENT IN SN4741 NEURONS

3.1. Introduction

24(*S*),25-epoxycholesterol is an unusual oxysterol. It is unusual as it is not an oxygenated metabolite of cholesterol but a product of a shunt in the mevalonate biosynthetic pathway. An epoxide group is introduced to squalene by squalene epoxidase during synthesis of cholesterol. The product of this reaction, 2,3-oxidosqualene (AKA 2,3-monoepoxysqualene), is then processed by a number of downstream enzymes to synthesise cholesterol. However, 2,3-oxidosqualene can be processed further in order to create 2,3:22,23-dioxidosqualene. This can then be cyclised by lanosterol synthase and further processed along the same enzymatic pathway in order to create 24(*S*),25-epoxycholesterol. 24(*S*),25-epoxycholesterol is a potent endogenous ligand of Insig and LXR (see sections 1.1.5.1. and 1.1.5.2. respectively). Therefore, an increase in the concentration of 24(*S*),25-epoxycholesterol results in up-regulation of genes with a LXR response element in their promoter and down-regulation of SREBP2 regulated genes.

24(*S*),25-epoxycholesterol appears to have a role in the development of the embryonic brain as 24(*S*),25-epoxycholesterol is present at relatively high levels in comparison to other oxysterols in the cortex and spinal cord of embryonic mice (Wang *et al.* 2009). The major oxysterol in adult mouse brain is 24(*S*)-hydroxycholesterol with a concentration of 2.53±0.05ng/μg 24(*S*)-hydroxycholesterol to cholesterol (Lütjohann *et al.* 2002). In the embryonic murine brain 24(*S*)-hydroxycholesterol is not the most abundant; at embryonic day 11 there was an observed level of 24(*S*)-hydroxycholesterol of 0.026μg/g wet weight in the cerebral cortex and 0.013μg/g wet weight in the spinal cord. In comparison, the concentration of 24(*S*),25-epoxycholesterol was 0.165μg/g wet weight in the cerebral cortex and 0.091μg/g wet weight in the spinal cord. It is unclear the role 24(*S*),25-epoxycholesterol, the most abundant oxysterol in foetal brain, plays in murine embryonic neural development though as LXR is present in embryonic brain (Annicotte *et al.* 2004) and that 24(*S*),25-epoxycholesterol is a potent ligand for this nuclear receptor (Janowski *et al.* 1999) it might play a role in neural development. Indeed, there is evidence to suggest

that the presence of LXR is essential to ventral midbrain neurogenesis (Sacchetti *et al.* 2009)

The mechanism by which LXR induces neurogenesis is unclear. Therefore, in order to investigate the role of 24(*S*),25-epoxycholesterol and LXR in neurogenesis a quantitative proteomic approach was employed. The proteomic technique stable isotope labelling in cell culture (SILAC) was used in order to identify changes in the proteome after treatment with 24(*S*),25-epoxycholesterol and GW3965. To this end, as a model for embryonic mouse brain, the murine neuronal cell line SN4741 was used. SN4741 cells are dopaminergic neurons derived from the substantia nigra of embryonic mouse (Son *et al.* 1999). The substantia nigra is located in the ventral midbrain. Therefore, SN4741 cells are a relevant model to the increased neurogenesis seen after LXR activation *in vivo*. Treatment of SILAC labelled SN4741 cells with either 24(*S*),25-epoxycholesterol or the synthetic LXR ligand 1μM GW3965 (which only activates LXR and has no effect on SREBP2) allows differentiation of effects as LXR dependent or independent. Thus, the aim of this work is to identify protein expression changes in SN4741 cells after 24(*S*),25-epoxycholesterol treatment and identify if these effects are LXR dependent or independent.

3.2. Results

3.2.1. Analysis of 24(*S*),25-epoxycholesterol Treatment on SN4741 Growth

To determine if 24(*S*),25-epoxycholesterol is toxic to SN4741 cells grown in culture cells were incubated with either 10μM 24(*S*),25-epoxycholesterol or with vehicle and the total cell number counted. In order to ensure that the cells survived in culture for a prolonged period but without introducing lipid small molecules that could affect the activity of 24(*S*),25-epoxycholesterol the media used contained charcoal stripped foetal bovine serum (FBS). After 76 hours there was no difference in cell number between 24(*S*),25-epoxychoelsterol and control (fig 3.1). However, incubation with charcoal stripped serum reduced the rate of growth and the vehicle and 24(*S*),25-epoxycholesterol treated cells in this media grew slower than control cells incubated in full media. Five days after seeding SN4741 cells at $2.5x10^4$cells/well in 24 well plates in full media they reached confluency and the plateau of the stationary phase of the curve. However, the 24(*S*),25-epoxycholesterol and control cells in stripped serum media did not reach confluency. However, as there were no statistical differences between control and 24(*S*),25-epoxycholesterol treatment ($p>0.05$ Student's t-test) it appears that 24(*S*),25-epoxycholesterol is non-toxic to SN4741 cells when measured by total cell number.

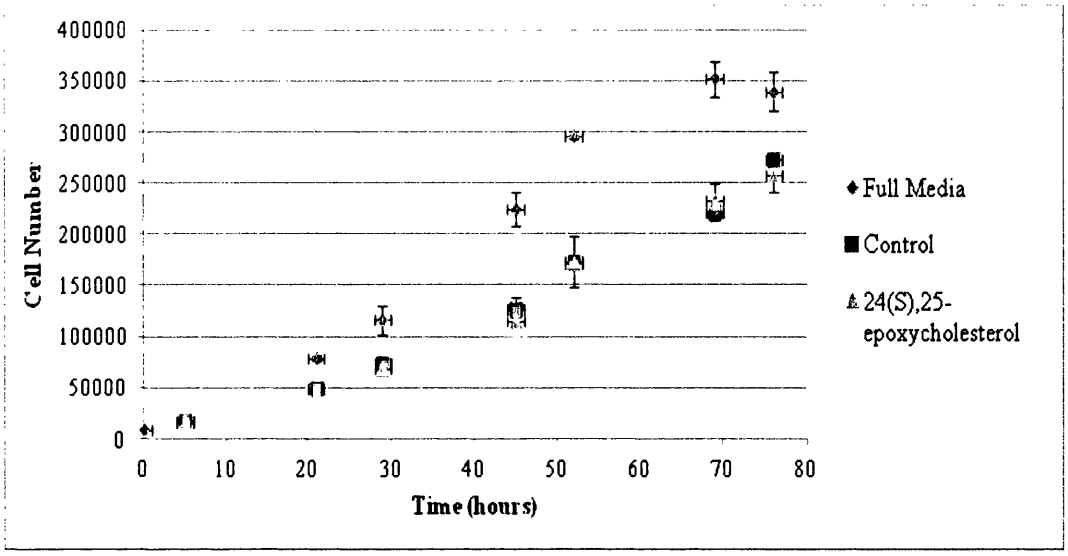

Figure 3.1. Effect of 24(*S*),25-epoxycholesterol on the rate of growth of SN4741 cells. 24 well plates were seeded at $2.5x10^4$ cells/well in media containg charcoal stripped media with either 10μM 24(*S*),25-epoxycholesterol or vehicle as control. Full media media was used to determine the effect of the charcoal stripped serum media on rate of cell growth. No difference in cell growth was observed with 24(*S*),25-epoxycholsterol and vehicle in charcoal stripped serum media. Cells grown in full media had a higher rate of cell growth compared with those grown in charcoal stripped serum media.

3.2.2. Analysis of 24(*S*),25-epoxycholesterol Treatment on SN4741 Viability

In addition the toxicity of 24(*S*),25-epoxycholesterol was measured using two other techniques – XTT (sodium 2,3,-bis(2-methoxy-4-nitro-5-sulfophenyl)-5-[(phenylamino)-carbonyl]-2H-tetrazolium inner salt) assay and Cell Titer Blue assay (a resazurin based assay marketed by Promega). Both techniques measure the ability of the cell to metabolise XTT or resoruzin respectively and induce a colour change that is proportional to the healthy cell number. XTT is not believed to enter the cell due to the net negative charge of the molecule and is believed to be reduced at the plasma membrane. Treatment with 24(*S*),25-epoxycholesterol led to no toxicity as shown by XTT assay (fig 3.2). After 24 or 48 hours of incubation with vehicle, 1μM GW3965, 10μM 24(*S*),25-epoxycholesterol, 10μM 24(*S*)-hydroxycholesterol no differences were observed. In the case of Cell Titer Blue again no toxicity was

observed (fig 3.3) after treatment with 1μM GW3965, 10μM 24(*S*),25-epoxycholesterol or 10μM 24(*S*)-hydroxycholesterol for 24 or 48 hours.

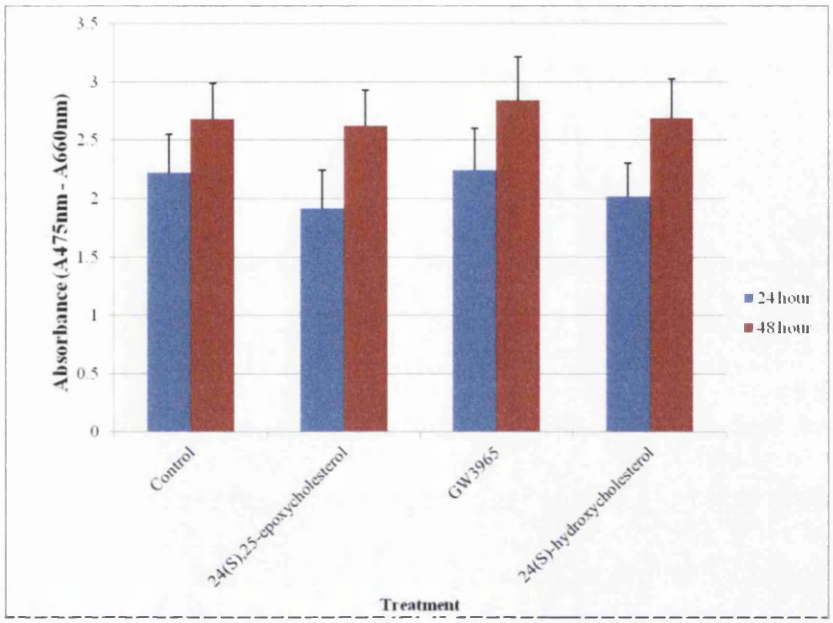

Figure 3.2. 24(*S*),25-epoxycholesterol is not toxic in SN4741 cells as measured by XTT assay (n=1). Measurements were conducted at the specific absorbance wavelength of reduced XTT (475nm) and at 660nm as a measure of non-specific absorbance. No differences were observed between control, 1μM GW3965, 10μM 24(*S*),25-epoxycholesterol, 10μM 24(*S*)-hydroxycholesterol after 24 or 48 hours.

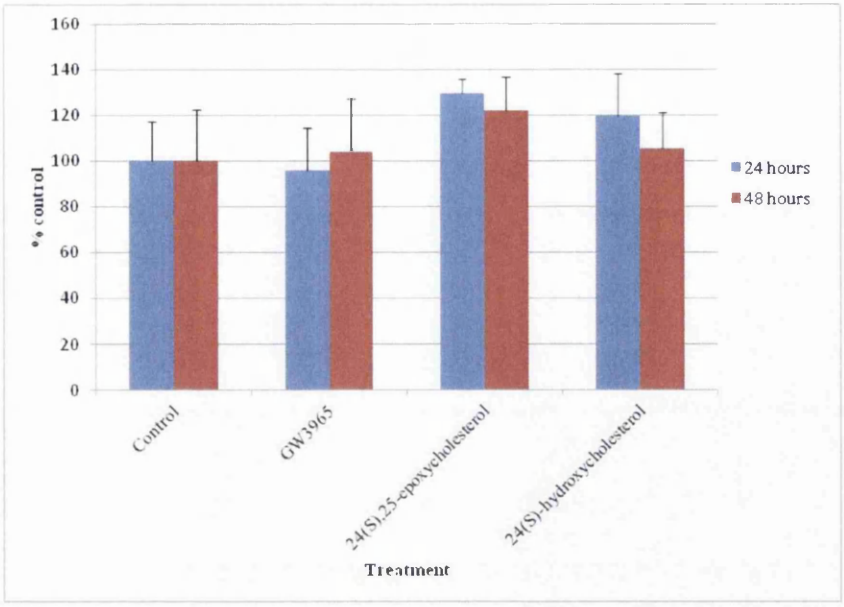

Figure 3.3. 24(*S*),25-epoxycholesterol is not toxic in SN4741 cells as measured by Cell Titer Blue assay (n=2). Measurements were conducted at fluorescent excitation wavlength (544nm) and emission wavelength (590nm) of resorufin (the metabolite generated by the reduction of resoruzin). No differences were observed between control, 1μM GW3965, 10μM 24(*S*),25-epoxycholesterol or 10μM 24(*S*)-hydroxycholesterol after 24 or 48 hours.

3.2.3. LXR Expression in SN4741 cells.

The aim of this study was to investigate LXR dependent and independent changes in protein expression. Therefore, the expression of LXRα and LXRβ was evaluated in SN4741 cells to ensure the appropriateness of the cell line as a model. The expression of both isoforms was evaluated by RT-qPCR to identify the presence of mRNA. In SN4741 cells both isoforms were present with LXRβ the predominant isoform with levels ~10 higher than LXRαwhich correlates with previously published data for the central nervous system (Whitney *et al.* 2002; table 3.1.).

Table 3.1. Threshold cycle for LXRα and LXRβ after RT-qPCR. Threshold cycle is inversely proportional to the abundance of mRNA. Therefore, more LXRβ mRNA is present than LXRα mRNA; LXRβ has a higher expression level.

Gene	Threshold Cycle
LXRα	21.1±0.9
LXRβ	17.8±1.1

In addition, after SN4741 cells were treated with either 10μM 24(*S*),25-epoxycholesterol or 1μM GW3965 the protein of the LXR responsive gene ABCA1 was increased (fig 3.4). The expression of ABCA1 is low in untreated cells. However, after 24 hours treatment with either 10μM 24(*S*),25-epoxycholesterol or 1μM GW3965 the protein level is increased markedly indicating activation of LXR. At the mRNA level RT-qPCR experiments showed that the LXRα regulated gene SREBP1c was up-regulated after treatment with both 24(*S*),25-epoxycholesterol and GW3965 indicating the expression of LXRα and the expected response (fig 3.12). GW3965 had a greater effect on SREBP1c expression with a ~7-fold increase over control whereas 24(*S*),25-epoxycholesterol only induced a ~3-fold increase.

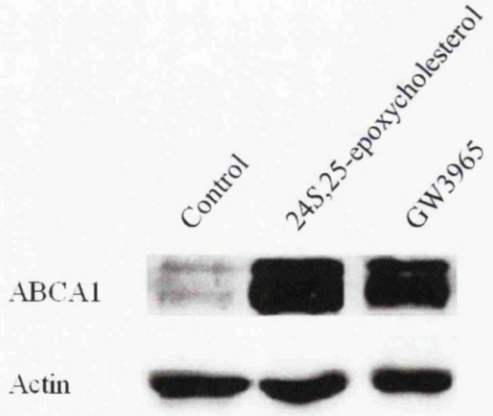

Figure 3.4. The protein level of ABCA1 is increased after 24 hours treatment with either 10μM 24(*S*),25-epoxycholesterol or 1μM GW3965 indicating that SN4741 cells express LXRα/β.

3.2.4. Strong Cation Exchange Fractionation of SILAC peptides

Treatment of SN4741 cells with 10μM 24(*S*),25-epoxycholesterol or 1μM GW3965 showed no toxic effects of these small molecules and SN4741 cells expressed LXRα/β. Thus, SN4741 cells were deemed suitable as a model for proteomic studies and grown in SILAC media for 5 passages. 5 passages is enough time to ensure full incorporation of the labelled amino acids to occur based on previous experience in our laboratory. SILAC SN4741 cells were treated with either vehicle, 1μM GW3965 or 10μM 24(*S*),25-epoxycholesterol for 24 hours in serum free SILAC media, before lysis and protein estimation. An equal amount of protein from each SILAC state was combined on a 1:1 basis and digested with trypsin to form a SILAC peptide mixture. This peptide mixture was then subjected to further analysis to elucidate proteomic changes.

Before the mass spectrometric analysis of the SILAC peptides 2-dimensional LC-MS/MS was performed. The first dimension of separation was performed using strong cation exchange chromatography. Strong cation exchange separates molecules by charge; anionic molecules elute first. Thus, the technique can be used as a fractionation step to reduce sample complexity prior to the second dimension of separation that is reverse phase C18 LC-MS/MS. In order to validate the strong cation exchange chromatography that was to be used on the SILAC samples the system was tested. A blank injection of solvent showed no detection of peptides eluting from the column (fig 3.5A) and therefore indicated lack of contamination of the system. In addition, to validate the ability of the column to separate peptides trypsin digested bovine serum albumin (BSA) was used. 50μg of peptide mixture was separated on the column and detected by UV (fig 3.5B).

A

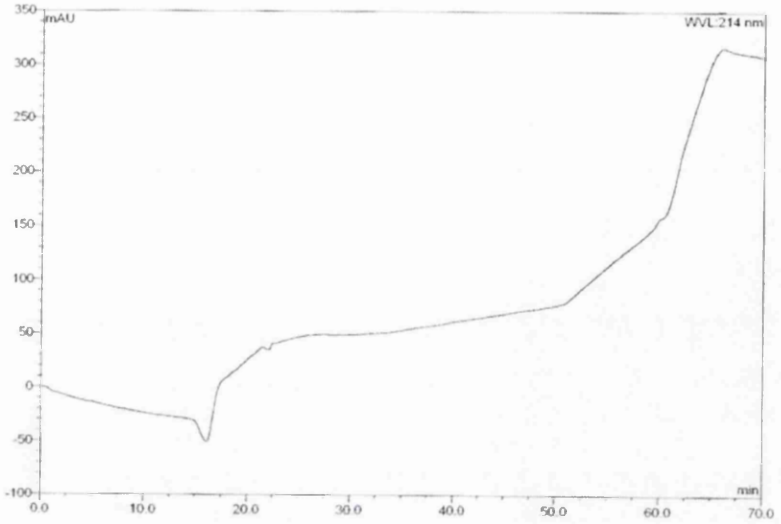

B

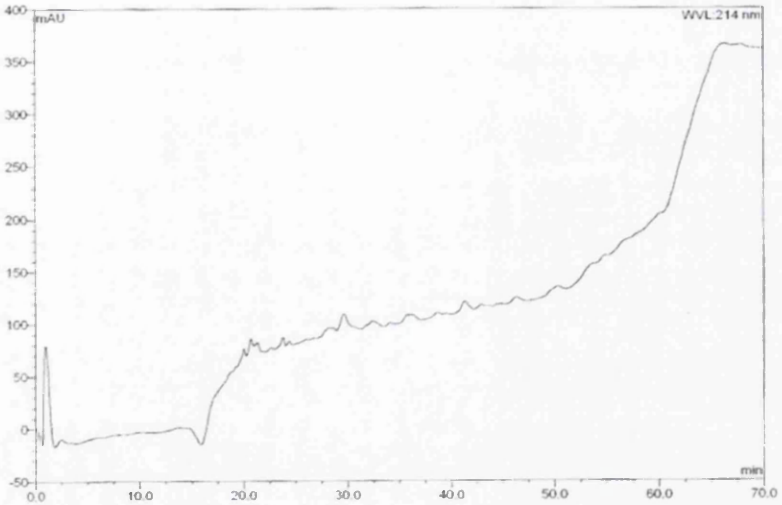

Figure 3.5. Strong Cation Exchange chromatography validation. Example UV (λ=214nm) chromatogram are shown highlighting expected instrument performance. A) A blank was run to ensure no carry over was present from previous experiments B) 50µg of BSA trypsin digested peptides loaded onto the column were separated by SCX.

Before fractionating the SILAC samples by SCX an additional blank run was to ensure that the column was free from BSA digest contamination. These procedures ensure no carry over from previous experiments and sufficient column performance. Once column performance was evaluated SILAC peptides were injected onto the column. From the UV chromatogram (fig. 3.6) it can be seen that there is a large amount of material present (c.f. blank and 50µg BSA chromatograms fig. 3.5) and that the material present has been separated. The majority of the peptides were eluted early in the run and therefore the time interval for fraction collection was shorter before increasing towards the end of the run where less material is present. The total number of peptides, compared to the number of unique peptides per fraction, can be seen in figure (fig. 3.6.). Therefore, the use of strong cation exchange chromatography was successful in reducing the complexity of the initial peptide mixture for subsequent LC-MS/MS steps. However, the number of peptides present in the fractions results in a complex mixture for reverse phase chromatography despite the fractionation.

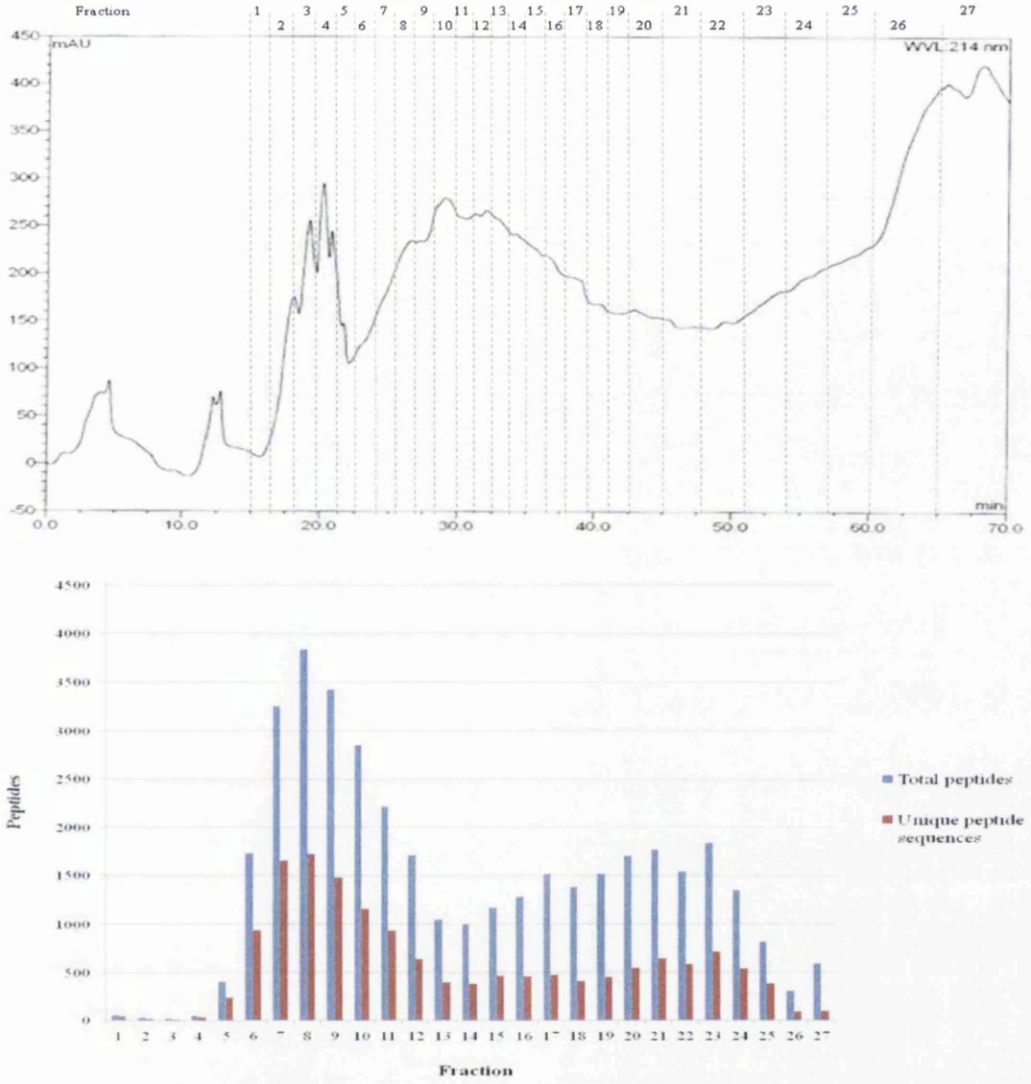

Figure 3.6. Strong Cation Exchange chromatography trace of SILAC peptides. Example of strong cation exchange chromatography fractionation from one experiment presented. A) The UV (λ=214nm) chromatogram highlights the large number of peptides present on the column. The time interval for fraction collection is indicated B) In this example a total 38458 peptides were identified. Of these 15526 were unique peptides. Strong cation exchange chromatography reduced the total number of peptides and number of unique peptides per fraction with ≤10% of the experiment total per fraction. Thus, each fraction is simplified compared to the initial mixture yet remains a complex peptide mixture in its own right.

3.2.5. C18 Reverse Phase LC-MS/MS of SILAC peptides

The peptide mixture fractions derived from strong cation exchange chromatography were desalted using Seppak C18 columns, dried under vacuum and resuspended in H_2O/0.1%formic acid to be analysed by LC-MS/MS. In order to test the performance of the reverse phase C18 column performance prior to running the SN4741 derived SILAC samples trypsin digested bovine serum albumin (BSA) was used. This allowed validation of both chromatography and mass spectrometry performance. The use of 5µl of a 20fmol/µl BSA trypsin digest gave a good signal in the mass spectra with sharp chromatographical peaks that indicate that the column performance is acceptable (a typical chromatogram is shown in fig. 3.7). In order to ensure the complete removal of the BSA peptides prior to running the SILAC SN4741 samples a blank run was performed injecting 80% acetonitrile.

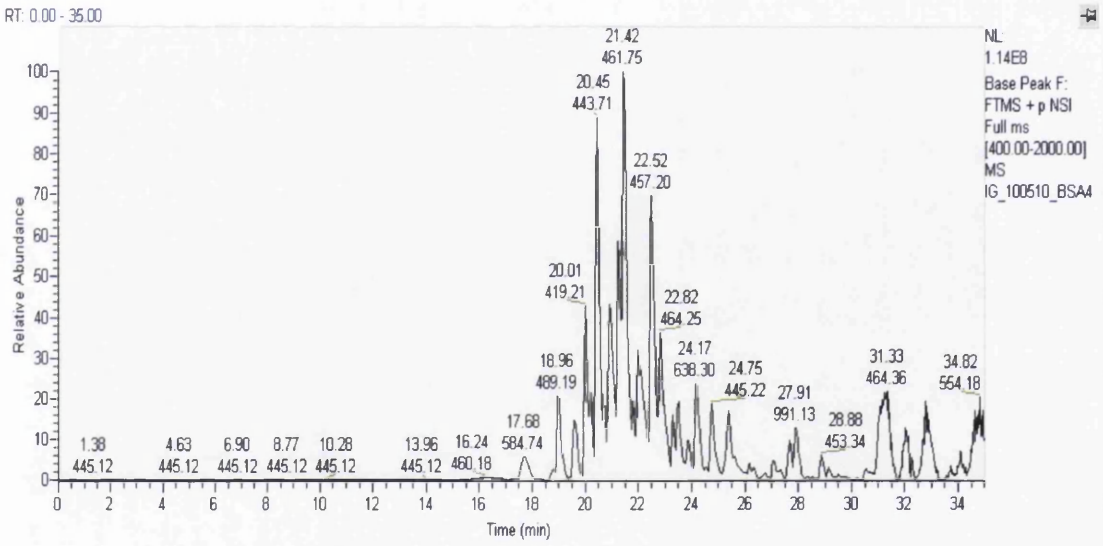

Figure 3.7. Reverse Phase LC-MS/MS validation. Example of column performance showing separation of peptides from a BSA trypsin digest. In order to ensure reverse phase column is clean a blank is run before initiating SILAC proteomic samples.

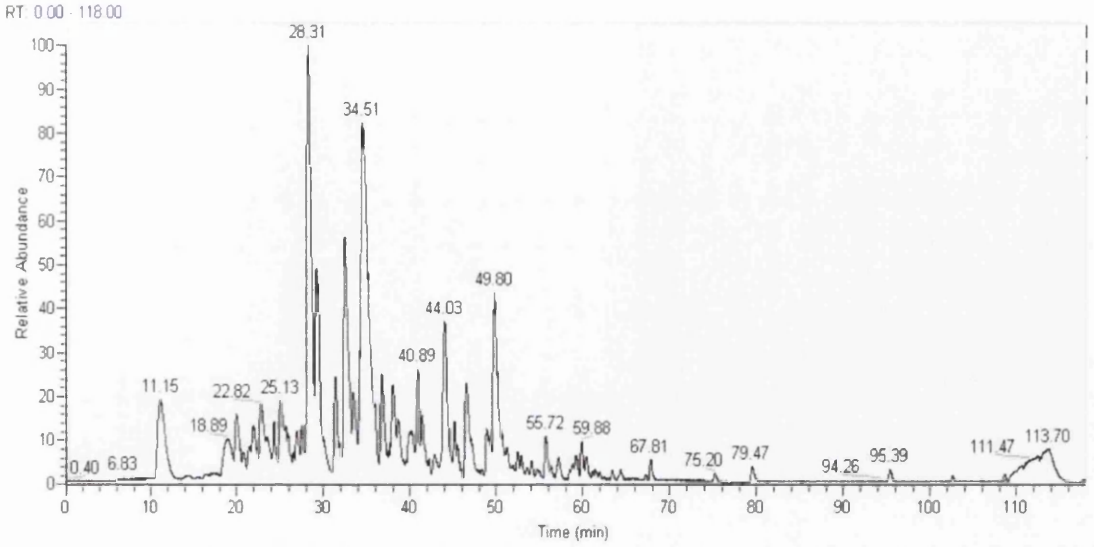

Figure 3.8. Reverse Phase LC-MS/MS SILAC peptide separation. An example chromatogram is shown that exemplifies the fact that peptides co-eluting from the strong cation exchange chromatography step can be separated by C18 reverse phase chromatography.

SILAC peptides were injected on to the HPLC system and separated over a 2 hour gradient. It can be seen from the example in figure 3.8 that a fraction obtained from strong cation exchange chromatography is still a very complex sample but the peptides present can be separated on the C18 column. Peptides eluting from the column are then analysed by mass spectrometry. Peaks with characteristic features of peptides were identified by the initial mass spectrometry scan and, if they conformed to the pre-selected criteria, were chosen for fragmentation (see Materials and Methods section 2.6.8.). The mass spectrometric scan of the fragments leads to the analysis of the backbone sequence and identification. However, the initial MS scan is critical to SILAC success as this scan is used for quantification. The SILAC envelope patterns have a triplet motif which are used for quantification. Indeed, the SILAC envelope patterns are indicative of labelled peptides (fig 3.9.). The use of differentially labelled arginine and lysine made it possible to distinguish between peptides terminating in different amino acids which contributes to the ease with which the bio-informatic software can identify peptides. It is possible to determine if a peptide contains arginine or lysine merely by examining the initial MS scan (fig 3.9) without any further information of sequence. For each technical replicate all raw spectrometric

data files were analysed simultaneously using MaxQuant software. This allowed the software to generate protein ratios derived from all the available spectra.

A

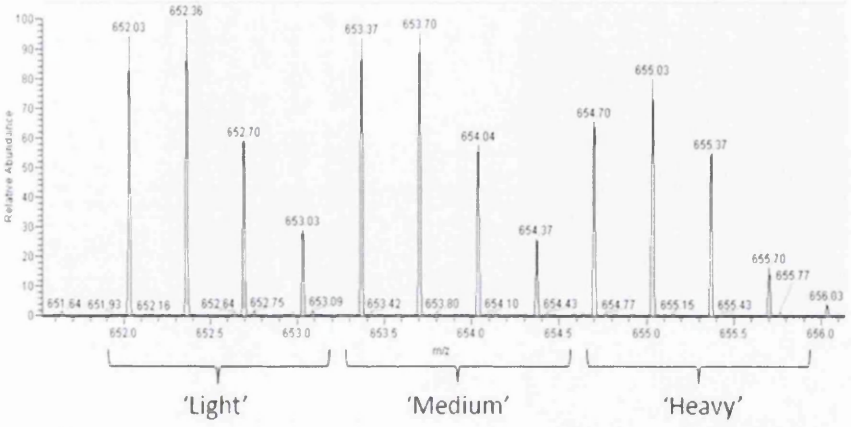

B

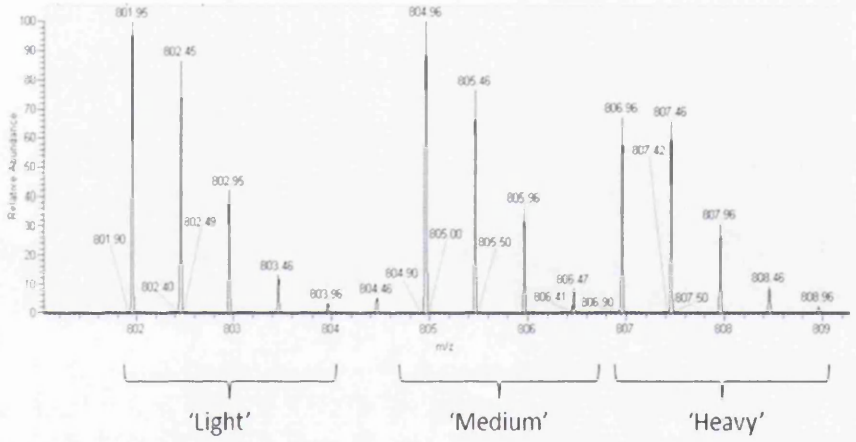

Figure 3.9. Example SILAC spectra for lysine and arginine containing peptides. The lysine containing spectra (A) is a triply charged peptide which, for the light peptide has a MW of 1953.057. It can be identified as containing lysine due to the mass shift between the SILAC states (medium +1.33m/z i.e. + 4Da; heavy = +2.66m/z i.e. +8Da). This peptide was identified by ms/ms fragmentation as having the sequence VAPDEHPILLTEAPLNPK from _-actin. The arginine containing spectra (B) is a doubly charged peptide which, for the light peptide, has a MW of 1601.889. It can be identified as containing lysine due to the mass shift between the SILAC states (medium +3m/z i.e. + 6Da; heavy = +5m/z i.e. +10Da). This peptide was identified by ms/ms fragmentation as having the sequence AAAAGALAPGPLPDLAAR from UDP-N-acetylhexosamine pyrophosphorylase-like protein 1.

3.2.6. Peptide and Protein Identifications

A large number of peptides were identified in each biological replicate and on each instrument though in these SILAC experiments the Orbitrap Velos instrument performed better than the LTQ-Orbitrap with regard to total number of peptide identifications. The LTQ Orbitrap identified in total 22,395 (10,495 unique), 38,458 (10,495 unique) and 75,322 (18,755 unique) peptides and the Orbitrap Velos 39,160 (18,671 unique), 52,249 (23,292 unique) and 105,952 (34,650 unique) peptides from each biological replicate respectively. This corresponds to an increase in the number of unique peptides identified on the Orbitrap Velos compared to the LTQ-Orbitrap of 77.9%,121.9% and 84.8% for each biological replicate. This increase in number of peptides identified corresponded to an increased number of proteins identified on the Orbitrap Velos instrument compared with the LTQ-Orbitrap (table 3.2). A large number of proteins were identified from the 3 biological replicates on both the LTQ-Orbitrap and the Orbitrap Velos instruments and, in each case, the majority of proteins were identified with ≥2 peptides (table 3.2). The Orbitrap Velos identified 1117, 971 and 1540 more proteins than the LTQ Orbitrap with ≥2 peptides in each of the 3 biological replicates respectively.

Table 3.2. Comparison of proteins identified between LTQ-Orbitrap and Orbitrap Velos instruments. The majority of proteins were identified with ≥2 peptides. A large proportion of proteins were identified with more peptides.

	Replicate	1		2		3	
	Instrument	LTQ-Orbitrap	Orbitrap Velos	LTQ-Orbitrap	Orbitrap Velos	LTQ-Orbitrap	Orbitrap Velos
Proteins identified with:-	≥ 1 peptide	2941	4211	3654	4672	3662	5219
	≥ 2 peptide	2039	3156	2739	3710	2879	4419
	≥ 3 peptide	1382	2334	2009	2844	2223	3622
	≥ 4 peptide	983	1763	1489	2223	1753	2985
	≥ 5 peptide	720	1392	1143	1755	1417	2501

There was a large overlap between the same lysates run on the two different instruments with the majority of leading proteins identified on both instruments. The number of proteins identified with ≥1 peptide from 3 biological replicates on both instruments was 2612 (59.0% of the 4425 proteins identified in total from both instruments), 3252 (64.7% of the 5025 proteins identified in total from both instruments) and 3098 (54.1% of the 5722 proteins identified in total from both instruments) respectively. The number of proteins identified with ≥2 peptides from the 3 biological replicates on both instruments was 1839 (54.8%), 2505 (63.5%) and 2473 (51.3%) respectively (fig 3.10.).

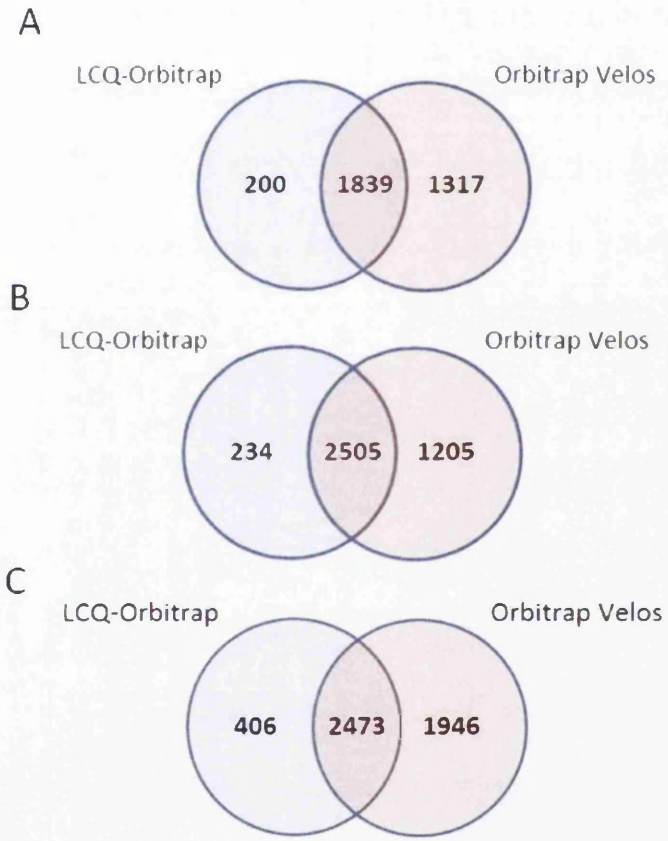

Figure 3.10. There was a large overlap between runs of the same biological replicate on different instruments (A, B, C); 90% (A), 91% (B) and 86% (C) of leading proteins identified on the LCQ-Orbitrap with ≥2 peptides were also identified on the Orbitrap Velos with ≥2 peptides

There was a large overlap between the three different biological replicates. The number of leading proteins identified and quantified with ≥1 peptide in all 3 biological replicates was 2096 proteins (44.3% total proteins) on the LTQ-Orbitrap. The number of proteins identified with ≥1 peptides in at least 2 of the biological replicates was unsurprisingly higher still; of the 4729 leading proteins identified 69.5% (3285) were identified in at least 2 biological replicates. In comparison, on the Orbitrap Velos 48.6% (3090) of the 6358 leading proteins identified with ≥1 peptide were observed in all 3 biological replicates. The number of leading proteins identified in at least 2 of the biological replicates with ≥1 peptide was 70.6% (4489). Therefore, these data demonstrate that the majority of proteins were quantified on at least 2 occasions from different biological replicates increasing the ease of discriminating between reproducible changes and rogue data points from a single biological sample.

However, the confidence in proteomic data is increased if multiple peptides are used for identification and quantification as relying on only 1 peptide can lead to error in identification and quantification due to error introduced by experimental variability or the software used during post-run analysis of the raw mass spectral data. The samples run on the LTQ-Orbitrap had 42.9% (1546) of the 3607 leading proteins identified with ≥2 peptides observed in all 3 biological replicates. The number of proteins identified with ≥2 peptides in at least 2 of the biological replicates was 69.4% (2504) of the total leading proteins identified with ≥2 peptides. In comparison, on the Orbitrap Velos 45.8% (2404) of the 5246 leading proteins identified with ≥2 peptides were observed in all 3 biological replicates (fig 3.11). The number of leading proteins identified in at least 2 of the biological replicates with ≥2 peptides was 69.3% (3635). It is clear, therefore, that the use of the SILAC proteomic methodology identified and quantified a large number of proteins suitable for further analysis. In addition, due to the large overlap between identifications from the three biological replicates, and the confidence inferred from multiple peptide protein identification these data are suitable for the analysis of up and down-regulation of protein as reproducible changes to the proteome should be apparent.

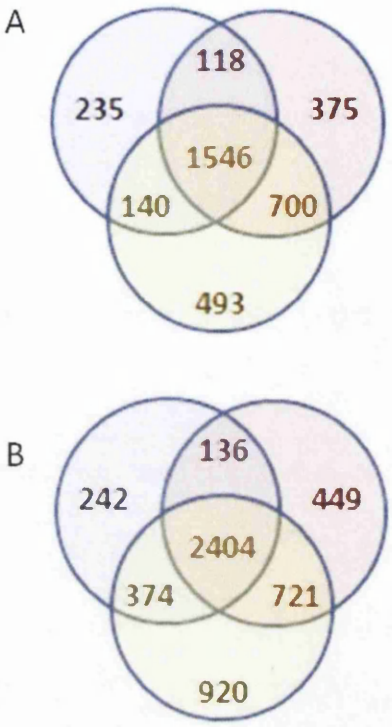

Figure 3.11. Overlap of leading proteins identified and quantified with ≥2 peptides using MaxQuant. A large overlap existed between 3 separate biological replicates run on a LTQ-Orbitrap (A) or an Orbitrap Velos instrument (B). 43% of proteins identified on the LTQ-Orbitrap and 46% of proteins identified on the Orbitrap Velos were present in all 3 replicates. 69% and 69% of proteins were identified in at least 2 replicates on the LTQ-Orbitrap and Orbitrap Velos instruments respectively.

3.2.7. Expression of Neurotrophins and Neuronal Markers in SN4741 Cells

The aim of the work is to elucidate the effect of 24(*S*),25-epoxycholesterol in neuronal development. A group of proteins with an established role in neuronal development are the neurotrophins (Hempstead 2006). Thus, the dataset was mined for the presence of the neurotrophins brain derived neurotrophic factor (BDNF), glial cell-derived neurotrophic factor (GDNF), ciliary neurotrophic factor (Cntf), neurotrophin 3 (Ntf3), neurotrophin 4 (Ntf4) and nerve growth factor (NGF). None of these neurotrophins were detected in the data set (table 3.3).

In addition, neuronal markers from different stages of neuronal development were present (table 3.3). Nestrin and SOX2 that are markers of neuronal progenitor cells were identified. Nestrin was down-regulated in some but not all of the biological replicates after treatment with 24(*S*),25-epoxycholesterol. Doublecortin a marker of early neuronal development was identified but another marker neurogenic differentiation 1 was not. The mature neuronal markers beta III tubulin (Tubb3) and microtubule-associated protein 2 (MAP2) were identified in all 3 biological replicates. Thus, a number of markers from different stages of neuronal development were identified although 24(*S*),25-epoxycholesterol had no reproducible effect on their expression.

No dopaminergic neuron markers were identified (table 3.3). However, it is important to note that a given protein may be expressed but not be present in the dataset due to the technicalities of proteomics. Low abundance proteins may not be identified. In addition, protein identification is reliant on the peptides generated by the action of trypsin. In this regard very short peptides do not furnish enough sequence information to allow confident identification from which protein they are derived. In addition, if a peptide is poorly ionised (e.g. due to a number of acidic amino acids) then it is unlikely to be detected.

Table 3.3. Neurotrophins and neuronal markers expressed in SN4741 cells identified in SILAC experiments. Normalised SILAC ratios shown are 24(*S*),25-epoxycholesterol:control. Neurotrophins (brain derived neurotrophic factor (BDNF), glial cell-derived neurotrophic factor (GDNF), ciliary neurotrophic factor (Cntf), neurotrophin 3 (Ntf3), neurotrophin 4 (Ntf4), nerve growth factor (NGF)) were not detected in any experiment. Markers of neuronal progenitor cells (Nestin (Nes), transcription factor SOX-2 (SOX2)) were detected. Early neuronal markers (doublecortin (DCX), neurogenic differentiation 1 (Neurod1). Mature neuronal markers (beta III tubulin (Tubb3), microtubule-associated protein 2 (MAP2)) were identified in all experiments, whereas (RNA binding protein fox-1 homolog 3 (Rbfox3; NeuN)) was not. Dopaminergic markers (GTP cyclohydrolase 1 (Gch1), aromatic L-amino acid decarboxylase (Ddc), tyrosine hydroxylase (Th) were not detected.

Biological Replicate	1		2		3	
Technical Replicate	1	2	1	2	1	2
Protein						
Bdnf	/	/	/	/	/	/
Gndf	/	/	/	/	/	/
Cntf	/	/	/	/	/	/
Ntf3	/	/	/	/	/	/
Ntf4	/	/	/	/	/	/
Ngf	/	/	/	/	/	/
Nes	0.535	0.665	0.786	0.771	0.868	0.916
Sox2	/	/	1.048	1.302	1.139	0.943
Dcx	/	/	0.927	0.865	/	1.151
Neurod1	/	/	/	/	/	/
Tubb3	1.117	1.226	0.957	1.015	0.888	0.798
Map2	1.086	0.990	0.951	0.783	0.831	/
Rbfox3	/	/	/	/	/	/
Gch1	/	/	/	/	/	/
Ddc	/	/	/	/	/	/
Th	/	/	/	/	/	/

3.2.8. Analysis of proteomic data

In each dataset the ratio of identified proteins had a normal distribution. The protein identification and quantification data generated from Maxquant was analysed to class proteins as 'no change', 'up-regulated' or 'down-regulated' using a previously published method (Graumann *et al.* 2008). The median was calculated and an increase or decrease the equivalent to 2 standards deviations (the arithmetic mean and standard deviation are not used in this method to prevent outliers having a pronounced effect) away from the median was classed as changed. Therefore, due to the use of the variation of the data in its calculation, the ratio between the heavy, medium and light SILAC states that serve as the boundary between 'no change' and 'up' or 'down-regulation' varied between datasets (table 3.4). This method identified a small portion of the total number of proteins as up- and down- regulated after treatment with 24(*S*),25-epoxycholesterol or GW3965 (table 3.4). The leading proteins identified as changed were then searched to determine reproducible trends in protein expression changes across the 6 datasets.

Table 3.4. Number of proteins identified as 'no change', 'up-regulated or 'down regulated' from each biological replicate on LTQ-Orbitrap or Orbitrap Velos instruments after treatment with 24(*S*),25-epoxycholesterol. The ratio cut-offs for what was classed as a change in protein expression (i.e. up or down regulation) are shown. Proteins were identified with ≥2 peptides.

Biological Replicate	1		2		3	
Instrument	LTQ-Orbitrap	Orbitrap Velos	LTQ-Orbitrap	Orbitrap Velos	LTQ-Orbitrap	Orbitrap Velos
Ratio Cut-off (up/down)	1.23/0.73	1.23/0.71	1.35/0.76	1.34/0.76	1.18/0.74	1.19/0.73
Up-regulated	78	158	116	195	227	233
No change	1855	2848	2534	3344	2471	3951
Down-regulated	106	150	89	171	181	235

In order to ensure no changes of interest were missed the proteomic datasets were also examined in detail by analysing every protein identified as up or down regulated to attempt to identify proteins of interest. In total, from all the biological and technical replicates, 1072 different proteins were identified as up–regulated in total and 864 proteins were identified as down-regulated (Appendix 1 and 2). No proteins were excluded from this analysis and therefore a large number of proteins were identified with only 1 peptide. For these proteins identified with 1 peptide there is the possibility of experimental error having a larger effect on the quantification. In addition, a number of proteins were only identified in only one biological replicate. For these proteins there is no contradictory data but conversely no validatory data. Therefore, it is important to recognise the limitations of these data however they could yield valuable information.

The proteins identified as up and down regulated (Appendix 1 and 2) were examined to determine which proteins had no contradictory data. In total, 229 proteins were classed as up-regulated and had no contradictory data (table 3.5) whereas 285 proteins were classed as down-regulated (table 3.6).

Table 3.5. Proteins identified as down-regulated. (Pep – Number of unique peptides, EC- SILAC ratio after treatment with 10μM 24(*S*),25-epoxycholesterol, GW - SILAC ratio after treatment with 1μM GW3965)

Biological Replicate			**1**						**2**						**3**					
Technical Replicate			**1**			**2**			**1**			**2**			**1**			**2**		
Protein Names	**Gene Names**	**Protein ID**	**Pep**	**EC**	**GW**	**Pep**	**EC**	**GW**	**Pep**	**EC**	**GW**	**Pep**	**EC**	**GW**	**Pep**	**EC**	**GW**	**Pep**	**EC**	**GW**
V-type proton ATPase subunit d 1	Atp6v0d1	IPI00313841	1	0.66	0.54	3	0.83	0.84	/			2	0.79	0.82	/			4	0.72	0.69
Intraflagellar transport protein 52 homolog	Ift52	IPI00459776	1	0.66	0.90	/			/			/			/			/		
Low-density lipoprotein receptor	Ldlr	IPI00312063	1	0.64	0.97	4	0.37	0.87	/			3	0.36	0.76	5	0.27	0.78	12	0.26	0.82
H-2 class I histocompatibility antigen, D-P alpha chain	H2-D1	IPI00126301	2	0.64	0.80	/			/			/			/			/		
Desmin	Des	IPI00130102	4	0.63	0.88	/			3	0.54	0.80	/			/			/		
AP-3 complex subunit delta-1	Ap3d1	IPI00117811	1	0.62	16.39	/			2	0.81	1.01	5	0.73	1.01	1	0.70	0.72	10	0.77	0.74
Acetyl-CoA acetyltransferase, cytosolic	Acat2	IPI00228253	5	0.62	1.35	6	0.62	1.05	7	0.53	0.97	8	0.55	0.97	9	0.63	1.03	12	0.64	1.10
Friend virus susceptibility protein 1	Fv1	IPI00137355	1	0.61	2.43	1	0.78	1.13	1	0.62	1.06	1	0.62	0.94	/			2	0.67	1.02
Retinol dehydrogenase 11	Rdh11	IPI00136098	1	0.61	1.09	2	0.64	0.95	1	0.79	1.04	2	0.74	0.88	/			4	0.60	1.07
Putative uncharacterized protein	Zbtb45	IPI00284393	1	0.61	0.72	/			/			/			/			/		
Mdm2-binding protein	Mtbp	IPI00330521	1	0.58	0.87	/			/			/			/			/		
Farnesyl pyrophosphate synthetase	Fdps	IPI00120457	5	0.51	1.08	8	0.55	1.07	7	0.53	1.02	9	0.52	1.03	12	0.51	1.07	14	0.54	1.06
Phosphomevalonate kinase	Pmvk	IPI00133709	1	0.50	1.22	1	0.48	0.94	1	0.54	1.20	/			/			1	0.76	1.22
WD repeat and SOF domain-containing protein 1	Wdsof1	IPI00129701	1	0.49	0.95	/			/			/			/			3	0.84	0.93
Kinetochore protein Spc24	Spc24	IPI00132177	1	0.48	0.78	1	0.67	1.03	/			/			/			2	0.82	0.99
Putative uncharacterized protein	Hsd17b7	IPI00474810	2	0.47	1.00	/			2	0.65	1.20	2	0.59	1.11	3	0.58	1.09	5	0.55	1.24
Sterol-4-alpha-carboxylate 3-dehydrogenase, decarboxylating	Nsdhl	IPI00128692	6	0.46	0.99	7	0.53	1.09	6	0.50	1.02	8	0.49	1.01	13	0.57	1.16	18	0.59	1.20
Protein C9orf140 homolog		IPI00462403	1	0.46		/			/			/			/			/		
Acyl-CoA synthetase short-chain family	Myh7b	IPI00752027	2	0.45	1.08	2	0.53	1.05	4	0.42	1.17	4	0.46	1.16	3	0.54	1.37	4	0.54	1.33

member 2																				
Lanosterol synthase	Lss	IPI00169958	4	0.43	1.06	7	0.40	1.07	3	0.44	1.05	6	0.52	1.03	6	0.50	1.10	9	0.51	1.24
Lanosterol 14-alpha demethylase	Cyp51a1	IPI00458711	3	0.42	1.02	5	0.42	1.02	3	0.26	0.93	3	0.24	1.01	6	0.29	1.02	9	0.29	1.01
Diphosphomevalonate decarboxylase	Mvd	IPI00319950	4	0.42	1.05	5	0.45	1.04	2	0.37	0.92	2	0.44	0.93	7	0.45	1.04	7	0.44	1.10
Isopentenyl-diphosphate Delta-isomerase 1	Idi1	IPI00849448	4	0.41	1.04	5	0.43	1.02	5	0.33	1.10	8	0.35	1.09	7	0.41	1.12	10	0.45	1.15
Beta-adrenergic receptor kinase 1	Adrbk1	IPI00320687	1	0.38	1.53	/			/			/			/			/		
Hydroxymethylglutaryl-CoA synthase, cytoplasmic	Hmgcs1	IPI00331707	11	0.32	1.02	11	0.30	0.99	5	0.17	0.97	8	0.24	1.06	10	0.20	1.08	13	0.22	1.08
UPF0470 protein C19orf51 homolog	6030429G01Rik	IPI00463244	1	0.31	0.99	1	0.36	1.20	/			/			/			/		
Alpha-actinin-3	Actn3	IPI00136701	5	0.09	0.85	/			/			/			/			/		
Novel protein	6230409E13Rik	IPI00750314	1	0.04	0.04	/			/			/			/			/		
Rotatin	Rttn	IPI00379692	1	0.02	0.09	/			/			/			/			/		
Cytochrome b-c1 complex subunit 6, mitochondrial	Uqcrh	IPI00129516	1	0.22	0.56	1	0.80	1.12	/			/			/			2	0.66	0.76
Amphoterin-induced protein 3	Amigo3	IPI00453796	1	0.02	0.02	/			/			/			/			/		
Ca(2+)-sensitive chloride channel 2	Clca2	IPI00914104	1	0.00	4.35	/			/			/			/			/		
NAD(P) transhydrogenase, mitochondrial	Nnt	IPI00874685	/			1	0.68	1.41	/			/			/			/		
Phosphatidylinositol-4,5-bisphosphate 3-kinase catalytic subunit beta isoform	Pik3cb	IPI00136110	/			1	0.68	0.70	/			/			/			/		
Mediator of RNA polymerase II transcription subunit 20	Med20	IPI00128183	/			1	0.68	1.06	/			/			/			/		
ATP-binding cassette sub-family G member 2	Abcg2	IPI00468691	/			1	0.68	1.05	1	0.84	0.85	/			1	0.79	0.68	2	0.66	0.50
Presenilin-1	Psen1	IPI00117124	/			1	0.67	0.83	/			/			/			/		
Golgin subfamily A member 7	Golga7	IPI00403747	/			1	0.67	1.10	/			/			/			/		
Cytochrome b5 type B	Cyb5b	IPI00315794	1	0.85	1.12	1	0.67	1.13	/			/			2	0.63	0.78	4	0.61	0.84
Lipin-1	Lpin1	IPI00308653	/			3	0.67	1.12	1	0.71	0.83	1	0.63	1.01	1	0.35	0.70	3	0.52	1.20

WD repeat-containing protein 3	Wdr3	IPI00221822	/			2	0.67	0.86	/			/			/			/		
CCR4-NOT transcription complex subunit 8	Cnot8	IPI00112188	/			1	0.67	0.61	/			/			/			/		
Heterogeneous nuclear ribonucleoproteins C1/C2	Hnrnpc	IPI00874321	/			10	0.66	0.94	/			/			/			11	0.71	0.88
Acetoacetyl-CoA synthetase	Aacs	IPI00135189	9	0.72	1.10	11	0.66	1.01	8	0.70	1.02	8	0.70	1.02	7	0.67	1.05	15	0.68	1.02
MHC class I-alpha	H2-D1	IPI00856542	/			3	0.66	1.08	/			/			/			/		
Mitofusin-2	Mfn2	IPI00312244	/			1	0.66	1.03	/			/			/			1	0.67	0.73
Putative S-adenosyl-L-methionine-dependent methyltransferase METT5D1	Mett5d1	IPI00187413	/			1	0.66	1.17	/			1	0.76	0.89	/			1	0.82	1.03
ATP-binding cassette sub-family B (MDR/TAP) member 11	Abcb11	IPI00828714	/			1	0.66	0.82	/			/			/			1	0.64	0.89
Sodium bicarbonate cotransporter 3	Slc4a7	IPI00664442	/			1	0.65	0.85	/			/			/			/		
Transcription elongation factor A protein 1	Tcea1	IPI00224168	/			9	0.65	0.71	/			/			/			/		
Protein tyrosine kinase 2 beta	Ptk2b	IPI00133132	/			2	0.65	1.05	/			/			/			/		
Anion exchange protein 3	Slc4a3	IPI00470963	/			1	0.65	0.80	/			/			/			/		
3-beta-hydroxysteroid-Delta(8),Delta(7)-isomerase	Ebp	IPI00137471	/			2	0.64	1.11	2	0.68	0.90	2	0.84	0.94	2	0.58	0.81	1	0.65	0.91
Zinc finger CCCH domain-containing protein 10	Zc3h10	IPI00153418	/			1	0.62	0.51	/			/			/			/		
Caveolin-1	Cav1	IPI00117829	/			1	0.61	0.76	2	0.67	0.75	3	0.63	0.85	2	0.60	0.57	3	0.60	0.65
Transcription factor SOX-13	Sox13	IPI00111162	/			1	0.61	0.09	/			/			/			/		
Kelch-like protein 13	Klhl13	IPI00776065	/			1	0.61	0.81	/			/			/			/		
UPF0404 protein C11orf59 homolog		IPI00315187	1	0.71	1.22	2	0.61	0.97	/			/			/			4	0.55	0.75
RNA/DNA-binding protein	Rnps1	IPI00122227	/			2	0.61	0.96	/			/			/			/		
Inhibitor of nuclear factor kappa-B kinase-interacting protein	Ikip	IPI00120310	/			3	0.61	0.97	/			/			/			/		
Tgm6 protein	Tgm6	IPI00468609	/			1	0.60	1.21	/			/			/			/		
Fumarylacetoacetate hydrolase domain-	Fahd2	IPI00121218	/			2	0.60	0.73	/			/			/			/		

containing protein 2A															
Transcription factor 4	Tcf4	IPI00400418	/	2	0.60	0.87	/	/			/	/			
MKIAA0429 protein	Mtss1	IPI00876025	/	1	0.60	1.19	/	/			/	/			
Transmembrane protein 97	Tmem97	IPI00122430	/	1	0.59	0.76	/	/			/	/			
Sodium/potassium-transporting ATPase subunit beta-1	Atp1b1	IPI00121550	/	1	0.57	0.90	/	/			/	2	0.62	0.80	
Ras-related protein Rap-2a	Rap2a	IPI00396701	/	1	0.56	1.06	/	/			/	4	0.61	1.06	
Inositol 1,4,5-trisphosphate 3-kinase B	Itpkb	IPI00263265	/	1	0.55	0.87	/	3	0.72	1.04	/	/			
3-keto-steroid reductase	Hsd17b7	IPI00316067	/	3	0.54	0.96	/	/			/	/			
MutS protein homolog 4	Msh4	IPI00118045	/	1	0.49	1.25	/	/			/	/			
Low density lipoprotein receptor adapter protein 1	Ldlrap1	IPI00454119	/	1	0.47	0.56	/	/			/	/			
Ubiquitin-conjugating enzyme E2 J1	Ube2j1	IPI00648249	/	1	0.47	0.92	/	/			/	1	0.75	0.82	
Protein FAM64A	Fam64a	IPI00221521	/	1	0.45	1.10	/	/			/	1	0.50	0.89	
Fibroblast growth factor 4	Fgf4	IPI00114434	/	1	0.44	0.13	/	/			/	/			
Acyl-CoA desaturase 2	Scd2	IPI00117142	/	2	0.41	1.42	/	/			/	/			
Serine/threonine-protein kinase Nek10	Nek10	IPI00844655	/	2	0.39	0.35	/	/			/	/			
Acyl-CoA-binding domain-containing protein 5	Acbd5	IPI00754110	/	1	0.33	1.11	/	/			/	1	0.64	0.90	
Matrix-remodeling-associated protein 8	Mxra8	IPI00310519	/	1	0.30	1.28	/	2	0.73	1.84	/	2	0.70	0.95	
Protein phosphatase PTC7 homolog	Pptc7	IPI00421081	/	1	0.29	0.43	/	/			/	/			
BMP-2-inducible protein kinase	Bmp2k	IPI00313513	/	1	0.28	0.69	/	/			/	/			
Rac/Cdc42 guanine nucleotide exchange factor (GEF) 6	Arhgef6	IPI00170221	/	2	0.26	1.16	/	/			/	/			
Leucine-zipper-like transcriptional regulator 1	Lztr1	IPI00272721	/	1	0.24	0.90	/	/			/	/			
Small proline-rich protein 3	Sprr3	IPI00114255	/	1	0.17	2.27	/	/			/	/			
Zinc finger protein RFP	Trim27	IPI00122244	/	1	0.12	1.08	/	/			/	/			
Putative uncharacterized protein	Srcap	IPI00620743	/	1	0.12	1.02	/	/			/	/			
Carbonic anhydrase 2	Ca2	IPI00121534	/	1	0.10	0.06	/	/			/	/			

FUN14 domain-containing protein 1	Fundc1	IPI00119124	/			/			1	0.73	0.73	1	0.66	0.82	1	0.73	0.81	2	0.81	0.85
ZAN	Zan	IPI00944148	/			/			1	0.73	0.93	/			/			/		
Pre-B-cell leukemia transcription factor-interacting protein 1	Pbxip1	IPI00153644	1	0.76	0.65	/			1	0.72	1.03	2	0.71	0.76	/			2	0.66	0.79
Cadherin 13, isoform CRA_a	Cdh13	IPI00775975	1	0.73	1.00	3	0.74	0.92	1	0.72	0.94	2	0.61	0.76	/			5	0.81	0.95
Mitochondrial carrier triple repeat 6	Mcart6	IPI00831068	/			/			1	0.70	0.10	/			/			/		
Sept5 protein	Sep-05	IPI00923056	/			/			1	0.70	1.31	3	0.73	1.19	4	0.81	1.10	/		
Talin-2	Tln2	IPI00421218	/			/			9	0.66	0.78	/			/			/		
UPF0577 protein KIAA1324	Kiaa1324	IPI00342908	/			/			1	0.65	0.84	1	0.61	0.81	/			/		
Protein AF-9	Mllt3	IPI00473183	/			/			1	0.65	1.10	/			/			/		
ELMO domain-containing protein 1	Elmod1	IPI00228907	/			/			1	0.64	0.86	/			/			/		
Cytochrome c oxidase subunit 6B1	Cox6b1	IPI00225390	/			/			1	0.59	0.72	1	0.62	0.75	2	0.48	0.65	/		
Mtch2 protein	Mtch2	IPI00807902	/			/			1	0.58	0.71	1	0.68	0.80	1	0.51	0.47	/		
Calcineurin binding protein 1	Cabin1	IPI00380107	/			/			1	0.56	0.85	1	0.65	0.79	1	0.64	0.91	1	0.59	0.84
Cornifin-A	Sprr1a	IPI00123458	3	0.80	0.98	6	0.73	0.96	8	0.55	0.91	7	0.59	0.91	8	0.70	0.87	10	0.72	0.93
Mevalonate kinase	Mvk	IPI00756996	3	0.74	1.02	5	0.69	0.98	4	0.53	0.90	6	0.55	0.89	4	0.60	1.02	10	0.58	0.99
B-cell receptor-associated protein 29	Bcap29	IPI00119980	/			/			1	0.50	0.82	/			/			/		
Retinoblastoma-like protein 1	Rbl1	IPI00137864	/			/			1	0.29	0.18	/			/			2	0.80	1.00
Synemin	Synm	IPI00469184	/			/			1	0.27	0.73	1	0.39	0.70	1	0.67	0.75	1	0.70	0.81
Tripartite motif-containing protein 75	Trim75	IPI00339960	/			/			1	0.26	0.22	/			/			/		
Brain-specific ankyrin-G	Ank3	IPI00623506	/			/			2	0.20	2.57	/			/			/		
Protein FAM63B	Fam63b	IPI00420796	1	0.82	1.01	1	0.69	0.75	1	0.19	0.45	1	0.79	0.64	2	0.68	0.90	3	0.60	0.97
		IPI00666788	/			/			1	0.09	0.16	1	0.02	0.00	/			/		
Putative uncharacterized protein	5830433M19Rik	IPI00954606	/			/			1	0.08	0.92	/			/			/		
Uncharacterized protein C20orf152 homolog	4921517L17Rik	IPI00828904	/			/			1	0.01	4.09	/			/			/		
Putative uncharacterized protein	Traf7	IPI00474945	/			/			1	0.01	0.01	1	0.02	0.01	/			/		
Myosin-IXa	Myo9a	IPI00928546	/			/			/			2	0.73	1.13	/			/		
Bardet-Biedl syndrome 7	Bbs7	IPI00648065	/			/			/			1	0.73	0.96	/			/		

DNA polymerase delta catalytic subunit	Pold1	IPI00323143	/	/	/	3	0.73	0.79	/			/		
DEP domain-containing protein 5	Depdc5	IPI00881403	/	/	/	1	0.72	0.92	/			/		
39S ribosomal protein L38, mitochondrial	Mrpl38	IPI00462925	/	/	/	1	0.72	0.76	/			/		
Sodium- and chloride-dependent glycine transporter 1	Glyt1	IPI00468633	/	/	/	1	0.71	0.85	/			1	0.46	0.87
Frizzled-1	Fzd1	IPI00118170	/	/	/	2	0.71	0.77	/			1	0.74	0.83
CCR4-associated factor 1	Caf1	IPI00121265	/	/	/	1	0.70	11.82	/			/		
PtdIns-4,5-P2 4-Ptase I	Tmem55b	IPI00356633	/	/	/	1	0.69	1.32	1	0.47	0.73	1	0.51	0.79
Protein tyrosine phosphatase, receptor type, D	Ptprd	IPI00608063	/	/	/	1	0.69	0.78	/			/		
Branched-chain acyl-CoA oxidase	Acox3	IPI00318108	/	/	/	11	0.68	0.90	/			/		
T-complex protein 11-like protein 1	Tcp11l1	IPI00225028	/	/	/	1	0.68	0.79	/			/		
SH3 domain-binding protein 2	3bp2	IPI00881074	/	/	/	2	0.68	1.20	/			/		
PDZ domain-containing protein GIPC3	Gipc3	IPI00154021	/	/	/	2	0.68	0.91	/			/		
Lysophospholipase-like protein 1	Lyplal1	IPI00153133	/	/	/	2	0.67	0.92	/			/		
Putative uncharacterized protein	Samhd1	IPI00653746	/	/	/	2	0.67	0.74	/			/		
Cytochrome c oxidase subunit 7A2, mitochondrial	Cox7a2	IPI00114377	/	/	/	1	0.66	0.68	/			1	0.44	0.46
Butyrate-induced protein 1	Ptplad1	IPI00322145	/	/	/	1	0.65	0.73	1	0.70	0.53	1	0.73	0.65
H-2 class I histocompatibility antigen, D-37 alpha chain	H2-T23	IPI00322542	/	/	/	2	0.65	3.65	/			/		
Fibulin-2	Fbln2	IPI00132067	/	/	/	1	0.64	0.92	/			/		
Putative uncharacterized protein	Crmp1	IPI00312527	/	/	/	3	0.64	0.86	/			4	0.72	0.72
MCG141096, isoform CRA_a	1700081L11Rik	IPI00649809	/	1	0.74 0.95	/	1	0.63	0.74	/		/		
Protein YIPF6	Yipf6	IPI00225621	/	/	/	1	0.62	0.96	/			/		
mTERF domain-containing protein 3, mitochondrial	Mterfd3	IPI00222753	/	/	/	2	0.62	1.04	/			/		
Cat eye syndrome critical region protein 5 homolog	Cecr5	IPI00314106	/	/	/	1	0.59	1.12	/			/		

CTP:phosphoethanolamine cytidylyltransferase	Pcyt2	IPI00311395	3	0.74	1.11	2	0.70	0.98	/	3	0.59	1.04	1	0.59	1.21	5	0.75	1.05
Putative uncharacterized protein	Cp	IPI00874570	/			/			/	3	0.58	0.78	/			/		
Angiomotin-like protein 1	Amotl1	IPI00669483	/			/			/	1	0.58	5.77	/			/		
Putative uncharacterized protein	Slc25a1	IPI00276926	/			/			/	1	0.58	0.65	/			1	0.40	0.54
Dynein, axonemal, heavy chain 9	Dnahc9	IPI00473970	/			/			/	1	0.57	0.37	/			/		
7-dehydrocholesterol reductase	Dhcr7	IPI00130988	/			/			/	1	0.56	0.92	/			/		
Rho GTPase-activating protein 6	Arhgap6	IPI00831349	/			/			/	2	0.56	0.12	/			/		
Mitochondrial fission regulator 1	Kiaa0009	IPI00162850	/			/			/	1	0.52	0.64	/			/		
Myosin-Id	Myo1d	IPI00408207	/			/			/	1	0.52	1.03	/			1	0.57	0.84
Anthrax toxin receptor 1	Antxr1	IPI00318636	/			/			/	1	0.52	0.70	/			/		
Mtm1 protein	Mtm1	IPI00944189	/			/			/	1	0.51	1.00	/			/		
2-hydroxyacyl-CoA lyase 1	Hacl1	IPI00316314	/			/			/	3	0.49	0.86	1	0.70	0.84	3	0.73	1.04
Delta(6) fatty acid desaturase	Fads2	IPI00129362	/			/			/	1	0.48	0.96	/			4	0.63	0.95
Glyoxylate reductase 1 homolog	Glyr1	IPI00817029	/			/			/	1	0.48	0.83	/			/		
Uncharacterized protein KIAA0819	Kiaa0819	IPI00858146	/			/			/	2	0.47	1.28	/			/		
67-11-3 protein	Lpts	IPI00153088	/			/			/	2	0.45	0.42	/			2	0.80	1.10
StAR-related lipid transfer protein 4	Stard4	IPI00320022	/			/			/	1	0.39	1.06	/			2	0.34	1.07
C-4 methylsterol oxidase	Sc4mol	IPI00133526	/			/			/	1	0.31	1.22	/			/		
Complex III subunit 8	Uqcrq	IPI00224210	/			/			/	1	0.22	0.95	1	0.45	0.85	/		
Protease, serine, 3	Prss3	IPI00130391	/			/			/	1	0.22	26.52	/			/		
High affinity cAMP-specific 3',5'-cyclic phosphodiesterase 7A	Pde7a	IPI00230552	/			/			/	1	0.21	0.07	/			/		
Probable G-protein coupled receptor 158	Gpr158	IPI00465871	/			/			/	1	0.20	0.22	/			/		
Arylsulfatase A	Arsa	IPI00118039	/			/			/	1	0.16	0.70	/			/		
Putative uncharacterized protein	Fdft1	IPI00338068	/			/			/	1	0.16	1.54	/			2	0.19	1.64
Zinc finger protein 182	Zfp182	IPI00775902	/			/			/	1	0.12	6.37	/			/		
Novel KRAB box and zinc finger, C2H2 type domain containing protein	OTTMUSG00000016626	IPI00850019	/			/			/	2	0.08	0.01	/			/		

Regulator of sex-limitation 2	AI929863	IPI00329967	/	/		/	1	0.06	3.98	/			/		
GABA-A receptor-associated membrane protein 1	Godz	IPI00172092	/	/		/	1	0.03	0.01	/			/		
Interleukin-4-induced protein 1	Fig1	IPI00759856	/	/		/	1	0.03	0.02	/			/		
Putative uncharacterized protein	Tspan15	IPI00775936	/	/		/	1	0.02	3.62	/			/		
Bcl-2 homologous antagonist/killer	Bak1	IPI00309183	/	/		/	/			1	0.69	0.80	1	0.69	0.80
Cytochrome c oxidase subunit 2	Mtco2	IPI00131176	/	/		/	1	0.78	0.74	1	0.68	0.48	2	0.62	0.52
Zfp597 protein	Zfp597	IPI00129554	/	/		/	/			1	0.67	0.73	/		
Probable cation-transporting ATPase 13A3	Atp13a3	IPI00850873	/	/		/	/			1	0.67	0.64	/		
H-2 class I histocompatibility antigen, K-W28 alpha chain	H2-K1	IPI00126458	/	/		/	/			2	0.64	1.03	/		
Ectonucleotide pyrophosphatase/phosphodiesterase family member 5	Enpp5	IPI00111163	/	/		/	/			1	0.64	0.82	/		
Tetratricopeptide repeat protein 35	Ttc35	IPI00133612	/	/		/	/			1	0.62	0.81	2	0.65	0.75
Carbonyl reductase family member 4	Cbr4	IPI00127227	/	/		/	/			1	0.56	0.55	/		
Mitochondrial inner membrane protein	Immt	IPI00381412	/	/		/	/			3	0.56	0.66	/		
Glucose-6-phosphate 1-dehydrogenase 2	G6pd2	IPI00228867	/	/		/	/			4	0.55	0.92	/		
Phosphatidylinositol-4-phosphate 3-kinase C2 domain-containing subunit gamma	Pik3c2g	IPI00115695	/	/		/	/			1	0.54	0.89	/		
Band 4.1-like protein 5	Epb41l5	IPI00469962	/	3	0.79	0.84	/	/		2	0.53	0.84	4	0.66	0.92
Ankycorbin	Rai14	IPI00453820	/	/		/	/			1	0.52	0.76	4	0.60	0.73
TBC1 domain family member 8	Tbc1d8	IPI00130023	/	/		/	/			2	0.35	185.8	/		
Transcription factor RFX3	Rfx3	IPI00121582	/	/		/	/			1	0.34	43.26	/		
Soluble calcium-activated nucleotidase 1	Cant1	IPI00113039	/	/		/	/			1	0.30	1.07	/		
Putative uncharacterized protein	Card6	IPI00351041	/	/		/	/			1	0.22	0.28	/		
		IPI00947579	/	/		/	/			2	0.18	0.98	/		

Putative uncharacterized protein	Fam184a	IPI00665988	/			/	/	/	1	0.09	0.01	/	
Melanocortin receptor 4	Mc4r	IPI00111301	/			/	/	/	1	0.09	0.04	/	
Ras-related protein Rab-39A	Rab39	IPI00221836	/			/	/	/	2	0.02	0.00	/	
MCG7443, isoform CRA_a	Gal3st4	IPI00626253	/			/	/	/	1	0.01	0.00	/	
Kinocilin	Kncn	IPI00656192	/			/	/	/	1	0.01	0.09	/	
Cyclin-D1-binding protein 1	Ccndbp1	IPI00653166	/			/	/	/	/			1	0.70	0.91
Nucleolar protein 14	Nop14	IPI00353010	/			/	/	/	/			2	0.70	0.89
Disrupted in renal carcinoma protein 2 homolog	Dirc2	IPI00221417	/			/	/	/	/			1	0.70	0.98
P2X purinoceptor	P2rx4	IPI00471089	/			/	/	/	/			3	0.70	0.52
Protein zyg-11 homolog A	Zyg11a	IPI00848714	/			/	/	/	/			2	0.70	2.88
AFG3-like protein 1	Afg3l1	IPI00468514	/			/	/	/	/			2	0.70	0.90
UPF0672 protein C3orf58 homolog	1190002N15Rik	IPI00875583	/			/	/	/	/			2	0.69	0.97
Anoctamin-10	Ano10	IPI00848909	/			/	/	/	/			1	0.69	0.57
Armadillo repeat-containing protein 8	Armc8	IPI00844808	/			/	/	/	/			4	0.69	1.22
Electrogenic sodium bicarbonate cotransporter 1	Slc4a4	IPI00314749	/			/	/	/	/			2	0.68	0.42
Bullous pemphigoid antigen 1, isoforms 6/7	Dst	IPI00623531	/			/	/	/	/			5	0.68	0.96
Vomeronasal 1 receptor, H4	V1rh4	IPI00153507	/			/	/	/	/			1	0.68	6.68
Endogenous murine leukemia virus	EG622147	IPI00854954	/			/	/	/	/			2	0.68	1.08
		IPI00807763	/			/	/	/	/			2	0.67	3.58
Solute carrier family 23 member 2	Slc23a2	IPI00165688	/			/	/	/	/			3	0.67	0.90
Stromal antigen 1	Stag1	IPI00466867	/			/	/	/	/			8	0.67	0.86
BAT2 domain-containing protein 1	Bat2d1	IPI00659535	/			/	/	/	/			29	0.67	1.19
Nucleolar protein 11	Nol11	IPI00153791	1	0.82	0.84	/	/	/	/			2	0.67	0.81
Gpsn2 protein	Gpsn2	IPI00875068	/			/	/	/	/			2	0.67	0.85
Geminin	Gmnn	IPI00131716	/			/	/	/	/			1	0.66	0.68
Conserved oligomeric Golgi complex	Cog1	IPI00129529	/			/	/	/	/			2	0.66	0.82

subunit 1											
Probable cation-transporting ATPase 13A1	Atp13a1	IPI00109891	/	/		/	/	/	2	0.66	0.98
Putative uncharacterized protein	Brwd1	IPI00654074	/	/		/	/	/	1	0.66	0.81
Sphingolipid delta(4)-desaturase DES1	Degs1	IPI00113731	/	/		/	/	/	2	0.65	0.61
Ferric-chelate reductase 1	FRRS1	IPI00322418	/	/		/	/	/	1	0.65	0.42
Putative sodium-coupled neutral amino acid transporter 10	Slc38a10	IPI00228647	/	/		/	/	/	1	0.65	0.42
Coiled-coil domain-containing protein 109A	Ccdc109a	IPI00655156	/	/		/	/	/	3	0.65	0.80
Melanoma antigen, family E, 1	Magee1	IPI00453948	/	/		/	/	/	1	0.65	0.88
Protein cornichon homolog 4	Cnih4	IPI00109447	/	/		/	/	/	1	0.64	0.73
Signal peptidase complex catalytic subunit SEC11A	Sec11a	IPI00894649	/	/		/	/	/	1	0.64	0.78
Adrenodoxin-like protein, mitochondrial	Fdx1l	IPI00132087	/	/		/	/	/	1	0.64	0.86
Patched domain-containing protein 2	Ptchd2	IPI00464195	/	/		/	/	/	1	0.64	0.85
UPF0539 protein C7orf59 homolog		IPI00229218	/	/		/	/	/	1	0.63	0.69
Calcium-binding protein p22	Chp	IPI00665857	/	/		/	/	/	2	0.63	0.76
Rab11 family-interacting protein 5	Rab11fip5	IPI00230238	/	/		/	/	/	6	0.63	1.31
F-box/LRR-repeat protein 8	Fbxl8	IPI00319775	/	1	0.77 0.82	/	/	/	1	0.62	1.19
WD repeat-containing protein 43	Wdr43	IPI00849919	/	/		/	/	/	4	0.62	0.79
Sterol regulatory element-binding protein cleavage-activating protein	Scap	IPI00856221	/	/		/	/	/	2	0.62	0.70
Transmembrane and coiled-coil domain-containing protein C6orf129 homolog		IPI00869365	/	/		/	/	/	1	0.62	1.87
		IPI00886331	/	/		/	/	/	2	0.62	0.54
Plasma membrane calcium-transporting ATPase 2	Atp2b2	IPI00831180	/	/		/	/	/	4	0.62	0.77
Putative uncharacterized protein	Gmeb1	IPI00123517	/	/		/	/	/	1	0.62	1.03
Translocon-associated protein subunit	Ssr4	IPI00122346	/	2	0.77 1.01	/	/	/	4	0.61	0.80

delta												
TLD domain-containing protein KIAA1609	Kiaa1609	IPI00157480	/	/	/	1	0.78	0.95	/	2	0.60	1.11
Syntaxin-2	Stx2	IPI00117112	/	/	/	/			/	2	0.60	0.79
Exoc6b protein	Exoc6b	IPI00224528	/	/	/	/			/	2	0.59	0.77
MOSC domain-containing protein 2, mitochondrial	Mosc2	IPI00123276	/	/	/	/			/	4	0.59	0.58
Leucine-rich repeat-containing protein 58	Lrrc58	IPI00751601	/	/	/	/			/	1	0.59	1.13
Proviral envelope protein	D17H6S56E-5	IPI00283900	/	/	/	/			/	2	0.58	0.71
Receptor tyrosine-protein kinase erbB-2	Erbb2	IPI00626433	/	/	/	/			/	1	0.58	0.70
Enhancer of polycomb homolog 2	Epc2	IPI00223821	/	/	/	/			/	1	0.57	0.50
Sucrase-isomaltase	2010204N08Rik	IPI00756791	/	/	/	/			/	2	0.56	1.89
Protein XRP2	Rp2	IPI00222852	/	/	/	/			/	1	0.56	0.67
Protein KRI1 homolog	Kri1	IPI00311761	/	/	/	/			/	1	0.55	0.66
Putative uncharacterized protein	Spcs3	IPI00420727	/	/	/	/			/	1	0.54	1.09
NADH dehydrogenase [ubiquinone] 1 alpha subcomplex subunit 11	Ndufa11	IPI00318645	/	/	/	/			/	1	0.52	1.13
Osteopetrosis-associated transmembrane protein 1	Ostm1	IPI00221706	/	/	/	/			/	2	0.52	0.80
Leucine-rich repeat serine/threonine-protein kinase 1	Lrrk1	IPI00756788	/	/	/	/			/	1	0.51	6.10
Interferon-activable protein 202	Ifi202	IPI00126725	/	/	/	/			/	2	0.51	0.25
Bcl10-interacting CARD protein	1110007C09Rik	IPI00315974	/	/	/	/			/	1	0.50	0.96
Equilibrative nucleoside transporter 3	Slc29a3	IPI00321909	/	/	/	/			/	1	0.50	0.78
N(6)-adenine-specific DNA methyltransferase 2	N6amt2	IPI00132944	/	/	/	/			/	1	0.50	0.78
Translocon-associated protein subunit gamma	Ssr3	IPI00120826	/	/	/	/			/	1	0.49	0.76

Collagen alpha-1(II) chain	Col2a1	IPI00828653	/	/	/	/		/	2	0.47	1.12
Envelope polyprotein	EG667538	IPI00845826	/	/	/	/		/	6	0.47	0.68
Mitochondrial carrier homolog 2	Mtch2	IPI00132039	/	/	/	/		/	4	0.46	0.44
Glycerol kinase	Gk	IPI00404687	/	/	/	/		/	1	0.46	1.71
Mitochondrial 2-oxoglutarate/malate carrier protein	Slc25a11	IPI00230754	/	/	/	/		/	2	0.45	0.61
Fibronectin type-III domain-containing protein C4orf31 homolog		IPI00330474	/	/	/	/		/	1	0.45	0.56
ORM1-like protein 2	Ormdl2	IPI00133384	/	/	/	1	0.82 1.07	/	1	0.45	1.31
snRNA-activating protein complex subunit 1	Snapc1	IPI00169634	/	/	/	/		/	1	0.45	0.97
Probable helicase with zinc finger domain	Helz	IPI00453654	/	/	/	/		/	1	0.45	0.30
Bromodomain-containing protein 8	Brd8	IPI00153722	/	/	/	/		/	2	0.45	1.12
		IPI00380986	/	/	/	/		/	2	0.43	0.12
Integrin beta-7	Itgb7	IPI00110508	/	/	/	/		/	1	0.42	0.79
THAP domain-containing protein 2	Thap2	IPI00135144	/	/	/	/		/	1	0.39	1.97
Family with sequence similarity 55, member B	4432416J03Rik	IPI00881975	/	/	/	/		/	1	0.39	0.21
Transcobalamin-2	Tcn2	IPI00136556	/	/	/	/		/	1	0.38	0.36
Zinc finger protein 541	Znf541	IPI00758325	/	/	/	/		/	1	0.28	0.38
		IPI00849452	/	/	/	/		/	3	0.27	0.21
Nebulin-related-anchoring protein	Nrap	IPI00135182	/	/	/	/		/	1	0.22	3.30
Zinc finger protein 536	Znf536	IPI00377726	/	/	/	/		/	2	0.20	0.14
NACHT-, LRR-, and PYD-containing protein 1 paralog c	Nlrp1c	IPI00665815	/	/	/	/		/	1	0.19	0.13
Zinc finger protein 397 opposite strand	Zfp397os	IPI00876362	/	/	/	/		/	1	0.18	0.96
		IPI00849706	/	/	/	/		/	3	0.17	0.39
Grifin	Grifin	IPI00134234	/	/	/	/		/	1	0.15	1.00
Sperm motility kinase 3	Smok3a	IPI00136957	/	/	/	/		/	1	0.11	0.29

Ankyrin repeat domain-containing protein 37	Ankrd37	IPI00229712	/	/	/	/	/	1	0.09	0.07
Ribonuclease H1	Rnaseh1	IPI00117308	/	/	/	/	/	1	0.08	0.17
Ig kappa chain V-V region HP R16.7		IPI00464383	/	/	/	/	/	1	0.06	0.23
Reck protein	Reck	IPI00890886	/	/	/	/	/	1	0.06	2.07
Voltage-dependent N-type calcium channel subunit alpha-1B	Cacna1b	IPI00466672	/	/	/	/	/	1	0.03	0.21
Tnik protein	Tnik	IPI00662721	/	/	/	/	/	1	0.03	0.03
		IPI00466185	/	/	/	/	/	10	0.03	0.02
Putative uncharacterized protein	Zbed4	IPI00848479	/	/	/	/	/	1	0.02	0.03
Zinc phosphodiesterase ELAC protein 1	Elac1	IPI00331197	/	/	/	/	/	1	0.01	0.07

Table 3.6. Proteins identified as up-regulated (Pep – Number of unique peptides, EC- SILAC ratio after treatment with 10μM 24(*S*),25-epoxycholesterol, GW - SILAC ratio after treatment with 1μM GW3965)

Biological Replicate			**1**						**2**						**3**					
Technical Replicate			**1**			**2**			**1**			**2**			**1**			**2**		
Protein Names	**Gene Names**	**Protein ID**	**Pep**	**EC**	**GW**	**Pep**	**EC**	**GW**	**Pep**	**EC**	**GW**	**Pep**	**EC**	**GW**	**Pep**	**EC**	**GW**	**Pep**	**EC**	**GW**
Cohesin subunit SA-1	Stag1	IPI00135921	1	23.72		3	22.64	0.80	/			/			/			/		
ATPase, Na+/K+ transporting, alpha 3 polypeptide	Atp1a3	IPI00752412	4	14.87	5.16	/			/			/			7	1.35	1.43	/		
Putative uncharacterized protein	EG641366	IPI00461390	2	9.41	1.26	/			/			/			/			/		
FRAS1-related extracellular matrix protein 2	Frem2	IPI00553703	1	7.08	13.23	/			/			/			/			/		
Aromatic-preferring amino acid transporter	Slc7a15	IPI00314366	1	3.30	0.53	/			/			/			/			/		
Putative uncharacterized protein	ENSMUSG0000 0053526	IPI00403867	1	2.33	13.72	/			/			/			/			/		
Putative uncharacterized protein	Khsrp	IPI00229109	1	1.98	3.21	/			/			/			/			/		
Putative uncharacterized protein	4933416I08Rik	IPI00136529	1	1.70	0.99	/			/			/			/			/		
Caprin-2	Caprin2	IPI00856547	1	1.64	0.77	/			/			/			/			/		
Aldehyde dehydrogenase family 3, subfamily A1	Aldh3a1	IPI00890112	5	1.40	1.31	7	1.27	1.22	6	1.86	1.23	7	1.76	1.23	5	1.51	1.22	11	1.58	1.21
Digestive organ expansion factor homolog	Def	IPI00225214	1	1.35	1.08	1	1.29	1.17	/			/			/			2	1.17	0.92
FERM domain-containing protein 4A	Frmd4a	IPI00222107	1	1.31	0.93	/			/			1	1.18	0.94	/			/		
Prolyl endopeptidase-like	Prepl	IPI00652834	3	1.26	1.02	/			/			/			/			/		
Putative uncharacterized protein	ENSMUSG0000 0079623	IPI00652501	/			1	19.78	63.89	/			/			/			1	20.75	1.11
ATP-binding cassette, sub-family A (ABC1), member 1	Abca1	IPI00889843	/			1	13.68	9.71	/			7	10.92	4.72	4	9.71	5.34	10	6.00	2.48

Activin receptor type-1	Acvr1	IPI00409269	/			1	11.83	0.91	/			/			/			/		
Integrin alpha 9 protein	Itga9	IPI00130117	/			1	8.40	6.34	/			/			/			/		
RNA-binding protein 40	Rnpc3	IPI00831482	/			1	7.46	9.61	/			/			/			/		
		IPI00890274	/			1	6.72	6.97	/			/			/			/		
Ankyrin repeat and BTB/POZ domain-containing protein 2	Abtb2	IPI00349814	/			1	2.63	5.20	/			/			/			/		
Ovarian cancer-associated gene 2 protein homolog	Ovca2	IPI00110207	/			1	2.30	0.77	/			/			/			/		
Tubulin polyglutamylase TTLL7	Ttll7	IPI00760054	/			1	2.22	1.00	/			/			/			/		
Nucleolar protein 4	Nol4	IPI00410916	/			1	2.17	2.16	/			/			/			/		
Tyrosine-protein phosphatase non-receptor type 6	Ptpn6	IPI00225419	/			1	2.17	0.74	/			/			/			/		
40S ribosomal protein S30	Fau	IPI00849113	/			1	1.83	1.62	/			/			2	1.40	0.88	2	1.36	1.03
Dedicator of cytokinesis protein 2	Dock2	IPI00117274	/			1	1.62	13.32	/			/			/			/		
AI607873 protein	AI607873	IPI00848965	/			3	1.57	1.21	/			/			/			/		
F-box only protein 9	Fbxo9	IPI00474493	/			1	1.51	1.13	/			/			/			/		
Transcription factor E2F1	E2f1	IPI00338528	/			1	1.50	1.00	/			/			/			/		
Glutathione peroxidase 1	Gpx1	IPI00319652	/			1	1.49	1.24	/			/			/			/		
ATPase family AAA domain-containing protein 5	Atad5	IPI00408664	/			1	1.45	1.03	/			/			/			/		
1-phosphatidylinositol-4,5-bisphosphate phosphodiesterase gamma-2	Plcg2	IPI00229848	/			1	1.42	0.91	/			/			/			/		
Sulfiredoxin 1 homolog (S. cerevisiae)	Srxn1	IPI00112189	/			1	1.42	1.39	/			3	1.61	1.21	/			1	1.40	0.90
Peroxisomal coenzyme A diphosphatase NUDT7	Nudt7	IPI00119755	/			1	1.39	1.15	/			/			/			/		
ATP-binding cassette sub-family A member 7	Abca7	IPI00125970	2	1.12	0.85	2	1.39	1.09	2	1.30	1.06	3	1.57	0.96	3	1.25	0.85	4	1.40	0.93
Dual specificity protein phosphatase 19	Dusp19	IPI00463211	/			1	1.38	0.93	/			/			/			/		
Zinc finger FYVE domain-containing protein 19	Zfyve19	IPI00119998	1	1.23	0.90	1	1.37	0.98	/			/			/			/		

Coiled-coil domain-containing protein 117	Ccdc117	IPI00321929	/			1	1.37	0.77	/			/			/			/		
Thioredoxin domain-containing protein 11	Txndc11	IPI00170006	/			1	1.35	0.84	/			/			/			/		
Molybdenum cofactor synthesis protein 2A	Mocs2	IPI00130416	/			1	1.34	0.98	/			/			/			/		
Uncharacterized protein C4orf21 homolog	4930422G04Rik	IPI00754519	/			1	1.34	0.91	/			/			/			/		
Retinoic acid receptor RXR-alpha	Rxra	IPI00849526	/			1	1.32	1.16	/			/			/			/		
CDGSH iron sulfur domain-containing protein 3, mitochondrial	Cisd3	IPI00649725	/			1	1.32	1.19	/			/			/			/		
Expressed sequence AU019823	AU019823	IPI00417063	/			1	1.31	1.21	/			/			/			/		
Golgi apparatus protein 1	Glg1	IPI00122399	3	1.18	0.91	8	1.31	0.98	5	1.37	0.87	7	1.29	0.87	10	1.51	1.06	22	1.50	1.04
Tropomyosin beta chain	Tpm2	IPI00123319	/			9	1.31	2.07	/			/			/			/		
Protein YIF1A	Yif1a	IPI00128941	/			1	1.31	1.22	/			/			/			/		
Protein KIAA0664	Kiaa0664	IPI00462594	/			8	1.31	1.19	/			/			/			/		
45 kDa calcium-binding protein	Sdf4	IPI00117754	/			1	1.30	1.12	/			/			/			/		
		IPI00808297	/			1	1.30	0.82	/			/			/			/		
DNA (cytosine-5)-methyltransferase 3A	Dnmt3a	IPI00172129	/			2	1.30	1.09	/			/			/			/		
Neuron navigator 1	Nav1	IPI00229599	/			1	1.30	1.07	/			/			/			/		
Oncoprotein-induced transcript 3 protein	Oit3	IPI00453489	/			1	1.29	1.81	/			/			/			/		
LIM domain-binding protein 3	Ldb3	IPI00323030	/			1	1.28	1.30	/			/			/			/		
Dynamin-1	Dnm1	IPI00272878	/			3	1.28	1.29	/			/			/			/		
Collagen type IV alpha-3-binding protein	Col4a3bp	IPI00111167	/			3	1.28	1.08	3	1.42	1.34	4	1.52	1.05	4	1.58	1.15	4	1.46	1.05
tRNA guanosine-2'-O-methyltransferase TRM13 homolog	Ccdc76	IPI00378506	/			1	1.27	0.87	/			/			/			/		
E3 ubiquitin-protein ligase MIB1	Mib1	IPI00330112	1	1.25	1.03	1	1.26	1.23	/			/			/			/		
Epidermal growth factor-containing fibulin-like extracellular matrix protein 1	Efemp1	IPI00515343	/			1	1.26	1.25	/			4	1.44	1.44	/			/		

Mediator of RNA polymerase II transcription subunit 24	Med24	IPI00857417	/	1	1.26	0.97	/			/			/			/			
Mannan-binding lectin serine protease 1	Masp1	IPI00475209	/	1	1.25	0.85	/			/			/			/			
MKIAA0628 protein	Zfp623	IPI00111118	/	/			1	34.11	6.69	/			/			/			
L(3)mbt-like (Drosophila)	L3mbtl	IPI00457726	/	/			1	13.29	91.27	/			/			/			
Ral GTPase-activating protein subunit alpha-1	Ralgapa1	IPI00460042	/	/			1	7.94	6.75	2	3.23	1.29	1	1.85	0.63	/			
Cingulin	Cgn	IPI00757790	/	/			1	4.04	1.14	/			/			/			
Putative uncharacterized protein	Spp1	IPI00625970	/	/			2	2.27	0.91	1	2.09	0.85	/			2	1.72	0.90	
Transcription factor E2F7	E2f7	IPI00420139	/	/			1	2.23	1.48	/			/			/			
Glutathione S-transferase A4	Gsta4	IPI00323911	/	/			1	2.17	1.48	2	2.02	1.35	2	1.55	1.07	5	1.48	1.03	
Aldehyde dehydrogenase, dimeric NADP-preferring	Aldh3a1	IPI00111222	/	/			5	2.04	1.26	7	1.76	1.26	5	1.84	1.28	/			
Bifunctional methylenetetrahydrofolate dehydrogenase/cyclohydrolase, mitochondrial	Mthfd2	IPI00109824	/	/			1	1.80	1.41	2	1.70	1.37	/			/			
Constitutive coactivator of PPAR-gamma-like protein 2	Fam120c	IPI00416125	/	/			2	1.75	0.11	/			/			/			
Fanconi anemia group I protein homolog	Fanci	IPI00225412	/	1	1.24	1.11	1	1.71	1.07	/			/			/			
CTD small phosphatase-like protein 2	Ctdspl2	IPI00454047	/	/			4	1.57	1.15	2	1.60	0.93	/			/			
Ankyrin repeat and SOCS box protein 6	Asb6	IPI00131423	/	/			1	1.56	1.21	/			/			/			
Pyridoxal-dependent decarboxylase domain-containing protein 1	Pdxdc1	IPI00336503	/	/			7	1.56	0.85	/			14	1.35	1.09	18	1.27	1.04	
FK506 binding protein 10	Fkbp10	IPI00944194	/	/			5	1.53	1.07	5	1.32	1.00	5	1.74	1.11	/			
Butyrate response factor 2	Zfp36l2	IPI00138319	/	/			1	1.53	1.07	/			/			/			
		IPI00622024	/	/			1	1.53	1.13	/			/			/			
Coiled-coil-helix-coiled-coil-helix domain-containing protein 6	Chchd6	IPI00313390	/	/			1	1.50	0.78	1	1.46	7.79	/			/			
Zfp384 protein	Zfp384	IPI00555146	/	/			1	1.50	0.89	/			/			/			
Sperm-associated antigen 5	Spag5	IPI00380243	/	/			1	1.49	1.04	1	1.76	1.08	/			/			

Leucine carboxyl methyltransferase 2	Lcmt2	IPI00914155	/			/			1	1.48	1.45	/			/			/		
Putative uncharacterized protein	Pfkp	IPI00927975	/			/			5	1.44	1.65	5	1.34	1.23	7	1.20	1.28	/		
Putative uncharacterized protein	Bnip2	IPI00473381	/			/			1	1.42	2.39	/			/			/		
		IPI00850044	/			/			/			1	61.97	1.31	/			/		
BTB/POZ domain-containing protein 6	Btbd6	IPI00110006	/			/			/			1	39.80	10.60	/			/		
FtsJ methyltransferase domain-containing protein 1	Ftsjd1	IPI00331208	/			/			/			1	13.01	4.49	/			/		
Connecdenn	Dennd1a	IPI00322415	/			/			/			1	5.62	0.98	/			/		
GRB2-associated binder 1	Gab1	IPI00406794	/			/			/			1	4.74	1.34	/			/		
UPF0461 protein C5orf24 homolog		IPI00330644	/			/			1	1.22	0.87	2	3.70	0.61	1	3.46	0.87	3	3.92	0.95
Putative uncharacterized protein	B930095I24Rik	IPI00405150	/			/			/			1	3.50	32.11	/			/		
Chromodomain helicase DNA binding protein 6	Chd6	IPI00457724	/			/			/			2	3.35	1.45	/			/		
mMRP63	Mrp63	IPI00132487	/			/			/			1	2.87	0.93	/			/		
ALL-1	All1	IPI00315032	/			/			/			1	2.39	1.46	/			/		
Liver X receptor beta	Lxrb	IPI00119090	/			/			/			2	2.09	3.11	1	2.04	2.29	/		
28S ribosomal protein S21, mitochondrial	Mrps21	IPI00115896	1	1.19	1.14	1	1.20	1.05	/			1	2.08	1.04	/			1	1.23	0.83
Putative uncharacterized protein	Faim	IPI00890905	/			/			/			2	2.05	1.19	/			/		
Protein ftsJ homolog 3	Ftsj3	IPI00119632	/			/			/			1	1.97	1.23	/			/		
Apolipoprotein J	Apoj	IPI00320420	/			/			/			1	1.97	0.94	/			/		
DnaJ (Hsp40) homolog, subfamily C, member 17	Dnajc17	IPI00943363	/			/			/			1	1.84	1.08	/			/		
Smoothelin	Smsmo	IPI00648499	/			/			/			1	1.79	1.11	/			/		
Folylpoly-gamma-glutamate synthetase	Fpgs	IPI00653390	/			/			/			1	1.78	40.42	/			/		
B aggressive lymphoma protein homolog	Bal	IPI00377563	/			/			/			1	1.77	1.06	/			/		
Kinesin family member 2C	Kif2c	IPI00648327	/			/			/			3	1.75	1.00	/			/		
Putative uncharacterized protein	Rps6ka1	IPI00648998	/			/			/			1	1.69	1.51	/			/		
G9 sialidase	Neu	IPI00315576	/			/			/			1	1.68	0.84	/			1	1.27	1.06

Lymphocyte antigen 6A-2/6E-1	Ly6	IPI00120592	/	/	/			1	1.65	1.85	/			/					
G2/mitotic-specific cyclin-B2	Ccnb2	IPI00314149	/	/	/			1	1.65	0.99	1	2.64	0.56	/					
MFLJ00163 protein	Maged1	IPI00556867	/	/	/			2	1.58	1.34	/			/					
Syndecan-3	Kiaa0468	IPI00135452	/	/	/			1	1.57	0.81	/			/					
Zinc finger MYND domain-containing protein 11	Zmynd11	IPI00775961	/	/	/			1	1.55	1.09	/			/					
DEAD (Asp-Glu-Ala-Asp) box polypeptide 21	Ddx21	IPI00652987	/	/	/			15	1.54	0.94	/			/					
DEAH box protein 32	Ddx32	IPI00127679	/	/	/			1	1.50	0.91	/			1	1.33	0.97			
		IPI00278864	/	/	/			1	1.49	1.14	/			/					
ATP-dependent RNA helicase ROK1-like	Ddx52	IPI00336965	/	/	/			2	1.49	1.12	/			/					
Putative uncharacterized protein	Nol14	IPI00785218	/	/	/			3	1.48	0.82	/			/					
Cyclooxygenase-2	Cox2	IPI00308785	/	/	/			1	1.48	1.12	/			/					
Surfeit locus protein 1	Surf1	IPI00319135	/	/	/			1	1.47	1.17	/			/					
Neuron navigator 2	Nav2	IPI00466984	/	/	/			2	1.46	1.52	/			/					
PAT1-like protein 1	Patl1	IPI00309059	/	/	/			1	1.46	1.04	/			2	1.22	1.15			
Brix domain-containing protein 5	Bxdc5	IPI00380313	/	/	/			1	1.46	0.81	/			/					
MCG9286, isoform CRA_b	Aagab	IPI00654197	/	/	/			1	1.45	1.12	/			/					
Citron Rho-interacting kinase	Cit	IPI00655040	/	/	/			2	1.44	1.02	/			/					
NOL1/NOP2/Sun domain family member 5	Nsun5	IPI00311260	/	/	/			1	1.43	1.82	/			/					
Uncharacterized protein C8orf59 homolog		IPI00785295	/	/	/			1	1.42	0.96	/			/					
TBC1 domain family member 25	Tbc1d25	IPI00222302	/	/	/			1	1.42	1.08	/			/					
Gene Y protein	Trific	IPI00463173	/	/	/			1	1.40	103.24	/			1	7.29	12.88			
		IPI00856470	/	/	/			2	1.40	1.02	/			2	1.25	1.37			
Pumilio homolog 1	Kiaa0099	IPI00400349	/	/	/			5	1.39	1.05	/			/					
Ankyrin repeat domain-containing protein 16	Ankrd16	IPI00221778	/	/	1	1.35	1.09	1	1.39	1.00	/			/					
MKIAA0480 protein	Cep350	IPI00928565	/	/	/			3	1.38	0.78	/			/					

ATP-dependent RNA helicase DDX55	Ddx55	IPI00453808	/			/			1	1.37	1.22	/			/		
		IPI00881767	/			/			/			1	122.9	11.59	/		
Membrane transport protein XK	Xk	IPI00135678	/			/			/			1	12.20	61.82	/		
Coiled-coil domain-containing protein 52	Ccdc52	IPI00170090	/			/			/			1	2.00	1.21	/		
WD repeat-containing protein 24	Wdr24	IPI00229321	/			/			/			1	1.91	0.90	/		
Receptor-type tyrosine-protein phosphatase gamma	Ptprg	IPI00114671	/			/			/			1	1.59	1.01	/		
60S ribosomal protein L36	Rpl36	IPI00869475	/			/			/			3	1.53	0.98	/		
60S ribosomal protein L18a	Rpl18a	IPI00880213	/			/			/			4	1.45	0.92	/		
Procollagen C-endopeptidase enhancer 1	Pcolce	IPI00120176	/			/			/			4	1.44	0.93	5	1.33	0.94
Macrophage colony-stimulating factor 1	Csf1	IPI00125138	/	2	1.23	1.00	1	1.34	0.92	2	1.35	1.43	1	1.43	0.96	2	1.36	1.01
Gamma-aminobutyric acid receptor-associated protein	Gabarap	IPI00120754	/			/			/			1	1.38	0.92	/		
Rho guanine nucleotide exchange factor 19	Arhgef19	IPI00226216	/			/			/			1	1.38	1.02	1	1.45	1.27
Amyloid beta A4 precursor protein-binding family A member 3	Apba3	IPI00135411	/			/			2	1.21	3.10	1	1.34	1.03	2	1.30	1.01
Prenylated Rab acceptor protein 1	Rabac1	IPI00129399	/			/			2	1.25	0.90	1	1.34	0.82	2	1.38	1.00
40S ribosomal protein S8	Rps8	IPI00466820	/			/			/			6	1.27	0.94	10	1.25	0.93
3222402P14Rik protein	Ppp2r3a	IPI00406107	/			/			/			1	1.25	0.86	/		
		IPI00858126	/			/			/			3	1.23	1.17	/		
Insulin receptor substrate 2	Irs2	IPI00923679	/			8	1.32	1.13	7	1.28	1.12	7	1.22	1.13	/		
Ribose-phosphate pyrophosphokinase	Prps1l1	IPI00900411	/			2	1.23	1.07	/			2	1.22	0.99	/		
Mediator of RNA polymerase II transcription subunit 13-like	Med13l	IPI00420457	/			/			/			/			1	44.54	10.66
Zinc finger protein 462	Zfp462	IPI00467729	/			/			/			/			1	41.05	4.63
Glucosamine--fructose-6-phosphate aminotransferase [isomerizing] 2	Gfpt2	IPI00278312	/			/			/			/			5	26.66	231.8
Mesenchyme homeobox 1	Meox1	IPI00649802	/			/			/			/			1	25.75	5.82

Syntaxin-binding protein 4	Stxbp4	IPI00125455	/	/	/	/		/	1	21.24	7.19
Serine/threonine-protein kinase ULK1	Ulk1	IPI00752067	/	/	/	/		/	1	19.83	0.86
		IPI00457415	/	/	/	/		/	3	12.35	1.41
Transmembrane protein 54	Tmem54	IPI00471083	/	/	/	/		/	1	7.66	2.50
Fascin homolog 2, actin-bundling protein, retinal (Strongylocentrotus purpuratus)	Fscn2	IPI00226453	/	/	/	/		/	1	3.57	1.05
Olfactory receptor Olfr1477	Olfr1477	IPI00313137	/	/	/	/		/	1	3.16	1.65
TRAF-interacting protein with FHA domain-containing protein A	Tifa	IPI00153104	/	/	/	/		/	1	2.70	0.73
Pcdhgc5 protein	Pcdhgc5	IPI00129572	/	/	/	/		/	2	2.61	0.86
Protein deltex-2	Dtx2	IPI00113171	/	/	/	/		/	1	2.58	1.26
Ubiquinone biosynthesis methyltransferase COQ5, mitochondrial	Coq5	IPI00379695	/	/	/	/		/	1	2.46	8.59
Gamma-tubulin complex component 3	Tubgcp3	IPI00396839	/	/	/	/		/	2	2.33	1.73
WD repeat-containing protein 7	Wdr7	IPI00120637	/	/	/	/		/	1	2.28	1.04
Brain-specific angiogenesis inhibitor 1	Bai1	IPI00850693	/	/	/	/		/	1	2.17	0.62
Dynein heavy chain 8, axonemal	Dnahc8	IPI00172328	/	/	/	/		/	1	1.96	5.98
Glucocorticoid modulatory element-binding protein 2	Gmeb2	IPI00118393	/	/	/	/		/	1	1.94	1.09
E3 ubiquitin-protein ligase UBR2	Ubr2	IPI00468701	/	/	/	/		/	2	1.90	1.09
Coiled-coil domain-containing protein 77	Ccdc77	IPI00112708	/	/	/	/		/	1	1.88	1.24
U6 snRNA-specific terminal uridylyltransferase 1	Tut1	IPI00153749	/	/	/	1	1.35	1.14 /	3	1.83	1.36
IRFD2	Ifrd2	IPI00469290	/	/	/	/		/	1	1.78	0.91
E3 ubiquitin-protein ligase NRDP1	Rnf41	IPI00308182	/	/	/	/		/	1	1.73	2.18
Uncharacterized protein C11orf61 homolog		IPI00279213	/	/	/	/		/	1	1.65	0.98
HN1-like protein	AY358078	IPI00396784	/	/	/	/		/	2	1.61	1.03
		IPI00751634	/	/	/	/		/	3	1.50	0.90

E3 ubiquitin-protein ligase Praja1	Pja1	IPI00309237	/			/			/			/			/			1	1.49	1.23
Nuclear prelamin A recognition factor-like protein	Narf1	IPI00309907	/			/			/			/			/			1	1.48	0.76
CDK5 regulatory subunit-associated protein 1-like 1	Cdkal1	IPI00163015	/			/			/			/			/			1	1.47	1.20
HMG box transcription factor BBX	Bbx	IPI00625898	/			/			/			/			/			2	1.46	3.35
Suppressor of fused homolog	Sufu	IPI00124718	/			/			/			/			/			2	1.46	66.24
Putative uncharacterized protein	Ttc13	IPI00895079	/			/			/			/			/			2	1.46	1.28
Arylsulfatase A	Arsa	IPI00607957	/			/			/			/			/			1	1.44	0.96
Clusterin-associated protein 1	Cluap1	IPI00277399	/			/			/			/			/			1	1.43	1.41
Inositol 1,4,5-triphosphate receptor-interacting protein	Itprip	IPI00420315	/			/			/			/			/			1	1.43	1.01
Arhgef5 protein	Arhgef5	IPI00855144	/			/			4	1.26	1.09	2	1.22	0.87	/			1	1.43	0.65
VPS10 domain-containing receptor SorCS2	Sorcs2	IPI00110262	/			/			/			/			/			1	1.43	0.54
Putative uncharacterized protein	Ugt2b1	IPI00153143	/			/			/			/			/			1	1.42	1.08
Vitamin K-dependent gamma-carboxylase	Ggcx	IPI00136012	/			/			/			/			/			1	1.39	1.45
Ankyrin repeat domain-containing protein 46	Ankrd46	IPI00225335	/			/			/			/			/			2	1.38	1.05
Ribosome biogenesis protein NSA2 homolog	Tinp1	IPI00468437	/			/			/			/			/			1	1.38	1.09
Metalloproteinase inhibitor 1	Timp1	IPI00114403	/			/			/			/			/			1	1.37	0.81
Kinesin-like protein KIF21A	Kif21a	IPI00454081	1	1.21	1.09	2	1.24	1.06	1	1.33	1.54	3	1.22	1.01	/			3	1.36	1.09
Sequestosome-1	Sqstm1	IPI00474373	/			/			/			/			/			11	1.35	1.15
Cartilage-associated protein	Crtap	IPI00111370	/			/			/			/			/			6	1.34	1.21
Retinitis pigmentosa 1-like 1 protein	Rp1l1	IPI00229529	/			/			/			/			/			4	1.34	0.88
UDP-glucuronosyltransferase 1-6	Ugt1a6	IPI00134432	/			/			/			/			/			2	1.34	1.07
Serine proteinase inhibitor mBM2A	Spi15	IPI00115683	/			/			/			/			/			2	1.33	1.26
Phosphatidylinositol-4-phosphate 5-	Pip5k1c	IPI00655177	/			/			/			/			/			2	1.32	1.27

kinase type-1 gamma										
MAP kinase-activating death domain protein	Madd	IPI00620097	/	/	/	/	/	1	1.32	1.06
		IPI00831560	/	/	/	/	/	1	1.30	0.95
Putative uncharacterized protein	Pi4ka	IPI00115875	/	/	/	/	/	3	1.30	1.10
Mps one binder kinase activator-like 2	Mob2	IPI00139718	/	/	/	/	/	1	1.29	1.04
Ras-related protein Rab-3B	Rab3b	IPI00113112	/	/	/	/	/	4	1.29	1.13
Calcium-transporting ATPase type 2C member 2	Atp2c2	IPI00849112	/	/	/	/	/	1	1.29	8.75
Alanine aminotransferase 2	Gpt2	IPI00265352	/	/	/	/	/	3	1.29	1.29
Glutathione S-transferase A1	Gsta1	IPI00554953	/	/	/	/	/	3	1.28	1.19
Plectin-1	Plec1	IPI00421271	/	/	/	/	/	180	1.28	1.31
MKIAA0480 protein	Cep350	IPI00118304	/	/	/	/	/	1	1.28	0.78
StAR-related lipid transfer protein 5	Stard5	IPI00284769	/	/	/	/	/	1	1.28	1.38
MKIAA0657 protein	Obsl1	IPI00403485	/	/	/	/	/	2	1.28	1.07
Putative uncharacterized protein	EG433762	IPI00463111	/	/	/	/	/	2	1.28	1.07
Carbohydrate kinase domain-containing protein	Carkd	IPI00894581	/	/	/	/	/	6	1.27	1.10
3-ketoacyl-CoA thiolase B, peroxisomal	Acaa1b	IPI00122139	/	/	/	/	/	9	1.26	1.14
Plakophilin-4	Pkp4	IPI00473693	/	/	/	/	/	2	1.24	1.52
Influenza virus NS1A-binding protein homolog	Ivns1abp	IPI00420559	/	/	/	/	/	1	1.24	1.60
DNA polymerase	Pold1	IPI00313515	/	/	/	/	/	8	1.24	0.93
PH and SEC7 domain-containing protein 3	Psd3	IPI00874973	/	/	/	/	/	1	1.24	1.76
TSC22 domain family protein 1	Tsc22d1	IPI00420803	/	/	/	/	/	3	1.23	1.11
Interferon-induced 35 kDa protein homolog	Ifi35	IPI00261188	/	/	/	/	/	1	1.23	0.96
RRP15-like protein	Rrp15	IPI00458958	/	/	/	/	/	2	1.23	1.09
GTP-binding protein 8	Gtpbp8	IPI00110725	/	/	/	/	/	1	1.23	1.23

Fibronectin type-III domain-containing protein 3a	Fndc3a	IPI00356888	/	/	/	/			/	1	1.23	1.14
Protein FAM122B	Fam122b	IPI00798493	/	/	/	/			/	1	1.23	1.21
Paired amphipathic helix protein Sin3b	Sin3b	IPI00608092	/	/	/	2	1.22	1.07	/	2	1.23	0.98
NEDD4 family-interacting protein 1	Ndfip1	IPI00850592	/	/	/	/			/	2	1.23	1.19
Autophagy-related protein 2 homolog B	Atg2b	IPI00377925	/	/	/	/			/	2	1.21	1.07
TATA box-binding protein-like protein 1	Tbpl1	IPI00131818	/	/	/	/			/	1	1.21	14.24

The data were then analysed using the bio-informatic software DAVID (http://david.abcc.ncifcrf.gov/) in order to determine if there are any links between the identified proteins that have previously been identified in the literature. The software identifies significant enrichment of gene ontology (GO) terms i.e. the process or processes in which the gene(s) function are over represented in the data set.

In total 15 GO terms were significantly enriched in the down-regulated proteins (table 3.7.) whereas no GO terms were identified as significantly enriched from the up-regulated proteins. It is obvious from the identified GO terms that the overarching factor in these terms is the effect on lipid small molecules. The 8 most significantly enriched terms are related to the biosynthesis and processing of sterols, cholesterol, steroid and lipids. Thus, it is clear, and unsurprising, that treatment of SN4741 cells with 24(*S*),25-epoxycholesterol results in alterations in the biosynthesis and processing of a variety of lipid molecules.

Table 3.7. Gene Ontology terms identified as enriched after DAVID bio-informatic analysis. GO terms significantly enriched after p-value correction (Benjamini) are shown. Proteins up and down regulated were analysed independently but all significantly enriched GO terms identified were from the down regulated proteins data.

Term	Count	Fold Enrichment	p-value	Benjamini
Sterol biosynthetic process	13	30.96	2.59E-15	3.32E-12
Cholesterol biosynthetic process	12	37.28	3.33E-15	2.17E-12
Sterol metabolic process	16	14.85	1.39E-13	6.05E-11
Cholesterol metabolic process	15	15.31	6.34E-13	2.06E-10
Steroid biosynthetic process	14	14.09	1.43E-11	3.72E-09
Steroid metabolic process	17	7.54	8.37E-10	1.82E-07
Lipid biosynthetic process	19	4.76	9.65E-08	1.80E-05
Lipid metabolic process	29	2.98	4.01E-07	6.53E-05
Alcohol metabolic process	19	3.77	2.93E-06	4.23E-04
Oxidation reduction	26	2.76	7.11E-06	9.25E-04
Isoprenoid biosynthetic process	6	19.49	1.08E-05	0.001
Isoprenoid metabolic process	7	10.21	5.74E-05	0.006
Transport	54	1.65	1.52E-04	0.015
Establishment of localization	54	1.64	1.81E-04	0.017
Cellular lipid metabolic process	18	2.67	4.19E-04	0.036

In addition to the GO terms identified the analysis of the down-regulated proteins identified a number of KEGG pathways as enriched (table 3.8) though only 2 pathways had significant Benjamini corrected p-values. Again, unsurprisingly, the most significantly enriched pathways were those related to steroid biosynthesis and terpenoid backbone synthesis. These pathways have a large number of previously identified SREBP2 regulated proteins. It is interesting to note that despite not being significantly enriched after correction of the p-value the KEGG pathways of both Alzheimer's and Parkinson's disease, 2 neurodegenerative diseases, were identified as enriched.

Table 3.8. KEGG Pathways identified as enriched by DAVID bio-informatic analysis of down regulated proteins. Benjamini is the corrected p-value required after multiple analysis.

Kegg Pathway	Count	IPI Number	Fold Enrichment	p-value	Benjamini
Steroid biosynthesis	8	IPI00338068, IPI00137471, IPI00474810, IPI00169958, IPI00130988, IPI00316067, IPI00128692, IPI00458711, IPI00133526	32.15	1.77E-09	**2.08E-07**
Terpenoid backbone biosynthesis	7	IPI00849448, IPI00319950, IPI00756996, IPI00120457, IPI00133709, IPI00331707, IPI00228253	34.15	2.09E-08	**1.22E-06**
Cardiac muscle contraction	6	IPI00224210, IPI00121550, IPI00131176, IPI00114377, IPI00129516, IPI00225390	5.25	5.18E-03	0.183
Oxidative phosphorylation	7	IPI00224210, IPI00131176, IPI00313841, IPI00114377, IPI00318645, IPI00129516, IPI00225390	3.68	0.01	0.275
Parkinson's disease	7	IPI00648249, IPI00224210, IPI00131176, IPI00923056, IPI00114377, IPI00129516, IPI00225390	3.60	0.01	0.249
Natural killer cell mediated cytotoxicity	6	IPI00133132, IPI00322542, IPI00881074, IPI00136110, IPI00856542, IPI00665857	3.36	0.03	0.461
Alzheimer's disease	7	IPI00224210, IPI00131176, IPI00114377, IPI00117124, IPI00665857, IPI00129516, IPI00225390	2.63	0.05	0.555
Calcium signalling pathway	7	IPI00471089, IPI00133132, IPI00466672, IPI00626433, IPI00831180, IPI00263265, IPI00665857	2.50	0.06	0.578
Biosynthesis of unsaturated fatty acids	3	IPI00129362, IPI00117142, IPI00318108	7.59	0.06	0.537
Focal adhesion	7	IPI00626433, IPI00117829, IPI00136110, IPI00828653, IPI00421218, IPI00136701, IPI00110508	2.41	0.07	0.550
Butanoate metabolsim	3	IPI00135189, IPI00331707, IPI00228253	5.54	0.099	0.672

The proteins identified as up-regulated were also analysed to identify enriched pathways (table 3.9). No significant changes in enrichment were identified after correction of the p-value. Thus, it appears that treatment of SN4741 cells with 10μM 24(*S*),25-epoxycholesterol fails to up-regulate specific pathways *en masse* but rather up-regulates single unrelated proteins.

Table 3.9. Kegg Pathways identified as enriched by DAVID bio-informatic analysis of up-regulated proteins. Benjamini is the corrected p-value required after multiple analysis.

Kegg Pathway	Count	IPI Number	Fold Enrichment	p-value	Benjamini
Metabolism of xenobiotics by cytochrome P450	5	IPI00323911 IPI00890112 IPI00111222 IPI00554953 IPI00134432 IPI00153143	7.01	0.005	0.415
Drug metabolism	5	IPI00323911 IPI00890112 IPI00111222 IPI00554953 IPI00134432 IPI00153143	6.17	0.008	0.344
Ribosome	4	IPI00880213 IPI00466820 IPI00849113 IPI00869475	4.16	0.068	0.916
Fc gammaR-mediated phagocytosis	4	IPI00272878 IPI00229848 IPI00655177 IPI00117274	3.78	0.086	0.904

As mentioned earlier some of the proteins identified had weak evidence of changes in expression either due to a low number of peptides or due to the fact that they were not identified in all biological replicates. Thus, in order to determine proteins with stronger evidence of expression changes the data presented in table 3.5. and table 3.6. were re-examined. Proteins identified with only 1 peptide were excluded. In addition, proteins only identified in 1 biological replicate were also excluded. Finally, proteins only identified with low-scoring peptides or where there was a large variability between peptides were excluded. The flowchart for data analysis is shown in figure 3.12. Thus, reliable, reproducible data was extracted from the data (table 3.10).

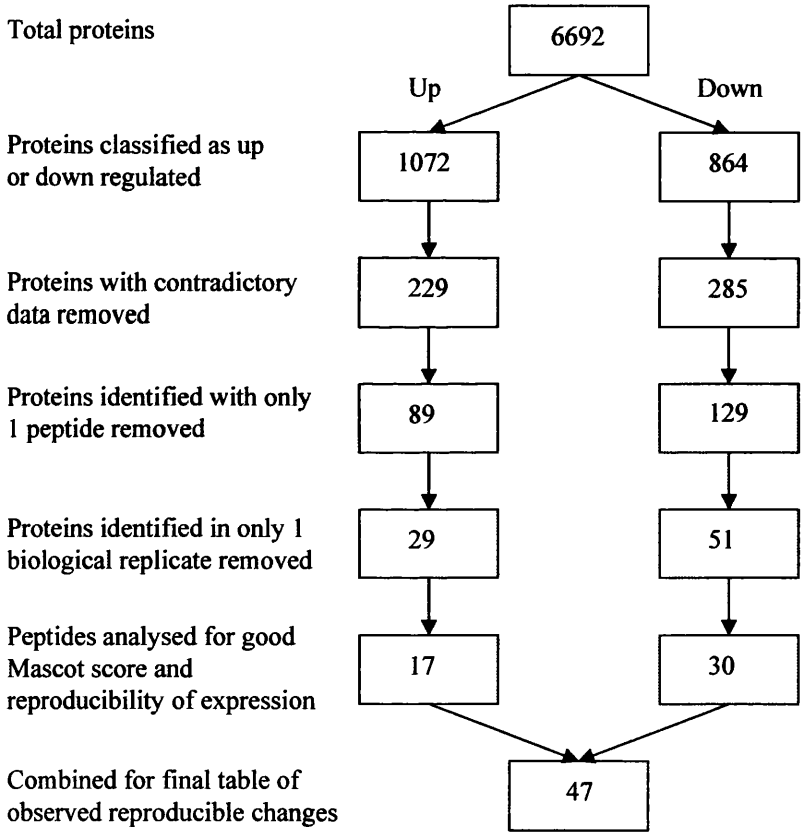

Figure 3.12. Flowchart of data analysis showing the process by which protein expression data was rejected in order to identify reproducible changes in the proteome. Of the 6692 unique proteins identified in the 3 biological replicates only 47 (0.7%) had strong, reproducible evidence of a change in protein expression.

It can be seen that previously identified changes associated with inhibition of SREBP2 processing by oxysterols are reliably observed in all 3 biological replicates after treatment with 10μM 24(*S*),25-epoxycholesterol (table 3.10). The synthetic LXR ligand GW3965, as expected, had no effect on the transcription of these genes. It is important to recognise that despite these proteins being previously identified and well characterised as regulated by SREBP2, and therefore, by oxysterols via INSIG, it is critical to the reliability of the SILAC experimental design that known changes expected with 24(*S*),25-epoxycholesterol are identified successfully in order to have confidence that other unexpected changes are true. In addition, ABCA1 expression was up-regulated after treatment with both 24(*S*),25-epoxycholesterol and GW3965. ABCA1 expression is dependent on LXR activation. As both 24(*S*),25-epoxycholesterol and GW3965 are ligands for LXR it again validates the methodology that a predicted change is observed after analysis of the proteomic data.

A number of proteins reproducibly identified as having a changed expression had links to cholesterol, phospholipids or fatty acids (table 3.10). However, other proteins, with no apparent link to lipids were also identified as having a changed expression. For example, two proteins that were reproducibly observed as being up regulated were Golgi apparatus protein 1 and macrophage colony stimulating factor.

Table 3.10. Summary of reproducible changes in protein expression. For the 3 biological replicates the mean SILAC ratio compared to control derived from the Orbitrap and Velos instruments is shown.

			24S,25-EC			GW3965			
Protein Name	Gene	PI Number	Biological Replicate						
			1	2	3	1	2	3	
Acetyl-CoA acetyltransferase, cytosolic	Acat2	IPI00128268	0.62	0.54	0.64	1.21	0.97	1.07	Cholesterol Synthesis
Acetoacetyl-CoA synthetase	Aacs	IPI00138189	0.69	0.70	0.68	1.06	1.02	1.04	
HMG-CoA synthase	Hmgcs1	IPI00331707	0.31	0.21	0.21	1.01	1.02	1.09	
Mevalonate kinase	Mvk	IPI00126732	0.72	0.54	0.70	1.01	0.90	0.99	
Phosphomevalonate kinase	Pmvk	IPI00139709	0.49	0.54	0.76	1.06	1.20	1.22	
PP mevalonate decarboxylase	Mvd	IPI00119960	0.44	0.41	0.45	1.04	0.93	1.07	
Isopentenyl-PP isomerase	Idi1	IPI00648448	0.42	0.34	0.43	1.03	1.10	1.14	
Farnesyl PP synthase	Fdps	IPI00130487	0.53	0.53	0.53	1.08	1.03	1.07	
Squalene synthase	Fdft1	IPI00338068	n.d.	0.16	0.16	n.d.	1.54	1.64	
Lanosterol synthase	Lss	IPI00169988	0.42	0.48	0.51	1.07	1.04	1.17	
Sterol 14-demethylase	Cyp51	IPI00458711	0.42	0.25	0.29	1.02	0.97	1.02	
Sterol-4-alpha-carboxylate 3-dehydrogenase, decarboxylat	Nsdhl	IPI00128692	0.50	0.50	0.58	1.04	1.02	1.18	
3-keto-sterol reductase	Hsd17b7	IPI00474810	0.51	0.62	0.57	0.98	1.16	1.17	
Cholestenol delta-isomerase	Ebp	IPI00127471	0.64	0.76	0.62	1.11	0.92	0.86	
Acetyl-CoA carboxylase 1	Acac	IPI00648448	1.11	1.05	1.08	1.28	1.26	1.21	Fatty Acid Synthesis and Metabolism
Fatty acid synthase	Fasn	IPI00118223	1.00	0.86	0.94	1.37	1.23	1.26	
Long-chain-fatty-acid CoA ligase 3	Acsl3	IPI00169772	0.84	0.82	0.86	1.34	1.38	1.39	
Fatty acid desaturase 2	Fads2	IPI00139963	n.d.	0.48	0.63	n.d.	0.96	0.95	
Acyl-CoA synthetase short-chain family member 2	Acss2	IPI00752027	0.49	0.44	0.54	1.07	1.17	1.35	Lipid Synthesis and Metabolism
Phosphatidate phosphatase LPIN1	Lpin1	IPI00328693	0.67	0.67	0.44	1.12	0.92	0.95	
Mid1-interacting protein 1	Mid1ip1	IPI00131884	1.03	n.d.	1.07	1.33	n.d.	1.92	
Phosphoethanolamine cytidylyltransferase	Pcyt2	IPI00111395	0.72	0.59	0.67	1.05	1.04	1.14	Phospholipid synthesis
CTP phosphocholine cytidylyltransferase A	Pcyt1a	IPI00118480	0.955	0.865	0.85	0.985	0.895	1.005	
6-phosphofructokinase type C	Pfkp	IPI00317875	n.d.	1.39	1.20	n.d.	1.44	1.28	Glycolysis
Low-density lipoprotein receptor	Ldlr	IPI00112063	0.52	0.36	0.27	0.92	0.76	0.90	Receptors and Plasma Membrane
Oxysterols receptor LXR-beta	Lxrb	IPI00119080	n.d.	1.00	1.04	n.d.	1.11	1.28	
CD44 antigen	Cd44	IPI00410801	n.d.	0.76	0.76	n.d.	0.85	0.99	
Integrin beta-5	Itgb5	IPI00377983	0.83	0.79	0.84	0.82	0.72	0.78	
Integrin alpha-V	Itgav	IPI00851185	0.82	0.82	0.78	0.94	0.73	0.80	
Caveolin-1	Cav1	IPI00117838	0.61	0.65	0.60	0.76	0.80	0.61	
ABCA1	Abca1	IPI00889648	3.69	10.82	7.96	8.71	4.78	8.91	Transport
ABCA7	Abca7	IPI00116970	1.48	1.26	1.28	1.03	0.89	0.96	
StAR-related lipid transfer protein 4	Star4	IPI00320032	n.d.	0.39	0.34	n.d.	1.05	1.07	
Collagen type IV alpha-3-binding protein	Col4a3bp	IPI00111167	1.28	1.47	1.52	1.08	1.20	1.10	
Wtch2 protein	Wtch2	IPI00307202	n.d.	0.63	0.49	n.d.	0.76	0.46	
Retinol dehydrogenase 11	Arsdr1	IPI00136098	0.63	0.77	0.60	1.02	0.96	1.07	Other
Cornifin-A	Sprr1a	IPI00123466	0.77	0.57	0.71	0.97	0.91	0.90	
V-type proton ATPase subunit d 1	Atp6d	IPI00128641	0.75	0.79	0.72	0.69	0.82	0.69	
Histone H3.3-like isoform 1	Gm6421	IPI00851232	n.d.	0.93	1.00	n.d.	0.69	0.72	
Alpha-1,3-mannosyltransferase ALG2	Alg2	IPI00111678	0.90	1.02	n.d.	1.28	1.40	n.d.	
Golgi sialoglycoprotein MG-160	Esl1	IPI00123898	1.25	1.33	1.51	0.94	0.87	1.05	
Annexin A6 isoform 8	Anx6	IPI00310340	1.16	1.18	1.29	1.23	1.32	1.46	
Kinesin-like protein KIF21A	Kiaa1708	IPI00454081	1.23	1.28	1.36	1.08	1.28	1.09	
Macrophage colony-stimulating factor 1	Csf1	IPI00115138	1.23	1.35	1.41	1.00	1.18	0.99	
Glutathione S-transferase A4	Gsta	IPI00229511	n.d.	1.30	1.52	n.d.	1.42	1.05	
Aldehyde dehydrogenase family 3, subfamily A1	Aldh3a1	IPI00880112	1.34	1.81	1.55	1.27	1.23	1.22	
FK506 binding protein 10	Fkbp10	IPI00944194	n.d.	1.43	1.74	n.d.	1.04	1.11	

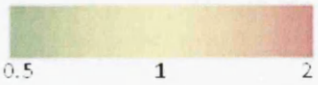

3.3. Discussion

The proteomic analysis of SN4741 cells after treatment with 24(*S*),25-epoxycholesterol and GW3965 identified a large number of proteins. In total, 6692 unique proteins were identified with ≥1 peptide in the 3 biological replicates (figure 3.12). However, the majority of proteins in each replicate were identified with 2 or more peptides (table 3.2). Thus, it is clear that the experimental approach of strong cation exchange to reduce the sample complexity followed by LC-MS was successful when judged by the total number of observed proteins in the experiments. In addition, the SILAC labelling adopted gave a wealth of data that required painstaking analysis to extract the most reliable data. From a technical perspective, it was clear that the Orbitrap Velos was the instrument that performed better as it consistently identified more peptides, and therefore proteins, than the LTQ-Orbitrap instrument (table 3.2).

A large number of proteins were identified as having an altered expression after treatment with 24(*S*),25-epoxycholesterol. In total 1072 up-regulated and 864 down-regulated proteins were identified in the 3 biological replicates (Appendix 1, Appendix 2). However, analysis of these proteins identified a significant number with contradictory data in a different data set (e.g. up-regulated in one dataset but no change in the others; Appendix 1, Appendix 2). The analysis of the data to remove these proteins led to a large proportion of them to be rejected as having a change in protein expression. After removal of contradictory proteins 229 (21.4%) up-regulated proteins and 285 (33.0%) down regulated proteins remained (table 3.5, table 3.6, fig 3.12). These data give a clear indication of the necessity of multiple biological replicates in proteomic studies.

The proteins identified as changed were then analysed by using the online software DAVID in order to identify GO terms and pathways significantly up or down-regulated in the data set. No GO terms or KEGG pathways were up-regulated with statistical significance. Therefore, it appears from these data that 24(*S*),25-epoxycholesterol up-regulates individual proteins and not whole pathways. In comparison, there was significant down regulation of 15 GO terms (table 3.7). In addition, 2 KEGG pathways were down-regulated after Benjamini correction - steroid biosynthesis and terpenoid backbone biosynthesis. It is unsurprising that these pathways are down-regulated as their expression is controlled by SREBP2.

The proteins identified in tables 3.5 and 3.6 have no contradictory data. However, the majority of the identified proteins have been identified as having a change in expression have only weak evidence to support the observation. A reliance on a SILAC ratio measurement from a single peptide can lead to experimental error. Similarly a protein observed in only one biological replicate can have an erroneous measurement. This is clear from the number of proteins with observed changes in expression being rejected as due to having contradictory data in a different biological replicate (figure 3.12). Thus, proteins that were only identified with one peptide or in one biological replicate were rejected.

The final analysis of the identified proteins was to examine their individual peptides used to identify the protein. The Mascot scores and the reproducibility of the SILAC ratios between peptides used to identify and quantify the same protein were examined. Proteins identified only with peptides with low Mascot scores were rejected. In addition, proteins identified with a number of unique peptides with a large variation in the SILAC quantification ratio were also rejected. This ensured that the proteins remaining were identified in multiple biological replicates, with multiple peptides and that the peptides used for identification had good Mascot scores and low variability of the SILAC ratio. Thus, the final 47 proteins presented in table 3.10 are the proteins with the most robust evidence of changes in expression. The rejection of the vast majority of the proteins identified as changed is a necessary evil in order to have the final outcome of a reliable, but much smaller, set of data.

It is clear that from the data presented here the SILAC proteomic approach was successful in identifying proteins, both known and novel, which are sensitive to 24(*S*),25-epoxycholesterol treatment and with a reproducible response (table 3.10). Both instruments identified expected SREBP2 regulated changes in protein expression of enzymes involved in the cholesterol synthesis pathway after 24(*S*),25-epoxycholesterol treatment. It is unlikely that any observed changes were due to toxicity as it was shown that 24(*S*),25-epoxycholesterol was non-toxic to SN4741 cells (fig 3.1; fig 3.2; fig 3.3). In addition, the rigorous criteria by which the data was analysed meant that the protein expression data presented here are trustworthy.

However, further validation of these data is required in order to determine how 24(*S*),25-epoxycholesterol induces the observed changes in protein expression. Thus

in the next chapter work will be conducted in order to elucidate the mechanisms involved.

CHAPTER 4: FURTHER ANALYSIS OF 24(*S*),25-EPOXYCHOLESTEROL INDUCED PROTEIN EXPRESSION CHANGES IN SN4741 NEURONS

4.1. Introduction

24(*S*),25-epoxycholesterol induces changes in the proteome of SN4741 cells. This effect is apparent in the proteomic data presented in Chapter 3 where 47 proteins were identified as changed reliably and reproducibly (table 3.10). Therefore, there is already evidence these proteins are sensitive to 24(*S*),25-epoxycholesterol. However, further analysis is required in order to validate the results and elucidate the mechanism by which 24(*S*),25-epoxycholesterol induces these changes.

It is already known that 24(*S*),25-epoxycholesterol can increase gene expression by activating the transcription factor LXR (section 1.1.5.2.). In addition, previous work has shown that oxysterols can prevent gene transcription regulated by SREBP2 (section 1.1.5.1). Thus, there is precedent for oxysterols inducing changes in gene expression by altering transcription of mRNA. Therefore, in order to investigate whether the observed changes in protein expression correlated with a change in the transcription of mRNA qPCR can be performed. These experiments will lead to understanding the mechanism by which 24(*S*),25-epoxycholesterol is inducing the observed changes.

In addition, further analysis of the protein expression changes at the protein level can be performed to validate and clarify the observed data in the SILAC proteomic experiments. An obvious example would be the use of Western blotting in order to confirm changes in protein expression. In addition, other techniques can be used to examine specific attributes of a protein observed as having changed. For example, ELISA can be used to examine if changes in expression correlate to changes in secretion of a given protein.

It is possible that secondary effects may influence changes in both protein expression and localisation as oxysterols reduce cholesterol synthesis due to inhibition of SREBP2. Thus, in the presence of 24(*S*),25-epoxycholesterol the cholesterol content of SN4741 cells will be reduced. Cholesterol is an essential component of membranes and therefore a reduction in the cholesterol level may disrupt the cellular membrane

and lead to changes in protein expression and localisation. Therefore, the observed protein expression changes in the SILAC experiments may be due to changes in the cellular cholesterol level. In this instance immunofluorescence may be used as an adjunct to examine changes in the localisation of a protein after treatment with 24(*S*),25-epoxycholesterol.

In summary, the aim of this chapter is to further investigate and discuss the changes identified in the SILAC quantitative proteomic experiments.

4.2. Results

4.2.1. Validation of Known Oxysterol Regulated Genes Identified by SILAC

The SILAC proteomic data led to the identification of known SREBP2 regulated genes in the cholesterol synthesis pathway to be identified reproducibly as down-regulated after treatment with 10μM 24(*S*),25-epoxycholesterol (table 3.10). The synthetic LXR ligand GW3965, as expected, did not down-regulate these genes. However, from these data it appears that GW3965 treatment resulted in the up-regulation of squalene synthase. It is important to recognise that despite these proteins being previously identified and well characterised as regulated by SREBP2, and therefore, by oxysterols via INSIG, it is critical to the reliability of the SILAC experimental design that known changes expected with 24(*S*),25-epoxycholesterol are identified successfully in order to have confidence that other unexpected changes are true.

Low density lipoprotein receptor (LDLR), another SREBP2 regulated gene, was observed as down regulated by 24(*S*),25-epoxycholesterol and not by GW3965 at the protein and mRNA level (table 3.10; figure 4.1). Interestingly, the protein expression of LDLR was not classed as down regulated after treatment with the LXR agonist GW3965 though it tended toward a reduced expression; LXR activation has been reported to increase LDLR protein degradation by inducing IDOL mediated ubiquitination in hepatocytes and macrophages (Zelcer *et al.* 2009). To determine if this effect on LDLR was a cell type specific effect initially IDOL expression was measured in SN4741 cells by qPCR. IDOL protein was not identified in the proteomic data set however IDOL mRNA was detected in SN4741 cells (figure 4.2). Therefore, these proteomic data indicate that in SN4741 cells the predominant mechanism of LDLR regulation is through SREBP2.

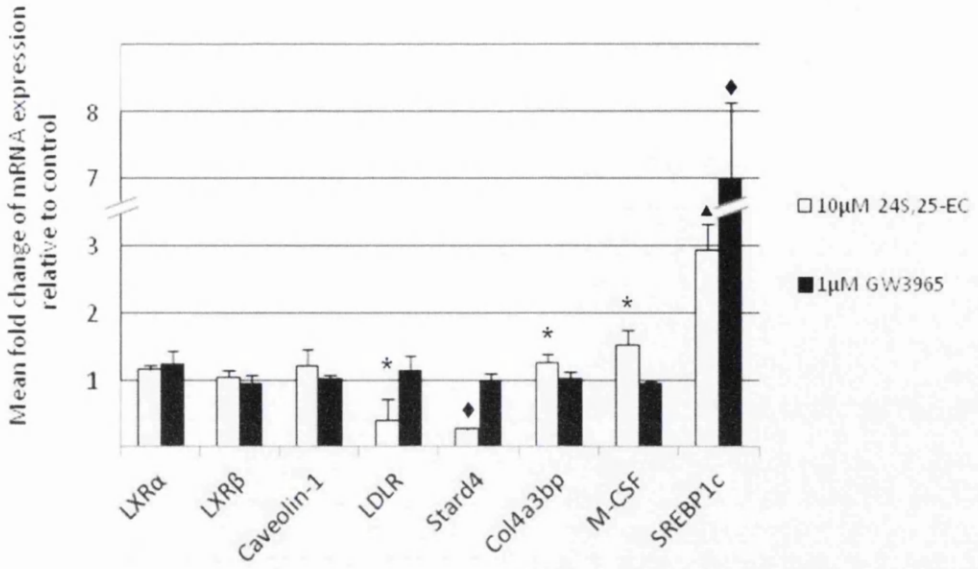

Figure 4.1. SN4741 reverse transcription qPCR. qPCR was performed on RNA extracted from SN4741 cells treated with vehicle, 1μM GW3965 or 10μM 24(*S*),25 epoxycholesterol. Data shown is presented as mean fold change in mRNA expression compared with control; n=3, compared with control * $p<0.05$, Student's t-test; ▲ $p<0.01$, Student's t-test, ♦ $p<0.001$, Student's two tailed t-test.

A number of other genes previously identified as regulated by oxysterols had changes in their expression identified. The LXR regulated gene ABCA1, when identified was up-regulated after treatment with 24(*S*),25-epoxycholesterol and GW3965 (table 3.10). StarD4 was down regulated in the presence of 24(*S*),25-epoxycholesterol but not with GW3965 at the protein and mRNA level (table 3.10; figure 4.1) which tallies with reported SREBP2 regulation (Soccio *et al.* 2005).

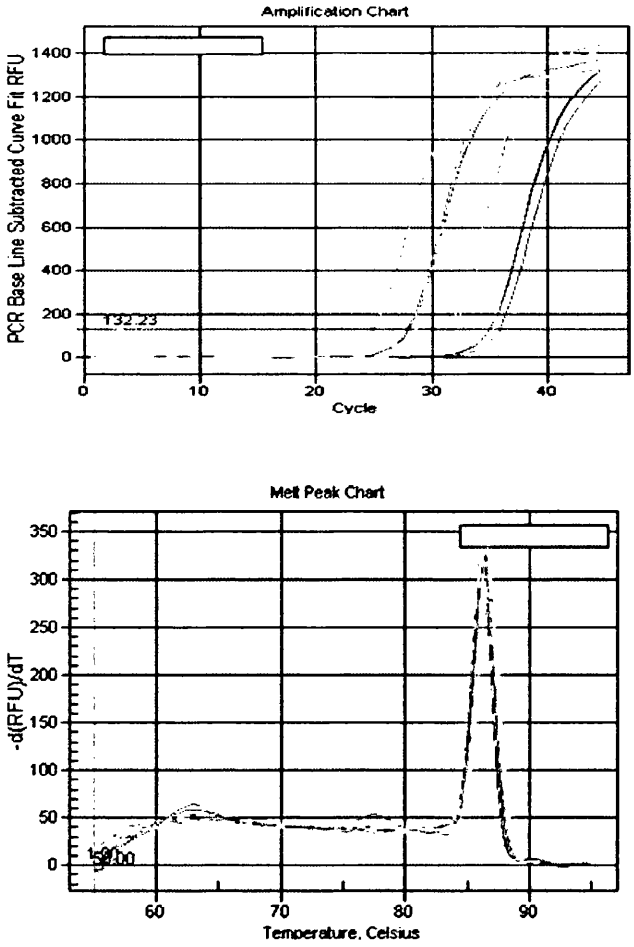

Figure 4.2. IDOL is expressed in SN4741 cells. RT-qPCR indicated the presence of IDOL mRNA in SN4741 cells. cDNA was used neat and at dilutions of 1:10, 1:100 and 1:1000 and qPCR amplification and melt curve plots are shown.

4.2.2. Ligand Binding Induces Up-Regulation of Liver X Receptor β (LXRβ)

Liver X receptor (LXR) is a nuclear receptor for which oxysterols are the natural ligand (see section 1.1.5.2). LXR has two isoforms LXRα and LXRβ. LXRα was not identified in any of the proteomic data sets. However, in the proteomic data LXRβ was identified as up-regulated in the presence of 10μM 24(*S*),25-epoxycholesterol and 1μM GW3965 (table 3.9). Therefore, it appears from these data that activation of LXRβ by either a natural or synthetic ligand causes an increase in its expression. Therefore, the effect of 10μM 24(*S*),25-epoxycholesterol and 1μM GW3965 on

LXRβ expression at the mRNA level was measured using RT-qPCR to examine if this change in the protein level was due to increased transcription. LXRα mRNA expression was also analysed as LXRα has been reported to be self regulating in human macrophages and murine adipose tissue (Laffitte *et al.* 2001, Whitney *et al.* 2001, Li *et al.* 2002, Ulven *et al.* 2004). However, in contradiction, there have been conflicting reports of no change in expression of LXRα after ligand activation in murine RAW264.7 macrophages and primary murine macrophages (Laffitte *et al.* 2001, Li *et al.* 2002). Therefore, this effect appears to be cell type specific. In SN4741 cells the expression of LXRα does not appear to self regulating; no change at the gene expression level of LXRα was observed after treatment with GW3965 or 24(*S*),25-epoxycholesterol. Treatment of SN4741 cells with the LXR ligands (24(*S*),25-epoxycholesterol or GW3965) did not affect the level of LXRβ mRNA expression.

4.2.3. Fatty Acid Synthesis

The complexity of fatty acid synthesis regulation is demonstrated in these data. Some SREBP1c regulated genes (acetyl-CoA carboxylase 1, long-chain-fatty-acid CoA ligase 3, fatty acid synthase) involved in fatty acid synthesis were increased after GW3965 treatment (table 3.10), but, despite the induction of SREBP1c mRNA (fig. 4.1) the expression of these genes were not changed after treatment with 24(*S*),25-epoxycholesterol. Similarly, the previously reported SREBP1 regulated gene, Mid1-interacting protein (Ecker *et al.* 2010) was up-regulated in the presence of GW3965 but not 24(*S*),25-epoxycholesterol. Interestingly, two genes, fatty acid desaturase 2 and lipin 1, that have been identified as SREBP1 regulated were unaffected by GW3965 (table 3.10; Horton *et al.* 2003). These genes, Fatty acid desaturase 2 and lipin 1 were however down-regulated after treatment with 24(*S*),25-epoxycholesterol (table 3.5.).

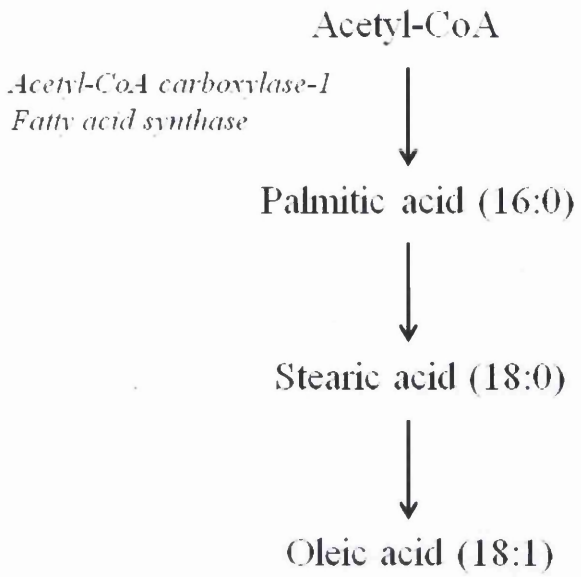

Figure 4.3. Synthesis of the monounsaturated fatty acid oleic acid. The enzymes fatty acid synthase and acetyl-CoA carboxylase-1 are regulated by SREBP1c and were identified as up-regulated after treatment with GW3965.

4.2.4. Phospholipid Synthesis

Reproducible changes were observed in the proteomic data of proteins involved in the synthesis of phospholipids (figure 4.4.) after treatment with 10μM 24(*S*),25-epoxycholesterol including ethanolamine-phosphate cytidylyltransferase and collagen type IV alpha-3-binding protein.

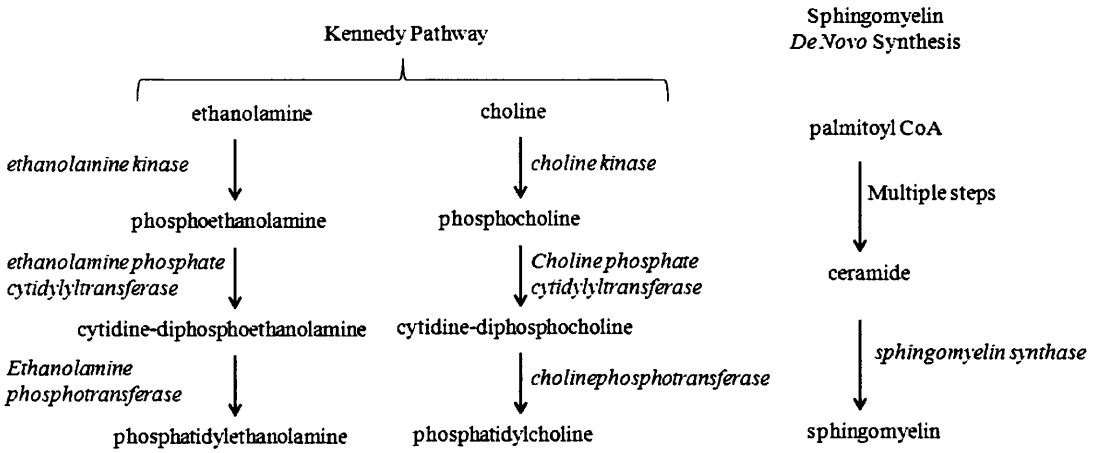

Figure 4.4. Simplified schematic of phospholipid synthesis. Ethanolamine-phosphate cytidylyltransferase was identified as down-regulated after treatment with 24(*S*),25-epoxycholesterol.

4.2.5. Decreased expression of Ethanolamine-phosphate cytidylyltransferase

Ethanolamine-phosphate cytidylyltransferase (PCyt2) is an enzyme involved in phospholipid biosynthesis and catalyses the reaction of cytidine triphosphate with ethanolamine phosphate yielding cytidine diphosphate-ethanolamine (CDP-ethanolamine) and diphosphate. CDP-ethanolamine is then processed further generating phosphatidylethanolamine. Phosphatidylethanolamine is major component of biological membrane and is found in all cells but is particularly abundant in the central nervous system (Bakovic *et al.* 2007 for review).

In the proteomics datasets PCyt2 was identified and quantified as down regulated reproducibly after treatment with 24(*S*),25-epoxycholesterol but not with GW3965 suggesting a SREBP2 mediated mechanism (table 3.10). The mean reduction in ethanolamine-phosphate cytidylyltransferase protein expression after 24(*S*),25-epoxycholesterol treatment was 33% less than that of control cell ethanolamine-phosphate cytidylyltransferase expression. In order to validate these data Western blotting was performed in SN4741 whole cell lysates. Treatment with 24(*S*),25-

epoxycholesterol was shown to down regulate PCyt2 correlating with the proteomics data (fig 4.5). Densitometry analysis showed that PCyt2 was reduced by 15% in 24(*S*),25-epoxycholesterol treated cells. This was less than observed in the proteomic experiments but highlighted the same trend. There was no significant change with GW3965

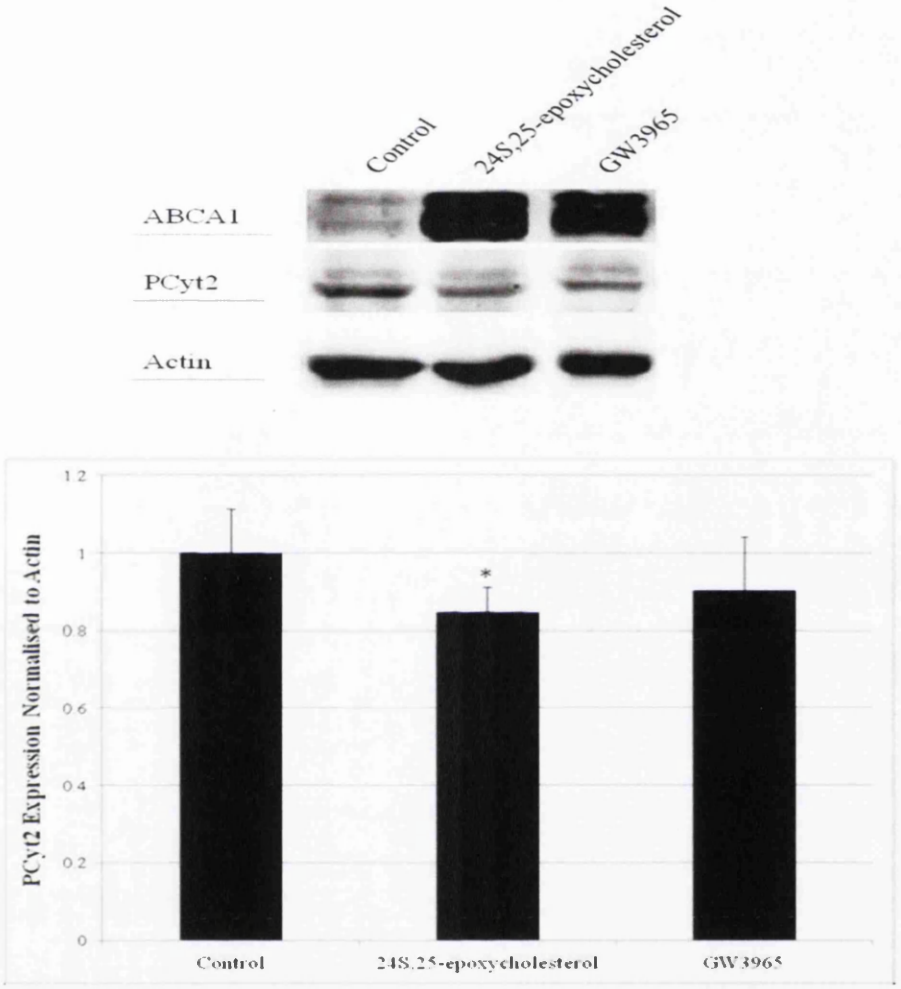

Figure 4.5. Western blotting confirmed the observed down-regulation of phosphoethanolamine cytidylyltransferase (PCyt2) in SN4741 cells. 10μM 24(*S*)25 epoxycholesterol decreased the expression of PCyt2 (lane 2) whilst 1 μM GW3965 had no effect on PCyt2 expression (lane 3). Both GW3965 and 24(*S*)25 epoxycholesterol induced ABCA1 (A lanes 2 and 3). Densitometry showed a significant ($p \leq 0.05$) decrease in PCyt2 expression of 15% compared with control (n=3, Student's t-test).

4.2.6. Increased expression of Collagen type IV alpha-3-binding protein

Collagen type IV alpha-3-binding protein (col4a3bp; Ceramide transfer protein; Goodpasture antigen-binding protein; StAR-related lipid transfer protein 11) transfers ceramide from where it is synthesised in the endoplasmic reticulum to the Golgi apparatus where it is utilised in the synthesis of the phospholipid sphingomyelin (Hanada *et al.* 2007 for review). Collagen type IV alpha-3-binding protein has been associated with oxysterol binding protein (OSBP) and the presence of 25-hydroxycholesterol promotes activation of collagen type IV alpha-3-binding protein mediated transfer of ceramide to the Golgi apparatus and, therefore, an increased rate of sphingomyelin synthesis (Perry & Ridgeway 2006). In addition, phosphorylation of OSBP at serine240 by protein kinase D impairs the Golgi localisation of collagen type IV alpha-3-binding protein (Nhek *et al.* 2010). These data suggest a regulatory role for oxysterols in ceramide processing. Interestingly, in some vertebrate species collagen type IV alpha-3-binding protein may have a role in embryo development as in a zebrafish knockout model it appears to play an anti-apoptotic role and is required for normal skeletal muscle and brain growth (Granero-Molto *et al.* 2008).

The proteomics showed that collagen type IV alpha-3-binding protein expression increased reproducibly after treatment with 24(*S*),25-epoxycholesterol (table 3.10). No change was observed after treatment with GW3965 suggesting an LXR independent mechanism. The identification of collagen type IV alpha-3-binding protein was from multiple peptides and from all biological replicates lending confidence that this observation is a true change (table 3.6). The mean increase in collagen type IV alpha-3-binding protein expression after 24(*S*),25-epoxycholesterol treatment was 45% more than that of control cell collagen type IV alpha-3-binding protein expression.

In order to determine if the increase observed at the protein level was due to increased transcription RT-qPCR experiments were performed. The mRNA expression of collagen type IV alpha-3-binding protein increased modestly after 24(*S*),25-epoxycholesterol treatment for 24 hours (fig. 4.1). The increase was of a similar magnitude to the change in protein expression seen in the proteomics data. And whilst this increase was statistically significant the p value was close to the 0.05 limit

(p=0.046). No change was observed in collagen type IV alpha-3-binding protein mRNA expression after treatment with GW3965.

4.2.7. 24(*S*),25-epoxycholesterol Effects Caveolin-1 Expression and Localisation

Caveolin-1, a 20-22kDa protein, is a membrane protein that has multiple functions including roles in endocytosis and cell signalling (reviewed in Parton & Simons 2007; Hansen & Nichols 2010). Caveolin-1 forms hairpin loops protruding from the plasma membrane into the cytoplasm by having the C and N termini of the protein anchored to the lipid bilayer. Caveolin can oligomerise with itself and these homooligomers associate with cholesterol and sphingomyelin in order to form caveolae. Caveolae are invaginations in the plasma membrane wall that have many intracellular functions. Each caveolae domain has been estimated to contain 100-200 caveolin proteins and ~10x the number of cholesterol molecules. These hydophobic parts of the membrane are termed lipid rafts.

Caveolin-1 was identified in the SILAC proteomic experiments as down regulated (table 3.10). Caveolin-1 was identified in all three biological and technical replicates. The mean reduction in caveolin-1 protein expression after 24(*S*),25-epoxycholesterol treatment was 30% less than that of control cell caveolin-1 expression. Western blotting was performed in order to validate this result. Caveolin-1 showed a decrease in protein expression after 24 hours when measured by immunoblotting (fig 4.6). Densitometry indicates that this observed decrease, when normalised to actin was similar to that observed in the proteomic data for both 24(*S*)25 epoxycholesterol and GW3965. Caveolin-1 was reduced by 32% in 24(*S*),25-epoxycholesterol treated cells and 15% in GW3965 treated cells. This was comparable to the observations in the proteomic experiments.

It has been reported that caveolin-1 expression is regulated, at least in part, by changes in the level of cholesterol (Hailstones *et al.* 1998). Moreover, it appears that oxysterols (7-ketocholesterol, 7α-hydroxycholesterol) can influence the transcription of caveolin-1 (Fielding *et al.* 1997). Therefore, to analyse whether the observed effects on caveolin-1 expression on SN4741 cells was due to changes in transcription RT-qPCR experiments were performed.

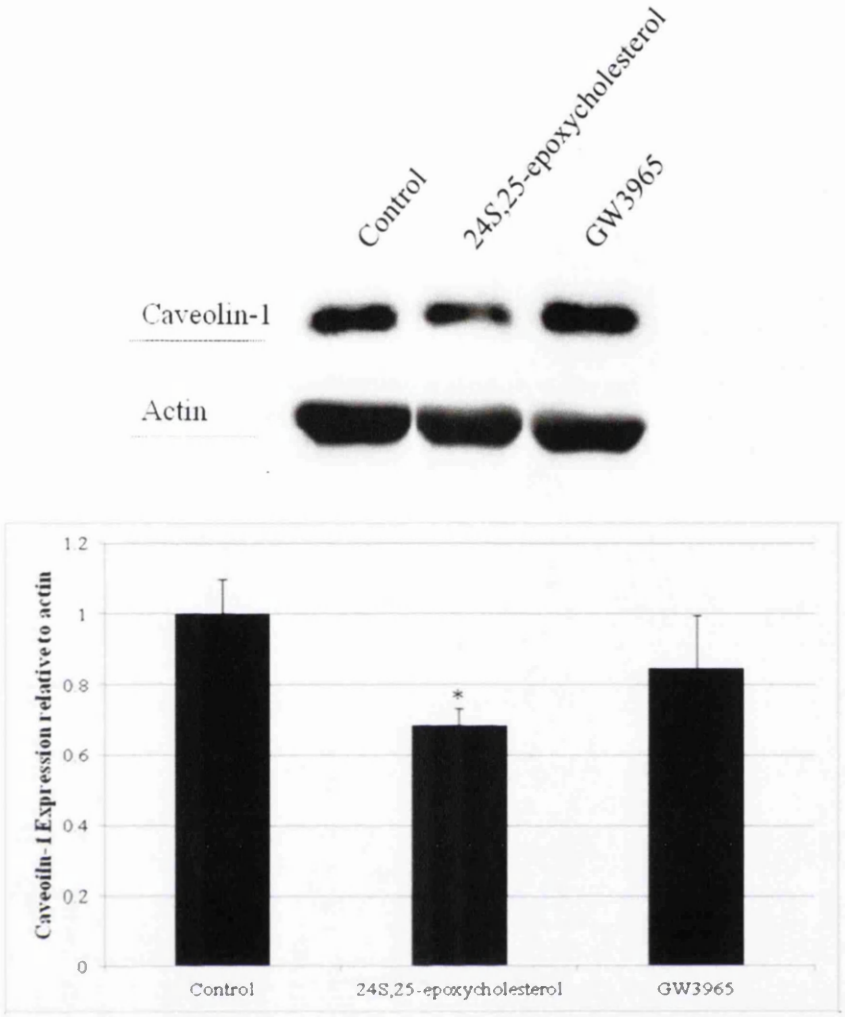

Figure 4.6. Western blotting confirmed the observed down-regulation of caveolin-1 in SN4741 cells. 10μM 24(*S*)25-epoxycholesterol and 1 μM GW3965 decreased the expression of caveolin-1 (lane 2). Results are indicative of 3 independent experiments. Densitometry showed a significant ($p \leq 0.05$) decrease in caveolin-1 expression of 32% after 24(*S*)25-epoxycholesterol treatment but no significant change after GW3965 treatment compared with control (n=3, Student's t-test).

Caveolin-1 expression showed no change at the mRNA level after treatment with GW3965 or 24(*S*),25-epoxycholesterol (fig 4.1). At the protein level 24(*S*),25-epoxycholesterol induced changes in caveolin-1 that was identified in the proteomics data (table 3.10) and by Western blotting (fig 4.6). This implies that the effect of 24(*S*),25-epoxycholesterol is due to post-translational effects. As mentioned earlier, lipid rafts that form the subcellular location of caveolin-1 have an abundance of

cholesterol and are usually found on the plasma membrane. Changes in the intracellular cholesterol could potentially affect caveolin-1 by disrupting the composition of lipid rafts. This implies that oxysterols could interfere with caveolin-1 localisation by inhibiting cholesterol synthesis. In order to test this hypothesis immunofluorescence confocal microscopy was undertaken in order to observe the effect in caveolin-1 localisation that oxysterols induced in SN4741 cells.

SN4741 cells fixed in 4% paraformaldehyde showed predominant plasma membrane labelling of caveolin-1 (fig 4.7) Exposure of the SN4741 cells to 24(*S*),25-epoxycholesterol led to a loss of caveolin-1 from the membrane and a predominantly intracellular location. Incubation with 1μM GW3965 did not change the localisation pattern observed. GW3965 induces ABCA1 to export cholesterol but does not reduce cholesterol synthesis. The experimental approach was performed in serum free conditions and therefore this observation might be due to the inability of media to accept the exported cholesterol. Whether there would be a different observation *in vivo* is unclear. In addition other oxysterols were tested. Oxysterols with the greatest affinity for Insig (Radhakrishnan *et al.* 2007) and, therefore, the greatest antagonism of SREBP2 regulated gene transcription led to a more pronounced change in localisation. 24*S*-hydroxycholesterol, 25-hydroxycholesterol and 27-hydroxycholesterol treatment (all at 10μM) resulted in localisation being disrupted similarly to 24(*S*),25-epoxycholesterol. In comparison, 7α-hydroxycholesterol and 19-hydroxycholesterol, 2 oxysterols that are classed as having intermediate or minimal SREBP2 inhibitory effects respectively, showed a negligible effect on the distribution of caveolin-1 (fig 4.8).

To analyse if the effects of 24(*S*),25-epoxycholesterol, 24*S*-hydroxycholesterol, 25-hydroxycholesterol and 27-hydroxycholesterol were due to inhibition of cholesterol synthesis, and therefore intracellular cholesterol depletion, SN4741 cells were co-incubated with 10μM oxysterol and 250μM cholesterol (fig 4.7; fig 4.8). The presence of cholesterol antagonised the changes in caveolin-1 localisation observed after oxysterol treatment alone with a normalisation of signal to the plasma membrane. This suggests that caveolin-1 localisation is regulated, at least partially, by changes in the intracellular cholesterol level. Therefore, these data show that 24(*S*),25-epoxycholesterol, and other oxysterols, can induce changes in protein

expression and localisation due to indirect effects either by inducing changes on the cellular cholesterol level or by disrupting lipid rafts.

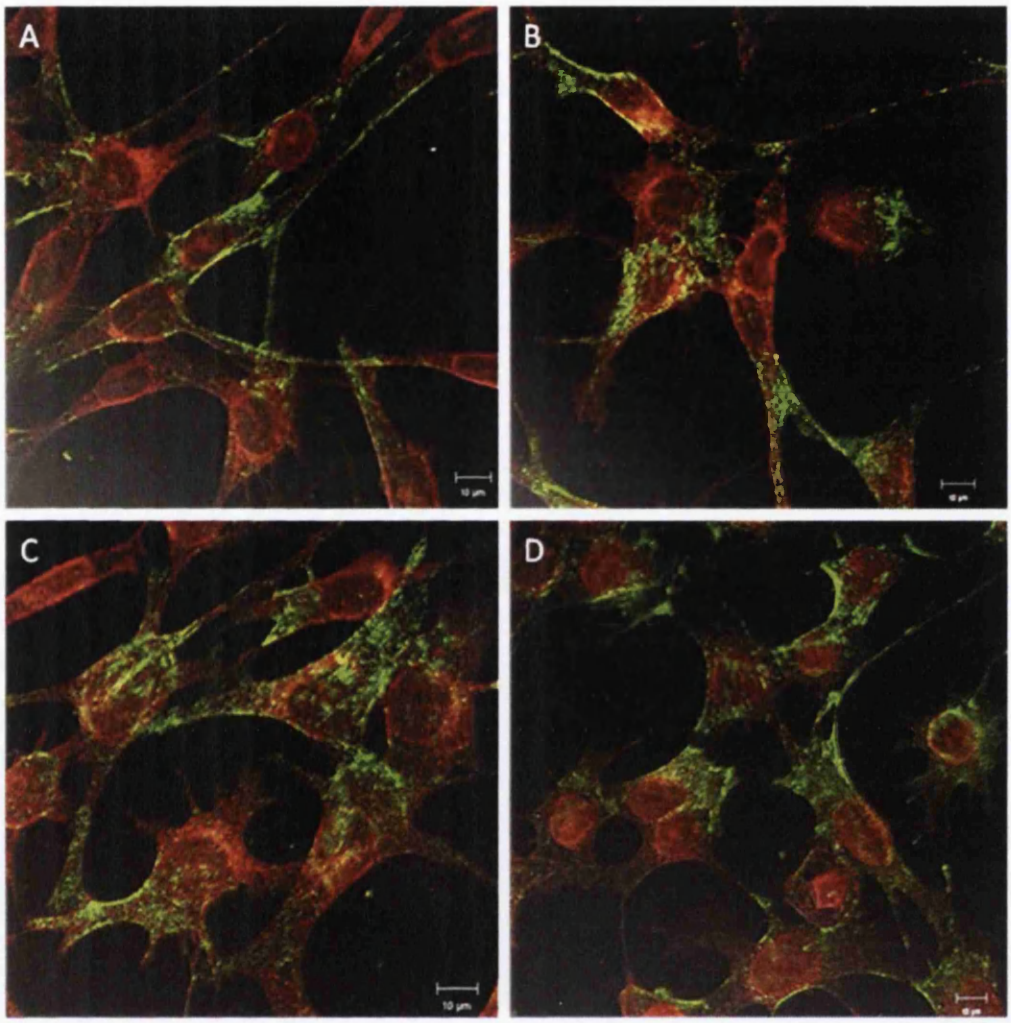

Figure 4.7. Confocal microscopy performed on paraformaldehyde fixed SN4741 cells. Caveolin-1 labelled with monoclonal antibody and using appropriate Alexa 488 labelled secondary. Vehicle treated control cells (A) has a predominant distribution of caveolin-1 on the plasma membrane. Treatment with 1μM GW3965 (B) and 10μM 24(*S*),25-epoxycholesterol (C) led to a reduction in signal located on the cell surface and to a predominantly internal distribution of caveolin-1. Co-incubation of 10μM 24(*S*),25-epoxycholesterol with 250μM cholesterol resulted in caveolin-1 localisation to partially normalise to the plasma membrane (D).

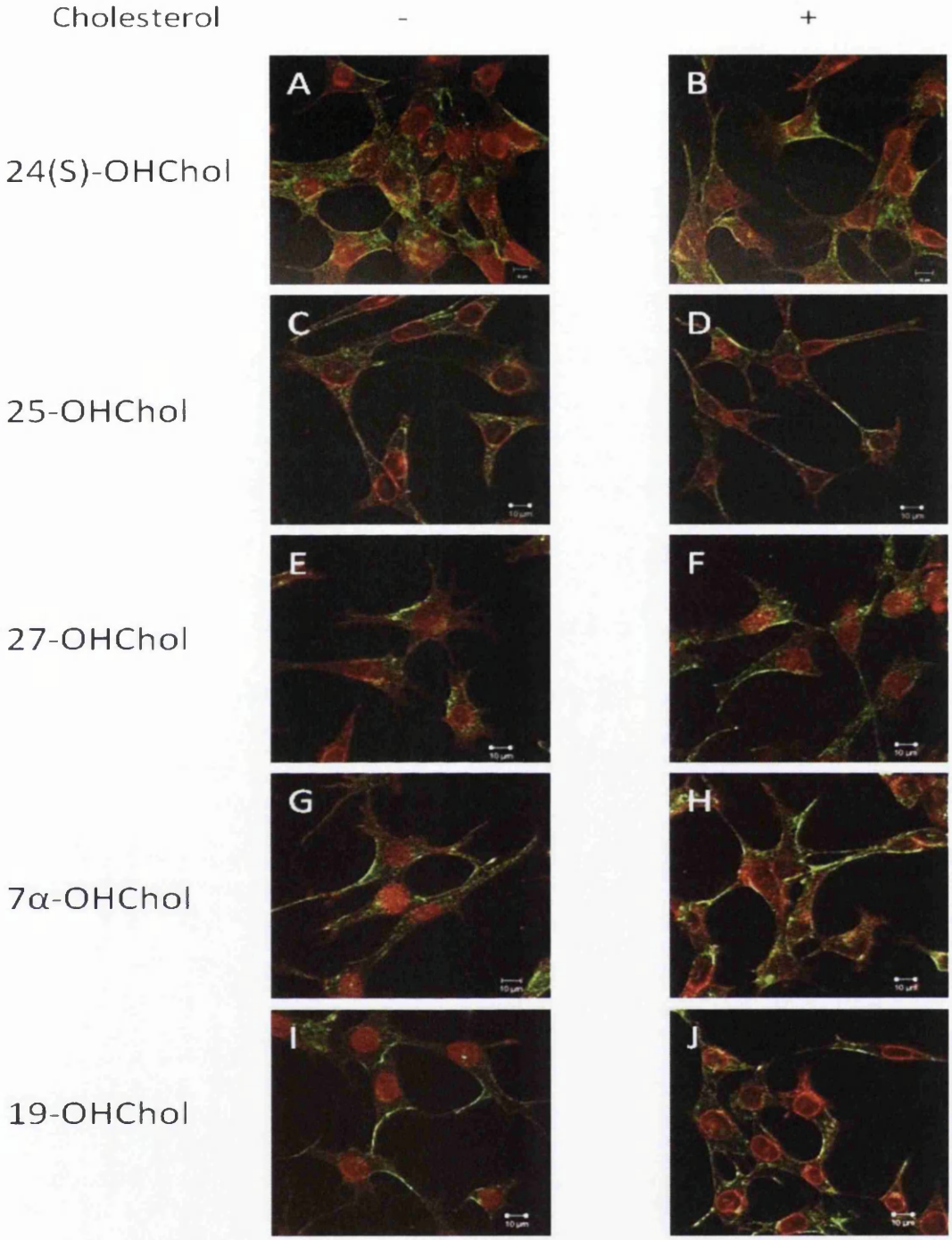

Figure 4.8. Confocal microscopy performed on paraformaldehyde fixed SN4741 cells. Caveolin-1 labelled with monoclonal antibody and using appropriate Alexa 488 labelled secondary. 10μM 24*S*-hydroxycholesterol (24(S)-OHChol, A), 10μM 25-hydroxycholesterol (25-OHChol, C), 10μM 27-hydroxycholesterol (27-OHChol, E) led to a reduction in signal located on the cell surface and to a predominantly internal distribution of caveolin-1. Co-incubation of 10μM 24*S*-hydroxycholesterol, 10μM 25-

hydroxycholesterol, 10μM 27-hydroxycholesterol with 250μM cholesterol resulted in caveolin-1 localisation to partially normalise to the plasma membrane (B, D, F). 10μM 19-hydroxycholesterol (19-OHChol, G) and 10μM 7α-hydroxycholesterol (7α–OHChol, I) showed no change in signal located on the cell surface. Co-incubation of 10μM 19-hydroxycholesterol and 10μM 7α-hydroxycholesterol with 250μM cholesterol had no effect (H, J).

4.2.8. Changes in miscellaneous proteins

Other proteins, with no apparent link to cholesterol, phospholipids or fatty acids were also identified as having a changed expression. 2 proteins that were reproducibly observed as being up regulated were Golgi apparatus protein 1 and macrophage colony stimulating factor.

4.2.8.1 Golgi sialoglycoprotein MG-160

Golgi sialoglycoprotein MG-160 (ESL1; GLG1; E-selectin ligand 1; Golgi apparatus protein 1) is a protein associated with the membrane of the Golgi apparatus though its function is unknown (Gonatas *et al.* 1989). It is however, expressed early in embryo development of some vertebrate species suggesting a potential role in development. In chick embryos Golgi sialoglycoprotein MG-160 has been observed as expressed after 3 days with high levels in the notochord, neural tube, somites, and cartilage (Stieber *et al.* 1995).

The proteomics showed that Golgi sialoglycoprotein MG-160 expression increased reproducibly after treatment with 24(*S*),25-epoxycholesterol (table 3.10). No change was observed after treatment with GW3965 suggesting an LXR independent mechanism. The mean increase in Golgi sialoglycoprotein MG-160expression after 24(*S*),25-epoxycholesterol treatment was 36% more than that of control cells Golgi sialoglycoprotein MG-160 protein expression. The identification of Golgi sialoglycoprotein MG-160 was from multiple peptides and from all biological replicates lending confidence that this observation is a true change. To identify this protein at least 3 unique peptides were used whilst the maximum was 22 unique

peptides and thus the large number of peptides identified lends weight to the observed changes in protein expression. However, as a note of caution, no further validation was undertaken.

4.2.8.2. Increased Expression of Macrophage Colony Stimulating Factor

Macrophage colony stimulating factor (MCSF; Colony stimulating factor 1, CSF-1), was identified in the SILAC experiments as up-regulated reproducibly in SN4741 cells after 10μM 24(*S*),25-epoxycholesterol but not 1μM GW3965 (table 3.10). MCSF is a α-helical cytokine whose primary role is a inducer of mononuclear cell activity by promoting the survival, proliferation and differentiation of monocytes and macrophages (Sweet & Hume 2003 for review) and acts through MCSF receptor (MCSF-R; c-fms). MCSF deficient mice are macrophage deficient but also suffer from osteopetrosis due to a reduction in osteoclast numbers (Yoshida *et al.* 1990; Wiktor-Jedrzejczak *et al.* 1990). In addition, MCSF deficient mice are infertile suggesting a role in reproduction (Pollard *et al.* 1991). The absence of MCSF results in mental retardation due to abnormal brain development (Michaelson *et al.* 1996). Thus, MCSF is essential for healthy development.

SN4741 cells are a neuronal cell line and therefore due to the implication of oxysterols in brain development the observed proteomic change in MCSF expression warranted further analysis. MCSF was identified in all three biological replicates and 5 of the 6 technical replicates. The mean increase in MCSF protein expression after 24(*S*),25-epoxycholesterol treatment was ~34% more than that of control cell MCSF expression (table 3.10). However, the change in the proteomic data was unable to be validated by Western blotting the same lysates (fig 4.9). Immunoblotting of SN4741 whole cell lysates showed no change in the level of MCSF after 10μM 24(*S*),25-epoxycholesterol or 1μM GW3965 treatment. Densitometry indicates that neither treatment had an effect on the observed level of MCSF.

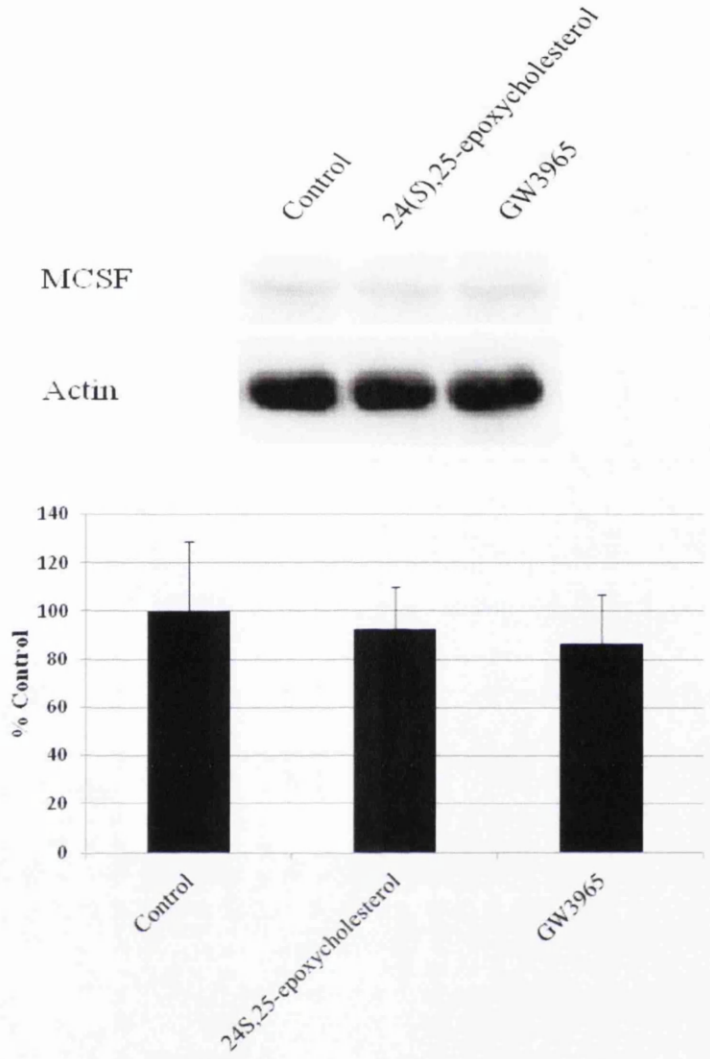

Figure 4.9. Western blotting of SN4741 lysates probing for MCSF. No significant change was observed in MCSF protein expression by Western blotting compared with control after treatment with 10μM 24(*S*),25-epoxycholesterol or 1μM GW3965 (n=3, Student's t-test).

To determine if the observed change in the proteomic data resulted from an increase to the transcription of the MCSF gene qRT-PCR was performed. The transcription of MCSF was not increased in the presence of GW3965, 7α-hydroxycholesterol and 7β-hydroxycholesterol. In contradiction a modest, but significant, increase was observed after treatment with 24(*S*),25-epoxycholesterol, 24(S)-hydroxycholesterol, and 25-

hydroxycholesterol (fig 4.10). 24(*S*),25-epoxycholesterol, 24(S)-hydroxycholesterol and 25-hydroxycholesterol led to a ~1.5 fold increase in the mRNA level after 24 hours of treatment. The oxysterols that caused an increase in MCSF were oxygenated on the side chain and natural efficacious ligands for LXR. However, as GW3965 did not induce any change in the mRNA level of MSCF it can be inferred that the mechanism of action is not through LXR.

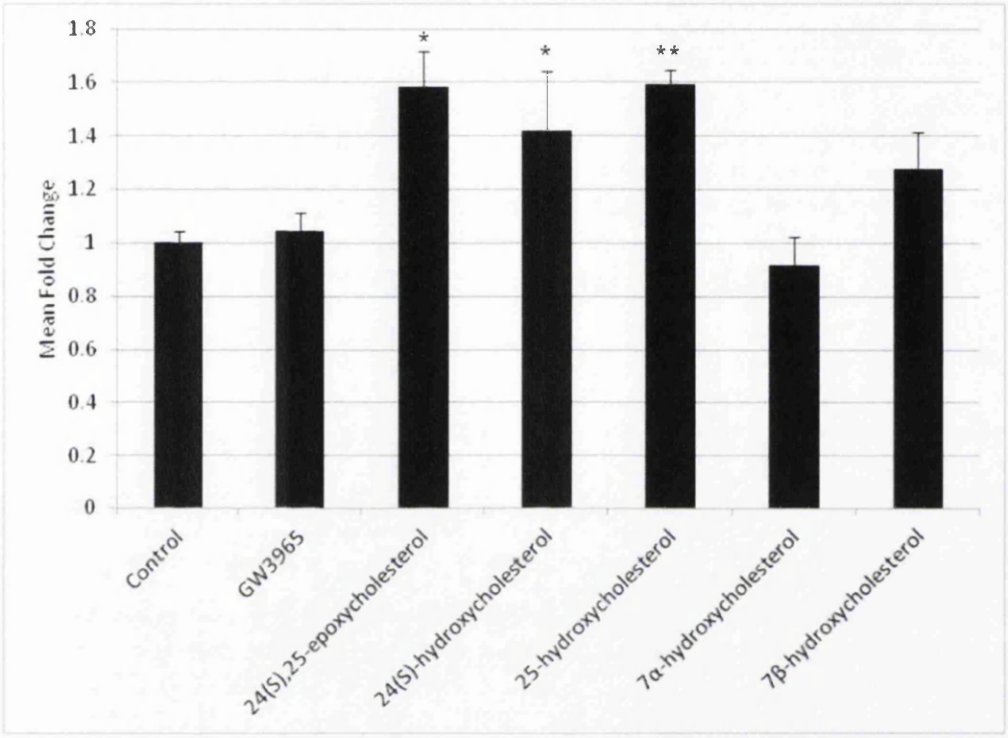

Figure 4.10. qPCR showing mean fold change in MCSF expression in SN4741 cells. Treatment with sidechain oxygenated oxysterols resulted in a modest but statistically significant increase in MSCF expression after 24 hours in an apparently LXR independent mechanism as 1μM GW3965 treatment did not result in an observable change in expression. 10μM 24(*S*),25-epoxycholesterol, 10μM 24(*S*)-hydroxycholesterol and 10μM 25-hydroxycholesterol increased expression of MCSF ~1.5fold. Ring oxygenated oxysterols (7α-hydroxycholesterol or 7β-hydroxycholesterol) did not significantly change the expression of MCSF. Compared with control, n=3, * $p<0.05$, Student's t-test; ** $p<0.01$, Student's t-test.

In order to determine if the increased expression of MCSF observed at the protein level in the SILAC proteomic data and at the mRNA level in the qPCR data resulted in an increased secretion from SN4741 cells an enzyme linked immunosorbant assay (ELISA) was performed (fig 4.11). The ELISA allowed the detection of MCSF in the cell culture medium of SN4741 cells treated with vehicle, 1μM GW3965 or 10μM oxysterol (24(*S*),25-epoxycholesterol, 24(*S*)-hydroxycholesterol, 25-hydroxycholesterol, 7α-hydroxycholesterol, 7β-hydroxycholesterol). The concentration of the internal control, supplied as part of the kit, calculated by standard curve fell into the acceptable limits for the assay. MCSF secretion was detected at low levels in SN4741 cells with the concentration in the cell culture media of ~70pg/ml. No differences were observed in the secreted MCSF level between different treatment groups (ANOVA $p>0.05$).

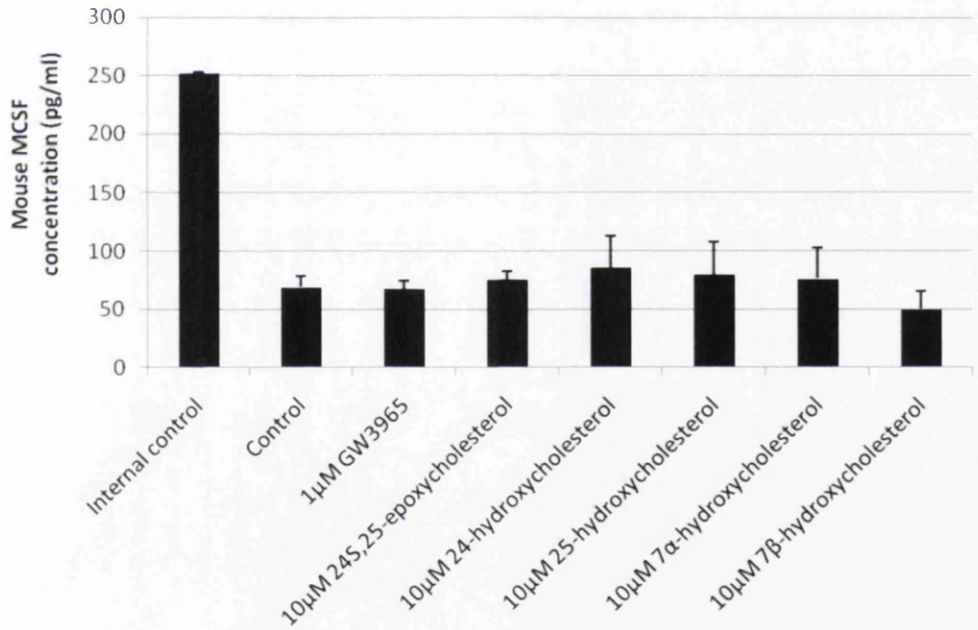

Figure 4.11. ELISA assay of secreted MCSF concentration in SN4741 cell supernatant. No significant difference in MCSF secretion was observed with 1μM GW3965 or 10μM oxysterol treatment (n=3, ANOVA).

4.2.9. Increased MCSF mRNA expression in THP1 human monocytes.

As mentioned earlier (section 4.2.8.2) MCSF is a cytokine and its biological role includes the inducement of monocytes to differentiate to macrophages. Therefore, following the data from the SN4741 cells that MCSF was modestly up-regulated after oxysterol treatment, experiments were undertaken in THP1 human monocytes in order to determine the effect, if any, oxysterols were inducing.

In THP1 monocytes there was a large response to oxysterols at the mRNA level (fig 4.12). All oxysterol treatments (24(*S*),25-epoxycholesterol, 24(*S*)-hydroxycholesterol, 25-hydroxycholesterol, 7α-hydroxycholesterol, 7β-hydroxycholesterol) resulted in an up-regulation in MCSF expression. The greatest response, with a 35 mean fold change compared with control was 25-hydroxycholesterol. The other oxysterols tested (24(*S*),25-epoxycholesterol, 24(*S*)-hydroxycholesterol, 7α-hydroxycholesterol, 7β-hydroxycholesterol) gave a reduced but still significant response. These oxysterols gave a varied response with 7α-hydroxycholesterol < 24(*S*),25-epoxycholesterol < 24(*S*)-hydroxycholesterol < 7β-hydroxycholesterol < 25-hydroxycholesterol. Interestingly, there was no change with GW3965 suggesting an LXR independent mechanism. This is supported by the data that shows that 7α-hydroxycholesterol, an oxysterol classed as a poor activator of LXRα and LXRβ (Janowski *et al.* 1999), is inducing changes in MCSF expression.

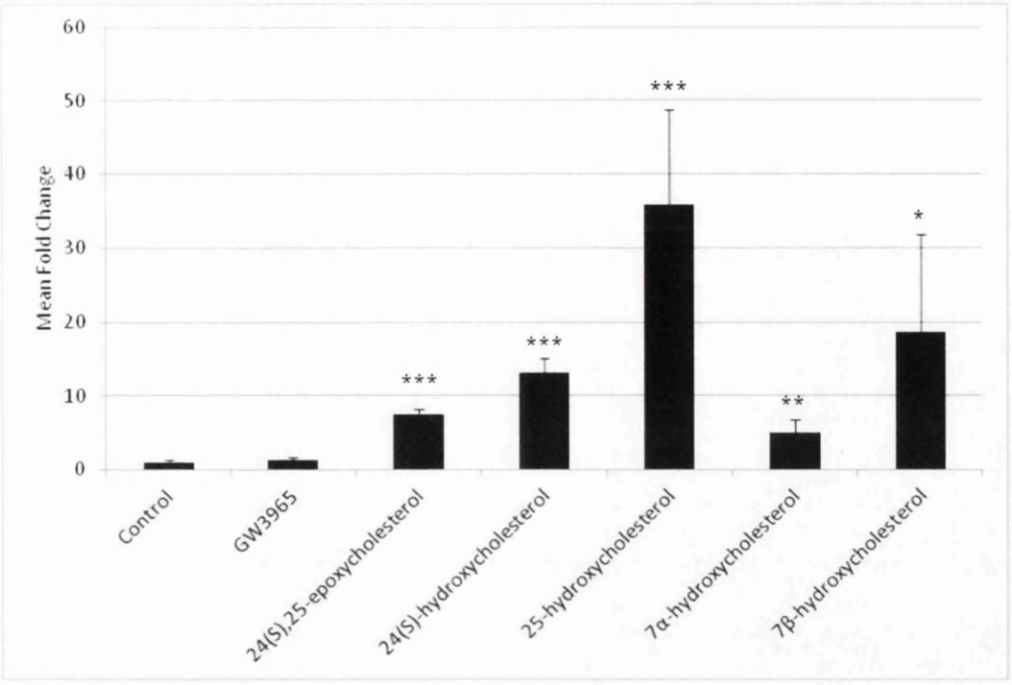

Figure 4.12. qPCR showing mean fold change in MCSF expression in THP1 monocytes. Treatment with sidechain oxygenated oxysterols resulted in a significant increase in MCSF expression. 25-hydroxycholesterol treatment resulted in the greatest observed change after 24 hours in an apparently LXR independent mechanism as 1μM GW3965 treatment did not result in an observable change in expression c.f. control. 10μM 24(*S*),25-epoxycholesterol, 10μM 24(*S*)-hydroxycholesterol ($p<0.05$, Student's t-test) and 10μM 25-hydroxycholesterol ($p<0.01$, Student's t-test) increased MCSF expression. Unlike in SN4741 cells the cholesterol ring oxygenated oxysterols 7α-hydroxycholesterol and 7β-hydroxycholesterol also induced significant increases in MCSF gene expression. Compared with control, n=3, * $p<0.05$, Student's t-test; ** $p<0.01$, Student's t-test, ***$p<0.001$, Student's t-test.

In order to determine if the observed increase in MCSF mRNA was coupled with an increase at the protein level immunoblotting was performed. Western blotting was performed using anti-MCSF primary antibody supplied with a MCSF ELISA kit for detection was used to probe for MCSF. The antibody is directly linked to horseradish peroxidase and therefore required no secondary antibody before detection using chemiluminescence. Western blotting of whole cell lysates did not identify a difference in the level of MCSF in THP1 monocytes after 24 hour treatment with

GW3965, 24(*S*),25-epoxycholesterol or 25-hydroxycholesterol (figure 4.13). Thus, the significant increase observed at the mRNA level appears not to be reproduced post translationally at the protein level.

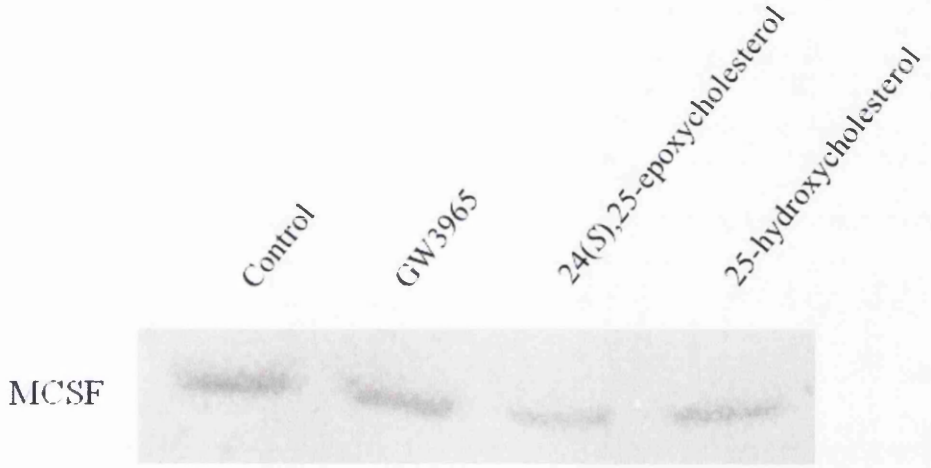

Figure 4.13. Western blot showing no change in MCSF protein expression in THP1 monocytes. No increase was observed in MCSF expression after treatment with 1μM GW3965, 10μM 24(*S*),25-epoxycholesterol or 10μM 25-hydroxycholesterol for 24 hours (n=1).

As shown previously in THP1 monocytes there is a large increase in MCSF mRNA expression following oxysterol treatment (fig 4.12) that is not corroborated at the protein level (fig. 4.13). It is possible, though unlikely, that no change in MCSF protein was due to increased secretion from the cells of newly synthesised protein. Thus, creating a situation whereby protein synthesis is increased but impossible to detect by examination of whole cell lysate due to the protein being secreted leading to no net change. Therefore, an enzyme linked immunosorbant assay (ELISA) was performed. The ELISA assay was performed on cell culture media taken from human THP1 monocytes treated with vehicle, GW3965, or various oxysterols (24(*S*),25-epoxycholesterol, 24(*S*)-hydroxycholesterol, 25-hydroxycholesterol, 7α-hydroxycholesterol, 7β-hydroxycholesterol; fig 4.14). This assay was performed in order to determine if the significant up-regulation of MCSF expression observed at

the mRNA level corresponded to an increase in secretion of MCSF. The MCSF concentration for all treatments, when quantified with a standard curve, fell below the concentration of the lowest concentration standard (78.125pg/ml) and therefore from these data it appears that oxysterol treatment alone does not directly stimulate MCSF secretion in THP1 cells.

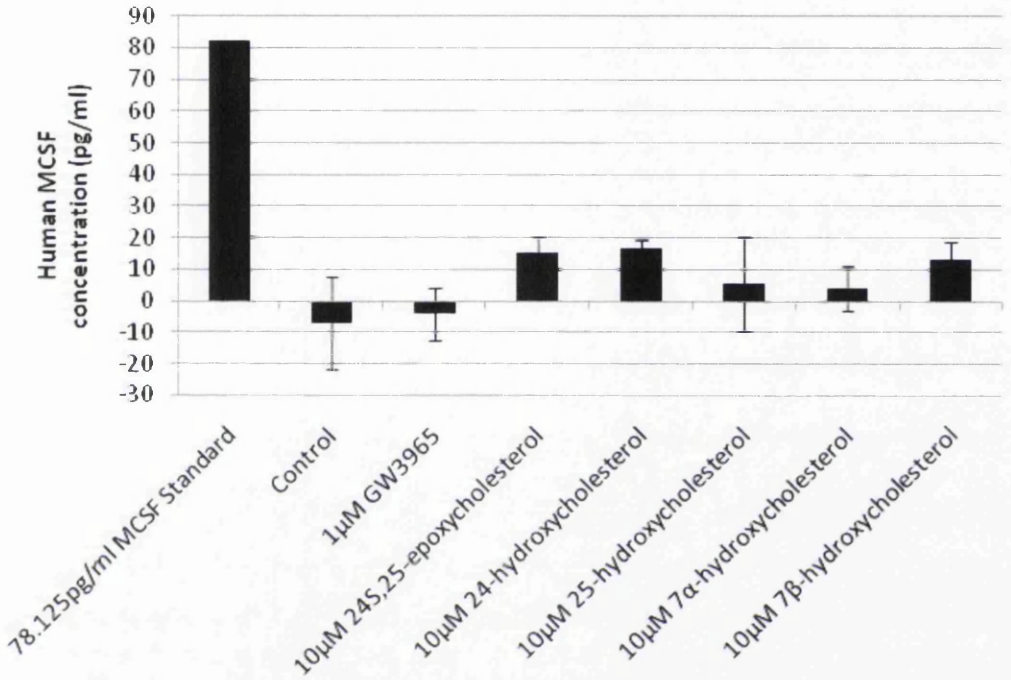

Figure 4.14. ELISA assay of secreted MCSF concentration in THP1 cell supernatant. All treatments were below the concentration of the most dilute MCSF standard. Thus, THP1 monocytes appear not secrete MCSF in the presence of oxysterols.

4.3. Discussion

SREBP1c is the main transcription factor responsible for the regulation of fatty acid synthesis. The transcription of SREBP1c is induced by LXRα, however the processing of SREBP1c is inhibited by Insig binding. As oxysterols mediate both LXRα activation and Insig inhibition there is a balance between the two opposing effects. In some cases, such as SREBP1c regulated genes acetyl-CoA carboxylase 1 and fatty acid synthase the net effect after 24(*S*),25-epoxycholesterol is no change at the protein level whilst GW3965 increased the expression of these genes due to the lack of the Insig inhibitory effect. However, for other genes also regulated by SREBP1c, such as fatty acid desaturase 2 (table 3.10), it appears that the binding of Insig overcome the effect of increased SREBP1 causing a reduction in gene expression after treatment with 24(*S*),25-epoxycholesterol. These effects may be cell type specific as the SREBP1c induction is due to LXRα whose expression varies between different tissues.

The nuclear receptor LXRβ, for which oxysterols are the natural ligand, was identified as up-regulated after treatment with both 24(*S*),25-epoxycholesterol and the synthetic ligand GW3965 suggesting a LXR dependent mechanism. It is interesting that LXRβ was not increased at the mRNA level (fig 4.1), i.e. that transcription was not increased, as there is some evidence that the binding of ligand to LXRβ prevents degradation of the nuclear receptor (Kim *et al.* 2009). Cells were transfected with FLAG tagged LXRβ and, after cycloheximide treatment to prevent new protein synthesis, the degradation of the protein was measured. The binding of ligand to LXRβ slowed the degradation of LXRβ. Therefore, we hypothesise that the increase at the proteomic level is due to a decrease in degradation of LXRβ but with no decrease in protein production. These data are the first to show that ligand binding can increase the level of endogenous LXRβ protein.

It appears that the presence of 24(*S*),25-epoxycholesterol has differential effects on members of the StAR-related lipid transfer protein family of transporters. StAR-related lipid transfer protein 4 (Stard4) is regulated by SREBP2 and transports cholesterol (Soccio *et al.* 2005). At both the protein and mRNA level Stard4 is down-regulated after 24(*S*),25-epoxycholesterol treatment (table 3.10; fig. 4.1).

Interestingly, the converse is true of Collagen type IV alpha-3-binding protein (col4a3bp; StAR-related lipid transfer protein 11, Stard11). At both the protein and mRNA level Collagen type IV alpha-3-binding protein is up-regulated after 24(*S*),25-epoxycholesterol treatment (table 3.10; fig. 4.1). Collagen type IV alpha-3-binding protein transports ceramide from the endoplasmic reticulum to the Golgi apparatus where it is synthesised to sphingomyelin. Interestingly, an LXR responsive gene, ABCG1, exports both cholesterol and sphingomyelin (Kennedy *et al.* 2001; Sabol *et al.* 2005; Sano *et al.* 2007). Therefore, the increase in Collagen type IV alpha-3-binding protein might be a homeostatic feedback to prevent reduced levels of sphingomyelin by increasing the rate of synthesis of the phospholipid. Indeed, this hypothesis fits the observation that the presence of 25-hydroxycholesterol promotes activation of Collagen type IV alpha-3-binding protein mediated transfer of ceramide to the Golgi apparatus and, therefore, an increased rate of sphingomyelin synthesis (Perry & Ridgeway 2006).

It appears that oxysterols have multiple roles in membrane homeostasis. It has been shown that the enzyme phosphoethanolamine cytidylyltransferase (PCyt2) that is required for phosphoethanolamine synthesis is down-regulated after 24(*S*),25-epoxycholesterol treatment. During the period where this work was undertaken it has been independently reported in the literature that PCyt2 is regulated by SREBP2 and, therefore, oxysterols in mouse NIH3T3 fibroblasts (Ando *et al.* 2010). Therefore, these data presented here corroborates the previously reported data generated from a different cell type and shows that 24(*S*),25-epoxycholesterol regulates PCyt2 in SN4741 neurons by modulating SREBP induced transcription. However, another enzyme previously reported to be regulated by SREBP2, phosphocholine cytidylyltransferase (Pcyt1) was identified in the proteomics data as having no change in expression (table 3.10.; Kast *et al.* 2001).

The expression and localisation of the membrane protein caveolin-1 appears to be influenced indirectly by 24(*S*),25-epoxycholesterol. Caveolin-1 was observed as down-regulated at the protein level but unchanged at the mRNA level (table 3.10; fig. 4.1; fig 4.6). Two major components of lipid rafts are caveolin-1 and cholesterol and thus we hypothesise that the level of the two are interdependent and that in this case a change in the intracellular cholesterol level is responsible for the observation of decreased protein expression. This hypothesis is supported by the confocal

microscopy data that demonstrates that oxysterols with a high affinity for Insig affect the localisation of caveolin-1 and that this effect can be negated by co-incubating with cholesterol (fig 4.7; fig 4.8). This relationship, could potentially explain the observation that in apolipoprotein E (ApoE) knockout mice there was an increased expression of brain caveolin-1 (Gaudreault *et al.* 2004). As ApoE is a cholesterol transporter this implicates a role for cholesterol homeostasis dysregulation in the observed up-regulation. An isoform of apolipoprotein E termed ApoE4 has been implicated in Alzheimer's disease. Thus, cholesterol dysregulation may explain the increased expression of caveolin-1 observed in the frontal cortex and hippocampus of Alzheimer's disease patients compared with age matched control patients (Gaudreault *et al.* 2004).

The SILAC data also identified changes unassociated with lipid metabolism and membrane homeostasis. It is interesting that MCSF was identified as increased at the protein and mRNA level after oxysterol treatment in SN741 neurons and, at the mRNA level, in THP1 monocytes (table 3.10; fig 4.10; fig 4.12). MCSF expression appears to be required for normal brain development in mice (Michaelson *et al.* 1996) and has been associated with two disease states also associated with oxysterols; artherosclerosis and Alzheimer's disease (section 1.1.6.). In artherosclerosis MCSF expression is increased in endothelial cells after treatment with low density lipoprotein (Rajavashisth *et al.* 1990). Indeed, in MCSF knockout mice there was a marked decrease in artherosclerotic lesions after feeding with an atherogenic diet (Qiao *et al.* 1997) and in low density lipoprotein receptor knockout mice artherogenesis was significantly reduced after MCSF was knocked out (*i.e.* double knockout LDLR -/-, op/op, Rajavashisth *et al.* 1998). Therefore, it is possible that the oxysterol component of low density lipoprotein is a mediator in this increase of MCSF due to the measured induction of MCSF mRNA in monocytes (fig 4.12).

MCSF has been associated with Alzheimer's disease though its role is unclear. The expression of MCSF has been shown to associate with Aβ plaques in Alzheimer's patients brains and that in the cerebrospinal fluid of Alzheimer's patients the level of MCSF is elevated ~5-fold compared with control (Du Yan *et al.* 1997). Also, in a mouse model of Alzheimer's increased expression of MCSF-R has been observed in microglia in transgenic AbPPV717F mice suggesting a role for its ligand MCSF

(Murphy *et al.* 2000). Indeed, in two studies from the same group it appears that MCSF is beneficial as knockout MCSF mice (these mice were not an Alzheimer's model) had an increased number of amyloid plaques (Kaku *et al.* 2003) and injection of MCSF to these mice reduced the deposition of Aβ (Kawata *et al.* 2005). However, there is contradictory evidence as an independent study did not observe Aβ deposits in MCSF knockout mice (Kondo *et al.* 2009). Transgenic mice with the chimeric human/mouse Aβ precursor protein (APPSwe) gene and the human presenilin 1 gene (A246E variant) injected with MCSF had reduced Aβ deposits and an increase in the number of microglia (Boissonneault *et al.* 2009). As microglia have been shown to be able to clear Aβ this increase might be relevant (Majunder *et al.* 2007). However, the benefit of MCSF activated microglia is unclear as there is evidence that they can augment toxicity induced by Aβ (Li *et al.* 2004).

The mechanism by which oxysterols increase the expression of MCSF appears to be independent of LXR as GW3965 shows no activity whilst ring oxygenated oxysterols such as 7β-hydroxycholesterol and 7α-hydroxycholesterol induce significant increases in MCSF mRNA in THP1 monocytes. A nuclear receptor that has been shown to regulate MCSF expression is PPARγ (Bonfield *et al.* 2008). Similarly to LXR, PPARγ is a nuclear receptor that requires heterodimerisation with RXR when activated. PPARγ activation causes a decrease in MCSF expression (Bonfield *et al.* 2008). Therefore it appears that PPARγ activation has an inverse effect to treatment with oxysterols. This leads to the hypothesis that oxysterols can inhibit PPARγ activity. Indeed, there has been recent evidence to suggest that 25-hydroxycholesterol can inhibit PPARγ (Xu *et al.* 2012).

The large (~35-fold) up-regulation in MCSF mRNA expression in THP1 cells after 25-hydroxycholesterol treatment may indicate that this is a part of an immune response. A large increase in the enzyme cholesterol-25-hydroxylase and its product 25-hydroxycholesterol is seen after exposure to lipopolysaccharide (section 1.1.7). The role of this increase in 25-hydroxycholesterol is currently unclear. Therefore, part of the response to infection may be to induce MCSF production to promote the differentiation of monocytes to macrophages and/or recruit macrophages to the site of infection. However, no increase in MCSF was identified in THP1 cells at the protein

level measured either by ELISA or Western blot. Therefore, it is possible that the synthesis and secretion of MCSF protein is controlled post-translationally and requires a secondary signal in order for the observed increase in mRNA expression to be converted to increased protein.

It is important to note that the experiments presented here were only conducted 3 times and that the low number of replicates may influence the statistical analysis. Ideally a sample size greater than 3 would have been used which would increase the power of Student's t-test. Unfortunately, time and financial constraints were in place limiting the number of replicates performed. It is however common for biological papers, even in high impact 'good' journals to combine a sample size of 3 with Student's t-test (*e.g.* Zelcer *et al.* 2009).

In summary, the SILAC proteomic approach has identified a large number of proteins with confidence in their quantification and identification due to the use of multiple peptides. This approach has led to the observation of expected changes such as down regulation of the cholesterol synthesis pathway. In addition, a number of the proteins observed as having their expression changed were related to the composition of cellular membranes. Thus, as 24(*S*),25-epoxycholesterol is the most abundant oxysterol in murine embryonic brain it is likely that it plays a role in embryonic lipid homeostasis. Increased expression of LXRβ after ligand binding and the LXR independent increase in MCSF expression were also observed. Therefore, as 24(*S*),25-epoxycholesterol induces LXRβ and MCSF and that these proteins are required for normal brain development we hypothesise that the role of this oxysterol is an important one for embryonic neurogenesis.

CHAPTER 5: PHOSPHOPROTEOMIC ANALYSIS OF 24(*S*),25-EPOXYCHOLESTEROL AND 25-HYDROXYCHOLESTEROL TREATMENT IN SN4741 CELLS

5.1. Introduction.

A common post-translational modification of proteins is phosphorylation. It has been estimated that around 30% of proteins will at some point during their expression (i.e. not simultaneously) be phosphorylated (Larsen *et al.* 2005). Protein phosphorylation is important for the transmission of signals within eukaryotic cells and thus, plays an important role in the regulation of diverse cellular processes. The reversible addition, or subtraction, of a phosphate group to proteins can result in the activation, or deactivation, of enzymes due to a conformational shift in their tertiary structure. This change can result in an enzyme having its activity restricted by altering the binding pocket that recognises the target molecule or by modifying the active site of enzyme activity. Serine, threonine and, less commonly, tyrosine amino acids can be phosphorylated in eukaryotic organisms. Protein phosphorylation is regulated enzymatically; enzymes classed as kinases add a phosphate group to a protein whereas a phosphatase does the reverse.

The major role for oxysterols is in cholesterol homeostasis (section 1.1.5). However, in addition to their regulatory role oxysterols can affect protein phosphorylation. There is evidence to show that oxysterols effect the phosphorylation of extracellular signal regulated kinase (ERK1/2) (Yoon *et al.* 2004, Lemaire-Ewing *et al.* 2009). Cholesterol stabilises a phosphatase complex containing oxysterol binding protein (OSBP) as a scaffold, the serine/threonine phosphatase PP2A and the tyrosine phosphatase HePTP that decreases the phosphorylation of ERK 1/2 (Wang *et al.* 2003, Wang *et al.* 2005). By competing with cholesterol 25-hydroxycholesterol causes the disassembling of the phosphatase complex and, therefore, the presence of oxysterol up-regulates ERK 1 phosphorylation at the thr202/tyr204 amino acid residues and ERK 2 at thr185/tyr187. ERK 1/2 is an important signalling molecule and a known oncogene. It has roles in a number of different biological functions including cell growth, differentiation and apoptosis (Avruch 2007). The up-regulation of ERK1/2 phosphorylation has been shown in a number of different cell lines either

by depletion of cholesterol with cyclodextrin or with treatment with oxysterols (table 4.1; Furuchi & Anderson 1998, Yoon *et al.* 2004, Agassandian *et al.* 2005, Calleros *et al.* 2006, Kim *et al.* 2007, Jin *et al.* 2008, Lemaire-Ewing *et al.* 2009). This effect seems to be a feature of oxysterols generally as a number of diverse oxysterols have been shown to initiate this effect including 7β-hydroxycholesterol, 22-hydroxycholesterol, and 25-hydroxycholesterol.

It is unclear whether treatment with oxysterols only affects ERK1/2 of the mitogen activated protein kinase (MAPK) family as there has been contradictory evidence regarding other MAPKs (e.g. JNK) (Ares *et al.* 2000, Yoon *et al.* 2004). In addition, it is unclear as to what pathways downstream of ERK1/2 are up/down-regulated due to the activation of ERK1/2. Furthermore, it is possible that phosphorylation on other proteins other than MAPKs could be affected by the destabilisation and deactivation of the PP2A/HePTP phosphatase complex. It has been demonstrated in the literature that oxysterols can cause changes to phosphorylation, however, the full extent and significance of these has yet to be assessed (table 5.1).

Table 5.1. Summary of studies analysing effects of oxysterol treatment or cyclodextrin cholesterol depletion on ERK phosphorylation. * = No information regarding conformation. All changes were demonstrated using Western blotting. MβCD= methyl-β-cyclodextrin. HβCD= 2-hydroxypropyl-β-cyclodextrin. OHChol = hydroxycholesterol.

Oxysterol	Cell-line	Condition	Effect on Phospho-ERK	Reference
n/a	Rat-1	Serum starved 24-40hrs 2% HβCD 1hr EGF 50ng/ml (0-10min)	Increase after 3min c.f. control.	Furuchi &Anderson 1998
7β-OHChol	Human aortic smooth muscle	5μg/ml 5-20min Serum starved 24hrs Serum free treatments	Increase after 5min c.f. control Max. response after 10min.	Ares *et al.* 2000
n/a	Fibroblasts /Hela	20μM PD98059 for 10min then 0.5-2% MβCD 15min	Increase with all concentrations MβCD c.f.control.	Wang *et al.* 2003
22(R)-OHChol	KMBC	30μM Serum starved 24hrs Time course	Increase after 2hrs. No control or total-ERK data presented.	Yoon *et al.* 2004
22-OHChol *	MLE	5-30μM Serum free treatments Time course	Increase after 15min. Persisted for 6hours.	Agassandian *et al.* 2005
25-OHChol	NIH3T3	2.5μM With serum 48hours	~2 fold increase No total-ERK data presented.	Calleros *et al.* 2006
n/a	HaCaT	10mM MβCD 1hr Serum starved 24hrs	Increase after 60min c.f. control.	Kim *et al.* 2007
n/a	Normal human melanocytes	1mM MβCD Time course. With serum.	Increase after 6 hours. Persisted for 48hours. No control data presented.	Jin *et al,* 2008
7β-OHChol 25-OHChol	THP-1	50μM Time course. With serum.	Max. increase at 6hours. 7β-OHChol = ~6-fold 25-OHChol = ~3-fold.	Lemaire-Ewing *et al.* 2009

In embryonic mouse brain 24(*S*),25-epoxycholesterol is present at a concentration greater than expected (Wang *et al.* 2009). The role that it plays is unclear it is possible that it acts beyond its activity as a ligand for SREBP and LXR and induces changes in post-translational modifications such as phosphorylation. Indeed, this is feasible as there is, as previously described, evidence that oxysterols can induce changes in ERK phosphorylation. Interestingly, previous work has shown a link between ERK activity and normal dopaminergic neuronal development. It has been shown that dopamine D_2 receptors in mesenphalic neuronal primary cell cultures activate ERK (Kim *et al.* 2006). This in turn activates the transcription factor Nurr1 that is important for normal dopaminergic neuron development, (Kim *et al.* 2006). Further work by the same group showed that striatal-enriched protein tyrosine phosphatase, a ERK phosphatase, also has an effect on normal dopaminergic neuron development (Kim *et al.* 2008). Gene silencing of striatal-enriched protein tyrosine phosphatase using siRNA reduced by ~25% the number of tyrosine hydroxylase positive mesenphalic neuronal primary cells. In addition, another paper, again by the same group, demonstrated that Wnt5a protein acted through dopamine D_2 receptors to increase the number of tyrosine hydroxylase positive cells in mesenphalic neuronal primary cell cultures by ~25% (Yoon *et al.* 2011). Wnt5a protein induced ERK phosphorylation that appeared to be mediated by EGFR signalling; small molecule inhibition of EGFR abolished the effect of Wnt5a on ERK phosphorylation and the increase in tyrosine hydroxylase positive neurons. It has also been shown, by an independent group, that ERK has a role to play in midbrain dopaminergic neurogenesis (Jaeger *et al.* 2011). In this case it appears that small molecule inhibition of ERK phosphorylation, for 2 days, triggers the differentiation of stem cells into dopaminergic neurons. However, ERK phosphorylation is then required in order to consolidate this effect. To demonstrate this, a small molecule MEK inhibitor PD0325901 used continuously for 5 days had no effect on *Lmx1a* and *Foxa2* (markers of dopaminergic neurogenesis) whereas 2 days treatment with PD0325901 followed by 3 days without significantly increased both. Thus, it appears that the regulation of ERK is important in normal dopaminergic neurogenesis.

Therefore, in order to evaluate changes to protein phosphorylation in SN4741 neuronal cells after treatment with oxysterols, 25-hydroxycholesterol and 24(*S*),25-

epoxycholesterol, a SILAC (section 1.2.3.1.) phosphoproteomic approach was employed.

Phosphoproteomics is the analysis of post-translational phosphorylation on a global protein level. However, phosphopeptides are difficult to analyze as the higher abundance of unmodified peptides leads to low signal intensities and low ionization efficiency (Thingholm *et al.* 2009). Therefore, phosphoproteomics relies on the enrichment of the phosphopeptides allowing the modified peptide to be observed rather than the much more abundant unmodified peptides. A number of phosphoenrichment techniques are available that allow the concentration of phosphopeptides (section 1.2.4.3.). In the work presented here a strong cation exchange fractionation step was used prior to immobilised metal ion affinity chromatography (IMAC). IMAC relies on the chelation of positively charged metal ions to beads creating a stationary phase that will bind to negatively charged phosphopeptides. Therefore, non-phosphorylated peptides will not bind to the metal ions and will be present in the initial flow through and phosphopeptides can be eluted subsequently and analysed using LC-MS/MS using a multistage activation method (section 1.2.2.3.).

Thus, the aim of the work is to investigate the phosphoproteomic changes in SN4741 cells, a neuronal cell line derived from the substantia nigra of embryonic mice, treated with 25-hydroxycholesterol and 24(*S*),25-epoxycholesterol.

5.2. Results

5.2.1. Effect of 25-hydroxycholesterol on ERK Phosphorylation

Initially Western blotting was performed examining the effect of 25-hydroxycholesterol in Hela cells. This was performed to observe previously reported changes in ERK phosphorylation in transfected Hela cells after 25-hydroxycholesterol treatment (Wang *et al.* 2005). An increase in phosphorylated ERK was observed after 6 hours treatment which persisted until 24 hours (fig. 5.1). This slow onset of action suggests a secondary or tertiary effect of 25-hydroxycholesterol on ERK phosphorylation. The phosphoERK1/2 antibody used detects phosphorylation on thr202/tyr204 (ERK1) or thr185/tyr187 (ERK2) when either amino acid residue or both are phosphorylated.

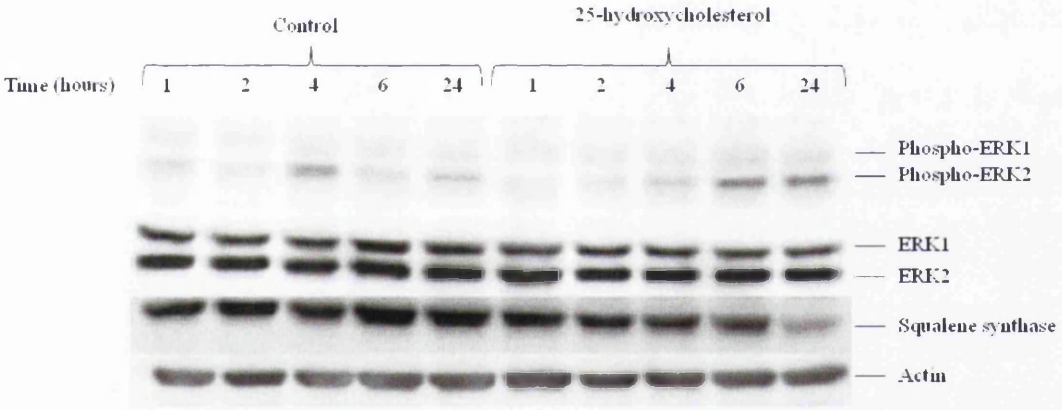

Figure 5.1 25-hydroxycholesterol treatment increases ERK1/2 phosphorylation in Hela cells. 10μM 25-hydroxycholesterol in serum free media increased ERK1/2 phosphorylation over time in Hela cells (20μg lysate loaded) with a corresponding decrease in the SREBP2 regulated gene squalene synthase (n=1). No serum starvation was performed prior to treatment.

The role of oxysterols in neuronal development is the area of interest in this research and therefore phosphoproteomic experiments were to be conducted in SN4741 cells derived from embryonic murine substantia nigra. SN4741 cells are dissimilar to Hela as they are neuronal not epithelial and are derived from mouse instead of human. Therefore, after the initial experiment in Hela cells the effect of 25-

hydroxycholesterol on phospho-ERK was examined in SN4741 cells. A number of experiments were performed (table 5.2) using different methodologies though these experiments proved inconclusive with a number of contradictory observations. However, the effect of 25-hydroxycholesterol on phospho-ERK might be cell type or species specific and therefore we proceeded with SILAC experiments to examine the phosphoproteome as a whole.

Table 5.2. Summary of Western blot experiments analysing effect of 25-hydroxycholsterol on SN4741 cell phospho-ERK levels. All treatments performed in serum free media. HβCD=2-hydroxypropyl-β-cyclodextrin; EGF=epidermal growth factor; 25-OHChol=25-hydroxycholesterol.

Treatment	Treatment time	Observed change in ERK phosphorylation c.f. control	Serum starved?
10μM 25-OHChol	24 hours	Down	No
10μM 25- OHChol	24 hours	No change	No
25μM 25- OHChol	2 hours	No change	24 hours
25μM 25- OHChol	3 hours	Down	24 hours
25μM 25- OHChol	3 hours	Up	24 hours
2% HβCD + EGF	2 hours	No change	24 hours
2% HβCD + EGF	1 hours	No change	24 hours
2% HβCD + EGF	1 hours	No change	24 hours

5.2.2. Strong Cation Exchange and IMAC

Strong cation exchange chromatography was used in order to reduce the complexity of the peptide mixture. The performance of the column was evaluated prior to use as shown previously (fig. 3.5). The presence of a phosphate group on serine/threonine/tyrosine residues of peptides results in a more anionic molecule. Strong cation exchange chromatography separates molecules based on their charge, with cationic molecules retained longer so phosphopeptides would elute earlier from the column. Therefore, the fraction collection was shortened at the beginning of the run when compared with the fractionation conducted for the protein expression

proteomics (fig. 3.6). It can be seen that the largest number of phosphopeptides as a percentage of the total number of peptides in the fraction were eluted at the beginning of the strong cation exchange run in both biological replicates (fig. 5.2; fig. 5.3).

In early fractions the majority of peptides eluted are phosphorylated (e.g. fractions 5 and 3 respectively for the 2 biological replicates). In addition, a large number of phosphopeptides eluted in the middle of the run. It can be seen that this is the time where the majority of peptides elute from the SCX column and therefore a large number of phosphopeptides here is unsurprising. However, as a proportion of the total this is much lower than early fractions. In these 'middle' fractions a large number of non-phosphorylated peptides were observed. The IMAC approach employed for phosphopeptide enrichment should, in theory, only bind phosphorylated peptides. Therefore, it is likely that the detection of these non-phosphorylated peptides is due to non-specific interactions between the IMAC beads and anionic residues.

A

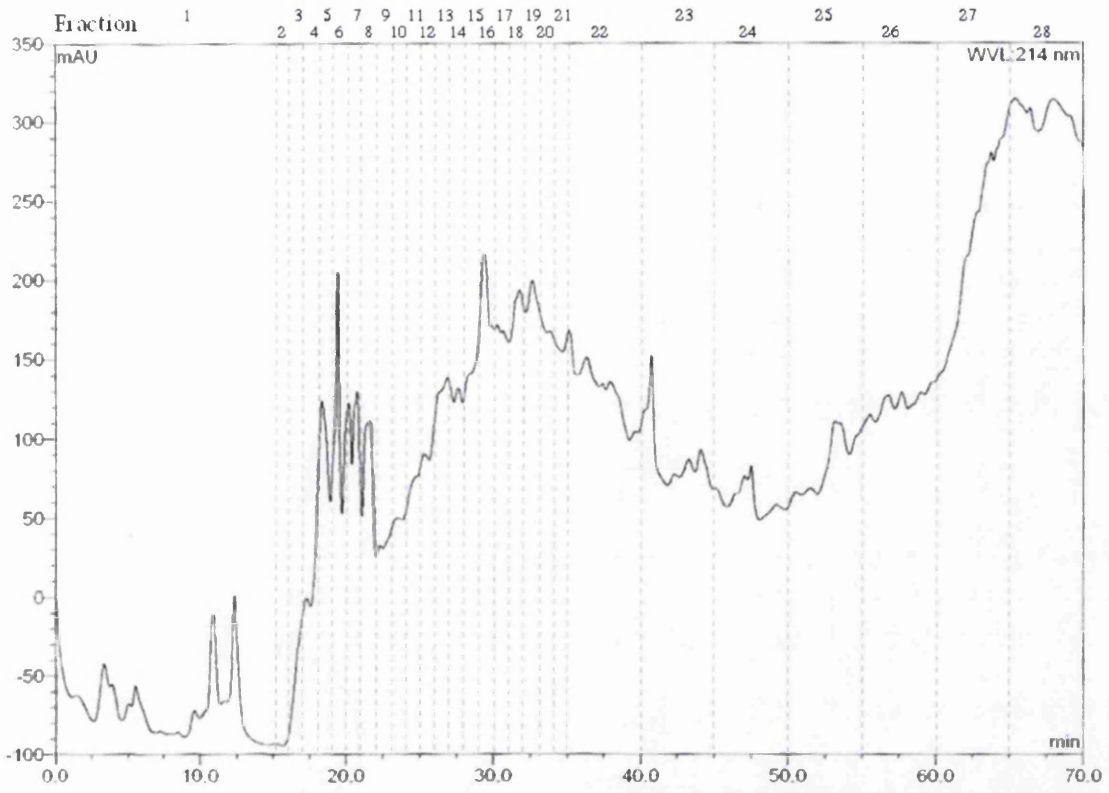
Fraction
1
2 3 4 5 6 7 8 9 10 11 12 13 14 15 16 17 18 19 20 21
22
23
24
25
26
27
28
mAU
WVL:214 nm
350
300
250
200
150
100
50
0
-50
-100
0.0
10.0
20.0
30.0
40.0
50.0
60.0
70.0
min

B

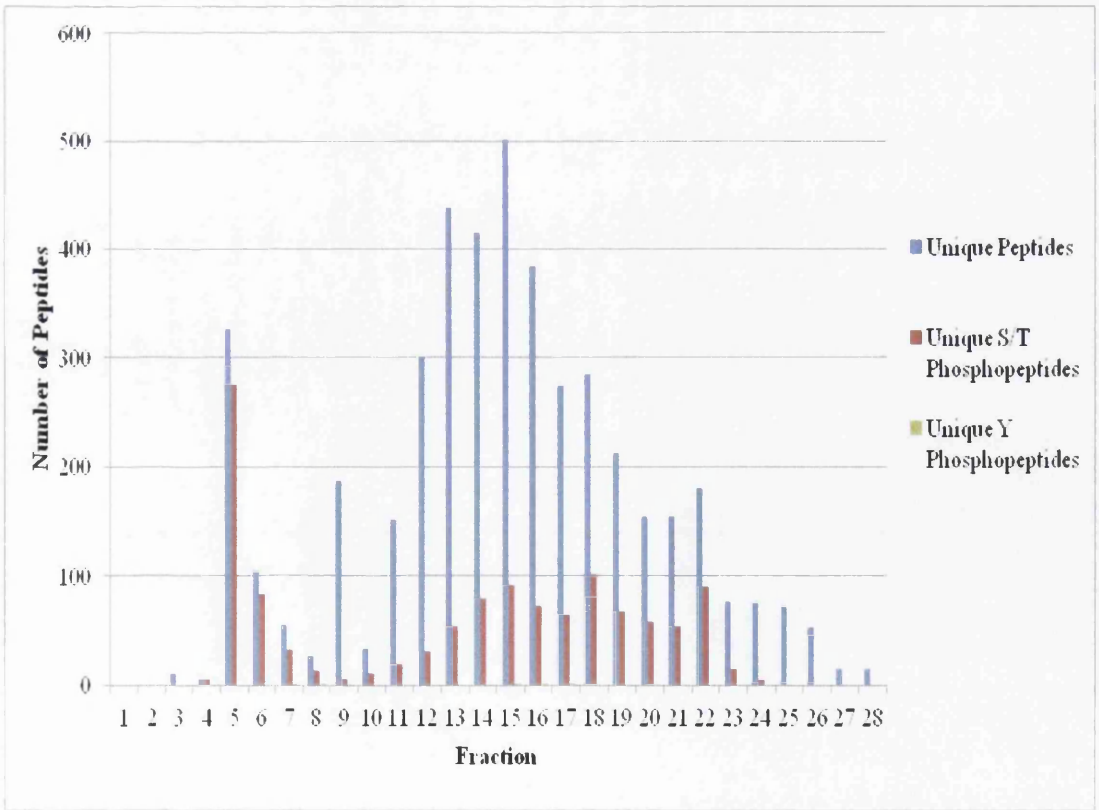
600
500
400
300
200
100
0
Number of Peptides
1 2 3 4 5 6 7 8 9 10 11 12 13 14 15 16 17 18 19 20 21 22 23 24 25 26 27 28
Fraction
Unique Peptides
Unique S/T Phosphopeptides
Unique Y Phosphopeptides

Figure 5.2. Strong Cation Exchange chromatography trace of SILAC peptides and phosphopeptides from the first biological replicate. A) The UV (λ=214nm) chromatogram highlights the large number of peptides present on the column. The time interval for fraction collection is indicated B) In this example a total of 4513 unique peptides were identified. Of these 1232 were unique phosphopeptides. Phosphopeptides eluted throughout the run but predominantly in early fractions. In fraction 5 the majority (84%) were identified as phosphopeptides. In later fractions very few phosphopeptides were detectable.

A

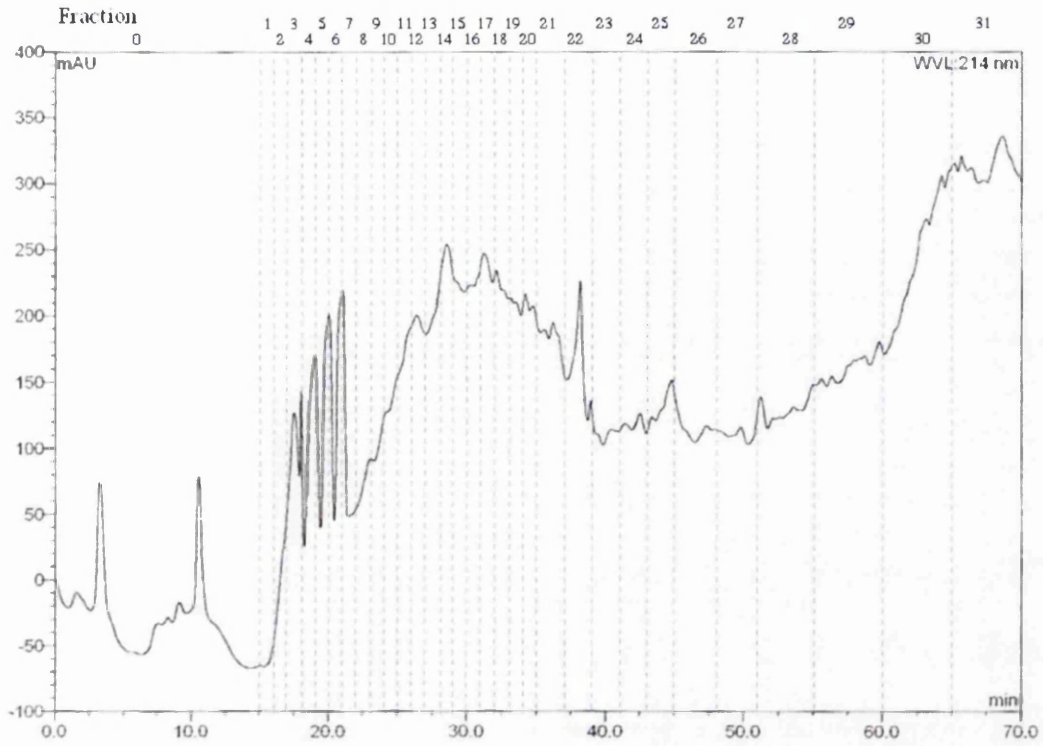
Fraction
0
1 3 5 7 9 11 13 15 17 19 21 23 25 27 29 31
2 4 6 8 10 12 14 16 18 20 22 24 26 28 30
mAU
WVL:214 nm
400
350
300
250
200
150
100
50
0
-50
-100
min
0.0
10.0
20.0
30.0
40.0
50.0
60.0
70.0

B

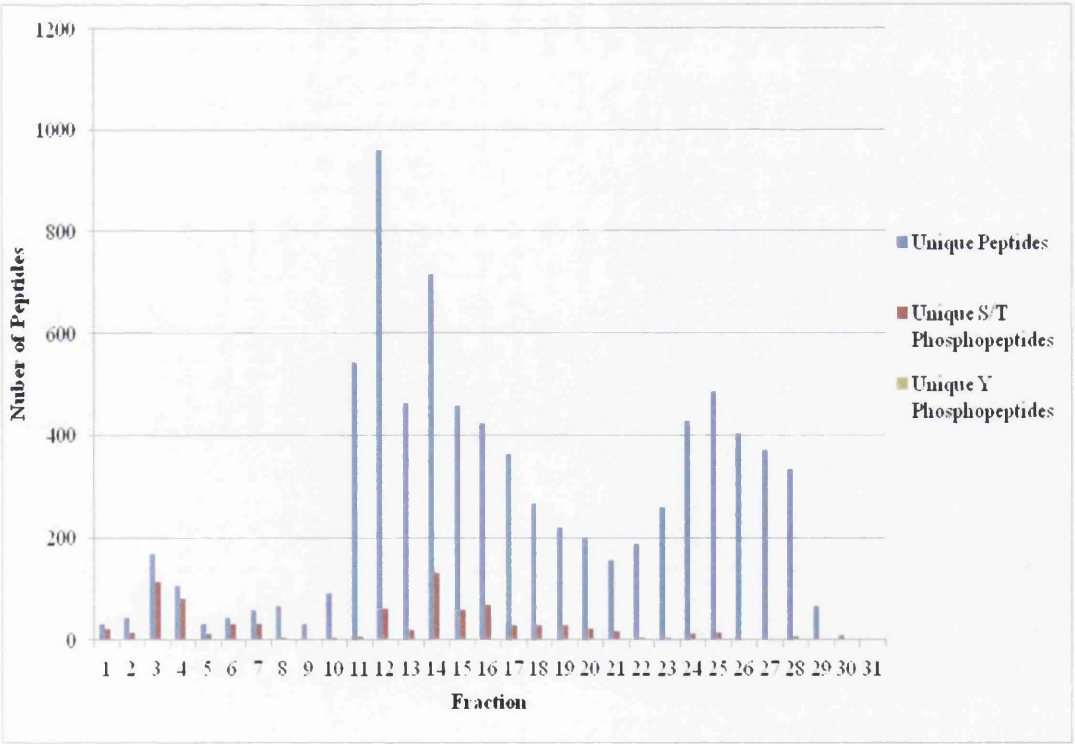
Number of Peptides
1200
1000
800
600
400
200
0
1 2 3 4 5 6 7 8 9 10 11 12 13 14 15 16 17 18 19 20 21 22 23 24 25 26 27 28 29 30 31
Fraction
Unique Peptides
Unique S/T Phosphopeptides
Unique Y Phosphopeptides

Figure 5.3. Strong Cation Exchange chromatography trace of SILAC peptides and phosphopeptides from the second biological replicate. A) The UV (λ=214nm) chromatogram highlights the large number of peptides present on the column. The time interval for fraction collection is indicated B) In this example a total of 7990 peptides were identified. Of these 845 were unique phosphopeptides. Phosphopeptides eluted throughout the run but predominantly in early fractions. In fraction 3 the majority (68%) were identified as phosphopeptides. In later fractions very few phosphopeptides were detectable.

5.2.3. C18 Reverse Phase LC-MS/MS of SILAC phosphopeptides

The peptide mixture fractions derived from IMAC phosphoenrichment were dried under vacuum and resuspended in H_2O/0.1% formic acid to be analysed by LC-MS/MS. In order to test the performance of the reverse phase C18 column performance prior to running the SN4741 derived SILAC samples trypsin digested bovine serum albumin (100fmol; BSA) was used. This allowed validation of both chromatography and mass spectrometry performance. In order to ensure the complete removal of the BSA peptides prior to running the SILAC SN4741 phosphopeptide samples a blank run was performed injecting 80% acetonitrile.

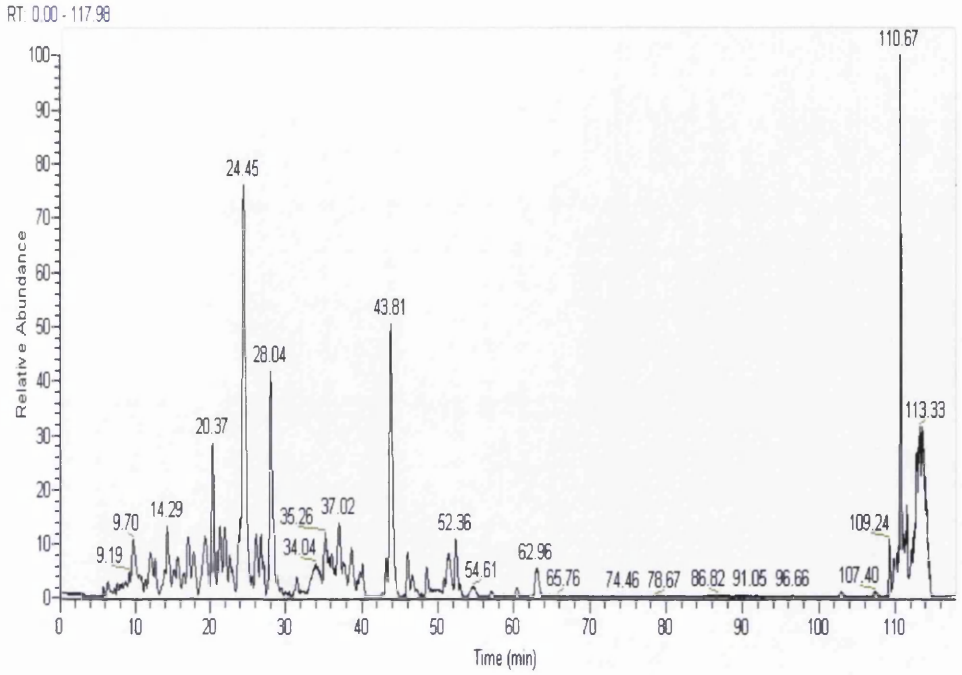

Figure 5.4. Reverse Phase LC-MS/MS SILAC phosphopeptide separation. An example chromatogram (fraction 5 of 1st biological replicate; fig. 5.2) is shown that exemplifies the fact that phosphopeptides co-eluting from the strong cation exchange chromatography step can be separated by C18 reverse phase chromatography.

SILAC phosphopeptides were injected on to the HPLC system and separated over a 2 hour gradient. It can be seen from the example in figure 5.4 that a fraction obtained from strong cation exchange chromatography and subsequently enriched using IMAC is still a complex sample but the peptides present can be separated on the C18 column. Peptides eluting from the column were then analysed by mass spectrometry. Peaks with characteristic features of peptides were identified by the initial mass spectrometry scan and if they conformed to pre-selected criteria were chosen for fragmentation (see Materials and Methods section 2.7.11). As previously described the initial MS scan is critical to SILAC success as this scan is used for quantification. Similarly to spectra observed in total protein these SILAC envelope patterns have a triplet motif that was indicative of labelled peptides (see fig 5.5. for example of a SILAC triplet). In the analysis of phosphopeptides fragmentation of the peptide is critical for the analysis of both the backbone sequence and identification of the location of post-translational modification(s). MS^2 fragmentation is often insufficient to identify both peptide sequence due to extensive neutral loss of the relatively labile

phosphate bond instead of backbone fragmentation. Thus, in MS^2 spectra the dominant peak is often the precursor ion with a neutral loss of 98Da or 80Da (representing H_3PO_4 or HPO_3 respectively). Therefore multistage activation was employed to allow identification of phosphopeptide sequence.

Multistage activation is a pseudo MS^3 process. In this process a selected precursor ion is selected for fragmentation then subjected to further fragmentation at the m/z where the neutral loss ion, in theory, should be. The fragments from both activations are then combined into one spectrum which is, in effect, a hybrid of MS^2 and MS^3 spectra. The peptide LLHEDLDES(ph)DDDVDEK has a monoisotopic mass of 1965.88Da and can be seen as doubly charged ion at 983.9 m/z (3.21ppm mass error; fig 5.5A) was selected for fragmentation. It can be seen that in the multistage activation spectra (fig 5.5B) that the peptide has been fragmented to yield sequence information. There is no dominant neutral loss peak. A number of ions are present that identify phosphorylated and neutral loss versions of the same peptide demonstrated by a neutral loss of 98Da (fig. 5.5B; fig 5.5C)

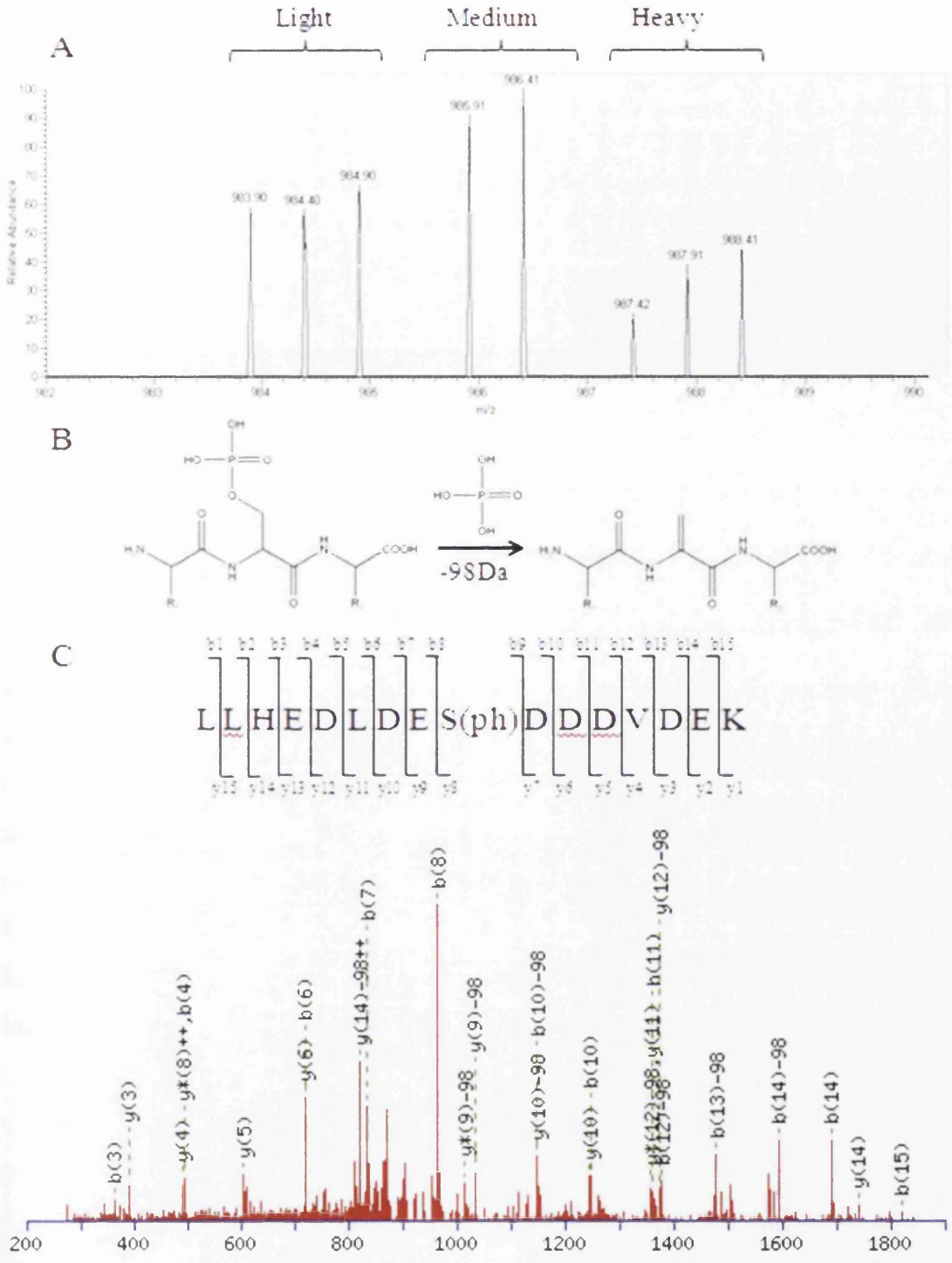

Figure 5.5. Phosphopeptide SILAC MS scan and multistage activation. The doubly charged phosphopeptide LLHEDLDES(ph)DDDVDEK is derived from Arf-GAP with SH3 domain, ANK repeat and PH domain-containing protein 2. The peptide has a monoisotopic mass of 1965.88Da was observed as a doubly charged ion (A). After the light SILAC phosphopeptide precursor ion at 983.90 *m/z* was selected for fragmentation it was analysed using multistage activation. Neutral loss of the

phosphate group(s) results in a loss of 98Da (B) and therefore multistage activation allows the observation of both neutral loss and backbone fragmentation resulting in identification of the sequence and phosphorylation site of the peptide (C).

The probability of the correct post-translational modification assignment is given by a post-translational modification (PTM) score. This value gives an indication of the probability differential between different amino acid residues on the peptide backbone. Examples of 'good', 'moderate' and 'poor' spectra are shown in figure 5.6. It can be seen from these spectra that the quality of the multistage activation fragmentation spectra is integral to the identification of sequence and phosphorylation that can be seen by the Mascot and post-translational modification scores of the 3 peptides. The Mascot scores are 89.71, 41.39 and 23.91 and the PTM score 341.18, 124.18 and 94.36 for the 'good' 'moderate' and 'poor' phosphopeptides. The 'good' spectrum has a large number of strong peaks above the background giving it high scores and making it a good spectrum for identification (fig 5.6A) as a large number of b and y ions were identified that allows identification of the phosphorylated amino acid. A neutral loss of 98 was observed from the y_4 to y_{17} but only on the b_{16} and b_{18} ions indicating the probable location of the phosphorylation on the GHSDSSASESEVSLLS(ph)PVK. It is clear that the 'poor' spectrum (fig 5.6C) has a lower peak intensity c.f. background that limits the reliability of the spectra for identification of b and y ions which is reflected in its lower scores.

A

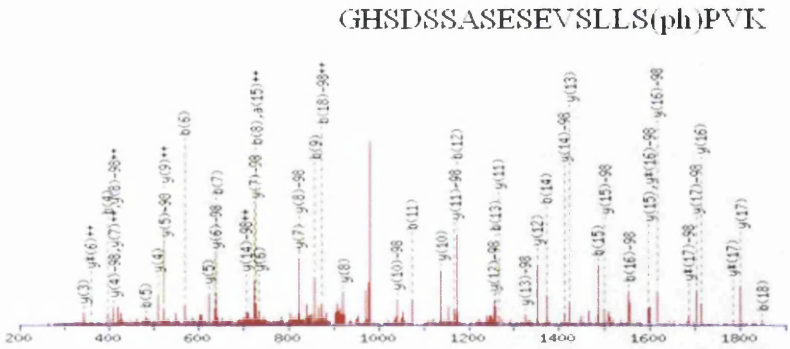

B

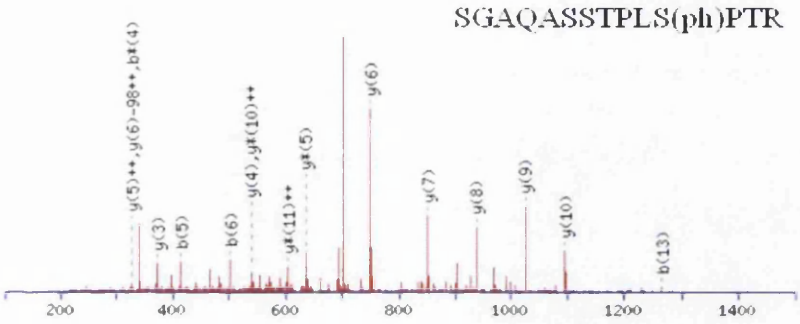

C

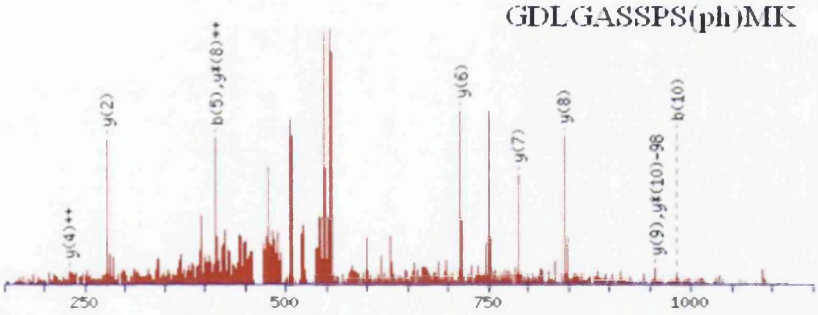

Figure 5.6. Phosphopeptide SILAC multistage activation MS/MS spectra. A) a 'good' spectra that identified the light SILAC peptide GHSDSSASESEVSLLS(ph)PVK from serine/threonine-protein phosphatase 4 regulatory subunit 2 (Mascot score = 89.71; PTM score = 341.18; Phospho site probability = GHSDSSASESEVSLLS(1)PVK). B) A 'moderate' spectra that identified the light SILAC peptide SGAQASSTPLS(ph)PTR from Lamin-A/C (Mascot score = 41.39; PTM score =124.18; Phospho site probability = SGAQASS(0.006)T(0.062)PLS(0.931)PTR). C) A 'poor' spectra that identified the peptide GDLGASSPS(ph)MK from Ahnak protein (Mascot score = 23.91; PTM score = 94.36; Phospho site probability = GDLGAS(0.048)S(0.048)PS(0.904)MK.

The PTM score does not, however, give an indication of whether the phosphorylation site identification site is unequivocal. It merely gives an indication of the differential between other sites on the peptide. For example, the peptide AS(ph)EDESDLEDEEEKSQEDTEQK derived from DNA replication licensing factor MCM3 was identified with a Mascot score of 96.69, and a high PTM score of 359.53 due to a large differential between the potential phosphorylation sites on the peptide (Phospho scores differentials = AS(0)EDES(0)DLEDEEEKS(-104.96)QEDT(-111.59)EQK). However, the correct phosphorylation site cannot be identified as by examining the phosphorylation probabilities on the peptide AS(0.5)EDES(0.5)DLEDEEEKSQEDTEQK it is not possible to distinguish between two serine residues (fig 5.7). These spectra are derived from the same sample and precursor ion therefore it is possible that this inability to distinguish is due to a mixed population being present. Alternatively, the phosphate group might be transferred during tandem MS to a different amino acid residue in the peptide which is a phenomenon that has been demonstrated to occur (Palumbo & Reid 2008). This effect could be the cause of these observed contradictory phosphorylation site identifications. Thus, spectra generated from multistage activation are can be used for identification of phosphopeptide sequence and site of post-translational modification though caution is required. All the scores and probabilities generated by the bio-informatic software need to be taken into account to avoid false identification of phosphopeptides.

A

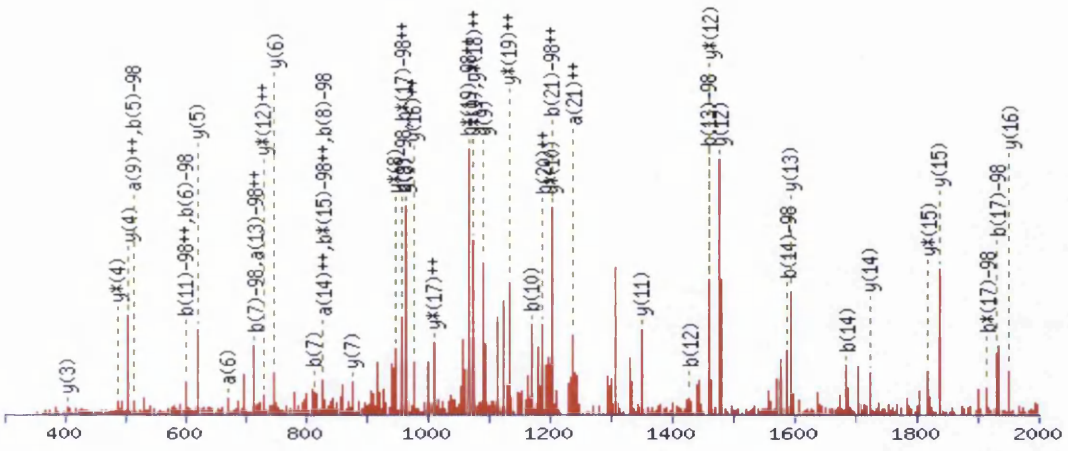

B

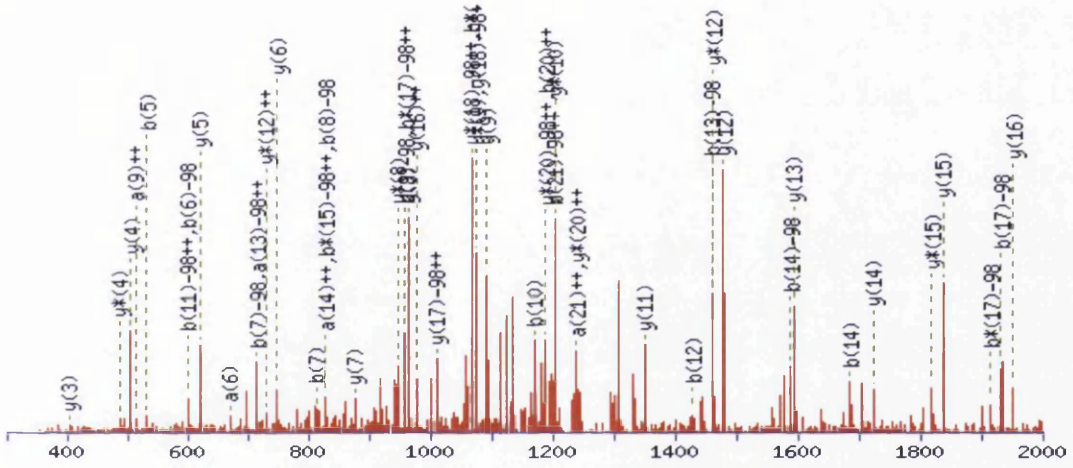

Figure 5.7. Phosphopeptide SILAC multistage activation scans for the phosphopeptide AS(ph)EDESDLEDEEEKSQEDTEQK. The peptide is derived from DNA replication licensing factor MCM3. The phosphopeptide was identified with a Mascot score of 96.69, and a high PTM score of 359.53. The phosphorylation site could not be identified unequivocally as equally probable were the peak assignment for the two phosphopeptides AS(ph)EDESDLEDEEEKSQEDTEQK (A) and ASEDES(ph)DLEDEEEKSQEDTEQK (B).Thus, the phosphorylation probabilities on the peptide AS(0.5)EDES(0.5)DLEDEEEKSQEDTEQK.

5.2.4. Phosphopeptide Identifications

Overall in the 2 biological replicates there were 7606 and 13499 peptides (table 5.3.). Of these 4513 (59%) and 7990 (59%) unique peptides were identified. However, not all of these peptides were identified as phosphorylated. In total 1266 (17% of total) and 1383 (10% of total) phosphopeptides were identified. The number of unique phosphopeptides was lower with 1232 (27% of total unique peptides) and 845 (11% of total unique peptides) identified respectively. The large majority of the phosphopeptides identified were phosphorylated on serine or threonine amino acid residues. For the 2 biological replicates <1% of the phosphopeptides identified were phosphorylated on tyrosine residues. These data suggest that the phosphoenrichment worked despite the obvious fact that a large number of non-modified peptides remain.

Table 5.3. The number of peptides identified in 2 biological replicates. Peptides had a mascot score ≥25 and had a ratio between the SILAC sates generated. Starting material refers to the total amount of protein trypsin digested in the biological replicate

Replicate	1	2
Starting Material	2mg	4mg
Total peptides	7606	13499
Unique	4513	7990
ST total	1261	1378
ST unique	1227	840
Y total	5	5
Y unique	5	5

A large number of phosphopeptides were identified in each biological replicate. The LTQ Orbitrap identified in total 1232 and 845 unique phosphopeptides in terms of peptide sequence and phosphorylation site from each biological replicate respectively. There was an overlap between samples with 414 unique phosphopeptides with identical peptide sequence and phosphorylation site identified (fig. 5.8.). Therefore, a total of 1663 unique phosphopeptides were identified in total.

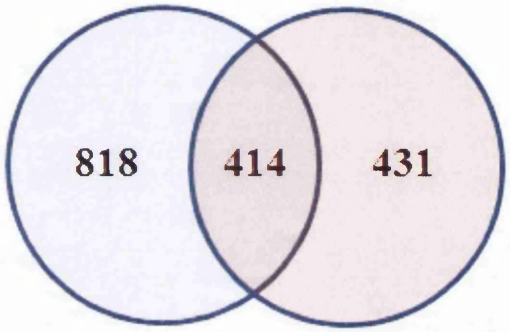

Figure 5.8. Venn diagram of phosphopeptides identified with unique sequence and site of modification. In the 2 biological replicates a total of 1232 and 845 unique phosphopeptides were identified with a Mascot score ≥25 and a SILAC ratio generated. 414 phosphopeptides were identified in both biological replicates.

5.2.5. Analysis of Phosphopeptides For Novel Phosphorylation Sites

The 414 phosphopeptides identified as being present in both biological replicates were examined further to determine if the observed post-translational modifications had been previously reported. The bio-informatic software MaxQuant generates data tables and one column is labelled 'Known Site'. This column indicates if the site has been previously reported to be phosphorylated. Of the 414 phosphopeptides 203 peptides were identified as phosphorylated on serine, 24 on threonine and 2 on tyrosine. Therefore, 185 phosphopeptides were classed as having a previously unreported phosphorylation site. In order to determine if any of these phosphorylation sites were novel the current canonical sequence and post translational modification status of each protein was examined using the protein database Uniprot (www.uniprot.org accessed 02-04-2012). Of the 185 phosphorylation sites 56 were

identified as not currently having experimental evidence to demonstrate phosphorylation i.e. 129 were listed on Uniprot as having been observed experimentally (table 5.4).

These 56 phosphopeptides can be split into phosphosites that have been predicted 'by similarity' (due to similarity with homologous sites on other proteins or species) and those that are not listed on Uniprot at present. 10 (of the 56) phosphopeptides gave experimental validation of 'by similarity' predicted sites whilst 46 peptides gave evidence for previously unknown post-translational modifications. The novel nature of these phosphorylation sites means that as they have not been elucidated experimentally previously it is impossible to validate them using antibodies as none are commercially available. However, the probability of the correct site of phosphorylation is calculated by the software and is shown in table 5.5. The majority (37/46, 80%), of phosphorylation sites were identified in both biological replicates with a probability of ≥0.9 indicating there is confidence in the identification of the phosphorylation site on these peptides. Indeed, for 13 of the phosphopeptides the probability of the phosphorylation site was 1, i.e. unequivocal, in both biological replicates. However, there was equivocal data on the phosphorylation site on 9 phosphopeptides (table 5.5). Therefore, for 37 phosphopeptides there is a high confidence in these data due to a high mascot score and phosphorylation site location probability

Table 5.4. Phosphopeptides identified in both replicates that are currently listed, on Uniprot.org (accessed 02/04/12), as not having experimental evidence to demonstrate post-translational modification at these phosphorylation sites. Some sites are listed as 'by similarity' as they have been predicted due to similarity to other sites or species. Mascot scores are listed to indicate probability of correct identification.

Gene	Sequence and Phosphorylation site	Amino Acid Position	Site known on Uniprot	Mascot Score from Replicate	
				1	2
Map4	AAVGVTGNDITT(ph)PPNK	658	Not listed	52.63	54
Pa1	AEEEGKGS(ph)QEEAGR	53	Not listed	55.03	51.41
Anln	AS(ph)SPVTAATFITENR	292	Not listed	34.63	64.27
Mcph1	ASSFYGSAS(ph)PNHLR	273	Not listed	43.29	35.01
Hirip3	AVES(ph)TDEDHQTDLDAK	134	Not listed	36.12	45.56
Flna	C(me)GQSAAVAS(ph)PGGSIDSR	16	Not listed	53.4	41.72
Larp1	ES(ph)PRPPAAAEAPAGSDGEDGGR	335	By similarity	47.37	46.24
Sntb2	GPAGEAS(ph)ASPPVR	88	Not listed	36.99	38.41
Gtf2f1	GTSRPGTPS(ph)AEAASTSSTLR	391	By similarity	43.03	35.53
Kiaa0913	HTGMASIDSSAPETTSDSS(ph)PTLSR	1158	Not listed	39.97	60.26
Tdp1	HVSS(ph)PDVTTAQK	119	Not listed	32.78	32.9
Ralbp1	IAQEIASLS(ph)KEDVSK	463	By similarity	48.23	52.17
Fzr1	INENEKS(ph)PSQNR	72	Not listed	35.33	36.45
Myo9b	KETPS(ph)PEMETAAQK	1142	Not listed	36.71	30.67
Spg20	KS(ph)PEQESVSTAPQR	126	Not listed	39.11	51.42
Camsap2	LDGES(ph)DKEQFDDDQK	1137	Not listed	42.61	35.62
Specc1	LGSSPTS(ph)SC(me)NPTPTK	136	Not listed	31.81	27.02
Rg9mtd2	LGTS(ph)DGEEER	24	Not listed	58.13	25.1
Thumpd2	LLQGS(ph)PEQGEAVTR	172	Not listed	35.55	40.41
Ranbp2	LNSNNSAS(ph)PHR	837	Not listed	40.56	51.76
Ppfibp1	LPTKPETS(ph)FEEGDGR	417	Not listed	28.15	30.17
Tp53bp1	LPTSEEERS(ph)PAK	1675	By similarity	25.34	25.63
Usp32	LSNS(ph)KENLDTSK	1423	Not listed	28.62	35.16
Zc3h13	NTEEPSS(ph)PVRK	110	Not listed	32.47	32.42
Phf3	NTVDIVDKPENS(ph)PQR	377	Not listed	50.04	50.63
Filip1l	PAS(ph)PSAPLQDNR	1080	Not listed	59.06	41.67
Irs1	PASVDGSPVS(ph)PSTNR	343	By similarity	27.92	42.29
Larp1	PATGISQPPTT(ph)PTGQATR	1315	Not listed	48.09	40.79
Chtf18	PC(me)PAGS(ph)PGNVNR	70	Not listed	43.42	38.29
Gigyf2	PGTPS(ph)DHQPQEATQFER	385	Not listed	64.14	47.33
Bop1	PHMS(ph)PASLPGK	11	Not listed	32.9	28.18

Zc3h11a	PLSSSSVLQES(ph)PTK	677	Not listed	67.72	34.78
Aff1	PVGNISHS(ph)PK	140	Not listed	35.66	31.23
Sos1	RPESAPAESS(ph)PSK	1153	Not listed	35.23	42.41
Rbmxrt	RSTPS(ph)GPVR	165	Not listed	53.29	40.18
Srrm2	RVPS(ph)PTPVPK	2535	Not listed	30.7	47.53
Kiaa0284	S(ph)GRSPEPDPAPPK	840	Not listed	33.59	25.25
Bag3	S(ph)GTPVHC(me)PSPIR	289	Not listed	42.66	40.41
Sqstm1	S(ph)RLTPTTPESSSTGTEDK	266	By similarity	69.05	74.88
Fra10ac1	S(ph)RSPPSEEASK	248	Not listed	43.14	33.29
Anln	SC(me)TKPS(ph)PSK	66	Not listed	29.48	28.03
Birc6	SDS(ph)VTGHTSQK	465	Not listed	25.93	37.29
Srrm2	SESDSSPDS(ph)KPK	1521	Not listed	48.28	35.64
Larp4	SNAVS(ph)PTR	642	By similarity	28.32	25.02
Fra10ac1	SRS(ph)PPSEEASK	250	Not listed	43.14	33.29
Chd8	T(ph)ASPSPLRPDAPVEK	1995	By similarity	25.73	27.58
Api5	TSEDTSS(ph)GSPPKK	462	By similarity	41.21	57.63
Papola	TSS(ph)PNKEESPK	648	Not listed	26.95	31.16
Prrc2b	TTHASSDGPET(ph)PSK	823	Not listed	25.72	29.61
Phldb2	TTPSLS(ph)PHFSSATMGR	958	By similarity	32.55	48.44
Cbx8	VDDKPSS(ph)PGDSSK	164	Not listed	47.38	33
Hdgfrp2	VMTVTAVTTTATS(ph)DR	137	Not listed	76.11	51.2
Dnmt1	VPALAS(ph)PAGSLPDHVR	15	Not listed	36.18	56.18
Arpp19	VT(ph)SPEKAEEAK	22	Not listed	34.2	28.94
Arpp19	VTS(ph)PEKAEEAK	23	Not listed	34.2	28.94
Anapc1	VTS(ph)TPQKPQAEQEENR	901	Not listed	52.09	26.45

Table 5.5. Probabilities of phosphopeptides identified in both replicates that are not currently listed, on Uniprot.org (accessed 02/04/12), as not phosphorylated at these sites. Underlined phosphopeptides indicate a high probability of correct phosphorylation site identification.

Sequence and Phosphorylation site	Gene	Phosphorylation Site Probabilities	
		1	2
AAVGVTGNDITT(ph)PPNK	Map4	AAVGVTGNDIT(0.07)T(0.93)PPNK	AAVGVTGNDIT(0.01)T(0.99)PPNK
AEEEGKGS(ph)QEEAGR	Pa1	AEEEGKGS(1)QEEAGR	AEEEGKGS(1)QEEAGR
AS(ph)SPVTAATFITENR	Anln	AS(0.5)S(0.5)PVTAATFITENR	AS(0.5)S(0.5)PVTAATFITENR
ASSFYGSAS(ph)PNHLR	Mcph1	ASSFYGS(0.001)AS(0.999)PNHLR	ASSFYGS(0.078)AS(0.922)PNHLR
AVES(ph)TDEDHQTDLDAK	Hirip3	AVES(0.994)T(0.006)DEDHQTDLDAK	AVES(0.997)T(0.003)DEDHQTDLDAK
C(me)GQSAAVAS(ph)PGGSIDSR	Flna	CGQSAAVAS(1)PGGSIDSR	CGQSAAVAS(0.903)PGGS(0.097)IDSR
GPAGEAS(ph)ASPPVR	Sntb2	GPAGEAS(0.994)AS(0.006)PPVR	GPAGEAS(0.992)AS(0.008)PPVR
HTGMASIDSSAPETTSDSS(ph)PTLSR	Kiaa0913	HTGMASIDSSAPETTS(0.001)DS(0.16)S(0.82)PT(0.019)LS(0.001)R	HTGMASIDSSAPETTSDS(0.007)S(0.993)PT(0.001)LSR
HVSS(ph)PDVTTAQK	Tdp1	HVS(0.044)S(0.956)PDVTTAQK	HVS(0.004)S(0.996)PDVTTAQK
INENEKS(ph)PSQNR	Fzr1	INENEKS(0.961)PS(0.039)QNR	INENEKS(0.5)PS(0.5)QNR
KETPS(ph)PEMETAAQK	Myo9b	KETPS(1)PEMETAAQK	KETPS(1)PEMETAAQK
KS(ph)PEQESVSTAPQR	Spg20	KS(1)PEQESVSTAPQR	KS(1)PEQESVSTAPQR
LDGES(ph)DKEQFDDDQK	Camsap2	LDGES(1)DKEQFDDDQK	LDGES(1)DKEQFDDDQK
LGSSPTS(ph)SC(me)NPTPTK	Specc1	LGS(0.014)S(0.098)PT(0.098)S(0.771)S(0.014)CNPT(0.002)PT(0.002)K	LGS(0.019)S(0.025)PT(0.106)S(0.712)S(0.106)CNPT(0.025)PT(0.006)K
LGTS(ph)DGEEER	Rg9mtd2	LGTS(1)DGEEER	LGTS(1)DGEEER
LLQGS(ph)PEQGEAVTR	Thumpd2	LLQGS(1)PEQGEAVTR	LLQGS(1)PEQGEAVTR
LNSNNSAS(ph)PHR	Ranbp2	LNSNNS(0.005)AS(0.995)PHR	LNSNNS(0.002)AS(0.998)PHR
LPTKPETS(ph)FEEGDGR	Ppfibp1	LPTKPET(0.08)S(0.92)FEEGDGR	LPTKPET(0.068)S(0.932)FEEGDGR
LSNS(ph)KENLDTSK	Usp32	LSNS(1)KENLDTSK	LSNS(1)KENLDTSK
NTEEPSS(ph)PVRK	Zc3h13	NTEEPS(0.005)S(0.995)PVRK	NTEEPS(0.057)S(0.943)PVRK
NTVDIVDKPENS(ph)PQR	Phf3	NTVDIVDKPENS(1)PQR	NTVDIVDKPENS(1)PQR
PAS(ph)PSAPLQDNR	Filip1l	PAS(0.994)PS(0.006)APLQDNR	PAS(1)PSAPLQDNR
PATGISQPPTT(ph)PTGQATR	Larp1	PATGISQPPT(0.066)T(0.928)PT(0.005)GQATR	PATGISQPPT(0.001)T(0.908)PT(0.091)GQATR
PC(me)PAGS(ph)PGNVNR	Chtf18	PCPAGS(1)PGNVNR	PCPAGS(1)PGNVNR
PGTPS(ph)DHQPQEATQFE	Gigyf2	PGT(0.062)PS(0.938)DHQPQEA	PGT(0.084)PS(0.916)DHQPQE

R		TQFER	ATQFER
PHMS(ph)PASLPGK	Bop1	PHMS(1)PASLPGK	PHMS(0.5)PAS(0.5)LPGK
PLSSSSVLQES(ph)PTK	Zc3h11a	PLSSSSVLQES(0.997)P T(0.003)K	PLSSSSVLQES(0.996)P T(0.004)K
PVGNISHS(ph)PK	Aff1	PVGNISHS(1)PK	PVGNISHS(1)PK
RPESAPAESS(ph)PSK	Sos1	RPESAPAES(0.054)S(0.892)P S(0.054)K	RPESAPAES(0.084)S(0.915)P S(0.001)K
RSTPS(ph)GPVR	Rbmxrt	RSTPS(1)GPVR	RST(0.001)PS(0.999)GPVR
RVPS(ph)PTPVPK	Srrm2	RVPS(1)PTPVPK	RVPS(1)PTPVPK
S(ph)GRSPEPDPAPPK	Kiaa0284	S(0.86)GRS(0.14)PEPDPAPPK	S(0.84)GRS(0.16)PEPDPAPPK
S(ph)GTPVHC(me)PSPIR	Bag3	S(0.827)GT(0.173)PVHCPSPIR	S(0.827)GT(0.173)PVHCPSPIR
S(ph)RSPPSEEASK	Fra10ac1	S(0.935)RS(0.065)PPSEEASK	S(0.919)RS(0.081)PPSEEASK
SC(me)TKPS(ph)PSK	Anln	SCTKPS(1)PSK	SCTKPS(1)PSK
SDS(ph)VTGHTSQK	Birc6	S(0.026)DS(0.974)VTGHTSQK	S(0.024)DS(0.976)VTGHTSQK
SESDSSPDS(ph)KPK	Srrm2	SESDSSPDS(1)KPK	SESDSSPDS(1)KPK
SRS(ph)PPSEEASK	Fra10ac1	S(0.001)RS(0.996)PPS(0.003)EE ASK	S(0.022)RS(0.975)PPS(0.002)EE ASK
TSS(ph)PNKEESPK	Papola	TSS(1)PNKEESPK	T(0.002)S(0.007)S(0.991)PNKE ESPK
TTHASSDGPET(ph)PSK	Prrc2b	TTHASS(0.007)DGPET(0.993)P S(0.001)K	TTHASSDGPET(1)PSK
VDDKPSS(ph)PGDSSK	Cbx8	VDDKPS(0.004)S(0.996)PGDSS K	VDDKPS(0.008)S(0.992)PGDSS K
VMTVTAVTTTATS(ph)DR	Hdgfrp2	VMTVTAVTTTAT(0.003) S(0.997)DR	VMTVTAVTTTAT(0.004) S(0.996)DR
VPALAS(ph)PAGSLPDHV R	Dnmt1	VPALAS(0.993)PAGS(0.007)LP DHVR	VPALAS(0.999)PAGS(0.001)LP DHVR
VT(ph)SPEKAEEAK	Arpp19	VT(0.929)S(0.071)PEKAEEAK	VT(0.955)S(0.045)PEKAEEAK
VTS(ph)PEKAEEAK	Arpp19	VT(0.045)S(0.955)PEKAEEAK	VT(0.045)S(0.955)PEKAEEAK
VTS(ph)TPQKPQAEQEEN R	Anapc1	VT(0.123)S(0.754)T(0.123)PQK PQAEQEENR	VT(0.098)S(0.805)T(0.098)PQK PQAEQEENR

5.2.6. Analysis of Phosphopeptide Motifs

Enzymes classed as kinases carry out phosphorylation of proteins. Kinases recognise amino acid sequences on their target that direct the phosphorylation of the site. The analysis of previously determined substrates of kinases has led to consensus sequences recognised by a given kinase. These amino acid sequences are termed motifs. The knowledge of the motif can be utilised to predict phosphorylation sites or the kinase responsible for a given phosphorylation. However, by analysing sequence alone they do not take into account secondary or tertiary structures present in the protein. Thus, the 3 dimensional structure of the protein is critical and caution is required if extrapolating kinase activity from amino acid sequence alone (Kennelly & Krebs 1991).

Despite this the simplicity of the consensus sequence of the motifs have made them useful tools in the study of kinases and prediction of their substrates. For example, in the case of ERK (MAPK) the motif required, as a minimum, for kinase activity is a serine or threonine residue followed by a proline at the C-terminal side (S/TP). However, a proline residue is often found at the -2 position. Thus, the optimum motif for ERK2 is PXS/TP, where X is any amino acid residue (Davis 1993).

The site of phosphorylation and its relationship to the amino acid sequence of identified phosphopeptides is analysed by the MaxQuant software in order to give a predicted kinase. This information is presented as a 'best motif'. Thus, the analysis of probable kinases acting on the phosphopeptides identified might yield information regarding the effect of oxysterol treatment on certain enzymes and pathways. From the datasets a large number of different kinases were identified as being probable enzymes for the phosphorylation sites identified (table 5.6).

Table 5.6. Frequency of phosphopeptide 'best motif' in each biological replicate.

	Biological replicate	
Best Motif	**1**	**2**
CAMK2	56	45
CDK1	46	37
CDK2	94	71
CHK1/2	19	10
CK1	116	75
CK2	163	68
ERK/MAPK	43	34
FHA KAPP	14	13
GSK3	41	27
NEK6	35	27
PKA	115	69
PKA/AKT	78	52
PKC	1	1
PKD	15	15
Polo box	47	41
WW GroupIV	75	69
Other	56	33
None	218	158

Therefore, in order to examine if there were any correlation between oxysterol treatment and changes in kinase/phosphatase activity the 6 most abundant motifs were examined in order to determine if they had a normal distribution when analysed with the SILAC ratio. The 6 best motifs analysed were CDK2, CK1, CK2, PKA, PKA/AKT, WW GroupIV (fig 5.9.). In addition, ERK/MAPK was analysed. The SILAC ratio had a normal distribution when plotted for the phosphopeptides identified with each motif. Therefore the data suggest that for peptides with these motifs the treatment with 24(*S*),25-epoxycholsterol are not having an effect on these

kinases. If the oxysterol was inducing changes in the phosphorylation a skewed distribution would be apparent.

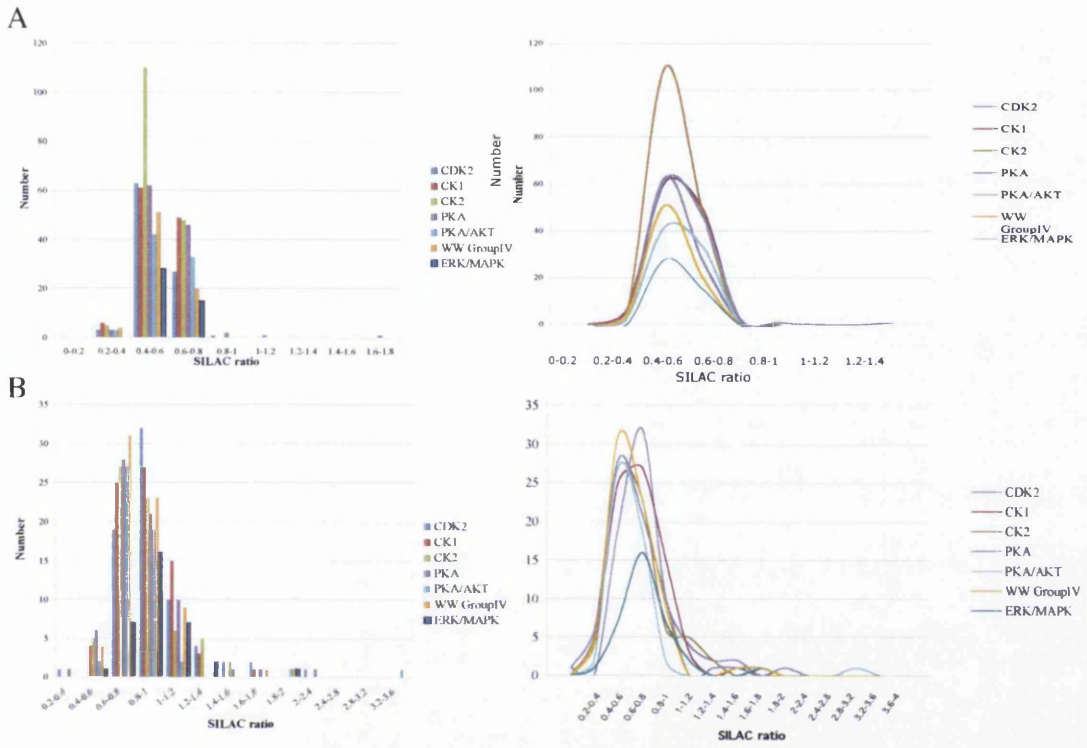

Figure 5.9. Distribution of phosphopeptide 'best motif' with SILAC ratio. Graphs indicate the distribution of motifs in the first (A) and second (B) biological replicate. Both biological replicates showed a normal distribution of the most abundant 'best' phospho motifs when plotted against un-normalised SILAC ratio after 24(*S*),25-epoxycholesterol treatment. These data suggest no effect of the oxysterols on these kinases. The median un-normalised SILAC ratio value for total peptides after 24(*S*),25-epoxycholesterol treatment was 0.59 and 0.81 respectively for the two biological treatments (15.87 percentile = 0.50 and 0.69 respectively, 84.13 percentile = 0.66 and 0.95 respectively).

5.2.7. Quantitative Analysis of Changes in Phosphorylation

As the samples were SILAC labelled this allowed the analysis of quantitative changes in the phosphorylation status of the SN4741 cells upon treatment with 25-hydroxycholesterol and 24(*S*),25-epoxycholesterol. Thus, in order to elucidate

reproducible changes in the phosphoproteome the data sets were examined for phosphopeptides reproducibly identified by the SILAC labelling as up or down regulated.

Due to the fact that phosphorylation in signalling pathways is transient and occurs without a change in total protein expression individual phosphopeptides were analysed instead of the overall protein expression in order to examine the phosphorylation state of the SN4741 cells. To this end, peptides common to both biological replicates with a Mascot score ≥25 and a SILAC ratio were examined for reproducible up or down regulation of the phosphopeptides. The un-normalised SILAC ratio was used for analysis. The median un-normalised SILAC ratio value after 25-hydroxycholesterol treatment (i.e. 25-hydroxycholesterol:control) was 0.66 and 0.75 respectively for the two biological treatments. The 15.87 percentile figure which gives an estimation of the standard deviation gave values of 0.53 and 0.61 for the 2 biological replicates. After 24(*S*),25-epoxycholesterol treatment the median un-normalised SILAC ratio value was 0.59 and 0.81 respectively for the 2 biological replicates. The 15.87 percentile figure was 0.50 and 0.69 respectively.

Table 5.7. Median SILAC un-normalised ratios for the 2 phosphoproteomic data sets. The median un-normalised 25-hydroxycholesterol:control and 24(*S*),25-epoxycholesterol:control ratios are shown as well as the 15.87 and 84.13 percentile ranges for the data.

	Ratio 25-OHChol :Control			**Ratio 24*S*,25-EC :Control**		
	Median	**15.87 Percentile**	**84.13 Percentile**	**Median**	**15.87 Percentile**	**84.13 Percentile**
Replicate						
1	0.66	0.53	0.77	0.59	0.50	0.66
2	0.75	0.61	0.93	0.81	0.69	0.95

A number of phosphopeptides were identified as being up or down regulated after treatment with 25-hydroxycholesterol or 24(*S*),25-epoxycholesterol. In total 87 unique peptides were identified as up-regulated and 65 down-regulated after treatment with 25-hydroxycholesterol. 101 unique phosphopeptides were identified as up-regulated and 68 down-regulated after treatment with 24(*S*),25-epoxycholesterol (a complete list of all phosphopeptides identified as changed is shown in appendix 3, appendix 4, appendix 5 and appendix 6). However, a number of these phosphopeptides had contradictory data between the 2 datasets. Therefore, these phosphopeptides were removed and the remaining peptides are shown below (tables 5.8, 5.9, 5.10, 5.11)

Table 5.8. Phosphopeptides identified as down-regulated after treatment with 24(*S*),25-epoxycholesterol (24(*S*),25-EC). Un-normalised SILAC phosphopeptide ratios are displayed

			Mascot Score		Ratio 25-OHChol :Control		Ratio 24(*S*),25-EC :Control	
		Replicate	1	2	1	2	1	2
Phosphopeptide	**Gene**	**IPI Number**						
EEVAS(ph)EPEEAASPTTPK	Nop56	IPI00318048	48.39	/	0.358	/	0.413	/
SQET(ph)PEKPR	Msl1	IPI00110256	30.08	/	0.650	/	0.408	/
GEGERS(ph)DEENEEK	Polr3g	IPI00463147	60.57	/	0.671	/	0.408	/
HS(ph)VTGYGDC(me)AAGAR	Jub	IPI00453693	35.36	/	0.440	/	0.404	/
GDVS(ph)EDEPSLGR	Rnmt	IPI00453849	32.67	/	0.598	/	0.400	/
RPMEEDGEEKSPS(ph)K	Ilf3	IPI00130591	34.61	/	0.410	/	0.400	/
RIS(ph)GLIYEETR	Hist1h4a	IPI00623776	35.15	/	0.267	/	0.400	/
SRLTPT(ph)TPESSSTGTEDK	Sqstm1	IPI00133374	69.05	/	0.392	/	0.398	/
ADS(ph)DSEDKGEESKPK	Cbx1	IPI00129466	40.05	/	0.347	/	0.393	/
NNVMT(ph)SPNVHLK	Cenpc1	IPI00114808	34.17	/	0.284	/	0.390	/
GVQAGNSDT(ph)EGGQPGR	Acin1	IPI00121136	32.19	/	0.811	/	0.387	/
NGLSQPS(ph)EEEVDIPKPK	Ddx21	IPI00120691	42.24	/	0.323	/	0.384	/
LPSGSGPASPTT(ph)GSAVDIR	Ahnak	IPI00553798	65.09	/	0.339	/	0.378	/
GSGEASSDSIDHS(ph)PAK	Suv39h2	IPI00111417	26.96	/	0.174	/	0.377	/
KTS(ph)LSDSTTSAYPGDAGK	Rab3gap1	IPI00749720	39.80	/	0.593	/	0.377	/
GHYEVTGS(ph)DDEAGK	Ahnak	IPI00553798	58.36	/	0.168	/	0.371	/
S(ph)ESSGNLPSVADTR	Akap1	IPI00230591	29.82	/	0.390	/	0.371	/
SNS(ph)FSDER	Ahnak	IPI00553798	29.85	/	0.154	/	0.366	/
RLS(ph)QSDEDVIR	Wdr26	IPI00226275	83.20	29.45	0.399	0.357	0.365	0.414
GGVTGSPEASISGS(ph)KGDLK	Ahnak	IPI00553798	43.68	/	0.119	/	0.363	/
LPSDSSASPPLSQT(ph)TPNKDADDQAR	Eya3	IPI00411085	40.03	/	0.518	/	0.348	/
S(ph)PSRPLPEVTDEYK	Ssb	IPI00134300	26.42	/	0.551	/	0.346	/
GGVTGSPEAS(ph)ISGSKGDLK	Ahnak	IPI00553798	43.68	/	0.135	/	0.346	/
AS(ph)AVSPEKAPM(ox)TSK	Tcof1	IPI00115660	34.02	/	0.345	/	0.346	/
DSVPAS(ph)PGVPAADFPAETEQSKPSK	Top2a	IPI00122223	25.31	/	0.116	/	0.342	/
KGDDS(ph)DEEDLC(me)ISNK	Stard13	IPI00857002	57.82	/	0.027	/	0.317	/
S(ph)SPPVEHPAGTSTTDNDVIIR	Rai14	IPI00453820	35.31	/	0.170	/	0.308	/
GDQVSQNGLPAEQGS(ph)PR	Sptbn1	IPI00319830	58.12	/	0.654	/	0.208	/

SHS(ph)LDDLQGDADVGK	Sash1	IPI00338954	/	58.75	/	0.525	/	0.538
LESHGSS(ph)EESLQVQEK	Vcan	IPI00875672	/	42.02	/	0.497	/	0.535
ANTSS(ph)DLEKDDDAYK	Ranbp2	IPI00337844	/	40.08	/	0.436	/	0.533
MSPNETLFLES(ph)TNK	Rragc	IPI00468702	/	32.32	/	0.407	/	0.530
AES(ph)PETSAVESTQSTPQK	Pds5b	IPI00845638	41.44	63.25	0.594	0.288	0.437	0.520
LEPAPLDSS(ph)PAVSTHEGSK	Renbp	IPI00124826	/	31.06	/	0.584	/	0.515
(ac)S(ph)ETAPVAQAASTATEKPAAAK	Hist1h1a	IPI00228616	/	53.02	/	0.439	/	0.514
PQSPVIQATAGS(ph)PK	Arfgef2	IPI00137087	/	41.94	/	0.350	/	0.511
VS(ph)PVPSPSQPAR	Mical1	IPI00116371	/	25.71	/	0.435	/	0.486
IDQGS(ph)HTAGESSTR	Tdp1	IPI00222253	/	34.56	/	0.416	/	0.476
S(ph)PASTSSVNGTPGSQLSTPR	Dclk1	IPI00468380	/	43.36	/	0.459	/	0.472
AQGHS(ph)PVNGLLK	Ccnl2	IPI00310772	/	25.94	/	0.493	/	0.464
HNS(ph)TTSSTSSGGYR	Abi1	IPI00798483	/	57.32	/	0.536	/	0.443
TASRPEDTPDSPSGPSS(ph)PK	Lrrc16a	IPI00474873	/	46.92	/	0.216	/	0.439
AGYTT(ph)DESSSSSLHTTR	Fxr2	IPI00126389	/	38.76	/	0.551	/	0.358
LYNSEESRPYT(ph)NK	Crkrs	IPI00648022	/	49.10	/	0.205	/	0.338
PQSAS(ph)PAKEEQK	Palm	IPI00129298	/	30.20	/	0.390	/	0.196

Table 5.9. Phosphopeptides identified as up-regulated after treatment with 24(*S*),25-epoxycholesterol (24(*S*),25-EC). Un-normalised SILAC phosphopeptide ratios are displayed

			Mascot Score		Ratio 25-OHChol :Control		Ratio 24(*S*),25-EC :Control	
		Replicate	1	2	1	2	1	2
Phosphopeptide	**Gene**	**IPI Number**						
KDS(ph)ISEDEMVLR	Wdtc1	IPI00108450	43.30	/	0.82	/	1.66	/
GGIDNPAIT(ph)SDQEVDDKK	Arhgap5	IPI00124298	40.63	/	0.92	/	1.13	/
KQIT(ph)VEELVR	Plec1	IPI00400215	38.61	/	0.62	/	1.07	/
PTGGLRDS(ph)EAEK	Hirip3	IPI00222813	29.49	/	1.03	/	1.06	/
DELADEIANSS(ph)GK	Myh9	IPI00123181	29.65	/	1.17	/	0.97	/
GPEVEGS(ph)PVSEALR	Brwd1	IPI00654074	37.76	/	0.55	/	0.95	/
LLQDSSS(ph)PVDLAK	Ncoa2	IPI00116968	29.72	/	1.12	/	0.92	/
IKPDEDLPS(ph)PGSR	Gli3	IPI00123429	42.62	/	0.78	/	0.91	/
IKDPDLT(ph)TPDSK	Ckap2	IPI00470092	44.82	/	0.79	/	0.85	/
SEVQAHS(ph)PSR	Mtap2	IPI00895965	31.21	/	0.91	/	0.85	/
ADS(ph)PAGLEAAR	Kiaa0284	IPI00380953	35.46	/	0.78	/	0.84	/
GGSS(ph)EELHDSPR	Hdgfrp2	IPI00116442	34.55	/	0.74	/	0.81	/
ASS(ph)EDTLNKPGSASSGVAR	Specc1	IPI00798550	33.64	/	0.89	/	0.80	/
KGS(ph)LDYLK	Luzp1	IPI00322204	30.67	/	0.71	/	0.80	/
HGPAQAVTGTSVTS(ph)PIK	Ccnt2	IPI00654257	47.80	/	0.74	/	0.79	/
NS(ph)PNNISGISNPPGTPR	Ssbp3	IPI00341944	51.85	/	0.82	/	0.79	/
KLS(ph)SGDLR	Phldb1	IPI00330246	30.55	/	0.68	/	0.79	/
RAS(ph)LSDIGFGK	Pctk3	IPI00111168	49.16	/	0.60	/	0.78	/
IKDPDLTT(ph)PDSK	Ckap2	IPI00470092	44.82	/	0.95	/	0.78	/
KGT(ph)GDC(me)SDEEVDGK	Myh9	IPI00123181	49.18	/	0.84	/	0.78	/
SQDATVS(ph)PGSEQSEK	Zc3hc1	IPI00465879	50.16	/	0.53	/	0.78	/
GQGT(ph)PPSGPGVGR	Wbp7	IPI00857289	27.74	/	0.61	/	0.77	/
QESLKS(ph)PEEEDQQAFR	Nes	IPI00453692	36.61	/	0.67	/	0.76	/
TQSSS(ph)C(me)EDLPSTTQPK	Cask	IPI00776341	25.68	/	0.46	/	0.76	/
RFS(ph)M(ox)EDLNK	Pctk3	IPI00111168	47.88	/	0.69	/	0.76	/
DDISEIQSLASDHS(ph)GR	Tjp1	IPI00135971	31.83	/	0.57	/	0.76	/
C(me)IFMSETQSS(ph)PTK	Pias2	IPI00453655	30.79	/	0.47	/	0.75	/
QDVDNAS(ph)LAR	Vim	IPI00227299	31.40	/	0.72	/	0.75	/
QEFSS(ph)EEMTK	Vcam1	IPI00126834	25.88	/	0.83	/	0.74	/
(ac)SDQEAKPST(ph)EDLGDKK	Sumo1	IPI00124593	33.58	/	0.78	/	0.73	/

DC(me)AKS(ph)DDEESLTLPEK	Nfkb1	IPI00719890	52.31	/	0.80	/	0.73	/
PAVVS(ph)PLSLSTEAR	Crtc1	IPI00469761	43.71	/	0.80	/	0.73	/
YVSGSS(ph)PDLVTR	Ptpn14	IPI00122168	49.84	/	0.73	/	0.73	/
ASPDQNASTHT(ph)PQSSAK	Clint1	IPI00648186	34.63	/	0.78	/	0.73	/
SSGSLS(ph)PGLETEDPLEAR	Tnks1bp1	IPI00459443	36.91	/	0.68	/	0.73	/
TASESISNLSEAGS(ph)VK	Clip1	IPI00857273	31.00	/	0.98	/	0.72	/
AQTPESC(me)GSVT(ph)PER	Filip1l	IPI00755058	30.92	/	0.94	/	0.72	/
SAT(ph)LETKPESK	Ifngr1	IPI00323231	25.38	/	0.64	/	0.72	/
SDEEDRAS(ph)EPK	Zc3h18	IPI00673693	27.94	/	0.79	/	0.72	/
VEESSEIS(ph)PEPK	Usp1	IPI00330276	40.56	/	0.57	/	0.72	/
S(ph)LEGENHDPLSSVVK	Nes	IPI00453692	45.85	/	0.68	/	0.72	/
MHASSTGSS(ph)C(me)DLSK	Cdgap	IPI00125505	27.19	/	0.54	/	0.72	/
AKT(ph)PVTLK	Tmpo	IPI00828976	41.32	/	0.58	/	0.72	/
SSS(ph)FGSVSTSSTSSK	Snx16	IPI00331029	/	54.62	/	1.42	/	5.00
SGFGGMSS(ph)PVIR	Nup107	IPI00221767	/	40.37	/	2.57	/	2.07
TEEDRENTQIDDTEPLS(ph)PVSNSK	Trp53bp1	IPI00229801	/	28.80	/	2.58	/	1.90
SEDRPS(ph)SPQVSVAAVETK	Trp53bp1	IPI00229801	/	48.56	/	2.07	/	1.70
PAS(ph)PLSGPR	D2Wsu81e	IPI00224127	/	29.84	/	1.80	/	1.65
GEVAPKET(ph)PKK	Marcksl1	IPI00281011	/	26.82	/	2.27	/	1.65
TVGNVS(ph)PTAQMVQR	Rbm7	IPI00133061	/	28.20	/	1.41	/	1.65
LHSAQLS(ph)PVDETPATQSQLK	Mlf1ip	IPI00459115	/	36.63	/	1.95	/	1.62
QEGAQENVKNS(ph)PVPR	Gmnn	IPI00131716	/	30.64	/	2.56	/	1.60
TTS(ph)PDLFESQSLTSASSK	Epn2	IPI00336844	/	27.33	/	1.25	/	1.55
AGS(ph)SPTQGAQNEAPR	Tcf20	IPI00407458	/	30.95	/	1.46	/	1.51
AS(ph)SHSSQSQGGGSVTK	Lmna	IPI00620256	/	58.67	/	2.60	/	1.51
C(me)QETESNEEQSIS(ph)PEKR	Akap12	IPI00123709	/	85.89	/	1.19	/	1.49
LATSS(ph)PEQSWPSTFK	Pml	IPI00229072	/	29.49	/	1.18	/	1.43
KQNETADEAT(ph)TPQAK	Nolc1	IPI00720058	/	43.74	/	1.50	/	1.42
EIITEEPS(ph)EEEADMPKPK	Ddx21	IPI00120691	/	31.38	/	1.69	/	1.38
AEEDEILNRS(ph)PR	Canx	IPI00119618	/	25.35	/	1.51	/	1.35
GPEVTSQGVQTSS(ph)PAC(me)K	Atxn2	IPI00117229	/	25.10	/	1.07	/	1.30
ASGQAFELILS(ph)PR	Stmn1	IPI00551236	/	30.07	/	0.87	/	1.30
AVGEEQRS(ph)EEPK	Akap12	IPI00123709	/	31.72	/	1.15	/	1.30

Table 5.10. Phosphopeptides identified as down-regulated after treatment with 25-hydroxycholesterol (25-OHChol). Un-normalised SILAC phosphopeptide ratios are displayed

			Mascot Score		Ratio 25-OHChol :Control		Ratio 24(*S*),25-EC :Control	
		Replicate	1	2	1	2	1	2
Phosphopeptide	**Gene**	**IPI Number**						
SPDEATAADQES(ph)EDDLSASR	Farp1	IPI00356904	26.44	/	0.349	/	0.465	/
TEEVLSPDGSPSKS(ph)PSK	Add3	IPI00387580	38.11	/	0.349	/	0.439	/
ADS(ph)DSEDKGEESKPK	Cbx1	IPI00129466	40.05	/	0.347	/	0.393	/
EELEQQT(ph)DGDC(me)DEEDDDK DGEVPK	Sec62	IPI00134398	57.28	/	0.346	/	0.532	/
EDAPPEDKES(ph)ESEAK	Cds2	IPI00468999	26.03	/	0.346	/	0.594	/
ERQES(ph)ESEQELVNK	Pdcd11	IPI00551454	39.77	/	0.345	/	0.560	/
AS(ph)AVSPEKAPM(ox)TSK	Tcof1	IPI00115660	34.02	/	0.345	/	0.346	/
ADS(ph)DSEDKGEESKPK	Cbx1	IPI00129466	40.05	/	0.344	/	0.451	/
LPSGSGPASPTT(ph)GSAVDIR	Ahnak	IPI00553798	65.09	/	0.339	/	0.378	/
IGPLGLS(ph)PK	Rpl12	IPI00463634	45.65	/	0.333	/	0.426	/
EIITEEPS(ph)EEEADM(ox)PKPK	Ddx21	IPI00120691	56.99	/	0.330	/	0.443	/
NGLSQPS(ph)EEEADIPKPK	Ddx21	IPI00120691	36.77	/	0.325	/	0.431	/
NGLSQPS(ph)EEEVDIPKPK	Ddx21	IPI00120691	42.24	/	0.323	/	0.384	/
NISEES(ph)PLTHR	Pask	IPI00400044	32.53	/	0.322	/	0.610	/
S(ph)PAKEPVEQPR	Spen	IPI00828562	25.27	/	0.321	/	0.464	/
RVSGS(ph)ATPNSEAPR	Ddx51	IPI00396728	58.55	/	0.306	/	0.460	/
S(ph)HTGEAAAVR	Bcl2l13	IPI00321499	35.83	/	0.288	/	0.467	/
NNVMT(ph)SPNVHLK	Cenpc1	IPI00114808	34.17	/	0.284	/	0.390	/
RVS(ph)GSATPNSEAPR	Ddx51	IPI00396728	58.55	/	0.278	/	0.427	/
YLEIDS(ph)DEESR	Sdad1	IPI00387439	33.64	/	0.276	/	0.529	/
DDS(ph)GAEDNVDTHQQQAENST VPTADSR	Rspry1	IPI00223590	27.35	/	0.275	/	0.445	/
LSQVNGATPVS(ph)PIEPESK	Mybbp1a	IPI00331361	33.48	/	0.272	/	0.461	/
RIS(ph)GLIYEETR	Hist1h4a	IPI00623776	35.15	/	0.267	/	0.400	/
GS(ph)HC(me)SGSGDPAEYNLR	Lmna	IPI00620256	32.11	/	0.257	/	0.488	/
LSQVNGAT(ph)PVSPIEPESK	Mybbp1a	IPI00331361	33.48	/	0.254	/	0.436	/
SST(ph)PLPTVSSSAENTR	Tmpo	IPI00896574	55.29	/	0.246	/	0.516	/
SPFNSPSPQDS(ph)PR	Nfic	IPI00137501	40.52	/	0.213	/	0.435	/
GSGEASSDSIDHS(ph)PAK	Suv39h2	IPI00111417	26.96	/	0.174	/	0.377	/

S(ph)SPPVEHPAGTSTTDNDVIIR	Rai14	IPI00453820	35.31	/	0.170	/	0.308	/
GHYEVTGS(ph)DDEAGK	Ahnak	IPI00553798	58.36	/	0.168	/	0.371	/
SNS(ph)FSDER	Ahnak	IPI00553798	29.85	/	0.154	/	0.366	/
GGVTGSPEAS(ph)ISGSKGDLK	Ahnak	IPI00553798	43.68	/	0.135	/	0.346	/
GGVTGSPEASISGS(ph)KGDLK	Ahnak	IPI00553798	43.68	/	0.119	/	0.363	/
DSVPAS(ph)PGVPAADFPAETEQS KPSK	Top2a	IPI00122223	25.31	/	0.116	/	0.342	/
SGAAEEDDS(ph)GVEVYYR	Pdcd11	IPI00551454	41.08	/	0.104	/	0.592	/
KGDDS(ph)DEEDLC(me)ISNK	Stard13	IPI00857002	57.82	/	0.027	/	0.317	/
MSPNETLFLES(ph)TNK	Rragc	IPI00468702	/	32.32	/	0.407	/	0.530
SPSPSPTS(ph)PGSLR	Dclk1	IPI00468380	/	51.87	/	0.398	/	0.582
PQSAS(ph)PAKEEQK	Palm	IPI00129298	/	30.2	/	0.390	/	0.196
LS(ph)PAYSLGSLTGASPR	Phldb1	IPI00330246	/	34.03	/	0.369	/	0.573
SGTSTPTTPGSTAITPGT(ph)PPSYS SR	Mtap2	IPI00895463	/	69.16	/	0.360	/	0.661
TASRPEDTPDSPSGPSS(ph)PK	Lrrc16a	IPI00474873	/	46.92	/	0.216	/	0.439
LYNSEESRPYT(ph)NK	Crkrs	IPI00648022	/	49.1	/	0.205	/	0.338

Table 5.11. Phosphopeptides identified as up-regulated after treatment with 25-hydroxycholesterol (25-OHChol). Un-normalised SILAC phosphopeptide ratios are displayed

			Mascot Score		Ratio 25-OHChol :Control		Ratio 24(*S*),25-EC :Control	
		Replicate	1	2	1	2	1	2
Phosphopeptide	**Gene**	**IPI Number**						
HGS(ph)DPAFGPSPR	Fam83h	IPI00227516	28.43	/	1.795	/	0.658	/
DELADEIANSS(ph)GK	Myh9	IPI00123181	29.65	/	1.166	/	0.970	/
S(ph)STSGSASSLESGVYR	Gtse1	IPI00268247	63.04	/	1.152	/	0.614	/
AQT(ph)PESC(me)GSVTPER	Filip1l	IPI00755058	30.92	/	1.120	/	0.637	/
LLQDSSS(ph)PVDLAK	Ncoa2	IPI00116968	29.72	/	1.118	/	0.919	/
RQS(ph)LTSPDSQSTR	Herc1	IPI00676574	33.46	38.87	1.064	0.991	0.698	0.776
GS(ph)PEDGSHEASPLEGK	Rbm20	IPI00849187	51.26	/	1.055	/	0.586	/
PTGGLRDS(ph)EAEK	Hirip3	IPI00222813	29.49	/	1.035	/	1.064	/
KLEVS(ph)PGDEQSNVETR	Gnl3	IPI00222461	73.45	/	0.988	/	0.431	/
TASESISNLSEAGS(ph)VK	Clip1	IPI00857273	31	/	0.975	/	0.725	/
IKDPDLTT(ph)PDSK	Ckap2	IPI00470092	44.82	/	0.954	/	0.782	/
AQTPESC(me)GSVT(ph)PER	Filip1l	IPI00755058	30.92	/	0.944	/	0.724	/
GGIDNPAIT(ph)SDQEVDDKK	Arhgap5	IPI00124298	40.63	/	0.924	/	1.125	/
SNS(ph)NSSSVITTEDNK	Filip1l	IPI00755058	77.83	/	0.922	/	0.623	/
SEVQAHS(ph)PSR	Mtap2	IPI00895965	31.21	/	0.907	/	0.849	/
TTSTSNPSS(ph)PAPDWYK	Atrx	IPI00857253	38.08	/	0.892	/	0.604	/
ASS(ph)EDTLNKPGSASSGVAR	Specc1	IPI00798550	33.64	/	0.887	/	0.805	/
YMSSDTT(ph)SPELR	Sin3a	IPI00117932	27.09	/	0.883	/	0.580	/
YIASVQGSAPS(ph)PR	Ranbp2	IPI00337844	36.79	/	0.875	/	0.596	/
EKEEEETS(ph)PDTSIPR	Arhgef5	IPI00855144	48.09	/	0.868	/	0.565	/
AS(ph)SHSSQSQGGGSVTK	Lmna	IPI00620256	/	58.67	/	2.595	/	1.511
TEEDRENTQIDDTEPLS(ph)PVSNSK	Trp53bp1	IPI00229801	/	28.8	/	2.576	/	1.904
SGFGGMSS(ph)PVIR	Nup107	IPI00221767	/	40.37	/	2.574	/	2.074
QEGAQENVKNS(ph)PVPR	Gmnn	IPI00131716	/	30.64	/	2.565	/	1.603
GEVAPKET(ph)PKK	Marcksl1	IPI00281011	/	26.82	/	2.274	/	1.651
SEDRPS(ph)SPQVSVAAVETK	Trp53bp1	IPI00229801	/	48.56	/	2.071	/	1.704
LHSAQLS(ph)PVDETPATQSQLK	Mlf1ip	IPI00459115	/	36.63	/	1.947	/	1.619
PAS(ph)PLSGPR	D2Wsu81e	IPI00224127	/	29.84	/	1.802	/	1.652

T(ph)SMGGTQQQFVEGVR	Ctnnb1	IPI00125899	/	48.59	/	1.721	/	1.130
EIITEEPS(ph)EEEADMPKPK	Ddx21	IPI00120691	/	31.38	/	1.693	/	1.383
HLFSS(ph)TENLAAR	Rab11fip1	IPI00169485	/	39.84	/	1.665	/	1.264
NWTEDIEGGISS(ph)PVK	Nfic	IPI00137501	/	32.95	/	1.656	/	1.073
TTVYYQS(ph)PLESKPR	Atad2	IPI00135252	/	41.56	/	1.532	/	1.139
T(ph)GSLQLSSTSIGTSSLK	Cobll1	IPI00762331	/	31.52	/	1.526	/	0.746
AEEDEILNRS(ph)PR	Canx	IPI00119618	/	25.35	/	1.506	/	1.350
KQNETADEAT(ph)TPQAK	Nolc1	IPI00720058	/	43.74	/	1.498	/	1.422
SRLTPTTPES(ph)SSTGTEDK	Sqstm1	IPI00133374	/	74.88	/	1.485	/	0.733
IALESVGQPEEQMESGNC(me)S(ph)GGDDDWTHLSSK	Sqstm1	IPI00133374	/	27.33	/	1.471	/	0.787
AGS(ph)SPTQGAQNEAPR	Tcf20	IPI00407458	/	30.95	/	1.457	/	1.514
KAPLTLAGS(ph)PTPK	Wiz	IPI00263016	/	39.77	/	1.455	/	1.147
KLDTFQSTS(ph)PK	Ddx24	IPI00113576	/	27.61	/	1.453	/	1.063
SRLT(ph)PTTPESSSTGTEDK	Sqstm1	IPI00133374	/	74.88	/	1.435	/	0.821
SSS(ph)FGSVSTSSTSSK	Snx16	IPI00331029	/	54.62	/	1.416	/	4.998
TVGNVS(ph)PTAQMVQR	Rbm7	IPI00133061	/	28.2	/	1.414	/	1.646
SRLTPTT(ph)PESSSTGTEDK	Sqstm1	IPI00133374	/	74.88	/	1.408	/	0.841
TEMDKS(ph)PFNSPSPQDSPR	Nfic	IPI00137501	/	35.42	/	1.371	/	1.118

Removal of the phosphopeptides only identified in 1 biological replicate reduced the total number of phosphopeptides considerably. In total 2 phosphopeptides were identified as changed (1 down-regulated, and 1 up-regulated) in both biological replicates after treatment with 25-hydroxycholesterol (table 5.12.). In the case of these phosphopeptides they are in the lowest or highest 15.87 percentile range and thus can be considered greater than 1 standard deviation away from the median. The median ratio after 24(*S*),25-epoxycholesterol was 0.59 (15.87 percentile = 0.5) and 0.81 (15.87 percentile = 0.69) for the two biological replicates respectively. Thus, only one peptide (RLS(ph)QSDEDVIR) was in the 15.87 percentile range in both biological replicates after treatment with 24(*S*),25-epoxycholesterol. It is interesting to note that the protein from which this phosphopeptide is derived has been associated with MAPK signalling (Zhu *et al.* 2004). There is evidence that MAPK (AKA ERK) phosphorylation can be influenced by oxysterols and, in addition, ERK appears to have a role in dopaminergic neurogenesis (section 5.1).

Table 5.12. Phosphopeptides identified as having change in expression after treatment with 25-hydroxycholesterol (25-OHChol) or 24(*S*),25-epoxycholesterol (24(*S*),25-EC). All the peptides had a probability of identification of the correct phosphorylation site of ≥0.98. Un-normalised SILAC phosphopeptide ratios are displayed. Values in bold were classed as changed

			Mascot Score		**Ratio 25-OHChol :Control**		**Ratio 24(*S*),25-EC :Control**	
		Replicate	**1**	**2**	**1**	**2**	**1**	**2**
Phosphopeptide	**Gene**	**IPI Number**						
RLS(ph)QSDEDVIR	Wdr26	IPI00226275	83.2	29.45	**0.36**	**0.36**	**0.40**	**0.41**
RQS(ph)LTSPDSQSTR	Herc1	IPI00676574	33.46	38.87	**1.06**	**0.99**	0.69	0.77.

Both phosphopeptides identified as changed (table 5.12) have no commercially available antibodies it was impossible to validate these changes. This inability to reproduce the observed changes by a different technique is critical as when analysed as a population the ratio of the phosphopeptides that were identified in both biological replicates were variable (fig. 5.10). Indeed, in some cases the phosphopeptides identified when quantified changed in opposite directions. Points in the upper left quadrant of the graph represent phosphopeptides that have increased in one replicate and decreased in the other (fig. 5.10). Thus, despite strong evidence to suggest that the peptide identification and phosphorylation site is correct without further experimental evidence it is difficult to have certainty to the changes in the quantification of the phosphorylation.

A

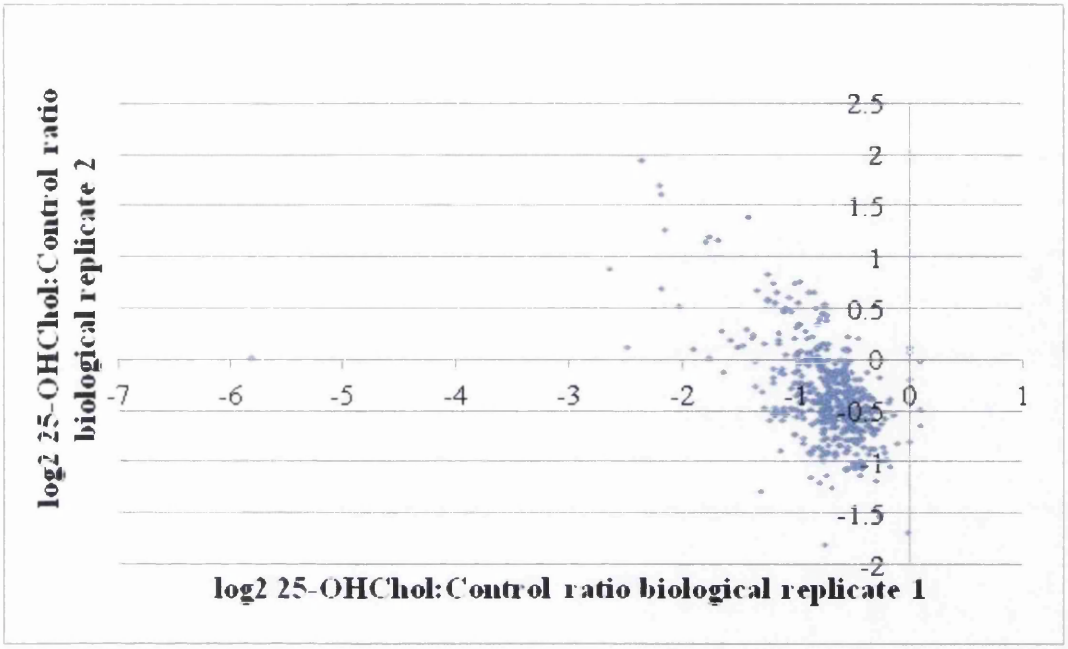
log2 25-OHChol:Control ratio biological replicate 2
2.5
2
1.5
1
0.5
0
-0.5
-1
-1.5
-2
-7
-6
-5
-4
-3
-2
-1
0
1
log2 25-OHChol:Control ratio biological replicate 1

B

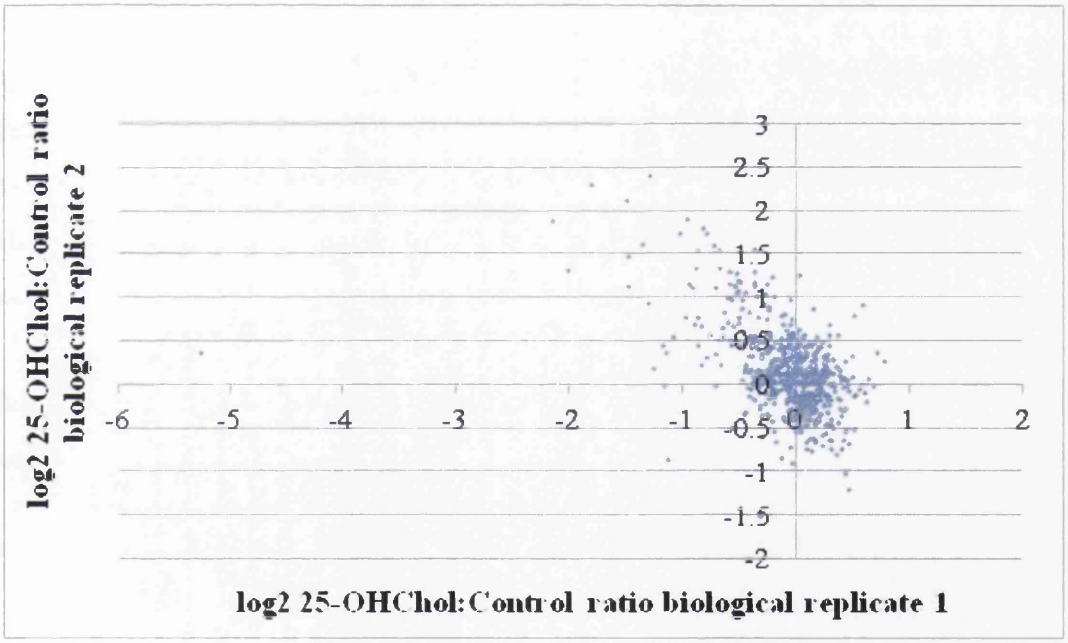
log2 25-OHChol:Control ratio biological replicate 2
3
2.5
2
1.5
1
0.5
0
-0.5
-1
-1.5
-2
-6
-5
-4
-3
-2
-1
0
1
2
log2 25-OHChol:Control ratio biological replicate 1

C

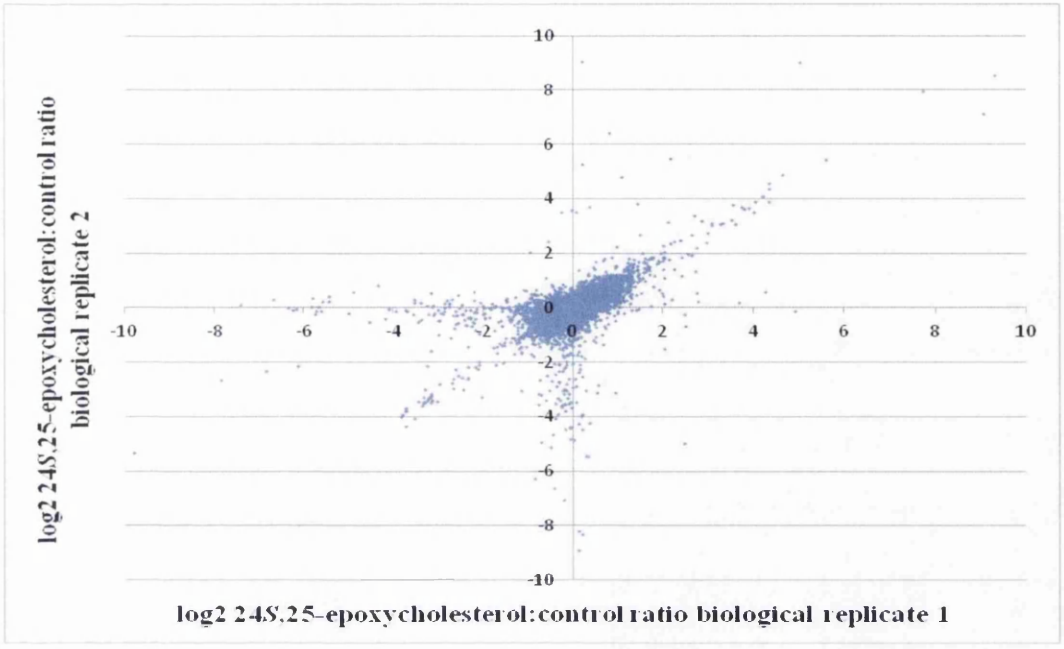

Figure 5.10. Poor correlation in peptide ratio between biological replicates. There is poor correlation in the ratios of the phosphopeptides common to both biological replicates after treatment with 25-hydroxycholesterol. The un-normalised ratio of the phosphopeptide (A) has a poor correlation with a number of peptides having opposite responses in a number of cases (top left quadrant). The normalised phosphopeptide ratios had a similar trend (B). Normalisation occurs in each experiment to take into account any error introduced by protein mixing. (C) As a contrast peptide ratios from 2 biological replicates treated with 24(*S*),25-epoxycholesterol and analysed for changes in protein expression (Chapter 3) showed a much better correlation in normalised peptide ratio between different biological samples.

5.2.8. Peptide Methylation

In an attempt to increase the specificity of the IMAC by reducing non-specific binding peptide methylation was undertaken. To methylate acidic amino acids and the C-terminus carboxylic acid peptides were incubated with methanolic hydrochloric acid. This methylation would, in theory prevent non-specific binding to the IMAC column as the non-phosphate negatively charged acidic moieties are blocked by the methyl group. Therefore to examine this method 2.25mg of SILAC SN4741 lysate was fractioned using strong cation exchange, treated with methanolic acid, phosphoenriched using IMAC and analysed by LC-MS/MS. This resulted in a total of 4510 peptides (2067 unique) being identified with a total Mascot score ≥25 and a SILAC ratio generated. 1082 of these 4510 peptides were phosphorylated. In total 609 unique phosphopeptides were identified. However, when examining peptide methylation only 716 of the total peptides were identified with a methylation either on an aspartic (D) or glutamic acid (E) residue or on the C-terminus. Of these only 425 were unique peptides. In addition, often the same peptide was methylated in different and/or multiple places. For example the peptide ALAAAGYDVEK from Histone H1.2 has 3 potential methylation sites one aspartic acid residue (D), one glutamic acid residue (E) and the C-terminus. This peptide was identified with 5 different combinations of methylation (table 5.13.). The 5 peptides eluted from the C18 column at different rates and therefore the total amount of peptide with the same amino acid sequence was split between the different retention times.

Table 5.13. Incomplete methylation increases complexity of the peptide mixture. In this example one peptide sequence was identified 5 times with different levels of methylation

Peptide Sequence	Mascot Score	Retention Time
ALAAAGYD(me)VE(me)K_(me)	58.27	55.025
ALAAAGYDVE(me)K_(me)	50.81	51.578
ALAAAGYD(me)VEK_(me)	34.84	50.173
ALAAAGYD(me)VE(me)K	41.49	52.224
ALAAAGYDVE(me)K	40.82	47.177

However, this dataset did contain some phosphopeptides and these were analysed to confirm the novel sites previously observed (table 5.5). Thus, analysis of the 609 unique phosphopeptides allowed further confirmation of 5 novel phosphorylation sites (table 5.14).

Table 5.14. Phosphopeptides with a novel site of phosphorylation identified in 3 independent experiments.

Sequence and Phosphorylation site	**Gene**	**Phosphorylation Site Probabilities**	**Mascot Score**
ASSFYGSAS(ph)PNHLR	Mcph1	ASSFYGS(0.007)AS(0.993)PNHLR	43.72
HVSS(ph)PDVTTAQK	Tdp1	HVS(0.054)S(0.946)PDVTTAQK	30.83
KS(ph)PEQESVSTAPQR	Spg20	KS(0.999)PEQES(0.001)VSTAPQR	38.85
NTVDIVDKPENS(ph)PQR	Phf3	NTVDIVDKPENS(1)PQR	58.37
RSTPS(ph)GPVR	Rbmxrt	RSTPS(1)GPVR	40.09

5.3. Discussion

The basis of these experiments was to identify changes in phosphorylation induced by oxysterols in SN4741 cells. Therefore, in order to elucidate reproducible changes in the phosphoproteome the data sets were examined for phosphopeptides reproducibly identified by the SILAC labelling as up-or down regulated. A limitation of the study was a use of only one time point for the SILAC experiments. As phosphorylation is a transient, reversible modification it is possible that some changes induced by oxysterol treatment were not observed due to examining the phosphoproteome at the 'wrong' time point.

However, 2 phosphopeptides were identified as having a changed expression after treatment with 25-hydroxycholesterol (table 5.12). The peptides identified had good Mascot scores and a high probability that the phosphorylation is assigned to the correct amino acid. Interestingly, WD repeat-containing protein 26 (Wdr26) which the previously reported phosphopeptide RLS(ph)QSDEDVIR (Sweet *et al.* 2009) is derived from has previously been associated with MAPK signalling (Zhu *et al.* 2004); a pathway also associated with oxysterols and dopaminergic neurogenesis. This phosphopeptide was classed as changed after treatment with 25-hydroxycholesterol or 24(*S*),25-epoxycholesterol. However, the independent validation of the observed change in these phosphopeptides was unable to be achieved due to the lack of a commercially available antibody.

With the lack of validation it is difficult to draw conclusions beyond unequivocal identification as in these experiments the reproducibility of the phosphopeptide quantification was ambiguous due to the fact that in some cases the same phosphopeptide was identified up or down regulated in different biological replicates (fig 5.10). Thus, these data throw into doubt the reliability of the very few reproducible changes observed after treatment with 25-hydroxycholesterol and 24(*S*),25-epoxycholesterol. To a certain extent these results are unsurprising as phosphorylation is a transient modification that can react quickly to a broad range of stimuli. These data highlight the technical difficulties in identifying reproducible changes in the phosphoproteome.

However, with this methodology, utilising strong cation exchange chromatography and IMAC phosphoenrichment, a large number of phosphopeptides were identified by mass spectrometry in each biological replicate. In the two biological replicates 1232 and 845 unique phosphopeptides were identified, 27% and 11% of the total unique peptides. In total 1663 phosphopeptides were identified with a Mascot score ≥25. Thus, in 2 biological replicates a proportion of the total phosphopeptides identified (414/1663, 24.9%) were observed in both data sets with Mascot scores ≥25. The reproducible observation of the same phosphopeptide in different biological replicates is a major challenge of phosphoproteomics and others have reported similar difficulties (Engholm-Keller *et al.* 2012).

Of the 414 phosphopeptides identified in both data sets 56 were identified as not currently having experimental evidence to demonstrate phosphorylation. Further analysis of these peptides allowed confident identification of 37 novel phosphorylation sites.

These data indicate that strong cation exchange chromatography followed by IMAC resulted in phosphopeptide enrichment. However, the number of phosphopeptides identified could be improved by improving the methodology. To this end peptide methylation was examined as a methodology to reduce the amount of non-specific binding to the IMAC column. However, from the data presented here the current methodology is unsuitable. The methylation is incomplete as shown by the data that only a subsection of the total population (716/4510) were identified as methylated. Furthermore, peptides identified as methylated did not react completely (table 5.13). Incomplete methylation means that unspecific binding to the column may still occur. Indeed, it appears that methylation, in some cases, does not prevent non specific binding (table 5.13). In addition the incomplete nature of the methylation may mean that some phosphopeptides have more than one retention time for the same sequence. This may lead to some of these low abundance, poorly ionisable peptides to not be detected at all. Thus methylation in some cases may be counterproductive. Therefore, other options to increase the number of phosphopeptide identifications may be preferable.

One option is to use another phosphoenrichment method sequentially after IMAC. In this case the peptide flow through from the IMAC columns would be subjected to

further stages of phosphoenrichment. Titanium dioxide (TiO_2) has previously been used for this purpose after IMAC phosphoenrichment and resulted in a greater number of peptides identified (Thingholm *et al.* 2008). Another option is to use multiple sequential rounds of phosphoenrichment using the same technique. This approach has recently been performed using titanium dioxide which resulted in the identification of ~4000 phosphorylation sites (Sharma *et al.* 2012). Using these approaches could increase the number of phosphopeptides identified and increase further the identifications common to independent biological replicates.

A second approach to improve the number of phosphopeptides identified might be to change the quantification approach. As shown in chapter 3 SILAC is a powerful technique for quantitative proteomics. However, in the case of phosphoproteomics some of its inherent characteristics might be considered weaknesses. SILAC is reliant on the triplet of peaks, seen in the MS scan, that are derived from the same peptide sequence but containing isotope labelled arginine or lysine in order to quantify peptides and, therefore, proteins. Therefore, this means for each peptide sequence there are 3 precursor ions in the spectra. For evaluation of total protein expression this is not an issue. However, the low abundance of phosphopeptides, coupled with their poor ability to ionise, might mean that due to splitting the total intensity from a given phosphopeptide over 3 peaks might result in the peptide being below the detection limit. Thus, an isobaric labelling, such as iTraq (section 1.2.3.2) might provide a better option for the quantitative analysis of phosphopeptides. iTraq labelling is performed on peptides prior to mixing and results in a covalent bond between amine groups of peptides and the iTraq reagent. The resultant labelling is isobaric between different groups and is only apparent in the MS^2 fragmentation spectra where reporter ions are used to quantify different treatment groups. Therefore, due to the isobaric nature of the iTraq labelling the initial precursor ion, unlike SILAC, is a single peak. This fact may increase the number of low intensity phosphopeptides identified whilst retaining the ability to quantify changes between different treatment groups.

One option to improve the reliability of the phosphopeptide quantification would be to analyse the non-phosphorylated peptide mixture eluted on the IMAC phosphoenrichment by LC-MS/MS. Therefore, they could be used in combination with the phosphoenriched samples, but processed by LC-MS/MS independently, in

order to normalise the phosphorylation of a given phosphopeptide to total protein expression. This can be done automatically by bio-informatic software whilst analysing data. This would give a more reliable estimation of the change in phosphorylation as the effect of experimental error in protein mixing would be adjusted for. By analysing the phosphopeptide alone this normalisation to protein is impossible as commonly the phosphopeptide is the only peptide used for identification of any protein and thus when normalised to protein results a ratio of 1.

In summary, the phosphoproteomic analysis of SN4741 cells led to the identification of a large number of phosphopeptides. Indeed, these data resulted in the identification of a number of novel phosphorylation sites in the mouse proteome. The work presented here does not investigate the role the identified phosphorylation sites play in the cell. It does, however, provide experimental evidence that these post translational modifications occur providing a basis for future elucidation. Unfortunately, the quantitative phosphoproteomics proved less successful. Phosphorylation is a transient and highly responsive post-translational modification and when compared to total protein expression that is, relatively, stable the analysis of the phosphoproteome is inherently more difficult. Thus, these data indicate the large technical challenge involved in quantitative phosphoproteomic studies.

CHAPTER 6: GENERAL DISCUSSION

Proteomics as a technology is still in its infancy. The power of this experimental approach is to analyse the global effects of treatments on protein expression and post-translational modifications. In this case the effect of 24(*S*),25-epoxycholesterol or GW3965 on protein expression and 24(*S*),25-epoxycholesterol or 25-hydroxycholesterol on the phosphoproteome. The data presented here highlight the effectiveness of proteomic experimental design in the ability to identify quantifiable changes in protein expression is clear. In the experiments analysing protein expression thousands of proteins were identified and quantified the majority of which with 2 or more peptides. The SILAC approach employed identified expected changes in protein expression after treatment with 24(*S*),25-epoxycholesterol or GW3965. These observations in known changes (e.g. the LXR regulated gene ABCA1) lend weight to the observed unexpected changes and, in addition, act as a positive control for treatment uptake. The SILAC methodology for quantifying protein expression changes presented here could easily be applied to any cell type or treatment.

Nevertheless, challenges remain. The selection of a peptide for fragmentation is reliant, to a certain extent, on chance as there is no guarantee that a protein of interest will be identified. This can be seen in tables 3.5. and 3.6 where a number of proteins are not identified in all three biological replicates. This is especially true of proteins of interest that are of low abundance as peptides with a weaker signal are at risk of not being selected for fragmentation and therefore identified. In addition, as SILAC data consists of light, medium and heavy peptides the spectra generated are inherently more complex. This could result in fragmentation of the same peptide in different SILAC states over a lower abundance unique peptide. In addition, the increased complexity might mask lower abundance peptides by having precursor ion peaks from other peptides superimposed on them. However, despite these potential limitations the SILAC data presented here identified a number of novel 24(*S*),25-epoxycholesterol induced protein changes.

Cholesterol itself is an integral part of cell membranes therefore it is perhaps unsurprising that a number of the novel 24(*S*),25-epoxycholesterol changes observed are related to membrane composition. The presence of 24(*S*),25-epoxycholesterol inhibits cholesterol synthesis and therefore may lead to membrane alteration (fig 6.1).

Two proteins involved directly or indirectly in phospholipid synthesis, phosphoethanolamine cytidylyltransferase and collagen type IV alpha-3-binding protein, were identified as changed after 24(*S*),25-epoxycholesterol treatment. Phosphoethanolamine cytidylyltransferase (PCyt2), a independently reported SREBP2 regulated gene identified whilst this work was being conducted (Ando *et al.* 2010), is required for phosphoethanolamine synthesis and is down-regulated after 24(*S*),25-epoxycholesterol treatment (table 3.10). Collagen type IV alpha-3-binding protein (col4a3bp; StAR-related lipid transfer protein 11, Stard11) is up-regulated after 24(*S*),25-epoxycholesterol treatment at both the protein and mRNA level (table 3.10; fig. 4.1). This protein transports ceramide from the endoplasmic reticulum to the Golgi apparatus where it is synthesised to sphingomyelin. In addition to the changes in the proteins involved in lipid synthesis caveolin-1, the lipid raft component, was identified as down-regulated after 24(*S*),25-epoxycholesterol treatment which based on confocal microscopy data appears to be related to changes in cholesterol levels (table 3.10; fig 3.17; fig.3.18; fig. 3.19). In order to investigate this hypothesis it could be possible to investigate the cholesterol level of 24(*S*),25-epoxycholesterol treated SN4741 cells to see if there is a correlation between cholesterol level and caveolin-1 expression. Indeed, mass spectrometry could be used to analyse all the components of the plasma membrane. Thus, quantification of phospholipids and cholesterol could determine the effect of the observed protein changes in relation to membrane lipids.

It is clear that 24(*S*),25-epoxycholesterol has an effect on caveolin-1 expression and localisation. Further investigations into the effect of 24(*S*),25-epoxycholesterol on protein localisation in SN4741 cells could be conducted using a proteomics approach. Subcellular fractionation could be used in order to examine the protein expression in certain parts of the cell. Subcellular fractionation allows different components of the cell to be isolated and therefore analysed separately. Thus, it could be possible to combine subcellular fractionation with, for example, SILAC labelling in order to quantify changes to protein distribution after a treatment. This approach would allow the identification of changes in membrane protein composition and protein translocation (e.g. cytoplasm to nucleus) where the total protein expression remains constant.

24(*S*),25-epoxycholesterol was shown to increase macrophage colony stimulating factor (MCSF) in SN4741 cells at both the protein and mRNA level. It is interesting

to note that MCSF is required for normal brain development and that, also, 24(*S*),25-epoxycholesterol is present at higher than expected levels in embryonic mouse brain (Michaelson *et al.* 1996; Wang *et al.* 2009). A role for LXR in ventral midbrain development has been demonstrated (Sacchetti *et al.* 2009) however, it is unlikely this increase in MCSF expression in SN4741 cells is LXR controlled as, the synthetic ligand, GW3965 had no effect. Indeed the ring oxygenated oxysterols 7β-hydroxycholesterol and 7α-hydroxycholesterol, which are considered weak LXR agonists, induced significant increases in MCSF mRNA in THP1 monocytes.

The lack of effect after GW3965 implies that a LXR independent mechanism is responsible for the observed increase in MCSF expression. Unfortunately, due to time restraints it was beyond the scope of this work to examine in detail the mechanism by which oxysterols induce this effect. However, a number of possibilities exist through which oxysterols could induce this observed effect on MCSF expression. A nuclear receptor that has been shown to regulate MCSF expression is PPARγ (Bonfield *et al.* 2008). Similarly to LXR, PPARγ is a nuclear receptor that requires heterodimerisation with RXR when activated. PPARγ activation causes a decrease in MCSF expression (Bonfield *et al.* 2008). Therefore it appears that PPARγ activation has an inverse effect to treatment with oxysterols. This leads to the hypothesis that oxysterols can inhibit PPARγ activity. Indeed, there has been recent evidence to suggest that this is the case with 25-hydroxycholesterol inhibiting PPARγ (Xu *et al.* 2012). It appears that PPARγ inhibits MCSF expression through repressing NF-kB mediated transcription (Bonfield *et al.* 2008). Furthermore, evidence of oxysterols inducing NF-kB translocation has recently been reported (Aye *et al.* 2012; Xu *et al.* 2012). Thus, one hypothesis is that the observed increase in MCSF expression is due to inhibition of PPARγ and increased translocation of NF-kB. Another potential mechanism for the increase in MCSF expression via NF-kB activation is through ERK signalling. Inhibition of ERK can decrease NF-kB activity (Vanden Berghe *et al.* 1998) therefore as oxysterols can increase ERK phosphorylation (Yoon *et al.* 2004, Lemaire-Ewing *et al.* 2009) it is possible that MCSF expression is increased through this pathway. Thus, it is possible that there is a link between the results observed for MCSF at the protein and mRNA level and the initial basis for the phosphoproteomic studies presented here. Experimental evidence would be required to confirm the pathway through the

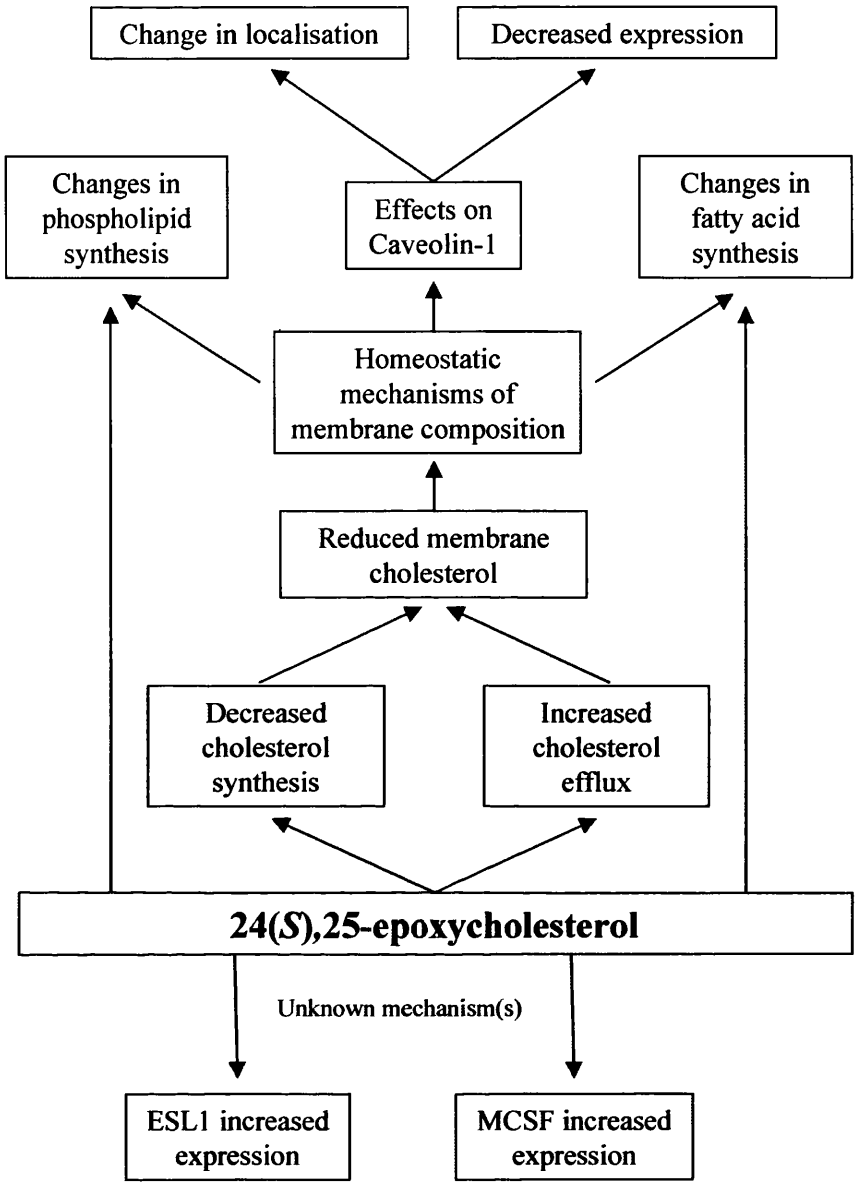

Figure 6.1. The effect of 24(*S*),25-epoxycholesterol on SN4741 neuronal cells. It is hypothesised that 24(*S*),25-epoxycholesterol induces a number of changes in cell membranes through direct (*e.g.* reducing the synthesis of cholesterol) and indirect (*e.g.* inducing changes in caveolin-1 expression and localisation) mechanisms. In addition, LXR independent up-regulation of Golgi sialoglycoprotein MG-160 (ESL1) and macrophage colony stimulating factor (MCSF) through an unknown mechanism was observed. MCSF has previously been reported to be important in brain development (Michaelson *et al.* 1996) and therefore it is hypothesised that this is an important effect of 24(*S*),25-epoxycholesterol on murine embryonic development.

use of small molecule inhibitors or RNAi in combination with oxysterol treatment. This approach would allow dissection of the mechanism by which oxysterols increase MCSF expression.

The use of SILAC in phosphoproteomic studies was also, albeit to a lesser extent, successful. A large number of phosphopeptides were identified with a Mascot score >25 and quantified (fig. 5.8). A number of these phosphopeptides confirmed predicted phosphorylation sites that had no previous experimental validation. In addition, a number of phosphorylation sites previously unreported on the canonical protein database Uniprot were identified (table 5.4; 5.5). The absence of a commercially available antibody for these previously unidentified phosphorylation sites means that validation is impossible. However, there is confidence in the mass spectrometry data and therefore it is probable that the sequence and phosphorylation site identifications are correct. The analysis of the function of these novel phosphorylation sites was beyond the scope of this work, however, a foundation is laid for future work. The identified phosphopeptides, novel and previously reported, can now be predicted as to where they will elute from both the strong cation exchange and C18 HPLC column. This allows, if required, a focused approach for a given phosphopeptide.

The identification of reproducible changes in the phosphoproteome proved difficult. A number of issues identified in these studies would be able to improve subsequent studies. The low abundance of phosphopeptides makes their analysis difficult. In addition, a large number of non-phosphorylated peptides were also identified in the phosphoenriched samples (table 5.3). Therefore, improvements in phosphoenrichment would be beneficial to improve the number of phosphopeptides identified. This would also improve the probability of identifying the same phosphopeptide in different biological replicates giving a greater overlap of phosphopeptides between different samples. This would be beneficial to identify reproducible changes in the phosphoproteome. The use of SILAC as a technique might not be ideal for phosphoproteomic work due to the characteristic 3 precursor ions in a SILAC peptide spectrum splitting the signal from low abundance phosphopeptides. In addition, as phosphopeptides are poorly ionisable there is a risk of not detecting phosphopeptides present in the sample. The use of an alternate labelling strategy, such as iTraq, could help to limit this due to peptides in different groups having the same mass and, thus, only distinguishable in the MS/MS spectra. One problem of the phosphoproteomic

methodology is the lack of an internal positive control in a similar vein to the SREBP2 regulated genes in the protein expression studies. ERK1/2, the only previously reported protein whose phosphorylation is induced by oxysterols, was not identified in any dataset. Therefore, due to the unknown effects of the oxysterols on phosphorylation beyond that reported for ERK1/2 there is a lack of known changes in the phosphoproteomic data set to look for as a validation. This makes it difficult to analyse quantifiable changes in the data set with confidence. In addition, the observed variation between different biological replicates meant that there is doubt in the few reproducibly observed changes in SILAC phosphopeptide quantification data without further experimental validation.

As a cautionary note it is important to recognise that as the experiments presented here were performed in serum free media the observed changes might be increased, reduced or absent, in the presence of serum. Serum is a complex mixture that contains a large number of components including cholesterol and oxysterols. Serum free media for *in vitro* studies allows the removal of the variability of batch to batch serum composition but might not necessarily portray the *in vivo* situation. However, these proteomic and phosphoproteomic studies provide a wealth of data regarding the effect of oxysterols on SN4741 neuronal cells and provide a large dataset to inspire further work. The role of oxysterols in membrane homeostasis, in subcellular protein localisation, and in immunity can be further elucidated and all stem from these data presented here. The most exciting discovery is that of a role of oxysterols in MCSF expression. This observation ties in with observed relationship between MCSF expression and neuronal development, neurodegenerative disease, and immunity. All of these are areas with which oxysterols have been associated and therefore their relationship with MCSF is an ideal subject for future work.

REFERENCES

Agassandian M, Zhou J, Tephly LA, Ryan AJ, Carter AB, Mallampalli RK. Oxysterols inhibit phosphatidylcholine synthesis via ERK docking and phosphorylation of CTP:phosphocholine cytidylyltransferase. J Biol Chem. 2005 Jun 3;280(22):21577-87.

Andersson S, Davis DL, Dahlbäck H, Jörnvall H, Russell DW. Cloning, structure, and expression of the mitochondrial cytochrome P-450 sterol 26-hydroxylase, a bile acid biosynthetic enzyme. J Biol Chem. 1989 May 15;264(14):8222-9.

Ando H, Horibata Y, Yamashita S, Oyama T, Sugimoto H. Low-density lipoprotein and oxysterols suppress the transcription of CTP: Phosphoethanolamine cytidylyltransferase in vitro. Biochim Biophys Acta. 2010 Apr;1801(4):487-95.

Annicotte JS, Schoonjans K, Auwerx J. Expression of the liver X receptor alpha and beta in embryonic and adult mice. Anat Rec A Discov Mol Cell Evol Biol. 2004 Apr;277(2):312-6.

Ares MP, Pörn-Ares MI, Moses S, Thyberg J, Juntti-Berggren L, Berggren P, Hultgårdh-Nilsson A, Kallin B, Nilsson J. 7beta-hydroxycholesterol induces Ca(2+) oscillations, MAP kinase activation and apoptosis in human aortic smooth muscle cells. Atherosclerosis. 2000 Nov;153(1):23-35

Avruch J. MAP kinase pathways: the first twenty years. Biochim Biophys Acta. 2007 Aug;1773(8):1150-60

Aye IL, Waddell BJ, Mark PJ, Keelan JA. Oxysterols exert proinflammatory effects in placental trophoblasts via TLR4-dependent, cholesterol-sensitive activation of NF-_B. Mol Hum Reprod. 2012 Jan 10. [Epub ahead of print]

Babiker A, Andersson O, Lund E, Xiu RJ, Deeb S, Reshef A, Leitersdorf E, Diczfalusy U, Björkhem I. Elimination of cholesterol in macrophages and endothelial cells by the sterol 27-hydroxylase mechanism. Comparison with high density lipoprotein-mediated reverse cholesterol transport. J Biol Chem. 1997 Oct 17;272(42):26253-61.

Bailey KM, Liu J. Caveolin-1 up-regulation during epithelial to mesenchymal transition is mediated by focal adhesion kinase. J Biol Chem. 2008 May 16;283(20):13714-24.

Bakovic M, Fullerton MD, Michel V. Metabolic and molecular aspects of ethanolamine phospholipid biosynthesis: the role of CTP:phosphoethanolamine cytidylyltransferase (Pcyt2). Biochem Cell Biol. 2007 Jun;85(3):283-300.

Bantscheff M, Schirle M, Sweetman G, Rick J, Kuster B. Quantitative mass spectrometry in proteomics: a critical review. Anal Bioanal Chem. 2007 Oct;389(4):1017-31.

Bauman DR, Bitmansour AD, McDonald JG, Thompson BM, Liang G, Russell DW. 25-Hydroxycholesterol secreted by macrophages in response to Toll-like receptor activation suppresses immunoglobulin A production. Proc Natl Acad Sci U S A. 2009 Sep 29;106(39):16764-9.

Björkhem I, Andersson O, Diczfalusy U, Sevastik B, Xiu RJ, Duan C, Lund E. Atherosclerosis and sterol 27-hydroxylase: evidence for a role of this enzyme in elimination of cholesterol from human macrophages. Proc Natl Acad Sci U S A. 1994 Aug 30;91(18):8592-6.

Boissonneault V, Filali M, Lessard M, Relton J, Wong G, Rivest S. Powerful beneficial effects of macrophage colony-stimulating factor on beta-amyloid deposition and cognitive impairment in Alzheimer's disease. Brain. 2009 Apr;132(Pt 4):1078-92.

Bonfield TL, Thomassen MJ, Farver CF, Abraham S, Koloze MT, Zhang X, Mosser DM, Culver DA. Peroxisome proliferator-activated receptor-gamma regulates the expression of alveolar macrophage macrophage colony-stimulating factor. J Immunol. 2008 Jul 1;181(1):235-42.

Bretillon L, Sidén A, Wahlund LO, Lütjohann D, Minthon L, Crisby M, Hillert J, Groth CG, Diczfalusy U, Björkhem I. Plasma levels of 24S-hydroxycholesterol in patients with neurological diseases. Neurosci Lett. 2000 Oct 27;293(2):87-90.

Brown J 3rd, Theisler C, Silberman S, Magnuson D, Gottardi-Littell N, Lee JM, Yager D, Crowley J, Sambamurti K, Rahman MM, Reiss AB, Eckman CB, Wolozin B. Differential expression of cholesterol hydroxylases in Alzheimer's disease. J Biol Chem. 2004 Aug 13;279(33):34674-81.

Brown MS, Goldstein JL. The SREBP pathway: regulation of cholesterol metabolism by proteolysis of a membrane-bound transcription factor. Cell. 1997 May 2;89(3):331-40.

Calleros L, Lasa M, Rodríguez-Alvarez FJ, Toro MJ, Chiloeches A. RhoA and p38 MAPK mediate apoptosis induced by cellular cholesterol depletion. Apoptosis. 2006 Jul;11(7):1161-73.

Chiang JY, Miller WF, Lin GM. Regulation of cholesterol 7 alpha-hydroxylase in the liver. Purification of cholesterol 7 alpha-hydroxylase and the immunochemical evidence for the induction of cholesterol 7 alpha-hydroxylase by cholestyramine and circadian rhythm. J Biol Chem. 1990 Mar 5;265(7):3889-97.

Chin DJ, Gil G, Faust JR, Goldstein JL, Brown MS, Luskey KL. Sterols accelerate degradation of hamster 3-hydroxy-3-methylglutaryl coenzyme A reductase encoded by a constitutively expressed cDNA. Mol Cell Biol. 1985 Apr;5(4):634-41.

Chisolm GM, Ma G, Irwin KC, Martin LL, Gunderson KG, Linberg LF, Morel DW, DiCorleto PE. 7□-Hydroperoxycholest-5-en-3□-ol, a component of human atherosclerotic lesions, is the primary cytotoxin of oxidized human low density lipoprotein. Proc Natl Acad Sci U S A. 1994;91:11452–11456.

Corcoran RB, Scott MP. Oxysterols stimulate Sonic hedgehog signal transduction and proliferation of medulloblastoma cells. Proc Natl Acad Sci U S A. 2006 May 30;103(22):8408-13.

Cox J, Matic I, Hilger M, Nagaraj N, Selbach M, Olsen JV, Mann M.A practical guide to the MaxQuant computational platform for SILAC-based quantitative proteomics. Nat Protoc. 2009;4(5):698-705.

Crisby M, Nilsson J, Kostulas V, Björkhem I, Diczfalusy U. Localization of sterol 27-hydroxylase immuno-reactivity in human atherosclerotic plaques. Biochim Biophys Acta. 1997 Feb 18;1344(3):278-85.

Cronin J, McAdam E, Danikas A, Tselepis C, Griffiths P, Baxter J, Thomas L, Manson J, Jenkins G. Epidermal growth factor receptor (EGFR) is overexpressed in high-grade dysplasia and adenocarcinoma of the esophagus and may represent a biomarker of histological progression in Barrett's esophagus (BE). Am J Gastroenterol. 2011 Jan;106(1):46-56.

Davis RJ. The mitogen-activated protein kinase signal transduction pathway. J Biol Chem. 1993 Jul 15;268(20):14553-6.

Diczfalusy U, Olofsson KE, Carlsson AM, Gong M, Golenbock DT, Rooyackers O, Fläring U, Björkbacka H. Marked upregulation of cholesterol 25-hydroxylase expression by lipopolysaccharide. J Lipid Res. 2009 Nov;50(11):2258-64.

Dix MM, Simon GM, Cravatt BF. Global mapping of the topography and magnitude of proteolytic events in apoptosis. Cell. 2008 Aug 22;134(4):679-91.

Du Yan S, Zhu H, Fu J, Yan SF, Roher A, Tourtellotte WW, Rajavashisth T, Chen X, Godman GC, Stern D, Schmidt AM. Amyloid-beta peptide-receptor for advanced glycation endproduct interaction elicits neuronal expression of macrophage-colony stimulating factor: a proinflammatory pathway in Alzheimer disease. Proc Natl Acad Sci U S A. 1997 May 13;94(10):5296-301.

Dwyer JR, Sever N, Carlson M, Nelson SF, Beachy PA, Parhami F. Oxysterols are novel activators of the hedgehog signaling pathway in pluripotent mesenchymal cells. J Biol Chem. 2007 Mar 23;282(12):8959-68.

Ecker J, Liebisch G, Englmaier M, Grandl M, Robenek H, Schmitz G. Induction of fatty acid synthesis is a key requirement for phagocytic differentiation of human monocytes. Proc Natl Acad Sci U S A. 2010 Apr 27;107(17):7817-22.

Emmett MR, Caprioli RM Micro-electrospray mass spectrometry: ultra-high-sensitivity analysis of peptides and proteins. J. Am. Soc. Mass Spectrom. 1994: 5 (7):

605–613.

Engholm-Keller K, Birck P, Størling J, Pociot F, Mandrup-Poulsen T, Larsen MR. TiSH--a robust and sensitive global phosphoproteomics strategy employing a combination of TiO2, SIMAC, and HILIC. J Proteomics. 2012 Oct 22;75(18):5749-61.

Espenshade PJ, Cheng D, Goldstein JL, Brown MS. Autocatalytic processing of site-1 protease removes propeptide and permits cleavage of sterol regulatory element-binding proteins. J Biol Chem. 1999 Aug 6;274(32):22795-804.

Fenn JB, Mann M, Meng CK, Wong SF, Whitehouse CM. Electrospray ionization for mass spectrometry of large biomolecules. Science. 1989 Oct 6;246(4926):64-71.

Fielding CJ, Bist A, Fielding PE. Caveolin mRNA levels are up-regulated by free cholesterol and down-regulated by oxysterols in fibroblast monolayers. Proc Natl Acad Sci U S A. 1997 Apr 15;94(8):3753-8.

Fourgeux C, Martine L, Björkhem I, Diczfalusy U, Joffre C, Acar N, Creuzot-Garcher C, Bron A, Bretillon L. Primary open-angle glaucoma: association with cholesterol 24S-hydroxylase (CYP46A1) gene polymorphism and plasma 24-hydroxycholesterol levels. Invest Ophthalmol Vis Sci. 2009 Dec;50(12):5712-7.

Fujiyama J, Kuriyama M, Arima S, Shibata Y, Nagata K, Takenaga S, Tanaka H, Osame M. Atherogenic risk factors in cerebrotendinous xanthomatosis. Clin Chim Acta. 1991 Aug 15;200(1):1-11.

Furuchi T, Anderson RG. Cholesterol depletion of caveolae causes hyperactivation of extracellular signal-related kinase (ERK). J Biol Chem. 1998 Aug 14;273(33):21099-104.

Gaudreault SB, Dea D, Poirier J. Increased caveolin-1 expression in Alzheimer's disease brain. Neurobiol Aging. 2004 Jul;25(6):753-9.

Gil G, Faust JR, Chin DJ, Goldstein JL, Brown MS. Membrane-bound domain of HMG CoA reductase is required for sterol-enhanced degradation of the enzyme. Cell. 1985 May;41(1):249-58.

Gill S, Chow R, Brown AJ. Sterol regulators of cholesterol homeostasis and beyond: the oxysterol hypothesis revisited and revised. Prog Lipid Res. 2008 Nov;47(6):391-404

Gonatas JO, Mezitis SG, Stieber A, Fleischer B, Gonatas NK. MG-160. A novel sialoglycoprotein of the medial cisternae of the Golgi apparatus. J Biol Chem. 1989 Jan 5;264(1):646-53.

Granero-Moltó F, Sarmah S, O'Rear L, Spagnoli A, Abrahamson D, Saus J, Hudson BG, Knapik EW. Goodpasture antigen-binding protein and its spliced variant, ceramide transfer protein, have different functions in the modulation of apoptosis during zebrafish development. J Biol Chem. 2008 Jul 18;283(29):20495-504.

Graumann J, Hubner NC, Kim JB, Ko K, Moser M, Kumar C, Cox J, Schöler H, Mann M. Stable isotope labeling by amino acids in cell culture (SILAC) and proteome quantitation of mouse embryonic stem cells to a depth of 5,111 proteins. Mol Cell Proteomics. 2008 Apr;7(4):672-83.

Hailstones D, Sleer LS, Parton RG, Stanley KK. Regulation of caveolin and caveolae by cholesterol in MDCK cells. J Lipid Res. 1998 Feb;39(2):369-79

Hanada K, Kumagai K, Tomishige N, Kawano M. CERT and intracellular trafficking of ceramide. Biochim Biophys Acta. 2007 Jun;1771(6):644-53.

Hannedouche S, Zhang J, Yi T, Shen W, Nguyen D, Pereira JP, Guerini D, Baumgarten BU, Roggo S, Wen B, Knochenmuss R, Noël S, Gessier F, Kelly LM, Vanek M, Laurent S, Preuss I, Miault C, Christen I, Karuna R, Li W, Koo DI, Suply T, Schmedt C, Peters EC, Falchetto R, Katopodis A, Spanka C, Roy MO, Detheux M, Chen YA, Schultz PG, Cho CY, Seuwen K, Cyster JG, Sailer AW. Oxysterols direct immune cell migration via EBI2. Nature. 2011 Jul 27;475(7357):524-7.

Hansen CG, Nichols BJ. Exploring the caves: cavins, caveolins and caveolae. Trends Cell Biol. 2010 Apr;20(4):177-86.

Hempstead BL. Dissecting the diverse actions of pro- and mature neurotrophins. Curr Alzheimer Res. 2006 Feb;3(1):19-24.

Horton JD, Shah NA, Warrington JA, Anderson NN, Park SW, Brown MS, Goldstein JL. Combined analysis of oligonucleotide microarray data from transgenic and knockout mice identifies direct SREBP target genes. Proc Natl Acad Sci U S A. 2003 Oct 14;100(21):12027-32.

Hu Q, Noll RJ, Li H, Makarov A, Hardman M, Graham Cooks R. The Orbitrap: a new mass spectrometer. J Mass Spectrom. 2005 Apr;40(4):430-43.

Hughes H, Mathews B, Lenz ML, Guyton JR. Cytotoxicity of oxidized LDL to porcine aortic smooth muscle cells is associated with the oxysterols 7-ketocholesterol and 7-hydroxycholesterol. Arterioscler Thromb. 1994 Jul;14(7):1177-85.

Jaeger I, Arber C, Risner-Janiczek JR, Kuechler J, Pritzsche D, Chen IC, Naveenan T, Ungless MA, Li M. Temporally controlled modulation of FGF/ERK signaling directs midbrain dopaminergic neural progenitor fate in mouse and human pluripotent stem cells. Development. 2011 Oct;138(20):4363-74.

Janowski BA, Grogan MJ, Jones SA, Wisely GB, Kliewer SA, Corey EJ, Mangelsdorf DJ. Structural requirements of ligands for the oxysterol liver X receptors LXRalpha and LXRbeta. Proc Natl Acad Sci U S A. 1999 Jan 5;96(1):266-71.

Jelinek DF, Andersson S, Slaughter CA, Russell DW. Cloning and regulation of cholesterol 7 alpha-hydroxylase, the rate-limiting enzyme in bile acid biosynthesis. J Biol Chem. 1990 May 15;265(14):8190-7.

Jensen ON. Modification-specific proteomics: characterization of post-translational modifications by mass spectrometry. Curr Opin Chem Biol. 2004 Feb;8(1):33-41.

Jin SH, Lee YY, Kang HY. Methyl-beta-cyclodextrin, a specific cholesterol-binding agent, inhibits melanogenesis in human melanocytes through activation of ERK. Arch Dermatol Res. 2008 Sep;300(8):451-4.

Kaku M, Tsutsui K, Motokawa M, Kawata T, Fujita T, Kohno S, Tohma Y, Ohtani J, Tenjoh K, Tanne K. Amyloid beta protein deposition and neuron loss in osteopetrotic (op/op) mice. Brain Res Brain Res Protoc. 2003 Oct;12(2):104-8.

Kast HR, Nguyen CM, Anisfeld AM, Ericsson J, Edwards PA. CTP:phosphocholine cytidylyltransferase, a new sterol- and SREBP-responsive gene. J Lipid Res. 2001 Aug;42(8):1266-72.

Kawata T, Tsutsui K, Kohno S, Kaku M, Fujita T, Tenjou K, Ohtani J, Motokawa M, Shigekawa M, Tohma Y, Tanne K. Amyloid beta protein deposition in osteopetrotic (op/op) mice is reduced by injections of macrophage colony stimulating factor. J Int Med Res. 2005 Nov-Dec;33(6):654-60.

Kennedy MA, Venkateswaran A, Tarr PT, Xenarios I, Kudoh J, Shimizu N, Edwards PA. Characterization of the human ABCG1 gene: liver X receptor activates an internal promoter that produces a novel transcript encoding an alternative form of the protein. J Biol Chem. 2001 Oct 19;276(42):39438-47.

Kennelly PJ, Krebs EG. Consensus sequences as substrate specificity determinants for protein kinases and protein phosphatases. J Biol Chem. 1991 Aug 25;266(24):15555-8.

Kim KH, Yoon JM, Choi AH, Kim WS, Lee GY, Kim JB. Liver X receptor ligands suppress ubiquitination and degradation of LXRalpha by displacing BARD1/BRCA1. Mol Endocrinol. 2009 Apr;23(4):466-74.

Kim S, Kim Y, Lee Y, Cho KH, Kim KH, Chung JH. Cholesterol inhibits MMP-9 expression in human epidermal keratinocytes and HaCaT cells. FEBS Lett. 2007 Aug 7;581(20):3869-74.

Kim SY, Choi KC, Chang MS, Kim MH, Kim SY, Na YS, Lee JE, Jin BK, Lee BH, Baik JH. The dopamine D2 receptor regulates the development of dopaminergic neurons via extracellular signal-regulated kinase and Nurr1 activation. J Neurosci. 2006 Apr 26;26(17):4567-76.

Kim SY, Lee HJ, Kim YN, Yoon S, Lee JE, Sun W, Choi EJ, Baik JH. Striatal-enriched protein tyrosine phosphatase regulates dopaminergic neuronal development via extracellular signal-regulated kinase signaling. Exp Neurol. 2008 Nov;214(1):69-77.

Kim WK, Meliton V, Amantea CM, Hahn TJ, Parhami F. 20(S)-hydroxycholesterol inhibits PPARgamma expression and adipogenic differentiation of bone marrow stromal cells through a hedgehog-dependent mechanism. J Bone Miner Res. 2007 Nov;22(11):1711-9.

Kim KH, Yoon JM, Choi AH, Kim WS, Lee GY, Kim JB. Liver X receptor ligands suppress ubiquitination and degradation of LXRalpha by displacing BARD1/BRCA1. Mol Endocrinol. 2009 Apr;23(4):466-74.

Kim WK, Meliton V, Tetradis S, Weinmaster G, Hahn TJ, Carlson M, Nelson SF, Parhami F. Osteogenic oxysterol, 20(S)-hydroxycholesterol, induces notch target gene expression in bone marrow stromal cells. J Bone Miner Res. 2010 Apr;25(4):782-95.

Kondo Y, Lemere CA, Seabrook TJ. Osteopetrotic (op/op) mice have reduced microglia, no Abeta deposition, and no changes in dopaminergic neurons. J Neuroinflammation. 2007 Dec 20;4:31.

Knight BL. ATP-binding cassette transporter A1: regulation of cholesterol efflux. Biochem Soc Trans. 2004 Feb;32(Pt 1):124-7

Laffitte BA, Joseph SB, Walczak R, Pei L, Wilpitz DC, Collins JL, Tontonoz P. Autoregulation of the human liver X receptor alpha promoter. Mol Cell Biol. 2001 Nov;21(22):7558-68

Larsen MR, Thingholm TE, Jensen ON, Roepstorff P, Jørgensen TJ. Highly selective enrichment of phosphorylated peptides from peptide mixtures using titanium dioxide microcolumns. Mol Cell Proteomics. 2005 Jul;4(7):873-86.

Lemaire-Ewing S, Berthier A, Royer MC, Logette E, Corcos L, Bouchot A, Monier S, Prunet C, Raveneau M, Rébé C, Desrumaux C, Lizard G, Néel D. 7beta-Hydroxycholesterol and 25-hydroxycholesterol-induced interleukin-8 secretion involves a calcium-dependent activation of c-fos via the ERK1/2 signaling pathway in THP-1 cells: oxysterols-induced IL-8 secretion is calcium-dependent. Cell Biol Toxicol. 2009 Apr;25(2):127-39.

Li M, Pisalyaput K, Galvan M, Tenner AJ. Macrophage colony stimulatory factor and interferon-gamma trigger distinct mechanisms for augmentation of beta-amyloid-induced microglia-mediated neurotoxicity. J Neurochem. 2004 Nov;91(3):623-33.

Li Y, Bolten C, Bhat BG, Woodring-Dietz J, Li S, Prayaga SK, Xia C, Lala DS. Induction of human liver X receptor alpha gene expression via an autoregulatory loop mechanism. Mol Endocrinol. 2002 Mar;16(3):506-14.

Liu C, Yang XV, Wu J, Kuei C, Mani NS, Zhang L, Yu J, Sutton SW, Qin N, Banie H, Karlsson L, Sun S, Lovenberg TW. Oxysterols direct B-cell migration through EBI2. Nature. 2011 Jul 27;475(7357):519-23.

Lund EG, Kerr TA, Sakai J, Li WP, Russell DW. cDNA cloning of mouse and human cholesterol 25-hydroxylases, polytopic membrane proteins that synthesize a potent oxysterol regulator of lipid metabolism. J Biol Chem. 1998 Dec 18;273(51):34316-27.

Lund EG, Guileyardo JM, Russell DW. cDNA cloning of cholesterol 24-hydroxylase, a mediator of cholesterol homeostasis in the brain. Proc Natl Acad Sci U S A. 1999 Jun 22;96(13):7238-43.

Lütjohann D, Breuer O, Ahlborg G, Nennesmo I, Sidén A, Diczfalusy U, Björkhem I. Cholesterol homeostasis in human brain: evidence for an age-dependent flux of 24S-hydroxycholesterol from the brain into the circulation. Proc Natl Acad Sci U S A. 1996 Sep 3;93(18):9799-804

Lütjohann D, Papassotiropoulos A, Björkhem I, Locatelli S, Bagli M, Oehring RD, Schlegel U, Jessen F, Rao ML, von Bergmann K, Heun R. Plasma 24S-hydroxycholesterol (cerebrosterol) is increased in Alzheimer and vascular demented patients. J Lipid Res. 2000 Feb;41(2):195-8.

Lütjohann D, Brzezinka A, Barth E, Abramowski D, Staufenbiel M, von Bergmann K, Beyreuther K, Multhaup G, Bayer TA. Profile of cholesterol-related sterols in aged amyloid precursor protein transgenic mouse brain. J Lipid Res. 2002 Jul;43(7):1078-85.

Majumdar A, Cruz D, Asamoah N, Buxbaum A, Sohar I, Lobel P, Maxfield FR. Activation of microglia acidifies lysosomes and leads to degradation of Alzheimer amyloid fibrils. Mol Biol Cell. 2007 Apr;18(4):1490-6.

Mann M, Wilm M. Error-tolerant identification of peptides in sequence databases by peptide sequence tags. Anal Chem. 1994 Dec 15;66(24):4390-9.

Masson D, Staels B, Gautier T, Desrumaux C, Athias A, Le Guern N, Schneider M, Zak Z, Dumont L, Deckert V, Tall A, Jiang XC, Lagrost L. Cholesteryl ester transfer protein modulates the effect of liver X receptor agonists on cholesterol transport and excretion in the mouse. J Lipid Res. 2004 Mar;45(3):543-50.

Metherall JE, Goldstein JL, Luskey KL, Brown MS. Loss of transcriptional repression of three sterol-regulated genes in mutant hamster cells. J Biol Chem. 1989 Sep 15;264(26):15634-41.

Michaelson MD, Bieri PL, Mehler MF, Xu H, Arezzo JC, Pollard JW, Kessler JA. CSF-1 deficiency in mice results in abnormal brain development. Development. 1996 Sep;122(9):2661-72.

Moreira EF, Larrayoz IM, Lee JW, Rodríguez IR. 7-Ketocholesterol is present in lipid deposits in the primate retina: potential implication in the induction of VEGF and CNV formation. Invest Ophthalmol Vis Sci. 2009 Feb;50(2):523-32.

Murphy GM Jr, Zhao F, Yang L, Cordell B. Expression of macrophage colony-stimulating factor receptor is increased in the AbetaPP(V717F) transgenic mouse model of Alzheimer's disease. Am J Pathol. 2000 Sep;157(3):895-904.

Nachtergaele S, Mydock LK, Krishnan K, Rammohan J, Schlesinger PH, Covey DF, Rohatgi R. Oxysterols are allosteric activators of the oncoprotein Smoothened. Nat Chem Biol. 2012 Jan 8;8(2):211-20.

Nakanishi M, Goldstein JL, Brown MS. Multivalent control of 3-hydroxy-3-methylglutaryl coenzyme A reductase. Mevalonate-derived product inhibits translation of mRNA and accelerates degradation of enzyme. J Biol Chem. 1988 Jun 25;263(18):8929-37.

Nelson JA, Steckbeck SR, Spencer TA. Biosynthesis of 24,25-epoxycholesterol from squalene 2,3;22,23-dioxide. J Biol Chem. 1981 Feb 10;256(3):1067-8.

Nhek S, Ngo M, Yang X, Ng MM, Field SJ, Asara JM, Ridgway ND, Toker A. Regulation of oxysterol-binding protein Golgi localization through protein kinase D-mediated phosphorylation. Mol Biol Cell. 2010 Jul 1;21(13):2327-37.

Ogundare M, Theofilopoulos S, Lockhart A, Hall LJ, Arenas E, Sjövall J, Brenton AG, Wang Y, Griffiths WJ. Cerebrospinal fluid steroidomics: are bioactive bile acids present in brain? J Biol Chem. 2010 Feb 12;285(7):4666-79.

Olkkonen VM, Lehto M. Oxysterols and oxysterol binding proteins: role in lipid metabolism and atherosclerosis. Ann Med. 2004;36(8):562-72

Olsen JV, Blagoev B, Gnad F, Macek B, Kumar C, Mortensen P, Mann M. Global, in vivo, and site-specific phosphorylation dynamics in signaling networks. Cell. 2006 Nov 3;127(3):635-48.

Olsen BN, Schlesinger PH, Ory DS, Baker NA. Side-chain oxysterols: from cells to membranes to molecules. Biochim Biophys Acta. 2012 Feb;1818(2):330-6.

Ong SE, Mann M.A practical recipe for stable isotope labeling by amino acids in cell culture (SILAC). Nat Protoc. 2006;1(6):2650-60.

Palumbo AM, Reid GE. Evaluation of gas-phase rearrangement and competing fragmentation reactions on protein phosphorylation site assignment using collision induced dissociation-MS/MS and MS3. Anal Chem. 2008 Dec 15;80(24):9735-47.

Park K, Scott AL. Cholesterol 25-hydroxylase production by dendritic cells and macrophages is regulated by type I interferons.J Leukoc Biol. 2010 Dec;88(6):1081-7.

Parton RG, Simons K. The multiple faces of caveolae. Nat Rev Mol Cell Biol. 2007 Mar;8(3):185-94.

Perry RJ, Ridgway ND. Oxysterol-binding protein and vesicle-associated membrane protein-associated protein are required for sterol-dependent activation of the ceramide transport protein. Mol Biol Cell. 2006 Jun;17(6):2604-16.

Pollard JW, Hunt JS, Wiktor-Jedrzejczak W, Stanley ER. A pregnancy defect in the osteopetrotic (op/op) mouse demonstrates the requirement for CSF-1 in female fertility. Dev Biol. 1991 Nov;148(1):273-83.

Prasanthi JR, Huls A, Thomasson S, Thompson A, Schommer E, Ghribi O. Differential effects of 24-hydroxycholesterol and 27-hydroxycholesterol on beta-amyloid precursor protein levels and processing in human neuroblastoma SH-SY5Y cells. Mol Neurodegener. 2009 Jan 6;4:1.

Qiao JH, Tripathi J, Mishra NK, Cai Y, Tripathi S, Wang XP, Imes S, Fishbein MC, Clinton SK, Libby P, Lusis AJ, Rajavashisth TB. Role of macrophage colony-stimulating factor in atherosclerosis: studies of osteopetrotic mice. Am J Pathol. 1997 May;150(5):1687-99.

Radhakrishnan A, Sun LP, Kwon HJ, Brown MS, Goldstein JL. Direct binding of cholesterol to the purified membrane region of SCAP: mechanism for a sterol-sensing domain. Mol Cell. 2004 Jul 23;15(2):259-68.

Radhakrishnan A, Ikeda Y, Kwon HJ, Brown MS, Goldstein JL. Sterol-regulated transport of SREBPs from endoplasmic reticulum to Golgi: oxysterols block transport by binding to Insig. Proc Natl Acad Sci U S A. 2007 Apr 17;104(16):6511-8.

Rajavashisth TB, Andalibi A, Territo MC, Berliner JA, Navab M, Fogelman AM, Lusis AJ. Induction of endothelial cell expression of granulocyte and macrophage colony-stimulating factors by modified low-density lipoproteins. Nature. 1990 Mar 15;344(6263):254-7.

Rajavashisth T, Qiao JH, Tripathi S, Tripathi J, Mishra N, Hua M, Wang XP, Loussararian A, Clinton S, Libby P, Lusis A. Heterozygous osteopetrotic (op) mutation reduces atherosclerosis in LDL receptor- deficient mice. J Clin Invest. 1998 Jun 15;101(12):2702-10.

Razzaque MS, Foster CS, Ahmed AR. Role of enhanced expression of m-CSF in conjunctiva affected by cicatricial pemphigoid. Invest Ophthalmol Vis Sci. 2002 Sep;43(9):2977-83.

Rodriguez IR, Alam S, Lee JW. Cytotoxicity of oxidized low-density lipoprotein in cultured RPE cells is dependent on the formation of 7-ketocholesterol. Invest Ophthalmol Vis Sci. 2004 Aug;45(8):2830-7

Rodriguez IR, Fliesler SJ. Photodamage generates 7-keto- and 7-hydroxycholesterol in the rat retina via a free radical-mediated mechanism. Photochem Photobiol. 2009 Sep-Oct;85(5):1116-25.

Roepstorff P, Fohlman J. Proposal for a common nomenclature for sequence ions in mass spectra of peptides. Biomed Mass Spectrom. 1984 Nov;11(11):601.

Rogers S, Girolami M, Kolch W, Waters KM, Liu T, Thrall B, Wiley HS. Investigating the correspondence between transcriptomic and proteomic expression profiles using coupled cluster models. Bioinformatics. 2008 Dec 15;24(24):2894-900.

Ross PL, Huang YN, Marchese JN, Williamson B, Parker K, Hattan S, Khainovski N, Pillai S, Dey S, Daniels S, Purkayastha S, Juhasz P, Martin S, Bartlet-Jones M, He F, Jacobson A, Pappin DJ. Multiplexed protein quantitation in Saccharomyces cerevisiae using amine-reactive isobaric tagging reagents. Mol Cell Proteomics. 2004 Dec;3(12):1154-69.

Sabol SL, Brewer HB Jr, Santamarina-Fojo S. The human ABCG1 gene: identification of LXR response elements that modulate expression in macrophages and liver. J Lipid Res. 2005 Oct;46(10):2151-67.

Sacchetti P, Sousa KM, Hall AC, Liste I, Steffensen KR, Theofilopoulos S, Parish CL, Hazenberg C, Richter LA, Hovatta O, Gustafsson JA, Arenas E. Liver X receptors and oxysterols promote ventral midbrain neurogenesis in vivo and in human embryonic stem cells. Cell Stem Cell. 2009 Oct 2;5(4):409-19.

Sano O, Kobayashi A, Nagao K, Kumagai K, Kioka N, Hanada K, Ueda K, Matsuo M. Sphingomyelin-dependence of cholesterol efflux mediated by ABCG1. J Lipid Res. 2007 Nov;48(11):2377-84.

Schönknecht P, Lütjohann D, Pantel J, Bardenheuer H, Hartmann T, von Bergmann K, Beyreuther K, Schröder J. Cerebrospinal fluid 24S-hydroxycholesterol is increased

in patients with Alzheimer's disease compared to healthy controls. Neurosci Lett. 2002 May 10;324(1):83-5.

Schroepfer GJ Jr. Oxysterols: modulators of cholesterol metabolism and other processes. Physiol Rev. 2000 Jan;80(1):361-554.

Scigelova M, Hornshaw M, Giannakopulos A, Makarov A. Fourier transform mass spectrometry. Mol Cell Proteomics. 2011 Jul;10(7):M111.009431

Sever N, Yang T, Brown MS, Goldstein JL, DeBose-Boyd RA. Accelerated degradation of HMG CoA reductase mediated by binding of insig-1 to its sterol-sensing domain. Mol Cell. 2003a Jan;11(1):25-33.

Sever N, Song BL, Yabe D, Goldstein JL, Brown MS, DeBose-Boyd RA. Insig-dependent ubiquitination and degradation of mammalian 3-hydroxy-3-methylglutaryl-CoA reductase stimulated by sterols and geranylgeraniol. J Biol Chem. 2003b Dec 26;278(52):52479-90.

Sharma K, Vabulas RM, Macek B, Pinkert S, Cox J, Mann M, Hartl FU. Quantitative proteomics reveals that hsp90 inhibition preferentially targets kinases and the DNA damage response. Mol Cell Proteomics. 2012 Mar;11(3):M111.014654.

Shimomura I, Shimano H, Horton JD, Goldstein JL, Brown MS. Differential expression of exons 1a and 1c in mRNAs for sterol regulatory element binding protein-1 in human and mouse organs and cultured cells. J Clin Invest. 1997 Mar 1;99(5):838-45.

Soccio RE, Adams RM, Maxwell KN, Breslow JL. Differential gene regulation of StarD4 and StarD5 cholesterol transfer proteins. Activation of StarD4 by sterol regulatory element-binding protein-2 and StarD5 by endoplasmic reticulum stress. J Biol Chem. 2005 May 13;280(19):19410-8.

Song C, Kokontis JM, Hiipakka RA, Liao S. Ubiquitous receptor: a receptor that modulates gene activation by retinoic acid and thyroid hormone receptors. Proc Natl Acad Sci USA 1994; 91: 10809-10813.

Son JH, Chun HS, Joh TH, Cho S, Conti B, Lee JW. Neuroprotection and neuronal differentiation studies using substantia nigra dopaminergic cells derived from transgenic mouse embryos. J Neurosci. 1999 Jan 1;19(1):10-20.

Spencer TA, Gayen AK, Phirwa S, Nelson JA, Taylor FR, Kandutsch AA, Erickson SK. 24(S),25-Epoxycholesterol. Evidence consistent with a role in the regulation of hepatic cholesterogenesis. J Biol Chem. 1985 Nov 5;260(25):13391-4.

Stieber A, Mourelatos Z, Chen YJ, Le Douarin N, Gonatas NK. MG160, a membrane protein of the Golgi apparatus which is homologous to a fibroblast growth factor receptor and to a ligand for E-selectin, is found only in the Golgi apparatus and appears early in chicken embryo development. Exp Cell Res. 1995 Aug;219(2):562-70.

Svensson S, Ostberg T, Jacobsson M, Norström C, Stefansson K, Hallén D, Johansson IC, Zachrisson K, Ogg D, Jendeberg L. Crystal structure of the heterodimeric complex of LXRalpha and RXRbeta ligand-binding domains in a fully agonistic conformation. EMBO J. 2003 Sep 15;22(18):4625-33.

Sweet MJ, Hume DA. CSF-1 as a regulator of macrophage activation and immune responses. Arch Immunol Ther Exp (Warsz). 2003;51(3):169-77.

Sweet SM, Bailey CM, Cunningham DL, Heath JK, Cooper HJ. Large scale localization of protein phosphorylation by use of electron capture dissociation mass spectrometry. Mol Cell Proteomics. 2009 May;8(5):904-12.

Tanaka, K.; Waki, H.; Ido, Y.; Akita, S.; Yoshida, Y.; Yoshida, T. Protein and Polymer Analyses up to m/z 100 000 by Laser Ionization Time-of flight Mass Spectrometry. Rapid Commun Mass Spectrom 1988: **2** (20): 151–3.

Theofilopoulos S, Wang Y, Kitambi SS, Sacchetti P, Sousa KM, Bodin K, Kirk J, Saltó C, Gustafsson M, Toledo EM, Karu K, Gustafsson JÅ, Steffensen KR, Ernfors P, Sjövall J, Griffiths WJ, Arenas E. Brain endogenous liver X receptor ligands selectively promote midbrain neurogenesis. Nat Chem Biol. 2013 Feb;9(2):126-33.

Thingholm TE, Jensen ON, Robinson PJ, Larsen MR. SIMAC (sequential elution from IMAC), a phosphoproteomics strategy for the rapid separation of monophosphorylated from multiply phosphorylated peptides. Mol Cell Proteomics. 2008 Apr;7(4):661-71.

Thingholm TE, Jensen ON, Larsen MR. Analytical strategies for phosphoproteomics. Proteomics. 2009 Mar;9(6):1451-68.

Torrini M, Marchese C, Vanzetti M, Marini V, Origone P, Garré C, Mareni C. Mutation analysis of oxisterol-binding-protein gene in patients with age-related macular degeneration. Genet Test. 2007 Winter;11(4):421-6.

Uhlen M, Ponten F.Antibody-based proteomics for human tissue profiling. Mol Cell Proteomics. 2005 Apr;4(4):384-93.

Ulven SM, Dalen KT, Gustafsson JA, Nebb HI. Tissue-specific autoregulation of the LXRalpha gene facilitates induction of apoE in mouse adipose tissue. J Lipid Res. 2004 Nov;45(11):2052-62.

UniProt Consortium. Ongoing and future developments at the Universal Protein Resource. Nucleic Acids Res. 2011 Jan;39:D214-9.

Vanden Berghe W, Plaisance S, Boone E, De Bosscher K, Schmitz ML, Fiers W, Haegeman G. p38 and extracellular signal-regulated kinase mitogen-activated protein kinase pathways are required for nuclear factor-kappaB p65 transactivation mediated by tumor necrosis factor. J Biol Chem. 1998 Feb 6;273(6):3285-90.

Vaya J, Schipper HM. Oxysterols, cholesterol homeostasis, and Alzheimer disease. J Neurochem. 2007 Sep;102(6):1727-37.

Wang PY, Liu P, Weng J, Sontag E, Anderson RG. A cholesterol-regulated PP2A/HePTP complex with dual specificity ERK1/2 phosphatase activity. EMBO J. 2003 Jun 2;22(11):2658-67.

Wang PY, Weng J, Anderson RG. OSBP is a cholesterol-regulated scaffolding protein in control of ERK 1/2 activation. Science. 2005 Mar 4;307(5714):1472-6.

Wang S, Yuan Y, Liao L, Kuang SQ, Tien JC, O'Malley BW, Xu J. Disruption of the SRC-1 gene in mice suppresses breast cancer metastasis without affecting primary tumor formation. Proc Natl Acad Sci U S A. 2009 Jan 6;106(1):151-6.

Wang Y, Sousa KM, Bodin K, Theofilopoulos S, Sacchetti P, Hornshaw M, Woffendin G, Karu K, Sjövall J, Arenas E, Griffiths WJ. Targeted lipidomic analysis of oxysterols in the embryonic central nervous system. Mol Biosyst. 2009 May;5(5):529-41.

Weiner ND, Noomnont P, Felmeister A. Autoxidation of cholesterol in aqueous dispersions and in monomolecular films. J Lipid Res. 1972 Mar;13(2):253-5.

Whitney KD, Watson MA, Goodwin B, Galardi CM, Maglich JM, Wilson JG, Willson TM, Collins JL, Kliewer SA. Liver X receptor (LXR) regulation of the LXRalpha gene in human macrophages. J Biol Chem. 2001 Nov 23;276(47):43509-15.

Whitney KD, Watson MA, Collins JL, Benson WG, Stone TM, Numerick MJ, Tippin TK, Wilson JG, Winegar DA, Kliewer SA. Regulation of cholesterol homeostasis by the liver X receptors in the central nervous system. Mol Endocrinol. 2002 Jun;16(6):1378-85.

Wiktor-Jedrzejczak W, Bartocci A, Ferrante AW Jr, Ahmed-Ansari A, Sell KW, Pollard JW, Stanley ER. Total absence of colony-stimulating factor 1 in the macrophage-deficient osteopetrotic (op/op) mouse. Proc Natl Acad Sci U S A. 1990 Jun;87(12):4828-32.

Wilkins MR, Pasquali C, Appel RD, Ou K, Golaz O, Sanchez JC, Yan JX, Gooley AA, Hughes G, Humphery-Smith I, Williams KL, Hochstrasser DF. From proteins to proteomes: large scale protein identification by two-dimensional electrophoresis and amino acid analysis. Biotechnology (N Y). 1996 Jan;14(1):61-5.

Wilm M, Mann M. Analytical properties of the nanoelectrospray ion source. Anal Chem. 1996 Jan 1;68(1):1-8.

Wong J, Quinn CM, Brown AJ. Statins inhibit synthesis of an oxysterol ligand for the liver x receptor in human macrophages with consequences for cholesterol flux. Arterioscler Thromb Vasc Biol. 2004 Dec;24(12):2365-71.

Wong J, Quinn CM, Guillemin G, Brown AJ. Primary human astrocytes produce 24(S),25-epoxycholesterol with implications for brain cholesterol homeostasis. J Neurochem. 2007 Dec;103(5):1764-73.

Xu L, Shen S, Ma Y, Kim JK, Rodriguez-Agudo D, Heuman DM, Hylemon PB, Pandak WM, Ren S. 25-Hydroxycholesterol-3-Sulfate (25HC3S) Attenuates Inflammatory Response via PPARgamma Signaling in Human THP-1 Macrophages. Am J Physiol Endocrinol Metab. 2012 Jan 24.

Yang T, Espenshade PJ, Wright ME, Yabe D, Gong Y, Aebersold R, Goldstein JL, Brown MS. Crucial step in cholesterol homeostasis: sterols promote binding of SCAP to INSIG-1, a membrane protein that facilitates retention of SREBPs in ER. Cell. 2002 Aug 23;110(4):489-500.

Yoon JH, Canbay AE, Werneburg NW, Lee SP, Gores GJ. Oxysterols induce cyclooxygenase-2 expression in cholangiocytes: implications for biliary tract carcinogenesis. Hepatology. 2004 Mar;39(3):732-8.

Yoon S, Choi MH, Chang MS, Baik JH. Wnt5a-dopamine D2 receptor interactions regulate dopamine neuron development via extracellular signal-regulated kinase (ERK) activation. J Biol Chem. 2011 May 6;286(18):15641-51.

Yoshida H, Hayashi S, Kunisada T, Ogawa M, Nishikawa S, Okamura H, Sudo T, Shultz LD, Nishikawa S. The murine mutation osteopetrosis is in the coding region of the macrophage colony stimulating factor gene. Nature. 1990 May 31;345(6274):442-4.

Zelcer N, Hong C, Boyadjian R, Tontonoz P. LXR regulates cholesterol uptake through Idol-dependent ubiquitination of the LDL receptor. Science. 2009 Jul 3;325(5936):100-4.

Zelenski NG, Rawson RB, Brown MS, Goldstein JL. Membrane topology of S2P, a protein required for intramembranous cleavage of sterol regulatory element-binding proteins. J Biol Chem. 1999 Jul 30;274(31):21973-80.

Zhou W, Merrick BA, Khaledi MG, Tomer KB. Detection and sequencing of phosphopeptides affinity bound to immobilized metal ion beads by matrix-assisted laser desorption/ionization mass spectrometry. J Am Soc Mass Spectrom. 2000 Apr;11(4):273-82.

Zhu Y, Wang Y, Xia C, Li D, Li Y, Zeng W, Yuan W, Liu H, Zhu C, Wu X, Liu M. WDR26: a novel Gbeta-like protein, suppresses MAPK signaling pathway. J Cell Biochem. 2004 Oct 15;93(3):579-87.

Appendix 1: All Proteins Identified as Down-Regulated in ≥1 Biological Replicate

Protein identities and expression ratio shown for proteins identified as down-regulated after SN4741 cells were treated with 10μM 24(*S*),25-epoxycholesterol. Pep = Number of unique peptides; EC = SILAC ratio after treatment with 24(*S*),25-epoxycholesterol; GW = SILAC ratio after treatment with GW3965.

Biological Replicate			1						2						3					
Technical Replicate			1			2			1			2			1			2		
Protein IDs	Gene Names	Uniprot	Pep	EC	GW	Pep	EC	GW	Pep	EC	GW	Pep	EC	GW	Pep	EC	GW	Pep	EC	GW
IPI00229801	Trp53bp1	A2AU91	2	0.678	0.929	8	0.705	0.899	4	1.752	0.729	13	1.484	0.788	9	0.918	0.963	21	0.897	0.965
IPI00471341	Ubl4a	P21126	2	0.678	0.555	1	1.007	0.864	3	1.058	1.022	2	1.080	0.949	2	0.915	1.019	5	1.005	0.954
IPI00136555	Ymel1l	O88967	2	0.677	0.867	/			1	1.410	0.852	2	1.326	0.852	1	0.804	0.920	6	0.860	0.939
IPI00124771	Slc25a3	Q8VEM8	2	0.677	1.230	5	0.720	1.180	5	1.394	0.832	7	1.365	0.870	7	0.587	0.692	12	0.596	0.742
IPI00553798	Ahnak	A0JLR7	39	0.676	0.869	73	0.684	0.891	82	1.216	0.950	102	1.237	0.970	120	0.729	0.878	189	0.739	0.900
IPI00129519	Basp1	Q91XV3	7	0.676	1.091	11	0.722	1.042	8	1.252	1.183	11	1.183	1.115	9	0.790	1.038	10	0.828	1.067
IPI00556827	Atp2b1	Q3TSK3	7	0.674	0.735	7	0.720	0.710	4	1.166	0.845	8	1.175	0.850	6	0.618	0.779	15	0.703	0.896
IPI00221688	Ublcp1	Q8BGR9-1	2	0.674	0.880	3	1.138	0.881	/			5	1.005	0.929	4	0.994	0.976	7	0.978	0.984
IPI00137336	Gpc1	Q9QZF2	2	0.671	0.970	5	0.655	0.909	3	1.407	0.522	6	1.358	0.614	9	0.817	0.832	13	0.797	0.877
IPI00278624	Mcm10	Q0VBD2	1	0.669	0.895	/			/			/			1	0.959	1.176	2	1.100	1.093
IPI00125960	Ndrg1	Q62433	3	0.667	1.044	2	0.887	1.078	4	0.841	1.113	5	0.838	1.039	6	0.829	1.136	6	0.890	1.081
IPI00271059	Rab4b	Q91ZR1	1	0.665	0.717	1	0.899	1.085	/			/			/			/		
IPI00377728	Tomm70a	Q9CZW5	2	0.664	1.106	5	0.614	1.107	5	1.307	0.904	5	1.337	0.831	6	0.733	0.780	7	0.719	0.788
IPI00135365	Zfand5	O88878	1	0.663	0.572	2	0.972	0.992	2	1.560	1.147	2	0.994	1.186	1	0.895	1.113	4	0.873	1.072
IPI00229911	Nradd	Q3TVC1	2	0.663	0.799	3	0.755	0.721	/			1	1.262	0.846	1	0.874	0.869	4	0.900	0.992
IPI00118018	Ehbp1l1	Q99MS7-1	2	0.662	0.908	3	0.813	1.048	2	0.999	1.012	3	1.130	0.948	3	0.923	1.330	4	0.890	1.038
IPI00221463	Hist3h2a	Q8BFU2	3	0.661	1.041	4	0.693	1.005	3	1.097	0.799	4	1.216	0.747	5	0.825	0.873	6	0.835	0.881
IPI00112460	Ndel1	Q9CZA6-1	2	0.661	0.973	3	0.683	1.012	2	1.410	1.146	5	1.305	1.064	1	13.38	1.187	4	1.121	1.110
IPI00124700	Tfrc	Q62351	6	0.661	0.927	12	0.775	0.957	8	1.880	0.944	9	1.871	0.888	9	1.011	0.982	18	1.048	0.981
IPI00313841	Atp6v0d1	P51863	1	0.658	0.542	3	0.829	0.844	/			2	0.788	0.817	/			4	0.716	0.689
IPI00459776	Ift52	Q62559	1	0.657	0.896	/			/			/			/			/		
IPI00121335	Akt2	Q60823	1	0.655	0.677	2	1.246	0.687	/			/			/			/		
IPI00119138	Uqcrc2	Q9DB77	4	0.655	1.432	3	0.720	1.288	4	1.420	0.722	6	1.413	0.786	8	0.468	0.665	11	0.466	0.697
IPI00321718	Phb2	O35129	2	0.651	1.465	4	0.746	1.399	2	1.599	0.860	4	1.304	0.913	3	0.580	0.694	6	0.620	0.744
IPI00473475	Gchfr	P99025	2	0.651	0.928	2	0.932	0.955	2	0.917	1.024	2	0.920	1.000	2	0.844	0.989	3	0.828	1.055
IPI00310518	Ccdc47	Q9D024-1	1	0.649	0.958	2	0.601	0.923	2	0.936	0.881	3	1.242	0.816	4	0.799	0.903	9	0.799	0.850
IPI00119892	Smarce1	O54941	2	0.648	0.737	4	1.047	0.946	1	1.023	0.846	3	1.056	0.919	3	0.808	1.132	7	0.842	0.885
IPI00130343	Hnrnpc	Q3U6P5	5	0.648	0.999	/			8	1.126	0.897	10	1.069	0.900	8	0.730	0.776	/		
IPI00408495	Bsg	P18572-1	1	0.644	0.817	2	0.755	0.724	4	1.186	0.956	6	1.189	0.945	6	0.769	0.953	6	0.767	0.892
IPI00133440	Phb	P67778	2	0.642	1.307	5	0.597	1.380	/			7	1.494	0.820	4	0.535	0.720	10	0.548	0.775
IPI00623776	Hist1h4a	P62806	4	0.640	1.007	6	0.661	0.987	6	1.030	0.751	5	0.979	0.745	9	0.832	0.871	9	0.863	0.894
IPI00312063	Ldlr	P35951	1	0.640	0.967	4	0.373	0.868	/			3	0.361	0.759	5	0.266	0.776	12	0.265	0.815
IPI00649005	Epb4.1	A2A841	2	0.639	0.853	3	0.618	0.803	3	1.412	1.136	4	1.318	1.051	5	0.836	0.925	5	0.827	1.029
IPI00126301	H2-D1	P14427	2	0.638	0.799	/			/			/			/			/		
IPI00109615	Nup37	Q9CWU9	2	0.633	1.043	2	1.000	1.102	1	1.027	0.959	/			2	1.015	1.056	5	0.997	1.000
IPI00311682	Atp1a1	Q8VDN2	8	0.632	0.845	14	0.619	0.835	11	1.000	0.808	15	1.032	0.842	15	0.661	0.830	25	0.689	0.882
IPI00387238	Crbn	Q8C7D2-1	1	0.632	0.799	1	1.109	0.971	1	0.770	0.774	2	1.045	0.932	2	1.051	1.025	3	1.036	1.064
IPI00129220	Epha2	Q03145	2	0.630	0.750	7	0.616	0.878	2	1.401	1.038	5	1.398	1.017	8	0.871	0.964	12	0.845	0.961
IPI00331577	Slc7a5	Q3UG45	2	0.629	0.811	2	0.690	0.862	1	0.962	1.012	2	1.027	1.162	2	0.958	0.767	4	0.940	0.878

IPI00130102	Des	P31001	4	0.628	0.881	/			3	0.539	0.805	/			/			/		
IPI00227582	Nrp2	O35375-4	1	0.626	0.660	2	0.928	1.016	1	1.965	0.709	1	0.970	1.064	/			6	0.918	0.883
IPI00885252	Pdcd5	P56812	2	0.626	0.775	2	1.036	0.897	3	0.929	0.918	/			4	1.095	1.011	/		
IPI00117811	Ap3d1	O54774	1	0.624	16.38	/			2	0.814	1.011	5	0.725	1.008	1	0.703	0.722	10	0.767	0.743
IPI00121277	Pi4k2a	Q2TBE6	1	0.621	0.810	/			/			5	1.004	1.027	2	0.698	0.929	8	0.833	0.996
IPI00228253	Acat2	Q8CAY6	5	0.619	1.350	6	0.617	1.055	7	0.528	0.967	8	0.548	0.966	9	0.635	1.032	12	0.636	1.096
IPI00126191	Lmnb2	P21619-1	3	0.618	0.884	4	0.793	0.780	5	1.452	0.776	6	1.479	0.828	8	0.665	0.807	10	0.651	0.814
IPI00399869	Ubl7	Q91W67	3	0.614	0.629	3	0.908	0.975	3	1.273	0.882	5	0.988	0.939	2	1.027	0.826	3	0.999	1.262
IPI00282848	H3f3a	P84244	3	0.614	1.068	2	0.645	1.044	2	1.141	0.740	2	1.098	0.697	2	0.983	0.775	4	0.953	0.813
IPI00313653	Maf1	Q9D0U6	1	0.612	1.054	1	1.155	1.232	/			/			/			/		
IPI00124221	Atp1b3	P97370	2	0.612	0.847	2	0.662	0.939	2	1.091	0.885	3	0.966	0.848	3	0.600	0.836	5	0.656	0.912
IPI00111842	Narf	Q9CYQ7	1	0.609	0.761	1	0.913	0.899	/			/			1	0.878	1.440	1	1.126	1.231
IPI00137355	Fv1	P70213	1	0.609	2.428	1	0.782	1.135	1	0.616	1.059	1	0.619	0.943	/			2	0.670	1.018
IPI00136098	Rdh11	Q9QYF1	1	0.607	1.092	2	0.644	0.950	1	0.787	1.040	2	0.741	0.884	/			4	0.598	1.069
IPI00284393	Zbtb45	Q3TLP9	1	0.605	0.721	/			/			/			/			/		
IPI00123755	Cbx5	Q61686	2	0.605	0.823	2	0.543	0.859	6	1.577	0.742	6	1.584	0.709	7	0.831	0.987	9	0.841	0.992
IPI00420597	Wapal	Q65Z40	1	0.604	0.961	/			/			/			/			6	1.028	0.960
IPI00123004	Pdk3	Q922H2	2	0.602	0.862	2	1.065	0.955	/			3	1.228	1.130	2	0.888	1.129	4	0.893	0.984
IPI00466588	Rap2c	Q8BU31	1	0.602	0.900	/			/			1	0.930	1.006	/			5	0.724	0.912
IPI00377290	Gmip	Q6PGG2-1	1	0.597	0.569	4	0.859	0.892	3	1.067	1.151	5	0.946	1.150	6	0.953	1.200	6	0.931	1.051
IPI00126883	Trps1	Q925H1	1	0.595	0.510	1	1.002	0.848	2	1.072	1.149	1	1.076	1.100	3	1.125	1.087	2	1.182	0.917
IPI00122491	Yipf3	Q3UDR8	1	0.593	1.018	1	1.084	0.969	/			1	1.103	0.807	/			1	1.008	1.077
IPI00125267	Vapa	Q9WV55	4	0.593	0.707	6	0.792	1.029	4	1.371	0.976	4	1.281	0.937	8	0.950	0.880	10	0.937	0.896
IPI00153201	Gga1	Q8R0H9	3	0.589	0.580	2	1.083	1.121	4	1.262	1.210	5	1.005	1.034	2	1.219	0.987	4	1.018	1.183
IPI00165794	Tmem48	Q8VCB1	1	0.583	0.829	2	0.751	0.851	3	1.157	1.469	2	0.767	1.067	1	0.899	0.963	3	0.778	0.945
IPI00330521	Mtbp	Q8BJS8-1	1	0.581	0.867	/			/			/			/			/		
IPI00130237	Arih2	Q9Z1K6	1	0.577	0.706	1	0.608	0.910	/			2	1.044	1.077	3	0.970	1.024	3	0.920	1.241
IPI00119680	Ap1m1	P35585	2	0.575		/			10	1.069	1.079	9	1.043	0.998	6	1.050	1.020	11	1.060	1.019
IPI00225371	Unc119b	Q8C4B4-1	3	0.569	0.979	2	1.138	1.040	1	1.150	0.950	3	1.121	0.983	2	0.986	0.951	5	1.014	1.019
IPI00120384	Klf4	Q3U2D6	1	0.560	1.032	1	0.655	1.029	/			/			/			1	0.938	1.362
IPI00750815	Fgfr1op	Q66JX5-1	2	0.555	0.682	2	0.821	0.976	5	1.128	1.053	3	1.015	0.954	3	0.867	1.078	4	0.924	1.087
IPI00113389	Niban	A0PJB3	2	0.553	1.004	2	0.899	1.332	/			/			/			3	1.450	2.939
IPI00310323	Scpep1	Q920A5	2	0.552	1.347	5	1.069	0.852	4	0.785	0.919	5	0.807	0.936	4	0.965	0.933	9	1.065	0.986
IPI00756198	Kntc1	Q8C3Y4	1	0.548	0.530	7	1.289	1.039	/			7	1.080	0.944	1	1.005	0.867	9	0.951	0.916
IPI00113812	Ifrd1	P19182	1	0.547	0.766	2	0.779	1.043	1	0.913	0.836	2	0.989	0.847	1	0.986	0.911	3	1.079	0.883
IPI00124695	Camk2g	Q923T9-1	2	0.542	0.659	/			/			7	1.044	1.040	7	1.193	1.024	9	1.144	1.002
IPI00112639	Ric8a	Q3TIR3-1	1	0.539	0.685	1	0.962	1.121	1	1.087	0.947	2	1.923	0.984	/			2	0.911	0.867
IPI00453692	Nes	Q6P5H2-1	4	0.535	0.806	17	0.665	0.925	11	0.771	1.009	10	0.787	0.970	12	0.868	1.097	22	0.916	0.962
IPI00111145	Uprt	B1AVZ0	1	0.531	0.637	2	1.103	1.010	3	0.929	1.083	4	1.092	0.964	2	1.127	1.305	7	1.124	1.088
IPI00421210	Stk25	Q3U6Y0	1	0.516	0.752	2	0.748	0.937	/			1	1.276	0.921	/			/		
IPI00120457	Fdps	Q920E5	5	0.515	1.080	8	0.554	1.069	7	0.531	1.017	9	0.520	1.030	12	0.507	1.073	14	0.543	1.059
IPI00133709	Pmvk	Q9D1G2-1	1	0.504	1.219	1	0.484	0.945	1	0.541	1.205	/			/			1	0.759	1.217
IPI00129701	Wdsof1	Q6PAC3	1	0.487	0.952	/			/			/			/			3	0.839	0.933
IPI00647978	Usp48	Q3V0C5-2	2	0.485	1.077	1	1.014	0.963	/			1	1.254	0.816	/			4	1.088	1.064
IPI00132177	Spc24	Q9D083-1	1	0.482	0.782	1	0.675	1.033	/			/			/			2	0.821	0.991
IPI00230353	Os9	Q8K2C7	1	0.481	1.087	1	0.979	0.960	/			/			/			5	0.945	0.929
IPI00655041	Exoc2	Q9D4H1	1	0.481	1.907	2	0.479	0.868	/			4	1.484	1.245	3	0.685	0.821	7	0.782	0.915
IPI00321005	Trim32	Q8CH72	2	0.476	0.674	/			/			2	1.092	0.899	/			4	1.057	0.992
IPI00458056	Ncbp1	Q3UYV9	1	0.472	0.417	7	1.097	1.124	4	1.117	1.243	6	1.056	1.182	2	0.821	0.996	3	0.949	0.943
IPI00115516	Emilin1	Q99K41	2	0.469	0.497	3	0.737	0.591	4	0.834	1.003	5	0.865	0.950	2	0.973	0.778	6	0.889	0.906
IPI00474810	Hsd17b7	Q8C5N9	2	0.466	0.998	/			2	0.646	1.196	2	0.587	1.113	3	0.580	1.092	5	0.554	1.245
IPI00128692	Nsdhl	Q9R1J0	6	0.465	0.993	7	0.525	1.091	6	0.502	1.016	8	0.489	1.008	13	0.573	1.164	18	0.594	1.196

IPI00462403		Q9D818-3	1	0.458		/			/			/			/			/		
IPI00111885	Uqcrc1	Q9CZ13	2	0.456	0.798	4	0.658	1.161	3	1.558	0.964	7	1.324	0.834	5	0.530	0.731	14	0.527	0.747
IPI00752027	Myh7b	A2AQN4	2	0.451	1.083	2	0.531	1.049	4	0.416	1.175	4	0.459	1.158	3	0.541	1.368	4	0.536	1.326
IPI00330840	Golga1	Q9CW79-1	1	0.448	0.776	2	1.115	1.035	3	1.084	0.980	1	1.101	0.783	/			3	1.206	0.966
IPI00169958	Lss	Q8BLN5	4	0.426	1.062	7	0.401	1.067	3	0.445	1.051	6	0.524	1.029	6	0.499	1.101	9	0.513	1.244
IPI00458711	Cyp51a1	Q8BSQ7	3	0.422	1.017	5	0.425	1.024	3	0.258	0.933	3	0.241	1.008	6	0.292	1.020	9	0.291	1.012
IPI00319950	Mvd	Q99JF5	4	0.419	1.051	5	0.446	1.042	2	0.375	0.924	2	0.442	0.925	7	0.451	1.043	7	0.436	1.103
IPI00848627	Akt1	A4FUQ9	2	0.414	0.604	4	0.856	1.051	/			3	1.094	1.061	1	0.874	0.978	3	0.756	1.184
IPI00849448	Idi1	P58044	4	0.405	1.040	5	0.426	1.022	5	0.332	1.098	8	0.355	1.087	7	0.408	1.121	10	0.447	1.150
IPI00474228	Stk3	Q9JI10-1	3	0.395	0.979	4	0.726	0.813	2	1.017	0.969	5	0.898	0.972	5	1.075	1.009	9	0.986	0.962
IPI00381495			1	0.381	0.820	3	0.974	1.086	3	1.342	0.900	2	0.892	0.964	1	0.917	0.897	5	0.842	0.980
IPI00320687	Adrbk1	Q99MK8	1	0.376	1.533	/			/			/			/			/		
IPI00114594	Rras	P10833	1	0.370	0.694	/			/			2	0.948	0.805	/			3	0.710	0.945
IPI00135132	Kif21b	Q9QXL1	1	0.343	256.570	1	0.863	5.847	/			/			/			/		
IPI00331707	Hmgcs1	Q8JZK9	11	0.318	1.024	11	0.303	0.986	5	0.168	0.969	8	0.243	1.059	10	0.200	1.076	13	0.220	1.080
IPI00321753	Gprc5a	Q8BHL4	1	0.313	0.490	1	0.343	0.925	/			2	1.155	0.998	1	0.634	0.830	3	0.602	0.974
IPI00463244	6030429G01Rik	Q3UYV8	1	0.313	0.987	1	0.363	1.196	/			/			/			/		
IPI00273767	Dars2	Q8BIP0	2	0.301	0.742	4	1.020	1.044	2	0.940	1.046	6	0.934	1.016	2	1.042	0.939	8	1.043	1.018
IPI00515370	Aldh3a2	B1ATI0	3	0.274	0.233	5	0.950	0.854	5	1.057	1.016	5	1.157	1.009	6	1.127	1.063	8	1.004	0.986
IPI00457532	Ppil3	Q9D6L8-1	1	0.256	0.201	2	1.111	1.282	2	0.996	0.686	2	1.078	1.010	2	1.001	0.919	6	1.050	0.972
IPI00157497	Odz4	Q3UHK6-3	1	0.254	0.194	/			/			/			/			/		
IPI00330763	Fam76b	Q80XP8-1	2	0.248	0.181	3	1.017	0.993	1	1.162	0.856	5	1.030	0.972	1	0.921	0.976	3	1.015	0.975
IPI00421085	Cpsf6	Q6NVF9	1	0.245	1.068	6	0.916	0.972	5	1.043	1.087	7	1.076	0.927	5	1.065	0.943	7	1.052	0.952
IPI00129927	Mcc	Q3TYX4	1	0.238	0.161	3	1.005	1.012	2	1.524	1.280	2	1.278	1.077	2	1.160	1.094	/		
IPI00129516	Uqcrh	P99028	1	0.215	0.564	1	0.802	1.119	/			/			/			2	0.662	0.757
IPI00649138	Bptf	A2A654	1	0.198	0.193	2	0.820	0.911	4	1.008	1.147	2	1.102	0.974	3	1.028	1.215	4	1.006	0.831
IPI00336310	Dtl	Q3TLR7-2	1	0.188	0.443	2	0.235	0.328	1	1.255	4.393	/			1	1.085	5.269	2	1.167	1.702
IPI00754308	Zfpm1	O35615	2	0.164	0.218	2	0.876	2.818	1	0.892	0.896	/			2	0.545	0.796	3	0.818	0.932
IPI00222809	H6pd	A2A7A7	1	0.148	1.955	2	1.052	0.944	/			/			/			3	0.987	0.901
IPI00875536	Vps8	Q0P5W1-1	1	0.132	0.222	1	1.125	1.004	/			1	0.846	0.923	/			/		
IPI00453829	Tmx4	Q8C0L0	1	0.127	0.717	2	1.056	0.892	1	0.806	0.933	2	0.938	0.949	1	0.868	0.972	4	0.895	0.981
IPI00417155	Eif4g3	Q80XI3-3	4	0.124	0.131	4	0.848	1.022	4	1.334	1.329	5	0.580	0.756	3	1.055	1.104	6	1.091	1.016
IPI00230439	Hps5	P59438-1	1	0.104	0.154	2	0.887	0.647	/			1	1.008	1.064	/			1	0.980	1.054
IPI00116701	Rad51l3	O55230	1	0.103	0.660	1	1.775	1.371	1	0.973	0.928	/			/			1	0.826	0.873
IPI00136701	Actn3	O88990	5	0.092	0.847	/			/			/			/			/		
IPI00123572	Nudt5	Q9JKX6	1	0.059	0.084	5	1.031	1.024	3	0.978	0.961	5	1.071	0.996	3	0.906	1.008	5	1.051	0.990
IPI00112125	Kiaa0907	Q3TCX3-1	1	0.038	0.074	2	1.163	1.094	2	1.049	1.030	2	1.066	0.930	2	1.115	1.279	2	0.959	1.015
IPI00750314	6230409E13Rik	Q3UMF9	1	0.038	0.042	/			/			/			/			/		
IPI00379692	Rttn	Q8R4Y8-1	1	0.024	0.091	/			/			/			/			/		
IPI00453796	Amigo3	Q8C2S7	1	0.018	0.019	/			/			/			/			/		
IPI00112674	1700074P13Rik	Q9D9G7	1	0.002	0.003	1	0.041	0.018	/			1	0.853	150.0	/			/		
IPI00914104	Clca2	Q9R070	1	0.002	4.346	/			/			/			/			/		
IPI00874685	Nnt	Q61941	/			1	0.680	1.411	/			/			/			/		
IPI00649329	Kpna6	O35345	/			2	0.679	0.804	4	1.191	0.927	6	1.252	0.928	6	0.925	0.953	9	0.926	0.922
IPI00124082	Ccdc115	Q8VE99	/			2	0.678	1.118	2	1.291	0.985	3	1.174	0.973	2	0.880	0.767	4	0.981	0.873
IPI00136110	Pik3cb	Q8BTI9	/			1	0.677	0.696	/			/			/			/		
IPI00128183	Med20	Q9R0X0-1	/			1	0.677	1.057	/			/			/			/		
IPI00761693	Mpp7	Q8BVD5-1	1	0.740	0.682	4	0.677	0.830	3	1.080	0.817	5	1.201	0.878	6	0.807	0.979	7	0.889	1.078
IPI00225912	Mki67ip	Q91VE6-1	/			1	0.677	1.319	/			2	1.063	0.796	/			2	0.832	0.719
IPI00110729	Chmp5	Q9D7S9	/			1	0.676	1.036	/			1	1.199	0.981	1	1.015	1.248	4	0.958	0.982

IPI00468691	Abcg2	Q7TMS5	/			1	0.676	1.048	1	0.840	0.846	/			1	0.786	0.678	2	0.665	0.500
IPI00133608	Ociad1	Q9CRD0-1	/			3	0.675	1.079	2	0.932	0.929	3	0.999	0.948	2	0.582	0.995	3	0.578	1.070
IPI00137331	Cap1	P40124	9	0.995	1.023	12	0.674	0.719	/			15	0.981	1.008	14	1.015	1.745	22	1.096	1.078
IPI00117124	Psen1	P49769-1	/			1	0.673	0.831	/			/			/			/		
IPI00403747	Golga7	Q91W53-2	/			1	0.673	1.102	/			/			/			/		
IPI00323134	Cdh2	P15116	/			2	0.672	0.658	2	1.396	0.818	2	1.287	0.830	5	0.777	0.811	6	0.774	0.899
IPI00315794	Cyb5b	Q9CQX2	1	0.848	1.116	1	0.672	1.127	/			/			2	0.630	0.779	4	0.613	0.837
IPI00308653	Lpin1	Q91ZP3-1	/			3	0.672	1.119	1	0.714	0.826	1	0.628	1.010	1	0.354	0.699	3	0.522	1.199
IPI00122273	Dag1	Q62165	/			3	0.672	0.730	3	1.152	0.956	4	1.182	0.905	5	0.801	0.955	7	0.798	0.981
IPI00459033	Dnajc3	Q91YW3	2	0.946	0.802	5	0.671	0.540	2	0.979	0.987	3	1.029	1.026	3	0.930	1.043	4	0.902	1.063
IPI00321597	Pelp1	Q9DBD5	/			5	0.670	0.854	4	1.181	0.941	5	1.154	1.044	4	0.879	1.083	15	0.961	1.056
IPI00121133	Cd80	Q00609-1	/			1	0.670	0.752	1	0.786	1.019	/			2	0.906	0.998	1	0.747	0.774
IPI00318485	Sri	Q6P069-1	2	0.990	1.113	2	0.668	1.089	2	0.888	1.052	2	0.940	0.947	4	1.073	1.052	7	1.007	1.052
IPI00221822	Wdr3	Q8BHB4	/			2	0.668	0.855	/			/			/			/		
IPI00849568	Zzef1	Q5SSH7-1	/			1	0.667	0.810	2	0.781	0.782	4	0.838	1.028	3	1.185	1.166	1	0.964	0.964
IPI00648295	Aof2	A3KG93	/			4	0.666	0.818	/			1	1.184	0.861	2	1.069	1.128	7	1.067	1.045
IPI00129466	Cbx1	P83917	2	0.712	0.834	2	0.666	0.791	2	1.288	0.795	3	1.264	0.800	2	0.739	0.924	5	0.876	0.913
IPI00112188	Cnot8	Q9D8X5	/			1	0.666	0.610	/			/			/			/		
IPI00348270	Hist2h2bb	Q64525	/			5	0.665	0.963	/			7	1.129	0.772	/			10	0.871	0.855
IPI00874321	Hnrnpc	Q9Z204-1	/			10	0.664	0.944	/			/			/			11	0.706	0.877
IPI00283817	Usp28	Q5I043-1	/			1	0.664	0.904	1	0.696	0.854	2	0.993	1.050	/			/		
IPI00309365	Acot8	P58137	1	0.952	0.847	3	0.663	0.800	/			1	0.786	1.135	/			2	0.913	1.182
IPI00621828	Rfwd2	Q9R1A8	/			2	0.662	0.590	/			1	0.917	0.896	/			/		
IPI00135189	Aacs	Q9D2R0	9	0.724	1.100	11	0.661	1.015	8	0.696	1.016	8	0.699	1.021	7	0.672	1.049	15	0.683	1.021
IPI00856542	H2-D1	Q31149	/			3	0.660	1.079	/			/			/			/		
IPI00109437	Pir	Q9D711	/			2	0.660	0.640	/			3	1.187	1.035	1	1.206	1.077	4	1.281	1.100
IPI00312244	Mfn2	Q80U63-1	/			1	0.660	1.028	/			/			/			1	0.671	0.732
IPI00115117	Stoml2	Q99JB2	1	0.735	1.194	4	0.660	0.981	2	1.141	0.867	3	1.168	0.884	4	0.718	0.848	6	0.765	0.942
IPI00313475	Atp5c1	Q91VR2	1	0.738	1.158	3	0.659	1.123	2	1.060	0.892	3	1.096	0.908	1	0.670	0.713	5	0.733	0.834
IPI00187413	Mett5d1	Q9DCL4	/			1	0.657	1.166	/			1	0.761	0.892	/			1	0.817	1.035
IPI00132330	Chchd1	Q9CQA6	/			1	0.656	0.704	1	0.877	0.981	1	0.931	0.962	1	1.056	1.102	/		
IPI00153756	Tspan8	Q8R3G9	2	0.740	1.058	1	0.656	1.000	1	0.786	0.933	1	0.776	0.997	1	0.871	0.975	2	0.801	0.975
IPI00828714	Abcb11	A2AUN4	/			1	0.655	0.821	/			/			/			1	0.643	0.888
IPI00134979	Chm	Q9QXG2	/			1	0.655	1.051	2	1.100	0.940	/			/			/		
IPI00664442	Slc4a7	Q8BTY2-2	/			1	0.654	0.853	/			/			/			/		
IPI00316159	F11r	O88792	/			2	0.653	1.008	1	0.982	0.849	3	0.928	0.910	2	0.777	0.965	3	0.809	0.918
IPI00453634	D030056L22Rik	Q8VCE4	/			1	0.651	0.786	/			1	1.155	1.136	/			1	1.078	1.146
IPI00845851	Syne2	Q640M5	/			2	0.651	0.949	2	1.009	0.905	6	0.898	0.989	/			21	0.644	0.809
IPI00224168	Tcea1	P10711-2	/			9	0.650	0.709	/			/			/			/		
IPI00133132	Ptk2b	Q9QVP9	/			2	0.650	1.046	/			/			/			/		
IPI00470963	Slc4a3	P16283-1	/			1	0.649	0.798	/			/			/			/		
IPI00330679	Ddrgk1	Q80WW9	/			1	0.647	0.995	1	1.623	15.383	1	1.736	1.078	/			2	0.865	1.604
IPI00169984	Kin	Q8K339	2	0.836	0.986	1	0.645	0.910	/			3	1.269	1.051	/			4	1.009	1.119
IPI00110456		Q9CXL3-1	/			1	0.642	0.692	1	1.120	1.556	2	0.925	1.224	2	1.161	0.866	3	1.113	1.059
IPI00556741	Tnfrsf10b	Q6GSD9	2	0.713	1.036	1	0.641	0.903	2	0.939	0.788	2	1.007	0.848	3	0.833	1.076	5	0.761	0.960
IPI00320011	Prc1	Q99K43-1	/			1	0.641	0.966	/			1	2.022	0.831	/			4	0.740	0.841
IPI00228719	Impad1	Q80V26	/			1	0.640	0.953	1	0.785	0.988	1	1.206	1.027	/			1	0.979	0.974
IPI00400017	Ppfibp2	O35711-4	1	0.934	0.836	2	0.639	0.714	2	0.771	1.208	/			2	0.927	1.502	2	1.235	1.518
IPI00420477	Arhgef18	Q6P9R4-1	/			2	0.638	0.999	2	0.968	0.951	4	1.309	1.062	4	0.968	0.880	9	1.006	1.061
IPI00453777	Atp5d	Q9D3D9	1	0.683	1.015	3	0.638	0.975	2	1.265	0.897	3	1.085	0.927	3	0.693	0.837	4	0.698	0.855

IPI00137471	Ebp	P70245	/			2	0.635	1.114	2	0.680	0.901	2	0.842	0.935	2	0.583	0.812	1	0.647	0.915
IPI00137194	Slc16a1	P53986	/			2	0.635	0.811	3	0.895	0.928	3	0.927	0.991	3	0.753	0.625	3	0.840	0.669
IPI00469000	Slc39a6	Q8C145	/			1	0.634	0.650	/			1	1.031	0.936	/			/		
IPI00229300	Epb41l3	Q9WV92-7	/			15	0.633	0.709	11	1.217	0.850	17	1.201	0.912	/			28	0.902	0.962
IPI00387427	Vps53	Q8CCB4-1	1	0.681	0.917	1	0.633	0.659	/			4	1.223	1.020	1	0.757	0.922	5	0.979	1.028
IPI00112128	Hdhd3	Q9CYW4	1	0.935	0.934	2	0.631	1.084	/			/			/			1	1.026	0.985
IPI00313525	Ncoa5	Q91W39	/			2	0.630	0.760	/			5	1.008	1.132	/			7	1.101	1.102
IPI00466570	Tmed10	Q9D1D4-1	1	0.744	0.998	1	0.630	1.177	/			3	1.054	0.939	3	0.785	0.694	3	0.808	0.669
IPI00222514	Mrps27	Q8BK72	/			3	0.629	0.900	3	0.891	0.882	4	0.853	0.814	3	1.046	1.072	8	0.976	0.890
IPI00111770	Atp5i	Q06185	/			1	0.627	1.596	1	1.009	0.819	1	0.952	0.823	/			1	0.594	0.812
IPI00315517	Seh1l	Q3TLC9	1	0.709	0.750	1	0.627	0.517	1	1.010	1.117	3	1.088	1.042	2	0.872	0.953	6	0.892	1.032
IPI00554845	Immt	Q8CAQ8-5	/			1	0.624	1.495	2	0.516	0.351	9	1.417	0.893	/			7	0.644	0.839
IPI00648654	Dusp3	B1AQF4	/			1	0.623	0.991	4	1.014	0.925	3	0.991	1.103	4	1.007	0.996	4	0.931	0.983
IPI00261638	Myl6b	Q8CI43	/			2	0.622	0.917	/			3	0.997	1.014	/			2	1.232	1.087
IPI00828892	Rbm27	Q5SFM8-1	/			2	0.621	0.647	1	1.251	1.262	1	1.133	0.996	2	0.958	1.080	3	1.001	0.966
IPI00311181	Klf13	Q9JJZ6	/			1	0.620	1.049	/			/			/			2	0.862	1.012
IPI00109506	Stx6	Q9JKK1-2	/			1	0.620	0.438	/			1	0.979	0.859	2	0.858	0.838	1	0.969	0.894
IPI00153418	Zc3h10	Q8R205	/			1	0.618	0.515	/			/			/			/		
IPI00402911	Mphosph10	Q810V0	/			1	0.616	0.778	/			2	1.725	1.159	1	0.829	1.121	4	0.863	1.098
IPI00230476	Diaph3	Q9Z207	/			1	0.615	0.912	/			2	0.338	0.990	/			5	0.849	1.133
IPI00454109	Erf	P70459	/			1	0.614	0.756	/			2	0.986	1.155	/			2	0.837	0.930
IPI00117829	Cav1	P49817-1	/			1	0.611	0.761	2	0.666	0.749	3	0.632	0.847	2	0.597	0.566	3	0.598	0.654
IPI00111162	Sox13	Q04891-1	/			1	0.611	0.090	/			/			/			/		
IPI00776065	Klhl13	A2AL88	/			1	0.610	0.813	/			/			/			/		
IPI00315187		Q9CQ22	1	0.713	1.217	2	0.610	0.972	/			/			/			4	0.548	0.753
IPI00118217	Stx7	O70439	/			1	0.609	0.800	/			/			/			1	0.943	0.629
IPI00122227	Rnps1	Q62150	/			2	0.609	0.957	/			/			/			/		
IPI00122223	Top2a	Q01320	/			4	0.607	1.108	4	3.181	0.851	10	3.296	0.933	5	0.795	0.964	11	0.780	0.967
IPI00469323	Dnmt1	P13864-1	10	0.861	1.003	19	0.606	0.739	19	1.496	1.241	26	1.364	1.141	22	1.095	1.007	35	1.073	1.020
IPI00120310	Ikip	Q9DBZ1-1	/			3	0.605	0.972	/			/			/			/		
IPI00119432	Smpd2	O70572	/			2	0.605	3.927	/			/			/			6	1.054	1.040
IPI00468609	Tgm6	Q14CG3	/			1	0.605	1.214	/			/			/			/		
IPI00758301	Th1l	Q3TW27	/			1	0.604	0.649	/			2	0.887	0.916	/			5	1.001	1.107
IPI00121218	Fahd2	Q3TC72	/			2	0.603	0.730	/			/			/			/		
IPI00138716	Rap2b	P61226	/			1	0.602	0.867	/			1	0.878	0.628	2	0.775	0.901	5	0.696	0.844
IPI00400418	Tcf4	Q60722-3	/			2	0.602	0.867	/			/			/			/		
IPI00126115	Sfxn3	Q91V61-1	/			3	0.598	1.236	4	1.328	0.917	6	1.271	0.859	6	0.654	0.742	9	0.606	0.757
IPI00460291	Unc84b	Q3TBU0	/			1	0.598	0.919	1	0.975	0.920	2	1.047	1.298	3	0.520	0.812	3	0.507	0.847
IPI00118986	Atp5o	Q9DB20	/			4	0.598	1.067	2	1.187	0.798	6	1.177	0.798	7	0.584	0.772	8	0.577	0.777
IPI00876025	Mtss1	Q6ZQB7	/			1	0.596	1.192	/			/			/			/		
IPI00222225	Sec24a	Q3U2P1-1	/			2	0.595	0.556	/			4	0.910	0.832	2	0.994	1.018	6	1.083	1.150
IPI00620227	Tapbp	Q3TCU5	/			1	0.595	1.035	1	0.879	0.839	1	0.966	0.870	/			2	0.646	0.970
IPI00128915	Cspg4	Q8VHY0-1	/			1	0.593	0.708	/			6	0.963	0.799	2	1.074	0.992	5	0.738	0.929
IPI00857073	Akt1s1	Q9D1F4	/			2	0.592	0.979	2	1.120	1.015	2	0.936	1.078	3	1.080	1.053	3	1.085	1.055
IPI00399958	Calu	Q3TL33	/			8	0.590	0.901	9	1.014	0.931	12	0.945	0.876	9	1.232	1.173	14	1.025	1.158
IPI00380817	Bcr	Q6PAJ1	2	0.897	0.710	2	0.589	0.389	/			/			/			4	0.947	1.023
IPI00108685	Ptpra	P18052-1	/			3	0.589	1.070	/			/			/			4	0.976	0.849
IPI00121576	Apoo	Q9DCZ4	/			1	0.589	0.574	/			1	1.104	0.884	/			1	0.772	0.858
IPI00122430	Tmem97	Q8VD00	/			1	0.588	0.757	/			/			/			/		
IPI00453582	Grsf1	Q8C5Q4	1	0.696	0.873	2	0.588	0.941	1	1.406	1.116	3	1.184	0.985	5	1.217	0.998	6	1.192	1.022
IPI00377618	Rpap1	Q80TE0-1	/			1	0.571	0.676	/			2	0.885	1.260	1	1.165	0.891	/		
IPI00121550	Atp1b1	P14094	/			1	0.567	0.898	/			/			/			2	0.619	0.804

IPI00378513		Q3TUU5	/			1	0.564	0.577	/			2	1.140	0.995	/			3	0.948	1.017
IPI00116968	Ncoa2	Q61026	2	0.794	0.988	4	0.564	0.803	/			2	1.221	1.002	/			6	0.961	0.937
IPI00230394	Lmnb1	P14733	2	0.797	0.772	8	0.558	0.847	7	1.459	0.822	6	1.706	0.842	15	0.567	0.723	21	0.607	0.735
IPI00396701	Rap2a	Q80ZJ1-1	/			1	0.557	1.057	/			/			/			4	0.607	1.065
IPI00331230	Ttc27	Q8CD92-1	/			2	0.557	0.926	/			3	1.132	1.065	1	0.944	1.032	3	0.961	1.124
IPI00816884			/			2	0.556	0.659	/			1	1.153	0.991	/			2	1.228	0.835
IPI00263265	Itpkb	B2RXC2	/			1	0.553	0.867	/			3	0.721	1.043	/			/		
IPI00338452	Col4a2	P08122	/			1	0.550	0.663	/			2	0.960	0.598	2	1.436	1.348	2	0.974	0.996
IPI00316067	Hsd17b7	O88736	/			3	0.538	0.956	/			/			/			/		
IPI00667471	Ppp2r2a	Q6P1F6	2	0.787	0.895	2	0.529	0.958	3	1.037	1.153	5	1.038	1.026	6	1.078	1.076	9	1.069	1.068
IPI00757830	Clcn5	B1ATV0	/			2	0.527	4.578	/			/			/			2	0.848	0.832
IPI00471423	Apbb2	Q9DBR4-1	/			2	0.526	0.565	/			/			2	1.067	0.866	2	0.957	0.987
IPI00308784	Unk	Q8BL48-1	1	0.888	0.900	2	0.508	0.504	/			2	0.933	0.952	1	0.967	1.054	3	1.137	1.106
IPI00136380	Zbtb7a	O88939-1	2	0.896	0.994	2	0.508	0.307	2	0.928	0.882	4	1.201	0.902	3	1.044	1.107	2	0.985	1.114
IPI00308332	Armcx3	Q8BHS6	/			1	0.505	0.776	1	1.661	1.028	/			/			1	0.620	1.012
IPI00310293	Bag1	Q60739-1	1	1.032	0.638	1	0.498	1.059	2	0.240	0.346	2	0.942	1.380	2	0.844	0.810	3	0.978	0.898
IPI00222793	Acaa1a	Q8BLD7	/			6	0.494	0.885	5	0.951	1.104	8	0.665	0.810	/			/		
IPI00348414	Ado	Q6PDY2	/			2	0.494	0.410	1	0.895	1.120	3	0.945	1.017	3	0.984	1.092	3	1.016	1.103
IPI00118045	Msh4	Q99MT2	/			1	0.492	1.253	/			/			/			/		
IPI00126796	Slc27a4	Q91VE0	/			1	0.484	25.588	/			1	1.263	0.965	/			/		
IPI00469218	Lamp1	Q3TX84	2	0.724	1.018	1	0.479	0.946	2	1.272	0.634	2	1.215	0.689	2	0.719	0.857	3	0.740	0.924
IPI00454119	Ldlrap1	Q8C142	/			1	0.470	0.561	/			/			/			/		
IPI00648249	Ube2j1	A3KG52	/			1	0.467	0.923	/			/			/			1	0.749	0.817
IPI00338854	Gnai3	Q9DC51	3	0.762	1.006	2	0.457	0.594	2	1.187	0.959	3	1.168	0.874	4	0.897	0.869	6	0.853	0.890
IPI00221521	Fam64a	Q8BFY7-1	/			1	0.454	1.100	/			/			/			1	0.495	0.886
IPI00135311	Mrpl19	Q9D338	/			1	0.454	0.175	/			2	1.050	1.160	/			2	0.936	0.934
IPI00114434	Fgf4	P11403	/			1	0.442	0.130	/			/			/			/		
IPI00132531	Ndufb5	Q9CQH3	/			1	0.440	0.976	/			1	1.828	1.193	/			/		
IPI00111416	Stx12	Q9ER00	/			2	0.432	0.648	2	1.367	1.551	2	1.221	1.081	2	0.895	1.315	2	0.981	1.409
IPI00117142	Scd2	P13011	/			2	0.412	1.423	/			/			/			/		
IPI00407252	Rad18	Q8CDH2	/			2	0.393	0.861	2	1.102	1.012	1	1.344	1.019	/			/		
IPI00844655	Nek10	Q3UGM2-1	/			2	0.387	0.355	/			/			/			/		
IPI00649972	Vps25	A2A4J8	1	1.074	1.024	1	0.378	0.672	1	1.514	0.939	2	0.987	1.134	/			2	0.889	1.038
IPI00109415	Ppp4c	P97470	2	0.829	0.927	2	0.361	0.538	3	1.005	0.957	6	1.061	0.984	4	1.047	1.059	8	1.035	1.026
IPI00404707	Rbm14	Q8C2Q3-1	2	0.888	0.962	2	0.359	0.902	2	1.196	1.013	4	1.128	0.983	5	0.945	0.923	4	0.919	1.006
IPI00221522	Znf629	Q6A085	/			1	0.349	0.332	1	1.125	1.589	1	1.017	1.956	/			2	1.087	1.328
IPI00124103	Ccs	Q9WU84	/			2	0.336	1.412	/			/			/			2	1.078	1.054
IPI00754110	Acbd5	Q5XG73-1	/			1	0.329	1.109	/			/			/			1	0.638	0.901
IPI00116804	Eif2b2	Q99LD9	5	0.911	0.930	3	0.327	0.385	4	1.031	0.973	7	1.128	0.984	4	1.094	0.966	6	1.042	1.045
IPI00653196		Q3U046	/			3	0.317	0.872	4	0.923	0.944	5	1.049	0.950	2	1.091	0.999	4	0.952	1.028
IPI00652900	Arhgef1	Q61210-5	/			5	0.311	1.156	/			/			/			9	1.034	1.755
IPI00226889	Utp15	Q8C7V3	/			1	0.300	0.825	1	1.511	0.996	2	1.562	0.817	3	0.744	0.801	5	0.700	0.818
IPI00310519	Mxra8	Q9DBV4	/			1	0.296	1.281	/			2	0.726	1.844	/			2	0.696	0.952
IPI00320259	Psrc1	Q9D0P7	/			2	0.295	0.402	/			2	1.032	0.930	/			/		
IPI00222090	Sh3pxd2b	A2AAY5	/			2	0.292	0.725	2	0.929	1.019	7	0.991	1.053	/			8	1.124	1.178
IPI00121341	Tmx1	Q8VBT0	1	0.870	2.578	2	0.289	1.630	1	0.933	0.732	1	1.153	0.929	/			3	0.983	0.992
IPI00421081	Pptc7	Q6NVE9-1	/			1	0.286	0.435	/			/			/			/		
IPI00313513	Bmp2k	Q91Z96-1	/			1	0.283	0.688	/			/			/			/		
IPI00355961	Tmed1	Q3V009-1	/			2	0.283	0.603	1	1.324	0.863	2	1.163	0.856	2	1.104	1.020	4	0.772	0.832
IPI00170221	Arhgef6	A2AFI0	/			2	0.260	1.157	/			/			/			/		
IPI00453578	Irf2bp1	Q8R3Y8-1	/			2	0.258	0.919	/			2	1.084	3.464	2	0.947	1.096	4	1.017	1.099

IPI00272721	Lztr1	Q9CQ33-2	/			1	0.239	0.896	/			/			/			/		
IPI00337955	Polr2e	Q80UW8	1	0.870	0.729	2	0.230	0.233	5	1.156	0.966	4	1.096	0.960	/			2	0.876	0.841
IPI00377455	Gcc2	Q8CHG3	/			2	0.201	1.058	3	1.035	0.959	5	1.106	1.006	1	1.135	12.955	5	1.123	1.327
IPI00311968	Frg1	P97376	/			1	0.198	0.302	/			/			1	0.964	1.051	1	0.969	0.999
IPI00272398	Bcorl1	A2AQH4	/			2	0.192	0.717	1	1.493	1.287	/			/			/		
IPI00308560	Wdr44	Q6NVE8-1	2	0.837	0.890	2	0.177	0.947	2	1.007	0.901	2	1.238	1.013	/			6	1.029	1.213
IPI00114255	Sprr3	O09116	/			1	0.166	2.272	/			/			/			/		
IPI00885521	Fam115a	Q8BNE1-1	2	0.910	0.939	2	0.137	0.569	1	0.972	1.060	2	1.001	1.042	1	0.714	0.927	2	0.790	0.989
IPI00895990	Stk38l	B2KFR5	/			2	0.130	0.075	/			/			/			2	0.899	1.081
IPI00122244	Trim27	Q62158	/			1	0.120	1.076	/			/			/			/		
IPI00620743	Srcap	Q8BKT0	/			1	0.116	1.018	/			/			/			/		
IPI00121534	Ca2	P00920	/			1	0.098	0.059	/			/			/			/		
IPI00127983	Tmed2	Q9R0Q3	/			2	0.095	0.805	/			3	1.092	0.857	/			4	0.818	0.814
IPI00312509	Axl	Q00993	2	0.990	0.892	2	0.093	0.065	2	1.360	0.943	2	1.459	1.068	2	0.946	0.880	4	1.001	1.908
IPI00881057	Runx1	Q3UM65	/			1	0.084	0.156	2	1.123	1.277	/			/			/		
IPI00109103	Bloc1s2	Q9CWG9	1	1.107	1.106	2	0.076	2.341	/			2	0.494	0.624	/			4	0.936	0.950
IPI00229849	Ppat	Q3TUW2	/			1	0.028	0.949	3	1.010	1.046	4	0.831	0.959	3	1.647	0.962	8	1.598	0.865
IPI00353998	Kif16b	B1AVY7	1	1.051	1.110	1	0.006	0.870	2	0.972	1.032	2	0.912	1.018	2	1.050	0.874	3	1.096	0.939
IPI00927982	Parp4	Q6A0B1	/			/			4	0.733	0.931	4	0.862	0.884	3	0.794	0.958	/		
IPI00461964	Aldh6a1	Q9EQ20	3	1.230	1.113	5	1.099	1.061	3	0.732	0.946	3	0.716	0.923	2	0.981	1.187	5	1.072	0.980
IPI00331555	Bckdha	P50136	/			/			1	0.732	0.847	2	0.925	1.001	4	1.047	0.962	7	1.011	0.915
IPI00133166	Nat9	Q3UG98	/			/			1	0.732	0.929	3	0.934	1.082	1	1.055	5.193	1	1.219	1.377
IPI00355673	Serpina3h	A2RTV1	/			3	1.110	0.963	1	0.731	1.547	5	0.793	1.476	/			4	1.245	1.868
IPI00120915	0610037L13Rik	Q8BHG2-3	/			1	1.203	0.990	1	0.729	0.985	2	0.859	0.911	/			2	1.034	0.885
IPI00119124	Fundc1	Q9DB70	/			/			1	0.729	0.732	1	0.664	0.819	1	0.735	0.808	2	0.814	0.854
IPI00314726	Naglu	A2BFA6	/			5	1.217	0.771	5	0.729	0.936	10	0.763	0.922	1	1.011	0.892	5	0.968	0.876
IPI00395140	Dcxr	Q91X52	4	1.314	1.093	7	1.272	1.069	6	0.729	0.912	7	0.738	0.907	5	1.061	0.970	10	1.055	1.079
IPI00319231	Rps15	P62843	1	1.005	1.370	3	1.183	1.204	1	0.728	0.929	3	0.960	1.004	5	1.042	0.895	5	1.114	0.879
IPI00944148	Zan	Q99ND0	/			/			1	0.728	0.928	/			/			/		
IPI00229349	Ate1	Q8CFP7	/			2	0.987	0.955	3	0.727	1.109	4	0.963	0.947	1	1.019	0.997	4	1.001	1.001
IPI00125505	Arhgap31	A6X8Z5	/			/			1	0.726	1.239	2	1.542	1.134	/			4	1.099	1.273
IPI00109109	Sod2	P09671	3	1.246	1.177	4	1.123	1.055	4	0.725	0.829	5	0.738	0.827	3	1.008	0.896	6	0.986	0.940
IPI00153644	Pbxip1	Q3TVI8	1	0.762	0.650	/			1	0.722	1.028	2	0.710	0.764	/			2	0.662	0.785
IPI00117842	Man2b2	O54782	/			/			2	0.721	0.876	4	0.708	0.897	2	1.024	1.109	5	0.994	1.099
IPI00230108	Pdia3	P27773	14	1.050	1.019	19	1.036	0.991	16	0.721	0.787	18	0.761	0.856	26	0.928	0.927	30	0.916	0.941
IPI00330599	Mtdh	Q80WJ7	3	1.196	1.113	6	1.179	1.092	4	0.721	0.895	5	0.713	0.904	6	0.783	0.833	8	0.847	0.910
IPI00125923	Ostf1	Q62422	4	1.082	1.037	4	1.074	1.061	2	0.721	0.753	4	0.967	1.012	4	0.945	1.027	6	0.995	1.002
IPI00134809	Dlst	Q9D2G2-1	4	0.914	1.008	7	0.991	0.988	5	0.720	1.007	7	0.769	0.945	6	0.922	0.912	9	0.904	0.901
IPI00307952	Cdkn1b	Q8BG74	/			/			6	0.720	0.974	7	0.784	1.015	4	1.140	1.006	5	1.156	1.010
IPI00111286	Creld2	Q9CYA0	4	0.825	0.942	3	0.915	0.925	2	0.719	0.878	4	0.739	0.864	2	0.891	0.941	6	0.881	0.892
IPI00116222	Hibadh	Q99L13	2	1.049	0.921	4	0.813	0.914	2	0.719	0.889	3	0.973	0.924	4	1.052	1.016	7	1.048	1.045
IPI00122548	Vdac3	Q3TTN3	/			2	0.908	1.713	3	0.719	0.693	4	0.726	0.805	/			5	0.502	0.446
IPI00348435	Mex3d	Q3UE17-2	/			2	1.068	0.954	1	0.716	0.730	2	0.932	0.928	2	0.922	1.103	2	0.964	1.121
IPI00775975	Cdh13	Q8BG11	1	0.735	0.997	3	0.744	0.921	1	0.716	0.938	2	0.613	0.758	/			5	0.814	0.952
IPI00331597	Hist1h1d	P43277	4	0.950	0.895	5	0.958	0.958	6	0.715	1.061	7	0.740	1.067	9	0.913	0.946	9	0.878	0.955
IPI00857151	9030617O03Rik	Q8BH86-1	8	1.217	1.007	13	1.139	0.999	9	0.714	0.925	14	0.717	0.876	15	0.908	1.013	20	0.913	0.998
IPI00338536	Sdhb	Q9CQA3	3	1.120	0.884	4	1.207	0.884	4	0.714	0.820	5	1.116	0.888	4	0.933	0.875	7	0.942	0.864
IPI00752812	Rnf7	Q9WTZ1	/			1	1.067	1.066	1	0.712	1.040	1	0.952	0.961	1	1.060	1.031	2	1.069	1.048
IPI00222430	Dbi	Q4VWZ5	/			/			3	0.712	0.954	2	0.742	0.889	3	0.906	1.015	/		
IPI00875492	Gpc4	P51655	3	0.845	1.024	5	0.870	0.963	6	0.707	0.679	6	0.754	0.634	6	0.801	0.891	12	0.761	0.900

IPI00323465	Amdhd2	Q8JZV7	2	1.415	1.080	/			4	0.705	0.866	3	0.880	1.005	4	1.007	0.990	7	0.993	0.968
IPI00126447	Map2k5	Q9WVS7-1	/			/			1	0.704	1.056	/			/			1	0.985	1.182
IPI00116254	Prdx4	O08807	4	0.955	0.994	6	0.994	0.962	6	0.702	0.950	7	0.758	0.938	8	0.936	0.879	12	0.934	0.901
IPI00831068	Mcart6	A2AF34	/			/			1	0.698	0.097	/			/			/		
IPI00923056	Sep-05	B7ZNM7	/			/			1	0.698	1.309	3	0.729	1.191	4	0.810	1.104	/		
IPI00387361	Tmem176b	Q9R1Q6	/			3	0.978	1.113	3	0.696	0.991	4	0.799	1.013	4	0.761	0.669	6	0.743	0.770
IPI00875672			/			/			1	0.695	1.664	3	0.731	0.866	/			1	0.861	0.915
IPI00655136	Arhgef7	Q9ES28-1	/			/			1	0.694	0.804	3	1.257	0.952	3	1.132	1.163	7	1.026	0.908
IPI00266752	Cpne3	Q8BT60	3	0.971	0.977	6	1.048	1.037	3	0.693	0.941	6	0.965	0.926	6	0.941	0.976	12	0.905	0.917
IPI00134426	Trappc6b	Q9D289	/			1	1.441	0.764	1	0.692	1.092	1	0.975	1.267	/			1	0.986	1.056
IPI00165834		Q8VE96	/			/			1	0.692	0.745	/			/			1	0.847	0.830
IPI00132938	Myadm	O35682	/			1	0.958	1.344	1	0.687	0.818	1	0.722	0.901	/			2	0.824	0.669
IPI00831223	Itsn1	Q9Z0R4-1	3	1.022	0.951	2	1.040	1.036	3	0.687	0.996	2	1.060	0.897	1	0.317	1.069	5	0.945	1.156
IPI00133776	Mcee	Q9D1I5	/			/			1	0.685	0.782	2	0.832	1.011	1	0.907	1.259	2	0.899	1.715
IPI00875998	Uck1	P52623	/			3	1.461	1.284	2	0.683	1.010	2	1.115	0.772	1	0.786	0.709	1	1.000	0.856
IPI00129186	Npc2	Q9Z0J0	2	1.022	0.864	2	0.955	0.924	3	0.683	1.003	2	0.737	0.995	2	0.873	0.961	4	0.908	1.037
IPI00652358	Arsb	P50429-1	/			1	1.134	0.907	3	0.682	0.792	6	0.678	0.814	3	0.898	0.878	8	0.844	0.938
IPI00223714	Hist1h1e	P43274	4	0.920	0.966	5	0.945	1.014	6	0.682	0.920	6	0.719	1.002	8	0.984	0.964	8	0.990	0.972
IPI00750091	Cln5	Q3UMW8	/			2	1.066	0.994	1	0.679	0.978	/			/			2	0.834	0.796
IPI00331564	Dld	Q3TIE8	6	0.992	0.952	/			5	0.674	0.850	/			/			/		
IPI00230133	Hist1h1b	P43276	4	0.990	0.932	5	0.879	0.914	6	0.674	0.832	6	0.729	0.892	7	0.961	0.861	7	0.958	0.915
IPI00918862	Pccb	A0PJE6	/			/			3	0.673	0.887	5	0.705	0.867	3	1.286	0.934	/		
IPI00652813	Fn1	B9EHT6	8	1.369	1.030	/			19	0.671	0.795	31	0.649	0.717	/			/		
IPI00130624	Pld3	O35405	3	1.168	1.050	4	0.974	0.949	4	0.671	0.714	7	0.715	0.808	4	0.837	0.968	5	0.832	0.944
IPI00331154	Tmem176a	Q9DCS1	1	1.010	1.211	1	1.011	1.191	2	0.670	0.924	1	0.746	0.828	1	0.881	0.687	2	0.891	0.740
IPI00856142	Ift122	Q6KAU2	/			1	1.241	1.588	1	0.667	1.177	1	0.662	0.704	1	1.211	0.820	1	0.478	0.615
IPI00896595	Cars2	Q8BYM8	/			2	1.260	0.978	1	0.665	0.789	/			/			/		
IPI00320462	Bphl	Q8R164	2	1.269	0.924	3	1.312	0.914	1	0.665	0.813	3	0.711	0.828	3	0.930	0.849	3	0.947	0.880
IPI00896604	Ddx10	Q80Y44	/			1	0.853	0.909	2	0.660	0.213	3	1.376	0.992	/			3	0.868	0.947
IPI00421218	Tln2	Q71LX4	/			/			9	0.660	0.781	/			/			/		
IPI00378120	Glrx5	Q80Y14	/			1	1.021	0.923	2	0.659	0.845	1	0.849	1.012	3	1.051	0.934	3	1.078	1.012
IPI00122549	Vdac1	Q60932-1	/			1	0.971	1.779	1	0.659	0.681	2	0.753	0.697	3	0.435	0.362	5	0.448	0.386
IPI00605187	Cp	Q2F3J4	/			2	1.568	1.079	2	0.657	0.763	/			3	0.813	0.746	5	0.858	0.715
IPI00828479	Acox1	A2A850	/			2	0.875	0.968	5	0.656	1.008	3	0.664	0.870	4	0.755	0.928	9	0.738	0.992
IPI00342908	Kiaa1324	A2AFS3-1	/			/			1	0.654	0.836	1	0.607	0.814	/			/		
IPI00130015	Ctsc	P97821	2	0.976	0.790	2	1.089	0.931	3	0.654	0.925	4	0.739	0.996	2	0.933	1.159	6	1.076	1.132
IPI00473183	Mllt3	A2AM29	/			/			1	0.653	1.101	/			/			/		
IPI00342603	Ogdhl	B2RXT3	4	1.234	0.957	6	1.417	0.960	5	0.652	0.918	8	0.712	0.859	7	1.041	0.978	12	0.941	0.846
IPI00128642	Cbr2	P08074	3	1.142	1.057	6	1.141	1.119	2	0.652	0.794	4	0.640	0.848	6	1.062	0.997	11	0.995	0.976
IPI00124027	A2ld1	Q923B0-1	/			1	1.162	1.027	1	0.648	0.887	1	0.740	0.902	1	0.920	0.923	1	0.876	0.973
IPI00269662	Hnrnpa3	Q8BG05-2	/			/			8	0.644	0.833	10	0.834	0.811	11	0.807	0.839	11	0.868	0.864
IPI00124428	Pla2g15	Q8VEB4	/			/			1	0.640	1.012	2	0.718	1.022	1	0.894	1.016	1	0.817	1.029
IPI00228907	Elmod1	Q3V1U8	/			/			1	0.639	0.862	/			/			/		
IPI00131606	Tmem165	P52875	1	0.961	1.341	1	0.959	1.125	3	0.637	1.019	3	0.682	1.010	2	0.801	0.967	5	0.773	0.605
IPI00462979	Fyttd1	Q91Z49-1	1	0.934	0.958	1	0.970	0.888	1	0.632	0.984	1	0.672	0.992	1	1.291	0.998	2	1.251	0.949
IPI00128689	Col5a1	O88207	/			/			3	0.630	0.957	/			/			1	1.294	1.133
IPI00405736	Cd81	Q3UWG5	2	1.000	1.124	/			1	0.628	1.205	1	0.807	0.951	1	1.123	0.827	3	1.000	0.920
IPI00754712	Aqp5	Q9WTY4	/			2	0.953	1.349	2	0.623	0.906	4	0.716	0.982	2	0.709	0.447	2	0.882	0.553
IPI00135231	Idh1	O88844	8	0.849	1.057	15	0.832	1.039	12	0.618	0.935	18	0.656	0.941	17	0.780	0.996	23	0.762	1.006
IPI00321858	Mrps15	Q9DC71	1	0.918	0.985	5	1.054	0.912	1	0.618	0.846	1	1.160	1.111	1	0.754	0.900	4	0.951	0.909
IPI00457659	Serpinb1a	Q9D154	5	1.336	1.142	8	1.325	1.168	7	0.615	0.924	5	0.580	0.922	7	0.987	0.878	10	0.865	0.890
IPI00111258	Mvp	Q9EQK5	2	1.039	0.957	9	1.073	0.978	10	0.611	0.913	18	0.681	0.929	13	0.874	0.687	22	0.900	0.727

IPI00342158	Nup210	Q9QY81	/			1	1.058	1.045	2	0.603	0.929	2	0.731	0.667	/			1	1.032	0.944
IPI00626834	Sh3glb2	Q8R3V5-4	/			/			2	0.599	0.738	3	0.885	0.848	5	1.026	1.024	/		
IPI00310684	Zerl	Q80ZJ6-1	1	1.213	1.065	1	0.733	1.096	1	0.599	0.829	/			1	0.825	1.170	1	0.778	0.656
IPI00468665	Myh13	B1AR69	/			/			2	0.598	0.664	/			/			3	1.094	1.037
IPI00755796	Ankrd44	B2RXR6	1	1.172	0.879	2	1.379	1.066	1	0.593	1.106	/			/			1	1.271	0.975
IPI00112986	Bcsll	Q9CZP5	/			1	0.864	0.960	1	0.593	0.869	3	0.829	0.887	/			6	1.127	1.078
IPI00225390	Cox6b1	P56391	/			/			1	0.591	0.722	1	0.618	0.752	2	0.485	0.645	/		
IPI00123967	Map3k7	Q3TXG1	1	1.044	0.899	2	1.139	1.114	2	0.587	0.479	2	1.147	1.037	/			3	1.112	1.040
IPI00329962	Fuk	Q7TMC8	2	1.192	1.387	2	1.121	0.960	1	0.587	1.081	1	0.887	0.941	3	1.004	0.967	6	1.054	1.020
IPI00807902	Mtch2	Q05C68	/			/			1	0.585	0.709	1	0.677	0.800	1	0.506	0.466	/		
IPI00323035	Fbln5	Q9WVH9	1	1.636	0.906	/			2	0.582	0.786	2	0.831	0.938	1	0.995	0.861	3	0.990	0.899
IPI00123140	Fyco1	Q8VDC1	4	1.099	1.058	6	1.033	0.880	2	0.574	0.950	4	0.692	0.761	/			3	1.018	0.989
IPI00112549	Acsl1	P41216	2	0.940	1.163	6	0.944	1.013	3	0.568	0.618	6	0.900	0.997	6	0.961	1.042	10	0.956	1.009
IPI00380107	Cabin1	B9EKC5	/			/			1	0.565	0.846	1	0.648	0.793	1	0.642	0.907	1	0.585	0.844
IPI00124979	Rbmx	Q9WV02	2	0.985	0.929	4	1.101	1.008	2	0.562	1.036	3	0.592	1.015	2	1.058	0.883	6	0.931	1.167
IPI00227299	Vim	P20152	27	0.744	0.869	30	0.746	0.818	27	0.555	0.748	31	0.616	0.786	37	0.863	0.895	38	0.871	0.908
IPI00453484	Wbscr27	Q3V1G0	4	1.003	0.978	3	0.910	0.943	1	0.552	0.951	3	0.781	0.965	/			2	0.769	1.004
IPI00123458	Sprr1a	Q62266	3	0.796	0.980	6	0.727	0.959	8	0.551	0.906	7	0.586	0.913	8	0.704	0.868	10	0.719	0.927
IPI00400143	Dgcr8	Q9EQM6	/			/			1	0.543	0.872	1	1.087	1.063	/			/		
IPI00153129	Gale	Q8R059	/			1	0.737	1.375	2	0.540	0.923	/			/			1	1.024	1.136
IPI00756996	Mvk	Q9R008	3	0.736	1.025	5	0.691	0.976	4	0.526	0.898	6	0.554	0.895	4	0.603	1.017	10	0.583	0.991
IPI00467914	H1f0	P10922	3	1.200	1.021	4	1.263	1.051	2	0.522	0.900	4	0.680	1.017	3	0.972	0.847	7	1.009	0.824
IPI00395047	Homer3	Q99JP6-2	5	1.031	0.979	6	1.183	0.988	2	0.519	0.558	1	0.843	0.875	2	0.966	1.020	4	0.940	1.007
IPI00109505	Murc	A2AMM0	/			1	1.464	1.028	1	0.515	1.102	/			/			1	0.664	1.283
IPI00119980	Bcap29	Q61334	/			/			1	0.504	0.821	/			/			/		
IPI00849833	Fam101b	Q5SVD0	1	0.970	0.775	1	1.053	0.997	1	0.497	0.860	3	0.509	0.843	/			2	1.060	1.060
IPI00114862	Thumpd1	Q99J36	/			2	1.143	1.031	2	0.469	1.112	3	1.128	1.039	2	1.060	0.977	5	0.956	0.973
IPI00315689	Dusp12	Q9D0T2	/			1	1.184	1.028	1	0.453	0.662	1	1.121	1.103	/			/		
IPI00228497	Mmab	Q9D273-2	/			2	0.938	1.062	2	0.408	0.887	3	0.420	0.806	1	0.502	0.920	3	0.498	0.914
IPI00884526	Sprr2b	A9JTY7	2	0.838	1.074	3	0.804	0.969	2	0.396	0.968	2	0.490	0.963	2	0.791	0.985	3	0.823	0.926
IPI00110265	Sirt2	Q8VDQ8-1	/			2	1.107	1.028	1	0.376	1.425	1	1.014	1.209	2	1.130	1.032	5	0.973	0.999
IPI00134334	Ptgr2	Q8VDQ1-1	/			1	1.281	1.057	1	0.363	1.069	3	0.857	0.870	/			2	1.004	1.015
IPI00124248	Clns1a	P97506	/			2	0.891	0.599	3	0.356	0.758	2	0.700	1.138	/			2	0.966	1.142
IPI00132950	Rps21	Q9CQR2	2	1.046	1.030	2	1.009	0.963	1	0.351	0.363	1	0.882	0.901	4	0.942	0.902	4	0.951	0.906
IPI00421052	Nipbl	Q6KCD5-1	/			/			2	0.329	0.682	1	1.205	1.159	/			1	0.855	0.974
IPI00121276	Mecr	Q9DCS3	/			/			1	0.307	1.191	2	0.744	1.002	/			6	0.989	0.979
IPI00137864	Rbl1	Q64701-1	/			/			1	0.287	0.177	/			/			2	0.798	1.000
IPI00762636	Acsf3	Q3URE1-1	/			/			2	0.274	0.833	/			/			4	1.337	1.033
IPI00469184	Synm	Q70IV5-1	/			/			1	0.270	0.730	1	0.393	0.705	1	0.665	0.754	1	0.698	0.812
IPI00339960	Trim75	Q3UWZ0	/			/			1	0.265	0.215	/			/			/		
IPI00930771	Htra1	Q8BN04	/			/			2	0.207	0.992	3	1.179	1.093	/			/		
IPI00623506	Ank3	Q9WUD7	/			/			2	0.204	2.567	/			/			/		
IPI00420796	Fam63b	Q6PDI6-1	1	0.823	1.014	1	0.695	0.745	1	0.188	0.448	1	0.792	0.636	2	0.676	0.899	3	0.601	0.974
IPI00666788			/			/			1	0.087	0.164	1	0.023	0.004	/			/		
IPI00954606	5830433M19Rik	Q3TUU0	/			/			1	0.079	0.918	/			/			/		
IPI00918972	Arhgap21	B2RWX1	/			/			1	0.050	0.268	1	0.894	0.836	/			/		
IPI00828904	4921517L17Rik	Q9D5U8-1	/			/			1	0.010	4.089	/			/			/		
IPI00474945	Traf7	Q8C2K8	/			/			1	0.007	0.007	1	0.021	0.011	/			/		
IPI00320241	Dnajb11	Q99KV1	4	0.935	0.935	8	0.935	0.964	8	0.768	0.861	5	0.734	0.861	6	0.857	1.003	9	0.945	1.019
IPI00132604	Scamp3	O35609	/			2	0.870	1.052	4	0.779	1.051	5	0.734	0.995	3	0.823	0.878	6	0.895	0.868
IPI00648755	Palm2	Q8BR92	2	0.821	0.964	3	0.895	0.928	1	0.877	1.560	4	0.732	1.085	/			1	0.897	1.327

IPI00338876	Efg2	Q8R2Q4-1	/			2	1.104	0.915	/			3	0.732	1.071	/			6	1.077	1.253
IPI00928546	Myo9a	Q8C170-2	/			/			/			2	0.731	1.132	/			/		
IPI00139994	Nup62	Q63850	/			2	1.031	1.001	1	0.890	0.861	3	0.731	1.003	5	0.943	0.946	7	0.967	0.983
IPI00648065	Bbs7	B1ATV5	/			/			/			1	0.729	0.962	/			/		
IPI00323143	Pold1	P52431	/			/			/			3	0.726	0.793	/			/		
IPI00830990	Pak3	A3KGC5	1	0.700	0.532	2	1.011	0.822	2	0.742	1.000	2	0.724	0.891	4	0.741	0.954	6	0.965	0.926
IPI00317932	Yif1b	Q9CX30-1	/			/			1	0.852	1.118	1	0.723	1.312	/			/		
IPI00396685	Dgkq	Q6P5E8-1	/			1	1.086	1.522	/			2	0.722	0.729	/			1	0.971	1.152
IPI00881403	Depdc5	P61460	/			/			/			1	0.721	0.918	/			/		
IPI00122313	Rbm38	Q62176	/			1	0.896	0.835	2	0.921	0.987	2	0.718	0.925	/			2	0.953	1.034
IPI00462925	Mrpl38	Q8K2M0-1	/			/			/			1	0.717	0.758	/			/		
IPI00831375	Ap1s2	Q3TIV9	/			1	1.059	7.548	/			1	0.713	1.078	/			1	1.065	0.954
IPI00120083	Tmem43	Q9DBS1	1	0.859	1.370	/			/			3	0.711	0.958	1	0.631	0.663	4	0.584	0.648
IPI00187257	Ube2q	Q7TSS2-1	/			/			1	1.226	0.913	1	0.710	1.028	/			2	0.959	1.021
IPI00468633	Glyt1	P28571-2	/			/			/			1	0.710	0.850	/			1	0.456	0.875
IPI00118170	Fzd1	O70421	/			/			/			2	0.708	0.767	/			1	0.735	0.829
IPI00653910	Cic	Q924A2-4	1	0.964	0.896	/			/			2	0.707	0.943	/			1	0.860	1.076
IPI00874456	Dld	O08749	/			9	1.052	1.002	/			8	0.705	0.853	9	0.950	0.925	11	0.943	0.955
IPI00121265	Caf1	Q60809	/			/			/			1	0.703	11.82	/			/		
IPI00406829	Gcc1	Q9D4H2	/			2	0.988	1.054	/			1	0.703	0.984	/			/		
IPI00623114	Fat1	A7ISQ0	5	0.879	0.860	7	0.801	0.824	5	0.737	0.773	3	0.701	0.785	1	0.505	0.579	14	0.754	0.944
IPI00886205	Kiaa4119	O88196	/			1	1.413	0.922	1	1.055	0.928	3	0.695	0.755	2	1.020	0.994	3	1.160	0.993
IPI00938479	Wdr81	Q5ND34-1	/			/			2	0.934	1.110	4	0.693	0.876	1	1.593	2.197	/		
IPI00119065	Lamb2	Q61292	2	1.010	0.910	7	1.115	1.035	3	0.787	1.138	6	0.693	0.865	2	0.858	0.954	10	0.844	0.939
IPI00132419	Tars2	Q3UQ84	/			2	1.049	0.953	2	0.743	0.801	3	0.691	1.054	1	1.128	1.629	3	0.914	0.988
IPI00653545	Acin1	Q3UZ28	/			/			/			1	0.690	0.164	1	1.099	4.237	1	0.914	1.790
IPI00356633	Tmem55b	Q3TWL2	/			/			/			1	0.689	1.315	1	0.475	0.733	1	0.510	0.794
IPI00608063	Ptprd	B9EJA3	/			/			/			1	0.689	0.781	/			/		
IPI00625954	Nt5dc2	Q91X76	/			1	1.350	0.941	/			2	0.687	0.891	/			4	1.329	0.912
IPI00648888	Rab3b	A2A7Z6	/			3	0.861	1.047	1	1.795	1.076	1	0.687	0.438	/			/		
IPI00136333	Oxsm	Q9D404	/			/			1	0.781	0.847	1	0.685	0.855	1	1.397	1.438	2	0.985	1.012
IPI00318108	Acox3	Q9EPL9	/			/			/			11	0.684	0.902	/			/		
IPI00458055	Gbl	Q9DCJ1	/			/			2	0.839	0.938	1	0.683	0.982	1	0.316	0.599	2	0.955	0.940
IPI00131954	D17Wsu104e	Q9CPT4	1	0.950	0.961	2	0.925	0.796	2	0.749	0.899	3	0.682	0.923	2	0.983	0.911	3	0.945	1.154
IPI00225028	Tcp11l1	Q8BTG3	/			/			/			1	0.681	0.791	/			/		
IPI00881074	3bp2	Q06649	/			/			/			2	0.680	1.198	/			/		
IPI00626501	Atsv	P33173	/			3	1.091	1.104	2	0.837	1.042	3	0.678	0.892	/			3	0.973	0.962
IPI00154021	Gipc3	Q8R5M0	/			/			/			2	0.677	0.908	/			/		
IPI00353579	Utp18	Q5SSI6	/			1	1.214	1.025	/			2	0.675	1.042	1	0.636	0.813	5	0.658	0.884
IPI00116247	mCG_17890	O08804	1	1.388	1.059	3	1.529	1.142	2	0.784	0.881	2	0.671	0.854	2	1.061	1.032	7	0.989	0.832
IPI00352163	Fn1	B7ZNJ1	/			19	1.483	1.006	/			31	0.670	0.797	33	1.027	0.772	44	1.046	0.811
IPI00322594	Ccn2	P29268	/			/			/			1	0.669	0.833	/			1	0.997	1.221
IPI00315808	Mrps36	Q9CQX8	1	0.764	1.048	/			3	0.824	0.975	3	0.667	0.980	4	0.886	0.881	5	0.874	0.840
IPI00153133	Lyplal1	Q3UFF7	/			/			/			2	0.666	0.921	/			/		
IPI00653746	Samhd1	Q3U754	/			/			/			2	0.666	0.744	/			/		
IPI00187434	Dut	Q8VCG1	2	1.174	0.991	5	1.407	1.055	4	1.166	1.069	6	0.662	1.265	4	0.888	1.053	/		
IPI00114377	Cox7a2	P48771	/			/			/			1	0.661	0.684	/			1	0.444	0.464
IPI00896060	Kiaa1882	Q3U0M1-1	/			/			/			2	0.656	0.776	/			1	0.884	1.272
IPI00322145	Ptplad1	Q8K2C9	/			/			/			1	0.654	0.728	1	0.704	0.534	1	0.733	0.654
IPI00554920	Kiaa0321	Q5DU37-1	1	0.803	0.944	3	1.267	1.020	5	0.875	0.988	3	0.654	0.905	1	0.888	0.845	1	0.860	0.911
IPI00282069	Crtc2	Q3U182	/			1	0.937	0.922	/			1	0.651	0.829	/			/		
IPI00331704	Eno2	P17183	/			/			4	0.848	1.145	6	0.650	0.934	/			8	0.846	1.005

IPI00322542	H2-T23	P06339	/			/			/			2	0.646	3.645	/			/		
IPI00461011		Q9D0A3	1	1.115	0.995	2	1.072	0.978	1	0.972	0.876	1	0.644	1.196	/			4	0.941	0.880
IPI00132067	Fbln2	P37889-1	/			/			/			1	0.643	0.921	/			/		
IPI00118413	Thbs1	P35441	/			/			/			4	0.642	0.699	/			16	0.984	1.480
IPI00226771	Bri3bp	Q8BXV2	/			/			/			1	0.639	0.660	/			2	0.965	1.045
IPI00312527	Crmp1	Q3TXY0	/			/			/			3	0.636	0.856	/			4	0.724	0.716
IPI00318750	D14Ucla2	Q99LB2	1	0.941	0.939	5	1.072	1.072	2	0.765	1.116	2	0.633	0.808	1	0.961	1.135	4	0.995	1.118
IPI00649809	1700081L11Rik	A2A5Y4	/			1	0.738	0.955	/			1	0.633	0.739	/			/		
IPI00875732	Nif3l1	Q9EQ80	3	1.087	0.962	2	1.040	0.937	3	0.981	1.086	3	0.629	0.792	3	0.991	0.976	6	0.966	0.991
IPI00320594	Kiaa1464	Q6VN19	/			2	1.031	1.087	1	1.302	1.204	3	0.628	1.027	1	1.109	0.718	3	1.043	1.226
IPI00126223	Jund	P15066	1	1.075	1.052	1	1.110	1.134	/			2	0.627	1.155	/			3	1.015	1.267
IPI00318154	Wdr35	Q8BND3-1	/			1	0.997	1.222	/			2	0.626	0.639	/			4	0.868	1.014
IPI00225621	Yipf6	Q8BR70	/			/			/			1	0.623	0.964	/			/		
IPI00877281	RP23-32C12.2-001	A2AE94	1	0.961	1.055	1	0.912	1.275	/			1	0.619	1.084	1	0.623	0.851	1	0.666	0.882
IPI00222753	Mterfd3	Q8BKY8	/			/			/			2	0.619	1.041	/			/		
IPI00113246	Aff4	Q9ESC8	/			1	0.973	0.883	/			2	0.615	1.020	/			/		
IPI00453577	Ipo13	Q8K0C1-2	/			/			/			2	0.611	0.774	/			5	0.953	0.958
IPI00124830	Cd47	Q61735-2	1	0.947	1.171	1	1.008	1.166	/			1	0.602	0.828	1	0.867	0.495	1	0.861	0.596
IPI00405699	Aldh4a1	Q8CHT0	2	0.981	1.015	4	1.122	0.998	/			3	0.596	0.919	/			4	0.947	1.073
IPI00221459	Katnb1	Q8BG40	/			6	0.795	0.885	1	1.129	1.069	2	0.590	0.715	1	1.133	1.134	2	0.924	2.054
IPI00314106	Cecr5	Q91WM2	/			/			/			1	0.589	1.124	/			/		
IPI00311395	Pcyt2	Q922E4	3	0.738	1.106	2	0.698	0.983	/			3	0.586	1.039	1	0.594	1.207	5	0.752	1.054
IPI00226726	Pcyox1l	Q8C7K6	/			2	1.356	1.146	/			1	0.585	0.757	1	0.892	1.080	2	0.834	0.948
IPI00830432	Mapre3	Q6PER3	/			2	0.979	0.997	/			3	0.584	0.907	/			/		
IPI00874570	Cp	Q8BU82	/			/			/			3	0.583	0.783	/			/		
IPI00131988	Mrpl49	Q9CQ40	/			1	0.877	0.803	/			2	0.582	2.962	/			4	1.096	0.855
IPI00315730	Dagk1	O88673	/			3	1.122	1.038	/			1	0.580	1.371	/			/		
IPI00112785	Sbdn	Q9ES56	/			2	1.181	0.991	/			1	0.579	0.862	/			3	1.002	0.962
IPI00669483	Amotl1	Q9D4H4	/			/			/			1	0.579	5.765	/			/		
IPI00403929	Hras1	Q6P716	/			/			1	1.025	0.815	1	0.578	0.972	1	0.993	1.159	/		
IPI00276926	Slc25a1	Q3TDH6	/			/			/			1	0.577	0.655	/			1	0.398	0.538
IPI00221739	Thnsl1	Q8BH55	/			/			/			1	0.577	0.889	/			1	0.976	1.440
IPI00473970	Dnahc9	B1AR51	/			/			/			1	0.569	0.365	/			/		
IPI00130988	Dhcr7	O88455	/			/			/			1	0.562	0.921	/			/		
IPI00345373	Fmnl2	A2APV2-3	/			2	1.101	1.064	/			1	0.561	0.681	/			/		
IPI00831349	Arhgap6	O54834-4	/			/			/			2	0.558	0.124	/			/		
IPI00881105	Gnpda2	Q9CRC9-1	/			/			/			2	0.536	0.779	/			3	1.026	0.757
IPI00138061	Crry	Q64735-1	/			1	1.104	0.931	/			1	0.528	1.472	/			3	0.854	0.972
IPI00162850	Kiaa0009	Q99MB2	/			/			/			1	0.523	0.644	/			/		
IPI00755238	Mafg	O54790	/			1	0.911	1.046	/			1	0.518	1.002	/			1	1.186	1.041
IPI00408207	Myo1d	Q5SYD0-1	/			/			/			1	0.516	1.029	/			1	0.566	0.842
IPI00318636	Antxr1	Q9CZ52-1	/			/			/			1	0.515	0.700	/			/		
IPI00308990	Cd14	P10810	/			1	1.073	1.597	/			1	0.515	0.835	/			/		
IPI00944189	Mtm1	Q5BKQ5	/			/			/			1	0.512	1.002	/			/		
IPI00316314	Hacl1	Q9QXE0	/			/			/			3	0.495	0.862	1	0.696	0.842	3	0.727	1.037
IPI00403352	Kiaa0421	Q8BKX6-1	/			/			/			1	0.493	1.071	/			2	0.946	0.991
IPI00121634	Atrc1	Q09143	/			2	0.682	0.983	/			1	0.491	0.645	1	1.072	0.582	2	0.908	0.804
IPI00129362	Fads2	Q9Z0R9	/			/			/			1	0.484	0.956	/			4	0.635	0.950
IPI00817029	Glyr1	Q922P9	/			/			/			1	0.477	0.833	/			/		
IPI00881096	Napg	Q9CWZ7	2	0.836	1.037	2	0.855	0.985	4	1.256	0.857	2	0.477	0.819	2	1.198	1.175	5	1.109	1.073
IPI00606760	RP23-13A13.2-	A2A837	3	0.948	1.009	6	0.921	1.029	2	1.115	1.512	2	0.475	0.678	2	0.876	1.135	3	1.005	1.107

	002																			
IPI00453611	Kiaa0676	Q5SVR0-1	/			1	1.282	1.192	1	1.027	0.940	2	0.472	0.907	/			1	0.882	0.958
IPI00858146	Kiaa0819	Q3UGQ8	/			/			/			2	0.465	1.282	/			/		
IPI00153088	Lpts	Q9CZX5	/			/			/			2	0.454	0.421	/			2	0.797	1.097
IPI00118834	H2-Ke4	Q31125	1	0.775	1.194	1	0.939	1.007	1	1.046	0.856	1	0.452	0.769	1	0.775	0.913	2	0.819	0.916
IPI00652288	I830012O16Rik	Q3UAB1	/			2	1.534	1.047	/			1	0.448	0.598	/			/		
IPI00119913	Apc	Q61315-1	/			2	0.851	1.313	1	1.016	0.943	2	0.438	0.787	/			2	1.864	1.380
IPI00226930	Hat1	Q8BY71	2	0.816	0.952	3	0.955	1.096	1	1.316	0.932	2	0.392	1.235	4	0.895	0.992	11	0.980	1.018
IPI00133241	Ints12	Q9D168	2	0.953	0.955	1	0.945	0.956	/			2	0.392	0.878	/			1	0.811	1.018
IPI00320022	Stard4	Q99JV5	/			/			/			1	0.390	1.056	/			2	0.339	1.066
IPI00124606	Ciz1	Q8VEH2	1	1.388	1.439	/			1	1.364	0.962	2	0.361	3.357	1	1.079	0.896	/		
IPI00310701	Lmf2	Q8C3X8	/			/			/			1	0.353	0.743	1	1.437	1.090	1	1.288	0.903
IPI00133526	Sc4mol	Q9CRA4	/			/			/			1	0.314	1.219	/			/		
IPI00318006	Serhl	Q9EPB5	/			1	0.899	0.678	1	0.943	1.254	2	0.282	0.819	/			/		
IPI00830611	Carm1	Q9WVG6-1	2	0.910	0.989	3	1.056	0.825	/			1	0.231	1.041	/			4	0.945	1.040
IPI00224210	Uqcrq	Q9CQ69	/			/			/			1	0.220	0.949	1	0.450	0.845	/		
IPI00130391	Prss3	B9EJ35	/			/			/			1	0.215	26.52 4	/			/		
IPI00265358	Dhx38	O89064	/			/			1	1.050	1.336	3	0.212	1.277	1	1.024	0.847	1	1.033	0.909
IPI00230552	Pde7a	P70453-2	/			/			/			1	0.208	0.074	/			/		
IPI00465871	Gpr158	Q8C419	/			/			/			1	0.203	0.224	/			/		
IPI00118039	Arsa	P50428	/			/			/			1	0.159	0.702	/			/		
IPI00338068	Fdft1	Q3TS40	/			/			/			1	0.158	1.544	/			2	0.186	1.644
IPI00225301	Hsdl1	Q8BTX9	/			/			1	0.853	0.744	1	0.136	0.930	2	1.516	0.864	3	0.962	0.964
IPI00775902	Zfp182	Q6P560	/			/			/			1	0.122	6.371	/			/		
IPI00750388	Sgce	O70258-2	/			/			/			1	0.105	1.284	/			1	0.938	1.056
IPI00850019	OTTMUSG000 00016626	A2ARX0	/			/			/			2	0.077	0.008	/			/		
IPI00329967	AI929863	Q7M6Y0	/			/			/			1	0.056	3.977	/			/		
IPI00172092	Godz	Q8R173	/			/			/			1	0.029	0.012	/			/		
IPI00759856	Fig1	O09046-2	/			/			/			1	0.028	0.022	/			/		
IPI00775936	Tspan15	Q3TA07	/			/			/			1	0.022	3.624	/			/		
IPI00387189	Vps18	Q8R307	2	1.184	1.358	2	0.880	0.986	/			4	1.129	1.014	1	0.699	0.792	3	0.927	0.807
IPI00113849	Cdc42	P60766-2	3	0.874	0.941	5	0.835	0.899	3	1.088	0.925	2	1.160	0.995	3	0.696	0.838	4	0.717	0.856
IPI00135648	Tmem59	Q9QY73	/			1	0.729	1.020	1	1.073	1.054	3	1.050	1.079	3	0.695	0.828	5	0.743	0.932
IPI00309183	Bak1	O08734	/			/			/			/			1	0.695	0.798	1	0.693	0.797
IPI00130409	Prpf6	Q91YR7-1	/			5	1.163	1.115	5	1.206	1.109	7	1.263	1.122	5	0.695	0.803	7	0.759	0.926
IPI00130246	Rrp1b	Q91YK2	/			/			/			1	1.783	1.044	1	0.693	0.779	4	0.794	0.902
IPI00133689	Wdr75	Q08EC1	/			/			/			/			1	0.690	0.836	1	1.164	0.938
IPI00420516	Tex2	Q6ZPJ0	/			1	0.923	0.789	/			2	0.969	0.680	1	0.690	9.604	/		
IPI00126449	Mapk7	Q9WVS8-1	/			5	1.095	0.935	3	0.872	1.000	1	1.069	1.018	2	0.690	0.873	7	0.879	0.877
IPI00460741	Mgrn1	Q9D074-3	/			/			/			1	1.162	1.003	1	0.689	1.022	4	0.886	1.299
IPI00130280	Atp5a1	Q03265	11	0.741	0.761	11	0.729	0.803	9	0.881	0.890	12	0.900	0.907	15	0.685	0.803	23	0.715	0.785
IPI00138860	Golga4	Q91VW5	/			2	1.010	0.873	1	0.760	0.705	/			1	0.685	0.611	3	1.016	0.914
IPI00154065	RP23-158O11.1	Q8QZV7	/			1	0.788	1.108	/			2	1.122	0.933	2	0.684	0.938	4	0.857	0.966
IPI00222429	Nomo1	Q3TKZ1	3	0.867	1.055	3	0.820	1.075	2	1.347	0.818	6	1.061	0.921	4	0.683	0.879	9	0.729	0.849
IPI00348488	Dennd4c	A2AJX5	1	0.830	0.780	3	1.095	1.079	/			4	1.070	1.171	2	0.682	0.479	6	0.987	0.980
IPI00131836	Copr5	Q9CQ13	/			1	1.056	1.025	2	1.121	1.050	2	0.926	1.024	1	0.681	0.882	1	0.958	0.908
IPI00117181	Flot1	O08917	2	0.756	0.959	2	0.798	0.798	3	1.131	0.800	4	0.948	0.774	3	0.680	0.691	7	0.743	0.666
IPI00263048	Numa1	Q3TH77	4	1.080	1.026	6	0.985	0.897	5	1.137	1.028	13	1.259	0.972	4	0.676	0.611	12	0.741	0.672
IPI00131176	Mtco2	P00405	/			/			/			1	0.781	0.738	1	0.676	0.481	2	0.621	0.515
IPI00890007	Akap1	B1AR25	/			/			1	1.391	1.129	1	1.545	0.813	2	0.675	0.651	4	0.654	0.732

IPI00223047	Ckap4	Q8BMK4	8	0.737	1.295	10	0.699	1.233	10	1.237	0.761	13	1.273	0.841	14	0.674	0.609	19	0.716	0.678
IPI00129554	Zfp597	Q2VPQ3	/			/			/			/			1	0.670	0.728	/		
IPI00313884	Podxl	Q9R0M4	/			/			/			/			1	0.668	0.634	4	0.938	0.893
IPI00845638	Pds5b	Q4VA53-3	1	1.341	1.172	2	1.329	1.107	4	1.033	1.194	4	1.051	1.156	2	0.668	0.867	9	0.722	0.850
IPI00170357	Afg3l2	Q8JZQ2	1	0.821	0.923	3	0.838	0.896	3	1.020	0.957	3	1.125	0.880	2	0.667	1.061	4	0.774	0.844
IPI00850873	Atp13a3	Q5XF89-2	/			/			/			/			1	0.667	0.644	/		
IPI00109335	Stx4	P70452	/			1	0.690	0.902	/			1	1.069	0.931	1	0.665	0.874	1	0.758	0.815
IPI00122075	Mavs	Q8VCF0	/			4	0.811	1.145	2	1.169	0.884	6	1.210	0.901	2	0.663	0.722	4	0.675	0.822
IPI00129298	Palm	Q9Z0P4-1	3	0.702	1.000	6	0.800	1.013	5	0.963	0.863	5	0.971	0.833	5	0.662	0.714	11	0.701	0.707
IPI00653643	Hnrnpl	Q3UMT7	/			/			8	0.977	0.874	12	0.980	0.896	14	0.659	0.894	15	0.662	0.733
IPI00122471	Gltscr2	Q3USL3	1	1.284	0.645	1	1.112	0.958	1	1.372	0.874	/			1	0.657	0.866	2	0.930	1.094
IPI00319933	Pacsin3	Q99JB8	3	0.787	1.563	3	0.906	1.148	4	1.129	0.888	6	1.051	0.877	6	0.654	0.830	8	0.795	0.909
IPI00134398	Sec62	Q8BU14	/			/			1	1.028	0.930	2	0.985	0.894	1	0.652	2.718	2	0.745	0.610
IPI00850433	Thoc7	Q7TMY4-1	1	0.997	0.978	1	1.067	0.860	/			1	1.128	1.073	1	0.651	1.084	/		
IPI00653745	Tmco1	Q3V4A0	/			/			/			1	1.283	0.810	1	0.650	0.820	1	0.731	0.714
IPI00848672	Sfrs11	Q3UIX4	2	1.036	0.957	3	0.951	0.960	2	1.007	1.114	2	0.929	1.079	3	0.649	0.979	4	0.947	0.917
IPI00124382	Elovl1	Q9JLJ5	/			/			/			1	1.050	0.830	2	0.649	0.878	1	0.658	0.745
IPI00221951	Rbm22	Q8BHS3	/			2	0.871	0.628	/			/			2	0.648	0.591	2	0.721	0.910
IPI00263106	Polr2g	P62488	/			1	0.851	0.942	1	0.912	0.775	/			1	0.648	0.749	2	0.845	0.764
IPI00467123	Timeless	Q9R1X4-1	1	0.903	1.040	/			/			3	1.454	1.031	1	0.647	0.817	5	0.715	0.823
IPI00126458	H2-K1	Q61894	/			/			/			/			2	0.645	1.033	/		
IPI00323748	Stom	P54116	/			2	0.961	1.251	/			/			3	0.644	0.665	5	0.747	0.705
IPI00788387	Mfge8	Q3U8S9	/			6	0.983	0.983	8	0.746	0.747	9	0.854	0.913	9	0.643	0.842	17	0.802	0.878
IPI00308162	Slc25a12	Q8BH59	/			3	0.723	0.919	4	1.272	0.768	7	1.292	0.786	3	0.640	0.853	16	0.643	0.711
IPI00108410	Atad1	Q9D5T0	/			/			/			1	1.407	0.676	1	0.638	0.520	3	0.698	0.572
IPI00111163	Enpp5	Q9EQG7	/			/			/			/			1	0.636	0.821	/		
IPI00118674	Ncstn	P57716	/			2	0.722	0.676	/			1	0.900	0.888	1	0.635	1.039	4	0.863	0.788
IPI00125929	Ndufa4	Q62425	1	0.872	1.000	3	0.964	1.028	1	1.073	0.839	3	0.875	0.802	2	0.633	0.820	5	0.758	0.894
IPI00890076	Maoa	B1AX52	3	0.989	1.596	4	0.936	1.501	4	1.703	0.866	4	1.540	0.855	4	0.632	0.577	8	0.612	0.635
IPI00111076			/			/			1	1.050	0.801	1	1.086	0.873	1	0.632	0.866	/		
IPI00331612	Hmga2	P52927	/			3	1.094	0.928	4	1.547	0.811	5	1.538	0.800	6	0.631	0.646	5	0.644	0.692
IPI00720003	Manbal	A2BGN7	/			1	0.932	1.103	/			1	0.922	0.698	1	0.631	0.704	1	0.696	0.743
IPI00312018	Mlec	Q6ZQI3	/			3	0.878	0.966	2	0.890	0.709	2	0.967	0.781	3	0.630	0.701	4	0.650	0.795
IPI00120653	Hmgn3	Q9DCB1-1	/			1	1.005	1.046	1	0.809	0.737	1	0.918	0.893	1	0.623	0.788	3	0.740	0.772
IPI00420464	Zeb2	Q9R0G7	/			/			1	1.031	1.032	3	1.096	1.077	1	0.621	1.143	2	0.949	0.902
IPI00172226	Ncapd2	Q8K2Z4-2	/			4	0.900	1.075	6	1.649	1.268	13	1.535	1.172	8	0.621	0.840	19	0.672	0.850
IPI00133612	Ttc35	Q9CRD2	/			/			/			/			1	0.617	0.808	2	0.652	0.754
IPI00125460	Atp5j	P97450	2	0.738	1.133	3	0.740	1.068	2	1.032	0.882	2	0.926	0.836	2	0.614	0.861	3	0.648	0.875
IPI00230507	Atp5h	Q9DCX2	3	0.702	1.244	4	0.722	1.168	9	1.002	0.774	6	1.006	0.780	7	0.612	0.849	9	0.628	0.823
IPI00331601	Cirh1a	Q8R2N2	/			/			1	1.443	0.915	1	1.299	1.144	2	0.611	0.783	3	0.842	0.888
IPI00953773	Ssr4	Q9D6F7	/			/			1	1.116	0.826	3	1.112	0.848	2	0.611	0.797	/		
IPI00153389	Tor2a	Q8R1J9-1	/			/			/			1	0.927	0.948	2	0.611	1.083	2	0.848	0.884
IPI00669709	Pds5a	Q6A026	2	0.929	0.941	5	1.193	1.011	5	1.472	1.218	5	1.510	1.151	4	0.607	0.796	7	0.653	0.732
IPI00131513	Ash2l	Q91X20	1	0.918	0.954	2	1.386	1.068	3	1.024	1.068	3	0.937	1.018	3	0.606	0.853	4	0.959	1.144
IPI00331361	Mybbp1a	Q7TPV4	4	1.235	1.121	6	0.985	1.275	6	1.848	1.071	15	2.052	1.073	8	0.605	0.838	17	0.624	0.846
IPI00132747	Hbxip	Q9D1L9	1	0.903	1.146	1	0.976	1.120	1	1.115	0.772	1	1.015	0.812	1	0.604	0.703	2	0.652	0.725
IPI00263878	Pik3r1	P26450	/			3	1.111	0.995	/			4	0.965	0.945	1	0.604	0.657	5	0.800	0.895
IPI00108811	Gba	P17439	3	0.882	0.721	3	0.870	0.819	4	0.893	0.941	5	0.859	0.850	4	0.597	0.873	6	0.680	0.884
IPI00271986	Atp5j2	P56135	/			/			/			1	1.123	0.730	1	0.597	0.806	2	0.623	0.873
IPI00114822	Ctu1	Q99J10	/			/			/			1	1.406	1.111	1	0.595	0.856	2	0.944	0.923
IPI00221540	Erlin2	Q8BFZ9	/			/			/			3	0.854	0.725	1	0.586	0.418	3	0.583	0.447
IPI00135345	Nudt2	P56380	/			2	1.482	1.112	1	0.830	0.999	1	0.877	1.064	1	0.583	0.832	2	0.936	1.411

IPI00229883	Ints4	Q8CIM8-1	1	1.079	0.994	1	1.111	1.205	1	1.726	1.423	3	1.449	1.401	1	0.583	0.935	1	0.841	1.663
IPI00165850	Smc6	Q924W5-1	/			/			1	1.243	0.975	2	1.077	0.977	1	0.581	0.813	4	0.831	0.827
IPI00407108	Rexo4	Q6PAQ4	/			/			/			2	1.392	0.904	1	0.581	0.932	3	0.841	0.911
IPI00169845	Mmgt1	Q8K273	/			/			/			1	0.811	0.992	1	0.574	0.670	1	0.888	0.668
IPI00153381	Uqcr10	Q8R1I1	/			/			1	1.342	0.788	1	1.439	0.823	1	0.571	0.774	2	0.542	0.801
IPI00135252	Atad2	Q8CDM1-2	/			/			1	1.631	1.061	1	2.204	1.018	1	0.565	0.831	2	0.685	0.845
IPI00127227	Cbr4	Q91VT4	/			/			/			/			1	0.564	0.546	/		
IPI00929902	Fas	A1Y9B2	/			/			1	0.841	0.822	1	0.793	0.683	1	0.559	0.724	/		
IPI00381412	Immt	Q8CAQ8-2	/			/			/			/			3	0.557	0.663	/		
IPI00127447	Scarb2	O35114	/			2	0.983	0.946	/			2	0.873	0.647	3	0.555	0.595	7	0.576	0.616
IPI00228867	G6pd2	P97324	/			/			/			/			4	0.549	0.922	/		
IPI00132728	Cyc1	Q9D0M3-1	/			/			/			1	1.472	0.882	2	0.542	0.701	2	0.498	0.705
IPI00620969	Tsc2	Q61037-1	1	1.060	0.946	3	1.100	1.006	3	0.900	1.065	2	0.859	1.133	2	0.540	0.869	3	0.881	1.136
IPI00128346	Cisd1	Q91WS0	/			/			/			1	4.020	1.015	1	0.536	0.821	3	0.579	0.784
IPI00115695	Pik3c2g	O70167-1	/			/			/			/			1	0.536	0.886	/		
IPI00469962	Epb41l5	Q8BGS1-1	/			3	0.791	0.841	/			/			2	0.533	0.835	4	0.661	0.919
IPI00453820	Rai14	Q9EP71	/			/			/			/			1	0.524	0.764	4	0.595	0.732
IPI00341282	Atp5f1	Q9CQQ7	/			3	0.718	1.073	4	1.023	0.853	2	1.050	0.811	1	0.523	0.841	4	0.598	0.799
IPI00464194	Fgd6	Q69ZL1-1	1	1.421	0.989	/			/			/			3	0.517	0.353	/		
IPI00133342	Atp5l	Q9CQY3	1	0.716	1.176	1	0.709	1.190	1	1.012	0.913	2	1.007	0.878	2	0.503	0.836	3	0.591	0.880
IPI00110298	Pold3	Q9EQ28	/			/			1	1.167	1.115	/			1	0.471	0.975	2	1.027	0.884
IPI00122362	Pdia5	Q921X9	/			2	1.377	1.122	/			2	0.976	0.941	2	0.465	0.942	4	1.126	0.962
IPI00110708	Ccdc51	Q3URS9-1	/			/			/			1	1.630	1.068	1	0.460	0.960	2	0.581	0.862
IPI00624711	Hmga1	P17095-1	/			/			/			2	1.008	0.949	1	0.445	0.995	2	0.866	0.870
IPI00132347	Uqcrb	Q9CQB4	/			/			2	1.237	0.786	3	1.370	0.872	2	0.436	0.690	6	0.486	0.755
IPI00396728	Ddx51	Q6P9R1	/			/			1	1.679	0.941	3	1.777	1.126	2	0.416	0.683	4	0.679	0.859
IPI00850362	Thada	A8C756-1	/			/			/			3	0.987	1.143	3	0.365	0.766	3	1.318	1.003
IPI00130023	Tbc1d8	Q9Z1A9	/			/			/			/			2	0.352	185.8	/		
IPI00121582	Rfx3	P48381-1	/			/			/			/			1	0.337	43.26	/		
IPI00467004	Stat1	P42225	2	0.978	0.926	5	1.045	1.010	3	0.934	1.012	5	0.953	1.031	3	0.332	0.331	4	0.928	0.885
IPI00113039	Cant1	Q8VCF1-3	/			/			/			/			1	0.302	1.072	/		
IPI00123531	Znf148	Q61624	/			1	0.892	0.473	1	1.362	0.930	/			1	0.284	0.479	/		
IPI00311611	Sos1	Q62245	/			2	0.793	0.805	/			3	1.216	1.170	1	0.254	0.431	/		
IPI00351041	Card6	Q8BWE0	/			/			/			/			1	0.220	0.283	/		
IPI00947579			/			/			/			/			2	0.178	0.984	/		
IPI00229571	Sltm	Q8CH25-1	/			/			/			/			1	0.170	0.252	5	1.020	1.045
IPI00665988	Fam184a	Q3UT79	/			/			/			/			1	0.094	0.014	/		
IPI00111301	Mc4r	P56450	/			/			/			/			1	0.086	0.039	/		
IPI00221836	Rab39	Q8BHD0	/			/			/			/			2	0.016	0.003	/		
IPI00626253	Gal3st4	Q3V1B8	/			/			/			/			1	0.014	0.002	/		
IPI00656192	Kncn	Q307W7	/			/			/			/			1	0.012	0.092	/		
IPI00129577	Aifm1	Q9Z0X1	6	0.861	1.013	8	0.778	1.030	6	0.996	0.790	7	1.013	0.780	8	0.712	0.806	13	0.703	0.814
IPI00227432	Dnm3	Q8BZ98-1	3	1.265	1.062	5	1.272	1.027	/			/			/			5	0.703	0.961
IPI00319980	Tmem175	Q9CXY1	/			/			/			1	0.853	0.664	/			1	0.702	0.733
IPI00321331	Taf10	Q8K0H5	1	1.045	1.033	1	0.988	1.058	1	1.120	1.043	1	1.069	0.962	1	0.859	0.963	1	0.702	0.873
IPI00653166	Ccndbp1	Q3TVC7-3	/			/			/			/			/			1	0.702	0.909
IPI00471372	Wasf1	Q8R5H6	/			1	1.030	0.971	/			4	0.905	0.965	2	0.803	1.160	3	0.702	1.099
IPI00117986	Slc12a9	Q99MR3	/			1	0.850	1.113	/			1	0.953	3.929	/			3	0.701	0.637
IPI00353010	Nop14	Q8R3N1	/			/			/			/			/			2	0.701	0.895
IPI00221417	Dirc2	Q8BFQ6	/			/			/			/			/			1	0.701	0.984
IPI00133047	Mapksp1	O88653	/			/			1	1.001	1.086	1	1.051	0.868	/			3	0.701	0.847
IPI00471089	P2rx4	Q3TR36	/			/			/			/			/			3	0.701	0.524

IPI00170128	Spg7	Q3ULF4	/			1	5.158	0.024	/			/			/			1	0.700	1.088
IPI00127408	Rac1	Q3TLP8	2	0.743	0.973	4	0.862	1.051	1	1.243	1.001	3	1.132	0.953	3	0.804	0.834	6	0.700	0.750
IPI00848714	Zyg11a	A2BFL2	/			/			/			/			/			2	0.698	2.877
IPI00468514	Afg3l1	Q920A7-1	/			/			/			/			/			2	0.697	0.898
IPI00116748	Ndufa10	Q99LC3	/			/			/			2	0.850	0.804	/			3	0.694	0.839
IPI00108450	Wdtc1	Q80ZK9	/			1	1.143	1.108	/			/			/			1	0.693	0.959
IPI00875583	1190002N15Rik	Q3USZ8	/			/			/			/			/			2	0.692	0.970
IPI00109108	Stt3a	P46978	/			2	1.008	1.232	2	1.239	1.021	/			2	0.711	0.635	4	0.692	0.682
IPI00848909	Ano10	Q8BH79-4	/			/			/			/			/			1	0.691	0.574
IPI00844808	Armc8	Q9DBR3-2	/			/			/			/			/			4	0.691	1.217
IPI00845689	Tmed9	Q9CZL0	1	0.772	1.112	1	0.864	1.506	2	0.994	0.719	/			2	0.764	0.719	4	0.690	0.819
IPI00121431	Hells	Q60848-1	/			3	0.921	0.882	3	1.523	1.089	4	1.710	1.213	/			4	0.690	1.003
IPI00463679	Mum1	Q6DID5	/			/			1	1.510	1.058	1	1.310	1.113	/			1	0.685	1.062
IPI00869441	RP23-263M10.5	Q8BZR9-1	/			1	0.990	0.993	/			2	1.140	2.803	1	0.760	0.964	2	0.684	0.982
IPI00225596		Q8BUR9	2	1.066	1.018	1	1.006	0.959	/			1	0.997	0.998	2	0.913	1.040	1	0.684	0.860
IPI00109293	Lactb	Q9EP89	/			/			/			2	0.862	0.898	/			4	0.683	0.748
IPI00314749	Slc4a4	O88343-1	/			/			/			/			/			2	0.680	0.418
IPI00623531	Dst	Q60824-2	/			/			/			/			/			5	0.679	0.962
IPI00828454	Jmjd2a	A2A8L8	/			1	0.901	1.091	/			/			/			1	0.679	0.983
IPI00856474	Gtf2h1	Q9DBA9	/			/			1	1.071	0.841	/			/			2	0.678	0.794
IPI00153507	V1rh4	Q8R280	/			/			/			/			/			1	0.677	6.683
IPI00110896	Fas	P25446	/			1	0.916	0.882	/			/			/			2	0.677	0.725
IPI00854954	EG622147	Q61533	/			/			/			/			/			2	0.676	1.081
IPI00807763			/			/			/			/			/			2	0.675	3.584
IPI00165688	Slc23a2	Q9EPR4-1	/			/			/			/			/			3	0.674	0.904
IPI00125681	Pigs	Q6PD26	/			/			/			1	1.273	0.681	/			4	0.673	0.740
IPI00466867	Stag1	Q6P5D1	/			/			/			/			/			8	0.673	0.858
IPI00659535	Bat2d1	Q3TLH4-5	/			/			/			/			/			29	0.673	1.192
IPI00153791	Nol11	Q8BJW5-1	1	0.818	0.837	/			/			/			/			2	0.671	0.813
IPI00420344	Rrp12	Q6P5B0	/			1	1.007	0.849	/			2	1.599	1.377	/			4	0.670	0.880
IPI00132957	Ddx56	Q9D0R4	/			/			1	1.484	1.302	2	1.330	1.063	1	0.761	0.803	2	0.670	0.916
IPI00128152	Abcb1	P06795	/			/			2	1.070	0.847	3	1.063	0.754	2	0.776	0.835	6	0.669	0.786
IPI00226829	Tmem19	Q91W52-2	1	1.103	1.297	1	1.088	1.475	1	0.770	0.808	/			/			1	0.669	0.526
IPI00875068	Gpsn2	Q52L67	/			/			/			/			/			2	0.668	0.848
IPI00228828	Guk1	Q64520	/			/			/			2	0.850	1.232	/			2	0.665	1.320
IPI00133365	Ergic2	Q9CR89-1	/			/			/			1	1.120	0.855	/			3	0.665	0.604
IPI00133074	RP23-349B15.2	Q9D136	/			/			/			2	1.209	0.783	/			2	0.664	0.759
IPI00338964	Atp2a2	O55143-1	2	0.991	0.969	5	0.959	1.275	2	1.234	1.044	3	1.295	0.844	3	0.803	0.801	16	0.663	0.714
IPI00131716	Gmnn	O88513	/			/			/			/			/			1	0.662	0.685
IPI00323822	Rras2	P62071	/			2	0.844	1.208	/			2	0.937	0.887	2	1.298	0.808	3	0.662	0.781
IPI00129529	Cog1	Q9Z160	/			/			/			/			/			2	0.661	0.818
IPI00135180	Cdca3	Q99M54-1	/			1	0.699	1.116	1	2.463	0.983	1	2.324	0.902	1	0.960	1.292	3	0.661	1.086
IPI00108147	Rock1	P70335-1	/			3	1.076	1.136	2	1.022	1.103	3	0.744	0.814	/			7	0.660	1.073
IPI00329986	Ireb2	Q811J3	1	1.014	0.876	2	0.905	0.959	/			3	1.015	0.991	3	0.713	1.020	8	0.659	1.026
IPI00109891	Atp13a1	Q9EPE9	/			/			/			/			/			2	0.659	0.978
IPI00654074	Brwd1	Q3UUZ7	/			/			/			/			/			1	0.657	0.809
IPI00113731	Degs1	O09005	/			/			/			/			/			2	0.654	0.606
IPI00187288	Echdc1	Q9D9V3-1	/			1	1.020	1.419	/			/			/			3	0.653	1.022
IPI00229647	Tln2	B2RY15	/			9	0.861	0.970	/			11	1.230	0.794	7	0.755	0.791	11	0.652	0.725
IPI00130322	Ndufa7	Q9Z1P6	/			/			1	0.884	0.709	/			/			1	0.651	0.732

IPI00322418	FRRS1	Q8K385	/			/			/			/			/			1	0.650	0.418
IPI00228647	Slc38a10	Q5I012-1	/			/			/			/			/			1	0.649	0.417
IPI00655156	Ccdc109a	Q3UMR5-1	/			/			/			/			/			3	0.649	0.805
IPI00453948	Magee1	Q6PCZ4	/			/			/			/			/			1	0.648	0.877
IPI00153101	Tmem109	Q3UBX0	/			/			/			/			1	0.901	0.755	1	0.646	1.069
IPI00109447	Cnih4	Q9CX13	/			/			/			/			/			1	0.643	0.725
IPI00894649	Sec11a	Q9R0P6	/			/			/			/			/			1	0.641	0.779
IPI00120744	Xab2	Q9DCD2	1	1.068	1.051	/			2	0.937	1.085	2	1.044	0.862	1	0.710	0.648	3	0.640	0.818
IPI00828950	Atp6v0a1	Q9Z1G4-2	/			1	1.379	1.435	/			/			/			2	0.639	0.728
IPI00132087	Fdx1l	Q9CPW2-1	/			/			/			/			/			1	0.638	0.860
IPI00464195	Ptchd2	A3KFU9-1	/			/			/			/			/			1	0.638	0.853
IPI00462465	ORF61	Q8CIV2-2	/			/			/			1	1.247	0.824	/			1	0.636	1.013
IPI00229218		Q8CF66	/			/			/			/			/			1	0.633	0.687
IPI00121477	Slc6a8	Q8VBW1-1	/			/			/			3	0.936	0.969	/			3	0.632	0.770
IPI00665857	Chp	P61022	/			/			/			/			/			2	0.630	0.757
IPI00880699	Ccdc9	Q8VC31	/			2	0.897	0.854	/			/			/			3	0.628	0.912
IPI00230238	Rab11fip5	Q8R361	/			/			/			/			/			6	0.627	1.307
IPI00136246	Pitpnm1	O35954	2	0.742	0.888	2	1.047	0.955	/			2	1.016	0.877	/			1	0.624	0.989
IPI00319775	Fbxl8	Q8CIG9	/			1	0.771	0.818	/			/			/			1	0.624	1.185
IPI00112527	Surf2	P09926	/			1	0.894	0.846	/			/			2	1.054	1.069	1	0.621	0.764
IPI00849919	Wdr43	Q6ZQL4	/			/			/			/			/			4	0.621	0.788
IPI00115454	Sfxn1	Q99JR1	/			/			1	2.800	1.015	2	1.363	0.823	/			7	0.621	0.709
IPI00856221	Scap	Q6GQT6	/			/			/			/			/			2	0.618	0.699
IPI00869365		Q9D162-1	/			/			/			/			/			1	0.617	1.871
IPI00886331			/			/			/			/			/			2	0.616	0.536
IPI00831180	Atp2b2	Q9R0K7	/			/			/			/			/			4	0.616	0.773
IPI00123517	Gmeb1	Q3UYV4	/			/			/			/			/			1	0.615	1.027
IPI00122346	Ssr4	Q62186	/			2	0.769	1.006	/			/			/			4	0.615	0.801
IPI00624653	Usmg5	Q78IK2	/			1	0.838	1.150	/			/			/			2	0.614	0.734
IPI00318428	Cenpv	Q9CXS4-1	/			/			1	1.003	1.075	/			/			2	0.612	0.768
IPI00222412	Zmpste24	Q80W54	/			1	0.899	1.333	/			1	0.915	0.841	/			1	0.609	0.632
IPI00157480	Kiaa1609	Q8K0P3-1	/			/			/			1	0.778	0.949	/			2	0.604	1.112
IPI00467530	Ablim1	Q8K4G5-1	/			3	0.945	1.024	/			3	0.839	0.969	/			3	0.598	0.933
IPI00117112	Stx2	Q00262	/			/			/			/			/			2	0.597	0.795
IPI00124959	Mki67	Q61769	/			/			/			3	1.154	1.001	/			3	0.596	0.817
IPI00122958	Mcl1	P97287	/			1	0.826	0.733	1	1.081	1.126	1	0.923	0.920	/			1	0.595	0.839
IPI00224528	Exoc6b	A6H5Z3	/			/			/			/			/			2	0.594	0.769
IPI00123276	Mosc2	Q922Q1	/			/			/			/			/			4	0.593	0.579
IPI00751601	Lrrc58	Q3UGP9	/			/			/			/			/			1	0.593	1.131
IPI00874376	Apool	Q9CZB4	/			/			/			1	1.290	0.865	/			6	0.590	0.712
IPI00720171	Kiaa0090	Q8C7X2-2	/			/			/			2	0.901	0.910	/			4	0.582	0.838
IPI00122547	Vdac2	Q60930	/			/			1	0.934	0.816	3	0.969	0.875	/			4	0.581	0.419
IPI00283900	D17H6S56E-5	P97406	/			/			/			/			/			2	0.580	0.713
IPI00626433	Erbb2	P70424	/			/			/			/			/			1	0.575	0.700
IPI00223821	Epc2	Q8C0I4	/			/			/			/			/			1	0.574	0.501
IPI00132564	Gemin6	Q9CX53	/			/			2	0.992	1.009	2	1.085	0.920	2	1.021	1.087	2	0.570	0.974
IPI00551399	Efr3a	Q8BG67-2	/			1	1.344	0.969	/			/			/			2	0.567	0.734
IPI00222125	Comtd1	Q8BIG7	/			/			/			2	1.371	0.948	/			5	0.562	0.844
IPI00135651	Slc25a13	Q9QXX4	/			/			1	1.211	0.815	/			/			10	0.559	0.734
IPI00756791	2010204N08Rik	B5THE3	/			/			/			/			/			2	0.559	1.886
IPI00222852	Rp2	Q9EPK2-2	/			/			/			/			/			1	0.557	0.666

IPI00311761	Kri1	Q8VDQ9	/			/			/			/			/			1	0.551	0.657
IPI00110852	Ssr1	Q52PE3	/			/			/			1	1.355	0.834	/			2	0.547	0.661
IPI00464317			7	0.962	1.030	8	1.047	0.930	6	1.058	1.025	9	0.994	1.032	10	1.139	1.334	15	0.541	0.583
IPI00121627	Clptm1	Q8VBZ3	/			1	1.035	1.239	1	1.004	1.056	2	0.985	1.017	/			3	0.539	0.695
IPI00420727	Spcs3	Q6ZWQ7	/			/			/			/			/			1	0.538	1.090
IPI00318645	Ndufa11	Q9D8B4	/			/			/			/			/			1	0.525	1.131
IPI00403228	Senp7	Q8BUH8-1	/			1	0.879	0.893	/			/			/			2	0.516	1.922
IPI00221706	Ostm1	Q8BGT0	/			/			/			/			/			2	0.516	0.798
IPI00756788	Lrrk1	Q3UHC2-2	/			/			/			/			/			1	0.510	6.096
IPI00126725	Ifi202	Q9R002	/			/			/			/			/			2	0.510	0.246
IPI00129580	Sumo3	Q9Z172-1	1	1.339	1.057	/			/			/			/			2	0.505	1.187
IPI00315974	1110007C09Rik	Q9D1I2	/			/			/			/			/			1	0.503	0.957
IPI00321909	Slc29a3	Q99P65	/			/			/			/			/			1	0.502	0.778
IPI00132944	N6amt2	Q9CY45	/			/			/			/			/			1	0.497	0.781
IPI00120826	Ssr3	Q9DCF9-1	/			/			/			/			/			1	0.491	0.758
IPI00228236	Spcs2	Q9CYN2	1	0.997	1.600	2	1.318	2.288	1	1.244	0.833	1	1.538	0.840	/			1	0.483	0.585
IPI00828653	Col2a1	P28481-3	/			/			/			/			/			2	0.473	1.121
IPI00262356	Fam76a	Q922G2-1	2	1.088	0.859	1	0.702	1.068	1	1.107	2.320	1	0.874	1.144	/			2	0.470	3.401
IPI00845826	EG667538	Q811N1	/			/			/			/			/			6	0.466	0.677
IPI00132039	Mtch2	Q791V5	/			/			/			/			/			4	0.464	0.443
IPI00404687	Gk	Q64516-3	/			/			/			/			/			1	0.463	1.714
IPI00230754	Slc25a11	Q9CR62	/			/			/			/			/			2	0.453	0.606
IPI00330474		Q8C119	/			/			/			/			/			1	0.452	0.563
IPI00133384	Ormdl2	Q9CQZ0-1	/			/			/			1	0.817	1.075	/			1	0.451	1.310
IPI00169634	Snapc1	Q8K0S9	/			/			/			/			/			1	0.449	0.969
IPI00453654	Helz	Q6DFV5-1	/			/			/			/			/			1	0.449	0.302
IPI00153722	Brd8	Q8R3B7	/			/			/			/			/			2	0.446	1.124
IPI00380986			/			/			/			/			/			2	0.431	0.118
IPI00110508	Itgb7	P26011	/			/			/			/			/			1	0.421	0.790
IPI00133581	Ube2c	Q9D1C1	/			3	0.879	0.827	1	2.493	1.283	2	1.522	0.879	/			1	0.405	0.938
IPI00459309	Tmx2	Q9D710	/			/			/			1	0.923	0.953	/			2	0.401	0.604
IPI00135144	Thap2	Q9D305	/			/			/			/			/			1	0.393	1.969
IPI00881975	4432416J03Rik	B2RU41	/			/			/			/			/			1	0.393	0.211
IPI00136556	Tcn2	O88968	/			/			/			/			/			1	0.377	0.360
IPI00113477	Col4a5	Q3TP61	/			/			3	0.985	1.118	3	0.968	0.985	/			3	0.364	0.945
IPI00224252	Sel1l	Q9Z2G6-2	/			/			1	1.442	1.557	/			/			4	0.291	0.633
IPI00758325	Znf541	Q0GGX2	/			/			/			/			/			1	0.285	0.384
IPI00849452			/			/			/			/			/			3	0.268	0.207
IPI00116921	Scarb1	Q61009	/			/			/			1	0.840	0.839	/			2	0.262	0.589
IPI00474617	Txlng	Q8BHN1-1	1	1.570	1.196	2	0.963	1.615	/			/			/			2	0.242	1.384
IPI00135182	Nrap	Q80XB4-1	/			/			/			/			/			1	0.216	3.302
IPI00114878	Dhrs7b	Q99J47-1	/			/			/			1	1.216	0.846	/			1	0.205	0.838
IPI00119242	Fnbp4	Q6ZQ03-1	/			3	1.160	0.761	/			3	0.947	1.315	/			2	0.203	1.160
IPI00377726	Znf536	Q8K083	/			/			/			/			/			2	0.197	0.144
IPI00127364	Epn3	Q91W69	/			/			/			2	1.223	0.708	/			2	0.195	0.010
IPI00665815	Nlrp1c	Q2LKU8	/			/			/			/			/			1	0.187	0.135
IPI00876362	Zfp397os	Q149X8	/			/			/			/			/			1	0.175	0.957
IPI00849706			/			/			/			/			/			3	0.170	0.387
IPI00134234	Grifin	Q9D1U0	/			/			/			/			/			1	0.148	1.003
IPI00136957	Smok3a	Q9QYZ5	/			/			/			/			/			1	0.109	0.287
IPI00229712	Ankrd37	Q569N2	/			/			/			/			/			1	0.092	0.075

IPI00117308	Rnaseh1	O70338	/			/			/			/			/			1	0.084	0.172
IPI00652977	Pten	Q3UUN5	/			1	1.191	1.082	/			/			/			2	0.071	1.864
IPI00464383		P01644	/			/			/			/			/			1	0.064	0.233
IPI00890886	Reck	A2RSP9	/			/			/			/			/			1	0.056	2.074
IPI00466672	Cacna1b	O55017-2	/			/			/			/			/			1	0.034	0.207
IPI00662721	Tnik	B2RQ80	/			/			/			/			/			1	0.029	0.032
IPI00466185			/			/			/			/			/			10	0.029	0.018
IPI00848479	Zbed4	Q3UPJ9	/			/			/			/			/			1	0.020	0.027
IPI00331197	Elac1	Q8VEB6-1	/			/			/			/			/			1	0.008	0.069

Appendix 2: All Proteins Identified as Up-Regulated in ≥1 Biological Replicate

Protein identities and expression ratio shown for proteins identified as up-regulated after SN4741 cells were treated with 10μM 24(*S*),25-epoxycholesterol. Pep = Number of unique peptides; EC = SILAC ratio after treatment with 24(*S*),25-epoxycholesterol; GW = SILAC ratio after treatment with GW3965

Biological Replicate			1						2						3					
Technical Replicate			1			2			1			2			1			2		
Protein IDs	Gene Names	Uniprot	Pep	EC	GW	Pep	EC	GW	Pep	EC	GW	Pep	EC	GW	Pep	EC	GW	Pep	EC	GW
IPI00135921	Stag1	Q9D3E6	1	23.71		3	22.63	0.802	/			/			/			/		
IPI00752412	Atp1a3	Q8VCE0	4	14.87	5.161	/			/			/			7	1.353	1.428	/		
IPI00461390	EG641366	Q3U4K5	2	9.409	1.262	/			/			/			/			/		
IPI00553703	Frem2	Q6NVD0-1	1	7.083	13.22	/			/			/			/			/		
IPI00109588	Col4a1	P02463	1	6.136	0.754	2	3.206	0.327	/			2	1.049	1.208	1	1.552	1.149	5	0.973	1.006
IPI00471246	Ivd	Q9JHI5	2	4.573	1.559	3	1.074	0.929	2	0.734	0.909	2	0.858	0.972	1	1.051	0.967	5	0.981	0.951
IPI00875295	4933425L03Rik	Q6GQV6	1	3.875	1.161	1	1.335	1.369	/			/			/			1	0.883	0.821
IPI00314366	Slc7a15	Q50E62	1	3.305	0.527	/			/			/			/			/		
IPI00313998	Sqrdl	Q9R112	2	2.513	2.371	2	1.090	0.825	3	0.927	1.125	7	0.924	1.019	/			6	0.960	1.054
IPI00126634	Poldip2	Q91VA6	3	2.426	1.850	3	1.104	1.006	2	1.090	1.103	5	1.014	0.966	4	1.114	0.973	10	1.042	1.027
IPI00403867	ENSMUSG00000053526	Q8BNL8	1	2.331	13.72	/			/			/			/			/		
IPI00468802	Mat2b	Q99LB6-1	2	2.255	1.041	/			/			/			2	1.042	1.010	6	1.082	1.043
IPI00109082	Dad1	P61804	1	2.052	1.747	1	0.801	1.072	1	1.168	0.907	/			1	0.833	0.707	3	0.839	0.794
IPI00229109	Khsrp	Q8CEN4	1	1.983	3.209	/			/			/			/			/		
IPI00116711	Rngtt	O55236	1	1.943		2	0.856	0.984	1	1.119	1.094	/			1	0.930	0.943	/		
IPI00749735	Wbp2	Q9DBP6	1	1.828	1.020	3	1.009	0.957	1	1.007	1.075	4	0.903	0.803	/			4	0.906	0.849
IPI00761611	Rnf213	B1ATE2	1	1.745	1.040	4	1.266	1.004	2	0.786	1.071	6	0.818	1.130	2	1.273	0.911	6	1.053	0.874
IPI00273491	Pdzd8	Q3UMB1	2	1.730	0.848	3	1.125	1.116	3	0.953	0.878	7	1.012	0.965	3	1.086	0.942	5	1.049	1.122
IPI00136529	4933416I08Rik	Q9D434	1	1.699	0.986	/			/			/			/			/		
IPI00310841	Prkar1b	P12849	1	1.692	0.670	/			/			/			/			3	0.799	0.950
IPI00116240	Serpinb8	O08800	1	1.657	1.027	2	1.399	1.063	3	0.978	1.018	4	0.963	1.032	3	1.105	1.065	4	1.023	1.002
IPI00453739	Tatdn1	Q6P8M1-1	1	1.651	1.233	1	0.990	0.814	1	1.145	1.458	2	0.780	1.234	1	0.808	0.848	2	1.011	0.970
IPI00856547	Caprin2	Q05A80-1	1	1.644	0.765	/			/			/			/			/		
IPI00323035	Fbln5	Q9WVH9	1	1.636	0.906	/			2	0.582	0.786	2	0.831	0.938	1	0.995	0.861	3	0.990	0.899
IPI00474617	Txlng	Q8BHN1-1	1	1.570	1.196	2	0.963	1.615	/			/			/			2	0.242	1.384
IPI00755905	Sec16a	A2AIX1	1	1.532	1.135	7	0.995	0.983	3	0.876	1.139	8	1.038	1.136	3	1.189	1.262	6	1.043	1.041
IPI00831049	Kiaa1033	Q3UMB9	2	1.531	0.968	6	1.244	1.008	3	0.845	1.060	9	0.898	1.158	3	1.473	1.201	9	1.162	0.964
IPI00137206	Actr10	Q9QZB7	1	1.529	1.000	1	1.214	0.976	3	0.911	1.201	4	0.889	0.942	3	0.920	0.996	7	1.052	0.942
IPI00171989	Pank2	Q7M753	1	1.518	1.218	1	1.307	1.098	1	0.966	0.951	3	1.018	0.799	/			2	1.027	0.801
IPI00849550	Rpl29	P47915	2	1.508	1.220	2	1.308	1.076	4	0.964	1.165	4	0.946	1.234	3	1.307	0.907	3	1.253	0.918
IPI00125899	Ctnnb1	Q02248	1	1.502	0.975	4	0.945	0.987	4	1.199	0.903	3	1.216	0.956	6	0.844	0.929	10	0.835	0.937
IPI00380829	Trip11	B2RY51	1	1.501	0.787	3	1.020	0.979	2	1.091	0.934	7	1.072	1.003	/			3	1.187	1.143
IPI00128154	Ctsl1	P06797	1	1.490	1.084	/			/			2	0.821	0.862	4	1.184	0.948	6	1.120	0.944
IPI00229645	Cytsa	Q2KN98	4	1.477	1.158	/			/			/			/			7	0.937	1.000

IPI00134746	Ass1	P16460	2	1.451	1.258	3	1.174	0.848	3	0.821	1.094	3	0.825	1.054	4	0.950	1.071	10	0.857	1.059
IPI00474116	Ppp3r1	Q63810-1	1	1.432	0.893	1	1.156	0.948	1	1.331	0.927	1	0.846	0.864	1	1.037	0.917	4	0.977	0.948
IPI00464194	Fgd6	Q69ZL1-1	1	1.421	0.989	/			/			/			3	0.517	0.353	/		
IPI00323465	Amdhd2	Q8JZV7	2	1.415	1.080	/			4	0.705	0.866	3	0.880	1.005	4	1.007	0.990	7	0.993	0.968
IPI00119152	Cpe	Q00493	1	1.412	1.032	2	1.311	1.000	3	0.983	0.986	4	0.999	0.934	3	1.426	1.102	7	1.421	0.995
IPI00108041	Stim1	P70302	1	1.411	1.323	1	1.072	0.963	2	1.098	0.780	2	1.034	0.935	/			7	1.016	1.134
IPI00111958	Urod	P70697	1	1.405	1.060	2	0.987	1.070	2	1.000	1.327	4	0.994	0.969	1	1.022	1.033	5	1.145	1.032
IPI00890112	Aldh3a1	B1ATI7	5	1.399	1.307	7	1.268	1.220	6	1.856	1.230	7	1.763	1.229	5	1.514	1.218	11	1.581	1.212
IPI00321848	Cc2d1a	Q8K1A6	1	1.395	1.429	3	1.007	0.964	3	1.316	1.172	4	1.326	1.140	/			3	1.026	1.161
IPI00664886	Thoc2	B1AZJ6	1	1.394	1.146	8	0.956	0.990	2	0.818	1.100	7	0.822	1.015	1	1.512	1.321	4	1.145	1.067
IPI00123278	Pycr2	Q922Q4	5	1.393	1.078	7	1.330	1.085	4	1.049	1.215	6	1.007	1.245	6	1.042	0.943	10	0.979	0.928
IPI00124606	Ciz1	Q8VEH2	1	1.388	1.439	/			1	1.364	0.962	2	0.361	3.357	1	1.079	0.896	/		
IPI00116247	Serpinb6b	O08804	1	1.388	1.059	3	1.529	1.142	2	0.784	0.881	2	0.671	0.854	2	1.061	1.032	7	0.989	0.832
IPI00126943	Stk38	Q91VJ4	1	1.384	1.221	2	1.064	0.797	2	1.067	0.876	3	0.952	0.913	4	0.824	0.948	4	0.902	0.991
IPI00349443	Tex264	Q99LS5	1	1.384	0.925	3	1.006	0.978	2	1.050	1.145	3	1.024	1.050	3	0.933	0.947	5	0.875	0.890
IPI00127766	Akap8l	Q9R0L7	1	1.383	1.299	4	1.340	0.932	1	0.907	0.704	2	0.909	0.765	1	0.871	0.864	3	0.782	0.722
IPI00170013	Acad10	Q8K370	3	1.377	1.065	1	1.279	1.027	1	1.264	0.963	6	0.820	0.858	1	0.929	1.013	4	0.984	0.885
IPI00330263	Aqr	Q8CFQ3	1	1.376	1.169	3	1.149	1.092	3	1.069	0.798	4	1.115	0.824	2	0.812	0.824	10	0.887	0.865
IPI00330688	Mrps7	Q80X85	1	1.374	1.239	3	1.030	1.026	4	0.914	0.999	5	0.902	0.961	2	1.027	1.126	4	1.061	1.031
IPI00331092	Rps4x	P62702	6	1.372	1.214	7	1.274	1.206	6	0.884	1.000	10	0.875	1.011	10	1.203	0.891	15	1.175	0.879
IPI00652813	Fn1	Q3UHL6	8	1.369	1.030	/			19	0.671	0.795	31	0.649	0.717	/			/		
IPI00137228	Anapc1	P53995	1	1.367	1.211	2	1.268	1.143	/			/			/			14	1.116	0.994
IPI00130948	Swap70	Q6A028	1	1.360	1.018	6	1.153	0.925	4	0.858	0.904	5	0.912	0.908	/			7	0.959	1.033
IPI00132005	Nenf	Q9CQ45	1	1.355	1.030	2	1.601	0.866	3	0.749	0.790	2	0.793	0.817	4	0.882	0.918	4	0.869	0.908
IPI00221663	Bpgm	P15327	1	1.352	0.991	3	1.106	1.184	2	1.053	1.279	1	0.874	0.935	/			2	0.931	0.924
IPI00225214	Def	Q8BTT6	1	1.351	1.080	1	1.287	1.171	/			/			/			2	1.172	0.917
IPI00228618	Gnaq	P21279	3	1.349	0.978	4	0.889	0.865	1	0.858	0.745	4	0.950	0.849	5	0.892	0.961	5	0.954	1.062
IPI00113655	Rps6	P62754	3	1.347	1.300	5	1.229	1.179	2	0.870	0.991	3	0.871	1.014	4	1.223	0.890	6	1.154	0.906
IPI00225796		Q8BVA5-1	1	1.342	0.965	2	1.365	0.887	1	1.164	0.897	2	1.108	1.042	/			1	1.117	0.966
IPI00133798	Necap2	Q9D1J1	1	1.341	1.216	1	0.774	0.823	3	0.902	0.990	3	1.030	0.998	2	0.916	1.053	4	0.975	1.053
IPI00845638	Pds5b	Q4VA53-3	1	1.341	1.172	2	1.329	1.107	4	1.033	1.194	4	1.051	1.156	2	0.668	0.867	9	0.722	0.850
IPI00129580	Sumo3	Q9Z172-1	1	1.339	1.057	/			/			/			/			2	0.505	1.187
IPI00788355	Pex5	O09012-1	1	1.339	1.193	/			2	0.950	1.145	5	0.905	0.977	2	0.897	0.994	6	0.908	1.002
IPI00311873	Ppp1cb	P62141	5	1.338	1.082	4	1.081	1.008	6	1.038	0.904	9	1.047	0.932	11	1.051	1.069	14	1.023	0.968
IPI00457659	Serpinb1a	Q9D154	5	1.336	1.142	8	1.325	1.168	7	0.615	0.924	5	0.580	0.922	7	0.987	0.878	10	0.865	0.890
IPI00113217	Ar	P19091	1	1.335	1.116	1	1.086	1.208	/			/			1	0.961	0.967	2	1.126	0.893
IPI00115895	Nadk	P58058	1	1.335	1.053	2	0.950	0.950	/			/			/			/		
IPI00420726	Rps9	Q6ZWN5	7	1.330	1.280	8	1.292	1.216	5	0.824	0.994	8	0.875	1.000	8	1.236	0.858	16	1.258	0.844
IPI00555047	1500010J02Rik	Q5SUQ9-1	1	1.326	1.157	3	1.179	1.071	3	0.923	1.089	8	0.971	0.967	7	1.085	2.294	12	0.987	0.706
IPI00459652	Ftsjd2	Q9DBC3	1	1.326	0.916	1	1.449	1.026	2	0.997	1.043	3	0.967	1.005	/			6	0.944	1.006
IPI00125901	Rps13	P62301	4	1.325	1.306	4	1.285	1.243	4	0.960	1.011	4	0.889	1.002	4	1.183	0.925	6	1.133	0.937
IPI00120546	Praf2	Q9JIG8	1	1.323	1.094	1	0.707	0.724	/			/			/			/		
IPI00461857	Tbcd	Q8BYA0	3	1.323	1.209	3	1.184	1.077	3	0.947	1.075	5	0.968	1.092	3	1.170	0.908	11	1.214	0.991
IPI00111169	Pla2g4a	P47713	2	1.321	1.145	5	1.068	1.067	1	1.177	1.037	4	1.177	1.039	4	0.901	0.958	12	0.905	0.864
IPI00320850	Mccc1	Q99MR8	3	1.317	1.044	4	1.282	1.061	5	0.792	0.972	6	0.816	0.933	8	0.959	1.099	9	0.993	0.970
IPI00313726	Polr1a	O35134	2	1.316	0.873	1	1.079	0.686	/			1	1.330	1.187	/			3	0.943	0.985
IPI00129085	Rad9a	Q9Z0F6	1	1.315	0.993	/			/			1	1.034	0.985	/			1	0.927	1.070
IPI00395140	Dcxr	Q91X52	4	1.314	1.093	7	1.272	1.069	6	0.729	0.912	7	0.738	0.907	5	1.061	0.970	10	1.055	1.079

IPI00222107	Frmd4a	Q8BIE6-2	1	1.312	0.925	/			/			1	1.181	0.937	/			/		
IPI00857891	Acox3	Q9EPL9	1	1.309	1.193	5	1.306	1.069	/			/			2	1.041	1.908	7	0.967	0.984
IPI00342766	Hp1bp3	Q3TEA8-1	4	1.302	1.051	/			3	0.927	1.080	7	0.868	1.001	2	0.944	0.819	6	0.930	0.825
IPI00121214	Ssna1	Q9JJ94	2	1.300	1.141	4	1.384	1.157	1	0.910	0.796	2	0.923	0.828	/			2	0.885	0.860
IPI00875923	Fam164a	Q8BJH1-1	1	1.300	0.936	1	1.291	0.959	/			/			/			2	0.961	0.838
IPI00137787	Rpl8	P62918	2	1.298	1.126	4	1.152	1.080	3	0.930	1.066	3	0.927	1.027	4	1.438	0.875	6	1.353	0.934
IPI00380503	Map3k7ip1	Q8CF89	1	1.294	1.514	/			/			3	0.955	1.000	/			4	1.008	1.210
IPI00762140	Heatr5b	Q8C547-1	1	1.294	1.156	2	0.951	1.031	2	1.316	1.320	2	0.960	0.996	1	1.441	0.650	3	0.992	0.811
IPI00263879	Rpl35	Q6ZWV7	1	1.292	1.143	1	1.353	1.188	1	1.059	1.081	2	1.078	1.071	2	1.199	0.893	4	1.157	0.881
IPI00761607	Hdhd2	Q3UGR5-1	2	1.288	0.805	3	1.031	0.936	2	0.845	0.972	3	0.912	0.981	3	1.053	1.098	5	0.997	0.997
IPI00133713	Dtd1	Q9DD18-1	1	1.287	0.910	1	1.598	0.943	1	0.746	0.785	1	0.807	0.745	2	0.966	1.007	/		
IPI00114982	Stat5b	P42232	2	1.287	0.783	3	1.160	1.040	/			3	1.058	0.965	/			5	1.109	1.077
IPI00396680	Psme4	Q5SSW2-1	2	1.286	1.089	6	1.103	1.148	3	0.787	1.319	3	1.064	1.008	2	1.100	0.879	7	1.094	0.869
IPI00118787	Atp6v1d	P57746	1	1.286	1.412	4	1.207	1.039	3	0.876	1.007	4	0.966	0.967	2	0.992	0.830	6	1.047	0.927
IPI00226787	Flad1	Q8R123-2	1	1.284	0.778	/			/			2	0.812	1.075	/			/		
IPI00122471	Gltscr2	Q3USL3	1	1.284	0.645	1	1.112	0.958	1	1.372	0.874	/			1	0.657	0.866	2	0.930	1.094
IPI00411102	Prps2	Q9CS42	2	1.283	1.173	5	1.092	1.001	3	1.078	1.058	4	1.154	1.035	4	1.163	0.966	10	1.130	0.982
IPI00459487	Suclg2	Q9Z2I8-1	4	1.280	0.944	5	1.301	0.953	3	0.926	0.900	3	0.858	0.896	6	1.027	0.917	9	0.976	0.951
IPI00117569	Rps11	Q9DB79	2	1.277	1.222	3	1.272	1.204	2	0.862	1.003	3	0.907	1.033	4	1.230	0.949	7	1.213	0.946
IPI00170055	Wdr32	A2AKB9-1	1	1.277	0.982	1	0.979	0.926	1	1.086	1.095	/			/			1	1.351	1.058
IPI00224505	Rpl13	P47963	4	1.276	1.135	5	1.252	1.065	5	0.925	1.109	6	0.950	1.159	5	1.381	0.921	8	1.358	0.964
IPI00129163	Tmlhe	Q91ZE0	1	1.271	1.052	2	1.131	0.965	3	0.865	0.881	4	0.869	0.882	/			4	0.995	0.913
IPI00109304	Ca13	Q9D6N1	1	1.271	1.029	3	1.133	0.915	/			4	1.170	1.034	1	2.106	1.285	3	1.192	1.034
IPI00465568	Rps24	P62849-1	2	1.270	1.090	3	1.237	1.168	2	0.878	0.977	3	0.912	1.011	2	1.147	0.894	5	1.150	0.929
IPI00379245	Gnpda1	O88958	5	1.270	0.951	4	1.371	0.892	3	0.842	0.914	4	0.829	0.885	3	0.946	0.899	7	0.992	0.934
IPI00678003	Itpa	Q9D892	2	1.270	1.222	2	1.076	0.933	2	1.184	1.080	4	1.002	1.034	4	1.069	0.903	5	1.034	0.958
IPI00380766	Rnf20	Q5DTM8-1	3	1.270	0.989	6	0.985	1.010	3	1.028	0.932	4	1.071	0.992	2	0.725	0.686	10	0.970	0.990
IPI00320462	Bphl	Q8R164	2	1.269	0.924	3	1.312	0.914	1	0.665	0.813	3	0.711	0.828	3	0.930	0.849	3	0.947	0.880
IPI00227432	Dnm3	Q8BZ98-1	3	1.265	1.062	5	1.272	1.027	/			/			/			5	0.703	0.961
IPI00652834	Prepl	Q8C167-4	3	1.264	1.015	/			/			/			/			/		
IPI00404551	Ctsd	Q8C243	3	1.264	1.051	7	1.091	1.008	7	0.848	0.905	9	0.835	0.918	7	0.981	0.942	11	1.000	0.998
IPI00471007	Arhgef11	Q5DU33	2	1.263	0.940	/			1	1.058	0.999	/			/			/		
IPI00469768	Kiaa0196	Q8C2E7-1	1	1.263	1.079	4	1.255	0.955	5	0.889	1.118	15	0.909	1.159	6	1.287	0.967	14	1.227	0.966
IPI00551495	Mtmr3	Q8K296-1	2	1.261	1.015	4	1.004	0.980	4	1.227	0.966	6	1.005	1.000	4	1.015	0.934	7	0.972	0.975
IPI00776276	Fhl1	A2AEY2	3	1.257	0.922	4	1.276	1.005	5	0.916	1.016	6	0.965	1.010	6	0.870	0.824	9	0.932	0.898
IPI00122421	Rpl27	P61358	2	1.255	1.102	4	1.233	1.094	3	0.831	1.033	4	0.845	1.029	3	1.448	0.910	5	1.322	0.927
IPI00131357	Rps23	Q497E1	3	1.255	1.227	4	1.196	1.163	3	0.908	0.899	3	0.905	0.988	2	1.231	0.893	4	1.177	0.925
IPI00114953	Cdk9	Q99J95-1	2	1.253	0.940	3	1.091	1.070	/			3	1.120	1.072	1	0.941	0.981	/		
IPI00408215	Myo1b	P46735-1	2	1.252	1.104	5	1.312	1.027	1	0.774	1.089	4	0.808	0.936	/			5	1.150	0.827
IPI00118372	Vamp4	O70480	1	1.251	1.049	1	1.102	0.941	2	1.338	0.750	2	1.254	0.949	/			3	1.063	0.936
IPI00126000	Fkbp3	Q62446	3	1.249	0.997	5	1.184	1.119	3	0.972	1.006	5	0.980	0.956	5	0.982	0.957	6	1.008	0.982
IPI00460453	Cgnl1	B2RY19	2	1.248	1.005	4	1.313	1.008	4	1.220	0.859	6	1.369	0.863	5	1.137	0.876	10	1.097	0.940
IPI00875938	Jmjd1b	Q3UI14	4	1.248	1.064	5	0.950	1.168	3	1.033	0.742	5	1.309	1.127	2	1.121	1.019	9	1.034	0.909
IPI00229810	Plekha5	Q6ZPK1	1	1.247	0.943	/			/			2	0.916	5.776	/			/		
IPI00652501	ENSMUSG00000079623	Q3UY87	/			1	19.78	63.89	/			/			/			1	20.74	1.114
IPI00889843	Abca1	B1AWZ8	/			1	13.67	9.711	/			7	10.92	4.720	4	9.709	5.338	10	5.997	2.481
IPI00409269	Acvr1	P37172	/			1	11.83	0.909	/			/			/			/		

IPI00130117	Itga9	Q91YD5	/			1	8.400	6.341	/			/			/			/		
IPI00831482	Rnpc3	Q3UZ01-1	/			1	7.457	9.606	/			/			/			/		
IPI00890274			/			1	6.723	6.973	/			/			/			/		
IPI00228026	Gan	Q8CA72	1	0.703	0.886	2	6.105	0.566	/			1	1.069	1.125	/			2	0.899	1.142
IPI00170128	Spg7	Q3ULF4	/			1	5.158	0.024	/			/			/			1	0.700	1.088
IPI00378206	Fbxw8	Q8BIA4-1	/			1	4.891	210.7	/			2	1.026	0.865	/			4	0.924	0.992
IPI00349814	Abtb2	Q7TQI7	/			1	2.630	5.205	/			/			/			/		
IPI00110207	Ovca2	Q9D7E3	/			1	2.305	0.772	/			/			/			/		
IPI00760054	Ttll7	A4Q9F0-1	/			1	2.222	0.998	/			/			/			/		
IPI00410916	Nol4	P60954	/			1	2.167	2.162	/			/			/			/		
IPI00225419	Ptpn6	P29351-2	/			1	2.166	0.743	/			/			/			/		
IPI00480329	Ep400	Q8CHI8-1	2	1.145	0.979	1	1.998	1.696	4	1.539	1.174	5	1.548	0.968	1	1.021	0.824	3	0.997	0.887
IPI00653931	Fah	Q3TY87	4	0.680	0.797	6	1.964	1.370	/			/			3	1.025	1.073	/		
IPI00453800	Znf828	Q8K327	/			1	1.889	0.976	3	1.218	0.894	4	1.164	0.971	3	0.908	1.043	3	1.004	0.972
IPI00223939		Q8BQR4-1	/			2	1.855	1.422	/			1	2.032	0.887	/			2	1.027	0.814
IPI00849113	Fau	P62862	/			1	1.830	1.621	/			/			2	1.401	0.885	2	1.365	1.026
IPI00109603	Uqcc	Q9CWU6-1	/			1	1.811	0.781	/			2	1.245	1.103	2	0.758	1.596	2	0.771	0.956
IPI00116701	Rad51l3	O55230	1	0.103	0.660	1	1.775	1.371	1	0.973	0.928	/			/			1	0.826	0.873
IPI00226384	Rbbp5	Q3TBL4	1	0.940	0.969	2	1.772	1.811	2	0.950	0.888	5	1.013	0.878	3	0.854	0.845	4	0.946	1.016
IPI00227152	Tdrd3	Q91W18-1	/			1	1.685	1.016	/			/			/			2	1.156	1.268
IPI00124593	Sumo1	P63166	2	1.238	1.085	4	1.678	1.110	3	0.921	0.785	3	1.024	0.769	3	1.066	0.966	3	1.019	0.913
IPI00169768	Wipf1	Q8K1I7	1	1.164	0.932	2	1.672	1.327	1	1.069	1.650	/			/			/		
IPI00224738	Klhl22	Q99JN2-2	2	1.001	1.185	1	1.658	0.444	1	1.130	0.949	4	1.312	1.069	3	1.033	0.962	6	1.133	0.893
IPI00117274	Dock2	Q8C3J5	/			1	1.617	13.31	/			/			/			/		
IPI00653721	Secisbp2	Q3TGQ4	/			1	1.592	0.990	/			1	0.910	0.721	/			/		
IPI00117801	Evc	P57680-1	/			2	1.583	2.019	1	1.042	0.836	/			1	0.902	0.779	1	1.050	0.895
IPI00848965	AI607873	B2RWU7	/			3	1.571	1.212	/			/			/			/		
IPI00605187	Cp	Q2F3J4	/			2	1.568	1.079	2	0.657	0.763	/			3	0.813	0.746	5	0.858	0.715
IPI00126860	Taok1	Q5F2E8	2	1.036	0.978	1	1.550	0.958	4	1.098	1.157	2	1.061	1.129	/			6	1.135	0.986
IPI00410844	9030624J02Rik	Q8BWQ6-1	/			2	1.535	0.962	1	1.043	1.160	3	0.999	0.977	/			7	0.988	0.914
IPI00652288	I830012O16Rik	Q3UAB1	/			2	1.534	1.047	/			1	0.448	0.598	/			/		
IPI00672924	Cttnbp2	Q69ZB2	/			2	1.531	1.002	1	0.950	0.881	/			/			/		
IPI00121674	Rilpl1	Q9JJC6	2	1.046	2.097	4	1.530	1.154	3	1.159	0.932	1	1.085	1.096	/			3	1.066	0.879
IPI00109233	Vhl	P40338	/			3	1.520	1.017	/			/			2	0.918	1.006	2	0.855	0.918
IPI00474493	Fbxo9	Q8BK06-1	/			1	1.513	1.127	/			/			/			/		
IPI00757586	Zc3h7b	Q3TZP6	3	1.007	1.255	1	1.509	0.925	/			3	1.013	0.963	3	1.256	1.182	6	0.959	1.006
IPI00121430	Col12a1	Q60847-1	/			4	1.505	1.065	/			/			/			4	0.949	0.961
IPI00338528	E2f1	Q61501	/			1	1.495	0.997	/			/			/			/		
IPI00119696	Tax1bp3	Q9DBG9	/			1	1.494	0.935	1	0.996	0.980	1	1.035	1.067	1	0.730	0.769	3	0.943	1.007
IPI00129075	Thumpd3	P97770-1	/			2	1.494	1.570	/			4	1.110	1.068	4	1.040	0.971	7	1.118	1.042
IPI00308882	Ndufs1	Q91VD9	/			1	1.492	1.453	/			/			/			4	1.086	0.823
IPI00319652	Gpx1	P11352	/			1	1.485	1.235	/			/			/			/		
IPI00352163	Fn1	Q3TBB4	/			19	1.483	1.006	/			31	0.670	0.797	33	1.027	0.772	44	1.046	0.811
IPI00135345	Nudt2	P56380	/			2	1.482	1.112	1	0.830	0.999	1	0.877	1.064	1	0.583	0.832	2	0.936	1.411
IPI00319131	Pex19	Q8VCI5-1	2	0.766	0.865	1	1.481	0.981	5	0.761	0.986	7	0.852	0.957	6	0.760	0.907	8	0.833	1.056
IPI00554855	Mark2	Q05512-1	/			2	1.479	0.872	2	1.032	1.125	2	1.125	1.115	4	0.999	1.015	6	0.989	0.889
IPI00337872	Cep110	Q7TSH4	1	1.205	1.094	1	1.477	1.056	1	0.856	0.872	1	0.887	0.928	1	1.019	1.038	2	0.993	1.020
IPI00223185	Prkab1	Q9R078	/			2	1.477	0.802	2	1.027	0.944	3	1.038	1.000	3	1.067	1.036	3	0.983	1.071

IPI00116459	Nat2	P50295	/			1	1.467	1.086	/			1	0.932	1.136	/			/		
IPI00274795	Ncor1	Q60974-1	/			1	1.466	1.797	4	1.152	1.114	3	1.054	1.090	2	0.940	0.959	/		
IPI00109505	Murc	A2AMM0-1	/			1	1.464	1.028	1	0.515	1.102	/			/			1	0.664	1.283
IPI00875998	Uck1	P52623	/			3	1.461	1.284	2	0.683	1.010	2	1.115	0.772	1	0.786	0.709	1	1.000	0.856
IPI00229794	Rps6ka5	Q8C050-1	/			2	1.458	0.744	/			1	0.964	0.956	1	1.195	1.047	3	0.998	1.065
IPI00453707	Ktelc1	Q8BYB9	2	1.154	0.951	1	1.454	1.248	1	0.922	0.932	2	0.843	0.948	2	0.837	1.200	3	1.031	1.050
IPI00408664	Atad5	Q4QY64-1	/			1	1.449	1.027	/			/			/			/		
IPI00134426	Trappc6b	Q9D289	/			1	1.441	0.764	1	0.692	1.092	1	0.975	1.267	/			1	0.986	1.056
IPI00652336	Pde4dip	Q80YT7-1	1	0.923	1.010	1	1.438	1.204	1	1.129	1.040	1	1.140	0.910						
IPI00119004	Iah1	Q9DB29	2	0.786	1.006	2	1.435	1.170	/			2	0.737	0.965	2	1.017	0.953	6	1.004	0.942
IPI00665734	Ppp1r12b	A6H644	/			1	1.433	1.212	2	1.102	0.946	/			2	1.080	0.933	/		
IPI00119795	Reps1	O54916-1	/			2	1.431	1.421	2	0.802	0.868	6	0.977	0.896	2	0.924	0.923	6	0.927	0.890
IPI00134420	Gdpd1	Q9CRY7	/			1	1.429	0.975	/			/			1	0.855	0.930	2	0.902	0.795
IPI00309224	Pik3ca	P42337	/			3	1.429	0.940	1	0.876	0.969	3	0.895	0.772	/			3	1.012	1.130
IPI00229848	Plcg2	Q8CIH5	/			1	1.422	0.910	/			/			/			/		
IPI00112189	Srxn1	A2AQU8	/			1	1.418	1.394	/			3	1.614	1.207	/			1	1.399	0.897
IPI00342603	Ogdhl	B2RXT3	4	1.234	0.957	6	1.417	0.960	5	0.652	0.918	8	0.712	0.859	7	1.041	0.978	12	0.941	0.846
IPI00886205	Ttc3	O88196	/			1	1.413	0.922	1	1.055	0.928	3	0.695	0.755	2	1.020	0.994	3	1.160	0.993
IPI00187434	Dut	Q8VCG1	2	1.174	0.991	5	1.407	1.055	4	1.166	1.069	6	0.662	1.265	4	0.888	1.053	/		
IPI00229428	Leprel1	Q8CG71	1	0.990	0.974	2	1.403	1.051	/			/			/			2	1.151	0.977
IPI00719890	Nfkb1	P25799-5	2	0.970	0.892	3	1.392	0.867	3	0.888	0.946	10	0.929	0.903	5	0.990	0.978	10	0.979	0.983
IPI00119755	Nudt7	Q99P30-2	/			1	1.390	1.152	/			/			/			/		
IPI00849760	Cdc42bpg	Q80UW5	1	1.071	1.068	2	1.389	0.962	1	0.860	1.117	3	0.751	0.955	1	0.892	1.128	/		
IPI00123138	Lars2	Q8VDC0	/			2	1.388	0.999	1	0.937	1.460	3	0.752	0.990	/			2	1.050	1.061
IPI00129159	Neo1	P97798-1	/			1	1.388	1.202	/			/			2	0.826	1.041	13	0.899	0.964
IPI00125970	Abca7	Q91V24	2	1.121	0.851	2	1.387	1.089	2	1.295	1.064	3	1.574	0.959	3	1.245	0.853	4	1.398	0.928
IPI00131513	Ash2l	Q91X20	1	0.918	0.954	2	1.386	1.068	3	1.024	1.068	3	0.937	1.018	3	0.606	0.853	4	0.959	1.144
IPI00133532	Exosc5	Q9CRA8	/			1	1.381	0.828	1	1.769	0.963	2	0.961	1.009	2	1.058	0.935	3	1.034	0.950
IPI00867808	Plekhh2	Q8C115-3	/			1	1.380	1.053	/			1	0.749	0.523	/			1	1.309	0.882
IPI00755796	Ankrd44	B2RXN6	1	1.172	0.879	2	1.379	1.066	1	0.593	1.106	/			/			1	1.271	0.975
IPI00828950	Atp6v0a1	Q9Z1G4-2	/			1	1.379	1.435	/			/			/			2	0.639	0.728
IPI00463211	Dusp19	Q8K4T5	/			1	1.378	0.930	/			/			/			/		
IPI00122362	Pdia5	Q921X9	/			2	1.377	1.122	/			2	0.976	0.941	2	0.465	0.942	4	1.126	0.962
IPI00119998	Zfyve19	Q9DAZ9	1	1.229	0.897	1	1.374	0.983	/			/			/			/		
IPI00230182	Angel2	Q8K1C0-1	2	1.109	0.994	1	1.373	1.059	1	0.950	0.980	1	0.814	1.053	2	1.049	0.876	3	0.994	1.071
IPI00227657	Sdf2l1	Q9ESP1	/			2	1.369	1.169	/			4	0.856	0.846	1	0.898	0.944	1	0.935	0.979
IPI00321929	Ccdc117	Q6PB51	/			1	1.367	0.773	/			/			/			/		
IPI00118959	Mitd1	Q8VDV8	/			1	1.365	1.357	/			1	0.939	1.000	1	5.024	0.992	2	1.115	0.907
IPI00169568	Mapkapk3	Q3UMW7-1	/			2	1.362	0.994	1	0.906	1.009	1	0.939	0.955	/			/		
IPI00756750	Fam160b1	Q8CDM8-1	/			2	1.360	0.864	2	1.182	1.141	2	0.992	0.956	1	0.890	1.144	2	1.039	0.955
IPI00119930	Prkag1	O54950	/			3	1.359	1.061	2	1.091	1.013	4	1.250	0.953	2	1.010	1.001	5	1.004	0.930
IPI00890036	Ahr	P30561	/			3	1.359	0.961	/			/			/			2	1.062	1.346
IPI00226726	Pcyox1l	Q8C7K6	/			2	1.356	1.146	/			1	0.585	0.757	1	0.892	1.080	2	0.834	0.948
IPI00153207	Vps37b	Q8R0J7	1	1.087	0.945	1	1.353	0.979	2	1.001	0.960	6	1.147	0.919	1	0.831	0.930	4	0.905	1.000
IPI00895320	Dctn6	Q9WUB4	/			1	1.351	0.208	/			/			1	1.195	1.063	2	1.150	1.276
IPI00828510	Znfx1	A2A5R3	/			1	1.350	1.348	/			/			/			2	1.046	0.833
IPI00170006	Txndc11	Q8K2W3-1	/			1	1.350	0.842	/			/			/			/		
IPI00625954	Nt5dc2	Q91X76	/			1	1.350	0.941	/			2	0.687	0.891	/			4	1.329	0.912

IPI00120923	Vps16	Q920Q4-1	/			2	1.349	0.923	/			2	1.023	0.924	/			5	0.929	0.914
IPI00468380	Dclk1	Q9JLM8-1	2	1.137	0.916	3	1.348	0.954	2	0.953	0.923	5	1.022	0.954	5	1.002	0.923	9	1.093	0.919
IPI00349293	Rc3h2	P0C090	1	0.955	0.960	1	1.344	1.372	2	0.962	1.007	1	0.968	0.891	/			2	0.980	1.041
IPI00165730	Plbd2	Q3TCN2-1	3	1.229	1.026	5	1.344	1.113	5	0.775	0.891	8	0.794	0.887	5	0.988	0.819	9	0.991	0.961
IPI00551399	Efr3a	Q8BG67-2	/			1	1.344	0.969	/			/			/			2	0.567	0.734
IPI00336291	Tecpr1	Q80VP0-1	1	1.200	0.885	1	1.343	0.958	2	1.054	0.953	6	0.949	1.032	1	1.428	1.193	3	0.982	0.937
IPI00131113	Kiaa1881	O88492-1	3	1.121	1.049	1	1.343	1.045	2	1.136	0.980	3	1.061	0.896	2	0.956	0.814	5	1.009	0.698
IPI00130416	Mocs2	Q9Z224	/			1	1.341	0.979	/			/			/			/		
IPI00112648	Csk	P41241	/			3	1.339	1.241	1	0.928	0.935	4	1.140	0.992	1	0.976	1.055	3	1.001	0.922
IPI00754519	4930422G04Rik	Q0VGT4	/			1	1.336	0.914	/			/			/			/		
IPI00469712	Smarca2	Q6DIC0	/			2	1.336	1.184	/			/			1	0.850	1.231	/		
IPI00849948	Rps8	P62242	3	1.240	1.193	5	1.327	1.163	5	0.876	0.985	6	0.895	0.992	/			/		
IPI00845840	Pkm2	P52480-2	24	1.245	1.204	27	1.327	1.106	/			31	0.842	0.783	31	0.838	0.777	33	0.839	0.833
IPI00283736	Cdkn2a	P51480-1	2	1.150	1.098	1	1.326	1.167	2	1.576	1.139	2	1.311	1.209	/			2	1.071	0.879
IPI00109169	Idh3g	P70404	/			2	1.322	1.313	2	0.983	0.964	4	0.892	0.951	6	0.995	0.909	8	1.029	0.953
IPI00849526	Rxra	P28700	/			1	1.321	1.160	/			/			/			/		
IPI00228236	Spcs2	Q9CYN2	1	0.997	1.600	2	1.318	2.288	1	1.244	0.833	1	1.538	0.840	/			1	0.483	0.585
IPI00649725	Cisd3	B1AR13	/			1	1.315	1.192	/			/			/			/		
IPI00417063	AU019823	Q6NX79	/			1	1.312	1.208	/			/			/			/		
IPI00122399	Glg1	Q61543	3	1.181	0.909	8	1.311	0.984	5	1.371	0.873	7	1.286	0.871	10	1.509	1.061	22	1.497	1.036
IPI00134747	Toe1	Q9D2E2-1	2	1.205	1.180	2	1.311	1.168	2	1.146	1.149	2	1.065	1.191	3	0.774	0.874	4	0.808	0.808
IPI00381071	Ddhd2	Q80Y98-1	/			3	1.311	1.015	/			6	1.020	0.901	5	1.118	1.122	8	1.136	0.938
IPI00127934	Pxk	Q8BX57-1	1	1.231	0.972	1	1.311	0.951	1	1.179	1.140	4	1.016	1.053	3	0.914	0.905	4	1.008	0.864
IPI00808098	Far1	Q922J9-4	3	1.114	1.118	4	1.310	1.146	3	1.019	1.077	6	0.960	1.066	2	1.126	1.039	4	1.098	1.001
IPI00110724	Rpl22l1	Q9D7S7-1	1	0.988	0.886	2	1.309	1.065	2	1.135	0.922	2	1.092	0.919	2	0.961	0.888	2	0.988	1.048
IPI00828779	Ap4e1	A2ASB4	/			1	1.309	0.975	/			/			/			2	0.967	9.011
IPI00123319	Tpm2	P58774-1	/			9	1.309	2.073	/			/			/			/		
IPI00128941	Yif1a	Q91XB7	/			1	1.309	1.224	/			/			/			/		
IPI00626782	Arfgef1	Q8BKL2	/			3	1.307	0.969	1	1.058	1.599	/			/			/		
IPI00133591	Vps28	Q9D1C8	1	0.954	0.991	1	1.307	0.978	3	0.952	1.108	3	1.045	0.949	2	1.019	1.019	7	0.928	0.973
IPI00462594	Kiaa0664	Q6GQX1	/			8	1.306	1.191	/			/			/			/		
IPI00654317		Q3U276	/			1	1.305	0.970	/			/			/			1	0.710	0.950
IPI00461460	R3hdm1	Q6P6J5	/			2	1.305	1.240	2	1.205	1.115	2	0.992	0.837	1	2.105	1.067	2	0.976	0.935
IPI00117754	Sdf4	Q61112	/			1	1.305	1.118	/			/			/			/		
IPI00119185	Med29	Q9DB91	/			1	1.304	0.999	1	1.005	1.141	1	1.102	0.855	1	1.210	1.342	/		
IPI00229315	Trafd1	Q3UDK1-1	1	1.162	1.046	2	1.301	1.111	1	1.084	0.915	1	1.069	1.073	1	1.148	0.971	3	1.086	1.013
IPI00808297			/			1	1.301	0.817	/			/			/			/		
IPI00187274	Ccdc91	Q9D8L5-1	/			2	1.301	1.094	1	0.880	1.095	1	1.060	1.010	1	1.234	1.133	/		
IPI00172129	Dnmt3a	O88508-2	/			2	1.299	1.088	/			/			/			/		
IPI00229599	Nav1	Q8CH77-1	/			1	1.298	1.074	/			/			/			/		
IPI00170051	Hscb	Q8K3A0	/			2	1.298	0.916	/			1	0.944	0.987	/			3	1.275	1.061
IPI00461642	Tjap1	Q9DCD5	1	1.200	0.990	4	1.296	1.094	3	1.047	0.997	6	1.018	0.909	2	0.962	0.987	7	1.012	1.037
IPI00119201	Ngdn	Q9DB96	/			1	1.293	1.013	/			/			/			3	0.737	1.000
IPI00109544	Ddx28	Q9CWT6	/			1	1.291	1.196	/			3	0.983	1.186	/			1	1.126	0.977
IPI00453489	Oit3	Q8R4V5-1	/			1	1.291	1.806	/			/			/			/		
IPI00223759	Vps26b	Q8C0E2-1	2	1.120	1.005	3	1.290	1.118	/			1	1.141	1.104	1	0.825	0.898	4	0.861	0.954
IPI00162781	Ahcyl1	Q80SW1	6	0.992	1.042	6	1.289	1.160	6	0.975	0.956	10	0.976	0.932	6	1.030	1.006	9	1.047	1.053

IPI00515170	Ttc28	Q80XJ3	/			2	1.289	1.064	/			/			/			3	1.100	0.970
IPI00756198	Kntc1	Q8C3Y4	1	0.548	0.530	7	1.289	1.039	/			7	1.080	0.944	1	1.005	0.867	9	0.951	0.916
IPI00474959	Rcn2	Q3TE95	5	1.098	0.951	9	1.288	1.003	7	0.882	0.891	7	0.881	0.880	10	0.979	0.977	12	0.946	0.972
IPI00308446	Ahcyl2	Q68FL4-1	/			4	1.283	1.068	/			/			5	1.085	1.045	9	1.020	0.982
IPI00453611	Tbc1d9b	Q5SVR0-1	/			1	1.282	1.192	1	1.027	0.940	2	0.472	0.907	/			1	0.882	0.958
IPI00457620	Loh12cr1	Q9D920	1	1.126	1.090	1	1.282	1.101	1	0.851	0.910	/			/			/		
IPI00323030	Ldb3	Q9JKS4-1	/			1	1.282	1.298	/			/			/			/		
IPI00131887	Ptgr1	Q91YR9	3	1.245	1.038	5	1.282	1.057	5	0.877	0.992	6	0.885	0.918	4	1.002	0.947	11	1.000	1.001
IPI00134334	Ptgr2	Q8VDQ1-1	/			1	1.281	1.057	1	0.363	1.069	3	0.857	0.870	/			2	1.004	1.015
IPI00272878	Dnm1	P39053-1	/			3	1.281	1.287	/			/			/			/		
IPI00881150	Taf8	Q9EQH4-4	/			1	1.280	0.711	/			2	1.110	1.195	1	0.951	0.916	2	1.040	1.158
IPI00459324	Cars2	Q8BW29	/			1	1.279	1.023	/			2	0.789	0.870	1	0.814	1.205	2	0.917	0.880
IPI00417173	Gtf3c5	Q8R2T8-1	/			4	1.277	1.187	/			1	0.965	1.548	/			4	0.895	0.894
IPI00111167	Col4a3bp	Q9EQG9-1	/			3	1.276	1.079	3	1.424	1.338	4	1.516	1.054	4	1.576	1.153	4	1.463	1.047
IPI00132574	Wdsub1	Q9D0I6	/			1	1.276	1.033	/			2	0.759	0.744	/			2	1.078	0.863
IPI00133061	Rbm7	Q9CQT2	/			1	1.275	1.133	1	1.018	1.158	2	1.070	0.890	/			2	0.992	1.040
IPI00230623	Rpl32	P62911	/			3	1.273	1.044	/			4	0.902	1.107	2	1.671	0.909	5	1.589	0.973
IPI00120202	Fbxo3	Q9DC63	/			1	1.273	1.048	1	0.969	1.170	1	1.014	0.931	/			3	1.118	1.096
IPI00828275	Serf2	A2ARQ4	/			1	1.271	0.929	/			/			/			2	0.873	0.903
IPI00330729	Csnk1a1	Q8BK63-1	1	1.145	1.097	1	1.269	1.119	2	1.090	1.015	/			2	1.159	0.927	4	1.249	0.903
IPI00136758	Fam175b	Q3TCJ1	/			1	1.269	1.162	1	0.972	0.992	4	0.925	1.077	3	1.112	0.926	3	1.048	0.990
IPI00111181	Vps35	Q9EQH3	9	1.237	1.041	12	1.269	1.063	13	1.222	1.070	19	1.178	1.081	13	0.734	0.833	28	0.759	0.861
IPI00128563	Dtnbp1	Q91WZ8-1	/			1	1.269	0.961	/			/			1	0.860	1.573	2	0.963	0.931
IPI00227851	Lrba	Q9ESE1	2	1.079	0.985	7	1.268	1.118	5	0.918	0.994	8	0.989	1.002	5	1.037	0.964	8	0.977	1.033
IPI00278153	Soat1	Q61263	/			1	1.268	1.428	/			3	0.988	0.869	/			/		
IPI00554920	Zfyve26	Q5DU37-1	1	0.803	0.944	3	1.267	1.020	5	0.875	0.988	3	0.654	0.905	1	0.888	0.845	1	0.860	0.911
IPI00135700	Dctpp1	Q9QY93	1	1.124	0.989	2	1.267	1.120	2	0.855	0.895	3	1.072	0.886	2	0.969	0.844	4	1.033	0.996
IPI00378506	Ccdc76	Q8BYH3	/			1	1.267	0.868	/			/			/			/		
IPI00275992	Htra2	Q9JIY5	/			2	1.266	1.003	4	0.855	1.109	4	0.856	1.083	3	1.225	1.009	3	1.173	1.020
IPI00462855	Scyl1	Q9EQC5	2	1.077	0.944	3	1.266	1.054	3	1.712	1.148	2	1.534	1.187	3	1.083	0.910	6	1.014	0.972
IPI00226952	Mars2	Q499X9	1	0.948	0.760	2	1.265	1.126	/			1	0.946	1.072	/			5	1.216	1.330
IPI00387484		Q8QZX2-1	/			2	1.264	1.507	/			2	1.511	1.568	1	1.006	1.050	2	1.058	1.162
IPI00312501	Osbpl2	Q8BX94	1	1.178	2.078	1	1.264	1.085	/			4	1.129	1.012	3	1.139	1.013	3	1.181	1.000
IPI00874398	Fam65a	Q68FE6	3	0.904	0.807	3	1.264	1.217	1	1.027	1.151	2	1.022	1.094	1	0.908	1.031	2	0.790	1.087
IPI00331528	Glrx	Q9QUH0	1	1.164	1.045	2	1.263	1.022	2	0.777	0.926	3	0.771	0.848	2	1.135	0.999	3	1.110	0.881
IPI00120264	Irgm	Q60766-1	1	1.069	0.916	1	1.263	1.016	1	0.811	0.844	2	0.789	0.877	1	0.933	0.827	4	0.907	0.871
IPI00467914	H1f0	P10922	3	1.200	1.021	4	1.263	1.051	2	0.522	0.900	4	0.680	1.017	3	0.972	0.847	7	1.009	0.824
IPI00222589	Ptk7	Q8BKG3	/			1	1.262	0.908	1	0.903	0.931	2	0.832	0.990	3	0.754	0.863	7	0.804	0.848
IPI00224128	Nmt1	O70310	5	1.120	0.934	7	1.261	1.046	7	0.972	1.037	12	1.000	0.989	13	0.980	0.947	15	1.025	0.983
IPI00330112	Mib1	Q80SY4	1	1.246	1.033	1	1.260	1.226	/			/			/			/		
IPI00896595	Cars2	Q8BYM8	/			2	1.260	0.978	1	0.665	0.789	/			/			/		
IPI00515343	Efemp1	Q5SNU0	/			1	1.260	1.252	/			4	1.437	1.444	/			/		
IPI00129164	Spr	Q64105	3	1.222	1.032	5	1.260	1.041	8	0.858	0.907	8	0.878	0.890	9	0.970	0.887	11	0.969	0.959
IPI00857417	Med24	Q99K74-2	/			1	1.260	0.965	/			/			/			/		
IPI00123744	Cst3	P21460	1	1.115	1.021	1	1.260	0.977	1	0.930	0.793	1	0.903	0.919	1	1.110	1.033	2	1.344	0.877
IPI00312076	Kif3a	P28741	/			6	1.259	1.022	2	0.976	1.027	4	0.992	1.001	2	1.181	1.150	4	1.113	1.044
IPI00662204	Thumpd2	Q9CZB3	/			2	1.259	0.984	2	0.863	0.928	1	0.833	1.005	1	1.142	0.970	3	0.932	1.070
IPI00762255	D11Wsu99e	A2A6P4	/			1	1.256	1.144	/			1	1.099	0.854	1	1.068	0.977	1	1.027	0.909

IPI00762483	Lrrfip1	Q8BLV4	2	1.138	0.912	5	1.256	1.023	4	1.055	1.022	/			5	1.070	0.825	8	0.863	0.834
IPI00378156	Rabgap1	A2AWA9-1	6	1.041	0.973	11	1.256	1.092	8	1.029	0.953	9	1.080	0.919	8	1.086	0.940	15	1.089	0.988
IPI00653709	Spin1	Q3UWM7	/			1	1.255	1.179	/			2	1.096	0.964	/			/		
IPI00475209	Masp1	Q8CD27	/			1	1.255	0.846	/			/			/			/		
IPI00130264	Uckl1	Q91YL3	/			2	1.254	1.137	/			2	1.011	1.069	/			3	1.085	1.145
IPI00221491	Trim65	Q8BFW4-1	/			1	1.252	1.293	1	0.963	1.057	2	0.937	1.031	/			3	0.842	1.121
IPI00406790	Camk2d	Q6PHZ2-5	3	1.114	1.038	5	1.252	1.086	5	1.132	1.043	7	1.094	1.005	5	1.181	0.967	8	1.128	1.003
IPI00850694	Ppm2c	A2AJQ0	1	1.033	0.837	1	1.252	1.016	/			3	0.896	0.932	1	0.948	1.033	4	1.053	0.989
IPI00654120	Dtx3l	Q3UIR3	1	1.082	1.024	1	1.250	1.055	/			/			/			/		
IPI00111118	Zfp623	Q6A033	/			/			1	34.11	6.689	/			/			/		
IPI00131061	Dfna5	Q9Z2D3	2	0.745	1.007	3	0.801	1.013	3	20.16	0.917	1	1.812	1.161	2	1.139	1.185	7	1.244	1.216
IPI00858099	Chd8	Q09XV5-1	3	1.016	0.997	1	0.906	1.004	2	18.11	0.703	3	1.259	1.050	/			/		
IPI00457726	L3mbtl	A2A5N8	/			/			1	13.29	91.27	/			/			/		
IPI00460042	Ralgapa1	Q6GYP7-2	/			/			1	7.935	6.749	2	3.233	1.287	1	1.847	0.633	/		
IPI00133025	Ccdc53	Q9CR27	3	0.920	1.005	2	0.944	1.016	1	5.482	0.876	3	1.052	0.881	1	0.969	0.923	2	0.972	0.970
IPI00128230	Mta2	Q9R190	/			/			2	5.244	1.166	/			2	0.873	0.915	4	0.866	0.887
IPI00757790	Cgn	P59242-2	/			/			1	4.043	1.144	/			/			/		
IPI00115998	Pbx1	P41778-1	/			/			1	3.462	0.700	2	0.963	0.904	3	0.923	1.156	4	1.098	1.002
IPI00122223	Top2a	Q01320	/			4	0.607	1.108	4	3.181	0.851	10	3.296	0.933	5	0.795	0.964	11	0.780	0.967
IPI00411164	Skt	A2AQ25-6	/			/			1	2.857	11.70	/			/			2	1.000	4.764
IPI00115454	Sfxn1	Q99JR1	/			/			1	2.800	1.015	2	1.363	0.823	/			7	0.621	0.709
IPI00225312	Msrb3	Q8BU85	1	1.053	1.299	3	0.928	1.168	1	2.591	0.913	2	0.975	0.857	/			3	1.074	0.911
IPI00133581	Ube2c	Q9D1C1	/			3	0.879	0.827	1	2.493	1.283	2	1.522	0.879	/			1	0.405	0.938
IPI00135180	Cdca3	Q99M54-1	/			1	0.699	1.116	1	2.463	0.983	1	2.324	0.902	1	0.960	1.292	3	0.661	1.086
IPI00118575	Ubqln4	Q99NB8	/			3	1.127	0.993	5	2.393	1.028	7	1.113	0.985	6	0.993	0.998	10	1.075	0.996
IPI00222461	Gnl3	Q8CI11-1	/			3	1.043	0.980	2	2.293	1.723	4	1.201	1.053	3	1.030	0.808	7	1.011	0.880
IPI00625970	Spp1	Q3TLP1	/			/			2	2.271	0.911	1	2.093	0.854	/			2	1.723	0.900
IPI00116757	Kif22	Q3V300	/			1	0.822	1.002	1	2.246	1.305	1	2.062	1.233	1	0.761	1.121	3	0.836	1.009
IPI00420139	E2f7	Q6S7F2	/			/			1	2.234	1.479	/			/			/		
IPI00120767	Plk1	Q07832	/			1	0.695	1.181	1	2.197	1.226	2	1.493	17.70	/			/		
IPI00323911	Gsta4	P24472	/			/			1	2.165	1.483	2	2.015	1.345	2	1.554	1.073	5	1.476	1.027
IPI00459381	Ddx18	Q8K363	2	0.963	1.188	3	0.936	1.064	3	2.121	1.067	8	1.666	1.030	2	0.776	0.822	9	0.943	0.858
IPI00114353	Fosl1	P48755	2	0.977	1.140	1	0.936	1.003	2	2.112	1.021	2	1.889	1.021	1	1.419	1.100	3	1.430	1.117
IPI00111896	Paf	Q9CQX4	/			/			1	2.101	1.481	1	2.294	1.121	1	0.731	1.047	4	0.936	1.093
IPI00118853	Mre11a	Q61216-1	3	1.118	1.052	7	1.136	0.993	2	2.095	0.845	5	0.982	0.940	3	0.971	0.858	5	0.934	0.953
IPI00111222	Aldh3a1	P47739	/			/			5	2.041	1.259	7	1.758	1.257	5	1.844	1.281	/		
IPI00123947	Kif20a	P97329	/			2	0.835	1.262	2	2.038	1.018	3	1.804	1.031	/			4	0.937	0.945
IPI00169684	Ect2	Q80VE4	/			/			1	2.032	1.152	1	1.696	1.050	/			3	0.930	1.180
IPI00122594	Ahctf1	Q8CJF7	/			3	0.897	1.067	1	2.027	0.826	4	1.569	0.739	1	1.140	0.770	9	0.721	0.803
IPI00172197	Anln	Q8K298	5	0.715	1.009	7	0.795	1.071	12	2.013	1.171	16	1.940	1.100	13	0.989	1.123	20	1.046	1.119
IPI00458852	Ccnb1	P24860	/			1	0.924	1.009	4	2.007	1.221	3	1.841	1.153	2	0.809	1.217	4	0.943	1.034
IPI00111953	Bola1	Q9D8S9	/			3	1.138	0.987	2	2.002	0.879	2	0.858	0.974	3	0.958	0.911	4	0.971	1.001
IPI00130218	Kif11	Q6P9P6	4	0.825	0.996	7	0.796	1.005	6	1.991	1.066	8	1.850	1.242	5	1.099	1.234	9	1.029	1.141
IPI00227582	Nrp2	O35375-4	/			2	0.928	1.016	1	1.965	0.709	1	0.970	1.064	/			6	0.918	0.883
IPI00130200	Uhrf1	Q8VDF2	1	0.798	1.065	2	0.986	1.144	1	1.936	1.220	7	1.700	1.148	6	1.013	1.083	9	0.966	1.034
IPI00320741	Ctcf	Q61164	/			1	0.820	1.109	1	1.922	0.828	/			2	0.906	0.663	4	0.833	0.985
IPI00124973	Kpna2	P52293	5	0.752	1.095	5	0.748	1.073	6	1.920	1.084	10	1.754	1.064	/			11	0.974	0.989
IPI00676143	Tmub2	A2AWT0	/			/			1	1.917	1.153	1	0.955	1.078	/			1	0.817	0.886

IPI00461832	Utp6	Q8VCY6	/			/			2	1.903	0.932	1	1.754	1.040	3	0.859	1.545	3	0.740	0.856
IPI00469755	Pwp2	Q8BU03	/			2	0.724	0.835	1	1.891	1.390	2	1.296	1.020	3	0.901	1.087	6	0.912	0.875
IPI00124700	Tfrc	Q62351	6	0.661	0.927	12	0.775	0.957	8	1.880	0.944	9	1.871	0.888	9	1.011	0.982	18	1.048	0.981
IPI00115477	Ccdc46	Q5PR68-1	/			/			1	1.848	1.273	/			/			1	1.074	0.833
IPI00331361	Mybbp1a	Q7TPV4	4	1.235	1.121	6	0.985	1.275	6	1.848	1.071	15	2.052	1.073	8	0.605	0.838	17	0.624	0.846
IPI00112645	Rrm2	P11157	/			4	0.878	1.053	3	1.824	1.070	5	1.801	1.250	4	1.004	1.155	6	0.981	1.033
IPI00132134	Pkp2	Q3TIY5	/			/			1	1.815	0.996	1	1.671	1.069	/			2	0.937	1.334
IPI00109824	Mthfd2	P18155	/			/			1	1.796	1.405	2	1.697	1.369	/			/		
IPI00648888	Rab3b	A2A7Z6	/			3	0.861	1.047	1	1.795	1.076	1	0.687	0.438	/			/		
IPI00318548	U2af1	Q9D883	2	0.909	1.041	3	1.010	1.061	1	1.783	1.084	5	1.089	0.970	4	0.938	0.893	6	1.024	0.895
IPI00114491	Cdc2	P11440	5	0.908	1.004	7	0.919	0.975	6	1.782	1.096	8	1.749	1.045	6	0.843	0.937	9	0.853	0.955
IPI00123365	Kif2c	Q922S8	/			3	0.794	1.129	2	1.780	1.154	4	1.781	1.229	3	0.988	1.019	3	1.020	1.126
IPI00653266	Rfc4	Q3UI84	4	0.888	1.424	8	0.834	0.936	2	1.762	0.865	4	1.069	1.013	4	0.887	0.919	6	0.905	0.955
IPI00123039	Ptpn1	P35821	/			2	0.748	0.894	3	1.755	1.131	3	1.175	0.817	3	0.929	0.935	7	0.850	0.928
IPI00229801	Trp53bp1	A2AU91	2	0.678	0.929	8	0.705	0.899	4	1.752	0.729	13	1.484	0.788	9	0.918	0.963	21	0.897	0.965
IPI00416125	Fam120c	Q8C3F2-3	/			/			2	1.751	0.113	/			/			/		
IPI00118827		Q9DAM7	/			2	0.949	0.923	1	1.740	0.925	2	1.516	0.927	2	1.229	0.955	3	1.137	0.948
IPI00330806	Bsdc1	Q80Y55	/			1	0.704	0.895	1	1.738	0.910	2	1.079	1.144	/			1	1.492	1.455
IPI00137018	Gle1	Q8R322	/			1	1.108	1.118	1	1.726	0.959	1	1.441	1.074	1	0.777	0.995	1	1.090	1.311
IPI00229883	Ints4	Q8CIM8-1	1	1.079	0.994	1	1.111	1.205	1	1.726	1.423	3	1.449	1.401	1	0.583	0.935	1	0.841	1.663
IPI00474439	Csda	Q64369	/			/			8	1.712	0.965	6	1.364	1.046	8	0.791	1.022	8	0.798	1.134
IPI00225412	Fanci	Q8K368-1	/			1	1.239	1.114	1	1.711	1.070	/			/			/		
IPI00459268	Mastl	Q8C0P0-2	/			/			1	1.708	1.225	2	0.927	1.571	1	1.204	1.151	/		
IPI00890076	Maoa	B1AX52	3	0.989	1.596	4	0.936	1.501	4	1.703	0.866	4	1.540	0.855	4	0.632	0.577	8	0.612	0.635
IPI00276866	Nat10	Q8K224	/			/			1	1.702	1.028	2	1.787	0.905	1	1.176	1.121	2	0.954	0.883
IPI00889961	Azi1	B1AXI9	/			2	0.978	1.110	1	1.697	1.178	6	1.396	1.059	2	1.249	1.776	4	1.115	0.931
IPI00453855	Topbp1	Q6ZQF0	1	1.134	1.108	/			3	1.694	0.954	/			2	0.983	2.994	5	0.978	0.932
IPI00222675	Kiaa0020	Q8BKS9	/			1	0.760	0.596	1	1.694	0.922	3	1.628	0.900	3	0.770	0.912	7	0.762	0.876
IPI00551454	Pdcd11	Q6NS46	/			/			3	1.686	0.919	3	1.970	0.913	1	0.747	0.692	4	0.850	0.921
IPI00396728	Ddx51	Q6P9R1	/			/			1	1.679	0.941	3	1.777	1.126	2	0.416	0.683	4	0.679	0.859
IPI00881456	Kif4	Q3UWH4	/			6	0.723	1.047	6	1.678	1.039	/			/			/		
IPI00225677	Lsm11	Q8BUV6	/			/			1	1.678	1.148	1	1.447	0.929	/			1	1.035	0.909
IPI00407413	Scand3	B2RPU8	1	0.990	0.710	2	0.962	0.785	2	1.663	1.142	3	1.588	1.092	3	1.430	0.976	4	1.343	0.850
IPI00828535	Atrn	A2AP43	/			/			1	1.662	1.682	/			/			2	0.815	0.924
IPI00308332	Armcx3	Q8BHS6	/			1	0.505	0.776	1	1.661	1.028	/			/			1	0.620	1.012
IPI00172226	Ncapd2	Q8K2Z4-2	/			4	0.900	1.075	6	1.649	1.268	13	1.535	1.172	8	0.621	0.840	19	0.672	0.850
IPI00467350	Pbk	Q9JJ78	/			2	0.801	0.941	2	1.645	1.214	/			/			/		
IPI00453589	Vamp8	O70404	1	0.788	1.007	1	0.688	1.089	1	1.640	0.898	2	1.339	0.911	1	0.845	0.883	4	0.860	0.863
IPI00124046	Mpp6	Q9JLB0-1	/			/			1	1.638	1.219	1	1.103	0.932	1	1.452	1.379	2	0.993	1.172
IPI00648030	Phactr4	Q501J7-3	1	0.695	1.120	3	0.752	1.050	2	1.637	0.893	4	1.596	0.943	2	0.836	1.001	4	0.848	1.012
IPI00135252	Atad2	Q8CDM1-2	/			/			1	1.631	1.061	1	2.204	1.018	1	0.565	0.831	2	0.685	0.845
IPI00131909	Pno1	Q9CPS7	2	0.911	1.025	3	0.958	1.067	3	1.630	0.954	3	0.972	1.075	3	0.939	0.911	3	0.973	0.928
IPI00665571	Rfc3	Q8R323	1	0.940	1.038	4	0.993	0.956	3	1.630	1.086	5	1.418	1.069	6	0.791	0.885	9	0.840	0.892
IPI00408781	Dhx37	Q5DTX1	/			2	0.822	0.974	1	1.627	1.017	1	1.494	1.067	1	0.970	0.890	1	1.171	0.886
IPI00115257	Psip1	Q99JF8-1	5	0.952	1.002	10	0.816	1.124	9	1.624	1.011	12	1.529	0.947	11	0.862	0.887	10	0.866	0.894
IPI00330679	Ddrgk1	Q80WW9	/			1	0.647	0.995	1	1.623	15.38	1	1.736	1.078	/			2	0.865	1.604
IPI00938448	Gnl2	B1ASC3	/			/			1	1.615	0.838	1	1.396	1.096	2	0.726	0.844	/		
IPI00135443	Top2b	Q64511	/			/			2	1.605	0.731	7	2.667	0.760	12	0.783	0.839	21	0.763	0.803

IPI00321718	Phb2	O35129	2	0.651	1.465	4	0.746	1.399	2	1.599	0.860	4	1.304	0.913	3	0.580	0.694	6	0.620	0.744
IPI00929813	Nap1l1	P28656	/			/			5	1.594	1.012	8	1.587	1.012	9	1.107	1.041	/		
IPI00321884	Nvl	Q9DBY8	2	0.957	1.091	5	0.956	1.445	4	1.581	1.041	3	1.433	0.978	2	0.988	1.015	6	0.944	0.981
IPI00453853	Bap1	Q99PU7	/			/			1	1.580	1.929	2	1.086	1.048	/			3	1.246	1.054
IPI00470138	Lrrc40	Q9CRC8	/			3	0.802	0.916	1	1.578	1.221	5	1.255	1.101	/			4	1.003	1.071
IPI00123755	Cbx5	Q61686	2	0.605	0.823	2	0.543	0.859	6	1.577	0.742	6	1.584	0.709	7	0.831	0.987	9	0.841	0.992
IPI00120691	Ddx21	Q9JIK5	5	0.724	1.049	10	0.865	1.084	13	1.571	0.962	/			16	0.829	0.808	22	0.897	0.850
IPI00453821	Nup155	Q99P88	3	0.874	0.982	/			4	1.570	1.089	12	1.413	1.042	8	0.769	0.852	16	0.823	0.851
IPI00354271	Ddx49	Q4FZF3	/			2	0.725	0.970	1	1.569	1.115	1	1.609	0.981	1	1.058	1.007	2	1.056	0.994
IPI00454047	Ctdspl2	Q8BG15-1	/			/			4	1.567	1.151	2	1.601	0.931	/			/		
IPI00850376	Memo1	Q91VH6	2	1.089	1.160	3	1.227	1.011	2	1.564	1.094	4	0.946	0.982	4	1.045	1.049	/		
IPI00131423	Asb6	Q91ZU1	/			/			1	1.563	1.206	/			/			/		
IPI00676074	Mphosph10	Q8K0Z2	/			/			1	1.562	0.975	2	1.602	0.866	1	0.839	0.910	4	0.804	1.001
IPI00135365	Zfand5	O88878	1	0.663	0.572	2	0.972	0.992	2	1.560	1.147	2	0.994	1.186	1	0.895	1.113	4	0.873	1.072
IPI00111885	Uqcrc1	Q9CZ13	2	0.456	0.798	4	0.658	1.161	3	1.558	0.964	7	1.324	0.834	5	0.530	0.731	14	0.527	0.747
IPI00336503	Pdxdc1	Q99K01-2	/			/			7	1.558	0.850	/			14	1.354	1.091	18	1.275	1.038
IPI00112414	Cse1l	Q9ERK4	6	0.966	1.022	13	1.017	1.042	11	1.554	1.159	18	1.494	1.097	14	0.754	0.813	27	0.740	0.827
IPI00133374	Sqstm1	Q64337-1	1	1.028	1.195	6	0.985	0.992	7	1.548	1.002	8	1.598	0.992	11	1.293	0.865	12	1.222	0.854
IPI00331612	Hmga2	P52927	/			3	1.094	0.928	4	1.547	0.811	5	1.538	0.800	6	0.631	0.646	5	0.644	0.692
IPI00121288	Ndufb10	Q9DCS9	/			1	0.722	1.102	1	1.542	0.982	1	1.595	0.956	1	1.043	1.138	3	0.950	0.957
IPI00308852	Dab2	P98078-1	1	1.003	1.089	4	0.971	0.964	3	1.539	0.917	2	1.290	1.113	/			1	0.998	1.171
IPI00944194	Fkbp10	A2A4I0	/			/			5	1.535	1.072	5	1.319	1.005	5	1.743	1.114	/		
IPI00623570	Trip12	O88380	2	1.106	1.118	6	1.102	0.937	5	1.533	1.065	5	1.206	1.035	4	0.758	0.956	8	0.836	0.836
IPI00138319	Zfp36l2	P23949	/			/			1	1.530	1.074	/			/			/		
IPI00622024			/			/			1	1.530	1.132	/			/			/		
IPI00134994	Fam111a	Q9D2L9	/			2	0.719	1.027	1	1.529	0.999	1	1.408	0.932	/			/		
IPI00129927	Mcc	Q3TYX4	1	0.238	0.161	3	1.005	1.012	2	1.524	1.280	2	1.278	1.077	2	1.160	1.094	/		
IPI00387234	Srpk1	O70551	2	0.847	0.973	3	0.892	0.979	1	1.524	1.213	5	1.414	1.118	2	0.948	1.092	6	0.982	0.965
IPI00121431	Hells	Q60848-1	/			3	0.921	0.882	3	1.523	1.089	4	1.710	1.213	/			4	0.690	1.003
IPI00322447	Cadm1	Q8R5M8-1	/			/			2	1.517	0.697	3	1.484	0.786	3	0.887	0.848	/		
IPI00331444	Ipo7	Q9EPL8	/			1	0.962	0.817	2	1.516	1.113	3	1.647	1.168	6	0.765	0.929	14	0.803	0.892
IPI00649972	Vps25	A2A4J8	1	1.074	1.024	1	0.378	0.672	1	1.514	0.939	2	0.987	1.134	/			2	0.889	1.038
IPI00226889	Utp15	Q8C7V3	/			1	0.300	0.825	1	1.511	0.996	2	1.562	0.817	3	0.744	0.801	5	0.700	0.818
IPI00463679	Mum1	Q6DID5	/			/			1	1.510	1.058	1	1.310	1.113	/			1	0.685	1.062
IPI00649326	Myo18a	Q9JMH9-6	/			6	0.932	1.024	2	1.509	0.821	4	1.614	0.909	3	1.244	0.874	6	1.146	0.925
IPI00828268	Cbx2	A2ABG2	1	1.046	0.716	1	1.077	1.171	1	1.508	1.106	2	1.332	0.843	3	0.784	1.540	1	0.957	0.818
IPI00313390	Chchd6	Q91VN4	/			/			1	1.504	0.777	1	1.458	7.792	/			/		
IPI00551348	Rapgef6	B2RUJ6	/			/			3	1.504	0.922	/			/			2	0.952	0.946
IPI00757998	Tacc3	Q99LH8	1	1.056	1.079	2	0.777	0.983	4	1.503	1.026	5	1.520	1.098	3	1.041	1.115	6	0.999	1.055
IPI00555146	Zfp384	Q6P3F1	/			/			1	1.501	0.888	/			/			/		
IPI00136252	Wdr18	Q4VBE8	1	0.688	0.835	3	0.778	0.899	2	1.499	1.034	4	1.076	0.974	/			5	0.998	0.986
IPI00120984	Ndufa8	Q9DCJ5	/			/			1	1.496	2.069	3	1.404	0.997	1	0.756	1.008	3	0.786	0.914
IPI00469323	Dnmt1	P13864-1	10	0.861	1.003	19	0.606	0.739	19	1.496	1.241	26	1.364	1.141	22	1.095	1.007	35	1.073	1.020
IPI00272398	Bcorl1	A2AQH4	/			2	0.192	0.717	1	1.493	1.287	/			/			/		
IPI00226149	Rsl1d1	Q3TAJ5	3	0.993	1.256	2	0.992	1.169	2	1.490	1.045	7	1.389	0.986	4	0.881	0.904	6	0.880	0.881
IPI00119079	Serpinb9b	Q3TJ69	5	0.740	0.955	8	0.728	1.000	7	1.489	1.529	9	1.392	1.344	5	1.236	1.276	15	1.255	1.217
IPI00380243	Spag5	Q7TME2	/			/			1	1.489	1.036	1	1.764	1.081	/			/		
IPI00622390	Eps8	Q08509	2	0.961	0.957	5	0.755	1.046	2	1.488	1.034	5	1.441	0.978	1	0.992	0.738	8	1.305	1.081

IPI00122202	Ncapg	B2RQA7	3	0.857	0.992	6	0.956	0.999	6	1.486	1.061	8	1.527	1.067	8	0.937	0.991	14	0.901	0.962
IPI00223457	Efemp1	Q8BPB5	2	1.048	1.115	2	1.027	1.162	4	1.485	1.070	6	1.419	1.052	8	1.377	1.061	10	1.375	1.079
IPI00947624	Aven	A2AGL4	/			/			1	1.485	1.075	5	1.121	0.877	2	1.136	1.076	/		
IPI00132957	Ddx56	Q9D0R4	/			/			1	1.484	1.302	2	1.330	1.063	1	0.761	0.803	2	0.670	0.916
IPI00649115	Nedd4l	Q8CFI0-1	/			/			1	1.481	1.016	2	1.506	1.029	1	1.054	0.918	/		
IPI00914155	Lcmt2	Q8BYR1-2	/			/			1	1.481	1.449	/			/			/		
IPI00136653	Stx8	O88983	2	0.862	0.958	2	0.835	0.995	2	1.477	0.897	1	1.119	1.008	1	1.502	1.140	2	0.966	1.018
IPI00669709	Pds5a	Q6A026	2	0.929	0.941	5	1.193	1.011	5	1.472	1.218	5	1.510	1.151	4	0.607	0.796	7	0.653	0.732
IPI00515257	Btf3	Q64152-1	3	1.187	1.090	1	1.033	1.057	2	1.472	1.003	3	1.324	1.029	6	0.953	0.903	5	0.939	0.905
IPI00170074		Q8K3D3	/			1	1.051	0.956	1	1.469	0.965	1	1.089	0.934	/			/		
IPI00127415	Npm1	Q61937	7	0.854	0.941	11	0.902	1.033	12	1.468	1.032	9	1.464	0.994	12	0.997	1.001	12	0.989	1.020
IPI00118534	Klf16	P58334	/			1	0.710	1.275	1	1.463	0.986	1	1.278	0.891	1	0.932	1.051	1	0.886	0.901
IPI00929869	Haus5	Q9D786-1	/			/			3	1.462	1.300	2	1.185	0.998	/			/		
IPI00129193	Ppl	Q9R269	/			3	0.948	1.049	5	1.460	1.122	5	1.063	1.082	3	0.827	0.873	12	0.865	0.967
IPI00230394	Lmnb1	P14733	2	0.797	0.772	8	0.558	0.847	7	1.459	0.822	6	1.706	0.842	15	0.567	0.723	21	0.607	0.735
IPI00466518	Cep55	Q8BT07-1	3	0.924	1.019	3	0.758	0.901	4	1.458	0.927	3	1.311	0.887	4	0.993	0.931	7	1.003	0.976
IPI00720058	Nolc1	Q6ZQK6	5	0.810	1.009	8	0.876	0.951	8	1.457	0.846	12	1.446	0.776	10	0.928	0.917	/		
IPI00116770	Rab18	P35293	3	1.141	1.134	4	0.945	1.007	4	1.456	1.105	4	1.455	1.014	2	1.086	0.929	5	1.178	1.003
IPI00126191	Lmnb2	P21619-1	3	0.618	0.884	4	0.793	0.780	5	1.452	0.776	6	1.479	0.828	8	0.665	0.807	10	0.651	0.814
IPI00128615	Gatad2b	Q8VHR5-1	1	0.964	1.086	3	1.051	1.065	2	1.451	1.004	4	1.406	1.036	4	0.908	0.853	6	0.836	0.884
IPI00169658	Znf280c	Q6P3Y5-1	2	0.981	0.894	/			1	1.450	0.959	1	1.494	0.995	2	1.097	0.946	2	0.895	0.931
IPI00224112	Frs2	Q8C180	1	0.968	0.991	1	1.075	1.269	1	1.450	1.041	/			/			/		
IPI00229472	Rbm28	Q8CGC6	/			/			1	1.449	1.013	2	1.161	2.558	/			/		
IPI00117454	Eps15	P42567-1	2	1.155	0.572	9	1.006	0.983	1	1.449	1.204	12	0.987	1.017	2	1.272	0.977	10	1.048	1.058
IPI00461384	Pxdn	Q3UQ28	/			/			1	1.446	0.636	2	0.890	0.749	/			2	0.965	0.829
IPI00330246	Phldb1	Q6PDH0-2	1	0.966	0.930	4	1.040	0.985	2	1.446	1.050	2	1.235	1.124	/			1	1.035	0.848
IPI00331601	Cirh1a	Q8R2N2	/			/			1	1.443	0.915	1	1.299	1.144	2	0.611	0.783	3	0.842	0.888
IPI00224252	Sel1l	Q9Z2G6-2	/			/			1	1.442	1.557	/			/			4	0.291	0.633
IPI00420734	Mff	Q6PCP5-1	/			/			1	1.440	0.890	2	1.470	0.864	/			2	0.730	0.783
IPI00263899	Nqo1	Q64669	2	0.955	0.956	4	0.937	0.970	1	1.439	1.077	4	1.275	1.204	2	1.089	1.035	8	1.015	1.019
IPI00927975	Pfkp	Q8C605	/			/			5	1.436	1.648	5	1.341	1.230	7	1.197	1.281	/		
IPI00268247	Gtse1	Q8R080	6	0.811	1.064	9	0.836	1.064	7	1.434	1.038	10	1.371	1.023	8	0.890	1.063	10	0.935	1.108
IPI00830807	Pcolce	Q61398	3	1.052	1.049	5	1.146	1.106	4	1.434	1.040	4	1.537	1.101	/			/		
IPI00169734	Eif1ad	Q3THJ3	/			/			1	1.433	1.832	1	1.194	1.019	1	0.804	0.919	1	1.089	1.210
IPI00874542	Stim2	B2RQE3	1	0.716	0.923	/			1	1.432	0.678	2	1.533	0.802	/			1	0.937	0.876
IPI00133262	Zeb1	Q64318	1	0.696	0.846	1	0.885	0.820	1	1.432	0.955	2	1.169	0.907	1	1.036	1.117	2	0.997	1.058
IPI00758413	Ard1a	Q3V4D5	2	1.101	0.609	3	1.012	0.973	3	1.430	1.521	3	1.268	1.001	/			3	1.199	0.944
IPI00331708	Mkl1	Q8K4J6-1	2	0.947	1.056	3	0.925	0.995	3	1.429	1.017	4	1.339	1.115	3	1.104	1.276	5	1.071	1.125
IPI00120257	Hspbp1	Q99P31	1	0.904	1.089	1	0.891	1.122	1	1.429	1.070	1	1.323	1.048	1	1.299	1.071	4	1.228	1.154
IPI00227314	Znf609	Q8BZ47	/			/			1	1.429	2.172	2	0.893	1.037	/			2	1.220	0.779
IPI00403864	Cep120	Q7TSG1-1	/			/			1	1.427	1.020	1	1.142	1.412	/			1	1.066	1.318
IPI00308691	Slc2a1	P17809	/			/			2	1.425	0.932	2	1.269	1.026	/			2	1.099	0.805
IPI00649191	Psme3	A2A4J1	2	0.967	1.035	2	0.960	0.979	4	1.424	1.040	5	1.138	0.998	2	1.081	0.884	8	1.092	1.072
IPI00135606	Cbx8	Q9QXV1	/			2	0.850	2.791	1	1.422	1.186	1	1.249	0.930	/			/		
IPI00115580	Eif3m	Q99JX4	2	0.867	0.940	2	0.790	0.775	1	1.421	1.560	7	1.144	1.072	5	1.083	1.048	8	1.021	1.026
IPI00473381	Bnip2	Q9D632	/			/			1	1.420	2.389	/			/			/		
IPI00119138	Uqcrc2	Q9DB77	4	0.655	1.432	3	0.720	1.288	4	1.420	0.722	6	1.413	0.786	8	0.468	0.665	11	0.466	0.697
IPI00757359	Caprin1	Q60865	1	0.952	0.925	3	0.934	0.972	5	1.418	0.926	7	1.377	0.985	8	0.961	0.947	10	0.924	0.961

IPI00396671	Abcf1	Q6P542	2	1.093	1.182	7	1.245	1.121	5	1.417	1.237	7	0.959	0.946	8	0.917	0.912	12	0.927	0.886
IPI00122251	Pdk2	Q9JK42	/			/			1	1.415	1.149	1	1.127	1.049	1	0.845	0.916	/		
IPI00120886	Ybx1	P62960	5	0.835	0.989	10	0.888	1.038	13	1.414	0.892	14	1.363	0.856	18	0.920	0.911	19	0.932	0.915
IPI00649005	Epb4.1	A2A841	2	0.639	0.853	3	0.618	0.803	3	1.412	1.136	4	1.318	1.051	5	0.836	0.925	5	0.827	1.029
IPI00121602	Bhlhe41	Q99PV5	1	0.822	0.852	1	0.896	1.008	1	1.412	1.458	2	0.931	1.010	1	0.916	0.912	2	1.030	0.889
IPI00138406	Rap1a	P62835	3	0.761	1.082	/			4	1.410	2.773	4	0.920	1.057	5	0.967	1.725	5	0.903	1.804
IPI00112460	Ndel1	Q9CZA6-1	2	0.661	0.973	3	0.683	1.012	2	1.410	1.146	5	1.305	1.064	1	13.38	1.187	4	1.121	1.110
IPI00136555	Ymel1l	O88967	2	0.677	0.867	/			1	1.410	0.852	2	1.326	0.852	1	0.804	0.920	6	0.860	0.939
IPI00466717	Thap4	Q6P3Z3-1	1	0.848	0.887	1	1.000	0.992	2	1.409	1.208	2	1.321	0.970	/			2	1.289	1.030
IPI00229294	Epb41l3	Q9WV92-2	/			/			10	1.409	0.780	17	1.480	0.793	17	0.967	0.781	/		
IPI00119776	Utp3	Q9JI13-1	1	0.724	1.119	2	0.741	1.067	2	1.408	0.818	4	1.367	0.826	1	0.965	0.933	4	0.852	0.854
IPI00137336	Gpc1	Q9QZF2	2	0.671	0.970	5	0.655	0.909	3	1.407	0.522	6	1.358	0.614	9	0.817	0.832	13	0.797	0.877
IPI00453582	Grsf1	Q8C5Q4	1	0.696	0.873	2	0.588	0.941	1	1.406	1.116	3	1.184	0.985	5	1.217	0.998	6	1.192	1.022
IPI00421179	Eif4g1	Q6NZJ6-1	14	0.918	0.999	/			21	1.406	1.152	/			27	1.099	1.026	/		
IPI00126343	Sparc	P07214	2	0.993	0.911	2	0.922	0.943	3	1.404	1.087	3	1.367	1.099	5	1.427	1.089	7	1.432	1.144
IPI00831133	Eif2b4	Q61749-2	/			2	0.768	1.886	3	1.404	1.507	3	1.056	1.212	2	1.066	1.018	4	1.006	1.000
IPI00230035	Ddx3x	Q62167	8	1.028	1.009	17	1.055	1.075	9	1.404	1.086	14	1.320	1.055	10	1.041	0.934	27	1.041	0.955
IPI00387212	Naa15	Q80UM3	5	0.992	0.975	11	0.925	0.909	7	1.403	1.095	8	1.300	1.151	5	0.967	0.914	18	0.918	0.968
IPI00129220	Epha2	Q03145	2	0.630	0.750	7	0.616	0.878	2	1.401	1.038	5	1.398	1.017	8	0.871	0.964	12	0.845	0.961
IPI00153919	Ppp1r14c	Q8R4S0	/			/			1	1.400	1.091	2	0.958	1.206	/			1	1.084	1.835
IPI00399663	Cenpe	Q6RT24	/			1	0.825	1.233	2	1.397	0.993	1	1.879	1.089	1	0.777	0.671	2	0.940	0.873
IPI00323134	Cdh2	P15116	/			2	0.672	0.658	2	1.396	0.818	2	1.287	0.830	5	0.777	0.811	6	0.774	0.899
IPI00396812	Exosc3	Q7TQK4	2	1.073	1.083	2	0.958	0.796	1	1.396	1.069	4	1.013	1.010	/			5	0.999	1.119
IPI00115366	Kif15	Q6P9L6	1	0.908	0.885	2	0.814	0.969	4	1.394	0.940	6	1.428	0.897	2	0.789	0.851	8	0.989	0.955
IPI00850044			/			/			/			1	61.96	1.309	/			/		
IPI00110006	Btbd6	Q8K2J9	/			/			/			1	39.80	10.60	/			/		
IPI00331208	Ftsjd1	Q8BWQ4	/			/			/			1	13.01	4.493	/			/		
IPI00664017	R3hcc1	Q8BSI6	/			/			/			1	10.15	1.208	2	1.118	1.100	2	1.148	1.082
IPI00874800	Akr1cl2	Q9DCT1	1	1.048	1.028	1	1.027	0.995	1	1.053	0.879	2	7.457	1.140	/			3	0.979	1.052
IPI00122992	Tfdp1	Q08639	/			/			1	1.198	0.902	1	6.275	1.130	/			1	1.079	0.983
IPI00138143	Cdkn2b	P55271	2	0.916	0.998	2	0.773	0.926	1	0.840	0.880	1	5.962	1.512	/			1	1.009	0.957
IPI00322415	Dennd1a	Q8K382	/			/			/			1	5.622	0.984	/			/		
IPI00406794	Gab1	Q9QYY0	/			/			/			1	4.738	1.336	/			/		
IPI00128346	Cisd1	Q91WS0	/			/			/			1	4.020	1.015	1	0.536	0.821	3	0.579	0.784
IPI00330644		Q80X32	/			/			1	1.219	0.865	2	3.702	0.609	1	3.465	0.867	3	3.918	0.947
IPI00177287	Rnf115	Q9D0C1	/			1	0.994	1.048	/			1	3.516	1.011	1	0.819	0.972	1	1.095	1.254
IPI00405150	B930095I24Rik	Q8C4T0	/			/			/			1	3.505	32.10	/			/		
IPI00457724	Chd6	A3KFM7	/			/			/			2	3.353	1.447	/			/		
IPI00132487	Mrp63	Q9CQF8	/			/			/			1	2.872	0.930	/			/		
IPI00407864	Kif23	Q05DU6	/			/			/			1	2.668	1.327	/			2	1.186	1.011
IPI00315032	All1	P55200-1	/			/			/			1	2.390	1.455	/			/		
IPI00118011	Bmn	Q8K2I4	/			2	0.944	0.811	/			1	2.171	0.867	/			1	1.109	0.713
IPI00120413	Hec1	Q9D0F1	/			/			/			1	2.104	1.360	/			3	0.907	1.450
IPI00119090	Lxrb	Q60644	/			/			/			2	2.095	3.112	1	2.043	2.288	/		
IPI00320204	2210023G05Rik	Q8R097	/			1	0.983	1.002	/			1	2.081	1.428	1	2.219	2.141	/		
IPI00115896	Mrps21	P58059	1	1.191	1.141	1	1.199	1.048	/			1	2.078	1.038	/			1	1.229	0.832
IPI00890905	Faim	Q3U119	/			/			/			2	2.051	1.192	/			/		

IPI00320011	Prc1	Q99K43-1	/			1	0.641	0.966	/			1	2.022	0.831	/			4	0.740	0.841
IPI00119632	Ftsj3	Q9DBE9	/			/			/			1	1.971	1.234	/			/		
IPI00320420	Apoj	Q06890	/			/			/			1	1.966	0.939	/			/		
IPI00112639	Ric8	Q3TIR3	1	0.539	0.685	1	0.962	1.121	1	1.087	0.947	2	1.923	0.984	/			2	0.911	0.867
IPI00227651	Zbtb11	Q8BZQ5	/			/			/			1	1.901	0.885	1	0.896	1.022	1	0.892	0.824
IPI00281538	Rab28	Q99KL7	/			/			/			1	1.898	1.006	/			1	0.788	0.635
IPI00122971	Ncam	P13595-1	/			4	0.709	0.847	4	1.265	1.097	5	1.878	1.192	/			15	0.875	1.017
IPI00121509	Orc2	Q60862	/			/			/			1	1.849	1.073	/			1	1.097	0.863
IPI00943363	Dnajc17	A3KGH2	/			/			/			1	1.842	1.080	/			/		
IPI00270376	Car	P97792-1	/			1	0.704	1.285	3	0.972	1.105	1	1.828	1.014	2	1.090	1.054	3	1.013	0.975
IPI00132531	Ndufb5	Q9CQH3	/			1	0.440	0.976	/			1	1.828	1.193	/			/		
IPI00122383	Imp3	Q921Y2	/			1	0.701	1.061	/			1	1.818	1.156	/			/		
IPI00318561	MNCb-1192	Q9D7Z3-1	/			1	0.928	1.104	/			1	1.817	1.024	/			2	0.950	0.854
IPI00648499	Smsmo	Q921U8-1	/			/			/			1	1.795	1.111	/			/		
IPI00461536	Nol8	Q3UHX0-1	/			/			/			2	1.789	0.927	/			5	0.829	0.947
IPI00130246	Rrp1b	Q91YK2	/			/			/			1	1.783	1.044	1	0.693	0.779	4	0.794	0.902
IPI00653390	Fpgs	P48760-2	/			/			/			1	1.779	40.41	/			/		
IPI00377563	Bal	Q8CAS9-1	/			/			/			1	1.769	1.063	/			/		
IPI00648327	Kif2c	Q3TTL2	/			/			/			3	1.753	1.001	/			/		
IPI00402911	Mphosph10	Q810V0	/			1	0.616	0.778	/			2	1.725	1.159	1	0.829	1.121	4	0.863	1.098
IPI00221714	Smndc1	Q8BGT7	/			/			2	1.343	0.908	2	1.705	0.962	1	1.194	0.895	3	0.972	0.854
IPI00133839	Caip150	Q9QWF0	/			/			/			1	1.702	2.277	/			3	0.874	0.943
IPI00648998	Rps6ka1	Q3TIM6	/			/			/			1	1.689	1.510	/			/		
IPI00315576	Neu	O35657	/			/			/			1	1.677	0.842	/			1	1.267	1.064
IPI00114667	Mov34	P26516	2	1.012	1.039	4	1.000	1.054	5	1.120	0.981	5	1.657	0.998	3	1.074	1.052	9	1.037	0.965
IPI00120592	Ly6	P05533	/			/			/			1	1.654	1.849	/			/		
IPI00314149	Ccnb2	P30276	/			/			/			1	1.647	0.991	1	2.637	0.555	/		
IPI00138068	Kiaa0938	Q80TN7	/			2	0.818	1.223	/			1	1.646	1.365	/			/		
IPI00228202	Dip	Q8CB44	1	1.080	1.018	2	1.205	1.219	/			1	1.632	0.989	/			/		
IPI00311453	Nol1	Q922K7	1	0.835	1.250	1	1.024	1.142	/			2	1.632	0.937	/			4	0.725	0.889
IPI00110708	Ccdc51	Q3URS9-1	/			/			/			1	1.630	1.068	1	0.460	0.960	2	0.581	0.862
IPI00311892	Ucrbp	Q00899	/			/			/			1	1.628	1.040	/			1	0.924	0.983
IPI00831121	Armc9	Q9D2I5-3	/			/			/			1	1.626	1.407	/			1	1.027	0.982
IPI00310474	Brp16	Q8C3I8	1	0.891	1.055	1	0.903	0.986	/			2	1.618	1.229	/			4	1.063	1.176
IPI00420344	Kiaa0690	Q6P5B0	/			1	1.007	0.849	/			2	1.599	1.377	/			4	0.670	0.880
IPI00461966	Fam132b	Q6PGN1	/			/			/			2	1.594	0.930	1	0.789	1.362	1	1.125	1.024
IPI00225974	Nob1	Q8BW10	/			1	0.904	0.859	1	1.237	1.272	1	1.590	1.209	2	0.957	1.151	3	1.067	1.000
IPI00136354	Dmahp	P70178	/			/			/			1	1.584	0.879	/			1	0.838	0.762
IPI00869399	Bub1b	A2ARS1	2	0.907	0.913	3	0.970	1.130	2	1.366	1.032	3	1.581	0.946	2	0.942	0.992	1	0.873	1.028
IPI00556867	Maged1	Q571N9	/			/			/			2	1.580	1.342	/			/		
IPI00830613	Epb4	Q9Z2H5-1	/			8	1.067	0.922	/			5	1.579	0.850	3	0.871	0.847	12	1.093	0.973
IPI00135452	Kiaa0468	Q64519	/			/			/			1	1.573	0.807	/			/		
IPI00124178	Lcb2	P97363	/			2	1.005	0.945	1	0.846	1.029	1	1.562	1.130	/			6	0.887	0.964
IPI00775961	Zmynd11	Q8R5C8	/			/			/			1	1.554	1.094	/			/		
IPI00890007	Akap1	B1AR25	/			/			1	1.391	1.129	1	1.545	0.813	2	0.675	0.651	4	0.654	0.732
IPI00125505	Arhgap31	A6X8Z5	/			/			1	0.726	1.239	2	1.542	1.134	/			4	1.099	1.273
IPI00652987	Ddx21	Q3TVJ3	/			/			/			15	1.535	0.936	/			/		
IPI00133679	Fam125a	Q78HU3	/			3	1.050	0.986	2	1.094	1.017	1	1.535	1.002	2	1.184	0.669	3	1.039	0.901

IPI00752277	D2Ertd750e	Q9D9Z1	/			/			/			3	1.523	1.116	/			1	0.993	0.919
IPI00653300	Tm9sf2	Q3TWB8	/			/			1	1.185	1.070	1	1.521	1.451	/			/		
IPI00330591	Csda	Q9JKB3-1	7	0.806	0.903	/			8	1.052	1.121	6	1.519	0.973	10	1.030	1.008	10	1.104	0.998
IPI00123040	Ptpk	P35822	1	0.901	0.745	1	1.012	0.957	1	1.394	1.026	2	1.518	1.045	2	0.905	1.089	2	0.964	0.702
IPI00112101	Stip	Q9ERA6	/			/			/			1	1.517	1.262	1	0.816	0.730	5	0.720	0.949
IPI00153445	Chmp7	Q8R1T1-1	/			/			/			1	1.511	0.902	/			1	1.195	0.978
IPI00132151	Apacd	Q9CQ79	2	1.000	0.988	2	0.929	0.872	1	1.157	0.918	2	1.504	1.067	2	0.878	1.047	3	1.041	0.984
IPI00828463	Noc2l	Q3UZI6	/			1	0.986	1.058	/			1	1.502	1.022	/			1	0.765	0.949
IPI00380696	Ckap2l	Q7TS74-1	/			1	0.854	0.714	/			1	1.501	1.293	/			/		
IPI00226564	Cip2a	Q8BWY9	/			/			/			1	1.499	0.919	/			4	0.880	0.962
IPI00331030	Fignl1	Q8BPY9	/			/			/			1	1.498	0.837	/			2	1.081	0.920
IPI00127679	Ddx32	Q8BZS9-2	/			/			/			1	1.497	0.909	/			1	1.327	0.969
IPI00224127	D2Wsu81e	Q3UHX9-1	/			2	0.837	1.091	/			1	1.494	0.840	/			1	0.955	0.899
IPI00133440	Phb	P67778	2	0.642	1.307	5	0.597	1.380	/			7	1.494	0.820	4	0.535	0.720	10	0.548	0.775
IPI00652944	Fxr2	Q3TA75	3	0.780	0.982	4	0.714	0.860	6	1.306	0.944	5	1.494	1.110	6	0.858	0.980	9	0.821	1.072
IPI00278864			/			/			/			1	1.493	1.143	/			/		
IPI00165762	Rbm19	Q8R3C6-1	1	0.979	1.201	2	0.970	1.136	/			5	1.491	0.923	/			7	0.903	0.996
IPI00123915	Rlim	Q9WTV7	/			/			/			1	1.488	1.044	1	1.014	1.093	/		
IPI00336965	Ddx52	Q8K301	/			/			/			2	1.487	1.118	/			/		
IPI00762434	Hectd1	Q05BY9	3	1.097	0.957	5	1.202	1.028	2	1.274	1.005	7	1.486	1.097	3	1.058	0.917	6	1.044	1.062
IPI00132770	Chaf1b	Q9D0N7	1	0.844	1.050	4	0.803	1.008	3	1.155	1.035	4	1.484	1.076	3	0.885	1.061	7	0.902	0.965
IPI00655041	Exoc2	Q9D4H1	1	0.481	1.907	2	0.479	0.868	/			4	1.484	1.245	3	0.685	0.821	7	0.782	0.915
IPI00223851	Papd5	Q68ED3	/			1	0.778	0.630	/			2	1.479	1.120	/			1	1.111	0.838
IPI00323045	Kiaa0175	Q61846	/			/			/			1	1.479	0.943	/			1	1.010	1.128
IPI00318537	Cuedc2	Q9CXX9	/			/			/			1	1.478	0.939	1	0.841	0.937	3	1.036	1.019
IPI00785218	Nol14	Q3TSX5	/			/			/			3	1.476	0.822	/			/		
IPI00308785	Cox2	Q05769	/			/			/			1	1.475	1.121	/			/		
IPI00126389	Fxr2	Q6P5B5	/			5	0.804	1.105	6	1.314	1.586	5	1.475	0.874	6	1.035	1.228	10	0.876	0.942
IPI00228584	Abin	Q9WUU8-1	/			/			/			1	1.474	0.805	1	0.899	0.852	1	1.063	0.795
IPI00224697	Kiaa4006	Q61151	/			1	0.869	1.140	/			2	1.474	1.264	/			5	0.903	0.964
IPI00132728	Cyc1	Q9D0M3-1	/			/			/			1	1.472	0.882	2	0.542	0.701	2	0.498	0.705
IPI00319135	Surf1	P09925	/			/			/			1	1.471	1.174	/			/		
IPI00120719	Cox5a	P12787	/			/			/			1	1.469	1.035	/			4	0.894	0.764
IPI00461329	Pex13	Q9D0K1	/			1	0.919	0.588	/			1	1.465	0.983	/			1	0.815	1.030
IPI00466984	Nav2	B2RWS4	/			/			/			2	1.464	1.521	/			/		
IPI00848508	Itfg2	Q91WI7-2	/			/			/			1	1.463	1.062	/			2	1.090	1.511
IPI00227880	Pkcd	P28867-2	/			/			/			2	1.461	1.129	/			1	1.182	0.913
IPI00120346	Rab27b	Q99P58	1	0.784	1.030	1	0.965	1.032	/			1	1.461	0.905	/			2	0.926	0.935
IPI00312509	Ark	Q00993	2	0.990	0.892	2	0.093	0.065	2	1.360	0.943	2	1.459	1.068	2	0.946	0.880	4	1.001	1.908
IPI00309059	Patl1	Q3TC46	/			/			/			1	1.458	1.042	/			2	1.222	1.147
IPI00380313	Bxdc5	Q7TND5	/			/			/			1	1.458	0.808	/			/		
IPI00467123	Tim1	Q9R1X4-1	1	0.903	1.040	/			/			3	1.454	1.031	1	0.647	0.817	5	0.715	0.823
IPI00462476	Ankhd1	Q5BJ28	2	1.023	1.045	6	0.945	1.082	/			3	1.451	0.981	/			5	1.025	1.092
IPI00654197	Aagab	Q3TW04	/			/			/			1	1.449	1.123	/			/		
IPI00462886	Ikbip	Q9DBZ1-2	/			/			/			3	1.443	1.038	/			4	0.917	1.282
IPI00655040	Cit	P49025-5	/			/			/			2	1.442	1.023	/			/		
IPI00474974	Dnmt	P13864-2	10	0.893	1.176	19	0.884	1.007	19	1.349	1.124	26	1.441	1.069	21	1.104	0.928	33	1.088	1.000
IPI00880430	Jmjd6	Q9ERI5-1	1	0.823	0.278	1	0.879	0.918	/			1	1.440	1.167	3	1.509	1.139	3	1.240	1.314

IPI00323231	Ifngr	P15261	/			/			/			1	1.440	0.724	2	0.940	1.026	2	1.088	1.142
IPI00153381	Uqcr10	Q8R1I1	/			/			1	1.342	0.788	1	1.439	0.823	1	0.571	0.774	2	0.542	0.801
IPI00126176	Mgcracgap	Q9WVM1	/			2	0.752	1.138	/			1	1.437	1.066	/			/		
IPI00461969	Cdc123	Q8CII2-1	/			2	0.902	0.965	/			3	1.436	1.097	2	1.088	1.021	5	1.073	1.047
IPI00311260	Nsun5	Q8K4F6	/			/			/			1	1.434	1.818	/			/		
IPI00124051	Mpp5	Q9JLB2	/			/			/			2	1.432	1.188	/			1	0.947	1.624
IPI00221790	Mapk1ip1l	Q8BH93	1	1.122	1.246	1	1.178	1.031	1	1.287	1.095	1	1.430	1.007	1	1.100	1.084	1	1.098	1.082
IPI00417158	Est1a	P61406	/			/			/			1	1.425	1.056	/			2	0.979	1.032
IPI00124245	G3bp2	P97379-1	5	0.865	1.047	5	0.853	1.054	7	1.367	1.129	7	1.424	1.153	4	1.025	0.921	7	1.019	0.987
IPI00112856	Nek7	Q9ES74	2	1.035	0.987	3	1.000	1.127	/			5	1.421	1.153	1	1.165	3.285	5	0.875	0.937
IPI00128880	Imp4a	Q8VI75	1	0.806	1.191	6	0.958	1.010	3	1.372	1.195	7	1.418	1.145	5	0.950	0.945	14	0.937	0.930
IPI00785295		Q0VG62	/			/			/			1	1.417	0.959	/			/		
IPI00554845	Immt	Q8CAQ8-5	/			1	0.624	1.495	2	0.516	0.351	9	1.417	0.893	/			7	0.644	0.839
IPI00752710	Cbf2	P53569-1	2	0.978	0.981	1	0.785	1.081	1	1.355	0.839	1	1.416	0.855	3	0.829	0.927	9	0.842	0.826
IPI00222302	Tbc1d25	A1A5B6	/			/			/			1	1.415	1.085	/			/		
IPI00132659	Dfrp2	Q9CQK7	3	1.086	0.988	3	0.991	0.912	/			1	1.415	1.028	/			3	1.175	1.037
IPI00380329	Kiaa1495	Q3UMG5-1	/			/			/			1	1.414	1.128	/			3	1.166	1.276
IPI00109419	Kif4	P33174	3	0.806	0.735	/			/			11	1.413	1.038	7	0.993	1.053	15	1.000	1.028
IPI00119509	Naa16	Q9DBB4	/			/			/			3	1.411	1.036	/			5	0.863	1.018
IPI00454030	Exoc3	Q6KAR6	/			/			/			3	1.409	1.175	/			4	0.735	0.985
IPI00108410	Atad1	Q9D5T0	/			/			/			1	1.407	0.676	1	0.638	0.520	3	0.698	0.572
IPI00114822	Atpbd3	Q99J10	/			/			/			1	1.406	1.111	1	0.595	0.856	2	0.944	0.923
IPI00222555	Cal1l	P08207	/			1	0.727	1.302	/			1	1.402	0.703	3	0.768	0.919	4	0.797	0.957
IPI00463173	Trific	Q7TNM2-2	/			/			/			1	1.401	103.2	/			1	7.288	12.87
IPI00469835	Impdh1	P50096	/			2	0.914	0.833	2	1.380	1.409	3	1.399	1.474	1	1.605	1.276	4	1.380	1.149
IPI00856470			/			/			/			2	1.398	1.021	/			2	1.246	1.367
IPI00652882	Ffr	Q3UVL4-1	/			2	1.058	1.186	/			1	1.397	1.467	/			3	0.917	0.807
IPI00133594	Rrp7a	Q9D1C9	/			/			/			1	1.397	1.202	/			2	0.941	0.982
IPI00134493	Zfx	P17012	/			/			/			1	1.397	0.963	/			1	0.971	1.149
IPI00407108	Gm111	Q6PAQ4	/			/			/			2	1.392	0.904	1	0.581	0.932	3	0.841	0.911
IPI00400349	Kiaa0099	Q80U78-2	/			/			/			5	1.392	1.047	/			/		
IPI00420601	Kiaa0190	P52479	/			/			/			5	1.392	1.138	3	0.954	1.184	4	1.046	0.982
IPI00135048	Vps33a	Q9D2N9	/			1	0.966	1.110	/			1	1.392	0.819	/			/		
IPI00858249	Eif4g1	Q3UZD9	/			23	0.997	1.059	/			31	1.392	1.109	/			44	1.121	1.037
IPI00221778	Ankrd16	A2AS55-1	/			/			1	1.353	1.085	1	1.389	1.000	/			/		
IPI00229465	Kiaa1561	Q8CGB3-3	/			2	1.004	0.902	/			1	1.388	0.877	/			2	0.985	1.001
IPI00830844	Maged2	Q3TFU3	/			4	0.985	1.016	/			1	1.384	1.243	1	1.159	1.217	4	1.098	1.004
IPI00321802	Tax1bp1	Q3UKC1	/			2	1.086	0.934	3	1.254	0.887	5	1.383	1.050	/			6	1.123	0.858
IPI00330289	Epb4.1l2	B6ZHD0	/			/			7	1.287	0.831	10	1.383	0.808	16	0.919	0.856	30	0.885	0.903
IPI00225915	D8Ertd233e	Q8C5L7	/			2	1.060	1.243	/			1	1.383	0.904	/			2	0.882	0.809
IPI00273851	Tlk1	Q8C0V0	/			/			1	1.098	1.230	2	1.379	1.093	2	0.783	0.855	3	1.164	1.050
IPI00896604	Ddx10	Q80Y44	/			1	0.853	0.909	2	0.660	0.213	3	1.376	0.992	/			3	0.868	0.947
IPI00928565	Cep350	Q6A062	/			/			/			3	1.376	0.783	/			/		
IPI00116199	Haus8	Q99L00-1	/			1	0.904	1.099	1	1.255	1.047	1	1.375	1.076	1	1.140	4.736	/		
IPI00457661	Kiaa0072	Q8BJY1	6	0.904	0.955	7	0.876	1.013	8	1.341	1.069	12	1.374	1.059	12	0.859	0.888	15	0.860	0.913
IPI00130489	Rab35	Q6PHN9	2	0.884	1.020	3	0.704	1.061	1	1.131	0.734	1	1.373	0.856	2	0.774	0.728	2	0.931	0.912
IPI00121225	Eml3	Q8VC03	4	1.036	0.970	1	0.932	0.475	1	1.072	0.954	3	1.372	1.016	2	1.478	0.937	3	1.300	1.476
IPI00273023	Ahsa2	Q8N9S3-1	2	1.073	1.053	3	0.976	0.947	/			1	1.372	1.161	/			4	1.040	0.997

IPI00222125	Comtd1	Q8BIG7	/			/			/			2	1.371	0.948	/			5	0.562	0.844
IPI00470092	Ckap2	Q3V1H1	7	0.808	1.126	10	0.839	1.039	13	1.383	0.975	14	1.371	0.987	15	0.902	1.097	18	0.932	1.056
IPI00453808	Ddx55	Q6ZPL9	/			/			/			1	1.371	1.215	/			/		
IPI00881767			/			/			/			/			1	122.9	11.59	/		
IPI00135678	Xk	Q9QXY7	/			/			/			/			1	12.20	61.82	/		
IPI00944702	Tsr2	Q8C8T8	/			/			1	0.920	0.921	4	0.950	0.918	1	10.60	1.105	/		
IPI00330404		Q80UY1	1	0.873	0.934	2	0.936	0.931	1	1.335	1.177	2	1.117	1.088	1	2.293	1.041	3	1.106	0.907
IPI00923659	Zmat3	B9EI21	/			/			/			2	0.964	0.997	1	2.016	1.236	/		
IPI00170090	Ccdc52	Q8C804	/			/			/			/			1	1.997	1.210	/		
IPI00275577	Trappc1	Q5NCF2	1	0.753	0.896	/			/			1	0.765	1.062	1	1.939	1.661	1	0.983	1.029
IPI00666034	Apob	Q3UH74	4	1.003	1.082	/			4	0.752	13.30	3	1.105	18.93	2	1.933	6.195	/		
IPI00229321	Wdr24	Q8CFJ9	/			/			/			/			1	1.906	0.904	/		
IPI00845788	Maea	Q4VC33-2	/			/			1	0.996	0.946	2	1.175	0.996	2	1.793	1.105	3	1.148	0.989
IPI00653791	Tbc1d22a	Q8R5A6-2	/			/			/			2	0.976	1.051	1	1.764	73.61	/		
IPI00135233	Akap10	O88845-1	/			1	1.081	1.208	/			1	1.243	0.833	1	1.729	1.554	2	1.090	0.942
IPI00624863	Paics	Q9CQ38	2	1.168	1.024	9	1.177	0.986	8	0.937	1.228	11	0.924	1.197	9	1.721	1.075	19	1.716	1.051
IPI00555113	Rpl18	P35980	4	1.211	1.144	4	1.212	1.110	5	0.855	1.055	5	0.846	1.011	6	1.680	0.908	7	1.631	0.911
IPI00120084	Dcaf6	Q9DC22	/			2	1.070	0.883	/			/			1	1.661	1.033	3	1.051	0.929
IPI00464128	Cdk13	Q69ZA1-1	/			/			/			2	1.060	0.891	1	1.659	1.017	2	1.017	0.900
IPI00229849	Ppat	Q3TKC5	/			1	0.028	0.949	3	1.010	1.046	4	0.831	0.959	3	1.647	0.962	8	1.598	0.865
IPI00124707	Fstl1	Q62356	/			/			2	0.820	0.984	3	0.839	0.891	2	1.640	1.377	4	1.386	0.997
IPI00381303	Man2b1	O09159	/			/			/			5	0.803	0.990	2	1.632	1.315	6	1.126	0.971
IPI00221580	1810063B05Rik	Q8BGD8	1	0.899	0.797	1	1.009	0.883	/			/			1	1.620	0.994	2	0.906	0.970
IPI00311591	Ube2z	Q3UE37	2	1.019	1.121	4	1.078	0.973	1	1.147	0.997	3	1.039	1.048	2	1.594	1.285	7	0.982	1.060
IPI00938479	Wdr81	Q5ND34-1	/			/			2	0.934	1.110	4	0.693	0.876	1	1.593	2.197	/		
IPI00114671	Ptprg	Q05909	/			/			/			/			1	1.589	1.006	/		
IPI00330363	Rpl7a	P12970	/			/			10	0.811	0.971	/			12	1.549	0.928	15	1.488	0.915
IPI00624030	Rpe	B2KGF0	1	0.954	1.036	3	0.994	1.026	2	1.000	1.031	3	0.960	1.013	1	1.547	1.156	1	1.102	1.082
IPI00400352	Ltbp3	Q61810-1	/			1	1.039	0.909	2	1.254	1.118	2	1.277	0.975	1	1.545	1.122	2	0.973	0.940
IPI00869475	Rpl36	Q5M9L1	/			/			/			/			3	1.534	0.981	/		
IPI00225301	Hsdl1	Q8BTX9	/			/			1	0.853	0.744	1	0.136	0.930	2	1.516	0.864	3	0.962	0.964
IPI00108254	Gins2	Q9D600	1	1.017	0.905	1	0.723	0.924	1	1.161	1.003	1	1.185	1.018	2	1.504	1.031	2	1.035	0.956
IPI00127902	Dhx30	Q99PU8-3	1	1.085	1.049	/			1	0.885	1.217	5	1.027	1.036	2	1.499	1.459	/		
IPI00111412	Rpl4	Q9D8E6	9	1.119	1.132	12	1.230	1.060	12	0.845	0.980	12	0.855	0.990	15	1.479	0.877	19	1.405	0.924
IPI00307907	Haus4	Q8BFT2	/			/			/			2	0.942	0.963	1	1.477	1.403	3	0.976	1.020
IPI00122740	Macrod1	Q922B1	/			/			1	0.927	1.041	/			1	1.475	1.430	2	1.010	1.278
IPI00342938	Mcat	Q8R3F5	/			/			/			3	0.989	0.980	1	1.472	1.393	4	1.033	1.026
IPI00115902	Rpl35a	O55142	2	1.201	1.090	3	1.223	1.160	1	0.974	1.195	2	0.911	1.007	2	1.470	0.944	4	1.276	0.919
IPI00473728	Rpl14	Q9CWK0	5	1.203	1.089	5	1.162	1.095	4	0.889	0.926	4	0.820	0.900	3	1.463	0.885	6	1.394	0.927
IPI00775775	Gripap1	A2AEW8	2	0.908	0.992	4	1.050	0.780	2	1.246	74.98	2	1.055	0.934	1	1.463	1.185	8	1.136	1.006
IPI00112701	Psmg3	Q9CZH3	1	1.175	1.080	2	1.064	1.100	3	1.126	1.025	4	1.027	0.957	2	1.453	1.004	4	0.939	0.948
IPI00119261	Dck	P43346	1	1.017	0.922	1	0.976	0.949	1	1.252	1.079	1	1.140	0.840	1	1.453	1.309	3	1.068	0.977
IPI00880213	Rpl18a	P62717	/			/			/			/			4	1.446	0.916	/		
IPI00120176	Pcolce	Q61398	/			/			/			/			4	1.442	0.927	5	1.325	0.936
IPI00310701	Lmf2	Q8C3X8	/			/			/			1	0.353	0.743	1	1.437	1.090	1	1.288	0.903
IPI00338452	Col4a2	P08122	/			1	0.550	0.663	/			2	0.960	0.598	2	1.436	1.348	2	0.974	0.996
IPI00222188	Col1a2	Q01149	4	0.814	0.844	8	0.994	0.929	3	1.241	0.899	3	1.107	0.826	2	1.434	1.373	3	1.526	1.046
IPI00323806	Rpl24	Q3UW40	2	1.197	1.083	4	1.156	1.114	3	1.006	1.064	6	1.040	1.025	5	1.430	0.928	6	1.344	0.947

IPI00223217	Rpl13a	P19253	4	1.114	1.113	4	1.040	1.071	4	0.794	0.987	4	0.836	0.988	3	1.430	0.887	7	1.345	0.906
IPI00125138	Csf1	P07141-1	/			2	1.225	1.002	1	1.338	0.917	2	1.350	1.433	1	1.429	0.961	2	1.357	1.013
IPI00626628	Rpl27a	Q9CQ16	3	1.123	1.054	4	1.172	1.099	3	0.938	1.041	3	0.946	1.058	4	1.429	0.958	5	1.350	0.975
IPI00387494	Hspa2	B7U582	/			9	1.108	1.084	8	0.791	0.902	8	0.962	1.076	9	1.426	1.406	14	1.091	1.090
IPI00222547	Rpl28	P41105	1	1.187	1.034	5	1.185	1.092	4	0.885	0.979	6	0.884	0.990	6	1.423	0.930	5	1.328	0.950
IPI00411004	Hdac4	Q6NZM9-1	/			1	0.949	0.699	/			/			1	1.421	1.064	3	1.032	0.925
IPI00311236	Rpl7	P14148	6	1.155	1.108	/			9	0.880	0.978	12	0.848	0.994	12	1.412	0.870	19	1.454	0.950
IPI00229662	Mgmt	P26187	/			2	0.828	0.984	2	0.822	1.044	2	0.873	0.996	1	1.410	1.346	2	0.962	1.108
IPI00649135	Gstm1	A2AE89	5	1.124	0.993	13	1.145	0.997	7	1.160	1.126	10	1.113	1.092	12	1.405	0.954	15	1.339	0.970
IPI00137831	Rcn1	Q05186	2	1.131	0.849	6	1.162	1.038	2	0.928	0.876	4	0.883	0.865	2	1.404	0.910	5	1.004	0.939
IPI00119524	Strn4	P58404-1	/			4	1.002	0.831	3	0.956	1.221	3	1.053	1.098	1	1.400	1.329	5	1.004	1.140
IPI00136333	Oxsm	Q9D404	/			/			1	0.781	0.847	1	0.685	0.855	1	1.397	1.438	2	0.985	1.012
IPI00128376	Akr1c14	Q91WT7	/			/			2	0.781	0.763	3	1.152	0.943	4	1.394	1.033	5	1.463	0.985
IPI00915054	Rpl10	Q3THJ6	/			/			4	0.982	1.191	3	1.010	1.040	4	1.390	0.907	/		
IPI00315593	Naga	Q9QWR8	1	1.229		2	0.962	0.863	/			3	1.000	1.145	2	1.387	1.005	5	1.333	1.080
IPI00120754	Gabarap	Q9DCD6	/			/			/			/			1	1.382	0.917	/		
IPI00226216	Arhgef19	Q8BWA8	/			/			/			/			1	1.381	1.024	1	1.447	1.265
IPI00123194	Bgn	P28653	2	1.168	0.918	5	1.047	0.855	5	1.251	0.919	6	1.175	0.866	7	1.372	0.806	8	1.360	0.836
IPI00120982	Fbxo22	Q78JE5	/			/			/			1	1.025	0.989	1	1.366	1.070	1	1.234	0.760
IPI00659860	Lrrfip2	Q8C062	/			3	0.961	0.886	3	1.146	0.971	3	1.184	6.789	2	1.366	0.903	4	1.015	1.056
IPI00134820	Drg2	Q9QXB9	1	1.203	1.027	3	1.239	1.105	3	1.106	1.151	7	1.033	1.090	3	1.364	1.275	10	1.350	1.199
IPI00889948	Ecm1	B7ZNR0	/			/			2	1.144	0.940	2	1.161	0.885	2	1.352	1.034	/		
IPI00313222	Rpl6	P47911	10	1.146	1.137	7	1.153	1.148	7	0.860	0.973	7	0.897	0.960	9	1.350	0.908	12	1.308	0.933
IPI00123264	Pole3	Q9JKP7	/			1	1.108	1.187	1	1.067	1.132	2	1.011	0.888	2	1.349	1.079	2	0.951	0.981
IPI00273803	Rpl15	Q9CZM2	4	1.075	1.303	5	1.153	1.019	5	0.797	0.944	5	0.873	0.939	7	1.349	0.866	10	1.314	0.906
IPI00798610	Gga3	A2A9W6	/			3	0.921	0.966	/			2	1.336	1.105	1	1.346	1.374	3	1.005	1.030
IPI00135411	Apba3	O88888	/			/			/			2	1.210	3.100	1	1.343	1.034	2	1.303	1.009
IPI00129399	Rabac1	Q9Z0S9	/			/			/			2	1.253	0.897	1	1.340	0.818	2	1.375	0.998
IPI00225526	Qrich1	Q3UA37	1	0.973	0.842	3	1.057	0.991	/			4	1.139	1.045	1	1.333	1.104	3	1.088	1.033
IPI00121517	Pter	Q60866-1	1	1.111	1.023	3	0.987	1.035	1	0.871	0.763	3	0.856	1.003	1	1.327	2.363	5	1.039	0.999
IPI00122426	Rpl19	P84099	2	1.170	1.010	3	1.154	0.957	1	0.842	1.097	1	0.873	1.116	4	1.325	0.948	4	1.408	0.949
IPI00849670	Myof	B9EK95	31	1.182	1.035	41	1.120	1.020	34	0.837	0.899	/			47	1.323	0.929	/		
IPI00474711	Pkn1	Q3UEA6	3	1.202	1.115	6	1.037	0.784	3	0.762	0.950	3	1.066	0.981	1	1.323	1.098	6	1.077	0.964
IPI00125534	Dok1	P97465	2	0.788	0.845	2	0.764	0.697	2	1.074	1.210	3	0.925	1.098	1	1.322	1.226	2	0.835	1.478
IPI00409393	Ltbp1	Q8CG19-1	2	1.096	0.747	3	0.802	0.772	/			/			1	1.322	1.052	/		
IPI00885334	Ecm1	Q3TXB7	2	1.098	1.096	4	1.021	0.967	/			/			2	1.321	1.080	3	1.677	1.551
IPI00124640	Grn	P28798	4	1.053	0.942	3	1.043	0.959	3	1.029	0.909	5	1.065	0.892	8	1.315	0.939	9	1.280	0.976
IPI00132452	Asf1a	Q9CQE6	2	1.048	1.046	3	0.924	0.977	2	1.094	0.869	3	1.350	1.000	2	1.314	0.853	1	0.986	0.943
IPI00117025	Cdk5rap3	Q99LM2	/			3	0.831	0.949	1	1.116	0.948	3	1.040	1.003	2	1.310	1.121	6	1.145	1.028
IPI00228548	Eno3	P21550	8	0.901	1.061	9	0.940	1.142	5	1.097	1.250	7	1.149	1.259	10	1.306	1.384	15	1.221	1.188
IPI00229690	Adssl1	P28650-2	4	1.135	0.983	7	1.213	1.006	6	0.947	1.084	8	0.995	1.047	6	1.302	1.080	13	1.178	1.062
IPI00395040	Kcmf1	Q80UY2-1	/			/			/			1	1.015	0.946	1	1.300	1.200	2	1.159	0.979
IPI00465884	Nploc4	P60670-1	4	0.897	0.898	5	1.077	1.077	3	1.068	1.168	6	1.006	0.966	5	1.299	1.137	9	1.043	1.028
IPI00113517	Ctsb	P10605	3	1.082	0.889	3	1.128	0.938	3	1.037	1.004	7	1.010	0.974	8	1.299	0.946	9	1.240	0.968
IPI00323822	Rras2	P62071	/			2	0.844	1.208	/			2	0.937	0.887	2	1.298	0.808	3	0.662	0.781
IPI00228343	Fech	P22315	/			2	0.829	0.945	5	0.796	0.978	4	0.779	0.957	4	1.296	1.083	7	1.224	1.013
IPI00122633	Acsf2	Q8VCW8	3	0.820	0.943	4	0.849	0.908	4	1.025	1.209	4	1.011	1.303	3	1.295	1.468	3	1.212	1.377
IPI00223231	Qsox1	Q8BND5-1	/			/			2	1.186	1.168	3	1.070	0.816	1	1.294	0.965	4	1.359	0.898

IPI00608021	Ddi2	A2ADY9	4	1.006	0.888	4	1.076	0.942	4	0.971	1.076	5	0.904	0.881	3	1.293	1.113	6	1.043	1.021
IPI00130627	Lgmn	O89017	/			/			/			/			2	1.292	1.136	3	1.135	0.963
IPI00555045	Rpl21	O09167	/			1	1.146	0.903	4	1.001	1.040	5	0.996	1.054	4	1.292	0.916	5	1.235	0.942
IPI00399761	Diaph2	O70566-2	/			/			/			1	0.871	0.952	1	1.291	0.968	4	1.097	0.962
IPI00462979	Fyttd1	Q91Z49-1	1	0.934	0.958	1	0.970	0.888	1	0.632	0.984	1	0.672	0.992	1	1.291	0.998	2	1.251	0.949
IPI00752148	2900010J23Rik	A2AN41	1	0.913	1.190	/			1	1.204	1.135	2	1.074	1.039	1	1.289	1.027	3	0.920	0.968
IPI00676243	Map1a	Q9QYR6-2	1	0.795	1.001	5	0.925	1.175	/			/			1	1.286	1.376	2	1.078	1.256
IPI00918862	Pccb	A0PJE6	/			/			3	0.673	0.887	5	0.705	0.867	3	1.286	0.934	/		
IPI00480275	Pfdn5	Q9WU28	1	1.072	1.123	2	1.120	1.036	/			2	0.950	0.966	2	1.284	1.159	4	1.059	0.985
IPI00854911	Max	B2RS19	1	0.891	0.945	1	1.149	2.534	/			1	0.851	0.792	1	1.283	1.015	1	1.174	1.056
IPI00222147	Rufy1	Q8BIJ7	2	1.072	1.052	4	0.900	1.047	3	1.144	1.056	3	1.169	1.025	1	1.283	0.980	5	1.257	0.949
IPI00387422	Zyx	Q3TCR9	7	0.909	0.956	11	0.899	0.969	12	1.175	1.272	15	1.181	1.258	14	1.282	1.281	14	1.283	1.263
IPI00858168	Mrpl39	A6X954	/			/			/			1	1.162	0.815	1	1.281	0.850	3	0.953	0.813
IPI00278600	Morf4l1	P60762-1	2	0.780	1.042	3	1.227	1.149	2	1.179	1.133	4	1.168	1.071	2	1.278	1.378	4	1.126	1.034
IPI00655217	Xdh	B2RUJ7	4	1.105	0.896	6	0.948	0.814	10	1.185	1.057	12	1.183	1.021	8	1.275	1.004	21	1.314	0.944
IPI00454015	Sf4	Q8CH02	/			2	1.019	1.001	2	1.131	0.867	11	1.220	1.019	3	1.275	1.327	6	1.059	1.067
IPI00466820	Rps8	P62242	/			/			/			/			6	1.272	0.935	10	1.254	0.927
IPI00133226	Zfand2b	Q91X58	1	0.866	1.306	2	0.919	0.954	1	0.881	0.926	2	0.932	1.078	3	1.271	1.219	3	1.008	1.196
IPI00118569	Gna13	P27601	3	0.868	0.942	2	0.834	0.923	1	1.071	0.892	3	1.218	0.940	1	1.265	0.928	4	0.862	0.987
IPI00118026	Ap1s1	P61967	/			1	1.152	1.156	1	1.132	0.900	1	0.933	12.04	1	1.264	1.477	2	1.121	0.943
IPI00845565	Vps37a	Q8CHS8-3	2	1.142	1.081	2	1.138	1.353	1	1.134	0.967	2	1.206	0.914	1	1.264	1.121	3	1.052	1.030
IPI00453981	Fdxr	Q61578	6	0.708	0.789	8	1.053	0.995	9	0.892	1.141	8	0.888	1.059	6	1.264	1.061	11	1.197	1.050
IPI00875296		A2RSX7-1	/			/			/			2	1.014	1.098	1	1.263	1.051	2	1.093	0.757
IPI00228616	Hist1h1a	P43275	6	0.865	0.986	6	0.862	0.968	5	0.818	1.032	7	0.838	0.967	7	1.262	1.060	8	1.195	1.095
IPI00310240	Anxa6	Q3V2Z4	7	1.075	1.274	15	1.237	1.190	8	1.189	1.320	/			10	1.260	1.409	21	1.321	1.503
IPI00127941	Smap	Q9R0P4	1	1.139	0.952	2	1.051	1.030	/			1	0.849	0.944	1	1.258	1.191	2	1.043	0.980
IPI00406107	Ppp2r3a	B2RXC8	/			/			/			/			1	1.252	0.865	/		
IPI00308607	Fbxo30	Q8BJL1	/			1	1.116	0.722	/			2	1.109	0.947	2	1.251	1.117	5	0.960	0.907
IPI00461189	Elp2	Q91WG4-1	/			/			2	0.971	0.739	1	0.814	0.998	1	1.251	1.018	5	1.364	0.982
IPI00330066	Edc4	Q3UJB9-1	7	0.963	0.967	13	1.008	0.977	11	0.976	0.938	18	1.001	0.932	15	1.250	1.051	22	1.062	1.095
IPI00331549	Dhrs1	Q99L04	1	0.913	1.083	2	0.832	1.256	3	1.227	1.157	3	1.169	1.269	3	1.250	1.325	7	1.338	1.291
IPI00229286		Q8CFE2	/			2	0.790	0.906	/			1	1.228	1.214	1	1.250	1.353	3	1.105	1.140
IPI00109401	Rpap3	Q9D706	3	0.998	1.050	5	0.904	0.970	4	1.281	1.167	7	1.282	1.009	3	1.247	1.128	13	1.026	1.087
IPI00229434	Tp53bp2	Q8CG79	/			2	0.978	0.988	/			2	1.044	1.061	1	1.243	2.312	1	1.068	1.742
IPI00153653	Nupl1	Q8R332-1	/			1	0.889	1.047	3	0.980	0.956	3	0.938	0.979	1	1.241	1.059	3	0.956	1.228
IPI00133034	Hint2	Q9D0S9	/			/			/			2	0.941	1.072	2	1.241	1.259	3	0.942	1.173
IPI00321170	Rpl3	P27659	5	1.168	1.110	8	1.216	1.095	6	0.936	0.973	10	0.931	1.003	10	1.240	0.894	15	1.235	0.922
IPI00321190	Psap	Q61207	6	1.191	0.997	8	1.157	0.977	9	0.939	0.929	/			13	1.235	0.936	17	1.213	0.959
IPI00858126			/			/			/			/			3	1.235	1.165	/		
IPI00463195	Atg7	Q9D906	1	0.992	0.842	3	0.989	0.953	2	0.885	1.225	6	0.990	1.094	7	1.234	1.048	8	1.196	1.162
IPI00399958	Calu	Q3TL33	/			8	0.590	0.901	9	1.014	0.931	12	0.945	0.876	9	1.232	1.173	14	1.025	1.158
IPI00410967	Wtap	Q9ER69-1	1	0.773	0.949	3	0.843	1.055	1	1.121	0.846	3	1.181	0.857	1	1.232	1.389	2	1.112	1.017
IPI00109388	Dph5	Q9CWQ0	/			/			/			1	1.038	0.971	1	1.231	1.816	2	1.078	1.029
IPI00322869	Abce1	P61222	10	1.099	0.920	12	1.144	0.940	13	0.990	1.028	14	0.959	1.027	15	1.230	0.980	19	1.239	0.993
IPI00230263	Dgcr14	Q3UFM6	1	0.735	0.963	4	0.965	1.062	2	1.101	1.016	3	1.144	0.978	1	1.230	1.101	6	0.838	1.092
IPI00119876	Dync1h1	Q9JHU4	47	1.182	1.047	70	1.201	1.043	67	0.898	1.075	92	0.914	1.065	70	1.229	1.000	131	1.190	0.986
IPI00923679	Irs2	B9EJW3	/			/			8	1.321	1.132	7	1.284	1.116	7	1.221	1.130	/		
IPI00336870	Mrpl55	Q9CZ83-2	1	0.802	0.799	1	0.925	1.061	/			/			1	1.219	0.869	1	0.885	0.935

IPI00153201	Gga1	Q8R0H9	3	0.589	0.580	2	1.083	1.121	4	1.262	1.210	5	1.005	1.034	2	1.219	0.987	4	1.018	1.183
IPI00323971	Impdh2	P24547	12	1.060	1.031	13	1.077	1.041	10	1.253	1.098	12	1.248	1.088	13	1.219	1.037	17	1.198	1.020
IPI00900411	Prps1l1	Q32M04	/			/			2	1.231	1.070	/			2	1.216	0.986	/		
IPI00131960	Pole4	Q9CQ36	1	0.978	0.873	1	0.894	1.083	1	1.292	0.951	2	1.233	0.896	1	1.215	0.952	2	1.154	0.960
IPI00132478		Q9CQF4	/			2	0.931	0.794	1	0.926	1.256	1	0.985	1.104	1	1.213	0.919	2	1.092	1.229
IPI00409255		B2RXC1-1	/			1	1.055	0.948	1	1.010	1.014	2	1.007	0.955	2	1.212	1.006	5	1.155	0.918
IPI00331439	Adh7	Q8JZP4	4	0.858	0.850	9	0.871	0.945	3	1.258	1.229	7	1.200	1.088	8	1.212	1.176	10	1.215	1.188
IPI00856142	Ift122	Q6KAU2	/			1	1.241	1.588	1	0.667	1.177	1	0.662	0.704	1	1.211	0.820	1	0.478	0.615
IPI00400432	Eif4a2	P10630-1	/			7	1.030	0.974	/			12	1.083	1.178	11	1.211	1.382	/		
IPI00750601	Usp8	A2AI52	3	1.014	1.039	2	1.065	0.943	3	1.033	1.105	5	1.011	1.021	2	1.211	1.095	7	1.236	1.118
IPI00845782	Ctc1	Q5SUQ9-2	1	0.847	0.823	3	1.027	1.152	3	1.060	1.259	8	0.947	1.077	7	1.210	1.127	12	1.179	1.114
IPI00121785	Lrch4	Q921G6	1	1.114	1.187	6	1.001	0.929	1	1.056	0.982	6	1.025	0.932	1	1.210	1.061	5	0.964	1.011
IPI00453682	Cdt1	Q8R4E9	1	0.948	0.928	4	0.939	0.913	3	1.283	1.031	3	1.123	0.910	2	1.208	0.919	3	1.116	1.038
IPI00170213	Abhd11	Q8K4F5	1	1.100	0.741	/			/			/			1	1.208	1.130	2	1.026	0.946
IPI00943373	RP23-293H17.3	B1ATT5	/			/			2	0.953	1.041	4	0.946	0.924	3	1.207	0.961	/		
IPI00113394	Rps15a	P62245	3	1.226	1.167	/			2	0.969	1.006	3	0.933	1.009	4	1.207	0.947	3	1.154	0.972
IPI00464280	Epn2	Q5NCM5	/			2	0.922	1.271	/			/			1	1.207	1.114	3	0.946	0.841
IPI00121814	MNCb-4931	Q9JJG9	/			3	0.974	0.928	3	1.057	1.027	1	0.833	0.919	1	1.207	1.024	3	0.946	1.055
IPI00109437	Pir	Q9D711	/			2	0.660	0.640	/			3	1.187	1.035	1	1.206	1.077	4	1.281	1.100
IPI00849604	Dcun1d1	Q9QZ73	1	0.995	1.369	/			3	1.158	0.990	3	1.102	0.984	2	1.205	0.971	3	1.010	1.041
IPI00138042	Lepre1	A2A7Q5	/			1	0.848	0.885	/			2	0.984	1.021	2	1.204	1.274	2	1.456	1.593
IPI00480235	Trim47	Q8C0E3-2	/			11	1.101	1.194	7	1.127	1.042	7	1.063	1.055	8	1.203	1.151	11	1.026	1.067
IPI00125658	Gclc	P97494	3	1.133	0.995	7	1.136	0.918	6	1.194	1.119	11	1.192	1.076	4	1.202	1.139	12	1.166	1.081
IPI00944724	Ttc28	Q80XJ3	/			/			1	1.295	0.907	2	1.018	0.984	2	1.202	0.895	/		
IPI00126349	Psmc3ip	O35047	/			/			/			1	1.192	1.028	1	1.199	0.890	2	0.806	1.039
IPI00420457	Med13l	Q6JPI3	/			/			/			/			/			1	44.54	10.65
IPI00467729	Zfp462	A2SW42	/			/			/			/			/			1	41.05	4.631
IPI00278312	Gfpt2	Q9Z2Z9	/			/			/			/			/			5	26.65	231.8
IPI00649802	Meox1	A2A5C5	/			/			/			/			/			1	25.74	5.819
IPI00125455	Stxbp4	Q9WV89-1	/			/			/			/			/			1	21.24	7.189
IPI00752067	Ulk1	O70405	/			/			/			/			/			1	19.82	0.865
IPI00457415		Q810K2	/			/			/			/			/			3	12.35	1.407
IPI00895965	Mtap2	B2KGT6	4	1.087	1.136	6	0.990	1.040	/			7	0.952	1.004	3	0.832	1.081	8	8.819	3.429
IPI00471083	Tmem54	Q9D7S1	/			/			/			/			/			1	7.661	2.504
IPI00761646	Abcb7	A2AC46	/			/			/			2	1.101	0.961	/			2	4.841	2.788
IPI00127492	Smap1	Q91VZ6	/			3	0.908	0.815	/			3	1.095	1.041	2	1.127	1.662	2	3.581	1.336
IPI00226453	Fscn2	Q32M02	/			/			/			/			/			1	3.566	1.054
IPI00313137	Olfr1477	Q7TQQ7	/			/			/			/			/			1	3.156	1.653
IPI00668529	Tmf1	Q3UMH8	/			/			/			2	0.779	0.926	/			2	2.834	0.824
IPI00123689	Mtmr6	Q8VE11	/			1	1.022	1.073	1	0.934	1.099	/			/			1	2.789	1.555
IPI00153104	Tifa	Q793I8	/			/			/			/			/			1	2.698	0.727
IPI00129572	Pcdhgc5	Q91XW9	/			/			/			/			/			2	2.610	0.865
IPI00113171	Dtx2	Q8R3P2-1	/			/			/			/			/			1	2.585	1.260
IPI00379695	Coq5	Q9CXI0	/			/			/			/			/			1	2.462	8.589
IPI00396839	Tubgcp3	P58854	/			/			/			/			/			2	2.331	1.727
IPI00120637	Wdr7	Q92019-1	/			/			/			/			/			1	2.277	1.039
IPI00453906	Efha1	Q8CD10	1	0.972	0.909	2	0.874	1.170	/			2	1.093	0.974	/			2	2.181	1.017
IPI00850693	Bai1	Q3UHD1	/			/			/			/			/			1	2.166	0.617

IPI00553773	Muc5ac	O88715	/			3	0.902	0.943	/			/			/			2	2.036	0.445
IPI00172328	Dnahc8	Q91XQ0-1	/			/			/			/			/			1	1.960	5.976
IPI00118393	Gmeb2	P58929	/			/			/			/			/			1	1.938	1.090
IPI00468701	Ubr2	Q6WKZ8-1	/			/			/			/			/			2	1.900	1.093
IPI00112708	Ccdc77	Q9CZH8-1	/			/			/			/			/			1	1.885	1.238
IPI00111328	Tsc22d4	Q9EQN3	/			5	0.893	0.864	/			3	1.122	1.003	/			3	1.882	0.462
IPI00915083	Cnot2	Q3TIJ0	/			/			2	0.931	0.977	4	1.066	1.096	3	1.058	1.175	2	1.881	4.210
IPI00119913	Apc	Q61315-1	/			2	0.851	1.313	1	1.016	0.943	2	0.438	0.787	/			2	1.864	1.380
IPI00608106	Numbl	Q3UH86	/			/			/			2	0.873	0.905	/			2	1.852	1.000
IPI00153749	Tutl	Q8R3F9-1	/			/			/			1	1.352	1.142	/			3	1.827	1.357
IPI00122493	Fkbp10	Q61576	3	0.711	0.870	5	0.767	0.903	/			/			/			10	1.814	1.298
IPI00464296	Epb41l3	Q9WV92-8	/			13	0.903	1.143	/			/			/			24	1.796	1.354
IPI00469290	Ifrd2	Q7TSB3	/			/			/			/			/			1	1.781	0.906
IPI00380799	Pde2a	Q3TXZ6	/			/			/			1	0.948	1.388	/			1	1.767	1.198
IPI00308182	Rnf41	Q8BH75-1	/			/			/			/			/			1	1.734	2.180
IPI00229852	Yrdc	Q3U5F4	/			2	0.932	1.035	/			2	1.225	1.268	/			1	1.721	1.943
IPI00279213		Q6NZR2-1	/			/			/			/			/			1	1.649	0.982
IPI00756386	Dhtkd1	A2ATU0	/			/			/			1	1.114	1.119	/			1	1.624	1.449
IPI00138084	Adk	P55264-2	/			/			/			/			7	1.041	1.062	11	1.623	0.988
IPI00402913	Ube2v2	Q9D2M8-1	/			6	1.065	0.962	6	1.094	0.977	7	0.987	0.992	5	1.060	1.002	8	1.619	1.371
IPI00396784	AY358078	Q6UY53	/			/			/			/			/			2	1.613	1.027
IPI00229539	Hist3h2bb	Q8CGP0	4	0.693	0.995	/			/			/			/			7	1.611	1.150
IPI00112032	Carkd	Q9CZ42-1	3	0.966	0.949	4	0.868	0.964	4	0.994	1.062	5	0.881	1.036	3	1.081	1.019	6	1.611	27.04
IPI00606952	Commd6	Q3V4B5	/			/			/			2	0.967	0.932	/			1	1.517	1.078
IPI00751634			/			/			/			/			/			3	1.498	0.897
IPI00309237	Pja1	O55176-3	/			/			/			/			/			1	1.491	1.233
IPI00309907	Narfl	Q7TMW6-2	/			/			/			/			/			1	1.480	0.756
IPI00163015	Cdkal1	Q91WE6-1	/			/			/			/			/			1	1.473	1.198
IPI00625995	Gatad2a	Q8CHY6	/			/			1	1.086	0.828	2	0.955	1.052	/			1	1.468	0.917
IPI00625898	Bbx	Q8VBW5-1	/			/			/			/			/			2	1.464	3.354
IPI00124718	Sufu	Q9Z0P7-4	/			/			/			/			/			2	1.464	66.23
IPI00169954	Nsl1	Q8K305	/			1	1.053	1.167	1	1.249	1.142	1	1.331	0.859	/			2	1.464	12.36
IPI00895079	Ttc13	Q3UMK4	/			/			/			/			/			2	1.463	1.275
IPI00914684	Rpl36	Q5M9L1	/			2	1.072	1.113	/			/			/			3	1.462	0.946
IPI00845679	Spg11	Q3UHA3-2	/			/			1	1.056	1.264	2	0.802	0.909	/			2	1.451	0.976
IPI00113389	Niban	A0PJB3	2	0.553	1.004	2	0.899	1.332	/			/			/			3	1.450	2.939
IPI00111501	Cplx2	P84086	/			2	0.993	0.996	1	1.098	1.417	3	1.047	1.073	/			2	1.446	1.205
IPI00676717	Btaf1	A0ZVB6	/			/			2	1.106	1.029	2	1.172	1.310	/			1	1.445	0.754
IPI00607957	Arsa	Q9DC66	/			/			/			/			/			1	1.445	0.961
IPI00277399	Cluap1	Q8R3P7	/			/			/			/			/			1	1.434	1.413
IPI00420315	Itprip	Q3TNL8-1	/			/			/			/			/			1	1.432	1.009
IPI00855144	Arhgef5	Q8R172	/			/			4	1.265	1.091	2	1.222	0.868	/			1	1.432	0.651
IPI00110262	Sorcs2	Q9EPR5	/			/			/			/			/			1	1.427	0.539
IPI00321357	Znf593	Q9DB42	/			1	0.952	1.099	/			1	1.098	0.938	2	0.785	1.206	4	1.424	0.895
IPI00554894	Anxa6	P14824	/			15	1.032	1.181	/			10	1.172	1.318	/			21	1.422	1.541
IPI00153143	Ugt2b1	Q8R084	/			/			/			/			/			1	1.422	1.082
IPI00162790	Rpl18a	P62717	3	0.901	0.918	4	1.119	1.078	3	0.734	0.838	6	0.886	0.957	/			7	1.418	0.972
IPI00224682	Elp3	Q9CZX0-2	/			2	1.085	0.849	/			3	0.773	0.816	/			6	1.418	1.019

IPI00113117	Cyr61	P18406	/			1	0.899	0.943	/			/			/			1	1.418	1.610
IPI00515708	Ptpn2	Q06180-1	/			1	1.006	0.950	/			/			/			1	1.400	1.021
IPI00469937	Prmt7	Q922X9	/			/			2	1.043	1.018	/			/			1	1.394	0.858
IPI00380838	Heca	Q3UYD2	/			/			/			1	0.989	0.836	/			2	1.393	1.169
IPI00136012	Ggcx	Q9QYC7	/			/			/			/			/			1	1.391	1.447
IPI00225335	Ankrd46	Q8BTZ5	/			/			/			/			/			2	1.380	1.048
IPI00468437	Tinp1	Q9CR47	/			/			/			/			/			1	1.378	1.092
IPI00463074	Shroom2	A2ALU4-1	/			5	1.046	1.074	/			3	0.982	0.990	1	0.945	1.240	5	1.378	1.250
IPI00466153	Rpl34	Q9D1R9	3	1.180	1.136	3	0.948	1.050	/			3	0.803	1.012	/			4	1.372	0.974
IPI00114403	Timp1	P12032	/			/			/			/			/			1	1.372	0.806
IPI00224078	Prepl	Q8C167-1	/			2	0.908	0.863	2	1.140	0.911	3	1.163	0.876	/			1	1.368	1.094
IPI00454081	Kif21a	Q9QXL2-1	1	1.214	1.089	2	1.236	1.057	1	1.328	1.537	3	1.219	1.014	/			3	1.361	1.091
IPI00474373	Sqstm1	Q64337-2	/			/			/			/			/			11	1.353	1.145
IPI00395213	Cugbp1	P28659-4	2	0.905	1.240	4	0.801	0.947	2	1.175	0.830	2	0.953	0.962	3	1.011	1.028	4	1.353	0.947
IPI00880228	Bola3	Q8CEI1	/			/			1	1.008	0.980	/			1	1.058	1.134	1	1.350	1.114
IPI00130331	L2hgdh	Q91YP0	/			3	1.090	1.116	1	1.381	0.818	/			/			2	1.348	1.239
IPI00111370	Crtap	Q9CYD3	/			/			/			/			/			6	1.343	1.215
IPI00754134	Bat2l	A2AN33	/			/			4	1.216	1.176	6	1.216	1.029	2	1.004	0.942	3	1.338	0.952
IPI00229529	Rpl11	Q8CGM2	/			/			/			/			/			4	1.338	0.883
IPI00134432	Ugt1a6	Q64435	/			/			/			/			/			2	1.338	1.067
IPI00762636	Acsf3	Q3URE1-1	/			/			2	0.274	0.833	/			/			4	1.337	1.033
IPI00115683	Spi15	O08798	/			/			/			/			/			2	1.328	1.264
IPI00655177	Pip5k1c	O70161-1	/			/			/			/			/			2	1.323	1.267
IPI00322302	Ttc15	Q8K2L8	2	1.022	0.829	7	1.108	1.039	3	1.069	0.883	3	1.068	0.967	1	1.148	0.935	6	1.320	1.106
IPI00229799	Rpusd3	Q14AI6-1	/			/			1	1.190	1.149	/			/			1	1.319	1.050
IPI00620097	Madd	Q80U28-2	/			/			/			/			/			1	1.319	1.060
IPI00459639	Frmd8	Q3UFK8	/			1	0.932	0.860	/			/			/			3	1.319	1.025
IPI00474637	Rpl10	Q6ZWV3	2	1.241	0.993	2	1.136	7.317	/			/			/			5	1.318	0.994
IPI00850362	Thada	A8C756-1	/			/			/			3	0.987	1.143	3	0.365	0.766	3	1.318	1.003
IPI00420389	Nubpl	Q3URR8	/			/			/			/			1	0.985	1.296	1	1.307	1.285
IPI00662244	Agl	Q8CE68	/			3	0.969	1.053	/			6	0.883	1.085	3	1.140	0.908	6	1.305	0.983
IPI00117416	Cox4nb	O70378	/			/			/			2	1.039	0.973	3	0.984	0.850	3	1.303	0.904
IPI00268676	Pias1	O88907	/			2	0.903	1.002	/			1	1.090	0.840	/			3	1.303	1.055
IPI00831560			/			/			/			/			/			1	1.301	0.950
IPI00133528	Golph3	Q9CRA5	1	1.010	0.919	1	0.767	1.176	/			2	1.219	0.854	1	1.024	1.178	1	1.297	1.328
IPI00115875	Pi4ka	Q3UVT5	/			/			/			/			/			3	1.297	1.101
IPI00128689	Col5a1	O88207	/			/			3	0.630	0.957	/			/			1	1.294	1.133
IPI00123321	D230025D16Rik	Q922R1	/			1	1.181	1.045	/			1	1.193	1.000	/			1	1.293	0.971
IPI00139718	Mob2	Q8VI63-1	/			/			/			/			/			1	1.292	1.038
IPI00113112	Rab3b	Q9CZT8	/			/			/			/			/			4	1.292	1.134
IPI00128570	Thtpa	Q8JZL3	/			2	1.060	0.939	/			1	0.745	0.998	/			2	1.292	1.304
IPI00464223	Myof	Q69ZN7-1	/			/			/			44	0.859	0.909	/			70	1.291	0.953
IPI00849112	Atp2c2	A7L9Z8	/			/			/			/			/			1	1.291	8.749
IPI00468517	Rnf31	Q924T7-1	/			/			1	1.035	1.063	1	1.015	1.269	/			1	1.290	1.014
IPI00265352	Gpt2	Q8BGT5	/			/			/			/			/			3	1.288	1.293
IPI00130160	Rbm5	Q91YE7-1	/			2	1.038	1.091	1	1.291	1.168	2	1.168	1.230	/			3	1.287	1.024
IPI00754663	Ube2l6	A2ATR9	/			/			/			1	0.779	1.181	/			1	1.282	1.343

IPI00554953	Gsta1	P13745	/			/			/			/			/			3	1.280	1.191
IPI00331006	Usp25	P57080	2	1.147	1.117	/			1	0.948	0.916	3	0.936	6.892	/			2	1.280	1.041
IPI00170232	Svil	Q8K4L3	4	0.758	0.988	9	0.904	1.054	4	1.145	1.061	7	1.116	1.068	4	1.077	1.093	10	1.280	1.219
IPI00421271	Plec1	Q9QXS1-13	/			/			/			/			/			180	1.279	1.312
IPI00121466	Naf1	Q3UMQ8	/			1	0.828	0.977	/			1	1.288	1.370	/			2	1.278	1.378
IPI00119036	Med27	Q9DB40-1	/			1	0.780	0.635	/			/			/			1	1.278	0.574
IPI00118304	Cep350	Q6A062	/			/			/			/			/			1	1.277	0.781
IPI00377729	Zfyve16	Q80U44	/			/			/			2	0.908	1.017	/			1	1.276	1.003
IPI00284769	Stard5	Q9EPQ7	/			/			/			/			/			1	1.276	1.385
IPI00662157	Synpo	Q8CC35-1	/			1	1.048	0.935	/			1	0.783	0.987	/			1	1.276	1.182
IPI00403485	Obsl1	Q80TU8	/			/			/			/			/			2	1.275	1.069
IPI00463111	EG433762	Q3U151	/			/			/			/			/			2	1.275	1.069
IPI00894581	Carkd	Q9CZ42-2	/			/			/			/			/			6	1.275	1.105
IPI00654261	Samd4	Q3UZ00	/			2	1.035	1.019	/			2	1.323	2.142	/			1	1.268	1.248
IPI00229726	Tarsl2	Q8BLY2	/			2	1.180	0.879	/			4	1.104	0.948	3	0.943	0.865	5	1.268	1.143
IPI00274186	Arrb1	Q8BWG8-1	/			/			/			2	0.830	1.008	/			1	1.267	1.598
IPI00229577	Eif2c5	Q8CGT7	/			2	0.985	0.962	/			/			/			2	1.261	1.079
IPI00894610	Stat5a	B2C3G8	/			/			1	1.043	0.856	/			/			5	1.260	1.584
IPI00420906	Kiaa1797	A2AKG8-1	/			/			/			3	0.801	0.857	2	0.884	1.928	1	1.258	0.904
IPI00406045	Pik3r4	Q8VD65	1	1.188	0.988	1	1.120	0.987	2	1.168	0.934	6	1.052	1.087	2	1.003	0.966	5	1.257	1.084
IPI00122139	Acaa1b	Q8VCH0	/			/			/			/			/			9	1.256	1.139
IPI00749954	Jmjd1c	Q69ZK6-1	1	0.955	1.172	2	1.206	1.098	4	0.988	1.060	2	1.069	1.165	/			4	1.255	1.073
IPI00228959	Znf276	Q8CE64-1	/			1	0.946	0.908	/			/			/			1	1.252	1.143
IPI00127547	Slc7a6os	Q7TPE5	/			1	1.133	1.136	/			1	1.138	1.141	1	1.089	0.931	2	1.251	1.114
IPI00309200	Gabarapl2	P60521	2	1.075	0.945	2	0.987	1.037	2	1.379	1.017	3	1.126	1.123	/			3	1.249	1.131
IPI00109744	Rpusd4	Q9CWX4	/			1	0.895	0.949	/			/			/			2	1.249	1.058
IPI00110679	Snx7	Q9CY18	/			2	1.037	1.063	/			1	0.896	0.791	/			2	1.249	1.413
IPI00133103	Creg1	O88668	/			/			1	0.893	0.829	1	0.940	0.884	/			3	1.247	0.925
IPI00387505	Fars2	Q99M01	1	1.159	1.272	2	0.996	0.874	1	1.209	1.195	1	0.931	1.002	/			3	1.247	1.399
IPI00355673	Serpina3h	A2RTV1	/			3	1.110	0.963	1	0.731	1.547	5	0.793	1.476	/			4	1.245	1.868
IPI00221825	Clic6	Q8BHB9	1	1.133	1.085	1	1.044	1.094	/			1	1.139	1.181	/			1	1.245	0.969
IPI00230074	Ofd1	Q80Z25	1	1.038	1.017	1	0.982	0.949	1	1.226	1.079	1	1.010	1.129	1	1.051	0.946	1	1.244	0.978
IPI00668902	Scaper	B2RXS3	/			/			/			3	0.952	0.912	/			1	1.243	0.907
IPI00473693	Pkp4	Q68FH0-1	/			/			/			/			/			2	1.242	1.523
IPI00420559	Ivns1abp	Q920Q8-1	/			/			/			/			/			1	1.241	1.595
IPI00313515	Pold1	Q3TFX6	/			/			/			/			/			8	1.241	0.930
IPI00469440	Rcbtb1	Q6NXM2	/			/			/			2	0.916	1.019	/			1	1.241	1.045
IPI00109434	Geft	Q9CWR0-1	/			1	1.054	1.012	/			/			/			3	1.238	1.161
IPI00874973	Psd3	Q2PFD7-1	/			/			/			/			/			1	1.238	1.757
IPI00400017	Ppfibp2	O35711-4	1	0.934	0.836	2	0.639	0.714	2	0.771	1.208	/			2	0.927	1.502	2	1.235	1.518
IPI00420803	Tsc22d1	P62500-1	/			/			/			/			/			3	1.234	1.109
IPI00261188	Ifi35	Q9D8C4	/			/			/			/			/			1	1.233	0.963
IPI00458958	Rrp15	Q9CYX7	/			/			/			/			/			2	1.232	1.092
IPI00127599	Terf2	O35144-1	/			2	0.941	1.011	/			3	1.154	1.052	1	1.056	0.978	2	1.232	1.141
IPI00261638	Myl6b	Q8CI43	/			2	0.622	0.917	/			3	0.997	1.014	/			2	1.232	1.087
IPI00875787	Becn1	Q99J03	/			1	1.121	0.892	1	1.145	0.974	1	1.100	0.865	/			2	1.231	0.888
IPI00110725	Gtpbp8	Q9CY28-1	/			/			/			/			/			1	1.231	1.225
IPI00356888	Fndc3a	Q8BX90	/			/			/			/			/			1	1.231	1.142

IPI00379844	Irs2	P81122	5	0.926	0.979	7	1.107	1.029	/			/			/			11	1.230	1.049
IPI00124444	Pfkp	Q9WUA3-1	2	1.036	0.814	7	0.947	0.873	/			/			/			17	1.230	1.192
IPI00133614	Nsmce2	Q91VT1-1	/			/			/			2	1.169	1.013	/			2	1.229	1.015
IPI00173167	2410091C18Rik	Q9CWG8-1	/			2	0.985	1.080	/			3	1.180	0.940	2	1.077	0.981	2	1.229	0.929
IPI00816884			/			2	0.556	0.659	/			1	1.153	0.991	/			2	1.228	0.835
IPI00798493	Fam122b	Q6NZE7-2	/			/			/			/			/			1	1.228	1.212
IPI00608092	Sin3b	Q62141-4	/			/			/			2	1.222	1.070	/			2	1.227	0.983
IPI00808125	Qser1	A2BIE1	1	1.096	1.034	1	0.788	1.001	/			/			/			2	1.226	1.084
IPI00850592	Ndfip1	Q8R0W6	/			/			/			/			/			2	1.226	1.188
IPI00515222	Bcas3	B1AR74	/			2	1.092	0.928	/			/			/			4	1.224	1.049
IPI00321396	Csnk1e	Q9JMK2	1	1.160	1.059	1	0.992	1.047	/			/			/			3	1.222	0.952
IPI00623304	Map3k4	O08648-1	/			/			/			2	1.142	0.927	/			2	1.222	1.029
IPI00889222	Rpl14	B0LAB8	/			5	1.196	0.897	4	0.740	0.894	4	0.791	0.921	/			6	1.221	0.769
IPI00121120	Col5a2	Q3U962	3	0.734	0.778	11	0.874	0.813	4	1.092	1.140	8	1.114	1.089	4	0.818	0.955	11	1.220	1.242
IPI00112176	Cutc	Q9D8X1	/			1	1.123	1.063	/			2	0.848	1.677	/			1	1.220	0.933
IPI00133166	Nat9	Q3UG98	/			/			1	0.732	0.929	3	0.934	1.082	1	1.055	5.193	1	1.219	1.377
IPI00120917	Zfand6	Q9DCH6	/			2	1.004	0.857	1	0.934	1.035	1	1.068	0.947	2	1.035	1.129	3	1.217	1.101
IPI00330164	Rbm16	Q3TTX6	4	0.973	1.015	3	1.098	1.142	/			/			/			7	1.215	1.018
IPI00114389	App	P12023-1	1	1.164	0.895	4	0.980	0.961	/			3	1.092	1.075	4	1.071	1.179	4	1.214	1.109
IPI00109119	Trmt11	Q9CWH5-1	/			/			/			2	1.064	2.062	/			1	1.214	1.746
IPI00124779	Tgs1	Q923W1	/			1	1.157	1.071	1	1.236	1.223	/			1	1.173	1.054	1	1.213	1.257
IPI00119095	Gm2a	Q60648	/			1	1.074	0.986	2	0.754	1.034	2	0.812	1.007	1	1.124	0.947	2	1.213	1.132
IPI00329846	Stk17b	Q8BG48	2	0.987	1.014	3	0.982	1.017	3	1.175	1.513	5	1.276	1.226	4	1.031	1.100	4	1.212	1.383
IPI00114254	Ttc37	Q3UYZ5	/			3	1.186	1.120	/			2	1.045	1.261	/			5	1.212	1.204
IPI00133338	Fam107b	Q3TGF2	4	1.028	1.157	6	0.990	1.021	4	1.216	1.117	6	1.124	0.975	3	1.129	1.122	6	1.212	1.073
IPI00225066	Rpl36a	P83882	/			/			/			2	1.002	0.947	1	1.199	0.933	4	1.209	0.970
IPI00228820	Gstm2	P15626	4	1.228	1.095	9	1.191	0.986	6	0.908	0.997	5	0.871	0.992	6	1.153	0.960	11	1.208	0.922
IPI00377925	Atg2b	Q80XK6-2	/			/			/			/			/			2	1.207	1.070
IPI00330840	Golga1	Q9CW79-1	1	0.448	0.776	2	1.115	1.035	3	1.084	0.980	1	1.101	0.783	/			3	1.206	0.966
IPI00122272	Ecm1	Q61508-1	2	1.121	0.972	/			/			/			/			3	1.206	1.050
IPI00131818	Tbpl1	P62340	/			/			/			/			/			1	1.206	14.23
IPI00127014	Terf2ip	Q91VL8	2	0.717	0.616	4	0.961	1.029	2	1.017	1.170	4	1.284	1.015	2	1.184	1.152	3	1.205	0.965
IPI00845626	Tle3	Q3TY99	2	0.958	0.885	4	1.161	1.044	2	0.999	0.923	2	0.923	1.225	2	1.085	0.979	4	1.205	0.958
IPI00330649	Myo1e	Q3TLJ4	2	1.013	0.926	6	1.022	1.025	3	0.912	1.167	2	0.826	1.069	/			5	1.204	1.030

Appendix 3. All phosphopeptides identified as down-regulated after treatment with 24(*S*),25-epoxycholesterol (24(*S*),25-EC) in ≥1 biological replicate. Un-normalised SILAC phosphopeptide ratios are displayed

			Mascot Score		Ratio 25-OHChol :Control		Ratio 24(*S*),25-EC :Control	
		Replicate	1	2	1	2	1	2
Phosphopeptide	**Gene**	**IPI Number**						
EEVAS(ph)EPEEAASPTTPK	Nop56	IPI00318048	48.39	/	0.358	/	0.413	/
RVS(ph)QEANLLTLAQK	C13003 9O16Rik	IPI00225777	36.98	65.16	0.628	0.889	0.412	0.796
SETAPAAPAAPAPAEKT(ph)PVK	Hist1h1e	IPI00223714	53.69	25.47	0.388	0.688	0.409	0.790
HGAPAAPS(ph)PPPR	Tbc1d10b	IPI00469012	43.89	50.35	0.521	0.574	0.408	0.770
SQET(ph)PEKPR	Msl1	IPI00110256	30.08	/	0.650	/	0.408	/
GEGERS(ph)DEENEEK	Polr3g	IPI00463147	60.57	/	0.671	/	0.408	/
HS(ph)VTGYGDC(me)AAGAR	Jub	IPI00453693	35.36	/	0.440	/	0.404	/
GDVS(ph)EDEPSLGR	Rnmt	IPI00453849	32.67	/	0.598	/	0.400	/
RPMEEDGEEKSPS(ph)K	Ilf3	IPI00130591	34.61	/	0.410	/	0.400	/
RIS(ph)GLIYEETR	Hist1h4a	IPI00623776	35.15	/	0.267	/	0.400	/
SRLTPT(ph)TPESSSTGTEDK	Sqstm1	IPI00133374	69.05	/	0.392	/	0.398	/
ADS(ph)DSEDKGEESKPK	Cbx1	IPI00129466	40.05	/	0.347	/	0.393	/
PMSVAGS(ph)PLSPGPVR	Irs2	IPI00379844	61.73	45.92	0.494	0.606	0.392	0.684
NNVMT(ph)SPNVHLK	Cenpc1	IPI00114808	34.17	/	0.284	/	0.390	/
LPTSEEERS(ph)PAK	Trp53bp1	IPI00229801	25.34	25.63	0.217	3.061	0.387	2.082
HLSTPSSVS(ph)PEPQDPAK	Arhgef12	IPI00754880	46.3	36.63	0.450	0.545	0.387	0.820
GVQAGNSDT(ph)EGGQPGR	Acin1	IPI00121136	32.19	/	0.811	/	0.387	/
SETLVNAQQTPLGT(ph)PK	Palm	IPI00129298	43.67	37.09	0.267	1.074	0.386	1.079
NGLSQPS(ph)EEEVDIPKPK	Ddx21	IPI00120691	42.24	/	0.323	/	0.384	/
LPSGSGPASPTT(ph)GSAVDIR	Ahnak	IPI00553798	65.09	/	0.339	/	0.378	/
GSGEASSDSIDHS(ph)PAK	Suv39h2	IPI00111417	26.96	/	0.174	/	0.377	/
KTS(ph)LSDSTTSAYPGDAGK	Rab3gap1	IPI00749720	39.8	/	0.593	/	0.377	/
S(ph)NSLPHSAVSNAASK	Wdr20a	IPI00153206	26.16	36.48	0.462	0.909	0.376	0.825
GHYEVTGS(ph)DDEAGK	Ahnak	IPI00553798	58.36	/	0.168	/	0.371	/
S(ph)ESSGNLPSVADTR	Akap1	IPI00230591	29.82	/	0.390	/	0.371	/
SNS(ph)FSDER	Ahnak	IPI00553798	29.85	/	0.154	/	0.366	/
RLS(ph)QSDEDVIR	Wdr26	IPI00226275	83.2	29.45	0.399	0.357	0.365	0.414
GGVTGSPEASISGS(ph)KGDLK	Ahnak	IPI00553798	43.68	/	0.119	/	0.363	/
LGSSPTS(ph)SC(me)NPTPTK	Specc1	IPI00798550	31.81	27.02	0.422	0.667	0.363	0.800
ETNVSKEDT(ph)DQEEK	Psip1	IPI00115257	37.57	44.98	0.386	0.996	0.362	0.871
LPSDSSASPPLSQT(ph)TPNKDADDQAR	Eya3	IPI00411085	40.03	/	0.518	/	0.348	/
S(ph)PSRPLPEVTDEYK	Ssb	IPI00134300	26.42	/	0.551	/	0.346	/
GGVTGSPEAS(ph)ISGSKGDLK	Ahnak	IPI00553798	43.68	/	0.135	/	0.346	/
GVTASSSS(ph)PASAPK	Ncam1	IPI00122971	43.46	34.3	0.244	1.437	0.346	1.195
AS(ph)AVSPEKAPM(ox)TSK	Tcof1	IPI00115660	34.02	/	0.345	/	0.346	/
SLS(ph)PSHLTEDR	Zc3h13	IPI00515528	44.78	33.98	0.317	0.922	0.344	0.904
DSVPAS(ph)PGVPAADFPAETEQSKPSK	Top2a	IPI00122223	25.31	/	0.116	/	0.342	/
PASVDGSPVS(ph)PSTNR	Irs1	IPI00119627	27.92	42.29	0.724	0.494	0.335	0.797
VDS(ph)SSEDGVDAKPDR	Casp7	IPI00130131	50.6	39.73	0.535	0.540	0.325	0.690
SPAPSNPTLS(ph)PSTPAK	Mybbp1a	IPI00331361	34.8	33.16	0.159	1.852	0.323	1.256

KGDDS(ph)DEEDLC(me)ISNK	Stard13	IPI00857002	57.82	/	0.027	/	0.317	/
S(ph)SPPVEHPAGTSTTDNDVIIR	Rai14	IPI00453820	35.31	/	0.170	/	0.308	/
APQS(ph)PTLAPAK	Cxadr	IPI00270376	25.52	30.84	0.219	1.618	0.291	1.103
GDQVSQNGLPAEQGS(ph)PR	Sptbn1	IPI00319830	58.12	/	0.654	/	0.208	/
SHS(ph)LDDLQGDADVGK	Sash1	IPI00338954	/	58.75	/	0.525	/	0.538
LESHGSS(ph)EESLQVQEK	Vcan	IPI00875672	/	42.02	/	0.497	/	0.535
ANTSS(ph)DLEKDDDAYK	Ranbp2	IPI00337844	/	40.08	/	0.436	/	0.533
SLPASGTPQS(ph)PPAVK		IPI00851031	49.32	62.59	0.747	0.487	0.582	0.533
MSPNETLFLES(ph)TNK	Rragc	IPI00468702	/	32.32	/	0.407	/	0.530
TSS(ph)PNKEESPK	Papola	IPI00266738	26.95	31.16	0.825	0.503	0.879	0.530
AES(ph)PETSAVESTQSTPQK	Pds5b	IPI00845638	41.44	63.25	0.594	0.288	0.437	0.520
LEPAPLDSS(ph)PAVSTHEGSK	Renbp	IPI00124826	/	31.06	/	0.584	/	0.515
(ac)S(ph)ETAPVAQAASTATEKPAAAK	Hist1h1a	IPI00228616	/	53.02	/	0.439	/	0.514
PQSPVIQATAGS(ph)PK	Arfgef2	IPI00137087	/	41.94	/	0.350	/	0.511
APS(ph)PSQPPK	Pds5b	IPI00845638	27.46	25.3	0.582	0.410	0.547	0.501
RIS(ph)DPLTSSPGR	Mcm2	IPI00323820	80.09	70.35	0.722	0.529	0.584	0.495
VS(ph)PVPSPSQPAR	Mical1	IPI00116371	/	25.71	/	0.435	/	0.486
IDQGS(ph)HTAGESSTR	Tdp1	IPI00222253	/	34.56	/	0.416	/	0.476
KPDQT(ph)LDEDDPGAAPLK	Bsg	IPI00408495	45.13	34.22	0.548	0.543	0.647	0.474
S(ph)PASTSSVNGTPGSQLSTPR	Dclk1	IPI00468380	/	43.36	/	0.459	/	0.472
KTS(ph)PASLDFPEPQK	Znf828	IPI00453800	36.79	46.94	0.541	0.805	0.638	0.471
AQGHS(ph)PVNGLLK	Ccnl2	IPI00310772	/	25.94	/	0.493	/	0.464
HNS(ph)TTSSTSSGGYR	Abi1	IPI00798483	/	57.32	/	0.536	/	0.443
TASRPEDTPDSPSGPSS(ph)PK	Lrrc16a	IPI00474873	/	46.92	/	0.216	/	0.439
RPDPDS(ph)DEDEDYER	Rbm17	IPI00170394	64.68	49.04	0.649	0.562	0.562	0.428
AGYTT(ph)DESSSSSLHTTR	Fxr2	IPI00126389	/	38.76	/	0.551	/	0.358
LYNSEESRPYT(ph)NK	Crkrs	IPI00648022	/	49.1	/	0.205	/	0.338
PQSAS(ph)PAKEEQK	Palm	IPI00129298	/	30.2	/	0.390	/	0.196

Appendix 4. All phosphopeptides identified as up-regulated after treatment with 24(*S*),25-epoxycholesterol (24(*S*),25-EC) in ≥1 biological replicate. Un-normalised SILAC phosphopeptide ratios are displayed

			Mascot Score		Ratio 25-OHChol :Control		Ratio 24(*S*),25-EC :Control	
		Replicate	1	2	1	2	1	2
Phosphopeptide	**Gene**	**IPI Number**						
KDS(ph)ISEDEMVLR	Wdtc1	IPI00108450	43.30	/	0.82	/	1.66	/
GGIDNPAIT(ph)SDQEVDDKK	Arhgap5	IPI00124298	40.63	/	0.92	/	1.13	/
KQIT(ph)VEELVR	Plec1	IPI00400215	38.61	/	0.62	/	1.07	/
PTGGLRDS(ph)EAEK	Hirip3	IPI00222813	29.49	/	1.03	/	1.06	/
DELADEIANSS(ph)GK	Myh9	IPI00123181	29.65	/	1.17	/	0.97	/
GPEVEGS(ph)PVSEALR	Brwd1	IPI00654074	37.76	/	0.55	/	0.95	/
LLQDSSS(ph)PVDLAK	Ncoa2	IPI00116968	29.72	/	1.12	/	0.92	/
IKPDEDLPS(ph)PGSR	Gli3	IPI00123429	42.62	/	0.78	/	0.91	/
TSS(ph)PNKEESPK	Papola	IPI00266738	26.95	31.16	0.82	0.50	0.88	0.53
IKDPDLT(ph)TPDSK	Ckap2	IPI00470092	44.82	/	0.79	/	0.85	/
SEVQAHS(ph)PSR	Mtap2	IPI00895965	31.21	/	0.91	/	0.85	/
ADS(ph)PAGLEAAR	Kiaa0284	IPI00380953	35.46	/	0.78	/	0.84	/
LPS(ph)PAQTQR	Micall2	IPI00280103	30.76	33.11	0.87	0.51	0.82	0.88
PATS(ph)TPDLASHR	Ptpn14	IPI00122168	51.69	67.48	0.57	0.67	0.81	0.73
GGSS(ph)EELHDSPR	Hdgfrp2	IPI00116442	34.55	/	0.74	/	0.81	/
ASS(ph)EDTLNKPGSASSGVAR	Specc1	IPI00798550	33.64	/	0.89	/	0.80	/
AYT(ph)HQVVTR	Cdk7	IPI00129222	26.40	28.51	0.98	0.31	0.80	0.63
KGS(ph)LDYLK	Luzp1	IPI00322204	30.67	/	0.71	/	0.80	/
HGPAQAVTGTSVTS(ph)PIK	Ccnt2	IPI00654257	47.80	/	0.74	/	0.79	/
NS(ph)PNNISGISNPPGTPR	Ssbp3	IPI00341944	51.85	/	0.82	/	0.79	/
KLS(ph)SGDLR	Phldb1	IPI00330246	30.55	/	0.68	/	0.79	/
ASSHSSQSQGGGS(ph)VTK	Lmna	IPI00620256	47.84	58.67	0.54	1.58	0.79	0.90
RAS(ph)LSDIGFGK	Pctk3	IPI00111168	49.16	/	0.60	/	0.78	/
IKDPDLTT(ph)PDSK	Ckap2	IPI00470092	44.82	/	0.95	/	0.78	/
S(ph)ASSDTSEELNSQDSPK	Slc9a3r1	IPI00109311	78.91	100.99	0.71	0.70	0.78	0.84
KGT(ph)GDC(me)SDEEVDGK	Myh9	IPI00123181	49.18	/	0.84	/	0.78	/
HVSS(ph)PDVTTAQK	Tdp1	IPI00222253	32.78	32.90	0.72	0.81	0.78	0.93
SQDATVS(ph)PGSEQSEK	Zc3hc1	IPI00465879	50.16	/	0.53	/	0.78	/
GQGT(ph)PPSGPGVGR	Wbp7	IPI00857289	27.74	/	0.61	/	0.77	/
SGALAS(ph)PTDPFQSR	Trim47	IPI00480235	32.36	36.30	0.59	0.77	0.77	0.80
QESLKS(ph)PEEEDQQAFR	Nes	IPI00453692	36.61	/	0.67	/	0.76	/
TQSSS(ph)C(me)EDLPSTTQPK	Cask	IPI00776341	25.68	/	0.46	/	0.76	/
RAS(ph)LEIGESFPEGTK	Myo9b	IPI00229766	60.85	42.49	0.99	0.58	0.76	0.71
RFS(ph)M(ox)EDLNK	Pctk3	IPI00111168	47.88	/	0.69	/	0.76	/
DDISEIQSLASDHS(ph)GR	Tjp1	IPI00135971	31.83	/	0.57	/	0.76	/
C(me)IFMSETQSS(ph)PTK	Pias2	IPI00453655	30.79	/	0.47	/	0.75	/
QDVDNAS(ph)LAR	Vim	IPI00227299	31.40	/	0.72	/	0.75	/
PQSPVIQATAGS(ph)PK	Arfgef2	IPI00137087	30.88	41.94	0.83	0.35	0.74	0.51
QEFSS(ph)EEMTK	Vcam1	IPI00126834	25.88	/	0.83	/	0.74	/
SLS(ph)TSGESLYHVLGLDK	Dnajc5	IPI00132206	50.50	47.88	0.51	1.70	0.74	1.20
(ac)SDQEAKPST(ph)EDLGDKK	Sumo1	IPI00124593	33.58	/	0.78	/	0.73	/
DC(me)AKS(ph)DDEESLTLPEK	Nfkb1	IPI00719890	52.31	/	0.80	/	0.73	/
PAVVS(ph)PLSLSTEAR	Crtc1	IPI00469761	43.71	/	0.80	/	0.73	/
YVSGSS(ph)PDLVTR	Ptpn14	IPI00122168	49.84	/	0.73	/	0.73	/
ASPDQNASTHT(ph)PQSSAK	Clint1	IPI00648186	34.63	/	0.78	/	0.73	/
SSGSLS(ph)PGLETEDPLEAR	Tnks1bp1	IPI00459443	36.91	/	0.68	/	0.73	/

TASESISNLSEAGS(ph)VK	Clip1	IPI00857273	31.00	/	0.98	/	0.72	/
AQTPESC(me)GSVT(ph)PER	Filip1l	IPI00755058	30.92	/	0.94	/	0.72	/
T(ph)SPTVATQTGASVTSTR	Fam117b	IPI00461475	68.26	64.54	0.73	0.73	0.72	0.89
S(ph)FEDLTDHPVTR	Adam17	IPI00314443	44.01	46.28	0.71	0.66	0.72	0.94
SAT(ph)LETKPESK	Ifngr1	IPI00323231	25.38	/	0.64	/	0.72	/
VMTVTAVTTTATS(ph)DR	Hdgfrp2	IPI00116442	76.11	51.20	0.60	0.72	0.72	0.89
SDEEDRAS(ph)EPK	Zc3h18	IPI00673693	27.94	/	0.79	/	0.72	/
VEESSEIS(ph)PEPK	Usp1	IPI00330276	40.56	/	0.57	/	0.72	/
S(ph)LEGENHDPLSSVVK	Nes	IPI00453692	45.85	/	0.68	/	0.72	/
MHASSTGSS(ph)C(me)DLSK	Cdgap	IPI00125505	27.19	/	0.54	/	0.72	/
KIS(ph)GTTALQEALK	Clip1	IPI00857273	33.36	67.72	0.88	0.77	0.72	0.74
AKT(ph)PVTLK	Tmpo	IPI00828976	41.32	/	0.58	/	0.72	/
SSS(ph)FGSVSTSSTSSK	Snx16	IPI00331029	/	54.62	/	1.42	/	5.00
TAS(ph)GSSVTSLEGTR	Ndrg1	IPI00125960	45.97	41.37	0.50	1.04	0.57	3.57
GGVTGS(ph)PEASISGSK	Ahnak	IPI00553798	43.68	27.58	0.21	3.27	0.47	2.79
SGFGGMS(ph)SPVIR	Nup107	IPI00221767	28.39	40.37	0.37	2.64	0.63	2.32
LPTSEEERS(ph)PAK	Trp53bp1	IPI00229801	25.34	25.63	0.22	3.06	0.39	2.08
SGFGGMSS(ph)PVIR	Nup107	IPI00221767	/	40.37	/	2.57	/	2.07
AS(ph)PALGSGHHDGSGDSLEMSSLDR	Tomm70a	IPI00751137	64.86	47.86	0.29	2.31	0.46	2.05
ASS(ph)HSSQSQGGGSVTK	Lmna	IPI00620256	47.84	58.67	0.19	3.86	0.52	1.95
TEEDRENTQIDDTEPLS(ph)PVSNSK	Trp53bp1	IPI00229801	/	28.80	/	2.58	/	1.90
KQQQEPTC(me)EPS(ph)PK	Hmga2	IPI00331612	26.67	30.20	0.29	2.23	0.43	1.72
SEDRPS(ph)SPQVSVAAVETK	Trp53bp1	IPI00229801	/	48.56	/	2.07	/	1.70
AEAKPGT(ph)PAK	Nolc1	IPI00720058	36.93	39.65	0.31	2.25	0.47	1.67
PAS(ph)PLSGPR	D2Wsu81e	IPI00224127	/	29.84	/	1.80	/	1.65
GEVAPKET(ph)PKK	Marcksl1	IPI00281011	/	26.82	/	2.27	/	1.65
TVGNVS(ph)PTAQMVQR	Rbm7	IPI00133061	/	28.20	/	1.41	/	1.65
LHSAQLS(ph)PVDETPATQSQLK	Mlf1ip	IPI00459115	/	36.63	/	1.95	/	1.62
QEGAQENVKNS(ph)PVPR	Gmnn	IPI00131716	/	30.64	/	2.56	/	1.60
GISQTNLITTVT(ph)PEK	Epb41l3	IPI00229299	50.15	40.47	0.46	1.55	0.52	1.55
TTS(ph)PDLFESQSLTSASSK	Epn2	IPI00336844	/	27.33	/	1.25	/	1.55
ATWGDGGDNS(ph)PSNVVSK	Snap23	IPI00113798	64.07	49.53	0.49	1.69	0.46	1.54
LEQHSQQPQLS(ph)PATSGR	Tor1aip1	IPI00762273	25.81	47.94	0.58	1.33	0.58	1.53
AGS(ph)SPTQGAQNEAPR	Tcf20	IPI00407458	/	30.95	/	1.46	/	1.51
AS(ph)SHSSQSQGGGSVTK	Lmna	IPI00620256	/	58.67	/	2.60	/	1.51
C(me)QETESNEEQSIS(ph)PEKR	Akap12	IPI00123709	/	85.89	/	1.19	/	1.49
AGGS(ph)PASYHGSTSPR	Epn2	IPI00336844	49.92	47.77	0.50	1.47	0.50	1.47
SLYSSS(ph)PGGAYVTR	Vim	IPI00227299	34.83	53.18	0.67	0.97	0.67	1.47
FGEYNSNIS(ph)PEEK	Nop14	IPI00353010	36.25	30.49	0.43	1.68	0.54	1.45
GEATAERPGEAAVASS(ph)PSK	Marcks	IPI00229534	53.11	53.46	0.60	1.36	0.58	1.45
LATSS(ph)PEQSWPSTFK	Pml	IPI00229072	/	29.49	/	1.18	/	1.43
KQNETADEAT(ph)TPQAK	Nolc1	IPI00720058	/	43.74	/	1.50	/	1.42
AAKES(ph)EEEEEEEETEEK	Nolc1	IPI00720058	93.93	73.89	0.42	1.80	0.46	1.41
EIITEEPS(ph)EEEADMPKPK	Ddx21	IPI00120691	/	31.38	/	1.69	/	1.38
LLKPGEEPSEYT(ph)DEEDTK	Pgrmc2	IPI00351206	39.74	35.31	0.39	1.61	0.48	1.36
AEEDEILNRS(ph)PR	Canx	IPI00119618	/	25.35	/	1.51	/	1.35
SSGS(ph)PYGGGYGSGGGSGGYGSR	Hnrnpa3	IPI00269661	113.25	92.56	0.42	1.50	0.58	1.35
SSSSLLAS(ph)PSHIAAK	Fam62b	IPI00266942	26.75	30.80	0.59	1.46	0.57	1.34
NVAEALGHS(ph)PK	Irf2bp1	IPI00453578	37.33	27.45	0.75	0.81	0.67	1.34
QKS(ph)DAEEDGVTGSQDEEDSKPK	Canx	IPI00119618	88.22	64.73	0.48	1.53	0.54	1.34
SKTS(ph)PVASGSTSK	Cep170	IPI00667973	51.13	43.40	0.68	1.18	0.68	1.34
AFGPGLQGGNAGS(ph)PAR	Flna	IPI00875567	36.73	27.19	0.68	0.82	0.60	1.33
GPEVTSQGVQTSS(ph)PAC(me)K	Atxn2	IPI00117229	/	25.10	/	1.07	/	1.30
ASGQAFELILS(ph)PR	Stmn1	IPI00551236	/	30.07	/	0.87	/	1.30
AVGEEQRS(ph)EEPK	Akap12	IPI00123709	/	31.72	/	1.15	/	1.30

Appendix 5. All phosphopeptides identified as down-regulated after treatment with 25-hydroxycholesterol (25-OHChol) in ≥1 biological replicate. Un-normalised SILAC phosphopeptide ratios are displayed

			Mascot Score		Ratio 25-OHChol :Control		Ratio 24(*S*),25-EC :Control	
		Replicate	1	2	1	2	1	2
Phosphopeptide	Gene	IPI Number						
NEKS(ph)EEEQSSASVK	Hnrnpc	IPI00874321	51.11	45.64	0.350	1.095	0.433	0.832
SPDEATAADQES(ph)EDDLSASR	Farp1	IPI00356904	26.44	/	0.349	/	0.465	/
TEEVLSPDGSPSKS(ph)PSK	Add3	IPI00387580	38.11	/	0.349	/	0.439	/
ADS(ph)DSEDKGEESKPK	Cbx1	IPI00129466	40.05	/	0.347	/	0.393	/
EELEQQT(ph)DGDC(me)DEEDDDK DGEVPK	Sec62	IPI00134398	57.28	/	0.346	/	0.532	/
EDAPPEDKES(ph)ESEAK	Cds2	IPI00468999	26.03	/	0.346	/	0.594	/
GEVAPKET(ph)PK	Marcksl 1	IPI00281011	33.28	26.82	0.345	2.274	0.556	1.651
ERQES(ph)ESEQELVNK	Pdcd11	IPI00551454	39.77	/	0.345	/	0.560	/
AS(ph)AVSPEKAPM(ox)TSK	Tcof1	IPI00115660	34.02	/	0.345	/	0.346	/
ADS(ph)DSEDKGEESKPK	Cbx1	IPI00129466	40.05	/	0.344	/	0.451	/
LPSGSGPASPTT(ph)GSAVDIR	Ahnak	IPI00553798	65.09	/	0.339	/	0.378	/
SPFNSPS(ph)PQDSPR	Nfic	IPI00137501	40.52	35.42	0.334	1.146	0.464	1.050
IGPLGLS(ph)PK	Rpl12	IPI00463634	45.65	/	0.333	/	0.426	/
EIITEEPS(ph)EEEADM(ox)PKPK	Ddx21	IPI00120691	56.99	/	0.330	/	0.443	/
NGLSQPS(ph)EEEADIPKPK	Ddx21	IPI00120691	36.77	/	0.325	/	0.431	/
NGLSQPS(ph)EEEVDIPKPK	Ddx21	IPI00120691	42.24	/	0.323	/	0.384	/
NISEES(ph)PLTHR	Pask	IPI00400044	32.53	/	0.322	/	0.610	/
S(ph)PAKEPVEQPR	Spen	IPI00828562	25.27	/	0.321	/	0.464	/
SLS(ph)PSHLTEDR	Zc3h13	IPI00515528	44.78	33.98	0.317	0.922	0.344	0.904
T(ph)GSESSQTGASATSGR	Eif4b	IPI00221581	79.96	77.19	0.314	1.215	0.474	0.757
AEAKPGT(ph)PAK	Nolc1	IPI00720058	36.93	39.65	0.308	2.251	0.470	1.673
RVSGS(ph)ATPNSEAPR	Ddx51	IPI00396728	58.55	/	0.306	/	0.460	/
AS(ph)PALGSGHHDGSGDSLEMSS LDR	Tomm7 0a	IPI00751137	64.86	47.86	0.293	2.308	0.464	2.047
S(ph)QEMVHLVNK	Cd44	IPI00410802	52.66	33.35	0.292	1.021	0.420	0.827
S(ph)HTGEAAAVR	Bcl2l13	IPI00321499	35.83	/	0.288	/	0.467	/
KQQQEPTC(me)EPS(ph)PK	Hmga2	IPI00331612	26.67	30.2	0.287	2.231	0.428	1.718
NNVMT(ph)SPNVHLK	Cenpc1	IPI00114808	34.17	/	0.284	/	0.390	/
RVS(ph)GSATPNSEAPR	Ddx51	IPI00396728	58.55	/	0.278	/	0.427	/
YLEIDS(ph)DEESR	Sdad1	IPI00387439	33.64	/	0.276	/	0.529	/
DDS(ph)GAEDNVDTHQQQAENST VPTADSR	Rspry1	IPI00223590	27.35	/	0.275	/	0.445	/
LSQVNGATPVS(ph)PIEPESK	Mybbp1 a	IPI00331361	33.48	/	0.272	/	0.461	/
SETLVNAQQTPLGT(ph)PK	Palm	IPI00129298	43.67	37.09	0.267	1.074	0.386	1.079
RIS(ph)GLIYEETR	Hist1h4 a	IPI00623776	35.15	/	0.267	/	0.400	/
GS(ph)HC(me)SGSGDPAEYNLR	Lmna	IPI00620256	32.11	/	0.257	/	0.488	/
LSQVNGAT(ph)PVSPIEPESK	Mybbp1 a	IPI00331361	33.48	/	0.254	/	0.436	/
SST(ph)PLPTVSSSAENTR	Tmpo	IPI00896574	55.29	/	0.246	/	0.516	/
GVTASSSS(ph)PASAPK	Ncam1	IPI00122971	43.46	34.3	0.244	1.437	0.346	1.195
ASSHS(ph)SQSQGGGSVTK	Lmna	IPI00620256	47.84	58.67	0.224	2.410	0.536	1.175
APQS(ph)PTLAPAK	Cxadr	IPI00270376	25.52	30.84	0.219	1.618	0.291	1.103
LPTSEEERS(ph)PAK	Trp53bp 1	IPI00229801	25.34	25.63	0.217	3.061	0.387	2.082
GGVTGS(ph)PEASISGSK	Ahnak	IPI00553798	43.68	27.58	0.215	3.272	0.474	2.790
SPFNSPSPQDS(ph)PR	Nfic	IPI00137501	40.52	/	0.213	/	0.435	/

ASS(ph)HSSQSQGGGSVTK	Lmna	IPI00620256	47.84	58.67	0.194	3.858	0.523	1.945
LRS(ph)EDGVEGDLGETQSR	Ahnak	IPI00553798	33.49	32.86	0.178	1.087	0.415	0.795
GSGEASSDSIDHS(ph)PAK	Suv39h2	IPI00111417	26.96	/	0.174	/	0.377	/
S(ph)SPPVEHPAGTSTTDNDVIIR	Rai14	IPI00453820	35.31	/	0.170	/	0.308	/
GHYEVTGS(ph)DDEAGK	Ahnak	IPI00553798	58.36	/	0.168	/	0.371	/
SPAPSNPTLS(ph)PSTPAK	Mybbp1a	IPI00331361	34.8	33.16	0.159	1.852	0.323	1.256
SNS(ph)FSDER	Ahnak	IPI00553798	29.85	/	0.154	/	0.366	/
GGVTGSPEAS(ph)ISGSKGDLK	Ahnak	IPI00553798	43.68	/	0.135	/	0.346	/
GGVTGSPEASISGS(ph)KGDLK	Ahnak	IPI00553798	43.68	/	0.119	/	0.363	/
DSVPAS(ph)PGVPAADFPAETEQSKPSK	Top2a	IPI00122223	25.31	/	0.116	/	0.342	/
SGAAEEDDS(ph)GVEVYYR	Pdcd11	IPI00551454	41.08	/	0.104	/	0.592	/
KGDDS(ph)DEEDLC(me)ISNK	Stard13	IPI00857002	57.82	/	0.027	/	0.317	/
FIQELSGSS(ph)PK	Tcfap4	IPI00121217	27.49	35.23	0.018	1.013	0.430	0.581
MSPNETLFLES(ph)TNK	Rragc	IPI00468702	/	32.32	/	0.407	/	0.530
SPSPSPTS(ph)PGSLR	Dclk1	IPI00468380	/	51.87	/	0.398	/	0.582
PQSAS(ph)PAKEEQK	Palm	IPI00129298	/	30.2	/	0.390	/	0.196
LS(ph)PAYSLGSLTGASPR	Phldb1	IPI00330246	/	34.03	/	0.369	/	0.573
SGTSTPTTPGSTAITPGT(ph)PPSYSSR	Mtap2	IPI00895463	/	69.16	/	0.360	/	0.661
PQSPVIQATAGS(ph)PK	Arfgef2	IPI00137087	30.88	41.94	0.827	0.350	0.742	0.511
AYT(ph)HQVVTR	Cdk7	IPI00129222	26.4	28.51	0.981	0.313	0.801	0.632
AES(ph)PETSAVESTQSTPQK	Pds5b	IPI00845638	41.44	63.25	0.594	0.288	0.437	0.520
TASRPEDTPDSPSGPSS(ph)PK	Lrrc16a	IPI00474873	/	46.92	/	0.216	/	0.439
LYNSEESRPYT(ph)NK	Crkrs	IPI00648022	/	49.1	/	0.205	/	0.338

Appendix 6. All phosphopeptides identified as up-regulated after treatment with 25-hydroxycholesterol (25-OHChol) in ≥1 biological replicate. Un-normalised SILAC phosphopeptide ratios are displayed

			Mascot Score		Ratio 25-OHChol :Control		Ratio 24(*S*),25-EC :Control	
		Replicate	1	2	1	2	1	2
Phosphopeptide	**Gene**	**IPI Number**						
HGS(ph)DPAFGPSPR	Fam83h	IPI00227516	28.43	/	1.795	/	0.658	/
DELADEIANSS(ph)GK	Myh9	IPI00123181	29.65	/	1.166	/	0.970	/
S(ph)STSGSASSLESGVYR	Gtse1	IPI00268247	63.04	/	1.152	/	0.614	/
AQT(ph)PESC(me)GSVTPER	Filip1l	IPI00755058	30.92	/	1.120	/	0.637	/
LLQDSSS(ph)PVDLAK	Ncoa2	IPI00116968	29.72	/	1.118	/	0.919	/
RQS(ph)LTSPDSQSTR	Herc1	IPI00676574	33.46	38.87	1.064	0.991	0.698	0.776
VDHGAEIITQS(ph)PSR	Mtap2	IPI00895965	61.57	80.97	1.062	0.717	0.679	0.989
GS(ph)PEDGSHEASPLEGK	Rbm20	IPI00849187	51.26	/	1.055	/	0.586	/
PTGGLRDS(ph)EAEK	Hirip3	IPI00222813	29.49	/	1.035	/	1.064	/
RAS(ph)LEIGESFPEGTK	Myo9b	IPI00229766	60.85	42.49	0.989	0.578	0.758	0.713
KLEVS(ph)PGDEQSNVETR	Gnl3	IPI00222461	73.45	/	0.988	/	0.431	/
AYT(ph)HQVVTR	Cdk7	IPI00129222	26.4	28.51	0.981	0.313	0.801	0.632
TASESISNLSEAGS(ph)VK	Clip1	IPI00857273	31	/	0.975	/	0.725	/
IKDPDLTT(ph)PDSK	Ckap2	IPI00470092	44.82	/	0.954	/	0.782	/
AQTPESC(me)GSVT(ph)PER	Filip1l	IPI00755058	30.92	/	0.944	/	0.724	/
GGIDNPAIT(ph)SDQEVDDKK	Arhgap 5	IPI00124298	40.63	/	0.924	/	1.125	/
SNS(ph)NSSSVITTEDNK	Filip1l	IPI00755058	77.83	/	0.922	/	0.623	/
C(me)QS(ph)PILHSSSSASSNIPSAK		IPI00875090	39.2	48.16	0.918	0.573	0.700	0.668
SEVQAHS(ph)PSR	Mtap2	IPI00895965	31.21	/	0.907	/	0.849	/
KS(ph)PEQESVSTAPQR	Spg20	IPI00153501	39.11	51.42	0.900	0.689	0.708	1.084
TTSTSNPSS(ph)PAPDWYK	Atrx	IPI00857253	38.08	/	0.892	/	0.604	/
ASS(ph)EDTLNKPGSASSGVAR	Specc1	IPI00798550	33.64	/	0.887	/	0.805	/
YMSSDTT(ph)SPELR	Sin3a	IPI00117932	27.09	/	0.883	/	0.580	/
KIS(ph)GTTALQEALK	Clip1	IPI00857273	33.36	67.72	0.882	0.770	0.720	0.745
NSGATADAGSIS(ph)PR	Ercc5	IPI00875692	46.69	47.1	0.881	0.485	0.627	0.883
HNSAS(ph)VENVSLR	Irs2	IPI00379844	53.04	55.86	0.877	0.752	0.615	0.720
YIASVQGSAPS(ph)PR	Ranbp2	IPI00337844	36.79	/	0.875	/	0.596	/
EKEEEETS(ph)PDTSIPR	Arhgef5	IPI00855144	48.09	/	0.868	/	0.565	/
LPS(ph)PAQTQR	Micall2	IPI00280103	30.76	33.11	0.865	0.509	0.816	0.876
ASS(ph)HSSQSQGGGSVTK	Lmna	IPI00620256	47.84	58.67	0.194	3.858	0.523	1.945
GGVTGS(ph)PEASISGSK	Ahnak	IPI00553798	43.68	27.58	0.215	3.272	0.474	2.790
LPTSEEERS(ph)PAK	Trp53bp 1	IPI00229801	25.34	25.63	0.217	3.061	0.387	2.082
SGFGGMS(ph)SPVIR	Nup107	IPI00221767	28.39	40.37	0.372	2.643	0.626	2.319
AS(ph)SHSSQSQGGGSVTK	Lmna	IPI00620256	/	58.67	/	2.595	/	1.511
TEEDRENTQIDDTEPLS(ph)PVSNSK	Trp53bp 1	IPI00229801	/	28.8	/	2.576	/	1.904
SGFGGMSS(ph)PVIR	Nup107	IPI00221767	/	40.37	/	2.574	/	2.074
QEGAQENVKNS(ph)PVPR	Gmnn	IPI00131716	/	30.64	/	2.565	/	1.603
ASSHS(ph)SQSQGGGSVTK	Lmna	IPI00620256	47.84	58.67	0.224	2.410	0.536	1.175
AS(ph)PALGSGHHDGSGDSLEMSSLDR	Tomm70a	IPI00751137	64.86	47.86	0.293	2.308	0.464	2.047
GEVAPKET(ph)PKK	Marcksl 1	IPI00281011	/	26.82	/	2.274	/	1.651
AEAKPGT(ph)PAK	Nolc1	IPI00720058	36.93	39.65	0.308	2.251	0.470	1.673
KQQQEPTC(me)EPS(ph)PK	Hmga2	IPI00331612	26.67	30.2	0.287	2.231	0.428	1.718
SEDRPS(ph)SPQVSVAAVETK	Trp53bp 1	IPI00229801	/	48.56	/	2.071	/	1.704
LHSAQLS(ph)PVDETPATQSQLK	Mlf1ip	IPI00459115	/	36.63	/	1.947	/	1.619

SPAPSNPTLS(ph)PSTPAK	Mybbp1a	IPI00331361	34.8	33.16	0.159	1.852	0.323	1.256
PAS(ph)PLSGPR	D2Wsu81e	IPI00224127	/	29.84	/	1.802	/	1.652
AAKES(ph)EEEEEEEETEEK	Nolc1	IPI00720058	93.93	73.89	0.420	1.796	0.464	1.406
T(ph)SMGGTQQQFVEGVR	Ctnnb1	IPI00125899	/	48.59	/	1.721	/	1.130
SLS(ph)TSGESLYHVLGLDK	Dnajc5	IPI00132206	50.5	47.88	0.508	1.703	0.739	1.197
EIITEEPS(ph)EEEADMPKPK	Ddx21	IPI00120691	/	31.38	/	1.693	/	1.383
ATWGDGGDNS(ph)PSNVVSK	Snap23	IPI00113798	64.07	49.53	0.493	1.687	0.455	1.545
FGEYNSNIS(ph)PEEK	Nop14	IPI00353010	36.25	30.49	0.434	1.684	0.539	1.451
HLFSS(ph)TENLAAR	Rab11fip1	IPI00169485	/	39.84	/	1.665	/	1.264
NWTEDIEGGISS(ph)PVK	Nfic	IPI00137501	/	32.95	/	1.656	/	1.073
APQS(ph)PTLAPAK	Cxadr	IPI00270376	25.52	30.84	0.219	1.618	0.291	1.103
LLKPGEEPSEYT(ph)DEEDTK	Pgrmc2	IPI00351206	39.74	35.31	0.393	1.606	0.475	1.357
KFS(ph)EEPEVAANFTK	Nop56	IPI00318048	35.3	31.73	0.442	1.595	0.504	0.850
ASSHSSQSQGGGS(ph)VTK	Lmna	IPI00620256	47.84	58.67	0.553	1.582	0.701	0.899
GISQTNLITTVT(ph)PEK	Epb41l3	IPI00229299	50.15	40.47	0.458	1.549	0.521	1.551
QKS(ph)DAEEDGVTGSQDEEDSKPK	Canx	IPI00119618	88.22	64.73	0.476	1.533	0.545	1.340
TTVYYQS(ph)PLESKPR	Atad2	IPI00135252	/	41.56	/	1.532	/	1.139
T(ph)GSLQLSSTSIGTSSLK	Cobll1	IPI00762331	/	31.52	/	1.526	/	0.746
VQTT(ph)PSKPGGDR	Cdc20	IPI00320406	30.44	31.01	0.417	1.516	0.586	0.870
AEEDEILNRS(ph)PR	Canx	IPI00119618	/	25.35	/	1.506	/	1.350
SSGS(ph)PYGGGYGSGGGSGGYGSR	Hnrnpa3	IPI00269661	113.25	92.56	0.420	1.501	0.581	1.346
KQNETADEAT(ph)TPQAK	Nolc1	IPI00720058	/	43.74	/	1.498	/	1.422
SRLTPTTPES(ph)SSTGTEDK	Sqstm1	IPI00133374	/	74.88	/	1.485	/	0.733
AAAT(ph)PESQEPQAK	Marcksl1	IPI00281011	38.45	26.81	0.438	1.477	0.531	0.964
AGGS(ph)PASYHGSTSPR	Epn2	IPI00336844	49.92	47.77	0.503	1.473	0.498	1.475
IALESVGQPEEQMESGNC(me)S(ph)GGDDDWTHLSSK	Sqstm1	IPI00133374	/	27.33	/	1.471	/	0.787
SSSSLLAS(ph)PSHIAAK	Fam62b	IPI00266942	26.75	30.8	0.594	1.465	0.568	1.344
AGS(ph)SPTQGAQNEAPR	Tcf20	IPI00407458	/	30.95	/	1.457	/	1.514
KAPLTLAGS(ph)PTPK	Wiz	IPI00263016	/	39.77	/	1.455	/	1.147
KLDTFQSTS(ph)PK	Ddx24	IPI00113576	/	27.61	/	1.453	/	1.063
GVTASSSS(ph)PASAPK	Ncam1	IPI00122971	43.46	34.3	0.244	1.437	0.346	1.195
SRLT(ph)PTTPESSSTGTEDK	Sqstm1	IPI00133374	/	74.88	/	1.435	/	0.821
SDAEEDGVTGS(ph)QDEEDSKPK	Canx	IPI00119618	88.22	64.73	0.467	1.430	0.557	1.215
SSS(ph)FGSVSTSSTSSK	Snx16	IPI00331029	/	54.62	/	1.416	/	4.998
S(ph)RPLNAVSQDGK	Csda	IPI00330591	47.17	44.25	0.563	1.416	0.553	1.041
TVGNVS(ph)PTAQMVQR	Rbm7	IPI00133061	/	28.2	/	1.414	/	1.646
S(ph)SGSPYGGGYGSGGGSGGYGSR	Hnrnpa3	IPI00269661	113.25	92.56	0.461	1.414	0.578	1.245
SRLTPTT(ph)PESSSTGTEDK	Sqstm1	IPI00133374	/	74.88	/	1.408	/	0.841
IAQEIASLS(ph)KEDVSK	Ralbp1	IPI00421132	48.23	52.17	0.463	1.392	0.539	1.266
KPAQETEETS(ph)SQESAEED	Hmga2	IPI00331612	40.72	28.37	0.482	1.384	0.484	0.886
TEMDKS(ph)PFNSPSPQDSPR	Nfic	IPI00137501	/	35.42	/	1.371	/	1.118
GDKS(ph)SEPTEDVETK	Tgoln2	IPI00408895	46.27	33.26	0.585	1.370	0.553	1.109
GEATAERPGEAAVASS(ph)PSK	Marcks	IPI00229534	53.11	53.46	0.600	1.362	0.576	1.450